IAEA-TECDOC-985

Accelerator driven systems: Energy generation and transmutation of nuclear waste

Status report

INTERNATIONAL ATOMIC ENERGY AGENCY

November 1997

The IAEA does not normally maintain stocks of reports in this series. However, microfiche copies of these reports can be obtained from

INIS Clearinghouse
International Atomic Energy Agency
Wagramerstrasse 5
P.O. Box 100
A-1400 Vienna, Austria

Orders should be accompanied by prepayment of Austrian Schillings 100,— in the form of a cheque or in the form of IAEA microfiche service coupons which may be ordered separately from the INIS Clearinghouse.

The originating Section of this publication in the IAEA was:

Nuclear Power Technology Development Section
International Atomic Energy Agency
Wagramerstrasse 5
P.O. Box 100
A-1400 Vienna, Austria

ACCELERATOR DRIVEN SYSTEMS: ENERGY GENERATION AND TRANSMUTATION OF NUCLEAR WASTE. STATUS REPORT
IAEA, VIENNA, 1997
IAEA-TECDOC-985
ISSN 1011–4289

Printed by the IAEA in Austria
November 1997

FOREWORD

One of the greatest obstacles facing nuclear energy is how to properly handle the highly radioactive waste which is generated during irradiation in reactors. In order for nuclear power to realize its full potential as a major energy source for the entire world, there must be a safe and effective way to deal with this waste. In the past years more and more studies have been carried out on advanced waste management strategy (i.e. actinide separation and elimination) in various countries and at an international level. An innovative concept of a hybrid system for transmutation of long-lived radioisotopes, i.e. the combination of a subcritical nuclear reactor with an high energy particle accelerator, has been suggested recently. It is claimed that accelerator-driven transmutation of waste (ATW), a concept which has being developed in different countries for a period of more than 30 years, offers new prospects for transmutation of high level nuclear waste. The system would convert highly radioactive materials, with half-lives as long as one million years, to non-radioactive materials or materials with much shorter half-lives. In addition, the hybrid system can generate electricity converting transuranium waste.

A Special Scientific Programme on "Use of High Energy Accelerators for Transmutation of Actinides and Power Production" was organized of the IAEA in Vienna on 21 September 1994 in conjunction with the 38th General Conference to present and investigate various technical options for transmutation of actinides and power production using high energy accelerators and to discuss their advantages and disadvantages together with prospects for their technical and economic viability and to understand what could be the role of the IAEA in the further development of this scientific area. Six experts presented their views on key issues of existing concepts and R&D programmes and discussed in depth short and long term perspectives of accelerator driven transmutation concepts.

As recommended by participants of the Special Scientific Programme, the IAEA has initiated work on a status report on accelerator driven systems (ADS). The general purpose of the status report is to provide, in particular for planners, decision makers, and other parties that are not directly involved in the development of ADS, an overview of ongoing development activities, different concepts being developed and their project status, as well as typical development trends.

In November 1994, the IAEA convened a consultants meeting on the status of accelerator driven systems, which brought together experts in this field from France, Japan, the Russian Federation, Sweden and CERN. The purpose was to review the current status of ADS technology and to evaluate the incentives and justifications for this technology in the light of present world energy demands. A draft report based on this review was prepared using input from the experts in areas such as the state of the art in ADS technology, the large scale technical feasibility and the economics of accelerator driven transmutation technology as well as their safety and related environmental aspects. These contributions were reviewed and discussed by the experts at a second consultants meeting and the results of this updated evaluation are summarized in the present TECDOC. This document includes the individual contributions by experts from six countries and two international organizations in many different areas of the accelerator driven systems technology. The report was written during a period of a very dynamic development of different ideas and conceptual designs of the accelerator driven transmutation technology. It is believed, however, that the report gives a comprehensive overview of the most interesting projects which were conducted in that time.

The IAEA would like to thank all those individuals who participated in the consultants meetings, and provided the written contributions from the various countries. Special thanks are due to W. Gudowski from Sweden, who compiled, processed and edited the input from the experts and to C. Rubbia, who provided a comprehensive report on the ADS concept elaborated by CERN. The valuable contributions from the ADTT-division (C. Bowman, F. Venneri and S. Wender) from the Los Alamos National Laboratory are to be acknowledged as well as H. Takahashi's (Brookhaven National Laboratory) invaluable assistance. V. Arkhipov from the IAEA's Division of Nuclear Power and the Fuel Cycle is the officer responsible for preparing this document. The IAEA would like to thank A. Soltan for his help in the final editing of this report.

EDITORIAL NOTE

In preparing this publication for press, staff of the IAEA have made up the pages from the original manuscripts as submitted by the authors. The views expressed do not necessarily reflect those of the governments of the nominating Member States or of the nominating organizations.

Throughout the text names of Member States are retained as they were when the text was compiled.

The use of particular designations of countries or territories does not imply any judgement by the publisher, the IAEA, as to the legal status of such countries or territories, of their authorities and institutions or of the delimitation of their boundaries.

The mention of names of specific companies or products (whether or not indicated as registered) does not imply any intention to infringe proprietary rights, nor should it be construed as an endorsement or recommendation on the part of the IAEA.

The authors are responsible for having obtained the necessary permission for the IAEA to reproduce, translate or use material from sources already protected by copyrights.

CONTENTS

A. INTRODUCTION 9

A.1. Statement of concept and goal 9
A.2. History and current status 10

B. PHYSICAL FEATURES 12

B.1. Classification of the ADS 12
B.2. Target and blanket - general issues 13
B.2.1. Liquid target/fuel and associated fuel cycle technologies 17
H. Katsuta
B.2.2. Concept of the neutron generating targets with molten metal circulation 23
E.I. Efimov, Yu.I. Orlov, V.T. Gorshkov, V.A. Shulyndin
B.2.3. Physical aspects of neutron generation in the target of an accelerator driven system 26
V.P. Eismont, S.G. Yavshits
B.2.4. Physical features of target and blanket 32
T. Nishida
B.2.5. The concept of a heavy water-PB grains fluidized bed neutron generating target 44
V.R. Mladov, M.L. Okhlopkov, V.D. Kazaritsky, V.F. Batyaev, P.P. Blagovolin, N.V. Stepanov, V.V. Seliverstov
B.2.6. Accelerator driven heavy water blanket on circulating fuel 48
V.D. Kazaritsky, P.P. Blagovolin, V.R. Mladov, M.L. Okhlopkov, V.F. Batyaev, N.V. Stepanov, V.V. Seliverstov
B.2.7. Chemical technology of the systems, partitioning and separation, disposal 54
V.I. Volk
B.3. Fuel and fuel cycles 58
B.3.1. Fuel cycle 59
T. Ogawa, Y. Suzuki
B.3.2. Solid TRU fuels and fuel cycle technology 63
T. Ogawa, Y. Suzuki
B.4. Accelerator driven systems (ADS): A principal neutronics and transmutation potential 69
I. Slessarev
B.4.1. Overall neutronics of the ADS 69
B.4.2. Deterministic safety aspects 70
B.4.3. Economics 70
B.4.4. Toxicity transmutation potential of the ADS 70
B.4.5. Conclusions 78
B.5. General accelerator issues 81
B.5.1. Cyclotron for proton accelerator 81

C. RESEARCH AND DEVELOPMENT - GENERAL ISSUES 82
H. Takahashi, W. Gudowski

C.1. Radiation damage 82
C.2 Nuclear data codes 84

D. PERFORMANCE OF THE ADS SYSTEM - REVIEW OF EXISTING PROJECTS, NATIONAL/INTERNATIONAL ACTIVITIES 87

D.1. JAERI and PNC - OMEGA Project (Japan) 87
D.1.1. JAERI accelerator driven system project 87
T. Takizuka
D.1.2. Development of the partitioning process at JAERI 106
M. Kubota
D.1.3. High intensity proton linear accelerator development for nuclear waste transmutation 108
M. Mizumoto et al.
D.1.4. Present status of integral spallation experiments in JAERI 117
H. Takada, S. Meigo, T. Sasa, T. Nishida, T. Takizuka, K. Ishibashi, T. Nakamoto
D.1.5. Demonstration experiments at PNC 130
S. Tani, H. Nakamura
D.1.6. PNC - electron linac concept 132
S. Tani, H. Nakamura
D.2. Los Alamos National Laboratory ADS projects 135
D.2.1. Basis and objectives of the Los Alamos accelerator driven transmutation technology project 135
C.D. Bowman
D.2.2. The Los Alamos accelerator driven transmutation of nuclear waste (ATW) concept development of the ATW target/blanket system 154
F. Venneri, M.A. Williamson, L. Ning
D.2.3. A small scale accelerator driven subcritical assembly development and demonstration experiment at LAMPF 179
S. Wender et al.
D.3. CERN-group conceptual design of a fast neutron operated high power energy amplifier . 187
C. Rubbia et al.
D.3.1. Introduction 187
D.3.2. Physics considerations and parameter definition 199
D.3.3. The accelerator complex 230
D.3.4. The energy amplifier unit 244
D.3.5. Computer simulated operation 267
D.3.6. Closing the fuel cycle 294
D.4. ADS program in Russia 313
D.4.1. Weapon plutonium in accelerator driven power system 313
O.V. Shvedov, B.P. Murin, B.P. Kochurov, Yu.N. Shubin, V.I. Volk, P.V. Bogdanov

D.4.2. ITEP concept of the use of electro-nuclear facilities in the atomic power industry 376
I. Chuvillo, G. Kiselev
D.4.3. Physical features and performance accelerator driven systems (ADSs) 389
D.5. Brookhaven National Laboratory ADS concepts (USA) 402
H. Takahashi
D.5.1. Accelerator driven energy producer (ADEP) 402
D.5.2. Phoenix concept 406
D.5.3. Accelerator driven particle fuel transmuter 408
D.5.4. Fuel and coolant materials and target 408
D.5.5. Subscriticality and safety issue 409
D.5.6. Use of thorium, cross progeny fuel cycle (^{233}U production and transmutation of minor actinides) and neutron economy 410
D.5.7. Issue of non-proliferation (separation of power production and fuel processing) ... 410
D.5.8. Accelerator 411
D.6. The European Community projects 415
D.6.1. Impact of accelerator based technologies on nuclear fission safety - share cost project of the European Community 415
D.6.2. Swedish perspective on the accelerator driven nuclear system 419
W. Gudowski, H. Condé
D.6.3. ADS programs in France 423
D.6.3.1. French programs for advanced waste management options 423
M. Salvatores, J.P. Schapira, H. Mouney
D.6.3.2. MUSE-1: A first experiment at Masurca to validate the physics of sub-critical multiplying systems relevant to ADS 430
M. Salvatores, M. Martini, I. Slessarev, R. Soule, J.C. Cabrillat, J. P. Chauvin, Ph. Finck, R. Jacqmin, A. Tchistiaakov
D.6.4. ADS program in the Czech Republic 437
D.6.4.1. Approaches to a national ADS program in the Czech Republic 437
F. Janouch, M. Hron, R. Mach, V. Valenta
D.6.4.2. Achievement on accelerator parameters needed for energy producing and waste transmuting ADS 443
M. Hron, M. Kuzmiak

E. SAFETY ASPECTS 447
H.U. Wider

E.1. Basic safety features of ADS 447
E.2. First investigations of the behaviour of an accelerator driven fast oxide reactor during an unprotected loss-of-flow accident 453
E.3. Investigation of reactivity accidents in a large sodium-cooled ADS 462

F. CONCLUSIONS AND RECOMMENDATIONS 471

LIST OF CONTRIBUTORS TO DRAFTING AND REVIEW 473

A. INTRODUCTION

A. 1. STATEMENT OF CONCEPT AND GOAL

The objective of the Status Report on Accelerator Driven Systems (ADS) is to present the state of the art of this technology by reviewing the current status and progress of national and international programmes in this field. The report aims at helping to identify and possibly stimulate important directions of national and international efforts in this area.

The experts working on this report noted the increasing interest among some Member States and international research groups in exploring possible accelerator impact on the nuclear fuel cycle and consequently on the future of nuclear energy.

This report is divided into several sections. The basic physical phenomena and physical aspects of ADS are described in the first parts (**Section A**) followed by a review of existing national/international projects. The most important research and development issues are also reviewed. Nonproliferation aspects, the impact of ADS on the future of nuclear power and the experts recommendations on the international cooperation are presented in the final part of the report.

The chapters written by invited experts are signed by their names, the parts in which names are not indicated are written or/and compiled by the editor, Mr. W. Gudowski of Sweden.

Section B - Physical Features of ADS describes the most important parts of these systems: target, blanket, fuel cycle, associated fuel cycle technologies and general accelerator issues. Special attention is focused on the neutron economy for different concepts of ADS.

Section C is dedicated to some research and development problems : radiation damage and computer code development necessary for the progress of ADS.

Section D - Performance of the ADS Systems - the most important national/international projects are presented by the respective project leaders. Some smaller efforts in ADS are also described. Contributions to this section were written by the managers/leading scientists of the selected national/international projects. Many issues from sections B and C are also extensively described in the context of the particular projects. Planned demonstration/integral experiments are also reviewed in this section.

Section E with two appendices address some selected safety problems connected to ADS projects proposed by CERN-group.

Section F - formulates briefly the expert recommendations.

A.2. HISTORY AND CURRENT STATUS

In a fission chain reaction the excess of neutrons - if available - may be used for converting non-fissile materials into nuclear fuel as well as for transmutation of some long-lived radioactive isotopes into short-lived or even nonradioactive ones. This excess of neutrons can also be used to facilitate incineration of long-lived waste components, for fissile material breeding or for extended burnup. One way to obtain excess neutrons is to use a hybrid subcritical reactor-accelerator system called just Accelerator-Driven System. In such a system the accelerator bombards a target with high energy protons to produce a very intense neutron source (a process called spallation), these neutrons can consequently be multiplied in a subcritical reactor (often called a blanket) which surrounds the spallation target.

The basic process of accelerator-driven nuclear systems is nuclear transmutation. This process was first demonstrated by Rutherford in 1919, who transmuted ^{14}N to ^{17}O using energetic α-particles. I. Curie and F. Joliot produced the first artificial radioactivity in 1933 using α-particles from naturally radioactive isotopes to transmute Boron and Aluminum into radioactive Nitrogen and Oxygen. It was not possible to extend this type of transmutation to heavier elements as long as the only available charged particles were the α-particles from natural radioactivity, since the Coulomb barriers surrounding heavy nuclei are too great to permit the entry of such particles into atomic nuclei. The invention of the cyclotron by E.O. Lawrence [1] removed this barrier and opened quite new possibilities [2]. When coupled with the spallation process, high power accelerators can be used to produce large numbers of neutrons, thus providing an alternative method to the use of nuclear reactors for this purpose. Spallation offers exciting new possibilities for generating intense neutron fluxes for a variety of purposes.

The first practical attempts to promote accelerators to generate potential neutron sources were made in the late 1940's by E.O. Lawrence in the United States, and W.N. Semenov in the USSR. The first such application for the production of fissile material was the MTA [3] project at the Lawrence Livermore Radiation Laboratory. This project was abandoned in 1952 when high grade Uranium ores were discovered in the United States. The Canadian team at Chalk River [4] has always been a strong proponent of such a producer of fissile material which could be used in conjunction with a conversion-efficient CANDU reactor.

When the United States administration decided to slow down the development the fast breeder to promote non-proliferation goals, Brookhaven National Laboratory presented several proposals for accelerator breeders such as the Na-cooled fast reactor target, the Molten Salt target, the He-gas-cooled target, as well as the LWR fuel regenerator.

This concept of the accelerator breeder has also been studied by Russian scientists. Under the guidance of V.I. Goldanski, R.G. Vassylkov [5] made a neutron yield experiment in depleted Uranium blocks using the accelerator at Dubna.

The original idea of exploiting the spallation process to transmute actinide and fission products directly was soon abandoned. The proton beam currents required were much larger than the most optimistic theoretical designs that an accelerator could achieve, which are around 300 mA. Indeed, it was shown that the yearly transmutation rate of a 300 mA proton accelerator would correspond only to a fraction of the waste generated annually by a LWR of 1 GWe.

To use only the spallation neutrons generated in a proton target, the fission products would be placed around the target. For the highest efficiency, depending on the material to be transmuted, either the fast neutrons would be used as they are emitted from the target or they would be slowed down by moderators to energy bands with higher transmutation cross-sections, for example, the resonance or the thermal region.

In the last few years hybrid systems were proposed for different purposes. ADS on fast neutrons for the incineration of higher actinides was proposed at Brookhaven National Laboratory (PHOENIX-project) and is now carried out in Japan as a part of OMEGA-programme. Los Alamos National Laboratory has developed several ideas to use the hybrid system on thermal neutrons with a linear accelerator for incineration of Plutonium and higher actinides, for transmutation of some fission products in order to effectively reduce long-

term radioactivity of nuclear waste as well as for producing energy based on the Thorium fuel cycle. In 1993 Carlo Rubbia and his European group at CERN proposed a cyclotron based hybrid system to produce nuclear energy with Thorium-based fuel. This is an attractive option reducing the concerns about higher actinides in the spent fuel and giving the possibility of utilizing cheap and quite abundant Thorium. First experiments have already been performed by the CERN-group.

Many countries are considering to permanently store long-lived highly radioactive material in stable geologic formations, e.g. such as the Yucca Mountain in Death Valley. However, there is concern that the waste remains dangerous for many tens of thousands of years. The concern that such repositories can become mines for Plutonium has become of even greater concern as the U. S. has made it known that nuclear weapons can be made from Plutonium generated in commercial power reactors [6]. Therefore, it is worthwhile studying an alternative approach that would separate the long-lived nuclei from the high-level waste by transmuting such nuclei into short-lived or non-radioactive wastes.

ADS operates in non self-sustained chain-reaction mode and therefore minimizes the power excursion concern. ADS is operated in a subcritical mode and stays subcritical, regardless of the accelerator being on or off. The accelerator provides a convenient control mechanism for subcritical systems than that provided by control rods in critical reactors, and subcriticality itself adds an extra level of operational safety concerning criticality accidents. As described later, a subcritical system driven with an accelerator decouples the neutron source (spallation neutrons) from the fissile fuel (fission neutrons). Accelerator driven systems can in principle work without safe-shutdown mechanisms (like control rods) and can accept fuels that would not be acceptable in critical systems.

The technology of accelerating a charged particle to high energy has been well demonstrated in recent years, as has the technology of the target. However, extension of this capability to high-current beam-acceleration is required.

B. PHYSICAL FEATURES

B.1. CLASSIFICATION OF THE ADS

Figure 1 shows a classification of existing ADS concepts according to their physical features and final objectives. The classification is based on neutron energy spectrum, fuel form (solid, liquid), fuel cycle and coolant/moderator type, and objectives for the system. ADS systems - like reactors - can be designed to work in two different neutron spectrum modes - on fast or on thermal neutrons. There are also attempts [7] to design a system which will exploit the neutron cross-section resonances in what could be classified as a "resonance neutron" mode. Both, fast and thermal systems are considered for solid and liquid fuels. Even quasi-liquid fuel has been proposed based on the particle fuel (pebble bed) concept developed by BNL [see later sections]. The objective for some nuclear transmutation systems is to transmute existing nuclear wastes from light water reactors, mainly Pu and minor actinides, with or without concurrent energy production. These projects can be classified as an attempt to close the LWR-fuel cycle. Other systems are designed to take advantage of the Thorium fuel cycle for energy production. As can be seen in Figure 1 most concepts are based on linear accelerators. However, the CERN-group and BNL propose to use a proton cyclotron. The choice of the accelerator is an important issue which is discussed later in this report.

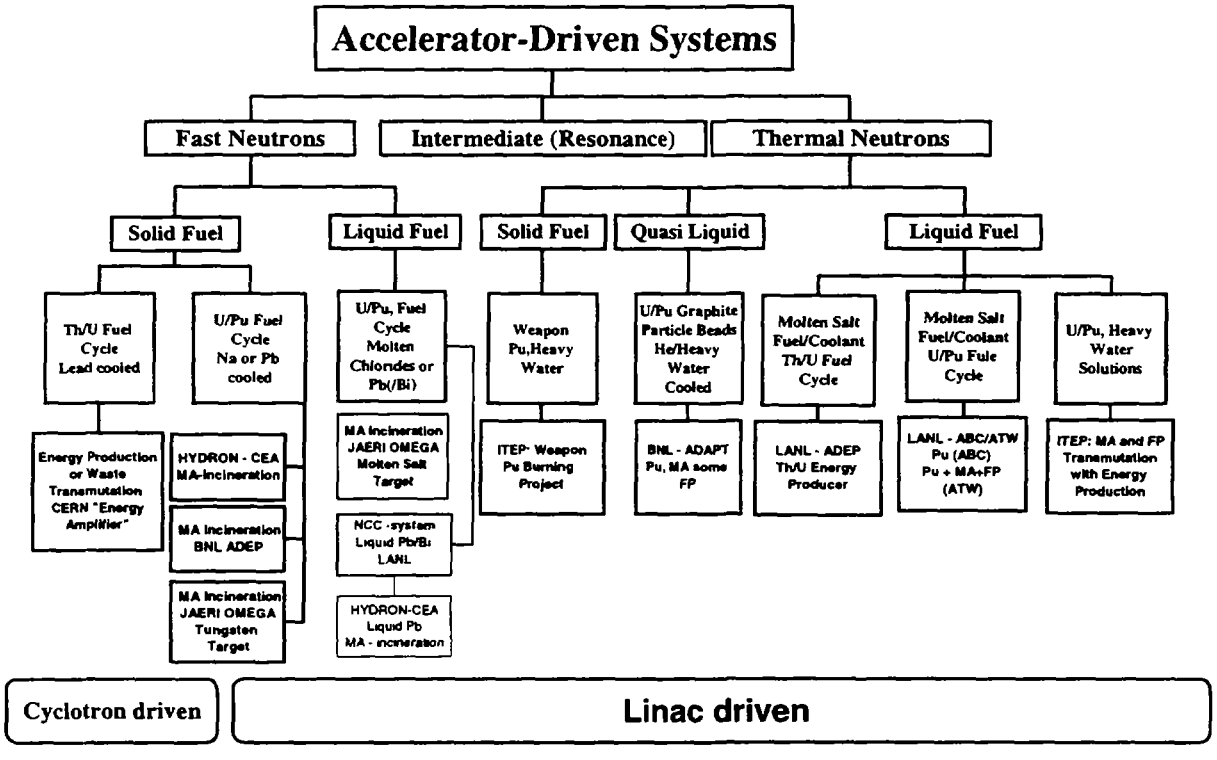

FIG. 1. Physical calssification of Accelerator-Driven systems

Spallation refers to nuclear reactions that occur when energetic particles (e g protons, deuterons neutrons, pions, muons, etc) interact with an atomic nucleus - the TARGET nucleus In this context, "energetic" means kinetic energies larger than about 100 MeV per nucleon At these energies it is no longer correct to think of the nuclear reaction as proceeding through the formation of a compound nucleus The initial collision between the incident projectile and the target nucleus leads to a series of direct reactions (intranuclear cascade) whereby individual nucleons or small groups of nucleons are ejected from the nucleus At energies above a few GeV per nucleon, fragmentation of the nucleus can also occur After the intranuclear cascade phase of the reaction, the nucleus is left in an excited state It subsequently relaxes its ground state by "evaporating" nucleons, mostly neutrons [1]

The spallation process is depicted in Fig 2, showing two stages of the process (intranuclear cascade and evaporation) For thick targets high energy (> 20 MeV) secondary particles (plus their progeny) can undergo further spallation reactions For some target materials, low energy (< 20 MeV) spallation neutrons (i e the cascade- evaporation neutrons) can enhance neutron production through low energy (n,xn) reactions For heavier nuclei, high energy fission can compete with evaporation in a highly-excited nucleus High-energy fission competition with evaporation in highly-excited nuclei is illustrated in Fig 2 Tantalum Tungsten, and Lead are examples of materials that can undergo spallation/high-energy fission

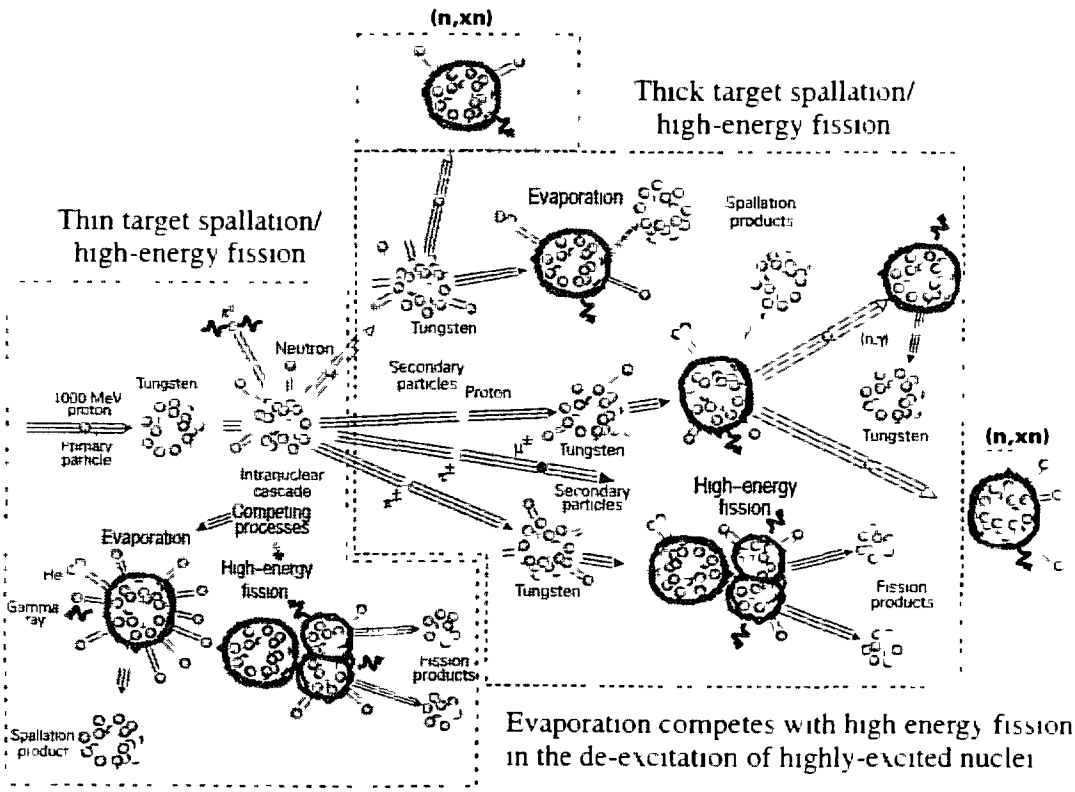

FIG 2 Illustration of the spallation process in thick targets, with evaporation competing with high energy fission in the de-excitation of highly excited nuclei

Some spallation-target fissionable materials such as Thorium and depleted Uranium can (in addition to undergoing high-energy fission) be fissioned by low-energy (~1 MeV to ~20 MeV) neutrons Spallation high -energy fission and low-energy neutron fission produce different nucelar debris (spallation and fission products)

These processes are calculated by intra- and inter-nuclear cascade codes developed by several

laboratories and described in the later sections.

Deuteron and triton projectiles produce more neutrons than protons in the energy range below 1-2 GeV; thus, the efficiency of transmutation can be increased using them. However, the high yield of neutrons among the low-energy deuterons and triton can easily contaminate the low-energy part of the accelerator with radio-activity from these spilled charged particles; this causes trouble in hand-maintaining the accelerator. Thus, the maintenance cost of the accelerator becomes high, unless spilling of the beam, which is more likely to occur in the low-energy section than in the high-energy section, is extremely limited. Figure 3 shows the neutron yield when deuterons or triton are injected into a finite-size U-target.

The function of the target in the ADS is to convert the incident high energy particle beam to low energy neutrons. These requirements can be summarized as [8]:

1. Compact size to enable good coupling to the surrounding blanket,
2. High power operation, of the order of 10 to 100 MW,
3. High neutron production efficiency,
4. Reliable and low maintenance operation,
5. Safe and low hazard operation,
6. Small contribution to the waste stream.

It is believed today that molten Lead or Lead-bismuth eutectic (LBE) are the best choices to meet most of these requirements. A significant problem with LBE, however, is the production of radioactive and highly mobile Polonium from high-energy proton and neutron reactions on Bismuth. This becomes a concern in accident scenarios where the polonim contained in the LBE is rapidly released at high temperatures. Lead, on the other hand, has a much reduced Polonium production, but higher operating temperatures. Experimental experience and further assessements are needed to make the best choice (see further sections).

In accelerator-driven transmution of MA (**M**inor **A**ctinides) or LLFP (**L**ong **L**ived **F**ission **P**roducts), a subcritical assembly (blanket) surrounding the spallation target can multiply the spallation neutrons. In quantitative terms, the total number of fissions N_{fiss} in the subcritical assembly can be expressed by:

$$N_{fiss} = N_h \Gamma_h \frac{k_{eff}}{(1-k_{eff})\nu}$$

where N_{fiss} = total number of fissions,

N_h = total number of fissions by high-energy proton reactions,

Γ_h = number of neutrons produced by high-energy proton reactions per fission in blanket (spallation, evaporation, and very high energy

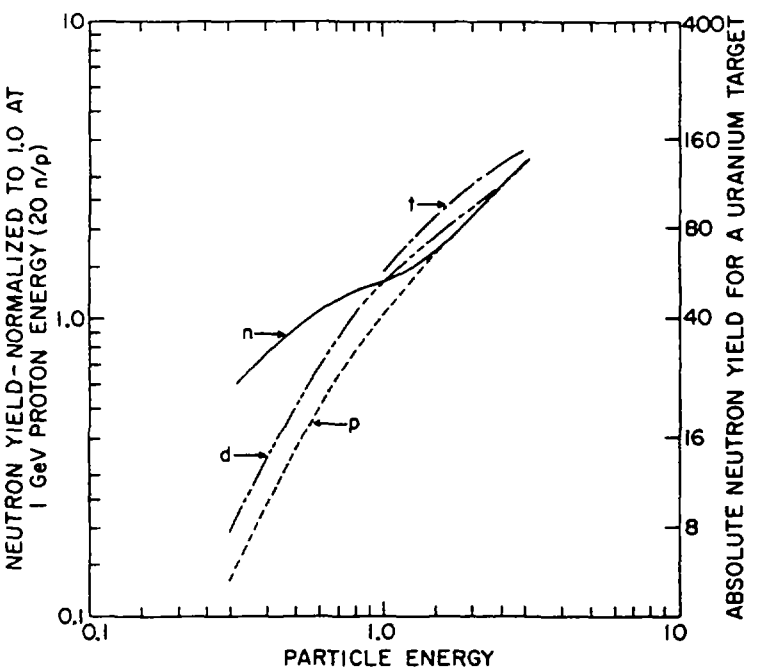

FIG. 3. Neutron yield vs. energy for proton, triton, deuteron, and neutron particles

fission)

ν = number of neutrons per 'regular' fission

k_{eff} = multiplication factor for 'regular' fission neutrons

By increasing the k_{eff} value of subcritical target, one can reduce the proton current required to incinerate the MAs If the k-value reaches 1, then the target becomes critical and does not require an outside source of neutron created by the proton accelerator; but instead the safety problem associated with criticality of "MA-reactor" has to be addressed So far, the k value that is most suitable for actinide incineration is under investigation Furthermore, it should be considered from many aspects, such as safety, the operational procedure, choice of material, and the cost of the incinerator k-values studied in many cases span over an interval of 0 9 - 0 98

The important issue in designing ADS is its inherent subcriticality and stability of reactivity This feature can significantly improve the safety of ADS and furthermore may eliminate the necessity of control rods Control rods are not only a safety concern (in most cases it is a mechanically driven device), they degrade - in the most of cases - the neutron economy of the system Good neutron economy is the crucial issue for ADS because it determines the power and consequently the cost of the accelerator

Similar to conventional nuclear reactors, ADS can operate in different neutron spectrum modes The thermal cross-section for transmuting MA and FP is larger than the fast neutron cross-section, so that the inventory of these materials in the core can be reduced substantially However, the thermal neutron cross-section of the transmuted products is also large, and, as soon as these daughter isotopes are produced in the core, it is desirable to remove them, otherwise the neutrons will be wasted by neutron capture by the poison isotopes The capture of fast neutrons by the fission products and the structural material is small, and from the point of view of neutron economy, the fast reactor is better than the thermal reactor Also, one would like to take advantage of the high η value for ^{239}Pu, the other actinides and MA to get extra neutrons produced by high-energy fission for transmuting the LLFP

The Thorium-Uranium fuel cycle is an attractive option for future ADS The Thorium-Uranium fuel cycle has advantages over the traditional Uranium-Plutonium cycle used in today's nuclear reactors, among them

1) The Thorium-Uranium cycle produces a relatively small amount of higher actinides compare with Uranium-Plutonium cycle, because of the small capture to fission ratio in ^{233}U and because of the presence of two other fissionable isotopes of Uranium (^{235}U and ^{237}U) in the chain leading to Plutonium and the other heavier actinides
2) The Thorium-Uranium cycle is regarded as safer than the Uranium-Plutonium cycle from a nuclear weapons proliferation standpoint, because of the presence of the hard-gamma emitter in ^{232}U decay chain as a minor product of the cycle, and because of the possibility of straightforward isotopic dilution of ^{233}U with depleted or natural Uranium in the feed or start-up fuel

However, Thorium-Uranium fuel cycle has less favourable overall neutron balance

These issues will be discussed in the later part of this report

REFERENCES

[1] E O Lawrence and N E Edlefsen, "On the Production of High Speed Protons", Science, LXXII, NO 1867, 376, October 10, 1939

[2] G J Russel, E J Pitcher and L L Daemen, "Introduction to Spallation Physics and Spallation Target Design", International Conference on Accelerator Driven Transmutation Technologies and Applications, Las Vegas, NV, July 25-29 1994

[3] C.M. van Atta, "A Brief History of MTA Project", ERDA Information Meeting on Accelerator Breeding , January 19-19 (1977)

[4] G.A. Bartholomew and P.R. Tunnicliffe, Eds, "The AECL Study for an Intense Neutron generator", Atomic Energy of Canada Limited, Report No. AECL-2600 (1966)

[5] R.G. Vassylkov, Vi.I. Goldanskii et al., Atomnaya Energiya 48, 329 (1978)

[6] Management and Disposition of Excess Weapons Pluronium, National Academy of Sciences, Committee on International Security and Arms Control, National Academy Press, Washington, DC 1994

[7] C. Rubbia (coordinator), "Neutron Driven Nuclear Transmutation by Adiabatic Resonance Crossing (TARC)", Proposal submitted to the European Union on 15th March, 1995.

[8] Venneri, F., et al., Accelerator-Driven Transmutation of Nuclear Waste (ATW): Status, New Concepts, and Future Development, LANL ADTT-Project Office presentation to DOE, December 1995

B.2.1. LIQUID TARGET/FUEL AND ASSOCIATED FUEL CYCLE TECHNOLOGIES

Hiroji Katsuta
Japan Atomic Energy Research Institute
Tokai-mura, Naka-gun, Ibaraki-ken 319-11 Japan

B.2.1.1. INTRODUCTION

Accelerator-driven transmutation systems with liquid target/fuel have advantages such as thecapability of establishinga continuous transmutation system without accompanying the batch reprocessing indispensable for solid target/fuel systems. In the liquid target/fuel systems, the nuclear waste from the system is designed to be restricted to only short-lived waste of fission products (FPs) and spallation products (SPs). The conceptional differences between solid and liquid systems in the fuel cycle technology are shown in Fig. 1. The concepts with liquid target/fuel systems may in principle have the advantage of

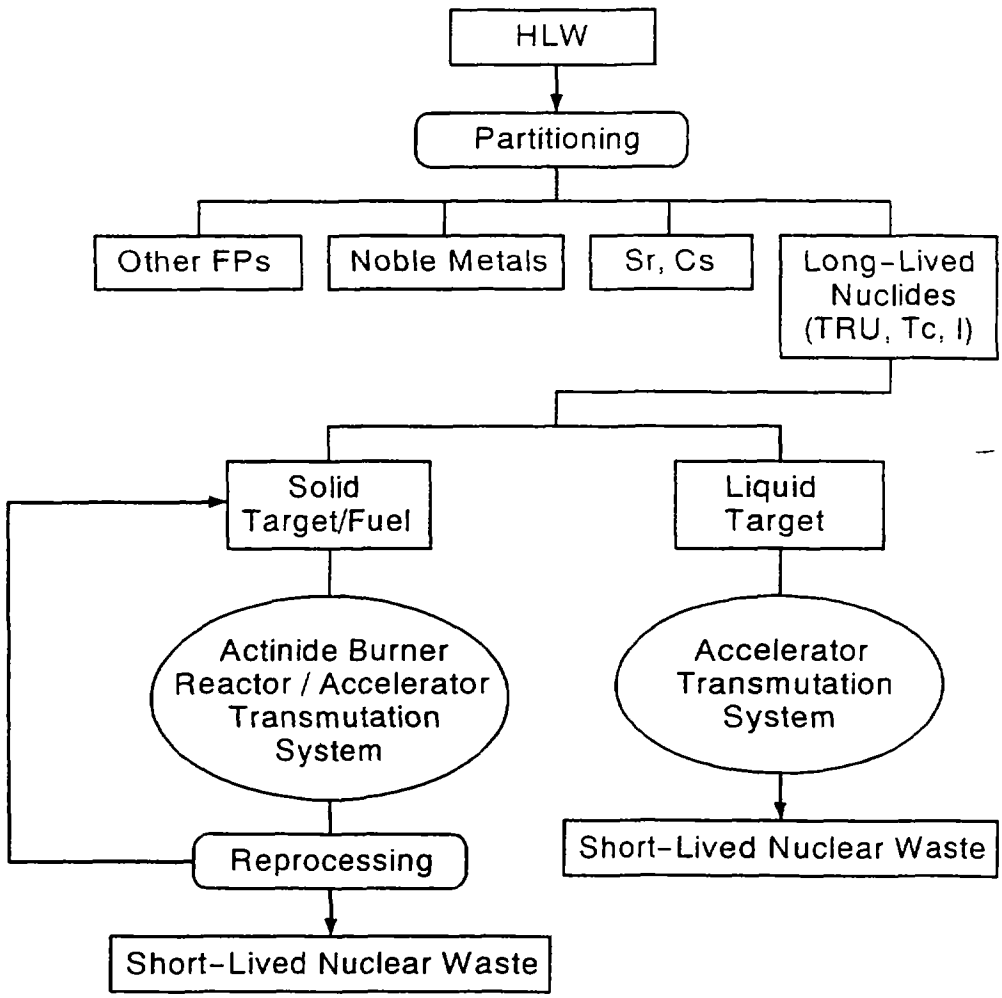

FIG. 1. Conceptual differences between the solid and liquid systems in the fuel cycle technology

eliminating the reprocessing processes for the spent fuel. However, since liquid target/fuel technology has not been proven, many R & Ds will be required to realize the liquid target/fuel system.

One of the JAERI proposed concepts with liquid target/fuel is the molten chloride salt system [1] and another is the liquid alloy system [2]. In the molten salt system, molten chloride salt dissolving transuranium (TRU) is adopted as the liquid target/fuel. In this system the heat exchangers are located in the target/blanket vessel to reduce the total TRU inventory. The TRU inventory in the system, however, is as large as 5,000 kg to transmute about 250 kg of minor actinides (MAs) per year. On the other hand, a liquid TRU alloy target/fuel of Pu-Np-Co-Ce is analyzed to examine the feasibility of a transmutation system with a small TRU inventory of less than 1,000 kg.

B.2.1.2. CONCEPT OF TRANSMUTATION TARGET/FUEL AND MATERIAL SELECTION

B.2.1.2.1. Molten salt target/fuel

Conceptional design studies on the transmutation system of TRU and long-lived FP of ^{99}Tc and ^{129}I have been performed. The technical feasibility of an accelerator-driven transmutation system with the molten chloride salt target/blanket has been assessed. To satisfy a requirement of the transmutation capacity of MA produced by about 10 units of 3,000 MW_t LWR, namely about 250 kg/a, fast neutron systems with an effective multiplication factor around 0.9 or more are needed.

To establish an efficient transmutation system with molten salt, molten chloride is selected from the point of view of the TRU solubilities and mass numbers of the component elements compared with the other possible salts such as fluorides. Concerning TRU solubilities in chloride salt systems reported, the $NaCl$-$ThCl_4$-$PuCl_3$ system [3] is attractive. The lowest melting temperature of the system is 325°C for the composition 46.5NaCl-18.5$PuCl_3$-35.0$ThCl_4$ as shown in Fig. 2. To make a preliminary analysis the NaCl-$PuCl_3$ system is adopted, whose eutectic temperature is

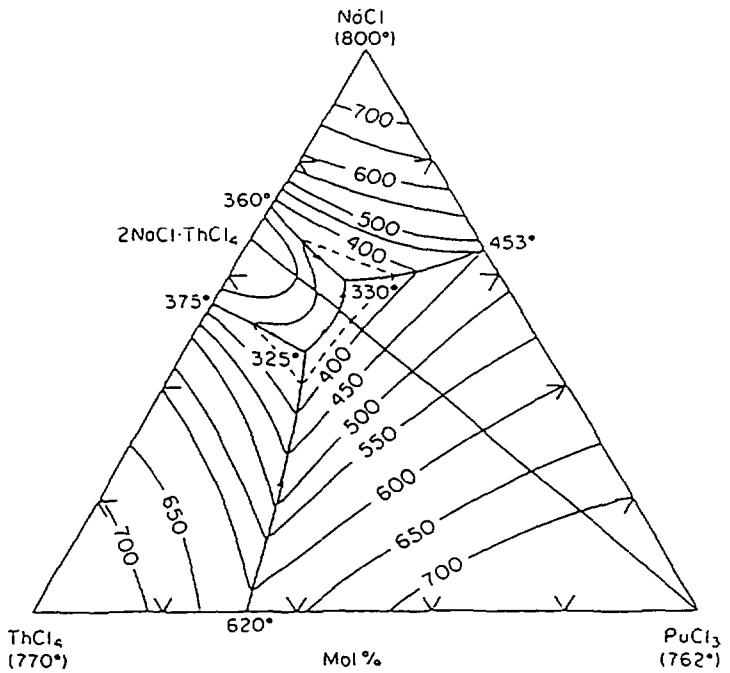

Temp. (°C)	Type	Composition (mol%) NaCl	$PuCl_3$	$ThCl_4$
330	Eutectic	58.5	18.5	23.0
325	Eutectic	46.5	18.5	35.0

The section $2NaCl·ThCl_4$-$PuCl_3$ was found to be binary with a minimum that occurs at 370°, 52%NaCl, 22%$PuCl_3$, 26%$ThCl_4$.

FIG. 2. Phase diagram of NaCl-$PuCl_3$-$ThCl_4$.

453°C for the composition 64NaCl -36$PuCl_3$. The solubilities of MAs in the salt are not reported, though Pu may be replaced by other actinides such as Np, Am, and Cm.

The parasitic neutron absorption cross section of the chlorine nuclide is not so large especially for fast neutrons. The amount of sulphur produced by the neutron absorption reaction of chlorine in the molten salt is estimated to be small enough and its effects on the target/blanket system will be ignored.

It is important for corrosion problems to be solved in the application of the molten salt technology to nuclear systems. Corrosion by chloride is a serious problem. It has been found, however, that low carbon steel may be usable as a structure material up to around 550°C, if water concentration in the salts can be controlled at sufficiently low values.

B.2.1.2.2. Alloy target/fuel

The liquid TRU target/blanket system is composed of a liquid TRU alloy target, a graphite blanket, and an upper plenum of molten fluoride salt. Eutectic alloys of Pu with Fe, Ni and Co make the melting temperature as low as around 450°C as shown in the phase diagram of Fig. 3. In the study, Pu-Co-Ce alloys [4] have been chosen as a fundamental alloy system and (15-45)Pu-25Co-(60-30)Ce is adopted for the nuclear calculation. The chemical properties of Pu and Np are very close at high temperatures and γ-Np and ε-Pu make a solid solution over a wide composition range. Accordingly, Pu in the alloy is considered to be easily substituted by Np without a significant change in the melting temperature of the alloy. The ratio of Pu to Np of 1 to 2.6 is adopted as the composition of the alloy. In this concept, transmutation of long lived FP of Tc is attempted by substituting Co by Tc in the alloy. The preliminary study has been performed on a target/fuel alloy with the composition (11-32.5)Np-(4-12.5)Pu-24Co-(60-30)Ce-Tc.

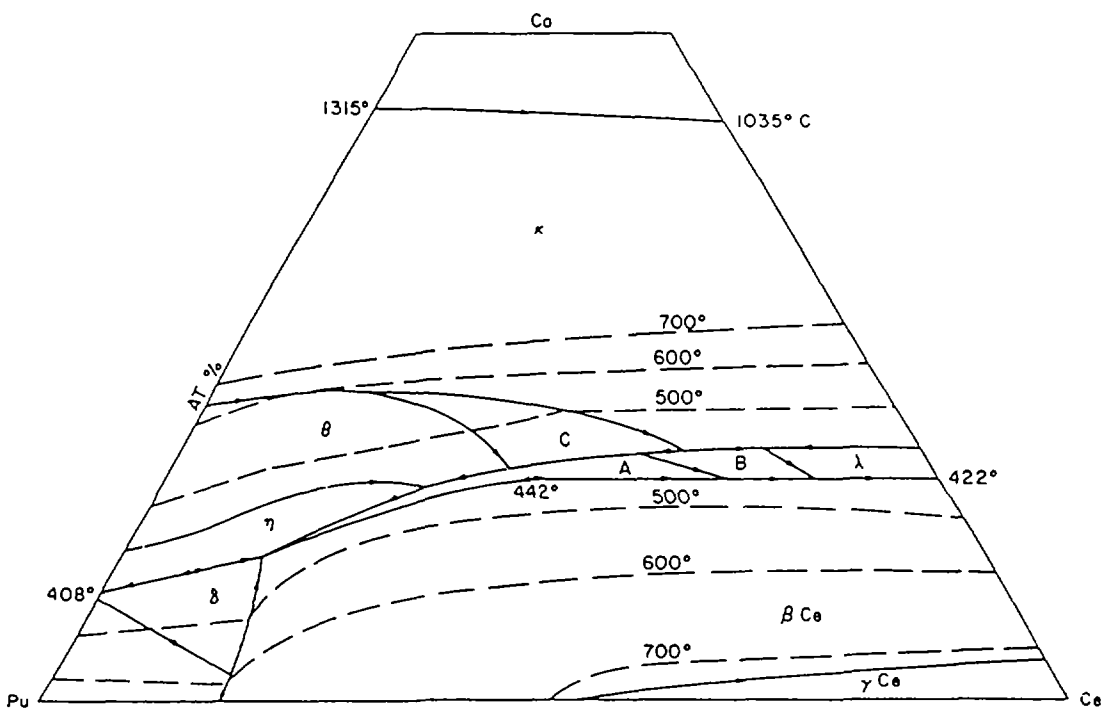

FIG. 3. Phase diagram of Pu-Co-Ce system.

The roles required of the secondary coolant in the system are heat removal from the liquid target alloy and material transfer to maintain the liquid alloy temperature and composition constant during operation. The TRU concentration in the secondary coolant has to be kept low enough from the safety point of view. In this study, molten salt of the LiF-BeF_2 system is selected for the secondary coolant. The solubility of

Pu (PuF_3) in Li_2BeF_4 has been measured to be about 0.5 atomic % at 600 °C.

B.2.1.3. REMOVAL OF FISSION PRODUCTS AND SPALLATION PRODUCTS

B.2.1.3.1. Molten salt target/fuel

In a target with an effective neutron multiplication factor of 0.92, more than ninety percent of MA is transmuted by the fission reaction, and several percent by the spallation reaction. The transmutation products in the molten salt are expected to be similar in composition to the FPs in fast reactors. The fission reaction of the TRU chloride may produce free chlorine according to the following reaction,

$$MACl_3 + n \rightarrow 3Cl + FPs.$$

Considerable amounts of FPs and SPs may react with the free chlorine and become chlorides in the molten-salt target/blanket. The major chlorides are shown in Table I arranged in order of the free energy of formation. In the table other chlorides such as actinide chlorides and alkali chlorides are also listed.

TABLE I. CHLORIDE IN TARGET SALT

Chloride -	ΔGf	Chloride	- ΔGf	Chloride	-ΔGf(kcal/g.Cl)
$BaCl_2$	83.4	$AmCl_3$	60.4	$CdCl_2$	30.4
KCl	81.4	$CmCl_3$	58.8	$FeCl_2$	26.6
RbCl	81.2	$PuCl_3$	58.5	$TeCl_2$	17.1
$SrCl_2$	81.0	$MgCl_2$	57.7	$MoCl_2$	8.0
CsCl	80.0	$NpCl_3$	54.1	$TcCl_3$	7.0
$SmCl_2$	80.0	UCl_3	51.8	RhCl	5.8
LiCl	78.8	$SnCl_2$	51.3	$PdCl_2$	3.8
$CaCl_2$	77.9	$ZrCl_2$	49.2	$RuCl_3$	1.4
NaCl	75.7				
$LaCl_3$	67.0				
$PrCl_3$	66.3				
$CeCl_3$	66.3				
$NdCl_3$	64.2				
YCl_3	61.2				

Owing to the chloride formation energy the FPs are qualitatively divided into the following 3 groups:

Group l: Inert gases and volatile chlorides.

Xe, Kr, I, $TeCl_4$, ZrCl2 (about 23% of total FP).

Group 2: Noble metals and transition metals (free energy of formation is smaller than that of Cd-chloride in absolute value).

Nb, Te, Mo, Tc, Rh, Pd, Ru (about 33% of total FP).

Group 3: Alkaline earth metals, Lanthanides and Y (free energy of formation is large in absolute value).

Ba, Rb, Sr, Cs, Sm, La, Pr, Ce, Nd, Eu, Gd, Y (about 44% of total FP).

For group 1, the He gas purge method will be applicable. $TeCl_4$, ZrCl2 and I are also expected to be purged away but the experiment has not been performed yet. For group 2, a reductive extraction method with liquid Cd may be applicable. The noble metals extracted to Cd metal may be removed continuously by a cold trapping. The elements in group 3 may immediately form stable chlorides after being produced by transmutation reactions. These chlorides can not be reduced by Cd metal. The cold trapping method may be applicable for group 3 elements, since the melting points of these chlorides are high enough to be compared with the target salt matrix. The separation methods applicable to the FPs of these three groups are listed in Table II. It is important in the FP removal from the target salt to remove the stable and short-lived FPs without contamination from the long-lived nuclides. If the contamination is low enough, the separated FPs may be easily disposed of.

TABLE II. SEPARATION METHODS FOR FISSION PRODUCTS

He Purge Method (Group 1) 23%		Reductive Extraction Method (Group 2) 33%		Cold Trap Method (Group 3) 44%	
	(%)		(%)		(%)
Kr	0.7	Nb	0.1	Rb	0.6
Xe	13	Mo	11.3	Sr	1.3
Te($TeCl_4$)	1.8	Tc	2.3	Y	0.7
I	1.0	Ru	8.7	Cs	10.7
Zr($ZrCl_2$)	7.3	Rh	2.5	Ba	4.4
		Pd	7.3	La	3.3
		Ag	0.7	Ce	6.0
				Pr	3.1
				Nd	10
				Pm	0.2
				Sm	3.1
				Eu	0.3
				Gd	0.4

B.2.1.3.2. Liquid alloy target/fuel

Fission products produced in the liquid alloy target are partly transferred to the secondary molten-salt coolant through direct contact between the liquid alloy and the molten salt according to the distribution coefficients of each of the elements between the two liquids. Considering the distribution coefficients the

following behavior and separation methods may be expected for the FPs.

(1) Gas species: Kr, Xe, T, I, volatile fluorides.

These elements are expected to move to the molten fluoride salt, and then the He purge method will be applicable.

(2) Noble metals and transition metals: Ru, Rh, Pd, Ag, Nb, Mo, Tc, Ta, W.

These elements may mostly remain in the liquid alloy phase, and then the cold trapping method may be applicable.

(3) Alkali and alkaline earth metals: Rb, Cs, Sr, Ba.

These elements may mostly move to the molten-salt phase, and remain in it.

(4) Lanthanides: La, Ce, Pr, Nd, Pm, Sm, Eu, Gd

The behavior of the lanthanides is difficult to estimate in the liquid alloy target system. The free energy of formation of the lanthanide fluorides is almost the same as those of the actinides or higher (in absolute value) than the actinides.

B.2.1.4. SUMMARY

Conceptual design studies on accelerator-driven transmutation systems with molten-salt target/fuel and liquid alloy target/fuel have been carried out at JAERI. In the design studies, molten salt and alloy selections, nuclear calculations, and thermal hydraulics calculations have been performed. The experimental studies on physical and chemical properties of the molten chloride salts are also underway.

REFERENCES

[1] KATSUTA, H., et al.: Proc.of OECD/NEA Information Exchange Meeting on Partitioning and Transmutation, ANL Chicago (1992).

[2] KATSUTA, H., et al.: Proc. of 7th Int. Conf. on Emerging Nuclear Energy System (ICENES '93), Makuhari (1993).

[3] ROTH, R.S.: Phase Diagrams for Ceramists, Volume V (1983), American Ceramic Soc.

[4] HANNUM W. H., and KIRKBRIDE, L. D.: "The Molten Plutonium Burn up Experiment", LA-3384-MS.

[5] THOMA, R. E.: ORNL-Tm-2256 (1968).

B.2.2. CONCEPT OF THE NEUTRON GENERATING TARGETS WITH MOLTEN METAL CIRCULATION

E.I. Efimov†, Yu. I. Orlov†, V.T. Gorshkov‡ and V.A. Shulyndin‡

†Institute of Physics and Power Engineering, Obninsk, Kaluga Region, Russia

‡ EDO "Hydropress", Podolsk, Moscow, Russia

The structure of a molten Lead-bismuth target has been developed for proton beam power - 10 MW (proton energy Ep=1.6 GeV, current I=6 mA, beam diameter ~ 100 mm). The target design is illustrated in Fig. 1.

The target itself is a cylindrical steel tube with inner diameter 242 mm and 1 m in length, containing an axis-symmetric tube with external diameter 204 mm. The coolant flows down the inner tube, cooling the steel hemispherical 1.5 mm thickness diaphragm on the guide, then flows up the circular gap between the external and inner tubes and enters the heat exchangers cooled with water. The circulation is achieved by electromechanical pumps.

The exchangers (3 units) and the pumps (3 units) are placed above the target in the same vessel.

The diaphragm (window) on the guide, in which the specific energy release rate calculated by code MARS-10 is ~1.5 kW/cm^3 is the most stressed unit in the target structure.

Special constructions - coolant flow rate "dividers" have been designed into the target to improve the window cooling and to achieve a conformity in the coolant flow rate profile in accordance with the energy release field.

The radiation damage stability of the window is a complicated problem. According to assessments the diaphragm might have to be replaced once every 3 months,

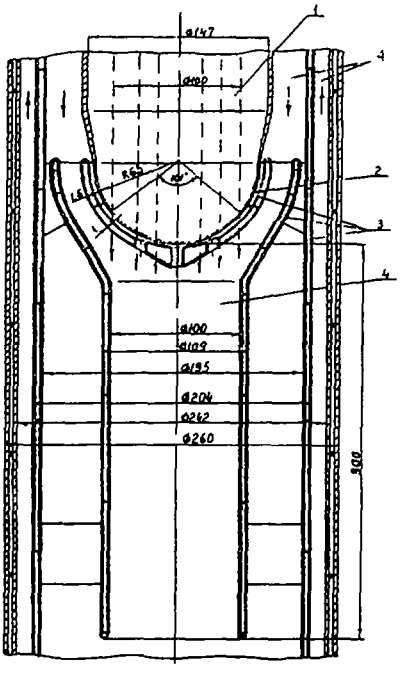

FIG. 1. Pb-Bi target design: 1- beam channel, 2 - diaphragm, 3 - dividers of flow rate, 4 - circulating alloy

The main heat engineering characteristics of the target circuit and the equipment have been evaluated. The coolant flow rate is ~150 m^3/hour, input temperature - 250°C, output temperature - 400°C.

Assessment of Polonium activity in the target circuit was also made. The specific activity is about several hundred curies per litre and is determined by ^{210}Po.

As a result of analysis and calculations by engineering methods a preliminary structure of the target without a window was proposed for a beam power ~100 MW. The target is a steel cylindrical vessel with 1 m diameter and 1.2 m height where the guide tube with diameter 175 mm enters. The target design is illustrated in Fig. 2. An axis symmetric inner tube is arranged in the vessel. The tube has diameter 320 mm and its funnel widens in the guide direction up to diameter 550 mm. The length of the transition part is 500 mm. The coolant enters the funnel from a circular nozzle, flows down to heat exchangers and is then pumped up along the circular area between the inner tube and the vessel. The coolant flow rate is 950 m^3/h, input temperature - 250°C, output temperature - 500°C.

Some preconceptual design of the target circuit has been made and the necessary equipment has been considered.

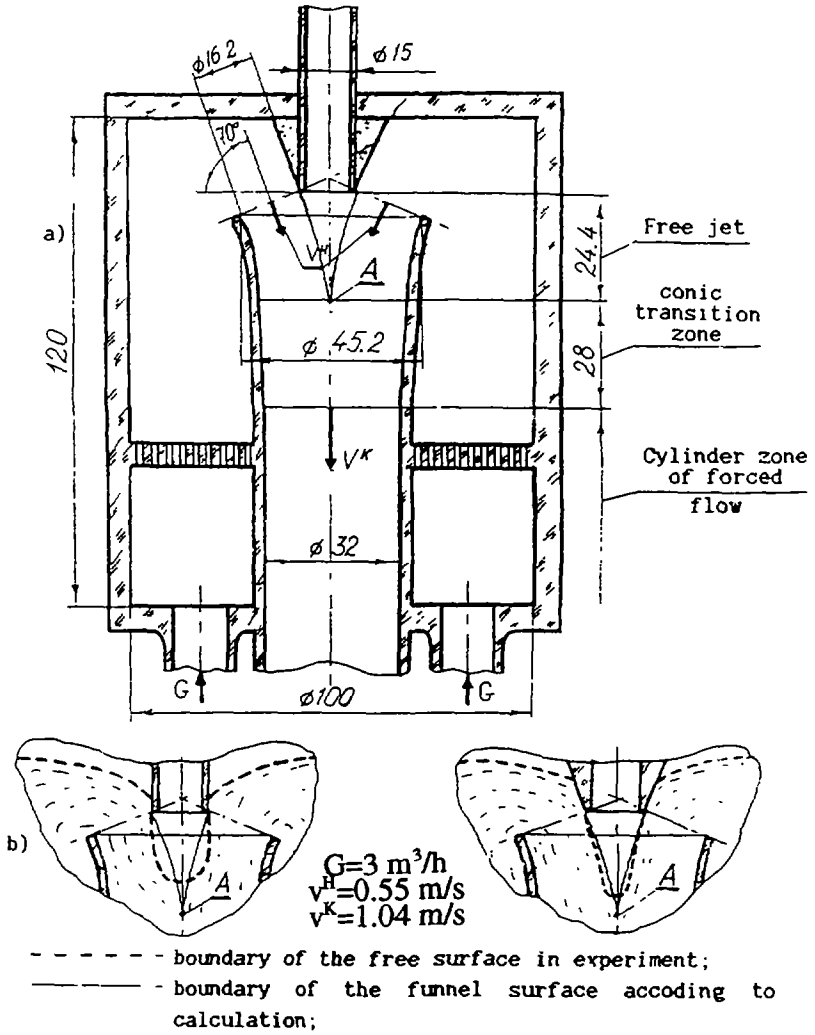

FIG. 2. a) Scheme of the experimental section; b) Forms of free surfaces for various designs of annular hole.

One of the main difficulties in the development of a target without a window is adjustment of the entrance geometry and the circuit parameters to ensure the coolant's continuous flow without vortexes and immobile areas. This requires numerical and experimental simulation of the coolant hydrodynamics in the entrance area.

The mock-up of the entrance unit was designed and manufactured for water modelling of the coolant. Preliminary experimental data were obtained.

Yet another important problem for a target without a window is evaporation of the coolant and radioactive admixtures into the guide tube.

A theoretical analysis of this problem has been made. For this purpose data on element vapour pressure and the Langmuire-Knudsen law on maximum evaporation rates into vacuum were used. The results of this analysis are presented in Table I.

A program of experimental research was developed. An experimental mock-up was manufactured for investigating the Lead-bismuth evaporation process in static conditions with use of a contact level gauge. Preliminary experiments were carried out. It was found that evaporation of (Pb-Bi) coolant components takes place mainly in the form of the intermetallic compounds Pb_xBi_y.

TABLE I. Calculated rates of evaporation of Pb, Bi and Po from their eutectic in g/cm^{2}h

Temperature, °C	130	300	500	700	1000
Pb	1.7E-15	2.7E-8	6.9E-4	2.6E-1	5.7E+1
Bi	8.1E-12	4.1E-5	5.0E-1	1.3E+2	1.8E+4
Po	2.9E-14	1.9E-9	1.6E-6	8.6E-5	3.1E-3

The molecular mechanism of evaporation was considered. The model of this vaporization is presented in Fig. 3.

A preliminary analysis of the problems of coolant quality maintenance was carried out for the target circuit operation conditions. A number of the elements accumulating in the target as spallation products (W,Ta, Hf, Ba etc.) have much higher oxygen affinity than Lead and Bismuth. This may cause a decrease of oxygen concentration in the coolant below the optimum value, which may require implementation of special measures.

From the point of view of corrosion strength stainless steels with chromium and nickel were recommended as construction materials for the target circuits.

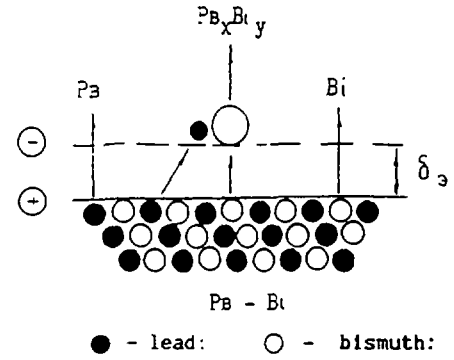

element	Pb	Bi	Po
Electro-negati-vity (eV) accor-ding to Poling	1.87	2.03	2.00

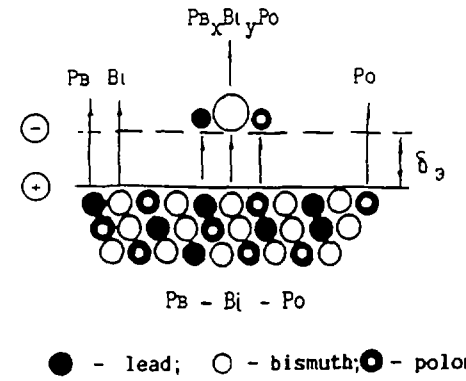

FIG.3. The model of Lead-Bismuth melt vaporization

B.2.3. PHYSICAL ASPECTS OF NEUTRON GENERATION IN THE TARGET OF AN ACCELERATOR DRIVEN SYSTEM

V.P.Eismont, S.G.Yavshits

V.G.Khlopin Radium Institute, St.-Petersburg, Russian Federation

B.2.3.1. INTRODUCTION

The massive target of an accelerator-driven system serves as a powerful neutron source for the irradiation of the subcritical reactor (blanket). The high-intensity neutron flux in the accelerator-driven system is caused by an interaction of incident protons with target nuclei which has an essentially cascade character at incident energies around 1 GeV. The primary proton knocks fast particles out from the nuclei with average energy about 100 MeV, which in turn can cause the same reactions on other nuclei. The residual nuclei have sufficiently high excitation energy to decay by particle emission or fission. If the cascade stage breeds 4-5 neutrons per primary proton then the multiplicity of evaporated neutrons is about 15 particles but the average kinetic energy is about 2-3 MeV only. The target neutrons are used for feeding the subcritical reactor. The residual nuclei in the target are mainly radioactive and they can decay by emission of electrons and γ-radiation. This leads to target activation and heat release after target irradiation. The construction parts of an accelerator-driven system also also activated by the primary and cascade particles. All of the processes mentioned are well-known in nuclear physics but their practical application needs precise nuclear data on the characteristics of secondary particles and residual nuclei obtained as from experiments and the theoretical simulation of processes inside the target. These data are necessary for a rather wide range of nuclei, from light to heavy nuclei, and the large energy range which should cover the region from the energy of the incident proton and down to energies in ten or hundred times lower. Some of the results obtained in the V.G.Khlopin Radium Institute are presented here.

B.2.3.2. THE SPALLATION AND FRAGMENTATION CROSS-SECTIONS

Spallation and fragmentation are the main reaction channels of the intermediate energy hadron interaction with middle and heavy nuclei. The cross-sections of radionuclide production in these reactions were measured by means of the γ-spectrometry method for the chemically unseparated products in the case of proton-induced reactions with energy 660 MeV (proton beams of the Joint Institute of Nuclear Research, Dubna synchrocyclotron) on thin targets of Al, Ti, V, Fe, Co, Ni, Cu, Zn, Zr, Mo, Ag, and Sn and with energy 1 GeV (St.-Petersburg Institute of Nuclear Physics synchrocyclotron) on targets of Al, Ti, Fe, Co, Cu, and Au. In the each case from 10 to 50 residual nuclei production cross-sections were measured in the both ground and isomeric states. Nuclear data on more than 400 reactions were obtained in these experiments (see, e.g. [1]). The compilation of our data as well as data of other authors gives us possibility to estimate the reaction excitation functions which can be used either directly or for the sake of model testing. The analysis shows that for reactions where the mass loss is less then half of the target mass the estimation accuracy is about 30 %. The discrepancy between experimental values and those obtained from semiempirical systematic and model calculations is often more than the experimental error.

B.2.3.3. FISSION CROSS-SECTIONS

Nuclear fission is a very important reaction channel for heavy nuclei, especially in the case of transactinide target nuclei. The relative fission cross-sections, $\sigma_f(^{232}Th)/\sigma_f(^{235}U)$, and $\sigma_f(^{238}U)/\sigma_f(^{235}U)$,

were measured with accuracy 15-20 % for neutron-induced fission with neutrons energies 1-100 MeV from the neutron spectrometer **GNEYS** (the St.-Petersburg Institute of Nuclear Physics) [2]. The absolute values of fission cross-section for ^{238}U and ^{209}Bi for neutrons with energies 135 and 160 MeV were obtained at the quasi-monochromatic neutron source of the TSL synchrocyclotron (Uppsala, Sweden) [3] with the same accuracy. The same measurements of ^{208}Pb fission cross-section are now in progress. The values of all of these fission cross-section are also important because they serve as secondary standards in the case of neutron flux measurements. Measurements on intermediate neutron energies are rather scarce due to the lack of neutron sources, the difficulties of neutron flux definition and the low neutron intensities as compared to those of proton beams.

More data were obtained on proton beams. With the proton beam of the Radium Institute synchro-cyclotron (E_p=10-100 MeV) fission cross-sections for ^{232}Th, $^{233,235,238}U$, ^{237}Np, ^{239}Pu, and $^{241,242,243}Am$ were measured with an accuracy of 10-15 % [4,5]. The results obtained are presented in Fig.1a-f in comparison with the data from other work. For all nuclei the fission cross-sections increase rapidly near the coulomb barrier, reach the maximum value at approximately 50 MeV proton beam energy and decrease for higher energies. On the basis of the data presented the total fission probability $\Gamma_f = \sigma_f / \sigma_{in}$, where σ_{in} is the cross-section for inelastic scattering, was calculated using the known systematic for σ_{in}. The total fission probability is shown in Fig.2a-f as a function of proton energy. An analysis of known data on fission cross-sections and probabilities of fission induced by neutrons and γ-quanta in the same target mass and projectile energy region was also performed. It was found that for all cases that the total fission probability increases with projectile energy and reaches saturation at some energy, as can be seen from Fig. 2a-f. The value of the fission probability in the saturation region, Γ_{max}, can be expressed as a function of the fissility parameter Z^2/A as follows:

$$\Gamma_{max} = 1 - \exp[-1.44(Z^2/A-34.0)].$$

The fission cross-sections of ^{nat}U, ^{209}Bi, $^{206,207,208}Pb$, and ^{197}Au were measured with the proton beam of the Institute of Theoretical and Experimental Physics (Moscow) synchrotron at energies 70, 100, 155, and 200 MeV as well as the fission cross-sections of ^{181}Ta at 155 and 200 MeV and the cross-sections of Sm, Sn, and Ag at 200 MeV [6]. The fission cross-sections of $^{235,238}U$, ^{232}Th, ^{209}Bi, $^{206-208}Pb$, ^{197}Au, ^{181}Ta, Yb, and Sm also were measured at the 1 GeV proton energy beam of the St.-Petersburg Institute of Nuclear Physics synchrocyclotron [7].

These results are now used as the basis for the modern fission cross-section estimation for the number of nuclei in the intermediate energy region.

B.2.3.4. YIELDS OF RESIDUAL NUCLEI AND NEUTRONS FOR THE MASSIVE TARGETS.

Residual nuclei inside the massive target and neutron radiation from the target arise as a result of elementary interactions between particles and nuclei inside the target volume. The radionuclide yields as well as their decay characteristics define the target activation and energy release which is converted into heat. There are few experiments carried out on massive targets. The measurements of the radioactive inventory due to irradiation of massive Pb cylinder with diameter 20 cm and height 60 cm by the 1 GeV proton energy beam of the St.-Petersburg Institute of Nuclear Physics synchrocyclotron were performed by the Radium Institute group [8]. The distribution of nuclide yields over the target radius and height has been obtained and the evaluation of yields for 22 nuclides inside the target volume were performed with an accuracy 20-40 %. Some results for radionuclide yields inside a massive Fe target irradiated by protons of the same energy can be found in [9] and mesurements for Al and U targets are now in progress.

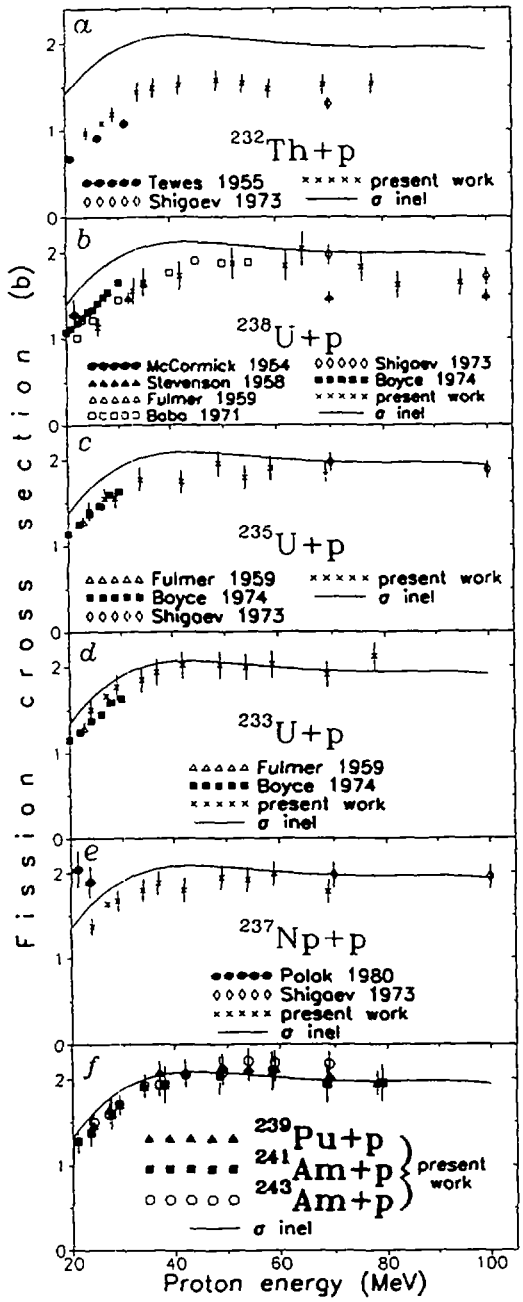

FIG. 1. The proton-induced fission cross sections of actinide nuclei

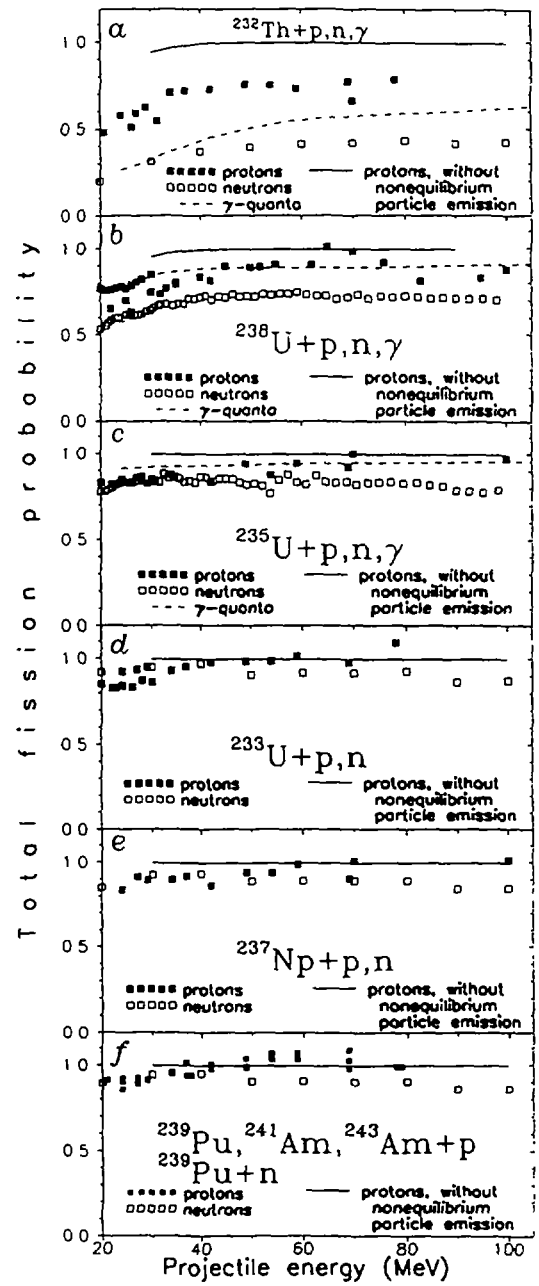

FIG. 2. The total fission probability in the reaction of actinide nuclei with protons, neutrons and γ-quanta

The most important features of a neutron-generated target are the neutron multiplicities and the spatial and energy distribution of neutrons escaping from the target. The energy spectra were measured on the surface of the 20x60 cm Pb target irradiated by 1 GeV protons and the spectra stiffness and neutron flux intensities were traced along the target axis [10]. A more detailed investigation of neutron flux from the Pb target has been performed with the proton and deuteron beams of the Joint Institute of Nuclear Physics syncrophasotron with energies 1-4 GeV [11]. The experiments have been carried out for the massive Pb cylinders with dimensions 20x60 cm and 20x20 cm and a cube 8x8x8 cm and for a thin target (the effective thickness was about 0.7 cm). The neutron yields from the 20x60 cm target are presented in Table I

TABLE.I EXPERIMENTAL NEUTRON YIELDS FROM A 20X60 CM PB TARGET

Neutron energy range	Proton energy , GeV			Deuteron energy, GeV		
	0.991	2.00	3.65	1.032	1.98	3.75
all	25.1 ±3.0	44.2 ±3.1	80.7± 6.9	24.9±5.0	58.5±8.2	98.9 ±14.0
> 1 MeV	16.3 ±2.1	27.5±2.0	49.9 ±4.5	13.9±2.8	31.3± 4.7	56.6± 8.5
> 20 MeV	2.1±0.3	4.7± 0.4	8.6±1.0	1.7±0.4	4.1±0.7	8.2 ±1.5

It was shown that 5 % of neutrons which have energies more than 50 MeV brings out the essential part of incident energy increasing from 12 % at E_{inc} = 1 GeV to 20 % at E_{inc} = 3 GeV. The average neutron energy increases from 8.8 MeV to 13.7 MeV when proton beam energy is changed from 1 GeV to 3.65 GeV. In the case of deuteron irradiation within the same energy range the mean neutron energy varies from 5.5 MeV to 9.4 MeV. The stiffness of neutron spectra increase for the smaller target and the fraction of neutrons with energies up to 1 MeV decreases from 38 % for the 20x60 cm target to 17 % in the case of the thin target at a proton beam energy near 2 GeV.

B.2.3.5. THEORETICAL SIMULATION OF HADRON-NUCLEUS INTERACTIONS AT INTERMEDIATE ENERGIES.

The description of hadron transport inside a massive target irradiated by intermediate-energy protons and therefore the choice of optimal neutron source parameters needs detailed knowledge of elementary interaction properties. There are two main reasons for the development of a theoretical set of nuclear data on these properties. First, the proton-nucleus interaction models give us the possibility to obtain data where they are still absent and (or) can not be extracted from experiments. The second reason is the possibility to investigate the characteristics of secondary particles for different targets vs. beam energy in order to find out the optimal combination from the point of view of neutron production, contents of residual radioactive nuclides, and so on.

The theoretical description of neutron generation inside a massive target can be divided into parts. The first is the simulation of hadron transport inside the target volume (internuclear cascade) and the second is the calculation of elementary (p,xn+yp) and (n,xn+yp) cross-sections as well as energy and angular spectra of secondary particles arising as result of hadron-nucleus interactions (intranuclear cascade). Monte-Carlo simulation of transport processes is a well-known method for the description of both inter- and intranuclear nucleon-nucleus interactions. The method was proposed in 1946 by M.Goldberger who suggested considering the intranuclear cascade as a series of quasi-elastic collisions of the fast primary particle with nucleons inside the nuclear volume. Now it is clear that such a algorithm is a numerical way to find the solution of the transport equation. In [12] the connection between the microscopic quantum theory of nuclear reactions and the intranuclear cascade model has been established and the physical and mathematical foundations and approximations of ICM were analyzed. It was shown in this work that ICM has at least the same degree of validity as, e.g. the optical model or disturbed wave approximation for target nuclei with A > 10-20 and beam energies E > 15-20 MeV.

Codes for both the intra- and internuclear cascade simulations were developed in the Radium Institute. The code for hadron transport inside the massive target (SITHA code [13]) is based on the semiempirical definition of the cross-sections for hadron-nucleus interactions and is intended for neutron transport simulation and energy release calculations inside the massive complex samples irradiated by intermediate-energy beams. The comparison of SITHA calculations with experimental results has shown [11] that the

distribution of neutron flux density at low energies is quite well described by the calculations but the high-energy part is underestimated.

Special efforts were made to improve the intranuclear cascade description (INTRA code) in the low energy region as compared to the commonly used approach [14]. At proton energies up to 250 MeV the effect of the nuclear potential should be taken into consideration. The consideration of trajectory refraction only on the edge of a diffuse nuclear potential leads to a significant discrepancy with the observed data and the reduction of final phase volumes due to nuclear centrifugal barriers has to be included. In the intranuclear cascade algorithm this effect can be accounted for together with the Pauli principle by means of the exclusion of forbidden states lying under the centrifugal barrier. Such a criteria increases the effective free path length and allows us to reproduce the phenomenological values of the imaginary part of the optical potential in a wide energy region and to apply the model in the low-energy region without any cut-off energy. The comparison of calculated data on the absolute cross-section of ^{197}Au (p,pn) reaction with the experimental ones [14] is presented in Fig. 3.

The consideration of isobar production at proton energies near 1 GeV also improves the description of pion cross-sections and spectra as compared to the approach [14]. The Monte-Carlo algorithm was also used to consider the evaporation stage of hadron-nucleus interaction after fast particle escape where neutron, proton, alpha-particle, and gamma emission were taken into account in competition with the fission channel.

The combined application of both codes allows us in principle to calculate all necessary parameters of the massive neutron-generated target irradiated by a proton beam with an energy around 1 GeV.

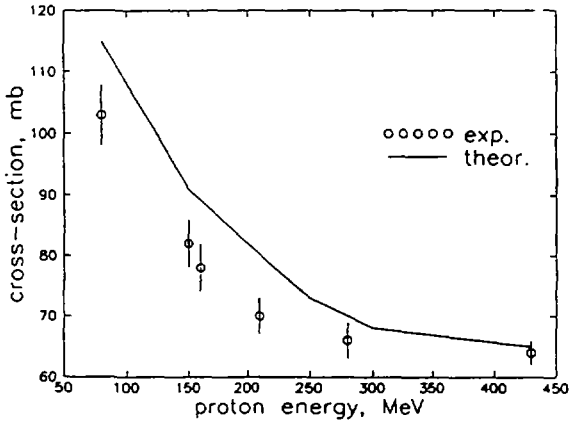

FIG. 3. Excitation function of ^{197}Au (p,pn) reaction

B.2.3.6. CONCLUSIONS

The above discussion of some nuclear physics aspects of target processes in the accelerator-driven system allows us to conclude that there are a number of experimental and calculated nuclear data necessary for the choice of optimal target parameters. But this data set is still far from complete and it is necessary to make additional experimental and theoretical efforts to obtain a detailed understanding of massive target physics.

REFERENCES

[1] Alexandrov Yu.V. et al. Proc. Int. Conf. on Nucl. Data for Science and Technology, Gatlinburg, 1994, v.1, p.371.

[2] Fomichev A.V. et al. Proc. Int. Conf. on Nucl. Data for Science and Technology, Julich, 1991, p.734.

[3] Eismont V.P. et al. Proc. Int. Conf. on Nucl. Data for Science and Technology, Gatlinburg, 1994, v.1, p.360.

[4] Gorshkov I.Yu. et al. Proc. Int. Conf. on Nucl. Data for Science and Technology, Julich, 1991, p.751.

[5] Eismont V.P. et al. Proc. Int. Conf. on Nucl. Data for Science and Technology, Gatlinburg, 1994, v.1, p.397.

[6] Obukhov A.I. et al. Preprint RI-17, 1973, Leningrad.

[7] Bochagov B.A. et al. Yad. Fiz., 1978, v.28, p.572.

[8] Bakhmutkin S.V. et al. Atomnaya Energiya, 1987, v.63, p.137.

[9] Alexandrov Yu.V. et al. Proc. Conf. on Nucl. Spectroscopy and Nucl.Structure. Abstracts, Tashkent, 1989, p.536.

[10] Bakhmutkin S.V. et al. Atomnaya Energiya, 1987, v.62, p.59.

[11] Yurevich V.I. PhD Dissertation, St.-Petersburg, 1992.

[12] Bunakov V.E. et al. LINP Communications N 1032, Leningrad, 1982.

[13] Daniel A.V. Preprint RI-181, M., 1984.

[14] Barashenkov V.S., Toneev V.D. Interactions of high-energy particles and atomic nuclei with nuclei. Moscow, 1972.

B.2.4. PHYSICAL FEATURES OF TARGET AND BLANKET

Takahiko Nishida
Japan Atomic Energy Research Institute
Tokai-mura, Naka-gun, Ibaraki-ken 319-11 Japan

B.2.4.1. TARGET

The target installed in the accelerator-driven transmutation system is directly irradiated by high energy protons with an energy of several GeV. Many spallation reactions in heavy metal targets such as minor actinides (MAs) occur with the emission of many neutrons. Almost all the spallation products have short half-lives but the spallation reactions are of the energy consumption type except for the high energy fission reaction. Results of our preliminary analysis showed that the target system based mainly on spallation reactions can transmute about 100 kg MA per year, which corresponds to the amount of MA from 4 units of 1 GWe LWR driven with a 1.5 GeV and 300 mA proton beam, but can not produce sufficient electricity to operate its own accelerator. It is thought that this system is a very interesting option for a waste disposal strategy in which a large weight is not given to energy balance.

To investigate the feasibility of an accelerator-driven transmutation system as an engineering system with more transmutation of MA and self sustaining energy generation, we adopted the hybrid system of an intense proton accelerator and a subcritical target/blanket fueled with MA. In this system, the spallation target acts mainly as a supplier of source neutrons to the subcritical blanket surrounding it. There the transmutation of MA by fission is major and the transmutation by spallation minor. The feasibility of an active target composed of MA metal alloy was examined in the design studies. The analytical result showed that the power peaking is generated around the target region due to ionization loss and fission reactions occurred locally by proton beam irradiation. This phenomenon restricts the beam current to the lower level to keep the target material temperature below the melting point. The existence of peak neutron flux makes the average neutron flux relatively low over the core and reduces the total amount of transmuted MA.

B.2.4.1.1. Nonactive target

In the solid target and solid fueled blanket system we used a nonactive target made of tungsten to avoid the power peaking restriction by taking into account that the transmutation of tungsten by spallation reactions is small and a tungsten target is a good neutron supplier. As a result the heat deposition in the target becomes lower due only to ionization energy loss of incident protons without fast fission.

For the solid MA alloy fuel transmutation system, the optimization design study [1] on the target structure was made to produce the largest number of spallation neutrons uniformly over the target surface and to achieve the highest transmutation rate. Here the cascade code NMTC/JAERI [2, 3] was used in the high energy range of 15 MeV to 1.5 GeV and the neutron transport code MORSE-DD in the energy range below 15 MeV. In the original design, the solid tungsten target composed of pin-bundle type subassemblies, like fuel subassemblies was chosen. The metal target subassembly should also be cooled by sodium coolant flow similar to the fuel subassembly in the blanket. The coolant flow channel parallel to the direction of the incident beam also provides the tunneling paths through which some of the incident protons escape from the bottom to the outer region. Neutronic survey calculations on four types of configuration: bulk, smear, disc and pin target configurations, were made to search for the optimum structure of the tungsten target in the solid MA alloy fuel system. The nucleon and neutron transport

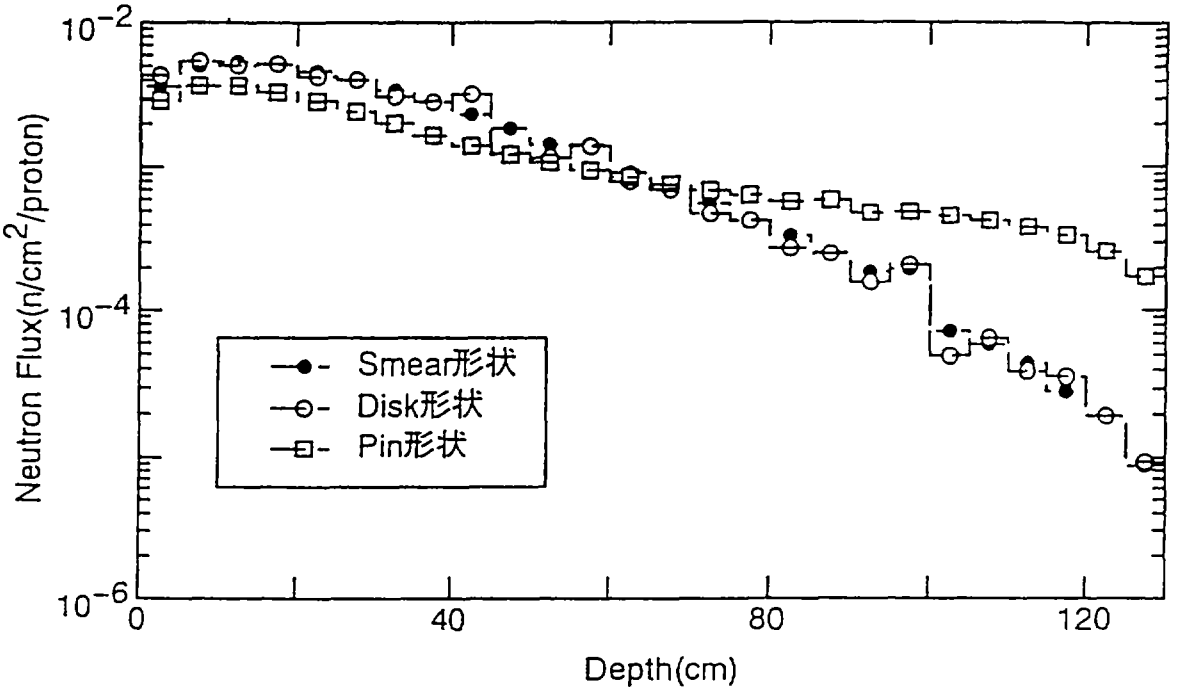

FIG. 1. Vertical neutron flux distributions for neutrons emitted from each type target surface.

calculations were made for cases where the uniform proton beam with 20 - 40 cm diameter is injected onto these targets. The target, in which the volume ratio of tungsten to sodium is assumed to be 1, has dimensions of 40 cm in diameter and 130 cm in height. The disk-type target gives the highest neutron yield of these targets. Figure 1 shows the axial flux distributions of neutrons emitted from the target surface to the blanket for three types of target beside the bulk case. In the modified disc target the number of disc layers and their thicknesses were adjusted to make a flat flux distribution . The thermal-hydraulics analyses on the disc type target were carried out, changing the size of coolant channel on the disc type target. Based on the thermal-hydraulic calculations, the disc has been designed to have 19 cooling holes with a diameter of 9 mm and a pitch of 15.4 mm, through which the sodium coolant flows upwards, whilst keeping the temperature at the hot spot in the target below the allowable temperature of 650°C. The target configuration was specified to achieve the maximum neutron gain by considering the results of both neutronics and thermal hydraulics calculations. As illustrated schematically in Fig. 2, the optimized target (135 cm in height and 40 cm in diameter) contains 13 discs, which are composed of 6 thin discs with a thickness of 1.5 cm and spacing of 5.1 cm and 7 thick discs with a thickness of 13 cm and spacing of 1.1 cm. About 30 spallation neutrons per incident proton are emitted from the target. Figure 3 represents the axial distribution of heat generation in the target [4] and the target withstands the maximum heat deposition generated by the proton beam with the allowable current of 68 mA. In the proposed design of the target subassembly, the tungsten discs are fixed in a wrapper tube. This is because the coolant pressure drop through the target subassembly is higher than those through the pin-bundle type fuel subassemblies. The pressure drop through the target subassembly is about 250 kPa at the maximum coolant velocity of 8 m/s. The coolant flow can sufficiently remove the heat deposited in the discs. The coolant hole pattern of successive discs is a

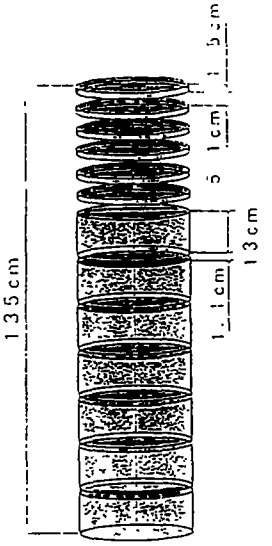

FIG. 2. Target model composed of 13 disc layers with two different thicknesses.

staggered arrangement so that the protons which pass a disc through the coolant holes should hit the next disc. The target composed of stacked discs with different thicknesses is a better choice than a target with pin-bundle type subassemblies, similar to those for fuel blankets because it reduces the proton loss due to channeling as seen in Fig. 4.

The time evolution process of main residual nuclides was also calculated to estimate the activity induced by products newly born in the target during and after proton irradiation using the SPCHAIN code. The calculated results showed that the residual's activities are negligibly small as shown in Fig. 5.

B.2.4.1.2. Active target

In liquid target/blanket transmutation systems such as those using molten salts and liquid metal alloys as described in a later section, there are no limitations for preventing a melt down accident of blanket and target due to local power peaking. MA concentration in molten-salt fuel or liquid metal alloy fuel is lower than in solid metal. For these cases, the power peaking around the irradiated zone is not a critical factor because of the relaxed heat condition for liquid fuel. So the high energy proton beam is injected directly into the center of the MA fueled zone where there is no target region with a definite boundary, the so-called "distributed target". The flowing fuel (MA molten salt or liquid

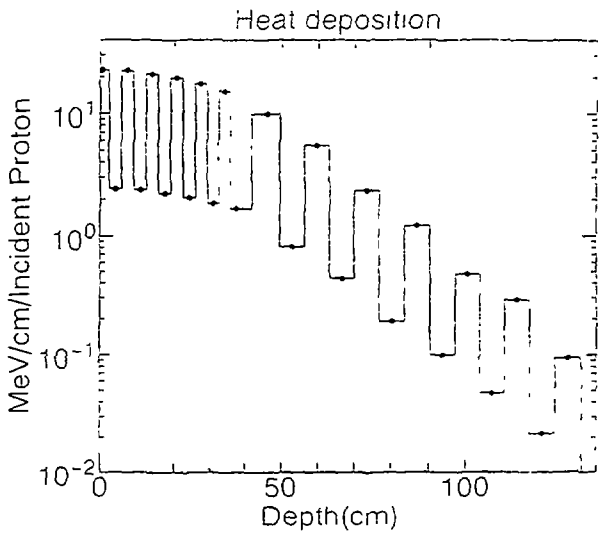

FIG. 3. Axial heat generation distribution in the disc type target.

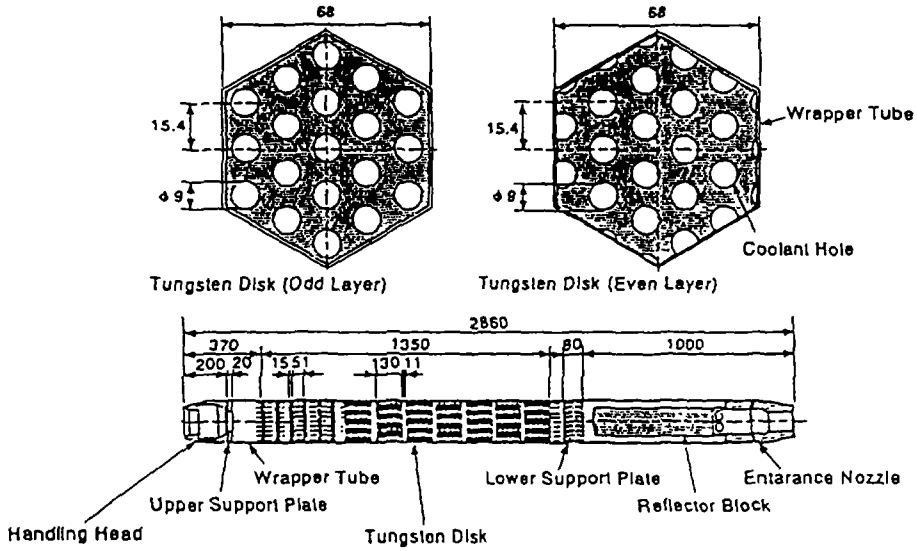

FIG. 4. Optimized tungsten target subassembly.

MA alloy) also forms the subcritical blanket and itself acts as a primary coolant which circulates through the target/blanket and heat exchangers.There are many light nuclides such as Cl or Ce in the active fluid targets in JAERI liquid transmutation systems. In the target region spallation reactions of MA and light nuclei such as Cl or Ce, of which the molten salt or liquid metal alloy mainly consists, occur simultaneously in addition to transmutation of MA. Cascade calculations of high energy hadron nuclear reaction in the light nucleus and transport processes in the dilute fluid target need to be analyzed with high precision. The QMD (Quantum Molecular Dynamics) code that is being developed at JAERI in collaboration with universities will give a more accurate solution for the cascade process in the light nucleus medium in the near future.

B.2.4.2. BLANKET

According to the national research and development program OMEGA, on partitioning and transmutation, conceptual design studies of accelerator-driven transmutation systems are being performed at JAERI for the following three types:

(a) Tungsten target and solid MA alloy fueled blanket system,

(b) MA molten-salt target/blanket system and

(c) Liquid MA alloy target and molten-salt blanket system.

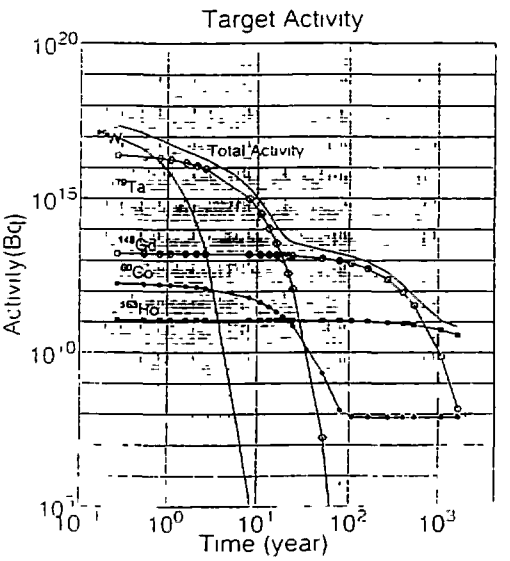

FIG. 5. Dependence of activities of residual nuclides in target on cooling time.

The solid MA alloy fueled system (a) is composed of a tungsten target and solid type fuel subassemblies like metal fueled fast reactors. Its R&D work is considered to be a relatively short term project so that the technologies and know-how about fast reactors already obtained can be applied to perform the design study of this type of system. The molten-salt system (b) and liquid alloy system (c) have a liquid fueled target/blanket without a solid target. These are expected to be more promising systems with the possibility of on-line fuel reprocessing but containing more problems that need to be resolved than the solid fuel one. Both systems have the active, subcritical blanket region with hard neutron energy spectra. The liquid alloy system (c) has a graphite moderator in the blanket to transmute long-lived fission products (LLFPs) by using thermalized neutrons.

Here we discuss the nuclear characteristics including the neutron energy and neutron fluxes in these accelerator-driven transmutation systems.

B.2.4.2.1. Neutron energies

The long-lived waste nuclides to be transmuted in the JAERI transmutation research program are MAs (^{237}Np, ^{241}Am, ^{243}Am, ^{243}Cm, ^{244}Cm, ^{245}Cm) and LLFPs (^{99}Tc, ^{129}I) with half-lives between a few hundred years and several million years. MA should be transmuted through fission reaction because the transmutation of MA by neutron capture has the possibility of increasing higher actinides. Figure 6 represents the comparison of ^{237}Np fission cross section and capture cross section data dependent on neutron energy between the nuclear data libraries of JENDL3.2, ENDF/B-VI and JEF-2. Fissioning of MA occurs dominantly in relation to neutron capture above the threshold energy of about 500 keV. JAERI selected the transmutation method of MA by fast fission induced by a spallation neutron source despite

requiring the large initial MA inventory In the ATW project at LANL, MAs and LLFPs are transmuted by thermalized spallation neutrons As illustrated in Fig 7 this method requires two or three neutrons per one MA fission since MA must be converted at first to a fissionable actinide through one neutron capture Its fission reaction after two thermal neutron absorptions occurs only with high thermal neutron flux of about 10^{16} n/cm^2/s This fact implies that neutron economy with fast fission is better than one with thermal fission for transmutation of MA by fission. LLFP can be transmuted only through thermal neutron capture to a stable nuclide as seen in Fig 8 because of the small capture cross section for fast neutrons For this reason, the thermalized neutron region needs to be included around the fast subcritical target/blanket to transmute MA and LLFP simultaneously in one system

Nuclear calculations in the accelerator-driven transmutation system must cover the wide energy range from several eV to a few GeV and calculate both high energy reaction and neutron transport process For the high energy region above 15 MeV the spallation reaction with many reaction channels is dominant but sufficient experimental and estimated nuclear data are not yet available for high energy neutron and charged particles At present, the best way to analyze the high energy process in the accelerator-driven transmutation system is to use the cascade codes, such as NMTC/JAERI, HETC/KFA2, and LAHET, based on the two-body collision approximation model JAERI are using the code NMTC/JAERI (High Energy Nuclear Reaction and Nucleon-Meson Transport Code) which treats the proton-induced nuclear spallation and subsequent internuclear transport process for energies above 15 MeV and also calculates high energy fission reaction as a competing process with evaporation Since most of these codes include, however, the old calculation model and data about the nucleus, which were installed before ~1975, they should be improved and upgraded by the newly developed nuclear theory and data based on recent high energy experiments, respectively So, JAERI is performing benchmark calculations, taking part in the OECD/NSC code benchmark task force work, and spallation integral experiments as basic studies relevant to accelerator-driven transmutation

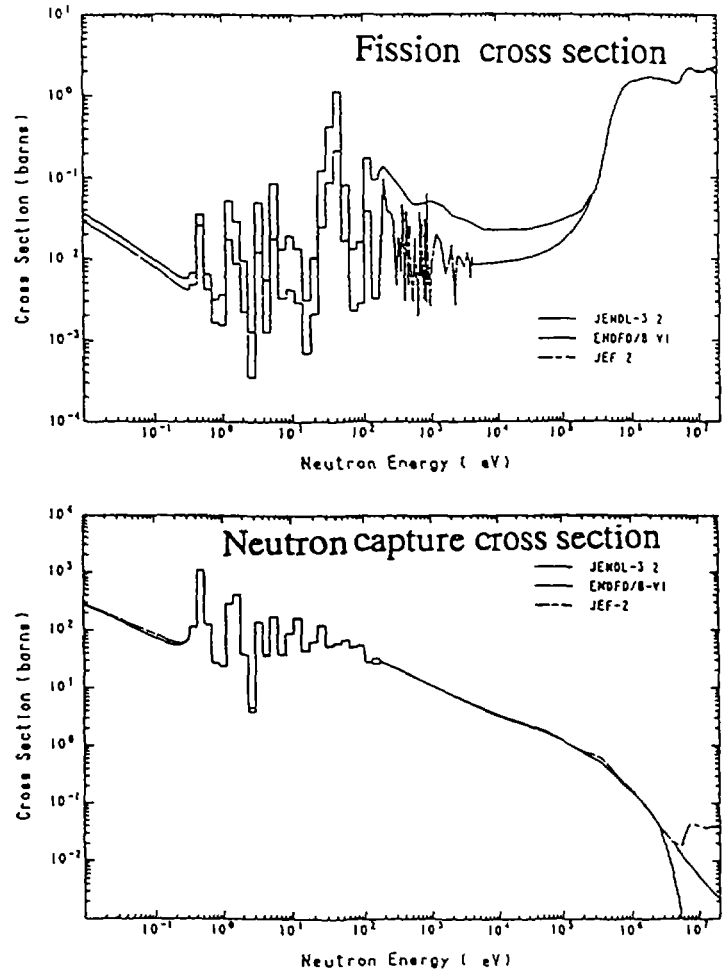

FIG 6 Comparison of fission and neutron capture cross sections for ^{237}Np.

To evaluate the validity of the simulation code and upgrade it, JAERI is carrying out spallation integral experiments at the National Laboratory for High Energy Physics (KEK) in Tsukuba [5, 6] The 500-MeV

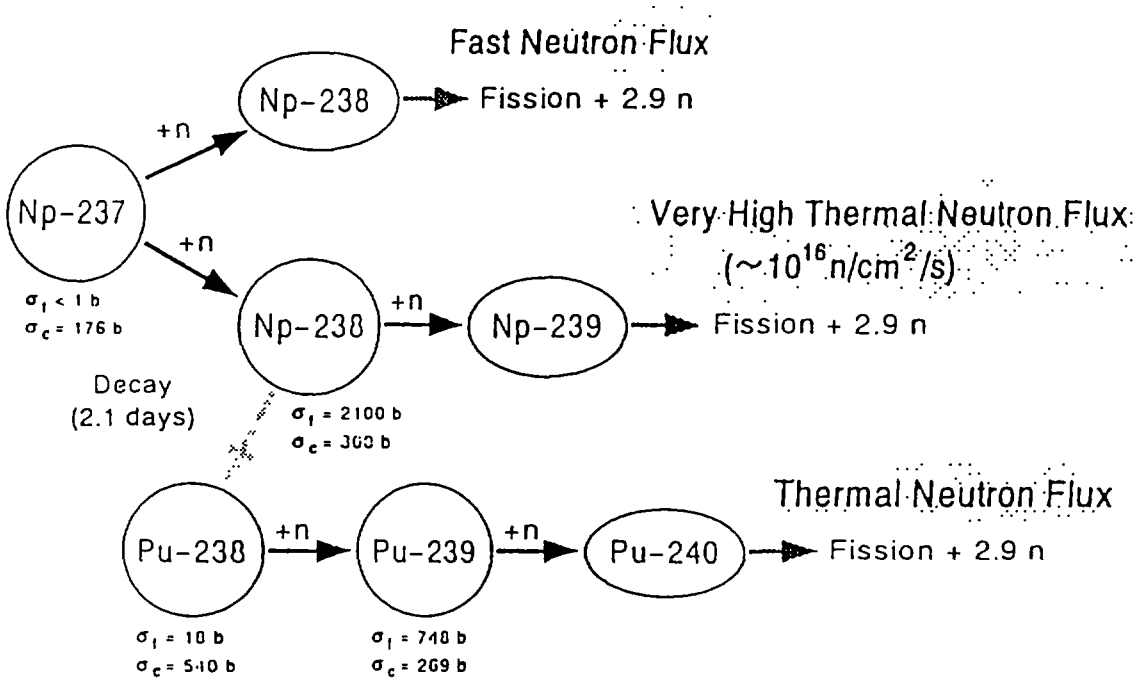

FIG.7. ^{237}Np *burning with fast and thermal neutron fluxes.*

booster synchrotron facility at KEK is used for the experiments. A Lead/tungsten target was installed in the center of a Lead assembly with a diameter of 600 mm and a length of 1000 mm. The activation samples of Al, Fe, Ni, and Cu were distributed in holes drilled through the assembly along the beam axis at various radial positions. The number of induced activities in the samples was obtained by measuring gamma rays with 100-cc Ge detector. Some experimental results agreed fairly well with predictions obtained using NMTC/JAERI. The double differential cross sections (DDX) of neutron emission in a thin Al sample irradiated by 800 MeV protons in the synchrotron facility at KEK were also measured by the time of flight method in cooperation with the Kyushu University, the Tohoku University, and KEK, and compared with calculations by the code HETC. It was found that the calculated results are in relatively good agreement with the experimental ones. The detection efficiency and the response function of the NE-213 scintillation counter for ~65 MeV neutrons were measured at the cyclotron in the JAERI Takasaki Research Establishment to improve the counting efficiency for neutrons with energies of tens of MeV. Detailed experimental results are

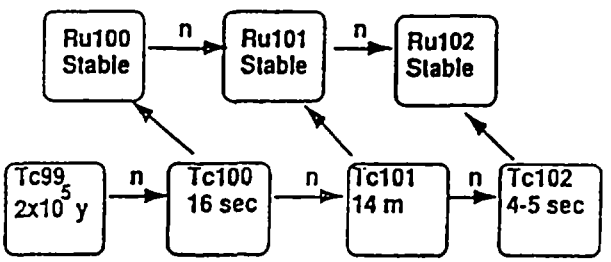

Isotope	σ (thermal)	σ (fast)
Tc99	20 barns	0.2 barns
I129	31	0.2
Sr90	1	(0.1)
Cs137	0.25	(<0.01?)

FIG. 8. Transmutation of LLFP using the thermal neutron flux.

described in a companion paper by Takada. The benchmark studies on the mass distribution of spallation products in thin and thick targets of Np for 800 MeV proton incidence and DDX of neutron or proton emission in Zr, induced by the 80 MeV proton bombardment, were carried out to verify and upgrade the accuracy of the predictions computed by the codes NMTC/JAERI and NUCLEUS.

Neutronic calculations on the transmutation system below 15 MeV are carried out using transport codes, Sn code TWOTRAN 2 or Monte Carlo code MCNP, since they were well prepared for analyzing the neutron transport process in a usual reactor. In the energy range below about 20 MeV the nuclear cross section libraries such as ENDF/B-V and JENDL3.2 are applicable to calculate the nuclear characteristics of the transmutation blanket. Figure 9 shows the code system ACCEL for analyzing an accelerator-driven transmutation system at JAERI. By using these codes we calculated the nuclear characteristics of three types of transmutation systems in the whole energy range. The spectrum of spallation neutrons evaporated from an excited heavy nucleus bombarded by high energy particles is similar to the fission neutron spectrum but shifts a little to higher energy, as seen in Fig. 10 in which the normalized neutron spectra for various reactions are compared. Information about spallation neutrons with energies below 15 MeV is transferred from the cascade code to the neutron transport code as source neutron terms.

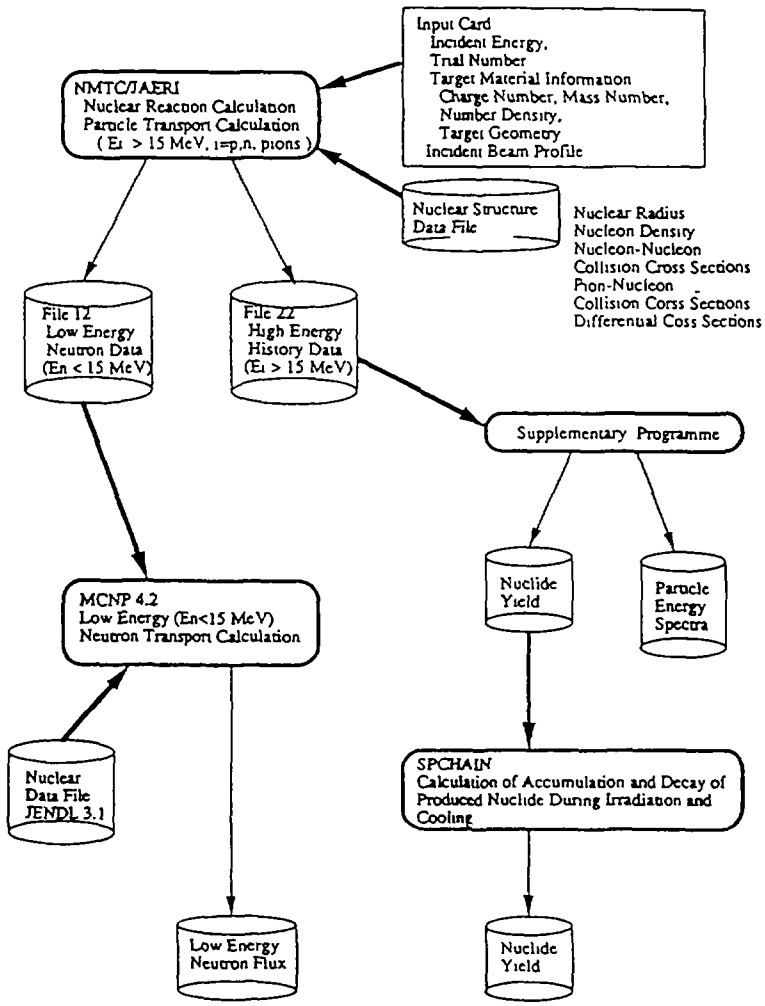

FIG. 9. Main part of upgraded ACCEL code system.

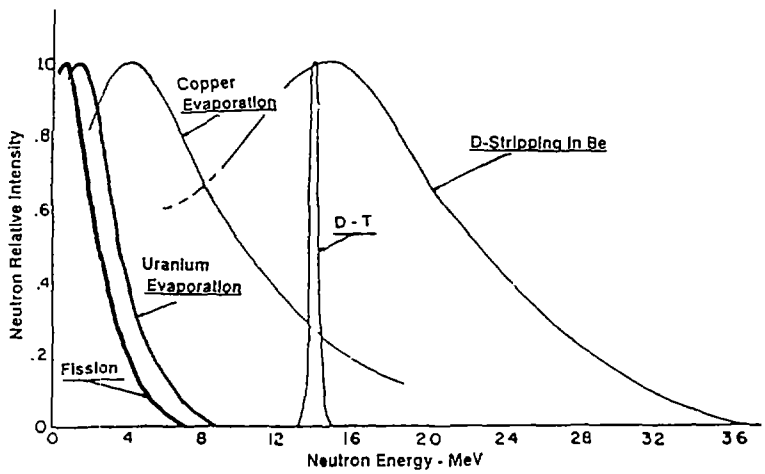

FIG. 10. Normalized neutron spectra in various neutron sources.

Figure 11 shows the calculated neutron energy spectrum averaged over the total target/blanket volume

in the MA metal fueled transmutation system with injection of 1.5 GeV protons. Apparently this curve represents a hard neutron spectrum with about 20 % higher than 1 MeV and about 70 % component higher than 0.1 MeV, which is useful to MA fast fission. The average neutron energy in this spectrum is 690 keV.

The two curves in Fig. 12 represent the neutron energy spectra in the target/blanket region filled with TRU chloride molten salt (NaCl-$TRUCl_3$) and the peripheral region where primary cooling system components (compact-type intermediate heat exchangers and molten-salt pumps) are installed. Both regions are separated by an inner reflector to protect the heat exchangers and pumps against high neutron flux. As seen from the figure, the neutron flux in the peripheral region is kept about two orders of magnitude lower than the one in the target/blanket. In the design, the primary cooling system components are located inside the target/blanket vessel to reduce the total inventory of MA molten salt.

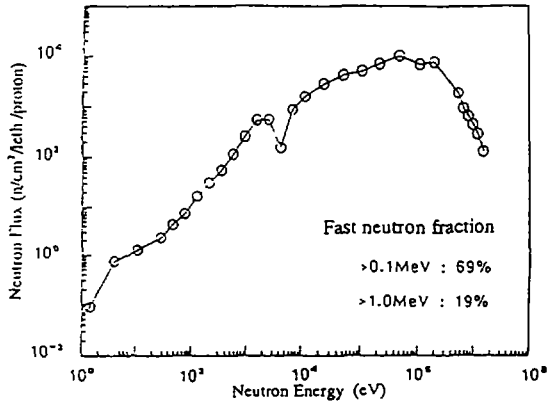

FIG. 11. Mean neutron energy spectrum of the MA metal fuelled system.

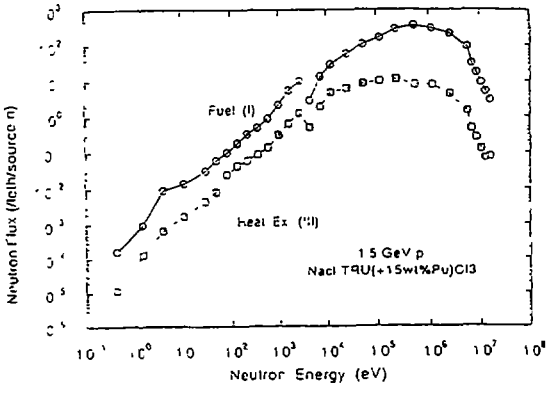

FIG. 12. Mean neutron energy spectra in the molten-salt target/blanket region and the heat exchanger region.

Figure 13 shows three neutron spectra in the target region filled with liquid metal alloy Np-Pu-Ce-Co-Tc, in the graphite moderated blanket region with channels through which liquid metal alloy and fluoride molten salt flow concurrently upwards, and in the upper plenum region of the molten-salt coolant in the liquid alloy system (c). A high neutron flux with a hard spectrum is distributed in the target region where most of MAs are transmuted by fission.

The blanket region has a high neutron flux in the intermediate energy range and MA neutron capture reactions occur more dominantly than in the target region. The molten-salt plenum above the target/blanket has a relatively high thermal neutron flux and provides the region for LLFP transmutation.

B.2.4.2.2. Neutron flux

In this study the neutron flux in the transmutation system was implicitly estimated through the heat deposition density distribution and MA transmutation rate (fast fission reaction rate) for each transmutation system.

B.2.4.2.2.1. Solid MA alloy fuel transmutation system [7, 8, 9]

The concept of the MA alloy fueled transmutation system with hard neutron spectrum, driven by an intense proton accelerator, has been proposed. This system consists of a sodium-cooled subcritical blanket with actinide fuel subassemblies and a spallation target of tungsten. The blanket is required to have an effective neutron multiplication factor more than about 0.9 for improving the burnup rate of MA and total

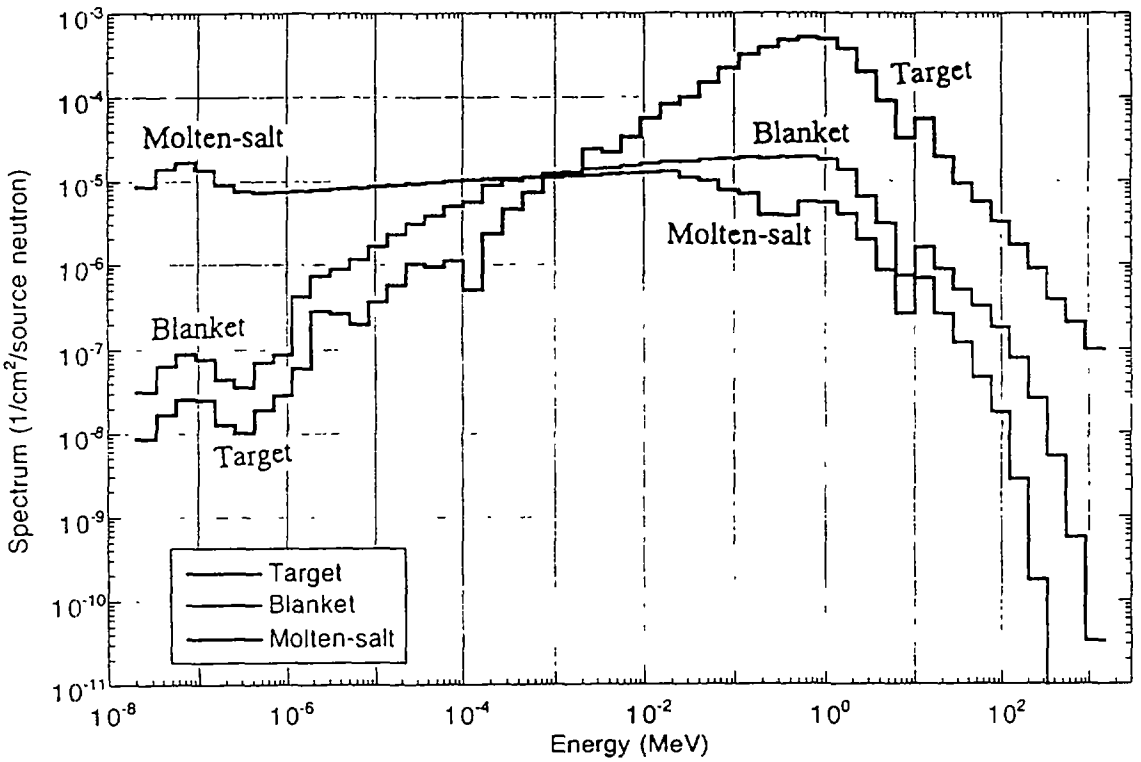

FIG. 13. Mean neutron energy spectra in the liquid alloy target, graphite blanket, and upper molten-salt plenum.

energy balance. When driven by a 39-mA proton beam with an energy of 1.5 GeV, a system with a mean blanket neutron flux of 4.6×10^{15} n/cm^2/s can transmute about 250 kg of MA after one year in operation and generate a thermal power of 820 MW, which is converted to an electric power of about 240 MW. This electricity is sufficient to power its own accelerator. The power density distribution is shown in Fig. 14. The maximum power densities are 930 MW/m^3 in the blanket region and 400 MW/m^3 in the target region. The power distribution is considered to be a measure of the neutron flux distribution in the blanket region. It is supposed that the neutron flux in the blanket around the target has become relatively flat without a peak. The mean neutron flux can be increased with the nonactive target.

B.2.4.2.2.2. MA molten-salt transmutation system [10, 11]

The concept of an advanced MA molten-salt transmutation system has been studied to take advantage of a simple fluid target/blanket for the transmutation system. This system has the target/blanket with a height 170 cm and a radius of 105 cm and the stainless steel reflector with thicknesses of 20 - 40 cm, including the internal heat exchanger. The MA chloride molten salt 64NaCl-36TRUCl$_3$ with a melting point of around 453 °C, was adopted as the fuel salt due to the high solubility of MA and a good nuclear characteristics for a hard neutron spectrum. MA molten salt is circulated between the target/blanket region and the heat exchangers by motor-driven mechanical pumps. MAs in the target/blanket region are transmuted mainly through fast fission reactions and less through spallation reactions. The high energy proton beam is injected vertically downward directly onto the molten salt which acts as the fuel and the spallation target material and serves also as the primary coolant. The fluoride molten salt NaBF$_3$-NaF is selected as the secondary coolant. The target/blanket with an effective neutron multiplication factor of 0.92

can transmute 250 kg of MA per year with a 1.5 GeV-25 mA proton beam, and produces 240 MW of electricity sufficient to power its own accelerator. The power density distribution in the target/blanket region is shown in Fig. 15. The maximum power density is 1,660 MW/m^3 at 25 mA.

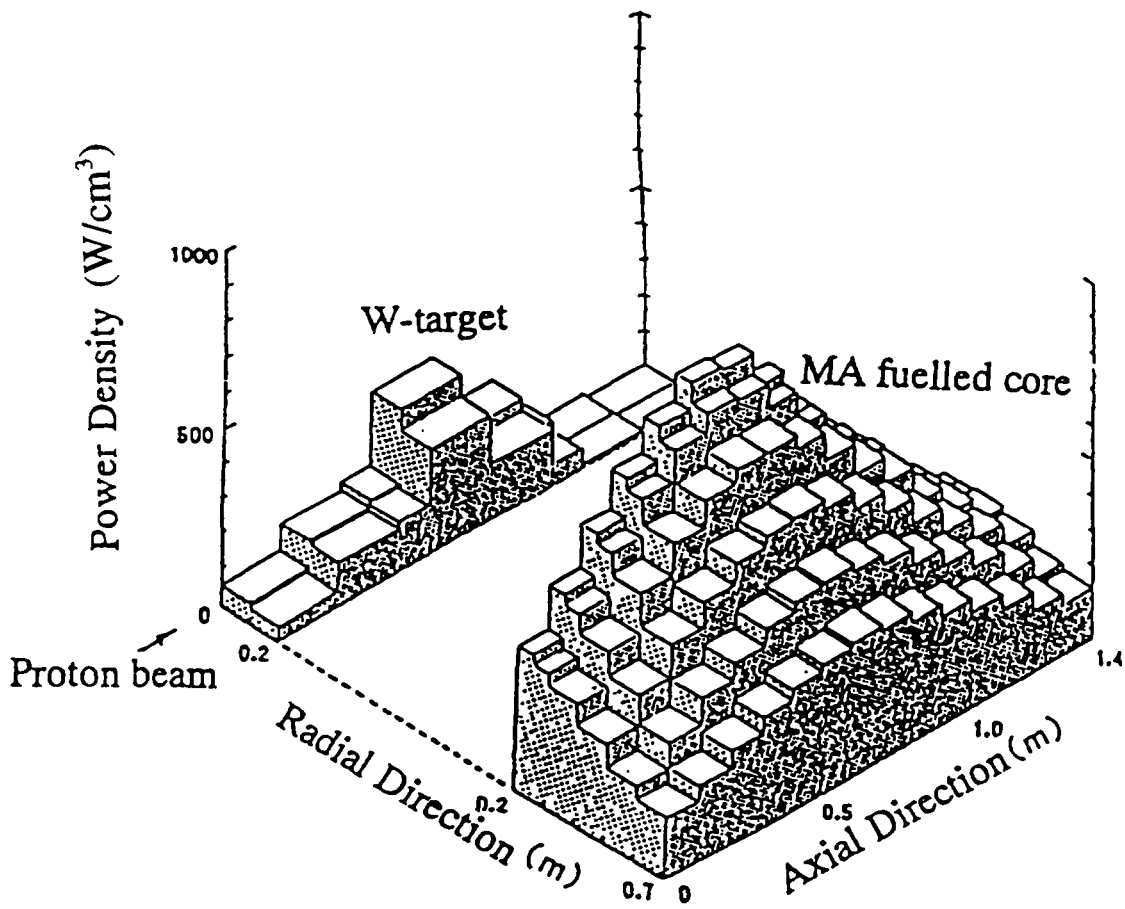

FIG. 14. Power density distribution in the target/blanket of the MA metal fuelled system.

The molten-salt transmutation system is expected to have the possibility of removing FPs from the system and controlling the MA in the system by the on-line processing.

B.2.4.2.2.3. Liquid MA alloy target transmutation system [12]

The preliminary neutronic calculations for the liquid alloy transmutation system have been started to examine the possibility of simultaneous transmutation of both MAs and LLFPs. A TRU alloy of Np-Pu-Co-Ce-Tc with melting point of around 450°C was selected as the target liquid which circulates through the channels in the graphite moderator and transfers the heat and reaction products to the secondary coolant of fluoride molten salt. A target/blanket with an effective neutron multiplication factor of 0.9 can transmute 70 kg of MA per year with 1.5 GeV-16 mA proton beam and the thermal power is 450 MW. The performance parameters of the liquid alloy system are summarized in Table I. The advantages of the liquid alloy system are small MA inventory, high transmutation rate and the simultaneous transmutation of MAs and LLFPs, together with the possibility of on-line charging of MA and removal of reaction products.

To examine the actinide burning performance of each transmutation system, the one group cross section library and the burnup code COMRAD has been prepared. The accelerator-driven transmutation plant

designing code system SPACE has been extended to calculate the burnup and transmutation characteristics of the accelerator-driven MA alloy fuel transmutation system. The one group cross section libraries needed for MAs and other nuclides in the burnup calculation have been produced by degenerating the 295 groups JSSTDL cross section libraries with the neutron spectra computed by the one-dimensional transport code ANISN. The new version of the burnup code COMRAD was prepared to speed up the computation. A preliminary burnup calculation was made for the proposed MA alloy fuel transmutation system.

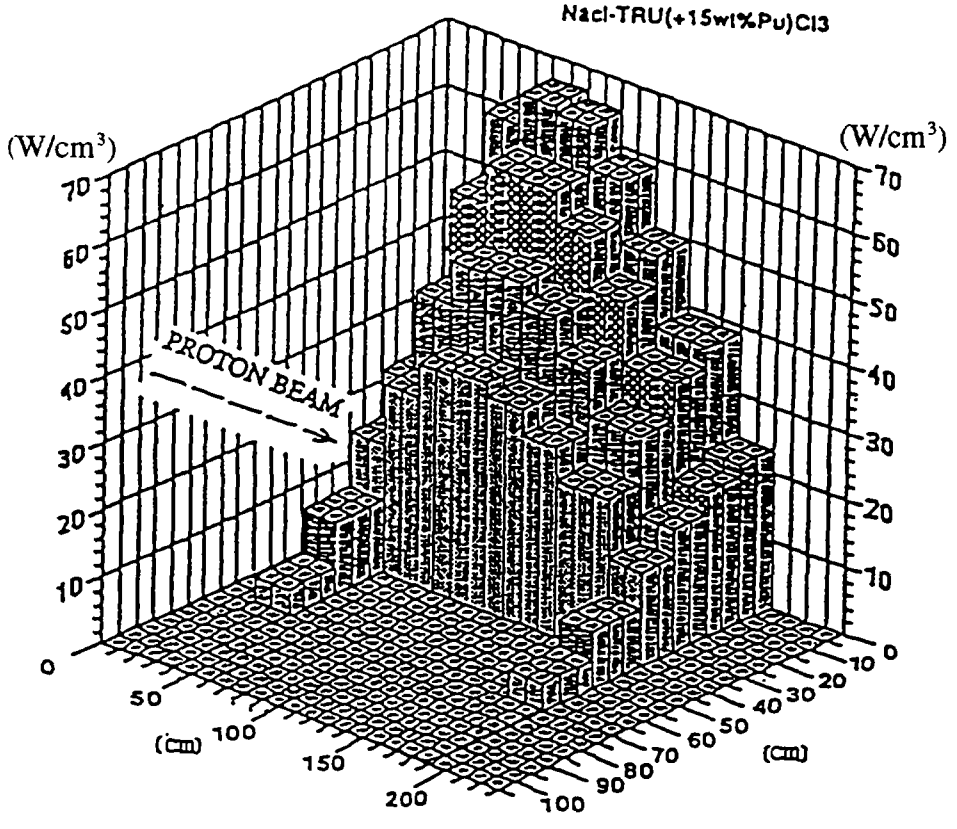

FIG. 15. Power density distribution in the target/blanket of the MA molten-salt system (1 mA proton beam).

TABLE I. MAJOR PARAMETERS FOR LIQUID ALLOY SYSTEM

Fuel	Liquid Metal Alloy
	12.5Np-4.8Pu-24Co-57.7Ce-Tc
Target	Liquid Metal Alloy
Secondary Coolant	Fluoride Molten Salt
Actinide Inventory	890 kg
Multiplication Factor	0.9
Spallation Neutrons	46.3 n/p
Proton Beam	1.5 GeV-15 mA
Thermal Power	450 MW
Burnup	141 kg/a (15.8 %/y)
Temperature, Target Inlet/Outlet	1050/1250 °C

REFERENCES

[1] NISHIDA, T., et al.: "Minor Actinide Transmutation System with an Intense Proton Accelerator", Proc. ICENES' 93, Makuhari (1993) 419.

[2] NAKAHARA, Y., TSUTSUI, T.: "NMTC/JAERI - A Simulation Code System for High Energy Nuclear Reactions and Nucleon-Meson Transport Process", JAERI-M 82-198 (1982) (in Japanese).

[3] NISHIDA, T., et al.: "Improvement of Spallation Reaction Simulation Codes NMTC/JAERI and NUCLEUS", 2nd Int. Symp. on Advanced Nuclear Energy Research, Mito (1990).

[4] NISHIDA, T., NAKAHARA, Y.: JAERI-M 84-154 (1984) (In Japanese).

[5] TAKADA, H., et al.: "Production of Radioactive Nuclides in a Lead Assembly wirh 500 MeV Protons", Proc. OECD/NEA Specialists' Meeting on Accelerator-based Transmutation (PSI, 1992).

[6] TAKADA, H., et al.: JAERI-M 93-181 (1993) 210.

[7] TAKIZUKA, T., et al.: " A Study of Incineration Target System", Proc. 5th Int. Conf. Emerg. Nucl. Systems, Karlsruhe (1989).

[8] MIZUMOTO, M., et al.: "High Intensity Proton Accelerator for Nuclear Waste Transmutation", 16th Int. Linear Accelerator Conf. LINAC-92 (Ottawa, 1992).

[9] TAKIZUKA, T., et al.: " Conceptual Design Study of an Accelerator-based Actinide Transmutation Plant with Sodium-cooled Solid Target/Core", Proc. 2nd OECD/NEA Information Exchange Meeting on P-T (1993) 397.

[10] KATSUTA, H., et al.: "A Continuous Transmutation System for Long-lived Nuclides with Accelerator-driven Fluid Target", ibid.

[11] KATO, Y., et al.: Proc. OECD/NEA Specialists' Meeting of Accelerator-based Transmutation, PSI (1992).

[12] KATSUTA, H., et al.: "A Concept of Accelerator Based Incineration System for Transmutation of TRU and FP with Liquid TRU-Alloy Target and Molten Salt Blanket", Proc. ICENES '93, Makuhari (1993) 424.

B.2.5. THE CONCEPT OF A HEAVY WATER - PB GRAINS FLUIDIZED BED NEUTRON GENERATING TARGET

V.R.Mladov, M.L.Okhlopkov, V.D.Kazaritsky, V.F.Batyaev, P.P.Blagovolin, N.V.Stepanov, V.V.Seliverstov

Institute for Theoretical and Experimental Physics, Moscow, Russian Federation

B.2.5 1. INTRODUCTION

The results of preliminary design, neutronic, thermal and hydraulic calculations of the target parameters are presented in this paper. The target is suggested on the basis of the following initial data, listed in Tables I and II.

TABLE I. BEAM DATA FOR PROTON LINEAR ACCELERATOR.

Energy, MeV	1000
Current, mA	100
Beam diameter at the target entrance, mm	200

TABLE II. BLANKET DATA

Thermal power, MW	2000
Moderator	Heavy water
Moderator pressure, MPa	0.1
Moderator temperature,°C	less than 100
Coolant	Heavy water
Coolant pressure, MPa	10
Coolant outlet temperature, °C	250
Fluid fuel	Heavy water + Minor actinides + Pu
Maximum temperature of fuel, °C	300

The present paper deals with the development of the target as a source of neutrons for the heavy water blanket of an accelerator driven plant. We propose to use a fluidized bed of spherical Lead grains in a heavy water flow. Preference is given to this concept of the target since it provides the possibility:

1) to create a target, containing materials with low neutron absorption;
2) to remove a reasonably large amount of the heat;
3) to remove the target from service reasonably quickly in case of accidents;
4) to combine the target technology with the heavy water technology of the blanket moderator;
5) to realize a reasonably handy scheme for replacement of Lead spheres by applying hydro-transportation;
6) to facilitate the complete process from production to the final disposal of the Lead spheres.

B.2.5.2. THE CONCEPT OF THE TARGET SCHEME

The basic design of the target is shown on Fig. 1. The heart of the target is a fluidized bed of Lead spheres in a heavy water flow, which circulates from bottom to top in a tube, isolating the target from the blanket moderator. The diameter and height of the fluidized bed are 500 mm and 2500 mm respectively, regardless of the fluidized bed porosity. The top line of the fluidized bed is located at a depth of 1000 mm from the top line of the blanket core. At the bottom of the target a Lead spheres receiver, a beam stop and a heat exchanger are located.

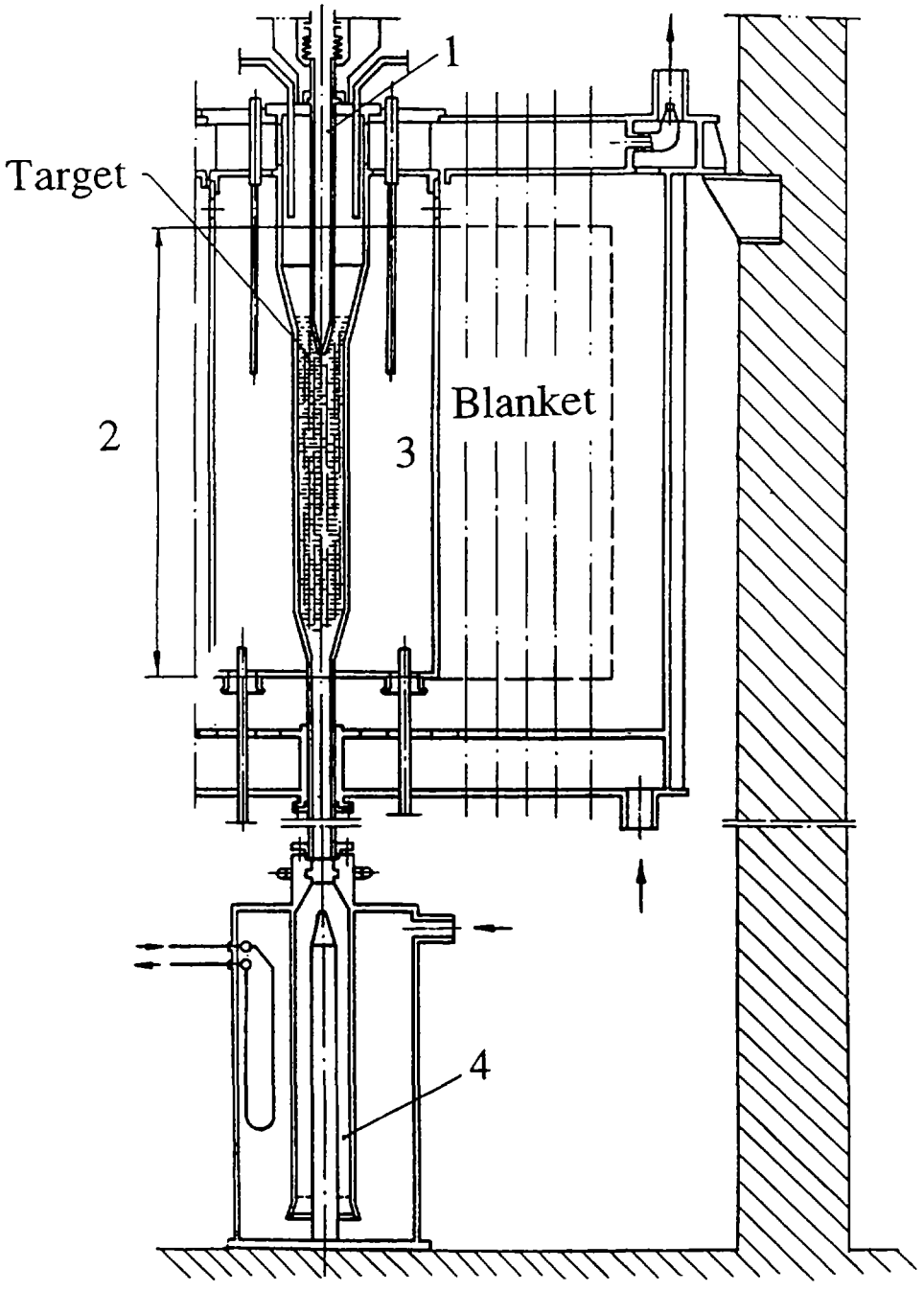

FIG. 1. Cros section of the heavy-water cooled target. 1 - proton beam channel with window, 2 - fluidized bed target (core), 3 - inner reflector, 4 - Pb-shot receiver tank and beam stop.

The proton beam finds its way into the target from above through a conical window, plunged into the fluidized bed. Non-neutron poisonous alloys are selected as structural materials for the target (compositions based on Aluminum and (or) Zirconium). Outside the blanket, stainless steel may be used.

B.2.5.3. THE HEAT REMOVAL

Fig. 2 shows a concept of heat removal from the blanket. The heavy water flow arrives from a pump at the bottom heat exchanger to the receiver and through a pipeline to the working zone of the target. The flow then passes to the top part of the moderator tank and the jet pump, is mixed with the moderator flow and goes to the basic heat exchanger, from which it goes to the bottom part of the tank. The jet pump, working from the excess pressure of the pump, assists the natural circulation of the blanket moderator. Two heat exchangers are needed to balance the parameters of the moderator and the target coolant.

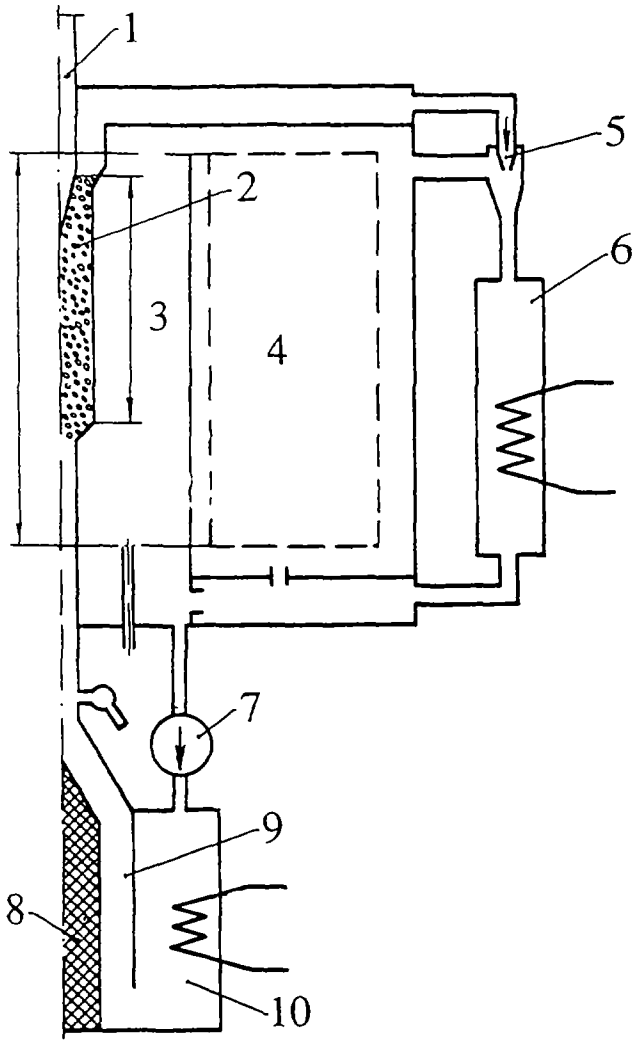

FIG. 2. Principal scheme of the target and moderator cooling. 1 - proton beam channel, 2 - fluidized bed target, 3 - internal heavy-water refelector, 4 - heavy water blanket, 5 - jet pump, 6 - heat exchanger for moderator and target cooling, 7 - pump, 8 - beam stop, 9 - Pb-shot receiver, 10 - the target heat exchanger

B.2.5.4. RESULTS OF NEUTRON YIELD AND THERMO-HYDRAULIC CALCULATIONS.

Calculations of neutron yield and energy deposition distributions, caused by a 1.0 GeV proton beam, were performed by two different Monte Carlo codes HETC [1] and PHOENIX [2] for various Pb-volume compositions of a target with 50 cm diameter and 200 cm height.

The proton beam was simulated as uniformly distributed within a radius of 10 cm. The results of the calculations by both codes are satisfactorily similar as far as the main target functions are concerned: neutron yield, total energy deposition and its longitudinal distribution. Longitudinal energy deposition, calculated by the PHOENIX code, is adopted for further thermodynamics calculations, because its values are greater than ones computed by the HETC code (approximately by 3%).

A flat top side (surface) to the target was assumed at the current stage calculations. In fact the target window should be made as a cone, which is sunk into the pseudo-liquid target for providing more efficient heat removal from the window. Such a window may be taken into account at the next stage of calculations of heat and neutron production distributions. The proton

beam, which is not distributed uniformly but by Gauss' law, should also be taken into account.

The number of neutrons that escape to the blanket is an important target quality. This quality is defined as the number of neutrons, that were produced by the initial proton, multiplied by a probability that the neutron reaches the target surface. The longitudinal distribution of neutrons, transmitted from the target to blanket, is another target quality. Results of the initial calculations of total neutron losses as a function of the porosity of the fluidized bed show that the longitudinal distribution of neutrons entering the blanket may be spread out. Though the neutron-to-proton efficiency of the proposed target goes down (about twice from 100% to 50% Pb-volume), the number of neutrons absorbed by construction materials is low.

Results of the tentative thermohydraulic calculations give the flow rate as a function of the diameters and porosity of the Lead spheres, as well as the dependence of the removed thermal power versus the Lead spheres diameter with the varied values of the porosity and flow pressure. The dependencies obtained are illustrated on Fig. 3. It can be seen that

- the porosity and flow pressure markedly affect the removed thermal power;

- for every value of the porosity there exists an optimum diameter of Lead spheres.

B.2.5.5. CONCLUSION

It is suggested that a heavy water-Pb grains fluidized bed be used as a neutron generating target. The preliminary design investigations, based on neutron yield and thermal hydraulic calculations, revealed that there is a possibility of a wide range of parameters to realize a fluidized bed target as an intensive neutron source of an accelerator driven subcritical nuclear reactor.

It should be noted that the proposed target provides for removal from service and replacement of the Lead spheres. This is an essential feature of the target for providing nuclear safety. The removed thermal power may be elevated as compared to the proposed design, if the directions of the proton beam and the heavy water flow are the same. Besides the non uniform porosity throughout the target height may be used to improve the efficiency of the neutron source.

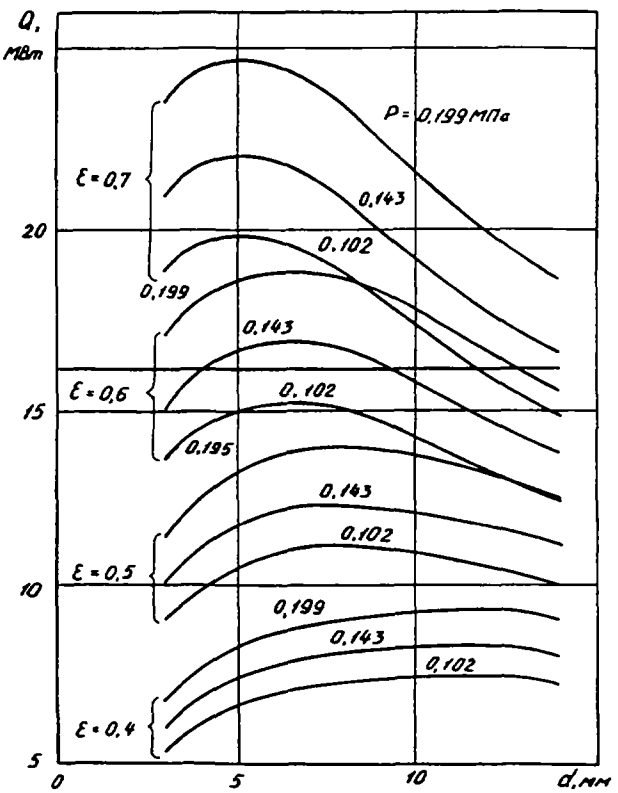

FIG. 3. Output power (MW_t) dependence on sphere diameter, Pb-volume of fluidized bed and output water pressure in MPa, e - Pb-volume in the target, P - water pressure

REFERENCES

1. T.W.Armstrong, K.C.Chandler - HETC - A High Energy Transport Code // Nucl.Sci.&Eng. 1972,49.p.110.
2. N.V.Stepanov - Computer Simulation of Fission of Exited Nuclei. 1. Description of the Model, M. Preprint ITEP 81-1987, 1987 (in Rus.).

B.2.6. ACCELERATOR DRIVEN HEAVY WATER BLANKET ON CIRCULATING FUEL

V.D.Kazaritsky, P.P.Blagovolin, V.R.Mladov, M.L.Okhlopkov, V.F.Batyaev, N.V.Stepanov, V.V.Seliverstov

Institute for Theoretical and Experimental Physics, Moscow, Russian Federation

B.2.6.1. INTRODUCTION

A conceptual design of a heavy water blanket with circulating fuel is described. Radiation safety for a reactor with fluid fuel is provided by the same means as in traditional nuclear power, namely by security in depth and control. As compared with fixed fuel reactors, the radiation situation in the suggested system can be improved, for, on the one hand, activity of the fission products is reduced through the continuous removal of the irradiated fuel for reprocessing, and, on the other hand, there is no need to open the reactor for reloading.

A design of a heavy water blanket with circulating fuel has been proposed in ITEP [1]. A lattice of power channels is placed inside a cold heavy water tank under about normal pressure. The channels made of proven Zr-Nb alloy isolate the fuel from the moderator and keep it constantly exposed to irradiation. Inside each channel there are two loops: a fuel loop (solution or slurry in heavy water) and a loop of pressurized heavy water coolant. The latter cools the fuel, circulating in the channel, while the fuel is continuously fed and removed in small portions for chemical reprocessing. After reprocessing the actinides come back to the fuel loop, while the remainder is fractionated and further sent for transmutation or storage and burial.

B.2.6.2. GENERAL CHARACTERISTICS OF THE FACILITY

The hybrid system consists of a high-current linear accelerator of protons and 4 targets, each placed inside a subcritical blanket. The plan view of target-blanket and its cross section are presented in Fig. 1 and 2. The accelerator current is 100 mA, the proton energy is 1 GeV and its power is 100 MW. The RF-to-beam conversion ratio is 40-50%.

Control magnets split the beam up into 4 separate beams, each of 25 mA current. After passing through defocusing magnets the beam of 30 cm in diameter goes through a diaphragm (window), isolating the accelerator vacuum from the target space, and strikes a 50 cm diameter target. The thermal power of such a separate beam is about 15 MW. The target consists of coated Pb elements or Pb grains cooled by heavy water flow. The Pb- heavy water volume ratio is 50%. The target, encased in a Zr tube, is surrounded by an inner reflector, made up of pure heavy water 70 cm thick. This heavy water layer is isolated from the blanket by a Zr cylinder wall. Control rods could be inserted into the inner reflector, and in a emergency some neutron poison for example, boric acid could be quickly released into the reflector water.

The subcritical blanket consists of a regular lattice of channels (modules), arranged with a step of 30 cm. The module design is shown in Fig. 3. The channel is constructed from Zr material. Heavy water coolant is pumped through an outer heat exchanger. Fluid fuel circulates inside the channel. The fuel is discharged in small portions for chemical reprocessing. Fresh fuel feeding and spent fuel discharge take place incessantly. The circulating fuel is either a heavy water solution of Pu, MA and fission products (FP) salts or their slurry.

The power of the channel, which is put under maximum load, is 5 MW. The depth of the active part of the channel is 4 m. The power of a channel in the blanket is on average about 3 MW (variation is 1.6). The blanket unit contains about 160 channels, the facility total being 640 channels.

The blanket is surrounded on an outer reflector. The subcriticality of the blanket is close to 5%. The thermal power is 500 MW (for the whole plant 2000 MW). Due to its heat-to-electricity conversion rate, close to 20%, the electric power of the whole plant will be 400 MW. An average thermal neutron flux in the blanket is expected to be about 3.* 10^{14} n/ cm^2 s.

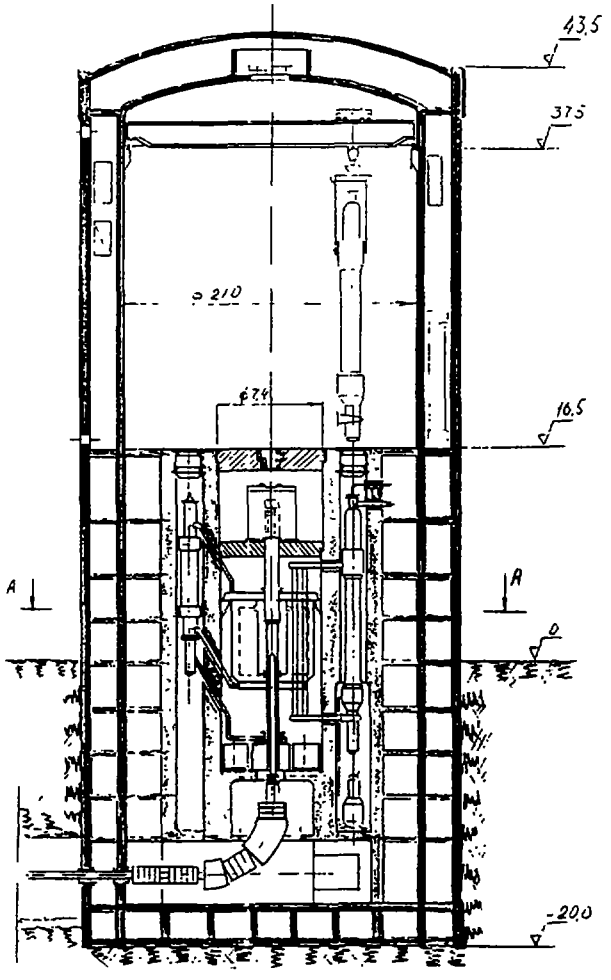

FIG. 1. Vertical cross-section of the accelerator driven heavy-water facility. The numbers show the approximate heights and diamaters in meters. The line A-A shows a cross section presented in Fig. 2

B.2.6.3. GENERAL PRINCIPLES OF THE SUGGESTED FLUID FUEL MODULE

The suggested fluid fuel module (FFM) is a unit of the blanket assembly of the accelerator driven nuclear plant containing circulating fluid fuel within the blanket core. Water solutions of salts or water slurry of oxides could be used as fluid fuel. The proposed design of the fluid fuel module is illustrated in Fig. 3.

The conceptual design scheme of FFM is as follows: the circuit of FFM contains a central 1.5 mm thick lifting tube of 83 mm in diameter (CLT) and 90 outlying 0.5 mm thick lowering tubes of 11 mm in diameter each (OLT). The OLT are joined with the CLT and arranged as a stringer with lattice spacing 13 mm. The forced circulation of the fluid fuel is realized by a centrifugal pump placed in the lower part of the CLT and driven by a hydraulic turbine, which uses the energy of a fluid fuel coolant. The FFM active zone is 4.0 m in height, the external diameter of the coolant channel is 165 mm.

The FFM is installed into an assembly channel, which is a component of the blanket structure.

The design scheme of the FFM also provides :

- continuous withdrawal of the irradiated fuel,
- compensation of the fluid fuel volume by changes of the temperature,
- support of the pressure drop between the coolant and the fluid fuel within hydraulic losses of the coolant,
- guide grids of the heat-exchange tubes.

The initial data for developing the blanket design are determined by the following factors:

- heavy water is the coolant and the fluid fuel carrier,
- production of electrical power for feeding the Linac.

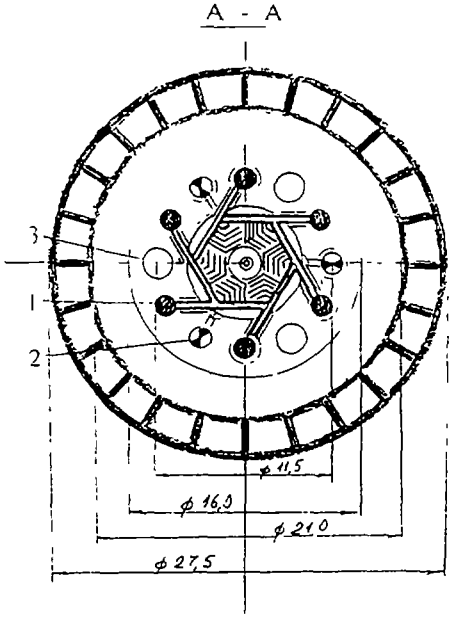

FIG. 2. Cross section of the facility. 1 - steam generator, 2 - heat exchanger, 3 - channel for inlet-outlet of fuel regeneration

On the basis of the literature on the subject and the preliminary calculatons of the design characteristics of the FFM, the following starting conditions are accepted:

- maximum temperature of the fluid fuel - 300 ;
- pressure - 10 MPa.

These conditions can provide:

- good enough characteristics for the power circuit of the plant (see an illustration of the suggested scheme on Fig. 4) ;
- practically complete suppression of the radiolytic gas release in the fluid fuel under normal operating conditions, moderate content of bivalent cuprous ions in fluid fuel (0.8 g/dm^3 and accordingly $\Sigma_c \leq 0.29 \cdot 10^{-4} cm^{-1}$);
- use of the Zirconium alloys such as H-1 and H-2 as construction materials;
- reasonable corrosion velocity (to 0.0107 mm\a by 280-300°C);

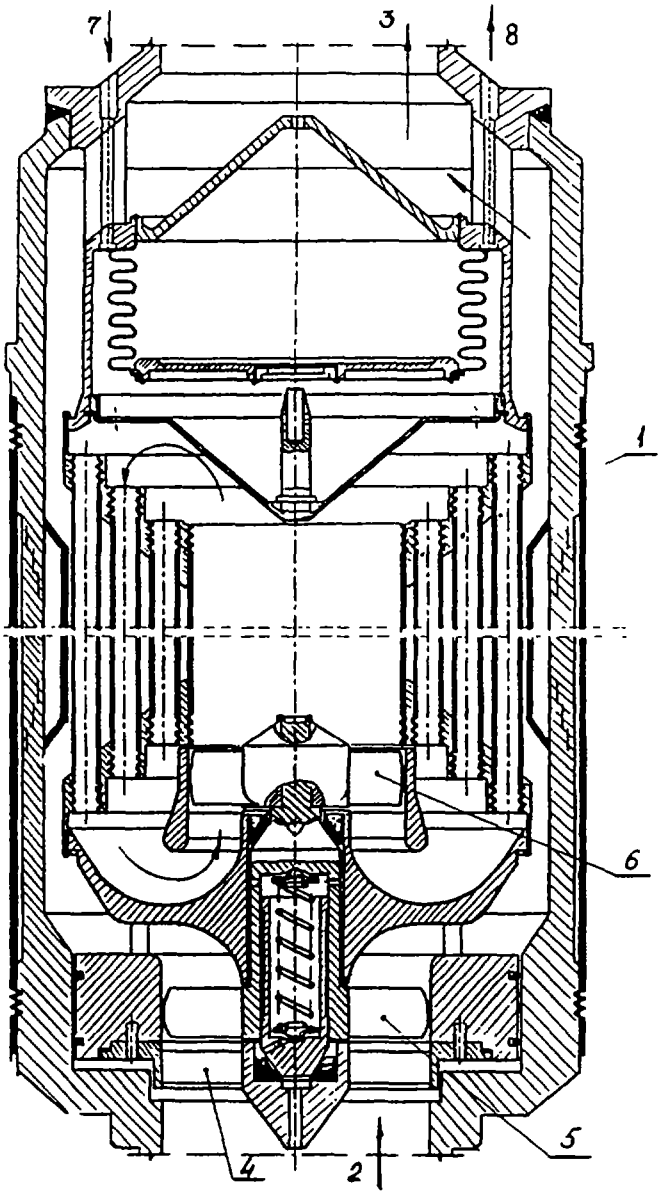

FIG. 3. Vertical cross section of the fluid fuel element. 1 - fluid fuel circuit, 2 - coolant inlet, 3 - coolant outlet, 4 - flow guider, 5 - turbo-drive, 6 - pump, 7 - feed inlet, 8 - fuel regeneration outlet

- good erosion resistance of the materials in the slurry with a flow velocity up to 6 m\sec.

Preliminary module design calculations show that the accepted above-mentioned parameters of the fluid fuel can be realized under the module parameters listed in Table I.

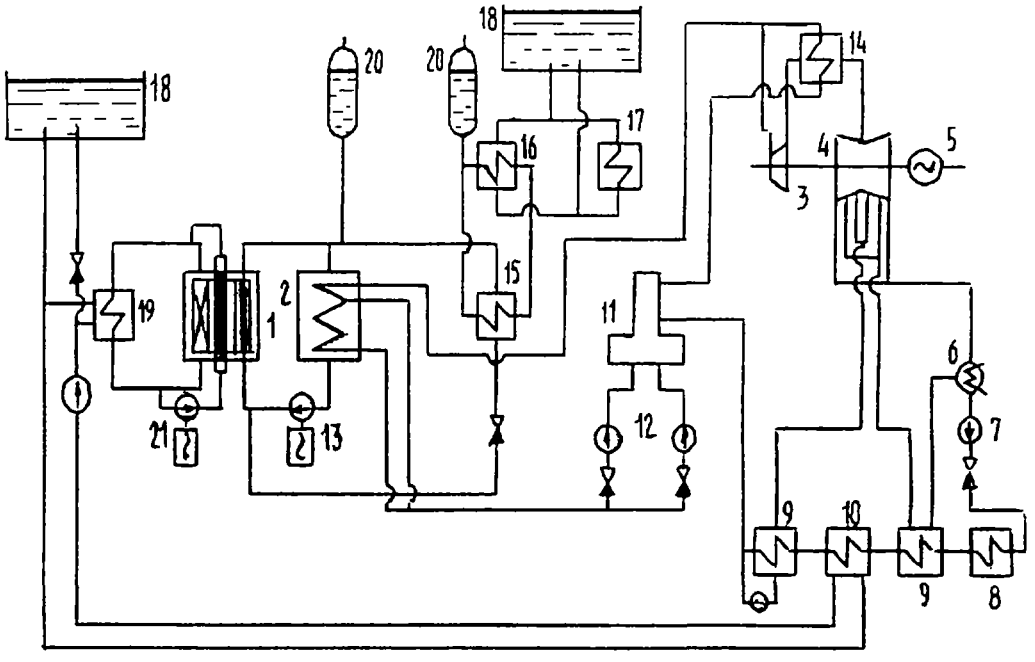

FIG. 4. Schematic thermodynamical layout of the facility. 1- target-blanket, 2 - steam generator, 3 - high pressure cylinder of the turbine, 4 - low pressure cylinder of the turbine, 5- electro-generator, 6 - condensor, 7 - condensation pump, 8 - condensation cooler, 9 - low pressure heater, 10 - heat exchanger of the moderator, 11 - deairator, 12 - water feeding pump, 13 - the first loop circulator, 14 -steam overheater, 15 - heat exchanger of coolant, 16 - water-water heat exchanger ocf coolant, 17 - water-air heat exchanger of coolant, 18 - reservoir of the emergency cooling, 19 - moderator cooling, 20 - comensator, 21 - target coolant circulator

TABLE I. PARAMETERS OF FLUID FUEL MODULE.

Thermal output, MW	5
Fuel circulation rate, kg/s	10
Coolant circulation rate, kg/s	35
Fuel velocity, m/s	2
Coolant velocity, m/s	6
Fuel temperature (av), °C	285
Coolant:	
outlet temperature, °C	250
average temperature, °C	230

Tentative estimates of parameters of the power circuit are shown in Table II. Figure 2 shows relative positions of steam generators and heat exchangers.

TABLE II. STEAM GENERATION SPECIFICATIONS

Steam temperature, °C	200
Feed-water temperature, °C	100
Steam pressure, MPa	1.6
Rankin's cycle thermal efficiency, %	22.6
Efficiency of the power plant, %	17.3

B.2.6.4 FUEL CYCLES

Two fuel cycles are considered: 1) military Pu and MA are loaded, only fission products (FP) are discharged (Cycle 1); 2) the same load, Pu of a worsened isotope composition is discharged additionally to FP (Cycle 2). In the blanket Pu, MA and FP are considered to be in equilibrium. With the given power of the facility equilibrium concentrations are maintained in stable working order with the choice of rates of feeding and discharge. Performance data for two fuel cycles are presented in Table III.

TABLE III. PERFORMANCE DATA FOR TWO CYCLES OF PU CONVERSION AND MA TRANSMUTATION.

	Cycle 1	Cycle 2
Pu load, kg/a	400	750
Pu withdrawal, kg/a	0	500
MA load, kg/a	200	350
FP discharge, kg/a	600	600
Core inventory of Pu and MA, t	4	2.9

It is assumed that the Pu in the load is Pu-239(100%). The composition of MA being loaded is ^{241}Am (47.47%), ^{237}Np(41.81%), ^{242m}Am(0.09%), ^{243}Am(8.57%), ^{244}Cm(1.67%), ^{245}Cm(0.09%). The equilibrium concentrations of Pu and MA mixtures in fluid fuel, which are obtained, are 125 g/l for Cycle 1 and 91.5 g/l for Cycle 2. The isotope composition of Pu is estimated to be as follows: ^{238}Pu(27%), ^{239}Pu(39,4%), ^{240}Pu (20%),^{241}Pu(5.8%), ^{242}Pu(7.8%).

It can be seen that in Cycle 2 the MA incineration rate to be achieved in the facility is approximately doubled due to a failure of complete Pu burn-down. The equilibrium compositions obtained are presented in Table IV. For Pu isolation in Cycle 2 the rate of chemical reprocessing needed, should be 46 l/day.

B.2.6.5. CONCLUSION

The suggested hybrid system offers a chance to fulfill safe and efficient incineration of all built Pu and MA stock. Resources of the facility performance can be considered by a wide variation of the load-withdrawal rate as well as the concentration of Pu and MA in the fluid fuel. Additionally, disposal of Cm

to interim storage and its return back to the blanket in 2 years' time are expected to be promising.

TABLE IV. EQUILIBRIUM ISOTOPE COMPOSITIONS (g/l) IN BLANKET CORE.

Element	Atom number	Cycle 1 (g/l)	Cycle 2 (g/l)
Np	237	9.33	17.15
Np	238	0.41E-1	0.76E-1
Pu	238	9.48	8.28
Pu	239	9.77	12.09
Pu	240	10.78	6.13
Pu	241	3.45	1.81
Pu	242	25.5	2.42
Am	241	3.075	5.58
Am	242m	0.33E--1	0.61E-1
Am	242	0.14E-1	0.25E-1
Am	243	7.99	4.15
Am	244	0.41E-3	0.23E-3
Cm	242	2.61	4.80
Cm	243	0.223	0.42
Cm	244	23.54	15.57
Cm	245	0.90	0.61
Cm	246	14.68	9.57
Cm	247	1.08	0.72
Cm	248	2.77	1.86

REFERENCE

[1] V.D.Kazaritsky, P.P.Blagovolin, V.R.Mladov et al. - Fluid Carrier Problem of Blankets on Circulating Fuel, Preprint ITEP 20-1994, M., 1994 (In Rus.).

XA9846556

B.2.7. CHEMICAL TECHNOLOGY OF THE SYSTEMS, PARTITIONING AND SEPARATION, DISPOSAL

V.I. Volk

Institute of Inorganic Materials, Moscow, Russian Federation

B.2.7.1. ASSESSMENT OF INSTALLATION STRUCTURE "REACTOR - ACCELERATOR REPROCESSING COMPLEX"

The general outline of the reprocessing complex is shown in Fig. 1. The complex comprises an electronuclear transmutation installation and chemical and technological support units, the function of which is maintenance of the steady-state of the blanket, separation of short-lived transmutation products to be disposed of from other components of the blanket, chemical conversion to relevant stable species of products to be disposed of for interim storage and disposal.

The objectives can be resolved as follows.

Pu that is fed to the complex from external sources is subjected to conditioning which involves formation of chemical species acceptable for membrane-extraction transport (e.g., Pu (IV) or Pu (III) nitrate solution not containing excess acid).

Minor actinides (MA) that arrive for transmutation from external sources need the same conditioning. In this case the MA flow can also contain Pu.

The conditioned flows enter the feeding and discharging unit of the blanket that comprises two stages, namely, those of feeding and discharging (Fig. 2.). Each stage is equipped with a membrane-extraction unit and necessary auxiliary equipment.

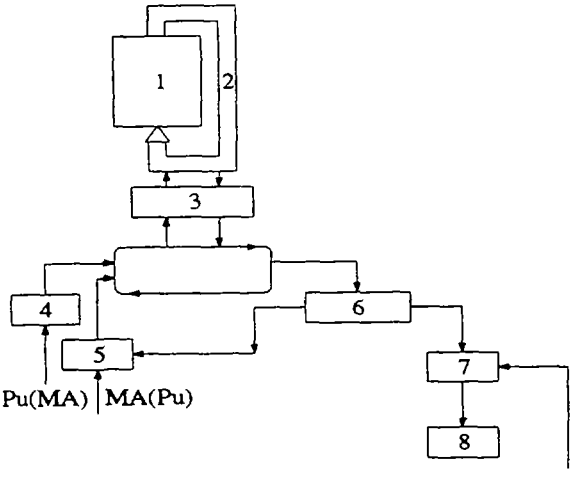

FIG. 1. General outline of reprocessing complex. 1- ELNU, 2 - out-reactor portion of heavy water blanket, 3- unit for blanket feeding and discharging, 4,5 - unit for Pu and minor actinides conditioning to be supplied to feeding and discharging unit, 6 - partitioning unit, 7 - unit for short lived transmutation product conditioning for disposal, 8 - disposal of short-lived transmutation products

At the blanket feed stage the membrane-extraction transport unit operates at a giving off/receiving flow ratio much less than 1 and at higher Pu and MA concentrations in the feeding solution. The joint impact of the two factors defines the direction of Pu and MA transport to the blanket. Evaporation of the feeding solution is feasible as the simplest way of reducing the flow amount and proportionally increasing concentration.

At the blanket discharge stage the membrane-extraction transport unit also operates at a relatively high flow of the receiving solution. The receiving flow is a by-pass flow of protium water sent to the partitioning unit.

A need for short-term cooling of the blanket flow prior to its entering the feeding and discharging unit

is not excluded. It is also possible to use the spent giving off flow from the discharge stage as a receiving flow at the blanket feed stage.

The aqueous flow from the discharge stage, containing practically all the components of the blanket flow (the membrane-extraction transport block of the discharge stage accomplishes non-selective transport of the elements), arrives at the partitioning unit. The function of the latter is to remove Pu and MA from the fraction of short-lived transmutation products, i.e., to shape a flow of radionuclides for supervised storage and subsequent disposal.

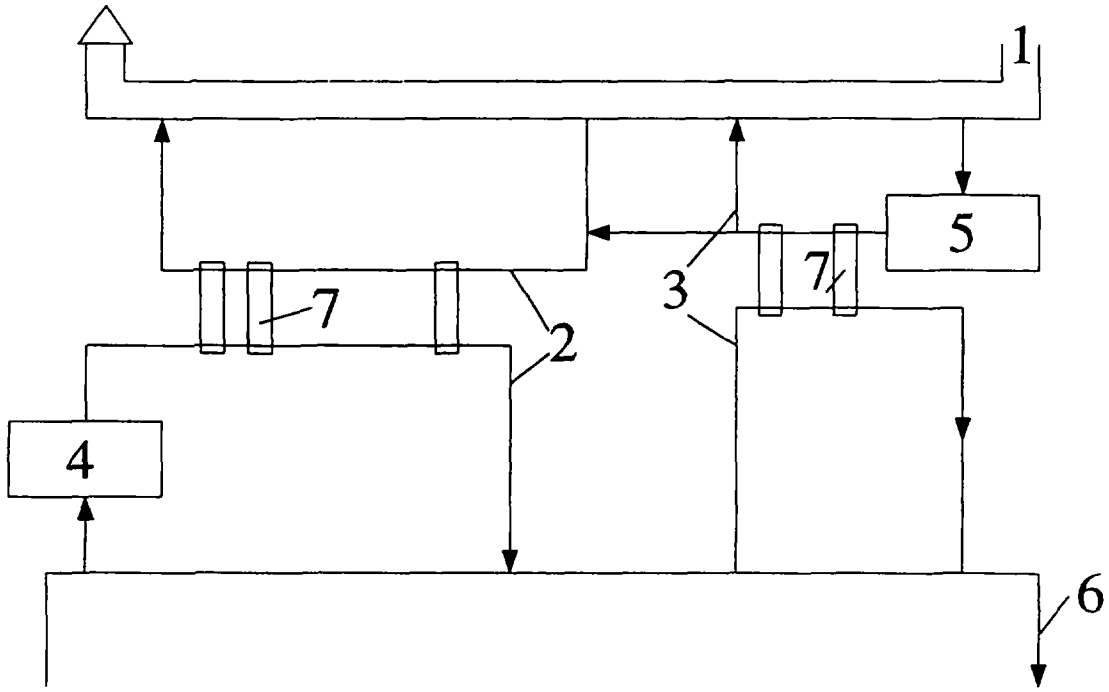

FIG. 2. Schematics of blanket feeding and discharging unit:
1 - out-of - reactor portion of blanket; 2 - by-pass lines of feeding unit; 3 - by-pass lines of discharging unit; 4 - evaporation of feeding flow; 5 - cooling of discharge flow; 6 - flow for partitioning

Pu and MA are brought back to the heavy water blanket through one of the conditioning units. The conditioning is accomplished together with those flows of Pu and MA that arrive at the complex from an external source, that is, together with the feeding flows.

The purified flow of short-lived transmutation products arrives at the waste chemical reprocessing unit, the function of which is to convert short-lived nuclides to chemically stable species and to incorporate them into special matrix materials having a high resistance to leaching and the necessary thermophysical and mechanical characteristics.

Waste chemical reprocessing comprises pre-conditioning (mixing) and evaporation of solutions, their concentration in a direct flow evaporator (DE) or calcination in a spray dryer (SD) and solidification of concentrates or calcinates in an induction melter having a cold crucible (IMCC).

Depending on the location of the complex in relation to a radiochemical spent fuel reprocessing plant a flow of short-lived fission products (SFP) can arrive at waste reprocessing operations from an external source.

The high initial heat release by solidified composite species containing short-lived nuclides demands a preliminary supervised storage with a forced transfer of heat. This storage could be realized on the basis

of the technical solutions used at "Mayak" and related to the interim storage of vitrified high activity level waste (Fig. 3.).

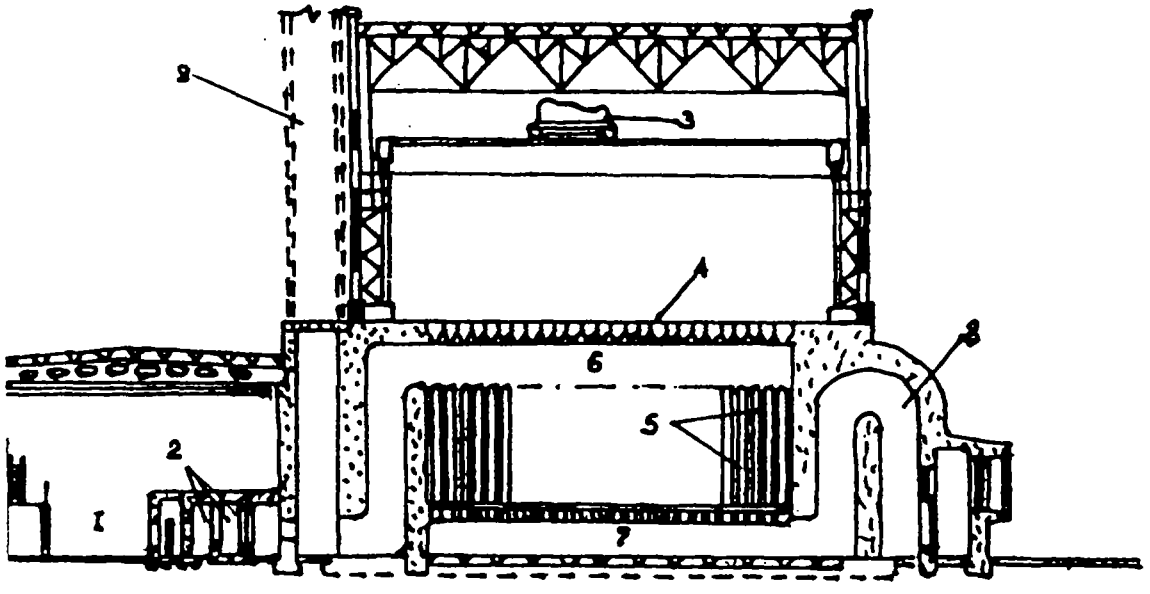

FIG. 3. Forced cooled storage facility. 1- blowers; 2 -shutters and filtration station; 3 - crane; 4 - dismantable floor; 5 - reinforced concrete wells for cans; 6,7 - air channels; 8 - air intake; 9 - vent pipe

B.2.7.2. EVALUATION OF INITIAL CHEMISTRY AND TECHNOLOGY REQUIREMENTS FOR EXTENT OF COMPONENT EXTRACTION

Components are extracted in the blanket feeding and discharging and partitioning units.

In the former unit (feeding and discharging) the intensity of removal from feeding solutions is only defined by technical and economical practicability. The necessary quantities of transmuted elements should be fed in the best way to the blanket feeding unit with an optional intensity of removal from the feeding solution. In the discharging unit the process is reversed for the intermediate and final products of transmutation.

Thus, the intensity of the removal of the elements at the stages indicated controls an additional parameter - the stable state of the blanket. Residual (not extracted) amounts of products circulate in the reprocessing complex as uncompleted products (UP), and the structure of the complex is optimized by the ratio between expenditures for complete extraction and UP amount.

In the latter unit the depth of extraction of the not transmuted Pu and MA from the flow of short-lived transmutation species that in the end are to be disposed, is governed by the radioecology requirements of a material which is in contact with the environment for an infinitely long period of time.

An analysis of the technical potentialities of the available and prospective technologies as well as protective properties of matrix materials already known and those under development produces the following requirements. The depth of long-lived alfa-emitter (Pu, MA) extraction has to meet the requirement that the activity ratio of long-lived active materials Ci_l to short-lived ones Ci_{sh} in a material to be disposed of is not higher than 5×10^{-2}, with the prospective improvement of Ci_l/Ci_{sh} to 1×10^{-2}.

B.2.7.3. ANALYSIS OF TRANSMUTATION PRODUCT COMPOSITION AND FEASIBLE METHODS OF IMMOBILIZATION OF RADIONUCLIDES TO BE TEMPORARILY STORED

The structure of the reprocessing complex provides chemical co-reprocessing and conditioning disposal of short-lived fission products from an external source and short-lived transmutation products. The full set of transmutation products has to be identified after defining the optimized steady-state of the blanket. However, even now one can be guided by specific constituents of the products to be disposed of (also including fission products of co-reprocessing), namely, isotopes of Cs, Sr, Sb, Te, Zr, Mo and rare-earth elements.

To immobilize radionuclides matrix materials are needed that comply with the rigid requirements for the following parameters:

- chemical stability, determined from the rate of the radionuclide leaching with natural water, to be not more than 10^{-6} g/cm^2 /day of ^{137}Cs, ^{90}Sr and not more than 10^{-7} g/cm^2/day of ^{239}Pu;
- radiation and thermal stability, determined from the invariability of material properties under the action of high irradiation doses and temperature (10^{+10} rad under β and γ-radiation at temperature higher than 559 °C);
- mechanical strength, Young modules not less than $5.4 \times 10^{+7}$ N/m^2 and compressive strength $(0.9\text{-}1.3)\times 10^{+7}$ N/m^2 ;
- thermophysical characteristics, namely, heat conductivity 1-2 W/m/K and linear expansion coefficient not more than 9×10^{-6} °C^{-1}.

These requirements are best met by matrices which are mineral-like systems of the ferrosilicate type, formed by (% mass) Fe_2O_3 - 40; CaO - 10; SiO_2 - 50.

In materials of this type isomorphic substitution is feasible: calcium by alkaline and alkaline earth nuclides, iron by nuclides of +3 and +4 valencies.

The level of possible incorporation of radionuclides in a matrix material of this kind is about 10^4 Ci/l of β and γ - nuclides and about 1 Ci/l of alfa- nuclides which represents the initial heat release of about 30 kW/m^3 .

The supervised storage continues until the heat release is reduced to 1.0-1.5 kW/m^3. After that the radionuclides, immobilized in a matrix material, are to be placed in an additional protection can and disposed of.

B.3. FUEL AND FUEL CYCLES

Any type of reactor can be arranged to be in a subcritical state. As shown in section B.1. Fig. 1 different fuel and fuel cycle concepts have been investigated. Los Alamos National Laboratory abandoned its earlier design based on slurry-type fuel suspended in the heavy water moderator (CANDU-reactor technology) and has developed a concept based on molten fluoride fuels in the thermal neutron spectrum with different fissile materials like: weapon-grade Plutonium, LWR-spent fuel (minor actinide and some fission product burner) and even Thorium fuels (based on molten salt reactor technology). JAERI has focused its attention on minor actinides burning in the fast neutron spectrum with a solid fuel (based on sodium-cooled fast reactor technology) or molten chloride fuel (unproven technology). The CERN-group advocates solid $ThO_2/^{233}UO_2$ fuel in the liquid Lead fast spectrum system (liquid Lead - liquid Lead/Bismuth reactor technology). Brookhaven National Laboratory has proposed several concepts based mainly on the fast spectrum, liquid sodium-cooling and oxide or metal solid fuels (sodium-cooled fast reactor technology). BNL also tried to implement the idea of a particle bed/bead fuel (space propulsion reactor technology) in the thermal neutron spectrum. In Russia, the Institute of Theoretical and Experimental Physics in Moscow is leading a big scientific project financed by the International Science and Technology Centre (ISTC) "Feasibility Study of Technologies for Accelerator Based Conversion of Military Plutonium and Long-Lived Radioactive Waste". Different types of systems and fuels are under investigation: like heavy water suspensions, molten fluoride systems and liquid Lead fast spectrum systems.

All these concepts require some sort of reprocessing of the fuel - more extensive for some projects, less for other. It is however believed that ADS can offer a reprocessing option which can accomplish high utilization of the nuclear fuel with reprocessing based on simple processes fulfilling non-proliferation objectives. In the case of weapons Plutonium incineration systems ADS can significantly contribute to the reduction of Plutonium stockpiles for ever.

The diversity and different objectives together with the different scientific and social perspectives make intercomparison of all these systems very difficult. Moreover, the scientific communities in many countries are still assessing what would be the best choice for ADS taking into account specific requirements. All the major projects and connected fuel cycle technologies are described in details in the following sections (partially in section B and for some of the projects - in section D).

B.3.1. FUEL CYCLE

Toru Ogawa and Yasufumi Suzuki
Japan Atomic Energy Research Institute
Tokai-mura, Naka-gun, Ibaraki-ken 319-11 Japan

B.3.1.1. DOUBLE STRATA CONCEPT AND ALTERNATIVE TRU FUEL SYSTEMS

The partitioning-transmutation (P-T) scheme is based on a double strata fuel cycle concept, where the minor actinides (MA: Np, Am, Cm etc.) from the commercial fuel cycle flow into the second-stratum transmutation ("actinide-burning") cycle, exiting only after being converted to fission products [1]. It is preferable to realize a dense fuel cycle for this second stratum, where high atom densities of the actinides are maintained throughout the whole cycle, and the system's volume and envelope are minimized.

The annual discharge of MA from 10 PWR units of 3410 MW_t each in open fuel cycle consists of 145 kg Np, 99 kg Am and 14 kg Cm. Burnup of PWR fuel is assumed to be 33 GWd/tHE; the irradiated fuel is reprocessed after 3 years and the MA is separated from high-level waste after an additional 5 years cooling. With a burnup of ~15 at% of the TRU fuel in an actinide burner, about 1.6 t of TRU (Pu and MA) would have to be reprocessed in order to incinerate the annual discharge of TRU elements given above (~250 kg). Even if one assumes a low plant load factor of 30%, only 15 kg TRU a day would have to be treated in the fuel cycle facility. If those actinides are treated in a condensed state, the total daily volume of TRU fuel is of the order of one liter.

One promising concept is the metal fuel cycle being studied by the Argonne National Laboratory, US, and the Central Research Institute of Electric Power Industry, Japan. JAERI is studying the feasibility of employing a mixed nitride fuel and pyrochemical reprocessing, with metal (alloy) fuel being regarded as an alternative. Another attractive concept is to use a liquid fuel such as a molten salt, where in-situ decontamination of the fuel from the fission products would be possible.

B.3.1.2. NITRIDE FUEL CYCLE

Figure 1 shows schematically the flow of the TRU-nitride fuel cycle. Actinide salts from the partitioning processes of high-level waste in commercial plants can be converted to mononitride microspheres via sol-gel techniques. Thus, a high-density liquid can be converted to a high-density solid. Problems associated with the actinide dust are minimized by the use of the sol-gel process. The irradiated fuel will be reprocessed with a molten-salt electrorefining technique, which is very similar to that used for metal fuels [2]. The nitride fuel is anodically dissolved in a LiCl-KCl eutectic melt, and the actinide metals deposit on the cathode. Solid and liquid-Cd cathodes will be used for recovering U and transuranium metals, respectively. The recovered metals are then nitrided in a liquid Cd bath.

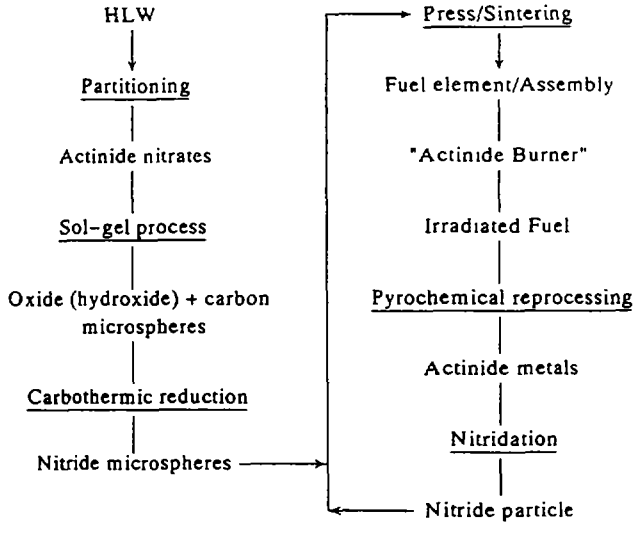

FIG. 1. Scheme of TRU nitride fuel cycle.

Though nitride fuels can be reprocessed by the PUREX process, pyrochemical reprocessing is preferable from the view of ^{15}N recycling. ^{15}N-enriched N_2 would have to be used to minimize ^{14}C production by the (n,p) reaction of ^{14}N. Then, the recycling of ^{15}N-enriched N_2 would be necessary, considering its predictably high price even at the mass production stage. In the electrorefining process the actinide nitrides are anodically dissolved into a molten salt; the actinide metals are deposited on the cathode. With such a process the N_2 liberated would be readily recovered for recycling.

B.3.1.3. IRRADIATED TRU FUEL CHARACTERISTICS AND THEIR ENGINEERING IMPLICATIONS

There is a significant difference in fuel characteristics between commercial power reactor fuels and "actinide burner" fuels. In the latter the larger concentration of minor actinides gives a higher dose rate and a-decay heat. These effects are illustrated in a study of a hypothetical alloy fuel system, where (Am, Cm, Pu)-5 at% Y and (Np, Pu)-20 at% Zr alloys are assumed [3,4]. The reason why two types of alloys are assumed is that Am and Np are predicted to be mutually insoluble [5]. Alloying elements, Y and Zr, are added to adjust the fuel power density. This is also expected to raise the melting points of the alloys, but has yet to be demonstrated. The solubility of Zr in Np might be much lower than previous expectation [6].

In the initial core, reactor-grade Pu is added to the alloys to adjust the core reactivity. Burnup of Pu compensates for the reactivity increase due to the generation of fissionable nuclides from the minor actinides. In succeeding cycles, no Plutonium is added, because sufficient fissionable nuclides are formed in the fuel: in the (Np, Pu)-Zr, for instance, loss of ^{239}Pu is compensated for by the generation of ^{238}Pu. In this core the neutron spectrum is very hard: the average neutron energy exceeds 0.76 MeV. Tables I and

TABLE I. ACTINIDE COMPOSITION IN IRRADIATED TRU FUEL AT 17.3 % OF HEAVY ATOM BURNUP AFTER TWO YEARS COOLING.

	(Am, Cm, Pu)-Y		(Np, Pu)-Zr	
	1st cycle	8th cycle	1st cycle	8th cycle
U-234			0.003	0.039
U-235				0.004
Np-237	0.002	0.007	0.625	0.569
Pu-238	0.061	0.134	0.113	0.264
Pu-239	0.150	0.039	0.114	0.068
Pu-240	0.157	0.174	0.106	0.038
Pu-241	0.025	0.013	0.019	0.004
Pu-242	0.033	0.069	0.015	0.007
Am-241	0.306	0.232	0.004	0.003
Am-242m	0.019	0.033		
Am-243	0.130	0.094		
Cm-242	0.0007	0.0006		
Cm-243	0.0008	0.0001		
Cm-244	0.107	0.154	0.0001	0.001
Cm-245	0.008	0.023		
Cm-246	0.0001	0.0024		

II give the characteristics of the irradiated fuels. The high dose rate requires that all fuel-cycle processes are performed remotely with heavy shielding. This is not considered a real disadvantage, since the metallic fuel cycle proposed for the commercial fast reactor also presumes the use of concrete cells for the whole

TABLE II. CHARACTERISTICS OF IRRADIATED TRU FUEL AT 17.3 % OF HEAVY ATOM BURNUP AFTER TWO YEARS COOLING.

	(Am, Cm, Pu)-Y		(Np, Pu)-Zr	
	1st cycle	8th cycle	1st cycle	8th cycle
γ strength (MeV/s.gHM)				
fission products	5.3×10^{10}	5.2×10^{10}	6.2×10^{10}	6.6×10^{10}
actinides	2.7×10^{9}	3.1×10^{9}	2.0×10^{8}	4.4×10^{8}
structural metals	8.8×10^{8}	1.0×10^{9}	1.3×10^{9}	1.5×10^{9}
Heat (W/gHM)				
fission products	0.029	0.028	0.033	0.035
actinides	0.47	0.62	0.066	0.15
structural metals	1.6×10^{-4}	1.8×10^{-5}	2.3×10^{-4}	2.7×10^{-4}
Neutron (n/s·gHM)	1.2×10^{6}	1.8×10^{6}	3.9×10^{3}	1.7×10^{4}

TABLE III. SOURCE STRENGTH OF IRRADIATED TRU ALLOYS AND REQUIRED NORMAL CONCRETE THICKNESS FOR SHIELDING TO ACHIEVE 0.625 MREM/H ON THE SURFACE.

			Point source strength	Thickness (cm)
(Am, Cm) alloys	Neutron		1.5×10^{10} n/s	130
8.14 kg HM	γ			
		total	6.2×10^{4} Ci	136
		actinides	9.9×10^{1} Ci	83
Np alloys	Neutron		1.2×10^{8} n/s	90
9.35 kg HM	γ			
		total	8.6×10^{4} Ci	140
		actinides	7.8×10^{2} Ci	100

process due to lower decontamination by pyrochemical reprocessing. Table III shows the source strength and required shielding. Though the neutron emission from the actinides is large, the wall thickness is mostly determined by the strength from the fission products. However there may be unexpected problems associated with high-energy neutrons such as those related to the life times of automated equipment.

Real difficulty comes from a large α-decay heat. With the assumed cooling time of two years, the α-decay heat is governed by that of ^{244}Cm in (Am, Cm, Pu)-Y and ^{238}Pu in (Np, Pu)-Zr alloys. It is needless to say that β/γ heating from the fission products predominates directly after the fuel discharge. However, the α-decay heat starts to predominate after some cooling time: after about 100 days for (Np, Pu)-Zr. We recall that U-Fs (Fs: fissium) alloy fuels of EBR-II after 2 at% burnup and 15 days cooling had a heat generation equal to that of the alloy fuels in Table II [7]. The EBR-II fuels could be successfully transported in a specially designed cask equipped with an argon blower for cooling. However, unlike the EBR-II fuel whose heat came from fission products, the heat comes from the actinides in the actinide burner fuels.

Therefore, it accompanies the fuel in all recycling stages. All processes, as well as the transportation of the recycled fuel to the core, should be designed with this problem of α-decay heat in mind. The design of the fuel assembly should also take this factor into account.

For the irradiated fuels with the compositions in Table I, the criticality is determined by ^{242m}Am. With a fully reflected but sufficiently dry condition, the subcriticality mass of the (Am, Cm, Pu) alloys is about 12 kg. A 91-pin assembly would contain about 4 kg HM. For the nitride fuels, water solution with a high heavy metal loading is used in the sol-gel process. The subcritical mass is then about 3 kg. In any case, the criticality problem would not be more severe than for a power reactor fuel cycle based on similar fuels and process schemes.

REFERENCES

[1] MUKAIYAMA, T., et al.: "Conceptual study of actinide burner reactors", 1989 Int. Reactor Physics Conf., Jackson Hole, Wyoming, Sept. 18-22, vol.4, 369.

[2] TILL, C. E. and CHANG, Y. I.: Conf-860422-1 (1986).

[3] TAKANO, H., et al.: JAERI-M 89-072 (1989).

[4] OGAWA, T., et al.: JAERI-M 89-123 (1989).

[5] OGAWA, T.: J. Alloys and Compds. 194 (1993) 1.

[6] GIBSON, J. K., et al.: J. Alloys and Compds., 213/214 (1994) 106.

[7] HESSON, J. C., et al : ANL-6605 (1963).

B.3.2. SOLID TRU FUELS AND FUEL CYCLE TECHNOLOGY

Toru Ogawa and Yasufumi Suzuki
Japan Atomic Energy Research Institute
Tokai-mura, Naka-gun, Ibaraki-ken 319-11 Japan

B.3.2.1. NITRIDES AND ALLOYS

Alloys and nitrides are candidate solid fuels for transmutation. The fuel element is the sodium-bonded type as shown in Fig. 1. Actinide metals and nitrides have good compatibility with Na. Since the lattice parameters of the nitrides are close to each other [1], one may expect that UN, NpN, PuN, AmN and CmN are miscible with each other. This is not the case for actinide metals. At present, Am-based and Np-based alloys are proposed, because the mutual solubility of Am and Np is considered to be small [2]. The lower melting points and rather low thermal conductivities of transuranium alloys would limit the linear heat rating of the fuel elements [3]. These are the reasons why the nitrides are preferred to the alloys. However, the alloy fuels are still considered important alternatives, since it would be easier to fabricate them than the nitrides. However, it is uncertain whether one may apply the simple method of injection casting, which has been successfully employed for the fabrication of the U-Zr and U-Pu-Zr alloy rods.

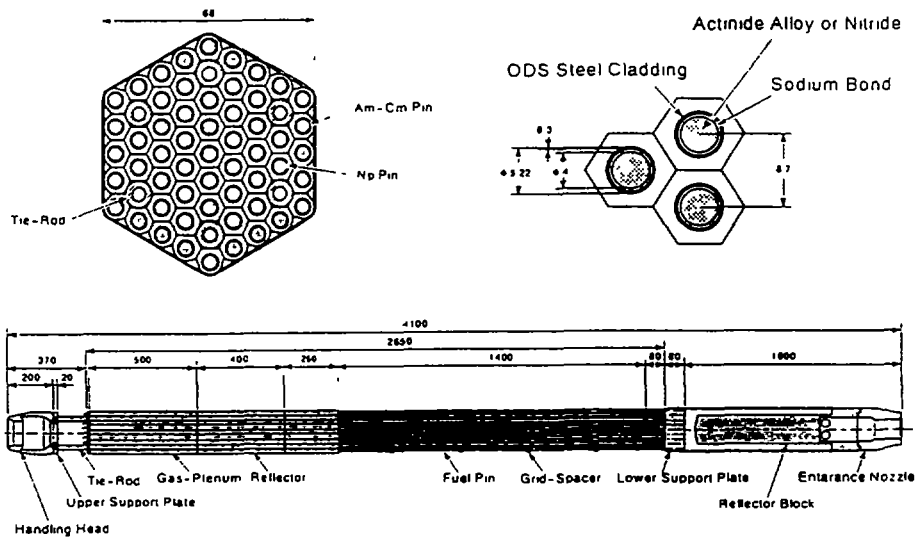

FIG. 1. Sodium-bonded fuel element and assembly.

The favorable thermal properties of the nitride fuels make full utilization of a cold-fuel concept possible [4]: (1) lower fuel temperatures and hence lower fission gas release and smaller swelling, and (2) a thinner cladding to achieve a high heavy-metal loading. A fuel would be called a "cold fuel", when its operating temperature is less than one third of the melting point. The melting point of the actinide nitrides is ~3000 K. There is an irradiation database of nitrides even for (U, Pu)N, but it is much smaller than those for the (U, Pu)O_2 and U-Pu-Zr alloys. However, the existing irradiation data suggest the tameness of (U, Pu)N under cold-fuel condition [4].

On the other hand, for the metallic fuels, there are phenomena whose mechanistic understanding has

not yet been reached the anisotropy in swelling, the component redistribution under a thermal gradient, the variation of apparent thermal conductivity with porous structure development and bond-sodium intrusion into pores etc [5] The reaction between stainless steel cladding and actinide alloys is also severe at higher temperatures, and imposes a performance limit [6] JAERI has prepared (U, Pu)N fuel elements and irradiated them in a thermal spectrum in JMTR [7] UN and PuN were prepared by carbothermic reduction of powder mixtures of respective oxides and carbon in flowing $H_2 + N_2$ Then UN and PuN were mixed and sintered to form (U, Pu)N The irradiation test of (U, Pu)N in the fast reactor, JOYO, was begun in August, 1994, as a JAERI/PNC joint program Suzuki et al [8] have prepared NpN by carbothermic synthesis Thermal conductivity [9] and high-temperature vaporization [10] of NpN have been studied by the same group The thermal conductivity of NpN was intermediate between UN and PuN Thermal properties will be further studied for (U, Pu, Np)N

B 3 2 2 NITRIDE FUEL CYCLE TECHNOLOGY

The scheme of the nitride fuel cycle is shown in Fig 2 For the nitride fuel cycle, technical developments are being made on (1) the internal gelation method to form (oxide + carbon) gel microspheres from the actinide nitrates and (2) the electrorefining process for reprocessing irradiated nitride fuels

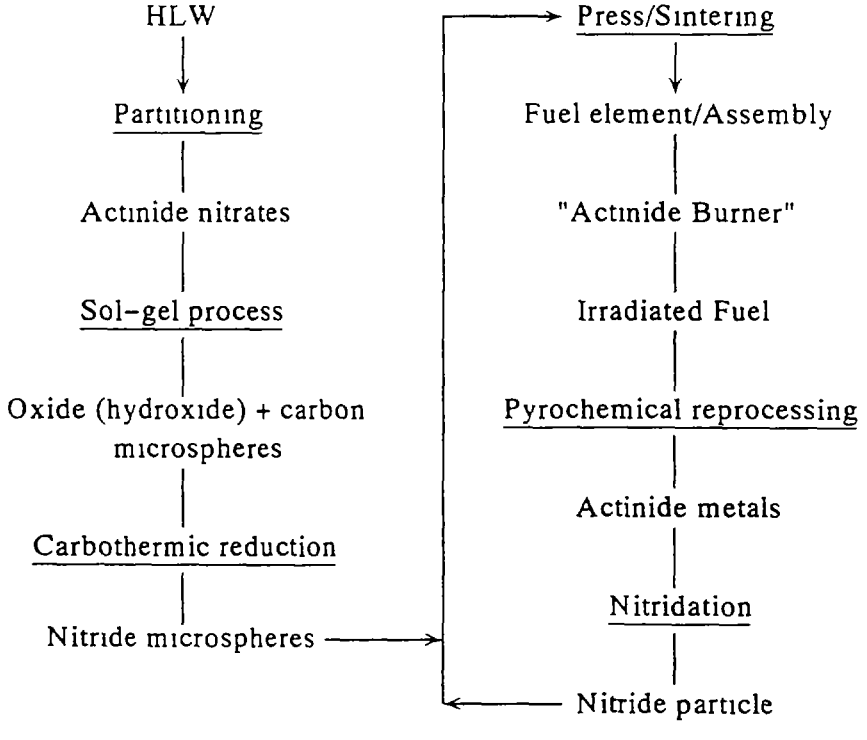

FIG 2 Scheme of TRU nitride fuel cycle

B.3.2.3.1. Nitride fabrication by sol-gel process

The internal gelation method is presently being studied because of the simplicity of feed solution preparation compared with the external gelation method, particularly when one wants to obtain multicomponent ceramics. In the internal gelation method, hexamethylenetetramine (HMTA), added to the solution, decomposes on heating to form ammonia which then reacts with the actinide nitrates. Then the solution of actinide nitrates with a carbon suspension turns into a solid mixture of oxide (hydroxide) and carbon in the form of microspheres. Normally the droplets of feed solution are heated in an oil column, but the use of a microwave heating for the internal gelation process has been proposed by Ledergerber et al. [11] Because of its potential to reduce the treatment of alpha contaminated oil, a 2.5 GHz microwave heating apparatus has been developed for this gelation process (Fig. 3) [12]. Also, in order to prevent the instability of the feed solution by the α-decay heat, techniques to mix the actinide nitrate solution and the HMTA solution right above the droplet-forming nozzle are being developed [13]. The gel microspheres are heat treated in a nitrogen atmosphere and converted to the nitride.

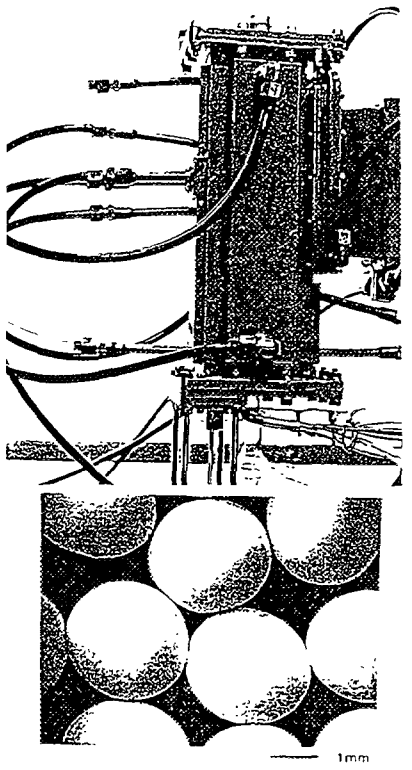

FIG. 3. Microwave gelation apparatus and ammonium uranate gel microspheres.

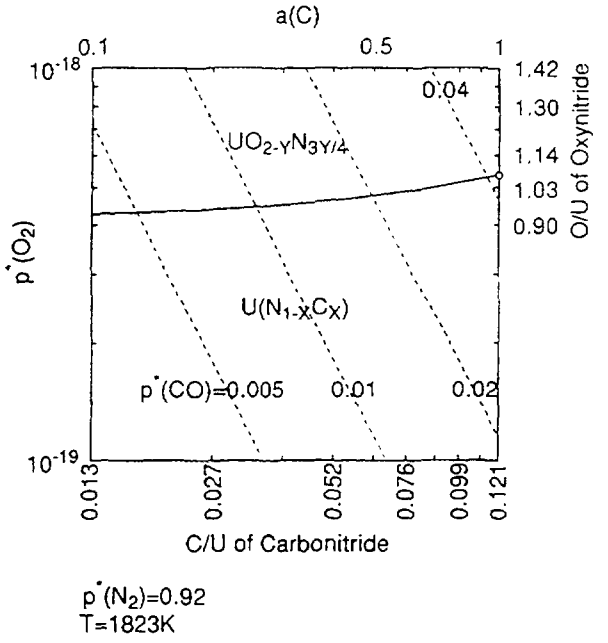

FIG. 4. Stability diagram of U-C-N-O system at 1823 K with p(N2) = 0.92 atm.*

It should be noted that the N_2 supply has to be in great excess for the carbothermic synthesis of the nitrides. This point can be illustrated by considering the case of UN synthesis. Figure 4 shows a stability diagram for the U-C-N-O system at an arbitrary nitrogen partial pressure of $p^*(N_2) = 0.1$ atm at 1823 K [14]. The mixture of UO_2 and carbon is heated in a nitrogen atmosphere to form Uranium carbonitride, U(C, N), and oxynitride, $UO_{2-Y}N_{3Y/4}$. The amount of the latter decreases with time; so does the fraction of UC in U(C,N). Carbon activity, a(C), and $p^*(O_2)$ are given by the upper abscissa and left ordinate, respectively. Progress of the carbothermic reaction is measured by the cumulative evolution of CO. The dashed line gives the equilibrium partial pressure of CO, p*(CO). p*(CO) at a(C)=1 is ~0.03 atm. As the reaction proceeds, C/U decreases to further reduce the equilibrium CO pressure, p*(CO). That is, in order to obtain UN, one has to supply nitrogen in a large excess to effectively remove CO from the system. Though excess N_2 from the process exhaust can be purified and circulated, the demand on ^{15}N-enriched N_2 makeup could be larger than that simply expected from the reaction stoichiometry. This is another incentive to recycle ^{15}N from the pyrochemical reprocessing.

B.3.2.3.2. Pyrochemical reprocessing

The irradiated fuels are reprocessed with molten-salt electrorefining techniques. The configuration of the electrorefiner can be common for the nitride and alloy fuels. For reprocessing nitride fuels, the electrorefiner has to be flushed with an inert gas to purge N_2 from the anode. ^{15}N-enriched N_2 is recycled to the nitride refabrication.

The anode basket contains either nitride or alloy fuels. The cathode is either a solid metal rod or a liquid metal bath such as molten Cd depending on the combination of actinide elements in the molten salt bath. A molten Cd cathode would be preferred to recover transuranium elements in the presence of U^{3+} in the molten salt phase.

The recovered N_2 can be fed to the process to convert actinide metals to nitrides. Conversion can be made in a liquid cadmium bath: actinide metals dissolve into Cd, react with N_2 which is in contact with Cd, and segregate as nitrides on the bottom of the bath. Cd can be readily distilled away from the nitrides.

The anodic dissolution of UN has been studied in laboratory-scale experiments [15]. UN powder was contained in a graphite anode basket. The counter electrode was a molybdenum rod. The LiCl-KCl-UCl_3 melt was contained in a recrystallized alumina crucible. The Ag/AgCl reference electrode consists of pure silver in LiCl-KCl-10 mol% AgCl. The measurements were done at 773 K. Fig. 5 shows that the anodic dissolution of UN occurs with the characteristic potential at about -0.66 V against the reference electrode. The pertinent reaction is the formation of solid UCl_3 on UN:

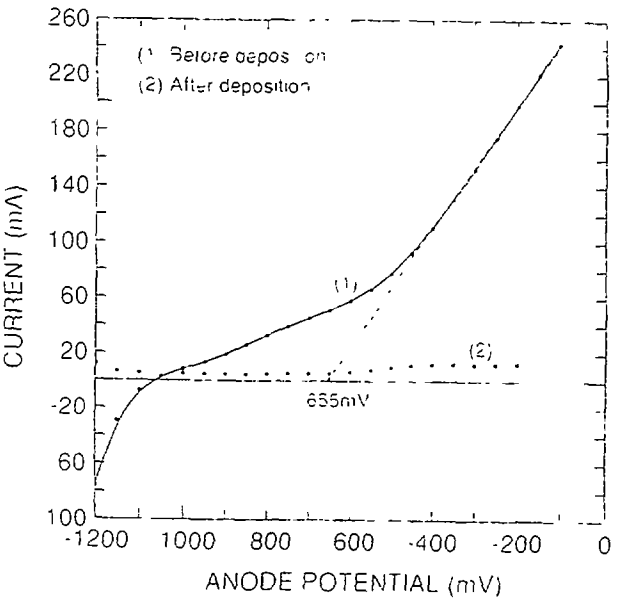

FIG. 5. Current and electrode potential for UN contained in a graphite anode basket in LiCl-KCl-UCl_3 melt at 773 K. The reference electrode was LiCl-KCl-10 mol% AgCl.

$$UN + 3[AgCl] = UCl_3 + N_2 + 3Ag \quad (1)$$

$$\Delta G = \Delta Gf^{\circ}(UCl_3) - \Delta Gf^{\circ}(UN) - 3\{\Delta Gf^{\circ}(AgCl) + RT \ln X_{AgCl}\}$$

$$= -192{,}030 \text{ J/mol}$$

$$E = \Delta G/3F = -0.66 \text{ V}$$

where ΔGf° is the free energy of formation, X_{AgCl} is the mole fraction of AgCl in the reference electrode, and F is the Faraday constant. Above this characteristic potential UN becomes unstable.

Electrolytic decomposition of UN was made with the working-electrode potential of -0.20 V. Almost all UN was dissolved, and α-U was deposited on the counter electrode. Similar runs have been made in LiCl-KCl-$CdCl_2$ melt, where Cd-U alloys were deposited on the cathode. Further tests with (U, Ln)N, PuN and NpN are scheduled (Ln: lanthanides). Table I shows the standard electrode potentials of actinide and

TABLE I. STANDARD ELECTRODE POTENTIALS IN LiCl-KCl EUTECTIC MELT AT 773 K.

Reaction	E°(Ag)/V
$Li^+ + e = Li$	-2.68
$La^+ + e = La$	-2.17
$Li^+ + e + (1/6)N_2 = LiN_{1/3}$	-1.88
$Pu^{3+} + 3e = Pu$	-1.81
$U^{3+} + 3e = U$	-1.61
$La^{3+} + 3e + (1/2)N_2 = LaN$	-1.42
$Pu^{3+} + 3e + (1/2)N_2 = PuN$	-1.00
$U^{3+} + 3e + (1/2)N_2 = UN$	-0.82
$Cd^{2+} + 2e = Cd$	-0.51
$Ag^+ + e = Ag$	0

fission-product metals and nitrides as well as those of structural metals, which were calculated from the thermodynamic data in the literature.

B.3.2.3.3. Fundamental database

In order to assess the feasibility of a P-T scheme, the database of basic properties has to be enlarged. The thermodynamic database has to be expanded in three major areas: (1) actinide alloys and intermetallics, (2) actinide-containing molten salts and (3) transuranium nitrides, particularly americium nitride. In JAERI, a pure substance and solid-solution database, related to actinide burning, is being created.

With our present knowledge, it is difficult to design a metal fuel with high concentrations of MA. Systematic studies of MA-transition metal alloying behavior are being made. Alloying behavior among U, Np, Pu and Am appears to be predicted with the Brewer model [2, 16], though the accuracy of prediction has yet to be examined for each system. Even with the U-Pu binary system, further refinement of the alloy theory seems to be necessary to realize satisfactory agreement with the experimental phase diagram [2]. Figures 6 and 7 show predicted ternary phase diagrams of U-Pu-Am and Np-Pu-Am, respectively. In the U-Pu-Am system, the liquid miscibility gap in the U-Am binary would close with the addition of a small amount of Pu. As for the Np-Am binary, the addition of small amount of Pu would not prevent the segregation of the Np-rich liquid at lower temperatures. Further theoretical refinement will be possible by referring the results of systematic experimental studies of the alloying behavior of transuranium elements such as those being made by Gibson and Haire [17].

The volatility of americium may be troublesome in any type of P-T scheme. For instance evaporative loss of americium during the sintering of the nitride fuel has to be avoided. Thermodynamic properties of AmN have to be studied to optimize the fabrication process. An initial estimate of the free energy of

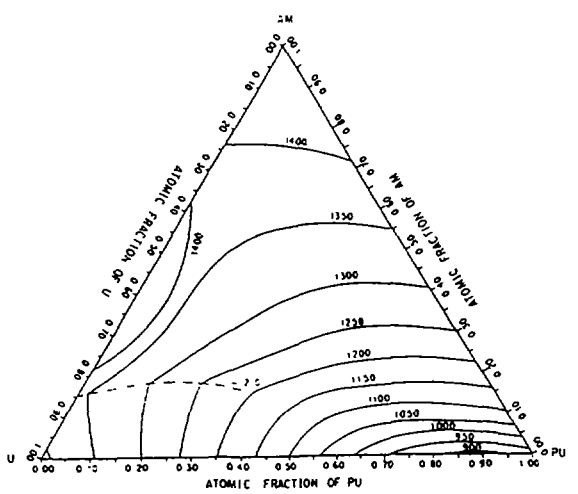

FIG. 6. Predict liquidus of U-Pu-Am ternary system.

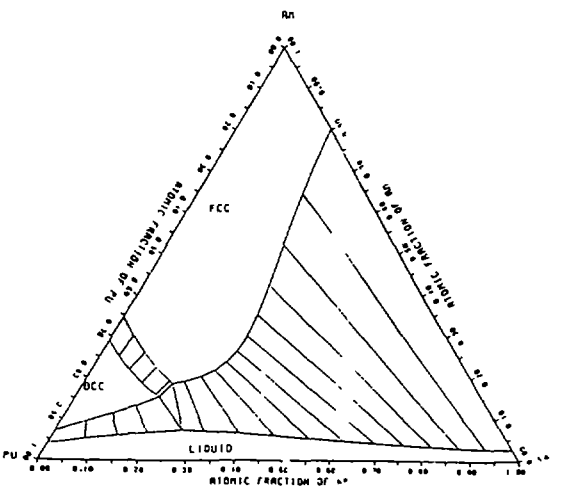

FIG. 7. Predicted isotherm of Np-Pu-Am ternary system at 1000 K.

formation, ΔGf°, of AmN has been made from the vaporization behavior of impurity ^{241}Am in reactor-grade PuN [18] ΔGf°(AmN) appears not to be significantly different from those of UN and PuN. This gives a much higher vapor pressure of Am over AmN compared with Pu over PuN. If so, either a technique to lower the sintering temperature has to be devised or the application of low-density fuel has to be considered.

As long as one seriously considers the use of Plutonium and the recycle of the other transuranium elements in nuclear technology, the thermodynamic behavior of actinide(An)-noble metal alloys such An-Pd alloys has to be better defined. The fission yields of noble metals are much greater from the transuraniums than from ^{235}U, and they form very stable intermetallics with actinides. The existence of stable intermetallics would cause a significant actinide loss during reprocessing.

REFERENCES

[1] KOCH, G., et al.: GMELIN Handbuch der Anorganishen Chemie, Transurane, Teil C: Die Verbindungen, Springer Verlag.

[2] OGAWA, T.: J. Alloys and Compds., 194 (1993) 1.

[3] OGAWA, T., et al.: JAERI-M 89-123 (1989).

[4] BLANK, H.: J. Less-Common Metals 121 (1986) 583.

[5] WALTERS, L. C.: Nucl. Technol. 65 (1984)179.

[6] VOHEN, A. B., et al.: Trans. ANS 66 (1992) 202.

[7] ARAI, Y., et al.: JAERI-Research 95-008 (1995).

[8] SUZUKI, Y., et al.: J. Nucl. Sci. Technol. 31 (1994) 677.

[9] ARAI, Y., et al.: J. Nucl Mater. 211 (1994) 248.

[10] NAKAJIMA, K., et al.: 1995 Annual Mtg. Atomic Energy Society of Japan, paper No. K9., Tokyo, March, 1995.

[11] LEDERGERBER, G.: Trans. ANS 40 (1982) 55.

[12] YAMAGISHI, S., et al.: JAERI-Tech 94-010 (1994).

[13] YAMAGISHI, S.: 1995 Annual Mtg. Atomic Energy Society of Japan, paper, No. L48, Tokyo, March, 1995.

[14] OGAWA, T., et al.: JAERI internal document.

[15] KOBAYASHI, F., et al.: J Am. Cer. Soc. (submitted).

[16] BREWER, L.: J. Alloys and Compds. 213/214 (1994) 132.

[17] GIBSON, J. K., et al.: J. Alloys and Compd. 213/214 (1994) 106.

[18] OGAWA, T., et al.: J. Alloys and Compds. (in press).

B.4. ACCELERATOR DRIVEN SYSTEMS (ADS): A PRINCIPAL NEUTRONICS AND TRANSMUTATION POTENTIAL

I. Slessarev

CEA, Cadarache, France

The proposed accelerator-based systems [1] use a beam of high energy protons to produce supplementary (external) neutrons as a result of spallation processes in a target. These neutrons are successively used to feed a subcritical blanket and can be used for the following goals:

- to create or to enhance a neutron surplus available for incineration of those long lived toxic nuclei which require neutrons (they can be long lived fission products, Minor Actinides (MA's) in the case when thermal neutron spectrum is applied, etc.);
- to enhance the deterministic safety features for reactivity-type of accidents.

B.4.1. OVERALL NEUTRONICS OF THE ADS

The external neutron source μ due to heavy nuclei spallation in a subcritical ($k_{eff} < 1$) medium can be defined as

$$\mu = \Gamma \cdot f \quad (\textit{neutrons per fission in the medium})$$

where Γ - is the number of neutrons returning to the ADS-medium if each fission has been transformed into proton current (spallation effectiveness),

f - is the fission fraction (fraction of energy) actually being used for spallation.

The following equations describe the neutronics of the ADS-blanket:

$$f = \frac{\left(\frac{1}{ke_{eff}} - 1\right)\nu}{\Gamma\varphi^*} \qquad (1)$$

$$I = \frac{\left(\frac{1}{ke_{eff}} - 1\right)5\nu W}{z\varphi^*}$$

where

ν - averaged secondary neutron number of fission process,

φ^* - importance of spallation neutrons in the given ADS,

I - proton current (mA),

W - ADS thermal power (MW),

z - the number of neutrons gained due to spallation per proton.

B.4.2. DETERMINISTIC SAFETY ASPECTS

One of ADS important potential is relating to deterministic safety concerning reactivity types of accidents. Evidently that all similar accidents can be certainly eliminated if ADS-reactivity could never exceed $k_{eff} = 1$. It means that the sum of the initial k^0_{eff} and all possible reactivity effects (burnup reactivity swing, including Np (or Pa) effect, power reactivity and void effects as well as other similar effects), taken for unfavorable situations, will never exceed critical value.

Obviously, subcriticality ($k^0_{eff} < 1$) can not guarantee these properties (except the case of a too low level k_{eff} when economics is not acceptable usually), while a combination of subcriticality and "stabilized reactivity" is a predisposition of deterministic safety features.

Further detailed simulations of all important accident scenarios are necessary in order to make a reliable deterministic safety potential analysis.

B.4.3. ECONOMICS

Economics puts an important impact on ADS-parameters choice [2,9].

For transmutation problems, which are not dependent on neutron surplus production (e.g. Pu burnup), it is important too keep k^0_{eff} - value close to critical state, because it allows to decrease requirements to proton beam power as well as to proton current. A benefit of ADS for these cases is relating to in the most cases deterministic safety enhancement. In turn, this is important to have small reactivity effects including burnup reactivity swing in ADS. Otherwise, one has to keep k_{eff} during a long core life at rather low level resulting in an economic penalty.

For example, in ADS with proton energy 1 GeV, the Γ is evaluated as 0.8 - 1.0 neutron/fission at $z = 25$ neutron/proton. It gives approximately 0.1 neutron/fission per each 10% of energy spent for the accelerator ($\varphi^* = 1$). Meanwhile, the analysis of a neutron surplus production potential shows (see paragraph B.1.4) that there is another way to enhance neutron surplus: ADS-blanket neutronics optimization.

Hence, both deterministic safety and economics considerations show an importance of "stable reactivity" concepts for ADS.

The economics of ADS depends upon the following negative factors: the necessity to have a "beam-target" system, as well as to spend a part of energy for proton current. Capital cost of the accelerator can affect ADS-economics. At the same time, enhanced safety potential of ADS allows to simplify reactor control.

A very rough preliminary estimation shows that a cost of the accelerator must not exceed 1/3 of the blanket cost to allow ADS to be economically acceptable.

Hence, a low capital cost of the accelerator, small fraction of consumed energy and a high k^0_{eff} - value may give an opportunity to be economically competitive with critical reactor.

In some Np-scenarios, even small fraction of ADS allows to reduce essentially MA-masses and fuel toxicity of all NP (as in the case of ADS/TransPu-Burners, see next paragraphs). For these cases, ADS-economic potentials will not be too important.

B.4.4. TOXICITY TRANSMUTATION POTENTIAL OF THE ADS

Minimization of the sources of a long-term toxicity in relation to energy production can be considered as the main goal of neutronics transmutation of both fuel and long-lived fission products (LLFP).

There are at least three types of long-term toxicity source [1]:

- fuel inventory in the nuclear reactors (systems),
- fuel wastes in the process of a discharged fuel reprocessing,
- long-lived radioactive fission products.

It seems that the last two sources mentioned are the most important due to toxicity accumulation during the normal functioning of the nuclear power industry [3].

For perspective development of nuclear power there is a state of "equilibrium", when similar operations (reactor fuel feeding, fuel burning, reprocessing, etc.) are constantly repeating. This leads inevitably to a "quasi-stabilization" of fuel and fuel waste contents.

B.4.4.1. Reduction of the long term toxicity of fission products

The neutron surplus potential of nuclear system depends on the overall neutron balance of every nucleus - "predecessor" (participating in reactor fuel feeding) and his "family", neutron "parasitic" losses (neutron leakage, absorption in construction materials (L + CM), et c.) and external neutron source μ [1 - 3].

For an equilibrium state, a neutron surplus potential G_J of a J-family being under irradiation can be expressed through the *"neutron consumption"* D_J (note: negative consumption means production) during family life (up to be fissioned completely):

$$G_J \text{ (neutrons/fission)} = - D_J - (L + CM)$$

The neutron consumption level D_J depends mostly on neutron spectrum and neutron flux level (the last one defines the competitiveness between neutron processes and radioactive decay). Generally, if a reactor is feeding by a set of nuclei, one has a total neutron surplus potential G of a system (in presence of an external source):

$$G(\textit{neutrons/fission}) = \sum_J (X_J \times G_J) + \mu = -\sum_J (X_J \times D_J) - (L+CM) + \mu = G_0 + \mu$$

where X_J is an *"enrichment"* of J-family "predecessor" (i.e. normalized fraction of J-nucleus) in the feed fuel and $_{Go}$ is a corresponding internal neutron surplus potential (for critical reactors $G \equiv G_0$).

A necessity to increase the neutron surplus potential (to increase LLFP-incineration rate) leads to ADS-concepts with a lower k^0_{eff} - level, which allows to increase the μ - value. It contradicts to some opinion, that the highest neutron "amplification" is more favorable for transmutation purposes. However, a low k^0_{eff} leads to a high energy consumption and the final value has to be chosen taking into account ADS-economics.

In practice, G-value reflects the neutron balance and its enhancement has a reasonable limit: for almost all realistic power reactors the (L + CM) value is roughly 0.3 neutrons/fission.

Criticality condition of a fissionable medium at equilibrium corresponds to $G_0 = 0$ and the G_0 value defines generally the potentially achievable multiplication factor k_{eff} as:

$$k_{eff} = \left(1 - \frac{G_0}{\nu}\right)^{-1}$$

Table I gives the G_0 - value potential (neutrons/fission) for fuel nuclei in different neutron spectra with "standard" and "high" averaged neutron fluxes F, when (L + CM) being taken equal to 0.3 neutrons/fission for all reactors and ADS.

TABLE I THE INTERNAL NEUTRON SURPLUS: G_0- VALUES FOR LWR AND FR SPECTRA FOR SOME IMPORTANT FAMILIES

J-families	The LWR-Spectrum $\phi = 10^{14} \div 10^{15}$ n/cm^2·s	The FR-spectrum $\phi = 10^{14} \div 10^{15}$ n/cm^2·s
^{235}U	+ (0.32÷0.35)	+ (0.58÷0.60)
^{238}U	- (0.37÷0.29)	+ (0.32÷0.35)
^{232}Th	- (0.06÷0.06)	+ (0.09÷0.09)
^{239}Pu	+ (0.42÷0.53)	+ (1.16÷1.21)
^{242}Pu	- (1.54÷0.98)	- (0.26÷0.41)
^{241}Am	- (1.37÷1.11)	+ (0.32÷0.43)
^{243}Am	- (0.59÷0.58)	+ (0.30÷0.70)

Table I shows that:

- fast spectrum is the most favorable for all families regarding on neutron surplus production
- ^{232}Th is the "poorest" among all natural fuels; its neutron production is 0.2 - 0.3 neutrons/fission less then of ^{238}U. The internal neutron surplus of the Thorium family is not very sensitive to the spectrum type,
- the sensitivity of the neutron surplus to the neutron flux level is not of a high importance; nevertheless it can be helpful for some special problem resolution.

A neutron surplus gained directly from spallation (μ) depends on blanket thermal efficiency and fission energy. Then fast spectrum blankets can give some supplementary advantage - about 20 - 30% in the μ - value when compared to thermal spectrum blankets [1].

Table II shows the neutron surplus potential of TransPu-fuel discharging from LWR's (closed cycle for U, Pu, Np) at different neutron flux levels for important neutron spectra. It can be seen that TransPu-fuel does not require a neutron surplus being burnt in a fast spectrum.

B.4.4.2. Fuel waste toxicity (FWT) reduction.

The source of fuel waste toxicity risk is originated from the *"losses"* of discharged fuel. In the case of an open cycle, *"losses"* represent 100% discharge to a repository. In the case of reprocessing, *"losses"* are related to the decontamination efficiency of the chemical fuel reprocessing. The Fuel Waste Toxicity (FWT) is the consequence of the losses of the equilibrium fuel mass. The FWT (per electricity production unit) can be easily evaluated by the following expression [3,4]:

$$FWT = \gamma(1-B)/B \times \sum_J \sum_I T_{JI} \times LOS_I \qquad (2)$$

TABLE II. NEUTRON PRODUCTION (NEUTRONS PER FISSION) POTENTIAL OF TransPu-BURNERS ((-D) VALUES [1]

Spectra	Flux level	^{239}Pu	^{241}Am	^{242m}Am	^{243}Am	^{244}Cm	$TransPu^B$ – $TransPu^E$
Fast	10^{15}	+1.46	+0.62	+1.36	+0.60	1.39	+0.68 – +0.80
	10^{16}	+1.51	+0.73	+1.48	+1.00	+1.84	+0.90 – +1.15
	10^{17}	+1.52	+0.78	+1.54	+1.07	+1.92	+0.96 – +1.22
Thermal	10^{14}	+0.72	-1.07	-0.11	-0.29	+0.68	-0.69 – -0.20
	10^{15}	+0.83	-0.81	+0.16	+0.28	+1.24	-0.31–+0.30
	10^{16}	+0.85	+0.02	+1.00	+0.45	+1.32	+0.26 – +0.58
Super-thermal	10^{14}	+1.01	-0.74	+0.25	-0.89	+0.10	-0.72 – -0.64
	10^{15}	+1.04	+0.04	+1.03	-0.53	+0.42	-0.11 – -0.18
	10^{16}	+1.07	+0.54	+1.53	-0.21	+0.48	+0.55 – +0.11
	10^{17}	+1.13	+0.66	+1.66	+0.36	+0.49	+0.45

($TransPu^B$) and ($TransPu^E$) are "neutron production" of the transplutoniums discharging from LWR-open fuel cycle (i.e. in the beginning "B" of the closing cycle procedure) and from LWR (closed fuel cycle for U+Pu+Np) at equilibrium "E".

In equation (2) we have summed up all nuclei which make up the feed fathers (^{235}U, ^{238}U, ^{239}Pu, MA's, TransPu, et c.) And we have used the following notations:

γ - mass (gram) of fission products per net electric energy production unit; its value depends mostly on a reactor thermal efficiency and varies between 0.9 $\times 10^6$ (fast reactors) and 1.2×10^6 gram/GW_e per year (thermal reactors),

B - fuel burnup (in 5 of heavy atoms, h.a.),

LOS_I - a fraction of I-nucleus being lost in fuel cycle operations,

$\Sigma_I T_{JI}$ - toxicity of J-family in a fuel (I - index of a family member) in one gram of reactor fuel at equilibrium (i.e. unit fuel mass toxicity after irradiation, see Table III).

Hence, fuel waste toxicity source depends mostly on neutron spectrum (through family toxicities), fuel burnup and losses during reprocessing. Subcriticality level does not play an important role in the FWT: it changes the fuel feeding relative concentration, but total FWT (for exception of special cases) usually varies slightly.

The fuel waste toxicities time-dependent distribution at equilibrium is shown on Fig. 1 for the main principal nuclear reactors with closed Uranium and Thorium fuel cycles. The standard LWR (open fuel cycle) and "conservative" fuel loss data have been taken as a reference: 0.1% for Uranium, 0.1% for Plutonium and 1% for MA's.

Closed fuel cycles give always the lower fuel waste toxicities when compared to the standard LWR (open cycle), having even more toxic fuel then the standard LWR due to much smaller losses (<1%) of the total fuel mass of the standard LWR discharge.

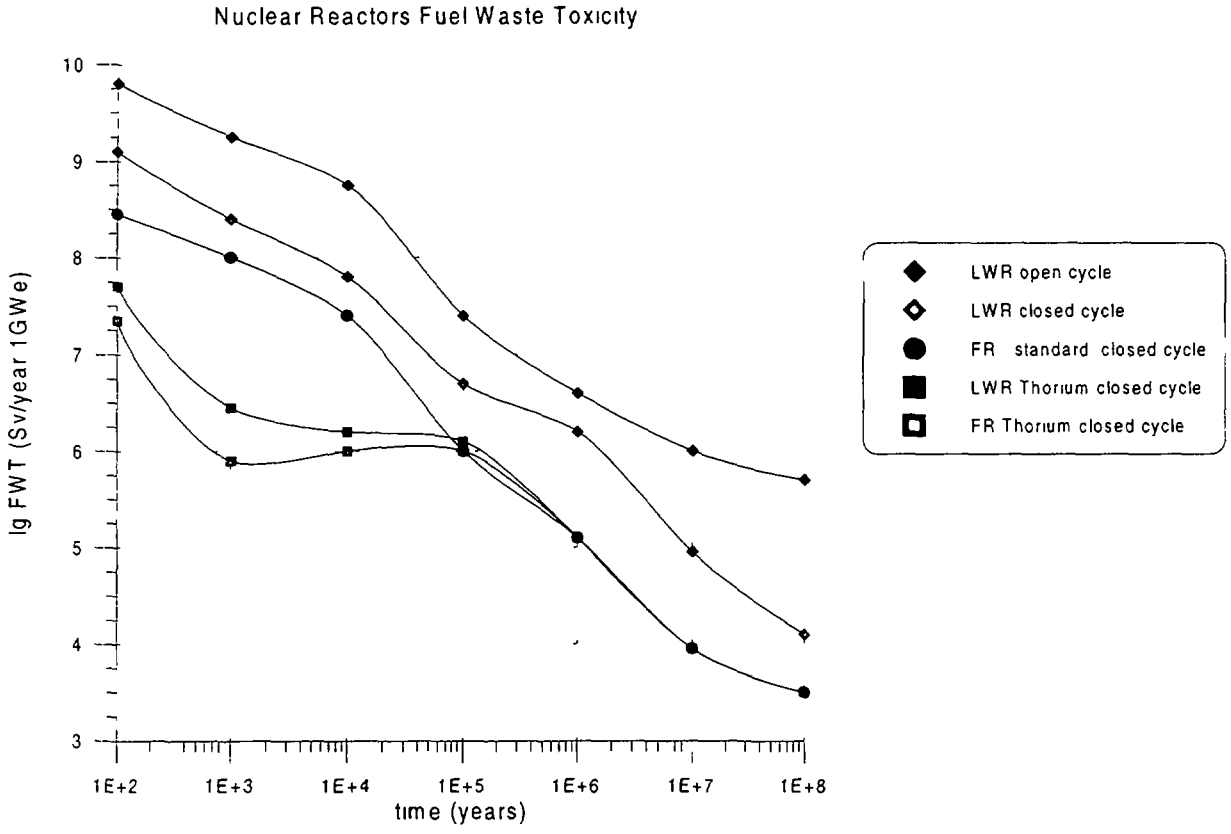

FIG 1 The fuel waste toxicities time-dependent distribution at equilibrium for the main principal nuclear reactors with closed Uranium and Thorium fuel cycles The standard LWR (open fuel cycle) is used as the reference

B.4.4.3. On ADS- "niches" in nuclear power

Considering possible "niches" for ADS in nuclear power, three stages of NP-development can be considering starting, long-term development and stagnation or power reduction

Let suppose that on starting stage (due to a power industry inertia) the share of new reactor generation (including fast reactors) can not be high enough and it will be possible to use a small option of new installations only Hence, the most realistic scenario of the ***"starting stage"*** of NP development can assume to use of all potential of the current reactor park for maximum FWT-reduction (to avoid Pu and MA accumulation)

It is not evident that LWR fully closing fuel cycle can be realized at an industrial scale, since the accumulation of MA affects strongly the LWR properties It seems that is more easy to close fuel cycle for U, Np and Pu fuel components only

Hence, at current stage, nuclear power can use

- ***the closed LWR fuel cycle (for U, Np and Pu) and a special reactor - TransPu-Burner to prevent an accumulation of transplutoniums.***

A preliminary assessment of the FWT-reduction potential shows that TransPu-burning is extremely important theoretically, closing of LWR fuel cycle (for U, Np and Pu components) in a combination with TransPu-burnout in a fast spectrum TransPu-Burner (closed cycle, burnup 15 % h a) Allows to reduce the FWT up to a factor 100

Due to some "negative" physics property (such as very low delayed neutron fraction, low Doppler

reactivity effect, positive void reactivity effects, et c.), due to some specific technologic difficulties, TransPu produces problems of being used in standard *critical* reactors. This can be the case to use subcritical ADS/TransPu-Burners.

Potentially, molten salt concepts are more suitable to play the TransPu-Burner role. They are:

- less sensitive (due to a possibility of continuous fuel feeding) to burnup reactivity swing effects. They do not demand a variable accelerator power due to constant subcriticality during burnup; can have a higher k_{eff} with an acceptable deterministic margin to reactivity type accidents. Hence, they can spent less energy for accelerator needs;
- less sensitive to "peaking" flux shape due to fuel mixing;

Besides, they have:

- the highest average to maximum burnup ratio (fuel mixing effect) that reduces the FWT-level; maximum neutron spallation importance φ^* due to possibility of proton beam insertion directly to region with maximum neutron importance and to fissile nuclei.

It was evaluated that Transplutonium fuel provides (see Table III) a rather high neutron surplus (ca 0.5 neutron per fission) in fast neutron spectrum, while other neutron spectra require additional fuel to support a k_{eff} as well as a higher fraction of Burners in NP.

TABLE III. NORMALIZED TOXICITIES OF J-FAMILIES T_j AT EQUILIBRIUM (in Sv/gram of family). T_j WAS AVERAGED ON SHORT ($10^2 \div 10^4$ YEARS) AND LONG ($10^2 \div 10^6$ YEARS) TIME INTERVALS (NEGLIGIBLE LOSS RATES) [2].

	Thermal reactors ($\phi=10^{14}$ n/cm^{2}s)		Fast reactors ($\phi=10^{14}$ n/cm^{2}s)		Superthermal reactors ($\phi=10^{14}$ n/cm^{2}s)		Natural toxicity ($\phi=10^{14}$ n/cm^{2}s)	
Predecessors of families	T_j Short	T_j Long	T_j Short	T_j Long	T_j Short	T_j Long	T_j Short	T_j Long
^{232}Th	21	4.6	38	11	41	3.8	0.0052	0.0052
^{233}U	221	53	117	62	168	23	111	46
^{235}U	372	19	92	19	173	2.5	0.037	0.48
^{238}U	97	1	841	5.7	275	3.5	0.0008	0.0068
^{239}Pu	4851	46	4290	28	4610	58	2300	13

Due to a small burnup reactivity swing, lack of Pa-Np types of reactivity effects, the following choice of subcriticality level seems to be reasonable, if TransPu burnout not demand an external neutron "help": $k_{eff} = 0.95 - 0.97$.

The principle parameters of fast spectrum ADS-TransPu-Burners can be the following:

$k_{eff} = 0.95$ and $z = 25$ n / 1 GeV-proton, $\varphi^* = 1.5$. Then one needs $\leq 5\%$ of ADS-TransPu-Burners in all park of reactors. Proton current is expecting to be 50 mA/GWe and the fraction of NP-energy spent for accelerator needs: 0.5 %. The system consisting of LWR's (closed cycle) and TransPu-Burners can produce (as a neutron surplus) 0.03 neutron per every fission in NP, which is available for partial LLFP-incineration.

Such ADS-Burner can be used as well for Pu-burnout (if needed). In this case, it will be reasonable to use a high neutron surplus of Pu for LLFP-incineration. However, the justification of ADS for Pu-burning is more difficult; it can be done in critical reactors also.

For comparison, one can assess a potential of the LWR standard neutron spectra for TransPu-burnout

($\varphi^* = 1.5$, $\Gamma = 0.8$ n/fission instead of $\Gamma = 1$/fission for fast spectrum systems) in the standard neutron flux level: 10^{14} n/cm^{2}s. One can get: $D_{TransPu} = 0.69$ (see Table III), $G_0 = -1$ n/fission, $k_{eff} = (1 - G_0/\nu)^{-1} = 0.7$, proton current I = 520 mA/GW$_e$. One needs all ADS energy to spend for the accelerator needs. As for "superthermal" neutron spectrum and elevated flux level (10^{15} n/cm^{2}s), one can get: $D_{TransPu} = 0.11$, $G_0 = -0.41$, $k_{eff} = 0.85$ and proton current I = 210 mA/GW$_e$. Moreover, there are no neutrons for LLFP-incineration and the FWT reduction potential is approximately one order lower than of fast spectrum (lower burnup, thermal efficiency, et c.).

In the hypothesis of continuation of nuclear power in **the long term future**, with the possibility to increase its energy output if required by eventual energy demand, one has to provide a system which be able:

- to breed fuel to make use of natural resources,
- to reduce LLFP toxicity in a large scale.

For this stage it is necessary to have a nuclear system with a sufficient neutron surplus to minimize fuel waste toxicity, LLFP-incineration and fuel breeding. It would be hopeful (particularly important for its public acceptability) if this system has deterministic safety features allowing to be definitely resistant to heavy accidents which lead to fuel disintegration.

ADS economics will play an important role if one wants to use a large park of innovative nuclear power installations. Competitive ADS (slightly subcritical: $k_{eff} \approx 0.98$) and reactivity stabilized blanket on the base of competitive fast reactor technology (i.e. lead coolant, dense fuel) seems to be attractive.

More important that supplementary neutrons of ADS can allow to compensate a drawback of oxide fuel - relatively large burnup reactivity swing. It means that fast spectrum ADS with oxide fuel can have deterministic safety features and can be economically acceptable.

To be sure in the optimum choice of ADS-spectrum, one can compare the potential of a thermal spectrum ADS ($\varphi^* = 1$, $\Gamma = 0.8$ n/fission for proton beam 1 GeV): the same subcriticality level ($k_{eff} = 0.98$) leads to higher proton current (factor of 1.3). Meanwhile, the reduction of the FWT is a factor of one order less than for fast spectrum, as well as many less neutrons are available for LLFP-transmutation.

B.4.4.4. On specific features of fuel cycles.

The Uranium fuel cycle

Potentially fast spectra have the following neutronics regarding transmutation problems:

- in fully closed Uranium fuel cycle (averaged burnup level B = 15%) the reduction of the FWT is assessed as two orders in magnitude when compared with standard LWR-open fuel cycle,
- neutron surplus for fuel self-sustaining fast reactors (zero breeding gain) is varying from 0.3 neutrons/fission for oxide fuel up to 0.5 neutrons/fission for metal fuel.

Example: the neutronic potential of an ADS - slightly subcritical lead cooled fast breeder system with nitride fuel and proton beam source (lead is used as a coolant as well as a liquid target for proton beam) and $k_{eff} = 0.98$ can be the following:

- neutron surplus - about 0.4 neutron per fission (zero breeding gain) in fuel plus 0.05 neutrons/fission due to spallation in lead target,
- relatively small (about 5% of the total energy) consumption for proton beam support.

The total neutron surplus (that can be available) both for breeding and for LLFP-incineration is assessed 0.45 neutrons/fission that seems to be enough to burnout all dangerous fission products and/or to reproduce new fuels for NP further development.

Economics of this system allows it to be rather competitive taking into account the simplicity advantage features: no needs in control rods, 2-circuits scheme, no needs in anti-coolant fire and anti-coolant

explosion protections, et c. Subcriticality plus a stabilized reactivity allow to increase a deterministic margin regarding reactivity type of accidents.

Hence, a reasonable compromise between safety features, reduction fuel waste potential and economics seems to be achieved for ADS with Uranium fuel cycle.

The Thorium fuel cycle

Thorium fuel cycle can have an attractive potential feature related to relatively small production of transplutonium [5,6] and, hence, to low MA concentrations (except ^{237}Np, ^{238}Pu) at equilibrium. As a result, the FWT level for both thermal and fast spectrum reactors during the first 10^3 years after incineration is much lower (see Fig. 1) than for Uranium fuel cycle. Later on, the advantage of Thorium cycle in the FWT is disappearing due to large concentrations of very long term toxic ^{233}U, ^{234}U, as well as ^{231}Pa.

^{232}Th-fuel has relatively tight neutron balance both in fast and thermal neutron spectra; for every fission it produces many fewer neutrons than ^{238}U (see Table I).

To use an advantage of subcriticality in deterministic safety features, one needs to have a burnup reactivity swing and reactivity effects as low as possible. A low burnup reactivity swing can be realized in traditional reactor designs if fuel concentration in the beginning of cycle (BOL) is "below" of equilibrium one (to compensate of core poisoning by fission products). It si more easy to realize this condition for subcritical ADS than for critical reactors. However, at a low k^0_{eff}, an accelerator energy consumption is too high. For example, for medium size fast reactors (0.5 - 1) GW_e with ^{232}Th- feeding, if equilibrium k^0_{eff} value is to be close to 0.95 and one has the reactivity stable (during burnup) core. If one propose to increase k^0_{eff} by ^{233}U-enrichment change, it leads to a loss of reactivity during core life and to a loss of reactivity margin regarding reactivity accidents.

Another disadvantage of thorium cycle is a high "protactinium effect" of reactivity (much higher than corresponding "neptunium effect" for Uranium cycle for standard fluxes), which demands to keep a low k^0_{eff} - value. To avoid problems with the protactinium effect and to increase neutron surplus, the Thorium cycle needs *"reduced flux level"* concepts.

Hence, for Thorium cycle, a compromise between deterministic safety, subcriticality level and economics will be more difficult as either one has a low k^0_{eff} and deterministic safety features with "weak" economics, or one has an acceptable economics (higher k_{eff}) with a "standard" safety level.

B.4.4.5. The long-term toxicity of fuel inventory.

The total fuel inventory toxicity is proportional to the mass of fuel inventory (per power unit) and to fuel toxicity. Fuel inventory INV is inversely proportional to the product $(\sigma_f \times F)$, where F is the averaged neutron flux. To minimize INV, one should increase $(\sigma_f \times F)$ both for thermal and fast neutron spectra. This gives an advantage to the high fluxes and thermal spectrum concepts. If the $(\sigma_f \times F)$ growth in a critical reactor can be achieved by a fuel concentration decrease (avoiding an increase of the specific power), then the neutron balance becomes tighter, and it leads to a burnup decrease and finally to the FWT increase.

One could increase F by decreasing k_{eff} (subcriticality effect), accounting for a possible fuel concentration drop, but the corresponding inventory reduction is expected to be relatively modest. For a reasonable level of subcriticality (k_{eff} = 0.8 - 0.9) the total effect will not exceed roughly a factor of $\cong$ 1.5 in inventory toxicity reduction.

B.4.4.6. Power Reduction or Stagnation Stage Scenarios.

In this type of scenarios, subcritical systems can be helpful due to their lower sensitivity to fuel mass inventory and isotopic content. Besides, they can give more flexibility for the elimination of residual fuel and LLFP toxicities.

The principal goal for this stage can be to approach a minimum (close to zero) mass inventory and zero toxicity of MA:s and LLFP:s.

It is very important to have the appropriate installations and one can use Burners (or a part of a reactor park) eventually used in previous stages, such as ADS/TransPu-Burners, FR-ADS with Uranium or Thorium fuels, et c.

For burning-out the residual toxic fuel (or stocked fuel) some versions of ADS can be particularly suitable since no critical mass is demanded, larger masses of LLFP (if one will use a large neutron surplus potential: low k^0_{eff} - options) can be eliminated, smallest fuel inventory (particularly, high neutron flux and thermalized neutron spectrum systems [7,8] can be exploited).

It has to be mentioned, however, that for high flux ADS concept with relatively short core lives (one-several months), a corresponding rapid reprocessing technology has to be available. Otherwise, standard (relatively long) cooling and reprocessing times leads to elimination of all advantages of these concepts. In the case of delayed reprocessing, the averaged neutron flux level is rapidly decreasing and fuel masses in fuel cycle is increasing.

B.4.5. CONCLUSIONS

Looking on futuristic fission systems with maximum reduction of long-term radiotoxicity risk for energy production unit one can conclude that the ACCELERATOR DRIVEN SYSTEMS are able to improve NP acceptability:

- ADS can increase the neutron surplus available for LLFP incineration. This is important for the fuel cycle with reduced neutron surplus production (e.g. Thorium fuel cycle). Meanwhile, this potential depends on ADS-economics, i.e. on a fraction of energy spent for accelerator and a capital cost of accelerator [9];
- The advantage of ADS - a tolerance to large reactivity insertion and to other anticipated reactivity transients without scram, seems to be essential. However, this advantage can be realized in the frame of economical acceptability if there is no large burnup-swing or other large "internal" sources of reactivity insertions;
- The potential of ADS in the fuel toxicity reduction and fuel inventory toxicity reduction seems to be important at near future (transPu-burnout), as well as for long-term perspective (regarding deterministic safety features realization) and for "reduction power" scenarios (residual waste burners with low inventories).

The most promising ADS (regarding neutron surplus production) is the fast spectrum system based on Uranium fuel cycle due to higher external (μ) and internal (G) neutron surplus production potentials. Thorium fuel cycle is the most attractive regarding on a fuel waste toxicity for 100 - 30000 years. This cycle seems to be attractive, if the importance of LLFP toxicity reduction and fuel breeding would be estimated as less important. ADS can help to compensate a shortcoming of Thorium cycle in neutron surplus production. However, deterministic safety feature concept realization can demand a higher fraction of energy.

According to the general transmutation potential, TransPu-Burner is one of the most promising system at near future for waste fuel toxicity reduction and LLFP-incineration. If one wants to minimize a park of these Burners and to reduce an energy consumption for proton beam; it needs to use fast spectrum ADS (slightly subcritical) with a stabilized (regarding reactivity swing) blankets. These ADS in a combination with LWR's (closed Uranium cycle) allow to reduce the fuel waste toxicity by a factor of 100 in magnitude and can be deterministic safe regarding reactivity type of accidents. Concluding, one has to reveal a necessity and profitability of ADS use in nuclear power. The corresponding "niches" for ADS can be formulated as the following:

- for transplutonium burnout (Uranium fuel cycle)

It seems that TransPu-fuel can not be used in critical reactors because an unacceptable neutronics (small delayed neutron fraction, small Doppler effect, positive void effect, et c.). Meanwhile, this fuel has some attractive features: lack of Np-Pa type effects, a low burnup reactivity swing, positive neutron surplus in fast spectrum. This stimulates to use the fast spectrum ADS with attractive economics.

Pu-burnup is also possible in similar ADS. However, Pu-fuel is rich of neutrons in any neutron spectra. Hence, a justification of this ADS application is more problematic.

- for wide deterministic safety principles application, fuel breeding and LLFP-incineration (Uranium fuel cycle) at the stage of long-term nuclear power development.

Breeding potential as well as LLFP-transmutation are sensitive to neutron surplus. ADS can enhance this surplus. However, spallation neutrons are rather expensive and it seems reasonable to increase neutron surplus firstly for the account of inherent neutronics potential of blankets (e.g. using fast spectrum advantages) and then to use an external source if needed. An attractive compromise can be achieved on the base of a fast spectrum slightly subcritical ADS with oxide or dense fuel.

- for a minimization both MA-production and fuel waste toxicity as well as for deterministic safety principles use (Thorium fuel cycle).

ADS plays a more important role for Thorium cycle concepts due to an inherent neutron "tightness" of Thorium family. The compromise between acceptable economics, deterministic safety and neutron surplus potential is more difficult to achieve than for Uranium cycle.

- for residual waste burnout ("reduction nuclear power" scenarios) with a high flux and/or thermalized neutron spectra ADS-concepts, due to a low fuel inventory requirement.

The potential niches of ADS are presented in the Table IV.

TABLE IV. ADS-PERSPECTIVE "NICHES"

Scenarios		
near future	*long-term future (Uranium and Thorium fuel cycles)*	*stagnation or nuclear power reduction*
◆ TransPu-Burners	**◆ Waste Reducer-Burner**	**◆ Residual Waste Burner**
(closed fuel cycle)	(closed Uranium fuel cycle)	–
Goals:	Goals:	Goals:
TransPu-intensive burnup;	Reduction of fuel waste and LLFP;	Minimization of residual waste masses;
Deterministic safety for reactivity accidents;	Deterministic safety for reactivity accidents;	Reduction of LLFP-toxicity.
Pu-rapid burnout (if needed).	Acceptable economics.	
	◆ Fuel Waste Toxicity Reducer	
	(closed Thorium fuel cycle)	
	Goals:	
	Small TRU-production:	
	Deterministic safety for reactivity accidents.	

REFERENCES

[1] International Information Exchange Meeting on Actinide and Fission Product Partitioning and Transmutation Cadarache, France, 12-14 Dec 1994

[2] M SALVATORES, I SLESSAREV, M UEMATSU A Global Physics Approach to Transmutation of Radioactive Nuclei NSE, 116, 1-18 (1994)

[3] M SALVATORES, I SLESSAREV, M UEMATSU, "Physics Characteristics of Nuclear Power Systems with Reduced Long-Term Radioactivity", *Nucl Sci Eng*, **120**, 18-39 (1995)

[4] M SALVATORES, I SLESSAREV, M UEMATSU, A TCHISTIAKOV, "the Neutronic Potential of Nuclear Power for Long-Term Radioactivity Risk Reduction", *Proc GLOBAL-95 Int Conf*, Versailles, France, September 11-14, 1995, V 1, p 686

[5] F CARMINATI et al , An Energy Amplifier for Cleaner and Inexhaustible Nuclear Energy Production Driven by a Particle Beam Accelerator CERN/AT/93-47(ET), (1994)

[6] C RUBBIA et al , "Conceptual Design of a Fast Neutron Operated High Power Energy Amplifier", CERN/AT/95-44(ET), European Organisation for Nuclear Research (1995)

[7] F VENNERI, C BOWMAN, S WENDER, "The Physics Design of Accelerator-Driven Transmutation Systems", *Proc GLOBAL-95 Int Conf* , Versailles, France, September 11-14, 1995, V 1, p 474

[8] C D BOWMAN et al , "Nuclear Energy Generation and Waste Transmutation Using an Accelerator-Driven Intense Thermal Neutron Source", LA-UR-91-2601, Los Alamos National Laboratory (1991)

[9] I SLESSAREV, M SALVATORES, "The potential of Nuclear Transmutation "Neutron Economics" of Critical Reactors and Hybrids",*Proc GLOBAL-95 Int Conf* , Versailles, France, September 11-14, 1995, V 1, p 482

B.5. GENERAL ACCELERATOR ISSUES

The high power accelerator technology required for ADS has been under continuous development over past decades. Linear accelerators, linacs, have been developed into highly reliable and efficient research (and military) tools. There is confidence that a high power (200 mA, 1.6 GeV), continuous wave (CW) accelerator can be built at a reasonable cost. On the other hand the technology of circular proton accelerators, such as the segmented cyclotron or synchrotron recently improved so that a proton beam of 10-15 mA is achievable. The cyclotron does not require a large physical area and has some other benefits compared to a linac. In a recent evaluation it was found that the most efficient operating current for a cyclotron-type machine would be ~10 mA and for a linear accelerator ~100 mA [see references in the accelerator chapters in section D - Project Review].

To provide external neutrons for a subcritical reactor, the proton beam must be stable, and the beam current well controlled so that there would be minimal power fluctuations in the subcritical assembly. Persistent power fluctuations may damage the fuel elements, especially in the case of metal fuel. The choice of the accelerator will be determined by economy and by the physical limitation of the proton current intensity.

The cyclotron is definitely cheaper, however, the space charge limitation puts the upper limit of the proton current - for the current state of the art - at about 10-20 mA. Linear accelerators do not have this limitation and it is believed that the construction of the linear accelerator with 100 mA proton current and energy of the order 1GeV is possible without an extensive R&D program. However, if one linear accelerator will drive a few subcritical reactors by splitting the beam, there is a serious safety concern in the case of malfunction of the dividers leading to dumping of the full beam power into one target. Moreover, malfunction of the single accelerator supplying several subcritical reactors with source neutrons shuts down the entire system. This is not a desirable situation for a commercial facility supplying electricity to the consumers.

B.5.1 CYCLOTRON FOR PROTON ACCELERATOR

Although one large accelerator can run several reactor targets, it might be practical to use a number of small cyclotrons. Cost might be increased by independently operating several small reactors, but it would alleviate several difficulties, such as splitting and controlling the high current beam. A cyclotron of 1.1 MW beam power has been developed in PSI for a 600 MeV proton accelerator.

Because of the nearly linear energy-dependence of the number, of spallation neutrons for protons with energies ranging from 1-3 GeV, beam current and beam energy can be traded off. These factors may favor the use of "multistage-parallel" cyclotrons over the linear accelerator.

While the price is almost proportional to the energy needed for the latter system, doubling or tripling the energy of a cyclotron is much less costly. On the other hand, the maximum achievable beam current of a cyclotron is rather limited, especially at low energies.

These conditions lead to the concept of the so-called "multistage-parallel" cyclotron arrangement, consisting of several low-energy, low-current cyclotrons feeding into one high energy cyclotron. (See Section D.3.)

C. RESEARCH AND DEVELOPMENT - GENERAL ISSUES

H Takahashi and W Gudowski

C 1 RADIATION DAMAGE

High-current medium-energy protons injected into the target generate, by spallation reactions, neutrons and charged particles with energies reaching the level of the accelerated protons This causes severe radiation damage in the section of the window, the target, and the wall material surrounding the target The most important type of radiation damage to materials stems from the displacement of lattice atoms resulting from the collision of the projectile particle upon the target atom or from the recoil energy that the atom receives upon emission of a nuclear particle, for example the atom recoil upon absorption of a neutron and emission of a capture γ-ray When an atom is displaced from its lattice site and comes to rest in between lattice atoms, a vacancy and an interstitial have been created [1] The vacancies may aggregate together, and similarly the interstitials, form vacancy-type and interstitial-type defect clusters These defect clusters are primary agents for causing radiation hardening and embrittlement The primary effects of concern with regard to the use of materials in the vicinity of the proton beam are changes in mechanical properties and dimensional stability The major mechanical property changes are hardening and embrittlement, and the embrittlement manifests itself in several ways radiation-produced defect clusters (aggregates of vacancies and interstitials), helium aggregation into bubbles and ductile-brittle transition defects A further type of radiation damages consists of the impurities introduced by the formation of transmutation products [2]

The analysis indicate that the surrounding wall as well as the window suffers high radiation damage, so that the former must be replaced frequently in a transmuter with a high current accelerator

The analysis of hydrogen and helium production indicates that hydrogen is deposited in the system by the spreading of the proton beam arising from multiple Coulomb scattering Hydrogen generated as a secondary proton of (n,xp) or (p,xp) as well as deuterons and He generated through evaporation processes, are slowed down and deposited mainly in the target

Because accelerated protons produce spallation neutrons and protons in the target and window areas with energies above the atomic displacement, and also produce hydrogen and helium, the problem of radiation damage is expected to be substantial when a high-power accelerator is used for a large subcritical reactor Using the small proton current associated with small sub-criticality avoids this serious problem

These findings indicate that, in designing the proton-accelerator based transmuter, the radiation damage to the beam window section and the side walls of the target should be investigated carefully Moreover, the radiation damages in structural materials of the accelerator-driven system can be higher than in corresponding critical reactors because of the existence of high energy spallation neutrons [3][4] Calculations of neutron energy spectra and fluxes are required so damage parameters can be determined and a better assessment of candidate alloys can be made

REFERENCES

[1] Monroe S Wechsler, Chubin Lin and Walter F Sommer, "Basic Aspects of Spallation Radiation Damage to Materials", AIP Conference Proceedings 346 on International Conference on Accelerator-Driven Transmutation Technologies and Applications, Las Vegas, NV, July 1994, AIP (1995)

[2] Wechsler, M S , Stubbins, J F , Sommer, W F et al, "Selection and Qualification of Materials for the Accelerator Transmutation of Waste Project", Report LA-UR-92-12-1211, Los Alamos

National Laboratory, Los Alamos, NM, (1992)

[3] Takahashi,H., Takashita, H., and Chen, X, "Transmutation of High_level Radioactive Waste and Production of ^{233}U Using an Accelerator-Driven Reactor", AIP Conference Proceedings 346 on International Conference on Accelerator-Driven Transmutation Technologies and Applications, Las Vegas, NV, July 1994, AIP (1995)

[4] DeVan, J.H., DiStefano, J.R. et al., "Materials Considerations for Molten Salt Accelerated.based Plutonium Conversion Systems", AIP Conference Proceedings 346 on International Conference on Accelerator-Driven Transmutation Technologies and Applications, Las Vegas, NV, July 1994, AIP (1995)

C.2 NUCLEAR DATA CODES

Proper calculations of accelerator-driven systems require more elaborate computer models than modeling for conventional critical reactors It is necessary to couple two transport problems the transport of the medium energy charged particle (1-3 GeV) in the spallation target with the transport of neutrons down to low energy range Neutron transport problems in the fission-range of the energies have been the subject of reactor physics for half of a century Transport problems with the charged particles were mainly the domain of accelerator physics and radiation protection

A description of fission neutron transport codes and burn-up codes is far beyond the scope of this report, we give here only a brief description of the codes which integrate/couple modeling of the charged particle transport and spallation processes with the neutron transport in the energy range up to the GeV region

Due to interest in accelerator-driven systems, as well as in other areas of application, such as radiooncology, accelerator shielding, astrophysics, and radiation during space travel, the nuclear reactor community undertook new initiatives to assess the reliability of the current nuclear models and to develop better transport codes, for example, the OECD NEA meeting (The findings are documented in the proceedings of a specialist meeting at Issy-Les Moulinaux, France, 30 May-1 June 1994)

When medium-energy protons collide with a nucleus, the nuclear reaction occurs by a two-step process of spallation and evaporation of the residual nucleus (see Fig 1 section B 2) When the residual nucleus has a large mass and a moderately high excitation energy, then it might undergo fission in competition with the evaporation reaction The third process is emission of the cluster and emission of the particle, the so-called pre-equilibrium emission particle, before reaching the thermal equilibrium state Neutron and photon transport below the energy of 20 MeV has been accurately estimated in conventional reactor calculations which are very familiar to the nuclear engineer

In the first step of the spallation process, the transport of the nucleon in the nucleus can be treated with the classical model because the nucleon's wavelength inside the nucleus is smaller than the average spacing The collision of the nucleon with a nucleon is treated as a two-body collision The π meson of π^+ and π which are created in the nucleon-nucleon collision are also included in calculations of the cascade process, thus, the basic data for a two-body collision between a pion and nucleon is required to describe the cascade process for the meson In the nuclear cascade codes NMTC [1] and HETC [2], [3], the evaluation of a nucleon-nucleon collision is obtained from Bertini's [4] data, and the production of a meson is treated by using the Isobar model developed by Sternheimer and Lindenbaum [5]

Since the nucleon is a fermion, the nucleon which is scattered below the Fermi energy is forbidden as a real scattering event Such events are discarded, and another scattering event is calculated When the kinetic energy of the scattered nucleon through the nuclear surface is above the binding energy of the nucleon, this nucleon escapes from the nucleus with kinetic energy minus its binding energy

When the nucleon's kinetic energy inside the nucleus is less than the binding energy , the nucleon gives kinetic energy to the nucleus as excitation energy This energy thermalises the nucleus, and neutrons, protons, or other light nuclei are evaporated When this excitation energy surpasses the fission barrier in the heavy nucleus, fission events will compete with the evaporation of light-element particles

The particle emitted from the collision of the nucleus travels until its next nuclear collision (called an inter-nuclear cascade) This process is repeated until the energy of the particle falls below the cut-off energy When the particle emitted or scattered from the nucleus is a charged particle, its energy is lost by exciting the electron surrounding its tracking path As the particle slows down its wavelength becomes longer than the average distance between the nucleons, then, the reaction cannot be described as a two-body collision of the nucleon or meson, and must be described by quantum mechanics, using

the optical potential model.

The NMTC and HETC codes are the system codes which calculate, by the Monte Carlo method, the nuclear reactions of protons, neutrons, and pions above the cut-off energy and the transport of these particles in heterogeneous media. In these codes, the cascade of a nucleon in the nucleus is calculated by the code MECC2, developed by Bertini; the evaporation process is calculated from the excited nucleus by EVAP developed by Dresner [6]. Particle transport within the heterogeneous medium is calculated by many subroutines developed in the O5R codes [7]. Furthermore, many subroutines were added to calculate the transport of the charged particle and the nuclear reactions associated with the pions.

The original NMTC and HETC codes cannot calculate high energy fission which is very important for targets with high atomic number, such as Uranium or the actinides. To treat this high-energy fission reaction, many authors have developed their own codes. By adding their own fission models to the NMTC code, the NMTC/JAERI [8]and NMTC/BNL [9] codes were generated. The LAHET code [10]was made by adding the Rutherford Appleton Laboratory (RAL) [11] and ORNL models [12] to the HETC code. Besides the NMTC and HETC, the ISABEL code [13] was developed from the VEGAS code [14] which can treat the refraction process. The LAHET code offers the option of using the ISABEL model in addition to the HETC code; LAHET treats the light mass nuclei's cascade by Fermi's break-up model. Furthermore NMTC/JAERI and LAHET (see section D) have the capability to handle the pre-equilibrium process based on the Exciton model.

Other nuclear cascade codes, such as FLUKA [15] (see also section D.3.) and CASIM [16] were developed by the high energy community and are continuously upgraded in order to be useful for ADS-calculations (e.g. through incorporation of the high energy fission processes).

At the OECD/NEA, conducted a study in two areas of microscopic nuclear physics, using the data from a thin target benchmark, and developing transport capability using thick target physics. Model codes such as ALICE92, PREQAQ2, GNASH, KAPSIES, FLUKA, FKK_GNASH, CEM92, and LAHET codes have been evaluated. In the evaluation of the thick target, the codes of LAHET(LANL) and FLUKA (CERN/Milano) and NMTC (JAERI) and HETC-THERMES (KFA-Jülich), LAHET-MCNP(LANL), CALOR(ORNL), SHIELD-SITHA(INR, Dubna) and SOURCE (Ansaldo, Italy) were discussed, as well as the group cross-section libraries -HILO86/400 MeV, LANL/800MEV and LAHI-KFA/2.8 GeV. As benchmark experiments, the following experimental data were described; COSMOTRON/ FERICON-LANL/CHALK RIVER, SUNNYSIDE-LANL, Stop Targets-LANL, Vassylkov experiments [17] (see also ICANS-XI, 1990, Shielding experiments at beam stop at PSI and LANL, a Japanese review of shielding experiments). For evaluating energy deposition and target heating, LANL-LANSCE and ANL/ RAL spallation sources provide very valuable data.

To evaluate calculations of radionuclide decay, it is desirable that the newly developed codes, such as ORIHET/PSI and CINDER 90/LANL, are available to the scientific community.

REFERENCES

[1] W.A. Coleman and T.W. Armstrong, "NMTC Monte Carlo Nucleon Meson Transport Code System", ORNL 4606 (1970)

[2] K.C. Chandler and T.W. Armstrong,, "Operating Instructions for the High-Energy Nucleon-Meson Transport Code HETC", ORNL-4744 (1972)

[3] Radiation Shielding Information Center, "HETC Monte Carlo High-Energy Nucleon-Meson Transport Code", Report CCC-178, Oak Ridge National Laboratory (1977)

[4] H.W. Bertini, "Monte Carlo Calculation of Intranuclear Cascade", ORNL-3383 (1963)

[5] R.M. Sternheimer and S.J. Lindenbaum, Phys. Rev. 105, 1974 (1957); Phys. Rev. 109, 1723 (1958); Phys. Rev. 123, 333 (1961)

[6] L. Dresner, "EVAP - A Fortran Program for Calculating the Evaporations of Various Particles from Excited Compound Nuclei", ORNL-TM-196 (1962)

[7] D.C. Irving et al., "O5R a General Purpose Monte Carlo Neutron Transport Code", ORNL-3622 (1965)

[8] Y. Nakahara and T. Tsutsui, JAERI Memorandum M82-198 (1982)

[9] H. Takahashi, "Fission Reaction in High Energy Cascade", BNL-NCS-51245 (1984)

[10] R. Prael and H. Lichtenstein, LA-UR-89-3014 (1989)

[11] F. Atchison, "Spallation and Fission in Heavy Metal Nuclei under Medium Energy Proton Bombardment", Meeting on Targets for Neutron Beam Spallation Sources, G. Bauer (Editor), KFA-Jülich, FRG, 11-12 June 1979, Jül-Conf.-34 (January 1980)

[12] R.G. Alsmiller, Jr. et al., "Neutron Production by Medium Energy (~1.5 GeV) Protons in Thick Uranium Targets", ORNL-TM-7527 (1981);
R.G. Alsmiller, Jr. et al, "A Phenomenological Model for Particle Production from the Collision of Nucleons and Pions with Fissile Elements at Medium Energies", ORNL-TM-7528 (1981)

[13] Y. Yariv and Z. Fraenkel, Phys. Rev. C, 20, 2227 (1979)

[14] K. Chen, Z. Fraenkel, G. Friedlander, J.R. Grover, J.M. Miller and Y. Shimamoto, Phys. Rev. 166, 949 (1968);
K. Chen, G. Friedlander, and J.M. Miller, Phys. Rev. 176, 1208 (1968)

[15] J. Ranft et al., "FLUKA82", CERN Divisional report TIS-RP/156/ CF (1985)

[16] A. VanGinnekin and T. Borak, IEEE Trans. Nucl. Sci. Vol. NS-18, No. 3, 746 (1971)

[17] R.G. Vassylkov et al., Atomnaya Energiya 44, 329 (1978)

D. PERFORMANCE OF THE ADS SYSTEM - REVIEW OF EXISTING PROJECTS, NATIONAL/INTERNATIONAL ACTIVITIES

D.1. JAERI AND PNC - OMEGA PROJECT (JAPAN)

D.1.1. JAERI ACCELERATOR DRIVEN SYSTEM PROJECT

Takakazu Takizuka
Japan Atomic Energy Research Institute
Tokai-mura, Naka-gun, Ibaraki-ken 319-11 Japan

D.1.1.1. INTRODUCTION

Among the issues relevant to development and utilization of nuclear energy, the management of high-level radioactive waste (HLW) arising from the reprocessing of spent nuclear fuels is the most important, as well as the safety assurance of nuclear installations. The hazard potential of transuranic actinides and fission products in the HLW is high due to their radioactivity. Of particular concern are the nuclides with very long half-life whose hazard potential remains high for millions of years.

The scheme, which is the main candidate for long-term waste management in most nuclear countries is the permanent disposal of unpartitioned HLWs, or unreprocessed spent fuels, into a stable geological formation to isolate them from the human environment. However, considerable attention has been directed towards partitioning and transmutation (P-T); separating long-lived nuclides from HLW and converting them into shorter-lived or non-radioactive ones. Improvements of long-term safety assurance in the waste management and possible beneficial use of valuable resources in the wastes can be expected through the establishment of the P-T technologies.

In Japan, a national program called OMEGA was started in 1988 for research and development of new technologies for P-T of nuclear waste. Under the OMEGA program, the Japan Atomic Energy Research Institute (JAERI) is carrying out research and development for proton accelerator-driven transmutation, together with transmutation with fast burner reactor and advanced partitioning technology.

The project on proton accelerator-driven transmutation at JAERI includes a conceptual design study of transmutation systems and development of an intense proton accelerator. Two types of accelerator-driven transmutation system are proposed: a solid system and a molten-salt system. They are dedicated systems specifically designed for the purpose of nuclear waste transmutation. In either system, an actinide loaded subcritical blanket is driven by a proton accelerator and utilizes a hard neutron spectrum to burn actinides efficiently.

In this report, an outline of the OMEGA program in Japan and the P-T studies at JAERI will be given to enable a good understanding of the background of the JAERI project. The description of proposed system concepts will then be presented in some detail.

D 1 1 2 OMEGA PROGRAM IN JAPAN

National policy for managing the HLW in Japan is based on disposal in a deep underground repository in a stable geological formation after solidification into a stable form and decay heat cooling for 30 to 50 years Many R&D efforts have been devoted to establishing technologies for safety disposal and methodologies for safety assessment

In addition to this national project, the Japan Atomic Energy Commission submitted in October 1988 a report entitled "Long-Term Program for Research and Development on Nuclide Partitioning and Transmutation Technology" to promote research and development on separation of nuclides contained in HLW according to their half-lives and potential usefulness, and transmutation of long-lived nuclides into short-lived or non-radioactive ones This program is nicknamed "OMEGA", which is the acronym derived from "Options Making Extra Gains from Actinides and fission products "

It was stated that the research on P-T is extremely important from the standpoint of conversion of HLW into a useful resource and improvement of the safety and efficiency of disposal The report plots a course for technological development up to the year 2000

The program aims to widen options for future waste management and to explore the possibility of utilizing HLW as useful resources The program is also expected to revitalize the nuclear option as we move into the 21st century In addition, the advancement of technologies such as accelerator technology, as advocated in this program, will provide potential spin-offs for other fields of science and technology

The program is led by the Science and Technology Agency (STA) with the collaboration of three major research organizations, JAERI, the Power Reactor and Nuclear Fuel Development Corporation (PNC) and the Central Research Institute of Electric Power Industry (CRIEPI) The program is to be conducted in two steps phase-I and II Phase-I covers a period up to about 1996, and phase-II covers a period from about 1997 to about 2000 In general basic studies and testing are to be conducted in phase-I to evaluate various concepts and to develop required technologies In phase-II, engineering tests of technologies or demonstrations of concepts are planned After the year 2000, pilot facilities will be constructed to demonstrate the P-T technology

It is to be noted that the program is conceived as a research effort to pursue benefits for future generations through long-term basic research and development, and hence not to seek a short-term alternative to established or planned fuel cycle back-end policies

The OMEGA program consists of two major R&D areas, the group separation of elements from HLW based on their physical and chemical properties and potential value of utilization, and the transmutation of minor actinides (MAs) and long-lived fission products (FPs) into shorter-lived or stable nuclides The outline of the program is shown in Fig 1

D 1 1 3 PARTITIONING AND TRANSMUTATION STUDIES AT JAERI

A partitioning process has been developed to separate elements in the HLW into four groups, transuranium elements (TRU), Sr-Cs, Tc-platinum group metals and the other elements [1] A series of laboratory-scale tests with the actual or synthesized HLW indicated that the proposed partitioning process was promising The hot test of the entire process is to be conducted with the actual HLW at the Nuclear Fuel Cycle Safety Engineering Research Facility (NUCEF), Tokai The chemical engineering test is also planned to start in 1996

A special transmutation device designed to operate with a very hard neutron energy spectrum and high neutron flux can be very efficient and effective for MA transmutation In this context, JAERI has been pursuing the concepts of an actinide burner reactor (ABR) [2] and an accelerator-driven system as dedicated transmuter, rather than transmutation schemes based on MA recycling to commercial power reactors

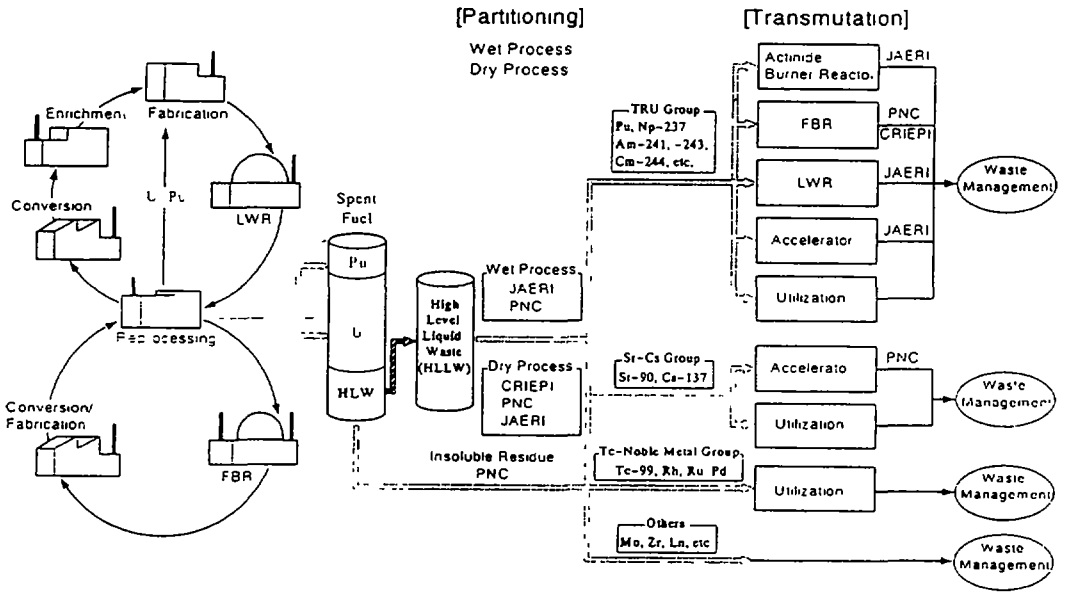

FIG. 1. P-T R&D activities under OMEGA Program.

With a dedicated transmuter, the troublesome MAs from the waste management view point could be confined in a P-T fuel cycle for transmutation, which forms a second stratum separated from the first one of a commercial fuel cycle for power generation. The concept of double-stratum fuel cycle is illustrated in Fig. 2. It can offer substantial advantages such as high transmutation rate, high transmutation capability, effective confinement of MAs, and no negative impact on the power reactor operation. There will be no additional shielding and cooling requirements to the existing commercial fuel cycle.

JAERI has proposed construction of an intense proton linear accelerator called the Engineering Test Accelerator (ETA) with 1.5-GeV beam energy and 10-mA average current. The main objective of ETA is to perform various engineering tests for accelerator-driven transmutation and other possible nuclear engineering applications. Toward this end, accelerator components have been developed and tested [3].

D.1.1.4. ACCELERATOR-DRIVEN TRANSMUTATION SYSTEM CONCEPTS

JAERI R&D includes the conceptual design study of an accelerator-driven transmutation plant, the development of a spallation simulation code system [4, 5], and the spallation integral experiments [6].

In the design study of the transmutation plant, two types of system concepts are being investigated; a solid system and a molten-salt system. In either system, an MA-loaded subcritical blanket is driven by a high-intensity proton accelerator and makes use of a hard neutron spectrum to transmute MAs efficiently by fission.

A small delayed neutron fraction in actinide fuel and a short neutron life-time, coupled with a small Doppler coefficient, tend to make the consequences of reactivity-initiated transient severe in critical fast reactors. The accelerator-driven subcritical system that is driven by external spallation neutrons can mitigate this safety problem and provide large margins for increasing flexibility in the design and operation. It also has an advantage in that the power of the subcritical blanket can be easily controlled by adjusting the power of incident proton beam.

The goal of the conceptual design study is to develop technically feasible concepts of the accelerator-driven transmutation system. The proposed plant is designed as a dedicated system that transmutes about

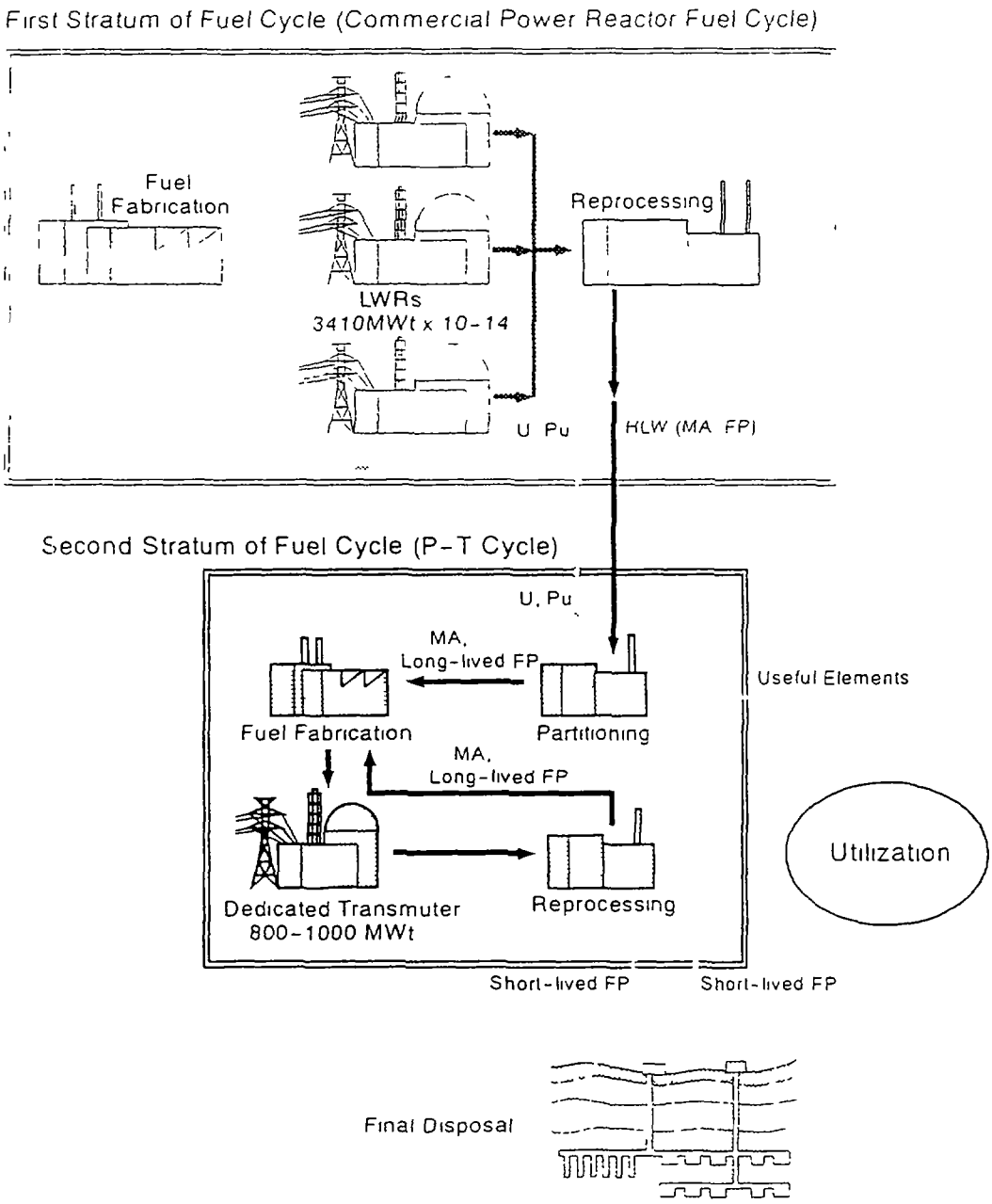

FIG 2 Concept of double stratum fuel cycle.

250 kg of MAs per year, which corresponds to the actinide production rate from operation of about 10 units of 3,000 MW_t light water reactor The capacity of the unit transmutation plant was chosen tentatively based on a preliminary strategic study of the partitioning and transmutation system [7] The subcritical blanket is required to operate at a multiplication factor of around 0.9 or more to reduce the scale of the proton accelerator and improve the energy balance of the total system.

A schematic diagram of the proposed transmutation system concept [8] is shown in Fig. 3. The design of the system is based on the state of the art technology for a sodium-cooled fast reactor.

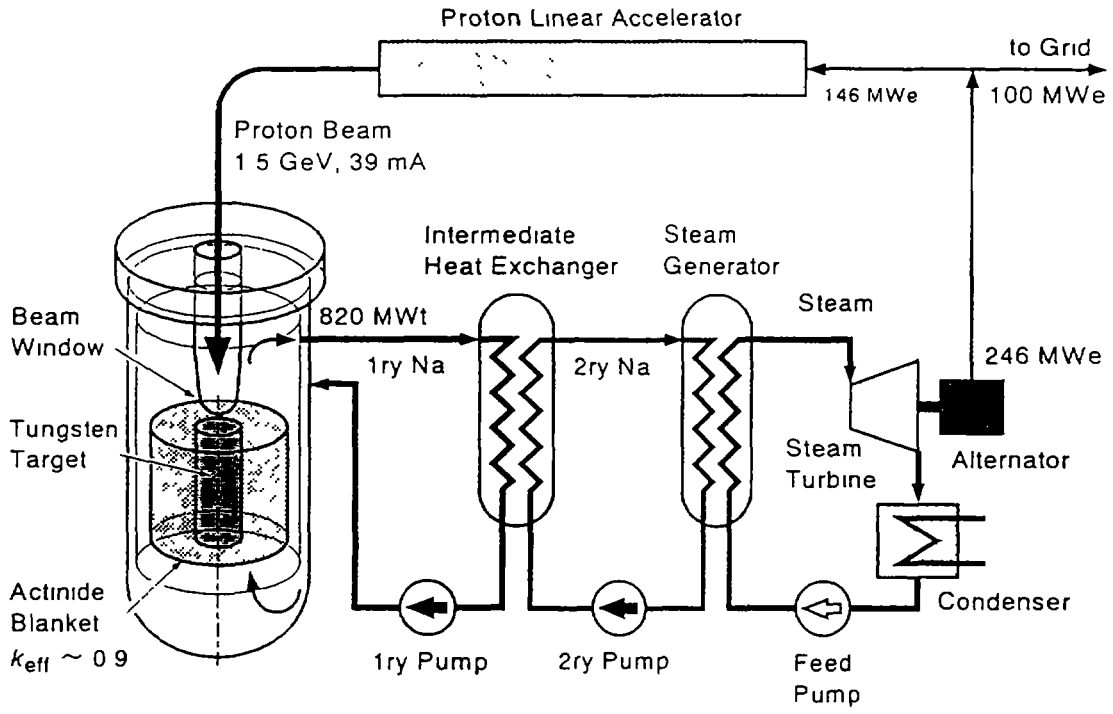

FIG 3 Concept of accelerator-driven transmutation system.

The accelerator injects a 1 5 GeV proton beam through the beam window into the target located at the center of the target/blanket The target is made of solid tungsten. Surrounding the target is the subcritical blanket loaded with actinide alloy fuel

A large number of neutrons are released by spallation reactions in the target, and induce further fission in the actinide blanket region The target/blanket generates a total thermal power of 820 MW, and is cooled by the forced upward flow of sodium primary coolant. Heat is transported through the primary and the secondary loops to the power conversion system. In the energy conversion system, thermal energy is converted into electricity A part of electric power is supplied to the systems own accelerator.

D.1.1.5.1. Actinide alloy fuel

A metallic alloy of MAs is used as the fuel in the reference design of the solid system. In order to maintain a sufficiently high phase stability of the alloy, the fuel is composed of two distinct alloy systems: Np-15Pu-30Zr and AmCm-35Pu-10Y. These alloy systems are proposed for a conceptual sodium-cooled actinide burner reactor [2]. Metallic fuel allows to implement a compact fuel cycle based on pyrochemical processes and provides a hard neutron spectrum.

In this design, the maximum fuel temperature is limited to 1173 K, because of the expected low melting point of MA alloy An actinide fuel slug with a diameter of 4 mm is sodium-bonded to cladding that is made of oxygen dispersion strengthened (ODS) steel. The outside diameter of the cladding is 5.22 mm, and the thickness is 0 3 mm The maximum cladding temperature is limited to 998 K.

A conceptual drawing of the fuel subassembly is shown in Fig. 4. The design of the fuel subassembly is of pin-bundle type, based on the current design practice for fast reactors. An unique design feature in the fuel subassembly containing highly heat generating actinides is the incorporation of measures to ensure sufficient cooling during out-of-blanket handling operations. The structure members are six tie-rods near the corners rather than a conventional hexagonal wrapper tube. The subassembly has 55 fuel pins arrayed in a relatively wide triangular pitch of 8.7 mm. Fuel pins containing Am and Cm are arranged on the outermost row of the array while Np-containing pins are arranged on the inner rows. The fuel subassembly has a dimension of 68 mm between flat faces.

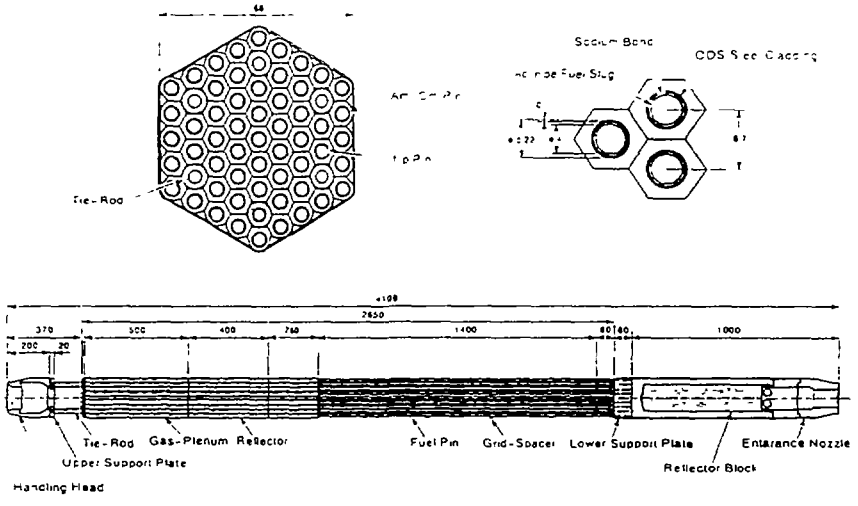

FIG. 4. Actinide fuel subassembly.

The active length of a fuel pin is 1.4 m. Each fuel pin contains a gas vent mechanism and upper reflector in its upper section. The gas vent mechanism releases excess internal pressure due to accumulation of gaseous and volatile fission products, allowing to achieve a very high burnup. Because of the relatively wide fuel pin spacing, grid type spacers are employed rather than wire wrap spacers.

Sodium coolant at 603 K enters the subassembly from the entrance nozzle at the bottom, and flows upward through the space between fuel pins, and exits from the handling head at the top. Maximum coolant velocity within the subassembly is limited to 8 m/s in the design to avoid the possibility of flow-induced vibration of fuel pins. The total length of the fuel subassembly is 4.1 m.

Fuel design parameters are summarized in Table I.

TABLE I. SOLID SYSTEM FUEL DESIGN PARAMETERS

Fuel Composition	Np-15Pu-30Zr AmCm-35Pu-10Y
Slug Diameter	4.0 mm
Cladding	
Material	ODS Steel
Outer Diameter	5.22 mm
Thickness	0.3 mm
Active Length	1400 mm
Pins/Subassembly	55
Pin Pitch	8.7 mm
Maximum Design Temperature	
Fuel	1173 K
Cladding	998 K

D.1.1.5.2. Target

A conceptual drawing of the target subassembly is shown in Fig. 5. Tungsten was chosen as the material for the solid target because of its high temperature capability. The target is inactive, or it does not contain any fissile or fissionable materials. This eliminates the high power peaking at the target, and thus considerably flattens the lateral power distribution in the target/blanket.

The target consists of layers of tungsten disk. This type of target configuration was chosen from the nuclear and thermal-hydraulic considerations. It is designed to maximize the number of emitted neutrons and to flatten the shape of axial distribution of neutron flux. The upper part of the target subassembly has six 15-mm thick disks spaced 51 mm apart and the lower part has seven 130-mm thick disks spaced 11 mm apart. Each disk has through holes with a diameter of 9 mm for coolant passage. They are arranged to stagger from layer to layer to avoid the possibility of direct penetration of high energy particles through the target.

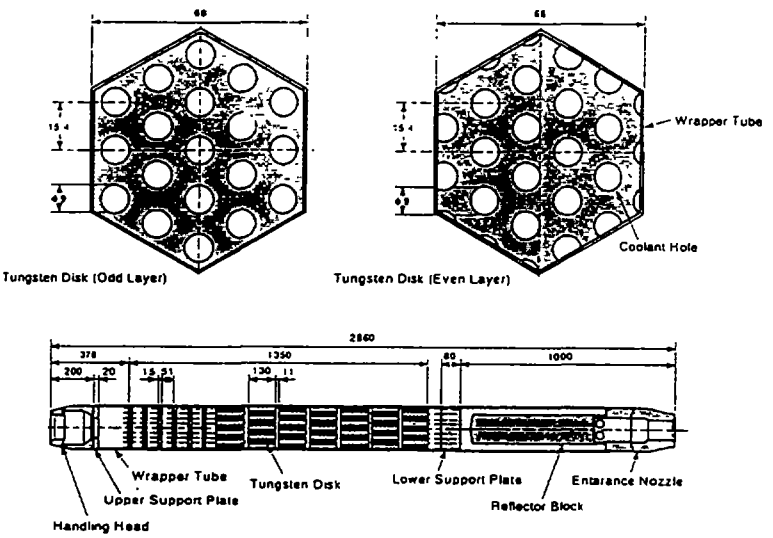

FIG. 5. Tungsten target subassembly

The target subassembly has the same dimension of 68 mm between flat facesas that of the fuel subassembly. Unlike the fuel subassembly, the target subassembly has a hexagonal wrapper tube to prevent an undesirable cross flow, which would be driven by lateral pressure difference due to the dissimilar hydraulic characteristics between the target and the fuel subassemblies.

In the target subassembly design, the maximum coolant pressure drop is limited to 250 kPa, and the maximum coolant velocity is limited to 8 m/s. The allowable peak tungsten temperature and maximum tungsten surface temperature are conservatively set at 1830 K and 950 K, respectively. The coolant temperature rise through the target is limited within the average coolant temperature rise through the target/blanket so that the target exit coolant flow can further cool the beam window sufficiently.

Sodium coolant at 603 K enters the subassembly from the entrance nozzle at the bottom, and flows upward through the coolant channels in the tungsten disks, and exits from the handling head at the top. The total length of the target subassembly is 2.86 m. The shorter total length compared with the fuel subassembly is due to the absence of upper reflector.

D.1.1.5.3. Target/blanket configuration

The target/blanket consists of a tungsten target region, an actinide fuel region, and reflectors. Figure 6 shows the plan view of the target/blanket. The target region is located in the center of the target/blanket. The target consists of 61 target subassemblies, which together form an approximate right circular cylinder,

with a diameter of about 0 56 m and a height of 1.4 m.

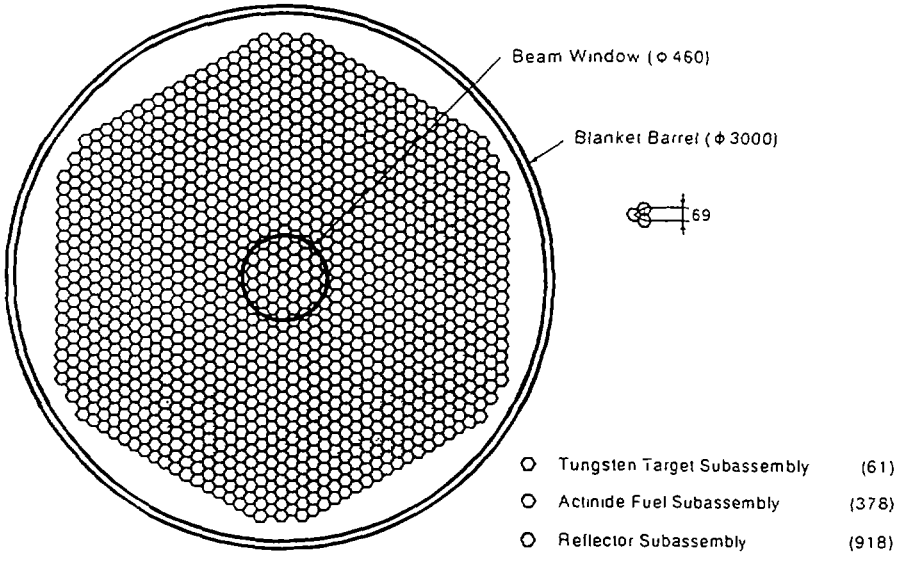

FIG. 6. Target/blanket configuration.

Surrounding the target region is the actinide fuel region having the form of an annulus, 1.52 m in outside diameter and 1.4 m in height. The fuel region is made up of 378 fuel subassemblies.

The actinide fuel region is in turn surrounded by reflectors made of stainless steel. The approximate thickness of the side reflector is 0.6 m. The side reflector is made up of 918 reflector subassemblies having the same cross sectional dimensions as the target and the fuel subassemblies. The upper and lower parts of the subassembly constitute the upper and lower axial reflectors, respectively. The thickness of the axial reflector is about 0.4 m. Above the target region, the upper reflector is not provided for an incoming high energy proton beam.

All of these subassemblies are arranged in a common triangular array with a pitch of 69 mm. The whole target/blanket including reflectors is contained within a target/blanket vessel made of steel as shown in Fig. 7 The vessel diameter is about 4.6 m and the height is about 14 m.

A vertical tube for the beam path is inserted into the target/blanket vessel down to just above the target region. The bottom end of the tube is the beam window which separates the accelerator vacuum and the target/blanket operating pressure. The beam window is made of ODS steel and has the form of a hemispherical shell. High energy protons are injected vertically downward through the beam window into the target.

The target/blanket has a loop type configuration. The inlet temperature of the primary sodium coolant is 603 K. The coolant enters the vessel through inlet nozzles, flows downward through the annular space along the vessel wall to the lower plenum. Then, it turns upward through the target/blanket, removing the heat from the target and fuel subassemblies. The beam window is cooled by impinging coolant flow from the target exit. The coolant then flows into the upper plenum and exits from the vessel through outlet nozzles. The outlet temperature of the coolant is 703 K on average.

The volume of active blanket is about 2 m^3. Maximum coolant flow velocity through the active target/blanket is set to 8 m/s. Sodium temperature at the target/blanket inlet is selected to be 603 K. This somewhat lower coolant temperature than in standard sodium-cooled reactors helps to achieve a high target/blanket power density, or a high transmutation rate, at the expense of degrading the power

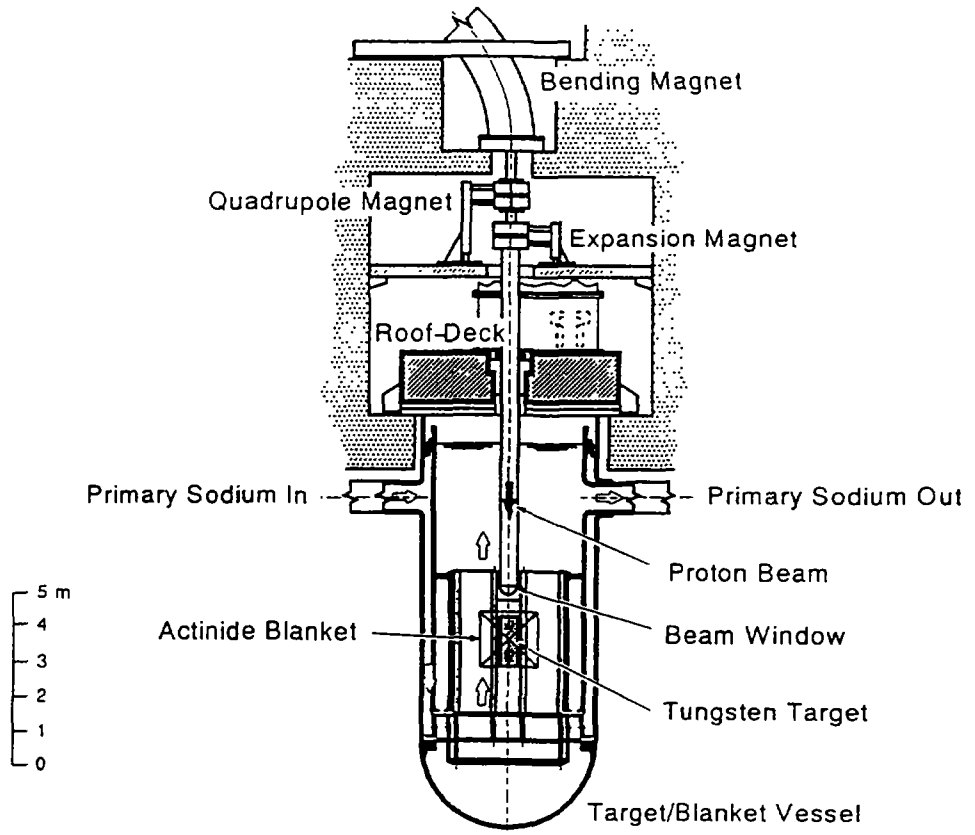

FIG. 7. Solid target/blanket system.

conversion efficiency.

Target/blanket design parameters of the solid system are summarized in Table II. A conceptual drawing of the target/blanket facility is shown in Fig. 8.

TABLE II. SOLID SYSTEM TARGET/BLANKET DESIGN PARAMETERS

Proton Beam		
	Energy	1.5 GeV
	Diameter	400 mm
Target	Tungsten	
Fuel		TRU Alloy
Reflector	Stainless Steel	
Active Blanket		
	Volume	2 m^3
	Height	1.4 m
Coolant	Sodium	
	Maximum Velocity	8 m/s
	Inlet Temperature	603 K

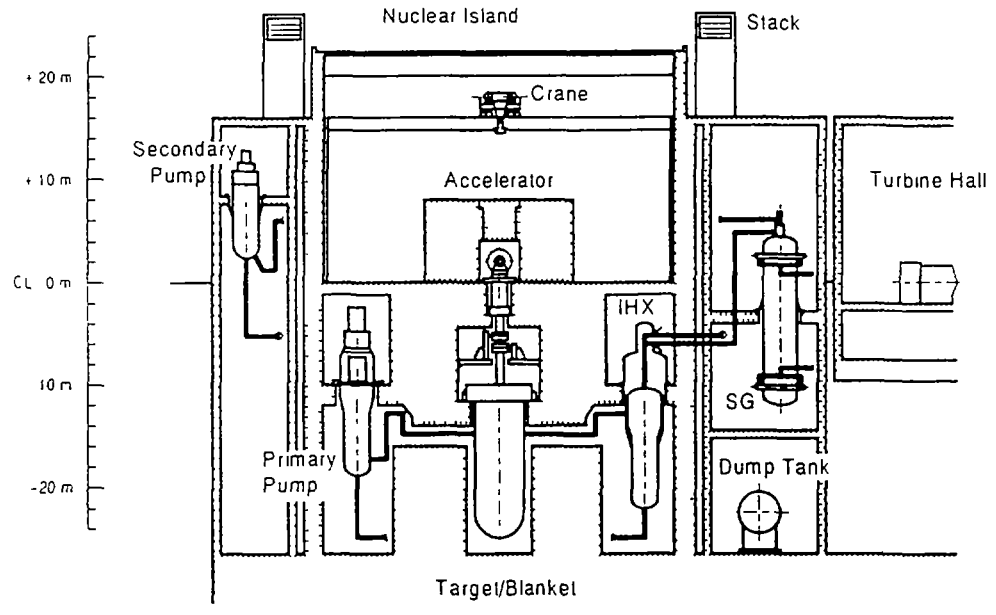

(a) Section View

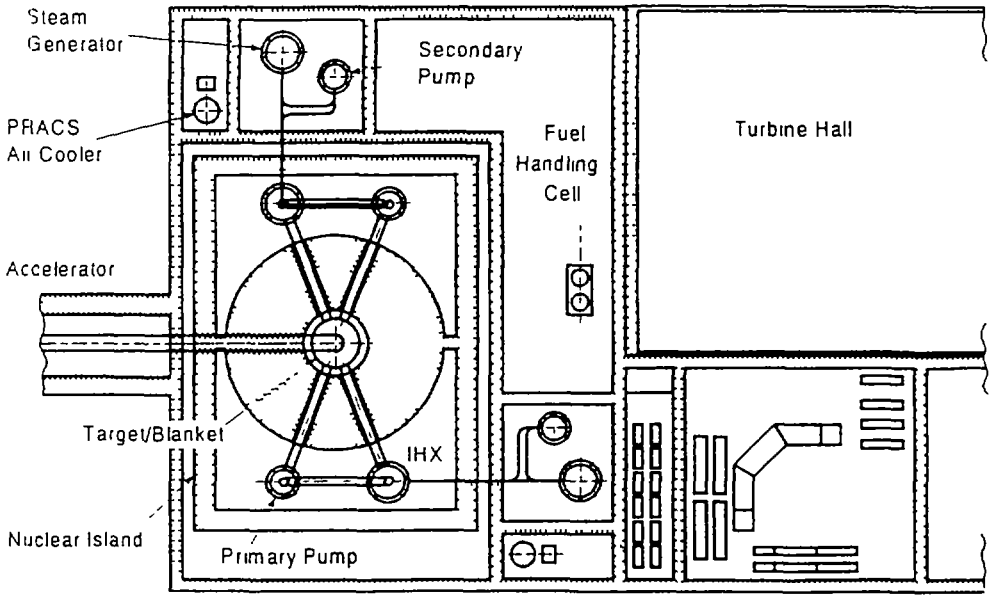

(b) Plan View

FIG 8 Target/blanket facility layout

D.1.1.5.4. Heat transport system

Heat transport and power conversion systems in the plant design is based on the current technology for a sodium-cooled fast breeder reactor plant. Figure 9 depicts the schematic flow diagram of the heat transport and power conversion systems.

The primary heat transport system consists of two sodium coolant loops. Each primary loop has an intermediate heat exchanger and a primary pump. The secondary system also consists of two sodium loops, with each having a steam generator and a secondary pump. Steam produced in the steam generators is supplied to the power conversion system.

A primary auxiliary cooling system consists of two NaK loops. This system is provided as an independent means of removing afterheat in the target/blanket. The afterheat is ultimately rejected from the air coolers to natural draft of atmospheric air through stacks

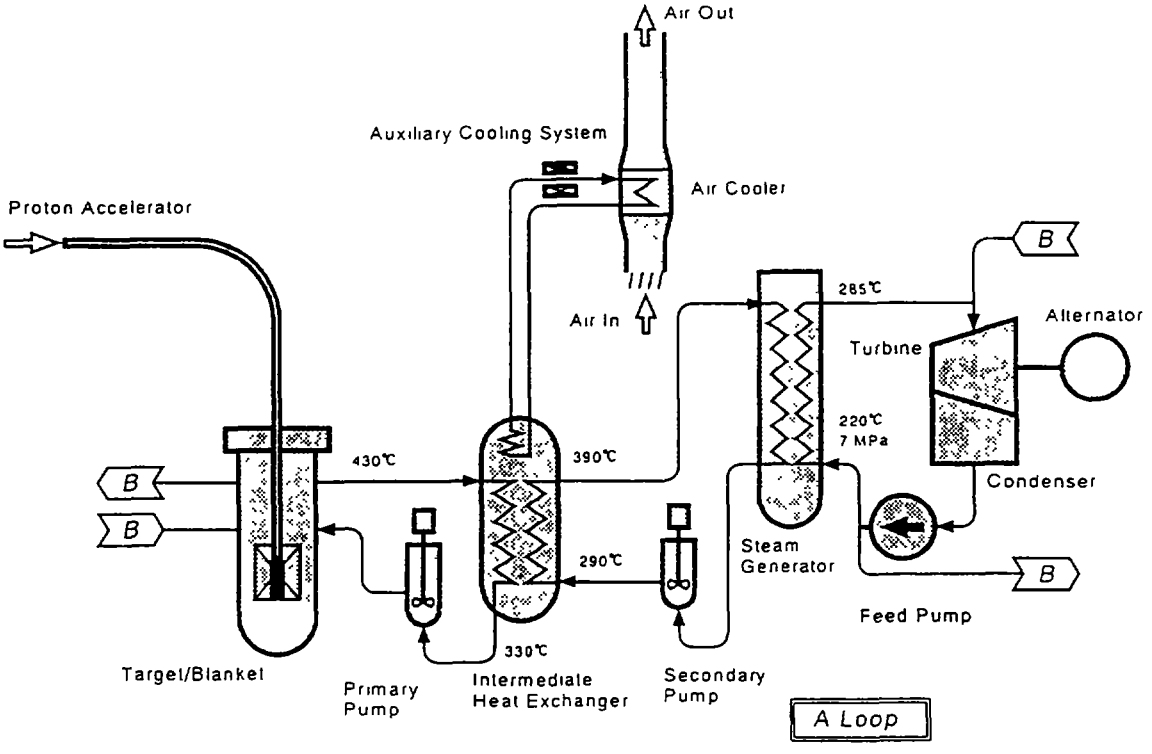

FIG. 9. Schematic flow diagram of heat transport and power conversion systems.

Parameters of the heat transport system are summarized in Table III

D.1.1.5.5. Power conversion system

In the power conversion system, steam raised in the steam generators drives a single turbine alternator to produce electricity Because of the relatively low operating coolant temperature for a sodium-cooled system, the steam condition is similar to that of a conventional light water reactor plant, thermal efficiency being roughly 30%.

TABLE III. HEAT TRANSPORT SYSTEM DESIGN PARAMETERS

Primary System	
Coolant Loops	2 x Na Loop
Temperature	
	IHX Inlet 703 K
	IHX Outlet 603 K
Components	IHXs, Primary Pumps
Secondary System	
Coolant Loops	2 x Na Loop
Temperature	
	SG Inlet 663 K
	SG Outlet 563 K
Components	SGs, Secondary Pumps
Auxiliary Cooling System	
Coolant Loops	2 x NaK Loop
Components	Air Coolers, EM Pumps

Parameters of the power conversion system are summarized in Table IV.

TABLE IV. POWER CONVERSION SYSTEM DESIGN PARAMETERS

Cycle	Saturated Steam Cycle
Working Fluid	Water/Steam
Turbine Inlet Temperature	558 K
Components	Turbine, Alternator, Condenser, Feed Pump
Electric Output	246 MW
Efficiency	30%

D.1.15.6. System performance

Figure 10 is the calculated power density distribution in the target/blanket. The target/blanket generates a total thermal power of 820 MW for the 1.5 GeV and 39 mA proton beam. The actinide fuel region generates 800 MW_t and the target region, 20 MW_t. In the fuel region, the maximum power density is about 920 MW/m^3 and the average power density, about 400 MW/m^3. The maximum power density in the target regions is about 360 MW/m^3, considerably lower than that in the fuel region.

The calculated temperature distributions along the fuel pin in the hot channel are shown in Fig. 11. Sodium coolant temperature at the hot channel exit is 746 K. The maximum temperature of the ODS steel

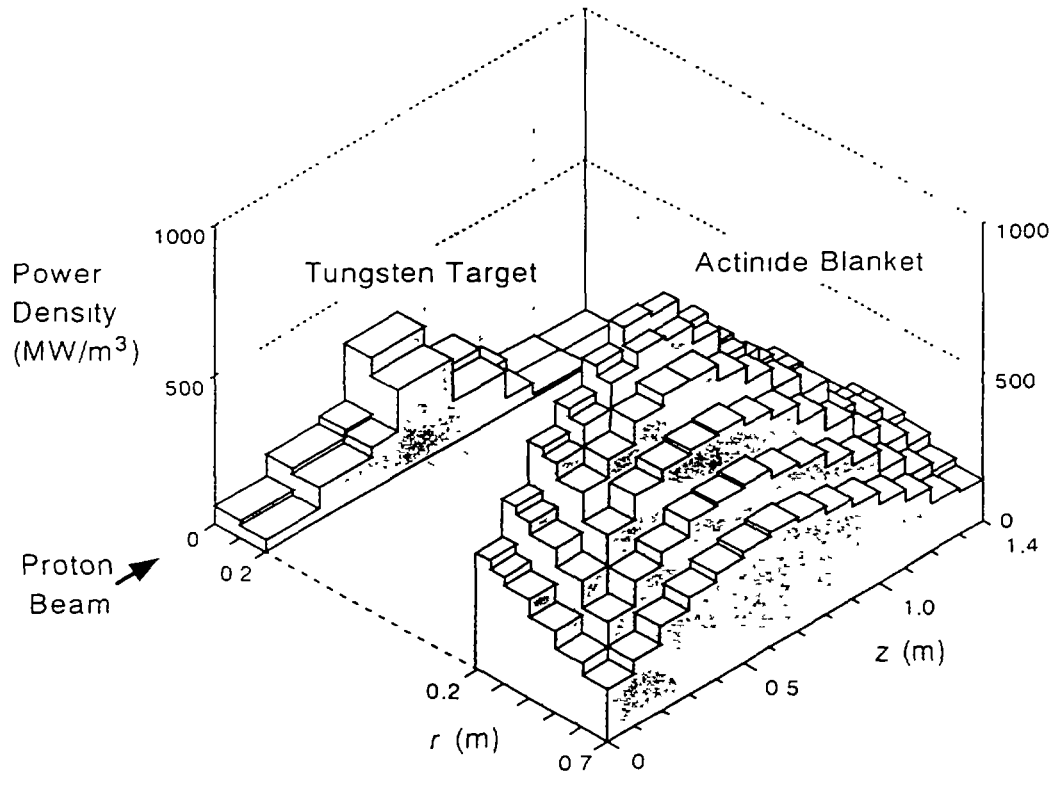

FIG. 10. Power distribution of solid target/blanket.

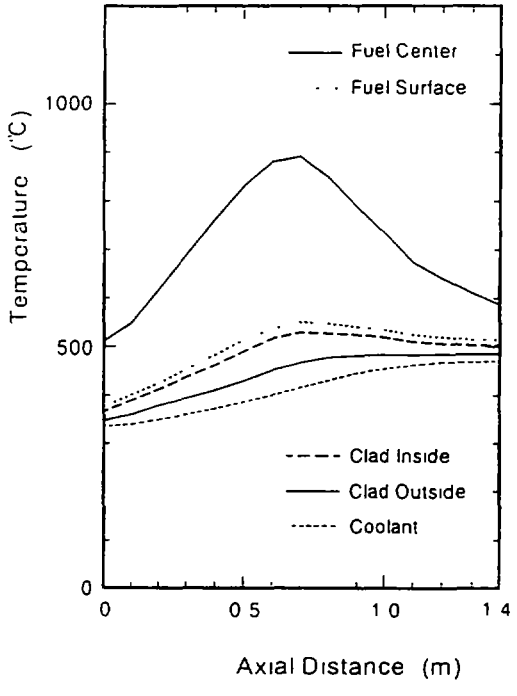

FIG. 11 Temperature distributions along the hot channel.

cladding is 801 K. This value is well within its design limit of 998 K. The maximum fuel center-line temperature is 1093 K, which is very close to the maximum allowable temperature of actinide alloy fuel. This indicates that the peak fuel temperature determines the maximum achievable thermal power in the target/blanket.

The target/blanket operating parameters are given in Table V.

TABLE V. SOLID SYSTEM TARGET/BLANKET OPERATING CONDITION

Proton Beam Current	39 mA
Actinide Inventory	3160 kg
Effective Multiplication Factor	0.89
Spallation Neutrons per Proton	40 n/p
Fissions per Proton	
(> 15 MeV)	0.45 f/p
(< 15 MeV)	100 f/p
Neutron Flux	4×10^{15} n/cm^2 s
Mean Neutron Energy	690 keV
Burnup	250 kg/y
Thermal Output	
Fuel Region	800 MW
Target Region	20 MW
Total	820 MW
Power Density	
Maximum	930 MW/m^3
Average	400 MW/m^3
Linear Rating	
Maximum	61 kW/m
Average	27 kW/m
Coolant Outlet Temperature	
Maximum	746 K
Average	703 K
Fuel Temperature	
Peak	1163 K
Surface Maximum	821 K
Clad Temperature	
Inside Maximum	801 K
Outside Maximum	757 K

The actinide inventory in the blanket is about 3,160 kg. The effective neutron multiplication factor is calculated to be 0.89. For an incident proton, approximately 40 neutrons are emitted by spallation reaction in the target region. About 100 fissions are induced per proton in the fuel region. Assuming a load factor of 80%, the actinide burnup is approximately 250 kg, corresponding to 8% of the actinide inventory, after one year in operation. Table VI shows the result of burnup calculation. With burnup, the effective neutron multiplication factor increases to 0.93 at 300 days, and then decreases to 0.83 at 1800 days.

A fairly hard neutron spectrum is achieved in the target/blanket. The average neutron energy is about 690 keV. Figure 12 depicts the neutron spectrum averaged over the target/blanket.

An electric power of 246 MW is produced with the 820-MW thermal power at a plant thermal efficiency of 30%. Assuming an efficiency of 40% for the 1.5 GeV-39 mA proton accelerator, the electric power required to operate the accelerator is about 146 MW. This means that the proposed system is more than self-sufficient in terms of its own energy balance, having the capability to supply some 100 MW surplus electricity to the external grid.

TABLE VI. BURNUP CALCULATION RESULTS

Nuclides	Initial Inventory (kg)	Mass Balance in EOC (unit: kg) BOC	EOC	EOC - BOC
Fuel				
Uranium				
U-235	0	0	0.9	+ 0.9
U-236	0	0	0.2	+ 0.2
U-238	0	0	0.0	+ 0.0
Plutonium				
Pu-238	13	13	470	+ 457
Pu-239	401	401	156	- 246
Pu-240	292	292	193	- 99
Pu-241	69	69	34	- 35
Pu-242	38	38	47	+ 8.9
Minor Actinides				
Neptunium				
Np-237	1861	1861	593	- 1268
Americium				
Am-241	292	292	95	- 197
Am-242m	0	0	9.5	+ 9.5
Am-243	133	133	57	- 77
Curium				
Cm-242	0	0	7.2	+ 7.2
Cm-243	0.3	0.3	1.0	+ 0.7
Cm-244	57	57	61	+ 4.8
Cm-245	5.1	3.1	10	+ 7.2
Other Actinides	0	0	0	0
Transmutation Capability (kg/GWt EFPY)			307	

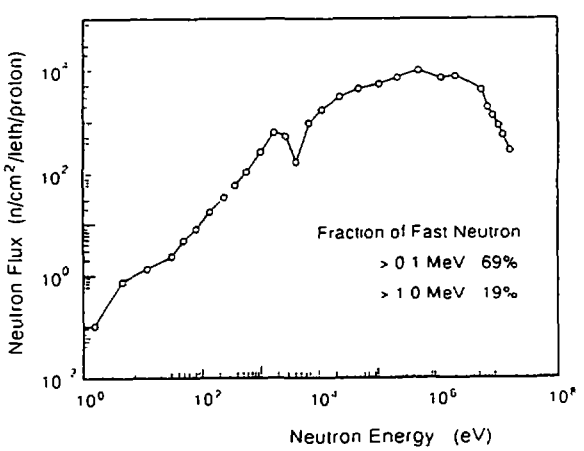

FIG. 12. Neutron spectrum of solid target /blanket.

D.1.1.6. MOLTEN-SALT SYSTEM

A preliminary conceptual design study is being performed on an 800-MWt molten-salt target/blanket system as an advanced option for an accelerator-driven nuclear waste transmutation system [9]. Figure 13 schematically shows the proposed molten-salt system concept. Chloride salt with a composition of 64NaCl-5$PuCl_3$-31$MACl_3$ (where MA represents Np, Am, and Cm) is chosen for the molten-salt system based mainly on the consideration of actinide solubility. The molten-salt acts both as fuel and as target material, and at the same time it also serves as coolant in the molten-salt system. This significantly simplifies the target/blanket

system configuration

A high energy proton beam at 1.5 GeV is injected into the central target/blanket region through the beam window The target/ blanket region is surrounded by an internal reflector Intermediate heat ex-changers and salt pumps are installed in the annular region around the internal reflector This in-vessel heat exchanger design minimizes the total actinide inventory in the system

The molten state of fuel provide the possibility of on-line processing of reaction product removal Fig 14 shows the conceptual flow diagram of on-line separation system for a molten-salt target/blanket

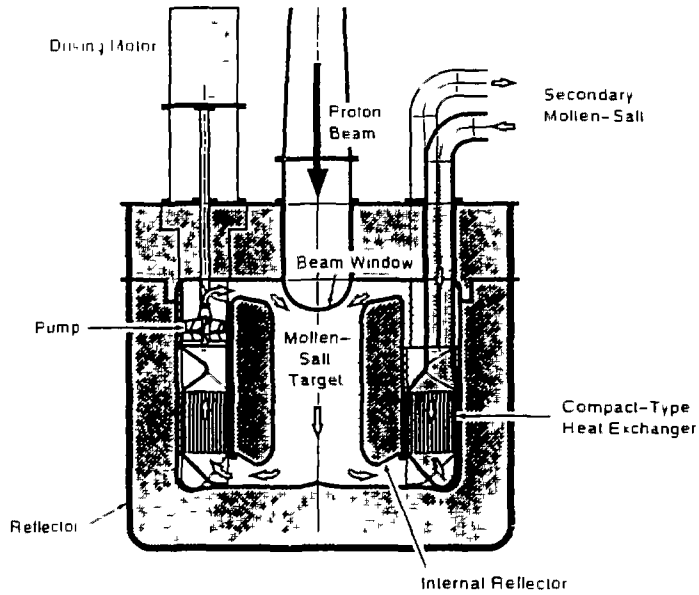

FIG 13 Concept of molten-salt target/blanket system

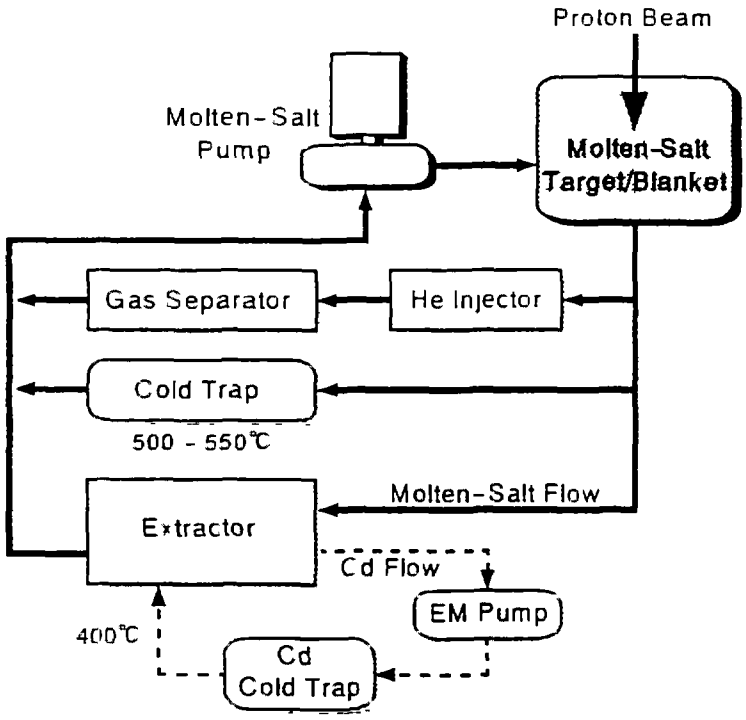

FIG 14 Conceptual flow diagram of on-line separation system for molten-salt target/blanket

D.1.1.6.1. Actinide fuel salt

Molten fluoride salt fuel of LiF-BeF_2-ThF_4-UF_4 has been demonstrated in the 1960s at the Oak Ridge National Laboratory in the Molten Salt Reactor Program The solubility of Th in the fluoride salt is sufficiently high (> 10 mol%) in the operating temperature range, whereas the solubilities of U and Pu are rather low (< 1 mol%) The solubilities of MAs in the salt are not expected to be sufficiently high The low solubilities of MAs together with the low mass numbers of constituent elements preclude the use of LiF-BeF_2 as fuel for fast neutron systems

Molten chloride salt is more attractive since it has high Pu solubility and the mass number of Cl is about twice of that of F The NaCl-

$PuCl_3$ system has an eutectic temperature of 726 K for the composition $64NaCl\text{-}36PuCl_3$. The solubilities of MAs in the salt are not known, but Pu in the chloride salt may be replaced by any MAs. The chloride salt selected for the design study of the molten-salt system is $64NaCl\text{-}5PuCl_3\text{-}31MACl_3$ (where MA represents Np, Am, and Cm).

One of the major problems with molten chloride salts is the material compatibility, which is vitally important in the application to nuclear systems.

D.1.1.6.2. Target/blanket configuration

The target/blanket is designed for 800-MW thermal power. As shown in Fig. 13, a high energy proton beam is injected downward into the central cavity filled with molten chloride salt through the beam window. The central cavity has the form of a right circular cylinder of 0.8 m in diameter and 1.7 m in height. The molten salt acts as target material and also as fuel. This eliminates the physical and functional separation between target and blanket, and thus significantly simplifies the target/blanket configuration. MA is mainly transmuted in this region by fast fission and spallation reactions.

The central cavity is surrounded by an internal reflector with a thickness of 0.3 m. The intermediate heat exchangers and molten-salt pumps are located around the internal reflector in the target/blanket vessel. The internal reflector protects the heat exchangers and pumps from the radiation damage. The intermediate heat exchangers are of compact type with plate-and-fin configuration, where heat in the primary molten salt is transferred to the secondary fluid of molten fluoride salt. The in-vessel heat exchanger design minimizes the total volume of the primary salt and the total inventory of actinides in the system. The molten-salt pumps are of a motor-driven mechanical type and circulate the primary salt through the heat exchangers to the central cavity. The dimensions of the target/blanket vessel are 2.9 m in diameter and 2.3 m in height. The thickness of the upper, lower, and side reflectors are 0.2 m, 0.4 m, and 0.4 m, respectively.

The beam window is a hemispherical shell of 0.4 m in diameter cooled by primary molten-salt flow.

D.1.1.6.3. System performance

The molten-salt target/blanket has an effective neutron multiplication factor of 0.92, and produces 800-MW thermal power with a 1.5 GeV-25 mA proton beam. In the molten-salt system, the maximum thermal power is limited not by the maximum fuel temperature or the maximum power density, but the heat transfer rate through the heat exchangers. The maximum power density in the target/blanket region is about 1660 MW/m^3. Assuming a load factor of 80%, the actinide burnup is approximately 250 kg/y, or 4.6%/y. The system operates at a molten-salt temperature in the range of 920-1020 K. With such a high operating temperature, a power conversion efficiency around 45% becomes feasible by using a supercritical steam cycle, which can improve the total energy balance of the system.

Table VII summarizes design parameters and operating conditions of the molten-salt system.

The molten state of the fuel salt offers several attractive features for the design of the transmutation system. The main advantage over a solid system is the capability of continuous on-line processing. The fuel composition can be continuously controlled and fission and spallation products can be continuously removed from the fuel. Furthermore, the rather laborious process of actinide fuel fabrication is not required for the molten-salt system. Blanket melt-down accidents would be impossible as the molten fuel is ready to be dumped from the blanket in case of emergency, which may add a high degree of safety.

D.1.1.7. SUMMARY

The accelerator-driven transmutation system project at JAERI has been presented. This project is being

carried out under the Japanese long-term R&D program on partitioning and transmutation, called OMEGA.

TABLE VII. MAJOR PARAMETERS OF MOLTEN-SALT TARGET/BLANKET SYSTEM

Fuel	Chloride Salt $64NaCl\text{-}5PuCl_3\text{-}31MACl_3$ (MA: Np, Am, Cm)
Target	Chloride Salt
Coolant	Chloride Salt
Actinide Inventory	5430 kg
Neutron Multiplication Factor	0.92
Spallation Neutrons per Proton	38 n/p
Proton Beam	1.5 GeV - 25 mA
Thermal Power	800 MW
Burnup	250 kg/y (4.6 %/y)
Power Density	
Maximum	1660 MW/m^3
Average	310 MW/m^3
Coolant Temperature	
Inlet	923 K
Outlet	1023 K
Coolant Maximum Velocity	3.6 m/s

In the design study for a transmutation plant, two types of dedicated system concepts are being investigated; a solid system and a molten-salt system. In either system, an MA-loaded subcritical blanket is driven by a high-intensity proton accelerator and makes use of a hard neutron spectrum to transmute MAs efficiently by fission.

The design of the solid system is based on the current status of liquid-metal fast reactor technology, whereas the design of the molten-salt system relies largely on next generation technology.

REFERENCES

[1] Kubota, M. et al.: "Development of Partitioning Process in JAERI", Proc. 2nd OECD/NEA Int. Information Exchange Meeting on Actinide and Fission Product Separation and Transmutation, ANL (1992).

[2] Mukaiyama, T. et al.: "Higher Actinide Transmutation using Higher Actinide Burner Reactor", Proc. Int. Conf. Physics of Reactors, Marseille, (1990).

[3] Mizumoto, M. et al.: "High Intensity Proton Accelerator for Nuclear Waste Transmutation", 16th Int. Linear Accelerator Conf. LINAC-92, Ottawa (1992).

[4] Nishida, T. et al.: "Improvement of Spallation Reaction Simulation Codes NMTC/JAERI and NUCLEUS", 2nd Int. Symp. on Advanced Nuclear Energy Research , Mito (1990).

[5] Nakahara, Y. and Tsutsui, T.: "NMTC/JAERI - A Simulation Code System for High Energy Nuclear Reactions and Nucleon-Meson Transport Process", JAERI-M 82-198 (in Japanese) (1982).

[6] Takada, H. et al.: "Production of Radioactive Nuclides in a Lead Assembly with 500 MeV Protons", Proc. Specialists' Mtg. on Accelerator-Based Transmutation, PSI (1992).

[7] YOSHIDA, H. et al.: "A Strategic Study of the Partitioning and Transmutation System being

Developed at JAERI", Proc. Int. Information Exchange Meeting on Actinide and Fission Product Separation and Transmutation, ANL (1992).

[8] Takizuka, T. et al.: "Conceptual Design Study of an Accelerator-based Actinide Transmutation Plant with Sodium-cooled Solid Target/Core", ibid.

[9] Katsuta, H. et al.: "A Continuous Transmutation System for Long-lived Nuclides with Accelerator-driven Fluid Targets", ibid.

D.1.2. DEVELOPMENT OF THE PARTITIONING PROCESS AT JAERI

Masumitsu Kubota

Japan Atomic Energy Research Institute

Tokai-mura, Naka-gun, Ibaraki-ken 319-11 Japan

D.1.2.1. INTRODUCTION

Partitioning of nuclides such as transuranium elements (TRU), Tc-99, Sr-90 and Cs-137 in a high-level liquid waste (HLLW) generated in nuclear fuel reprocessing and transmutation of long-lived nuclides by nuclear reactions are expected to increase the efficiency of high-level waste disposal and will allow utilization of existing resources in spent fuel.

Since 1985, much effort has been directed to developing an advanced partitioning process for separating elements in HLLW into four groups; TRU, Tc-Platinum group metals (PGM), Sr-Cs and the other elements [1,2]. The most recent studies are mainly focused on how to increase the efficiency of TRU separation with diisodecylphosphoric acid (DIDPA) solvent.

D.1.2.2. SEPARATION OF TRU, ESPECIALLY NEPTUNIUM

Effectiveness of DIDPA for the complete extraction of Am, Cm, Pu and U had been already demonstrated with an actual HLLW before 1984. Therefore much attention has been given to how to increase Np extraction with DIDPA. Penta-valent Np, which is dominant in HLLW, is the TRU most difficult to extract with general organic solvents. We found that the addition of hydrogen peroxide to the TRU extraction with DIDPA accelerated penta-valent Np extraction. Through experiments on counter-current continuous extraction using a mixer-settler, more than 99.96% of penta-valent Np was found to be extracted when hydrogen peroxide was fed at a level to compensate for its decomposition.

The behavior of fission and corrosion products in continuous counter-current extraction with DIDPA was also tested with a simulated HLLW. More than 99.99% of Nd, which was used as a stand-in for rare earths, Am and Cm, was found to be extracted and recovered by back-extraction with 4 M nitric acid. Most of the Fe was extracted with DIDPA, but not back-extracted with 4 M nitric acid. Therefore, Fe could be separated from Nd with a decontamination factor of about 100. About 6% of Ru and 11% of Rh were extracted in this experiment. Their extraction behavior might change in a practical application because their chemical forms seem to differ in actual HLLW. Almost all Cs and Sr were transferred to the raffinate fraction and Nd was found to be completely separated from these heat generating nuclides in HLLW.

D.1.2.3. SEPARATION OF AMERICIUM AND CURIUM FROM RARE EARTHS

In order to produce a more continuous process, we are developing a preferential back-extraction of Am and Cm, leaving rare earths in the DIDPA solvent, by using a stripping solution which contains 0.05 M DTPA (diethylenetriaminepentaacetic acid), 1 M lactic acid and ammonia.

The continuous back-extraction experiment was performed with the DIDPA solvent containing Nd and La, which are stand-ins for Am-Cm and rare earths respectively. The experimental results revealed that more than 99.9% of Nd was back-extracted, while more than 98% of La was left in the solvent, and the Nd and La concentration profiles agreed very closely with calculated profiles.

These findings show that the estimation of the back-extraction behavior of Am, Cm and rare earths by calculation would be valid enough for optimization of the back-extraction process.

The calculated back-extraction behavior of Am-Cm and rare earths in the optimized process showed that 99.995% of Am-Cm was back-extracted and only 1.1% of rare earths accompanied Am-Cm. As the weight ratio of Am and Cm to rare earths is only 3.3% in HLLW, it would become about 75% after separation.

We are going to confirm this estimation by performing a continuous experiment with a solvent containing both Am and rare earths.

D.1.2.4. BACK-EXTRACTION OF URANIUM

After Am and Cm back-extraction with DTPA solution, all rare earths and other TRU (Np and Pu) can be back-extracted with 4 M nitric acid and 0.8 M oxalic acid solution, respectively. As for the back-extraction of U, the effectiveness of phosphoric acid has already been studied. However, it has some difficulties in practical use.

We are developing the application of a sodium carbonate solution to the back-extraction of U from the DIDPA solvent.

Batch experiments showed that the distribution ratio of U became lower than 0.1 when the 0.8 to 2 M sodium carbonate solution was used as back-extractant. However, an emulsion was formed. We found that this could be avoided by increasing temperature and/or adding alcohol.

When the temperature was increased to 65°C, no emulsion was observed. When ethanol was added with a ratio of 15 vol%, the temperature could be lowered to 15°C and the distribution ratio of U became lower than 0.1. U could be back-extracted in a small number of stages in a mixer-settler.

D.1.2.5. CONSTRUCTION OF PARTITIONING PROCESS

Through these fundamental studies, the advanced four group partitioning process was constructed and its effectiveness will be demonstrated with an actual HLLW at the NUCEF (Nuclear Fuel Cycle Safety Engineering Research Facility) in 1996.

REFERENCES

[1] KUBOTA, M., et al.: "Development of a partitioning process for the management of high-level waste", Future Nuclear Systems: Emerging Fuel Cycles and Waste Disposal Options GLOBAL '93 (Proc. Int. Symp. Seattle, 1993), 588.

[2] KUBOTA, M.: "Recovery of technetium from high-level liquid waste generated in nuclear fuel reprocessing", Radiochimica Acta 63, 91 (1993).

D.1.3. HIGH INTENSITY PROTON LINEAR ACCELERATOR DEVELOPMENT FOR NUCLEAR WASTE TRANSMUTATION

M. Mizumoto, K. Hasegawa, H. Oguri, N. Ito, J. Kusano, Y. Okumura, H. Murata and K. Sakogawa

Japan Atomic Energy Research Institute

Tokai-mura, Naka-gun, Ibaraki-ken 319-11 Japan

D.1.3.1. INTRODUCTION

Design studies of accelerator-driven nuclear waste transmutation system have been carried out for the OMEGA project (Options Making Extra Gains of Actinides and Fission Products). The high-intensity proton linear accelerator (ETA: Engineering Test Accelerator) with an energy of 1.5 GeV and an average current of 10 mA has been proposed for various engineering tests for the transmutation system by JAERI. Nuclear spallation reactions with high energy proton beams will produce various intense beams that can also be utilized for other nuclear engineering applications. These include material science, radio isotope production, nuclear data measurements and other basic sciences with the proton, neutron and other secondary beams in addition to nuclear waste transmutation.

In the course of the accelerator development, the R&D work for the low energy portion of the accelerator (BTA: Basic Technology Accelerator), with an energy of 10 MeV and a current of 10 mA, has been made, because the maximum beam current and quality are mainly determined by this low energy portion. R&D for the main accelerator components such as the high current hydrogen ion source, radio-frequency quadrupole (RFQ), drift tune linac (DTL) and RF power source is in progress.

The conceptual and optimization studies for the high energy accelerator ETA have been performed simultaneously with regard to proper choice of operating frequency, high b structure, mechanical engineering considerations and RF source aspects in order to ensure low beam loss, hands-on maintenance and low construction cost.

D.1.3.2. ACCELERATOR DEVELOPMENT

The conceptual layout of the ETA is shown in Fig. 1. In the case of a high intensity accelerator, it is particularly important to maintain good beam quality (low emittance; small beam size and divergence) and minimize beam losses to avoid damage and activation of the accelerator structures. Because the beam quality and maximum current are mainly determined by the low energy portion of the accelerator, the accelerator (BTA) will be built as a first step in the ETA development [1]. The layout of BTA is shown in Fig. 2.

The basic specification of BTA is given in Table I. The beam dynamics design calculations for the BTA, which will consist of the ion source, RFQ and DTL including the beam transport system, have been made with the computer codes PARMTEQ and PARMILA [2]. Because of the high beam current and high duty factor, the problem of heat removal from the accelerator structure is also an important issue for the mechanical design. The electromagnetic field distribution, temperature distribution and thermal stresses are carefully studied with the three dimensional modelling codes, MAFIA and ABAQUS. The beam energy for the BTA is chosen to be 10 MeV in order to avoid proton induced reactions in accelerator structural materials where the Coulomb barriers are barely exceeded. The acceleration frequency of 201.25 MHz is selected both for RFQ and DTL mainly due to the large bore radius, manageable heat removal problem and the availability of an RF source

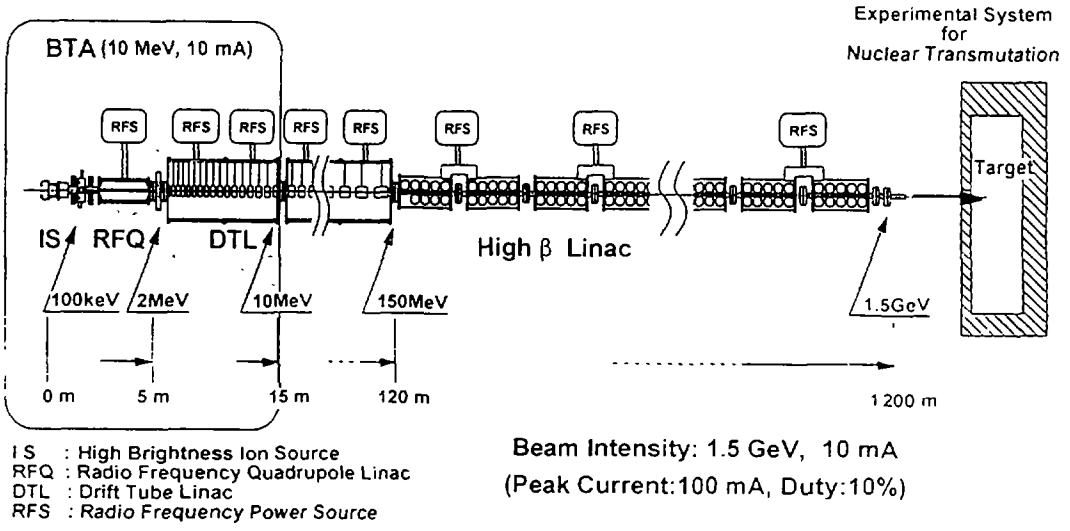

FIG. 1. A conceptual layout of the ETA

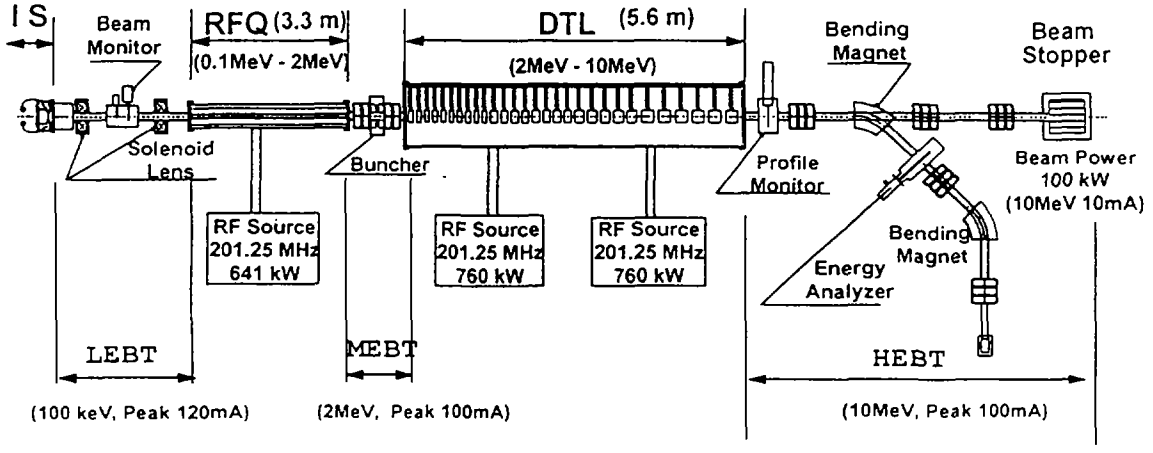

FIG. 2. A layout of the BTA.

D.1.3.2.1. Ion source

Figure 3 shows a prototype ion source which was constructed based on the experience from the NBI (Neutral Beam Injectors) for Fusion Research [3]. The ion source consists of a multicusp plasma type generator with four tungsten filaments and a two stage extractor. The dimension of the plasma chamber is 20 cm in diameter and

TABLE I. A BASIC SPECIFICATION OF BTA

Output energy	10 MeV
Operation mode	pulse
Duty factor	10 %
Average beam current	10 mA
Peak beam current	100 mA

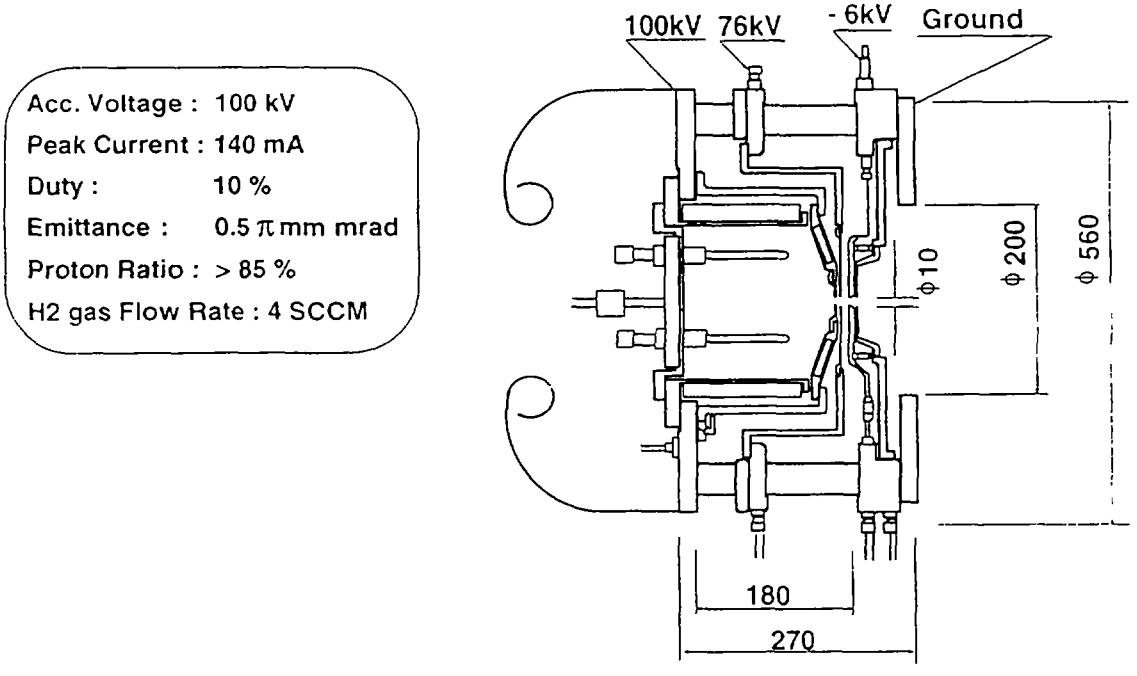

FIG. 3. A prototype of a high brightness ion source.

17cm in length. The chamber is surrounded by 10 columns of SmCo magnets with a field strength of about 0.2 T at the inner surface. The other basic specifications for the source are given in Table II.

The high brightness hydrogen ion beam of 140 mA was extracted using the 100 kV high voltage power supply. The beam profile was measured with a multi-channel calorimeter and the observed normalized emittance was about 0.45 pmm.mrad (90%). The proton ratio and impurity were found to be 80% and less than 1%, respectively, using a Doppler shifted spectroscopy method

TABLE II. ION SOURCE

Energy	100 keV
Current	120 mA
Duty factor	CW
Emittance	0.5 pmm.mrad (normalized 100%)
Proton ratio	> 90%
Impurity	< 1%

D.1.3.2.2. RF source

Three sets of 201.25 MHz RF sources with about 1 MW peak amplifiers are needed for BTA (641 kW for RFQ and two 760 kW for DTL). The tetrode tube 4CM2500KG (EIMAC), which was originally developed for fusion plasma heating, is used with a multistage amplifier configuration [4]. The block diagram of the RF source is shown in Fig. 4. The RF source was designed and one set of amplifiers was manufactured. The high power amplifier (HPA) is driven by a 60 kW intermediate amplifier (IPA of RS2058CJ) which is fed by a master oscillator and a 3 kW solid state drive amplifier. The accelerator voltage and phase control loop with an accuracy of < 0.1% in amplitude and < 1 in phase were constructed. The high power test was successfully made with a peak power of 1 MW at 0.6% duty and 830 kW at 12%

duty obtained using a dummy load.

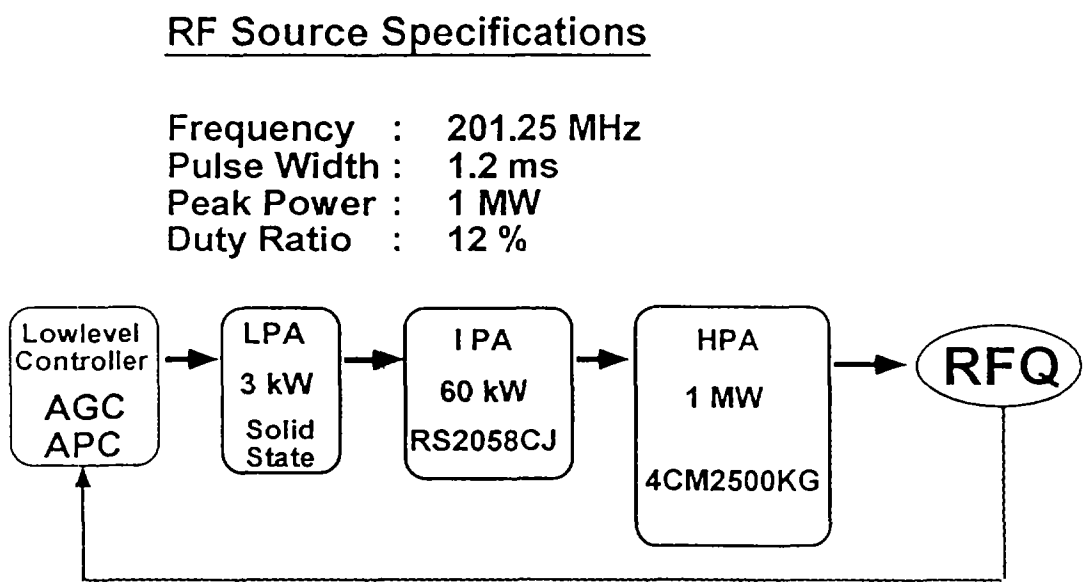

FIG. 4. A block diagram of the RF source.

D.1.3.2.3. DTL high power test

Design studies were made under various mechanical constraints for DTL such as the resonant frequency, magnetic field strength and the problem of heat removal. The DTL parameters are given in Table III. A hollow conductor type coil with 5*5 mm^2 was chosen for the electric quadrupole magnet. The configuration of this quadrupole magnet was optimized with conditions on the coolant water (temperature rise 25 K in the coil, pressure drop 50 N/cm^2 and velocity 3.4 m/s). The hot test model with 9 cells was fabricated with 8 drift tubes inside the DTL tank and 2 drift tubes in the end plates. The first drift tube and the one at the front end plate were installed with actual quadrupole magnets. The cross cut view of the DTL hot test model is shown in Fig. 5 [5].

The drift tube alignment was made with a laser telescope and an accurate longitudinal scale. Alignment errors in the transverse plane and the longitudinal direction were within 0.1 and 0.08 mm, respectively. The cold test was performed to examine the RF characteristics such as resonance frequency, Q value and electric field distribution on the beam axis. The resonant frequency of the TM01 mode was measured to be 201.178 MHZ when the tuner displacement was 100 mm. The measured frequency shifts were in good agreement with those predicted by calculation. The resonant frequency could be shifted with the tuner by about 200 kHz, which is enough to compensate the frequency change due to RF heating. The measured Q value was 42000 (83% of the SUPERFISH calculation). This result indicates that an RF power of 130 kW is required to obtain an average strength of 2 MV/m. The electric field distribution on the beam axis was measured by the bead perturbation method with an aluminum spherical bead of 7 mm in diameter. The average field strength over the whole region was deduced to be 2.03 MV/m which is in good agreement with the designed value of 2 MV/m. Deviation of the average field in each cell was within 2.3%. A high power test was carried out to examine the cooling capability. Various quantities were monitored during the high power conditioning; RF signals from a pickup loop and a directional coupler, temperature of the cooling water, total vacuum pressure using an ionization gauge, partial pressure using quadrupole mass spectrometer and bremsstrahlung X-ray spectrum. During the conditioning, an input RF power up to 154 kW with a duty factor of 12% was achieved in the DTL model, which exceeded the prescribed nominal

power level of 130 kW. The relation between the input power from the RF monitor and the gap voltage from the X-ray spectrum agrees well with the calculation using the SUPERFISH code.

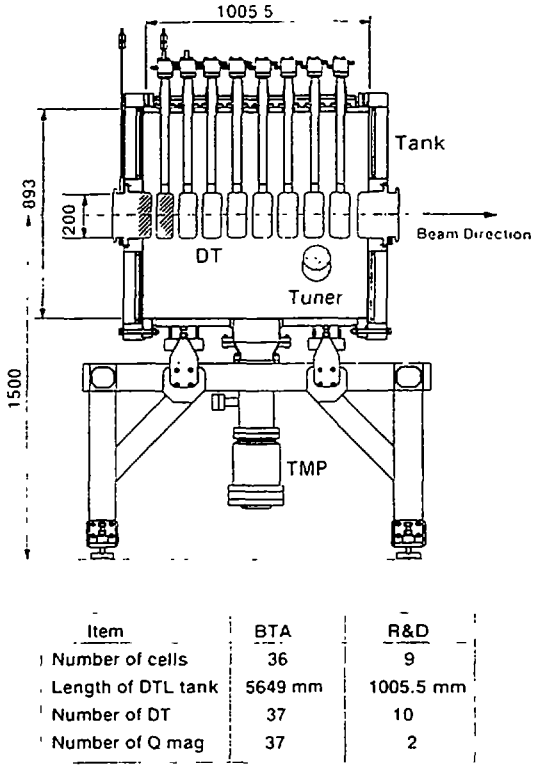

Item	BTA	R&D
Number of cells	36	9
Length of DTL tank	5649 mm	1005.5 mm
Number of DT	37	10
Number of Q mag	37	2

TABLE III. DTL PARAMETERS

Frequency	201.25 MHz
Energy	2 - 10 MeV
Beam current	100 mA
Average field	2.0 MV/m
Tank diameter	89.3 cm
Tank length	564.9 cm
Cell length	9.86 - 21.55 cm
g/L	0.234 - 0.293
DT outer diameter	20 cm
DT inner diameter	2 cm
Synchronous phase	-30
DT cell number	36
Focus magnetic field	80 - 35 T/m
Q	69800
Wall loss	720 kW
Beam power	800 kW

FIG. 5. A cross cut view of DTL hot test model.

A high power test was carried out to examine the cooling capability. Various quantities were monitored during the high power conditioning; RF signals from a pickup loop and a directional coupler, temperature of the cooling water, total vacuum pressure using an ionization gauge, partial pressure using quadrupole mass spectrometer and bremsstrahlung X-ray spectrum. During the conditioning, an input RF power up to 154 kW with a duty factor of 12% was achieved in the DTL model, which exceeded the prescribed nominal power level of 130 kW. The relation between the input power from the RF monitor and the gap voltage from the X-ray spectrum agrees well with the calculation using the SUPERFISH code.

The cooling capability was examined by feeding an RF power of 130 kW. To obtain the distribution of the power dissipation, the temperature rise and cooling water flow rate through each path were measured using platinum resistance thermometers and a flow meter, respectively. The experimental distribution of the power dissipation among the 9 drift tubes (including 2 in the end plates) is generally in good agreement with the SUPERFISH calculation.

D.1.3.2.4. RFQ beam test

The basic specification of the RFQ is given in Table IV. The first beam test with the ion source and RFQ was carried out at the test shop of Sumitomo Heavy Industries (SHI), Ltd. [6] in February, 1994. After this first beam test had been completed, the whole apparatus was transferred to Tokai, JAERI and reassembled. The beam test was restarted again in November, 1994 and various beam properties are being studied.

The layout of the 2 MeV RFQ beam test is shown in Fig. 6. The 100 keV H^+ beam was extracted by a multi-cusp type ion source to the RFQ. Two focusing solenoids in the low energy beam transport (LEBT) were used to match the ion source beam emittance to the RFQ acceptance. The transmission was deduced from the RFQ input and output currents measured with the two Faraday cups. The RFQ acceleration current as a function of the normalized vane voltage (a normalized vane voltage of unity corresponds to nominal gap voltage of 113 kV) is shown in Fig. 7. The results of the measured beam transmission were lower by 20 - 30% than the design values with PARMTEQ. The various causes of these lower transmissions are being investigated. The beam

TABLE IV. RFQ PARAMETERS

Frequency	201.25 MHz
Energy	0.1 - 2 MeV
Beam current	110 mA
Duty Factor	10 %
Synchronous phase	-90- -35
Vane voltage	0.113 MV
Focusing parameter B	7.114
Number of cell	181
Cavity diameter	36.6 cm
Vane length	334.8 cm
Quality factor (Q)	13000 (100% Q)
Wall loss power	432 kW (60% Q)
Beam power	209 kW

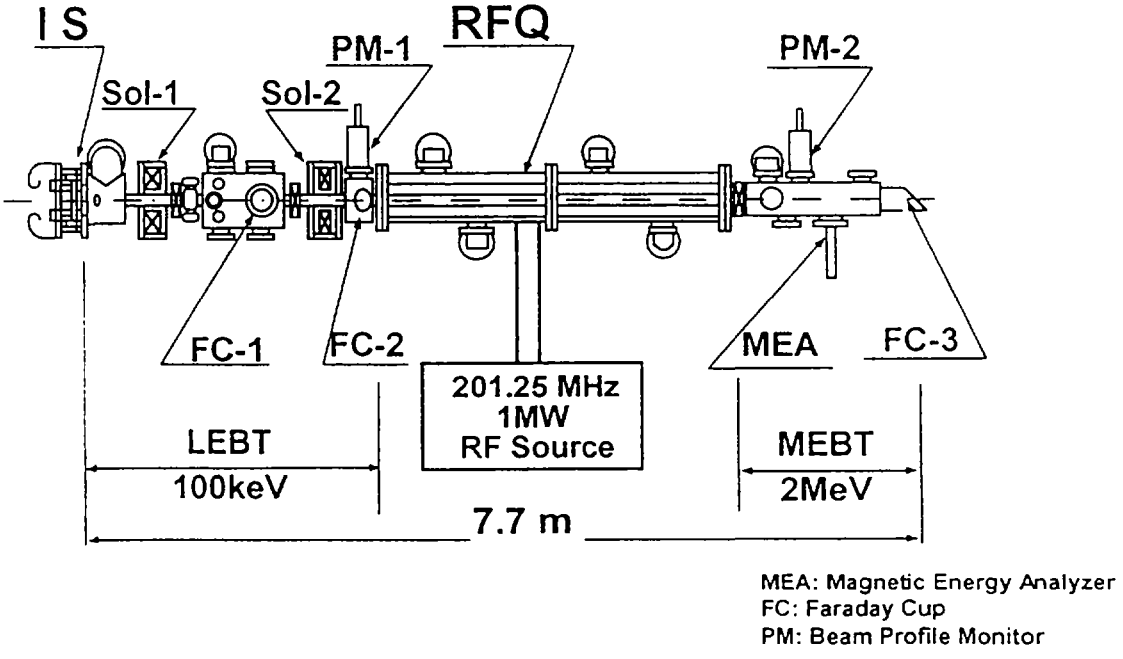

FIG. 6. A layout of the 2 MeV RFQ beam test.

energy spectra from the RFQ were also measured using a compact magnetic energy analyzer (MEA), with a pole radius and gap length of 40mm and 6mm, respectively. The deflection angle was 25° and the energy resolution was assumed to be 5% for a 2 MeV proton beam. The 100 keV H^+, H^{2+} and H^{3+} beam from the ion source through the RFQ (without RF) was used as an energy calibration source for five vane voltages. The intervane voltage dependence of the proton energy spectra is shown in Fig. 8. As the intervane voltage was reduced, the energy spectrum shifted to lower energies with a prominent discrete energy distribution. This interesting phenomenon was well predicted by PARMTEQ as indicated in the figure.

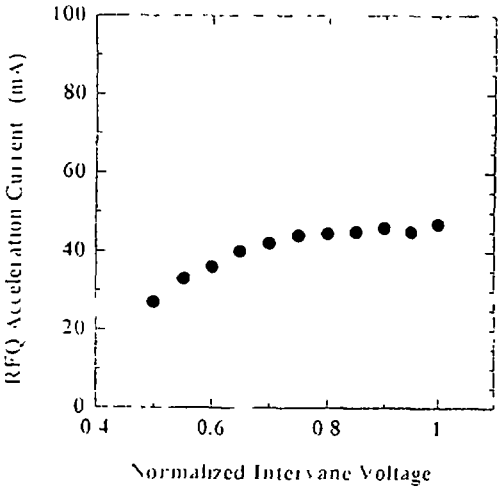

FIG. 7. Intervane voltage dependence of RFQ acceleration current.

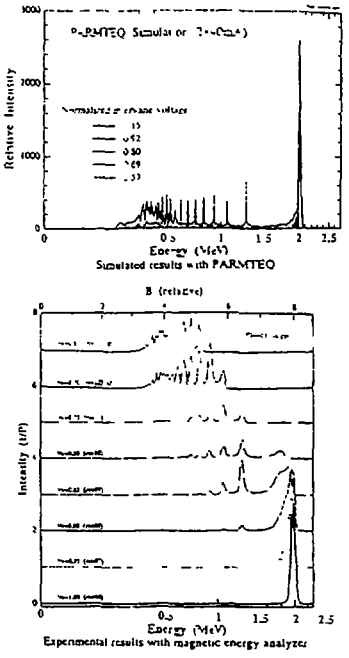

FIG. 8. Intervane voltage dependence of proton energy spectra from the RFQ.

D.1.3.3. SUMMARY

R&D work has been carried out on the design and construction of prototype accelerator structures (Ion source, RFQ, DTL and RF source). The low-power tests were made to study the RF characteristics for the RFQ and DTL accelerating structures and have verified the design prediction. The first 2 MeV beam test with the ion source and RFQ in combination with a single high power RF source unit was successfully carried out with a peak acceleration current of 52 mA (for the duty factor of 5%). For the DTL high power test, measurements of the electromagnetic characteristics were made satisfactorily. Problems of heat dissipation and heat removal in the structure were studied. Table V summarized the major results of the R&D work. The detailed design work for the BTA construction will follow in the next stage based on these R&D results. Further improvement is however still required to increase the average beam current (the goal is 10 mA) by improving the peak current and duty factor. More detailed studies of the beam properties are needed to improve transmission.

TABLE V. THE PRESENT STATUS OF THE PROTON LINAC DEVELOPMENT FOR THE JAERI OMEGA PROGRAM

(1) Ion source: Multi-cusp ion source	
High voltage	100 kV
Accelerating current	140 mA
Emittance	0.5 π mm.mrad (90%)
Proton ratio	> 80 %
(2) Radio frequency quadrupole (RFQ): 4 vane type	
Q	9,420 (71% Q)
Electromagnetic field distribution	
Field balance	< 2.5 %
Field flatness	< 7.1 %
(3) DTL: hollow conductor type DT	
Magnetic field center	< 30 μm
Temperature rise	< 25° C
Heat expansion	< 4 μm
Hot test model (9 cell)	
Q	42,000 (83% Q)
Electromagnetic field distribution	
Field flatness	< 2.3 %
High power test	154 kW (duty 12%)
(4) RF source	
Maximum power	830 kW (duty 12%)
	1 MW (duty 0.6%)
The RFQ beam test	
Methods	
Energy spectrum	Analyzing magnet
Vane voltage	X-ray detection with NaI and Ge detector
Profile	Profile monitor
Beam current & transmission	Faraday cup

	Present status	Goal
Current	52 mA	100 mA
Duty	5 %	10 %
Pulse width	1.0 ms	1.0 ms
Rep. rate	50 Hz	50 Hz

REFERENCES

[1] MIZUMOTO, M., et al.: "High Intensity Proton Accelerator for Nuclear Waste Transmutation", 1992 Linear Accelerator Conf. Proc., 1992 August 24-28, Ottawa, Ontario, Canada, C.R. Hoffman Editor, AECL-10728, 749.

[2] Los Alamos Accelerator Code Group: "Computer Codes for Particles Accelerator Design and Analysis", LA-UR-90-1766, 1990.

[3] OGURI, H., et al.: "A High Brightness Hydrogen Ion Source for the BTA at JAERI", Proc. of 1994 Int. Linac Conf., August 21-26, 1994, Tsukuba, Japan, K. Takata Editor, 381.

[4] TOUCHI, Y., et al.: "A High Power RF System for the JAERI BTA", 4th European Particle Accelerator Conf., June 27 - July 1, 1994, London, edited by V. Suller and C. Petit-Jean-Genaz.

[5] ITO, N., et al.: "Fabrication and Tests of the DTL Hot Model in the R&D Works for the Basic Technology Accelerator (BTA) in JAERI", Proc. of 1994 Int. Linac Conf., August 21-26, 1994, Tsukuba, Japan, K. Takata Editor, 119.

[6] HASEGAWA, K., et al.: "First Beam Test if the JAERI 2 MeV RFQ for the BTA", ibid., 113.

D.1.4. PRESENT STATUS OF INTEGRAL SPALLATION EXPERIMENTS IN JAERI

Hiroshi Takada, Shin-ichirou Meigo, Toshinobu Sasa,
Takahiko Nishida and Takakazu Takizuka
Japan Atomic Energy Research Institute
Tokai-mura, Naka-gun, Ibaraki-ken 319-11 Japan

Kenji Ishibashi and Tatsushi Nakamoto
Kyushu University
Hakozaki, Higashi-ku, Fukuoka-shi, Fukuoka-ken 812 Japan

D.1.4.1. INTRODUCTION

Interest is growing for the use of accelerator-driven subcritical systems for the transmutation of long-lived radioactive nuclear wastes The subcritical blanket design is generally one [1-5] in which high energy protons with energies of 0 8 to 1 6 GeV are injected into a spallation target surrounded by a fuel blanket region made of actinides and/or fission products. The actinide nuclides are transmuted by the fission reactions induced by the neutrons produced via the spallation reactions in the target.

There are many options for the choice of both target materials and fuel elements. One is the solid system [2] which consists of a tungsten target and the actinide metal alloy fuel with a pin bundle structure Another is the liquid system which employs a liquid heavy metal or a molten salt target with molten salt actinide/fission products fuels [1, 4] As for the neutron energy, thermal neutrons [1, 4] and fast neutrons [2, 3] produced by the use of heavy water coolant or of liquid sodium coolant respectively are studied

In the design study, it is necessary to use a code system which can estimate such quantities as neutron yield, neutron energy spectrum and nuclide yield with high accuracy because these are important factors determining the performance of the system However, since there is little evaluated nuclear data available in the energy region above 20 MeV,, the neutron transport codes which have been used in the neutronic design of commercial reactors cannot be applicable. Therefore, a Nucleon Meson Transport Code such as NMTC/JAERI [6] or LAHET [7] which simulates nuclear reactions and the subsequent particle transport have been used in connection with the neutron transport code for the neutronics calculation of the accelerator-driven subcritical system

In order to study the accuracy of the physical model used in the Nucleon Meson Transport Code, several neutron double differential cross section measurements have been carried out for a variety of targets with proton energies up to 800 MeV [8-15]. With these experimental data, an international code comparison [16, 17] was organized and has been carried out by OECD/NEA to test the predictive power of various physical models and codes applicable for the calculation of intermediate energy nuclear reactions

Some integral experiments [18-21] have been carried out to validate the accuracy of the code system. At JAERI, an spallation integral experiment using a large-scale Lead assembly is in progress using 500 MeV protons to estimate the accuracy of NMTC/JAERI A supplemental neutron energy spectrum measurement has been carried out as a part of neutron differential cross section measurements by Kyushu University [22, 23] with the protons of 0 8, 1.5 and 3.0 GeV.

There is a proposal [24] by the Proton Engineering Center in which high energy protons of 1.5 GeV with a maximum current of 10 mA are available at the OMEGA Nuclear Energy Development Facility. This intense proton beam enables us to make a variety of experiments ranging from differential ones to

demonstration tests of the accelerator-driven subcritical system. This paper describes the present status of the integral experiments in JAERI and shows the results of preliminary analysis for engineering experiments in the OMEGA Nuclear Energy Development Facility .

D.1.4.2. EXPERIMENTS

D.1.4.2.1. Measurement of nuclide yield in Lead assembly

In order to validate the accuracy of the nucleon meson transport code NMTC/JAERI, an integral spallation experiment has been carried out using a Lead assembly bombarded with 500 MeV protons at the beam dump room of the booster synchrotron facility of the National Laboratory for High Energy Physics (KEK). Figure 1 shows the cross sectional view of the Lead assembly. Lead was melted into a mould of stainless steel with a thickness of 2.5 mm. The size of the assembly was 60 cm in diameter and 100 cm in length. The protons were transported through the beam entrance hole of 10 cm in diameter and 20 cm in length and were injected perpendicular to the target of 16 cm in diameter and 30 cm in length installed in the assembly. Lead and tungsten alloy were used as targets, respectively.

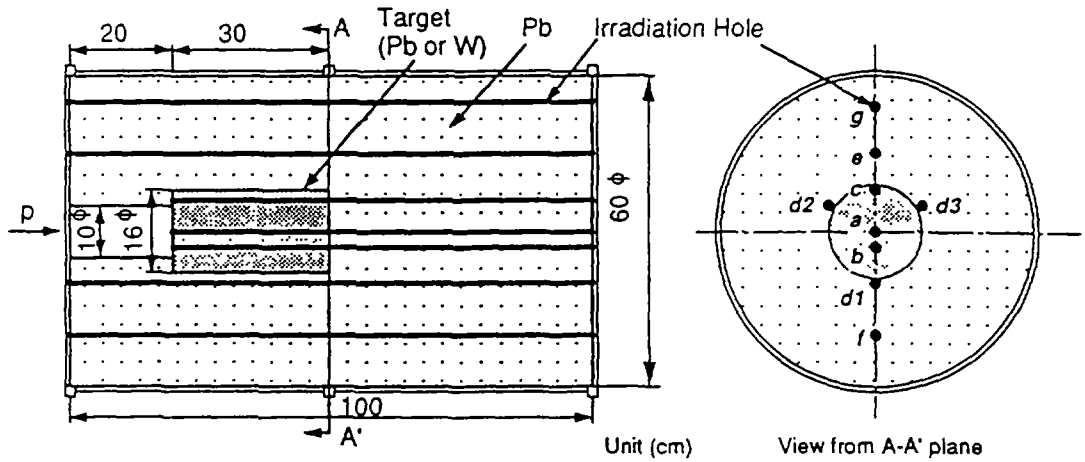

FIG. 1. Cross sectional view of Lead assembly. Thin and thick hatched areas indicate the Lead assembly and the target in which Lead or tungsten is installed. Thick solid lines of 'a' to 'g' represent the irradiation holes for activation samples.

In order to study the transport of the secondary particles induced by spallation reaction using an activation method, some irradiation holes were made along the beam axis of the assembly at the radial distances of 0, 3, 6, 10, 15, 20 and 25 cm. Using of various high purity metal activation samples of Al, Fe, Ni, Cu and Au, yields of the nuclides produced in the samples were measured by the technique of γ-ray spectrometry. The size of the samples was 6 or 8 mm in diameter and 4 or 10 mm in length. The samples were packed together with Pb samples into an aluminum capsule having an outer diameter of 8 or 9.4 mm with a thickness of 0.5 mm and a length of 500 mm so that they could be placed with a ratio of 1 to 2 cm per 10 cm in the Lead assembly to suppress the perturbation of the neutron field in the irradiation hole as much as possible.

During irradiation, the number of injected protons was monitored by a calibrated pick up coil set in the booster beam line. The experiment was made using 2×10^{14} to 3×10^{15} protons. The γ-ray spectrum from the activated samples was measured with a 100 cm^3 Ge detector with 20% efficiency relative to NaI detector. Peak area counting in the measured γ-ray spectrum was made with the code BOB-73 [25].

Nuclide yield was obtained by considering the time relative to the irradiation time, the cooling, the measurement and the half life. Here, the correction for the self-absorption of γ-rays in a sample was made by a Monte Carlo calculation. The estimation of the systematic error on the γ-ray spectrum measurement is still in progress. For this reason, preliminary results including only the statistical error are shown in this report.

D.1.4.2.2. Measurement of neutron energy spectrum from thick target

Measurements of the energy spectrum of leakage neutrons from a thick Lead target bombarded with protons of 500 MeV and 1.5 GeV were carried out by the time of flight (TOF) technique in a series of neutron double differential cross section measurements at the π2-line of the 12 GeV proton synchrotron facility of KEK. The protons used in this experiment were produced at an internal target which was placed in the synchrotron accelerator ring. The intensity of the protons was quite weak as low as fA level. The experimental setup is illustrated in Fig. 2. The size of the Lead target was 20 cm in length and 15 cm by 15 cm in cross section. Pilot U scintillation detectors were set just in front of the target and at a point 20 m upstream. These pilot U scintillation detectors enable us to separate protons from charged pions and to give the start signal for the neutron counting systems consisted of NE213 scintillation detectors of 5 inches in diameter with 5 inches in thickness. Here, NE102A plastic scintillation detectors were employed as VETO counters to remove charged particle induced events from the counting system. The bias given to the NE213 detectors was set at the value of the half height of the ^{137}Cs Compton edge.

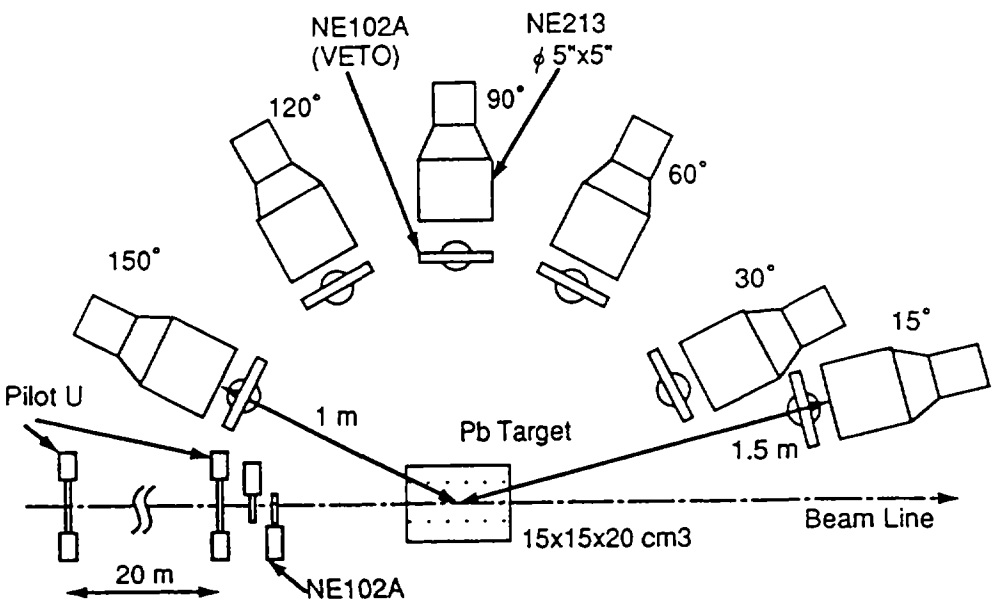

FIG. 2. Illustration of the experimental arrangement for neutron energy spectrum measurement by the time of flight method.

In the data acquisition procedure, a two-gate integration method [26] was employed to give n-γ discrimination in the measured pulse height data. The fast gate was 50 ns and the slow gate was 500 ns after a delay of 130 ns. In the data analysis, the detection efficiency calculated with the code SCINFUL [27] was employed for the energy region below 80 MeV; the accuracy of the code was confirmed to be about 10%. Since the applicable energy range of SCINFUL is up to 80 MeV, however, the detector efficiency above 80 MeV was determined by results calculated using the code CECIL [28] which was normalized to the value of SCINFUL at 80 MeV. The resultant detector efficiency is shown in Fig. 3.

In the TOF measurement with a thick target it should be noted that the scattering of the neutrons in the

target delays their flight time so that they might give a different energy from the real one. This effect makes the low energy component of the neutron energy spectrum increase. In order to remove the scattering effect, an unfolding method was also employed in the data analysis because the energy of the emitted neutrons was determined merely from the pulse height irrespective of the flight time. A saturation was observed in the pulse height signals for neutrons with the energies higher than several tens of MeV. The unfolding method was applied to the energy region below 14 MeV. Here, the calculation was carried out with the code FORIST [29] by the use of the response matrix obtained by the code SCINFUL.

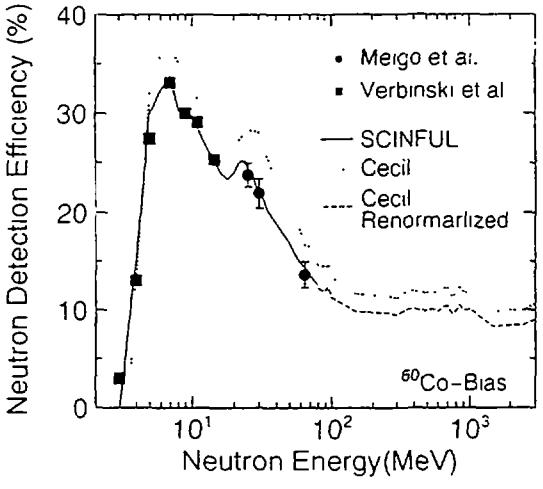

FIG. 3. The detector efficiency based on the calculation with the code SCINFUL and CECIL. Solid marks indicate the experimental results [38].

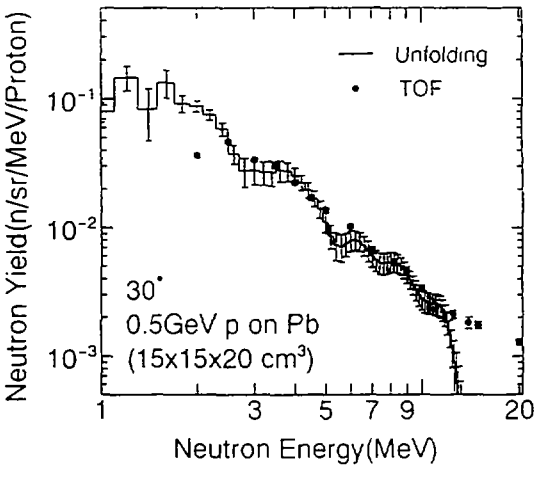

FIG. 4. Comparison of measured neutron energy spectrum at 30° for 500 MeV proton incidence on thick Lead target of 15 by 15 cm in width and 20 cm in length. Solid circle stand for the results obtained by time of flight method. Solid line represents the ones obtained by unfolding method.

In Fig. 4, the neutron energy spectrum at 30° obtained by the unfolding method is compared to the one obtained by the TOF method for 500 MeV proton incidence. An oscillation seen in the results for the unfolding method is due to the poor statistics of the detected events. A difference of more than 50% is observed in the energy region below 3 MeV between the two methods. This is because of the ambiguity of the efficiency near the threshold of ^{137}Cs bias used in the TOF method. It has been concluded from this result that the neutron spectrum obtained by the unfolding method is more reliable below 3 MeV than that obtained by the TOF method. Since good agreement is seen in the neutron spectrum above 3 MeV between the two methods, the results of the TOF method were adopted as final results. It has been found that there is no influence of the scattering effect in the measured neutron energy spectrum above 3 MeV.

D.1.4.3. CALCULATION

The calculation were made with the codes NMTC/JAERI and MCNP4.2 [30]. In the calculation of the nuclide yield in the Lead assembly, the beam profile was the Gaussian shape whose FWHM is 1.75 cm. The value was determined by the measurement of the activity induced in an aluminum foil put on the surface of the target. The irradiation hole was divided into 40 cells in the longitudinal direction with a radial thickness of 1.5 cm. In the calculation of the neutron leakage spectrum from thick target, the profile of the beam had a uniform circular shape with a diameter of 3 cm. The neutron energy spectrum was obtained by a surface crossing estimation at a curved surface with a width of 5 inches formed on a sphere

obtained by a surface crossing estimation at a curved surface with a width of 5 inches formed on a sphere of 1 m in radius.

NMTC/JAERI simulates the nuclear reaction and nucleon transport in the energy region above 20 MeV. The nuclear reaction is simulated by intranuclear cascade evaporation including the high energy fission model. MCNP4.2 calculates the transport of neutrons with energies below 20 MeV based on the cross section library processed from JENDL3.1 [31]. A calculation of 1,000,000 events was made to estimate the neutron energy spectrum in NMTC/JAERI.

It should be noted in the calculation with NMTC/JAERI that a modification was made to take into account the total cross section and the elastic cross section of nucleon-nucleus reactions by using Pearlstein systematics [32]. Since the geometric cross section was as the default value so far, irrespective of the incident energy, the code was improved by this modification so that it could accurately estimate the mean free path of neutrons travelling in matter. Figure. 5 compares the total cross sections evaluated by Pearlstein systematics with the geometric ones for ^{56}Fe and ^{208}Pb. Figure. 6 shows the calculated neutron energy spectra at a depth between 30 and 32.5 cm in radial positions of 10 and 20 cm. The influence of the inclusion of Pearlstein systematics is seen to be significant in the calculated neutron energy spectrum

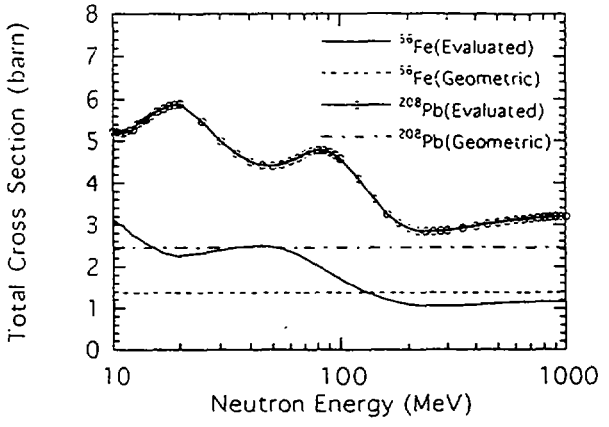

FIG. 5. Total cross sections for incident neutrons on ^{56}Fe and ^{208}Pb. The solid lines represent the values obtained by Pearlstein [1]. The dotted and dot-dashed lines denote the geometric cross sections.

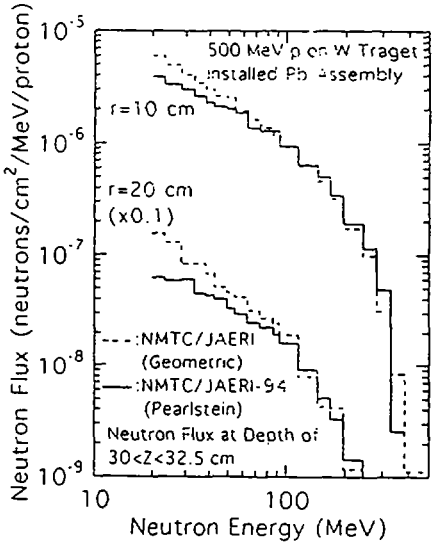

FIG. 6. Calculated neutron energy spectra at the depth between 30 and 32.5 cm at radial distances of 10 and 20 cm for 500 MeV protons incident on a tungsten target installed in the Lead assembly having a size of 60 cm in diameter and 100 cm in length.

in the energy region between 20 and 50 MeV. In order to obtain the nuclide yield, the evaluated nuclide production cross sections compiled in JENDL3.1 and the ones calculated by the code NUCLEUS [33] are employed in the energy region below and above 20 MeV, respectively. NUCLEUS is based on the intranuclear cascade evaporation model and corresponds to the nuclear reaction calculation part of NMTC/JAERI. In this calculation, the level density parameters derived by Baba were employed. The energy bins above 20 MeV were 20 groups with lethargy width of 0.05 up to 54 MeV and 30 groups with that of 0.075 above 54 MeV.

In this description, we focus on nuclide yields induced by the spallation neutrons which were obtained at radial distances greater than 8 cm, that is the region out of the target. Figure 7 shows the measured spatial distribution of the yields of ^{57}Ni in ^{nat}Ni samples for both Lead and tungsten targets. It is observed that the yields obtained around the depth of 20 to 35 cm are almost the same independent of the target materials. On the other hand, the differences of a factor of 2 to 3 are seen at longitudinal positions deeper than 50 cm in all radial positions. The neutron yield estimated by the calculation differs about 10 % between tungsten and Lead. The major differences between those materials are the range of 500 MeV

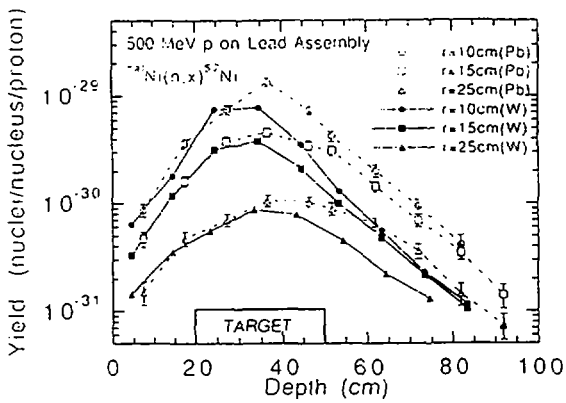

FIG. 7. Comparison of measured yields of ^{57}Ni produced in ^{nat}Ni samples between Lead and tungsten targets at radial positions of 10 to 25 cm for 500 MeV protons incident on the Lead assembly. The open and solid marks stand for the results for Lead and tungsten targets, respectively. The lines are a guide for the eye.

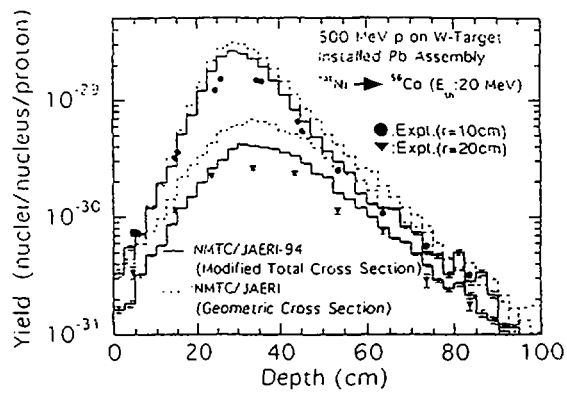

FIG. 8. Experimental and calculated yields of ^{56}Co in ^{nat}Ni samples inserted into a tungsten target installed in the Lead assembly for 500 MeV proton bombardment. The solid marks stand for the experimental data at radial positions of 10, 15, 20 and 25 cm, respectively. The solid lines represent the calculated results of NMTC/JAERI and MCNP4.2.

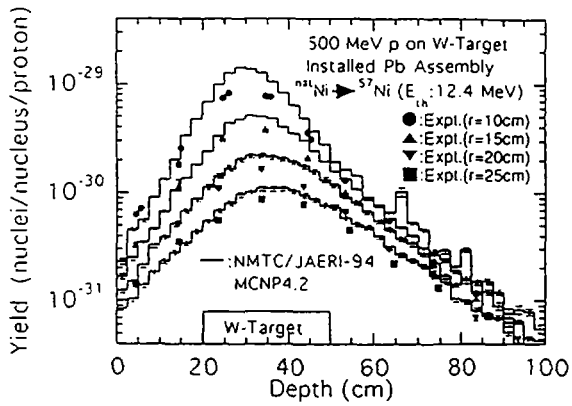

FIG. 9. Experimental and calculated yields of ^{57}Ni in ^{nat}Ni samples inserted into a tungsten target installed Lead assembly for 500 MeV proton bombardment. The solid marks stand for the experimental data at the radial positions of 10, 15, 20 and 25 cm, respectively. The solid lines represent the calculated results of NMTC/JAERI and MCNP4.2.

protons and the macroscopic total cross sections. The range is 12 cm in tungsten and 19 cm in Lead. The macroscopic total cross section of tungsten is about twice as large as that of Lead. Therefore, the spallation neutron has a much greater possibility to lose its energy by collision in tungsten than in Lead.

Figure 8 shows the measured and the calculated spatial distributions of the yield of ^{56}Co in a ^{nat}Ni sample at the radial positions of 10 and 20 cm in the tungsten target installed Lead assembly. The threshold energy of the reaction is 20 MeV. It is observed that the results calculated with the modified total cross sections improve on the ones obtained with the geometric cross sections and are in reasonable agreement with the measured data, although overestimations up to about 40% are seen.

In Figs 9 to 12, comparisons are made between the calculated and the measured results for the reactions of ^{nat}Ni(n,x)^{57}Ni and Al(n,x)^{24}Na,

respectively. The threshold energies for these reactions are 12.4 and 3.9 MeV, respectively. In the results for $^{nat}Ni(n,x)^{57}Ni$, good agreement is obtained between experimental and the calculated results for both tungsten and Lead targets although slight overestimation is observed in the calculated results for the tungsten target in comparison with those for the Lead target. For the yield of $Al(n,xn)^{24}Na$, the calculated results are in good agreement with the experimental results for the tungsten target. For the Lead target, however, the calculation underestimates the experiment by about 50%. This discrepancy becomes significant as the longitudinal distance increases.

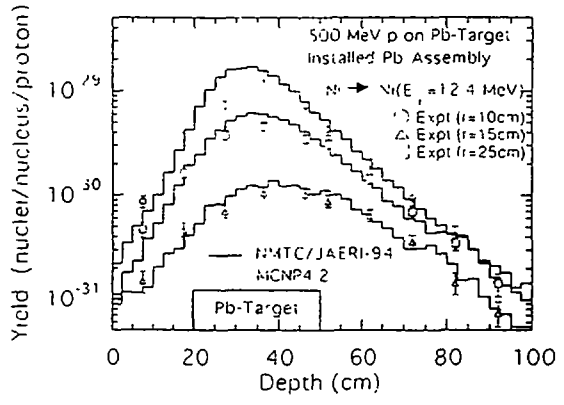

FIG. 10. Experimental and calculated yields of ^{57}Ni in ^{nat}Ni samples inserted into a Lead target installed Lead assembly for 500 MeV proton bombardment. The open marks stand for the experimental data at the radial positions of 10, 15 and 25 cm, respectively. The solid lines represent the calculated results of NMTC/JAERI and MCNP4.2.

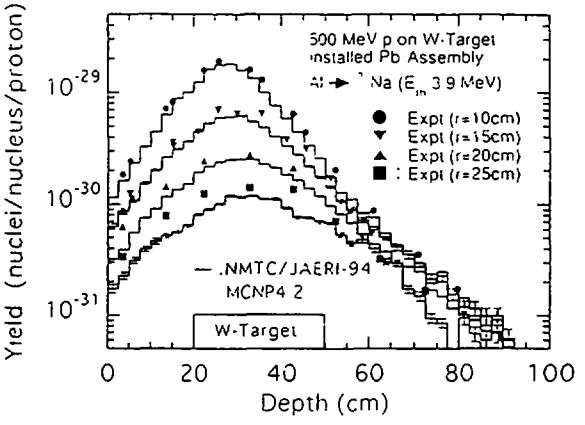

FIG. 11. Experimental and calculated yields of ^{24}Na in Al samples inserted into a tungsten target installed Lead assembly for 500 MeV proton bombardment. The solid marks and the solid lines represent are the same as for Fig. 9.

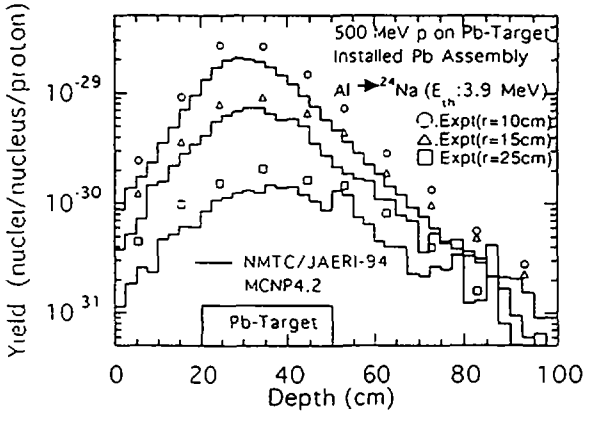

FIG. 12. Experimental and calculated yields of ^{24}Na in Al samples inserted into a Lead target installed Lead assembly for 500 MeV proton bombardment. The open marks and the solid lines represent are the same as for Fig. 10.

Figures 13 and 14 show the cross sections of the reactions of $^{nat}Ni(n,x)^{57}Ni$ and $Al(n,x)^{24}Na$, respectively. The results of NUCLEUS, which were used in the calculation of nuclide yield in the Lead assembly, are compared with the measured cross sections [34, 35] in these figures. It is observed that the calculated results overestimated the measured data of $^{nat}Ni(n,x)^{57}Ni$ by about a factor of 2. In contrast, NUCLEUS gives a cross section lower than the experimental one by about 40% for $Al(n,x)^{24}Na$. These discrepancies indicate that the approximation made in the intranuclear cascade evaporation (INCE) model is too crude to predict nuclear reactions in the tens of MeV region.

In Figs 15 and 16, calculated neutron energy spectra are compared with the experimental ones for 500 MeV and 1.5 GeV incident protons, respectively. In both cases, the calculated results reproduce the experimental ones successfully in

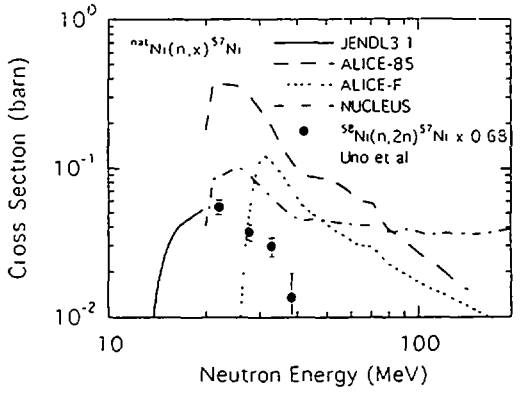

FIG. 13. Cross section of $^{nat}Ni(n,x)^{57}Ni$ reaction. Solid lines represent the values compiled in the JENDL3.1. The dotted, dashed and dot-dashed lines stand for the calculated results of ALICE-F, ALICE-85 and NUCLEUS, respectively. The solid circle indicates the measured data [34] for $^{58}Ni(n,2n)^{57}Ni$ reaction normalized to the fraction of ^{58}Ni in ^{nat}Ni.

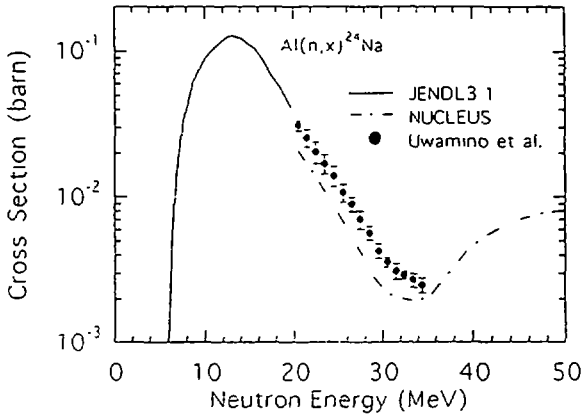

FIG. 14. Cross section of $Al(n,x)^{24}Na$ reaction. Solid lines represent the values compiled in the JENDL3.1. The dot-dashed line stand for the calculated results of NUCLEUS. The solid circle indicates the measured data [35].

the energy region below 10 MeV although a slight underestimation is seen in the results at backward angles beyond 90°. On the other hand, the calculation underestimates the experimental results in the energy region between 20 and 100 MeV at all angles. Since the similar discrepancies are observed between the calculated and experimental results on the differential cross section measurements, it is necessary to improve the INCE model.

Judging from the present predictive power for the neutron energy spectrum and the nuclide production cross sections shown in Figs 13 to 16, it is consistent that the calculated nuclide yields are lower than the experimental results for the $Al(n,x)^{24}Na$ reaction in the case of a Lead target. As for the results for $^{nat}Ni(n,x)^{57}Ni$, reasonable agreement is obtained as a result of a cancellation of the overestimated nuclide production cross section and the underestimation of the neutron energy spectrum.

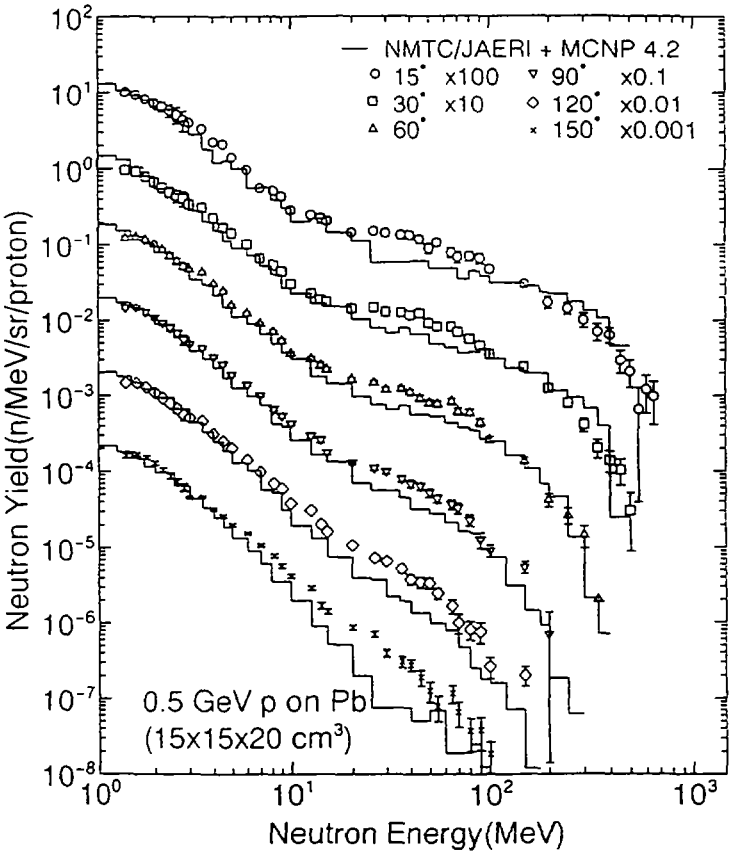

FIG. 15 Experimental and calculated leakage neutron energy spectrum from thick Lead target of 15 by 15 cm width and 20 cm in length bombarded by 500 MeV protons. Open marks indicate the experimental results at emission angles from 15° to 120°. Solid lines stand for the calculated results with NMTC/JAERI and MCNP4.2.

D.1.4.4. PRELIMINARY STUDY FOR TARGET-BLANKET EXPERIMENTS IN OMEGA NUCLEAR ENERGY FACILITY

In this section, we give an overview of the experimental subjects through a preliminary neutronic and hydraulic analysis of the subcritical blanket of the solid system [3] which is composed of a tungsten target and actinide metal alloy fuels cooled with liquid sodium. The size of the subcritical blanket was 140 cm in diameter and 140 cm in length; the diameter of the tungsten target installed at the center of the blanket was 40 cm. The effective multiplication factor of the blanket is 0.89. The calculated results were obtained under the condition that 1.5 GeV protons with a current of 10 mA were injected in the tungsten target with a uniform circular configuration. Figures 17 and 18 show the neutron flux distribution in the subcritical blanket with energies above 1 and 50 MeV, respectively.

It is seen that the high energy neutrons are produced near the point of incidence and diverge in the forward direction. The distribution of the neutrons above 1 MeV has a peak value in the blanket region near the surface of the tungsten region. This is because the multiplication of neutrons by the fission reaction contributes predominantly near the surface of the tungsten target. From the experience of the integral experiment described in the previous section, the neutronic characteristics of the subcritical blanket, such as neutron spectra, flux distribution and fission reaction distribution can be experimentally investigated by the foil activation method with a current of nA to mA.

For a real accelerator-driven transmutation system, the target must be durable enough to be irradiated continuously for a long period. The following issues should be studied in detail: the evolution of neutronic characteristics during irradiation, the change of mechanical characteristics induced by radiation damage and the corrosion in the cooling system. It is reported [36] that a water cooled spallation target made of tantalum has been irradiated through 1500 mAh without observing any radiation damage at ISIS, but corrosion was found in the cooling system in the case of a bare tungsten target used at LANSCE.

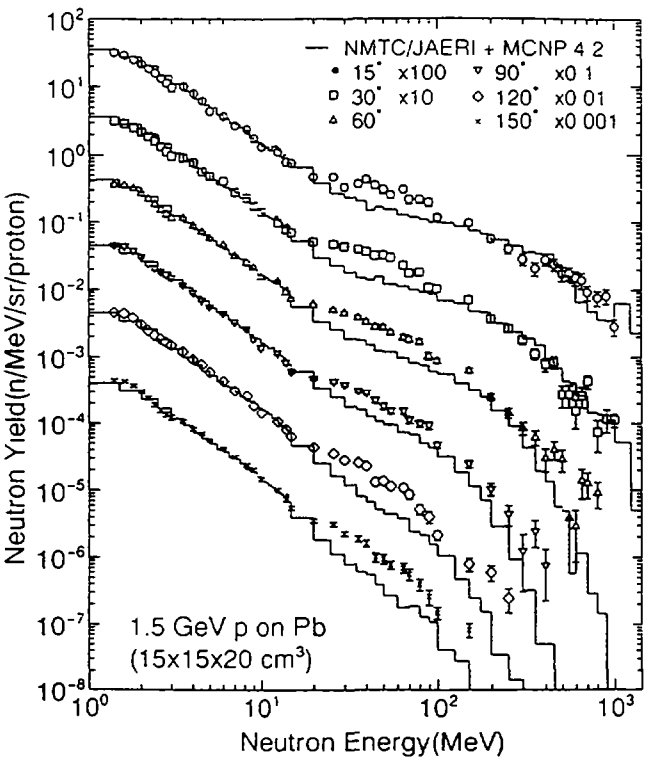

FIG. 16. Experimental and calculated leakage neutron energy spectrum from thick Lead target of 15 by 15 cm width and 20 cm in length bombarded by 1.5 GeV protons. Open marks indicate the experimental results at emission angles from 15° to 150°. Solid lines stand for the calculated results with NMTC/JAERI and MCNP4.2.

In order to estimate the strength of the target, it is necessary to know the accumulation of spallation products during the irradiation time. Figure 19 shows the calculated nuclide yield by spallation reactions above 15 MeV in a tungsten target after 10 days operation with a current of 10 mA. This calculation was made without taking into consideration the change of composition of the target nuclides. It is expected from these results that the neutron yield might not decrease as fast because most of the products have a mass number close to tungsten.

When an accelerator is used a beam window is required to separate the high vacuum regime and the

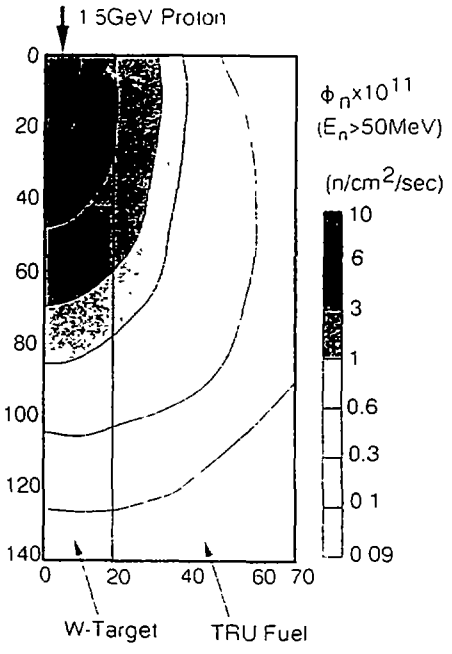

FIG. 17. Calculated neutron flux distribution with the energies higher than 1 MeV for 1.5 GeV protons with the current of 10 mA incidence on the tungsten target installed subcritical blanket [3] for actinide transmutation.

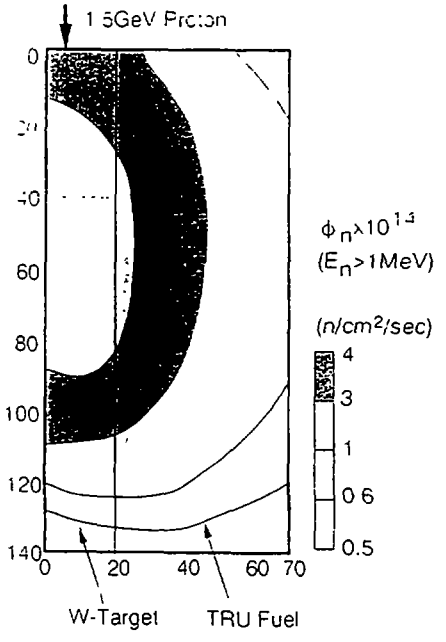

FIG. 18. Calculated neutron flux distribution with the energies higher than 50 MeV for 1.5 GeV protons with the current of 10 mA incidence on the tungsten target installed subcritical blanket [3] for actinide transmutation.

environment. Since the beam window is exposed to a high current beam, it is necessary to cool the window to remove the heat produced. In the design of a solid target system, the window is assumed to be cooled by slightly pressurized coolant which flows from the target region. In a spallation neutron source facility, it is ensured [36] that the allowable current density is 80 μA/cm^2 at the beam window. In a transmutation system the proton beam injected in the target is designed to have diameter of several tens of cm so that heat production is suppressed. This reduces the current density limit to 3 μA/cm^2 for a total current of 10 mA through a semi-spherical beam window of 46 cm in diameter.

In Fig. 20, the calculated stress generated in oxide dispersed strengthened (ODS) steel is shown as a function of beam current. It is evident that the stress increases as the beam current increases. In order to use ODS steel safely, the amount of stress has to be suppressed below the creep rupture strength. The result indicates that the window can be used in the allowable range even at 80 mA if the thickness is chosen to be 1 mm. As the radiation damage evolves with irradiation, however, the creep rupture strength becomes smaller than 230 MPa. If the strength decreases down to 100 MPa, a beam current of 40 mA cannot be allowed. It is important therefore to obtain elemental data on the change of mechanical characteristics as radiation damage accumulates. The use of a high current beam is expected to shorten the irradiation time within which the required amount of damage is accumulated.

D.1.4.5. CONCLUDING REMARKS

The neutron energy spectrum from a thick Lead target and nuclide yield distributions of various threshold reactions in a Lead assembly have been measured using 500 MeV protons. Calculations using the codes NMTC/JAERI and MCNP4.2, which are used for the neutronics calculation of the accelerator-driven subcritical system, reproduced the low energy component with the energy lower than 10 MeV well but underestimated the neutron yield from 20 to 100 MeV.

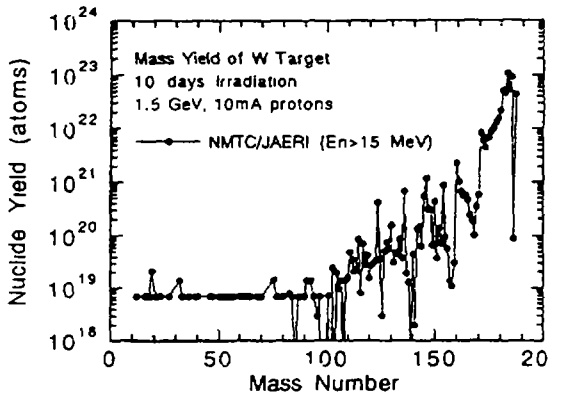

FIG. 19. Calculated mass yield in a tungsten target of 40 cm in diameter and 140 cm in length which contains sodium coolant of 50 vol%. The solid marks indicate the calculated results of NMTC/JAERI in the energy region above 15 MeV.

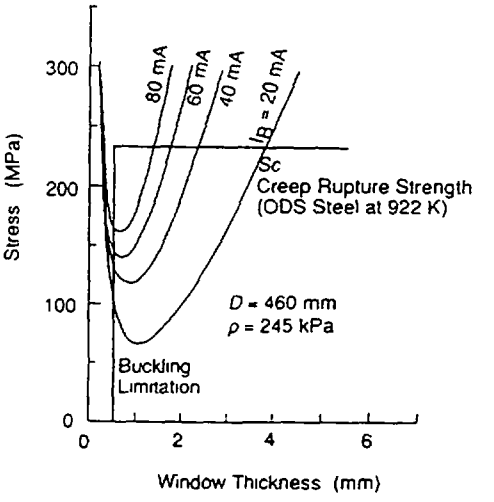

FIG. 20. Estimated stress generated in oxide dispersed strengthened steel with the configuration of a semi-sphere of 460 mm in diameter under a pressure of 245 kPa.

In the analysis of the nuclide yield distribution in the Lead assembly, the calculated results reproduced the shape of the measured nuclide yield distribution. Because of the ambiguity in the predictive power of the INCE model for the nuclide production cross section, the degree of the agreement differs from reaction to reaction. Based on the present results, it has been concluded that the code system composed of NMTC/JAERI and MCNP4.2 can estimate the nuclide yield through neutron induced reactions with a threshold energy up to a couple of tens of MeV, within a factor of two.

It has been found from the integral experiment that further improvements are required for the INCE model to remove the discrepancies in both the nuclide production cross section and the neutron energy spectrum. As has been reported in the international code comparison, inclusion of the pre-equilibrium analysis and reassessment of the various cross sections employed in the calculation code, may lead to the improvement of the predictive power of NMTC/JAERI. Moreover, a study to introduce the technique used in quantum molecular dynamics (QMD) seems likely to improve on the INCE model since the QMD has achieved a successful description of various nuclear reactions [37].

From the experimental point of view, a comparison of the yield of proton induced spallation products is being planned as the next step in our integral spallation experiment to obtain further understanding of the predictive power of NMTC/JAERI.

At the OMEGA Nuclear Energy Facility of the Proton Engineering Center, we expect to carry out a variety of experiments concerning the effect of radiation damage not only the neutronic characteristics but also the mechanical characteristics of the accelerator-based subcritical system.

REFERENCES

[1] BOWMAN, C. D., et al.: "Nuclear Energy Generation and Waste Transmutation Using an Accelerator Driven Intense Thermal Neutron Sources", Nucl. Instr. and Meth., A320 (1992) 336.

[2] TAKIZUKA, T., et al.: "Conceptual Design Study of an Accelerator-based Actinide Transmutation Plant with Sodium-cooled Solid Target/Core", (Proc. of OECD/NEA Mtg., Argonne, 1992) (1993) 398.

[3] TAKAHASHI, H., RIEF, H.: "Concept of Accelerator Based Transmutation Systems", (Proc. of Specialists' Mtg., Villigen, 1992) (1992) 2.

[4] CHUVILO, I. V., et al.: "Nuclear Fuel Cycle Using Nuclear Power Facilities Based on Subcritical Blankets Driven by the Proton Accelerator", (Proc. of Int. Conf. and Exhibition (Global '93), Seattle, 1993) (1993) 924.

[5] TAKASHITA, H., et al.: "Transmutation of Long-Lived Radioactive Nuclides", ibid. 797.

[6] NAKAHARA, Y., TSUTSUI, T.: "NMTC/JAERI A Simulation Code System for High Energy Nuclear Reactions and Nucleon Meson Transport Code", JAERI-M 82-198 (1982), (in Japanese).

[7] PRAEL, R., LICHTENSTEIN, H.: "User Guide to LCS: The LAHET Code System", LA-UR 89-3014 (1989).

[8] MEIER, M.M., et al.: "Differential Neutron Production Cross Sections and Neutron Yields from Sto pping Length Targets for 113 MeV Protons", Nucl. Sci. Eng., 102 (1989) 310.

[9] MEIER, M. M., et al.: "Differential Neutron Production Cross Sections and Neutron Yields from Stopping Length Targets for 256 MeV Protons", LA-11656-MS (1989).

[10] MEIER, M. M., et al.: "318 and 800 MeV (p,xn) Cross Sections, Radiation Effects", 96 (1986) 73.

[11] MEIER, M. M., et al.: "Differential Neutron Production Cross Sections for 597 MeV Protons", LA-UR 91-3410 (1991)

[12] AMIAN, W. B., et al.: "Differential Neutron Production Cross Sections for 800 MeV Protons", Nucl. Sci. Eng., 112 (1990) 78.

[13] TRABANDT, M.: "Preequilibrium Neutron Emission in the Reactions ^{90}Zr, ^{208}Pb(p,xn) with 80 MeV Projectiles", et al., Phys. ReV. C39 (1989) 452.

[14] SCOBEL, W., et al.: "Preequilibrium (p,n) Reactions as a Probe for the Effective Nucleon Nucleon Interaction in Multistep Direct Processes", Phys. Rev. C41 (1992) 2010.

[15] STAMER, S., et al.: "Double Differential Cross Sections for Neutron Emission Induced by 256 and 800 MeV Protons", Phys Rev. C47 (1993) 1647.

[16] BLANN, M., et al.: "International Code Comparison for Intermediate Energy Nuclear Data", OECD/NEA (1994).

[17] OECD/NEA, "Intermediate Energy Nuclear Data: Models and Codes", (Proc. of Specialists' Mtg., France) (1994).

[18] STRATTON, T. F., et al.: "Targets for Accelerator Transmutation for Waste", LA-UR 94-1182 (1994).

[19] ULLMANN, J. L., et al.: "Thick Target Spallation Product Yields From 800 MeV Protons on Tungsten", LA-UR-94-1575 (1994).

[20] VASSYLKOV, R. G., YUREVICH, V. I.: "Neutron Emission from an Extended Lead Target under the Action of Light Ions in the GeV Region.", (Proc. of 11th Mtg. of Int. Collaboration on Advanced Neutron Sources, KEK, Tsukuba, October 22-26) 1990.

[21] BELYAKOV-BODIN, V. I., et al.: "Heat Deposition in Targets Bombarded by Medium-energy Protons", Nucl. Instr. and Meth., A335 (1993) 30.

[22] ISHIBASHI, K., et al.: "Measurement of Neutron Production Double Differential Cross Sections for Incident Protons of 0.8, 1.5 and 3.0 GeV", (Proc. Int. Conf, Gatlinburg, 1994) (1994)

[23] NAKAMOTO, T., et al.: "Spallation Neutron Measurement by the Time of Flight Method with a Short Flight Path" (to be published).

[24] Proc. 1st Workshop on Proton Engineering Center, 1995, JAERI-CONF (to be published).

[25] BABA, H., et al.: "A Method of the Gamma-ray Spectrum Analysis: FORTRAN IV Programs "BOB73" for Ge(Li) Detectors and "NAISAP" for NAI(Tl) Detectors", JAERI 1227 (1973).

[26] ZUCKER, M. S., et al.: "An n-γ Pulse Discrimination System for Wide Energy Ranges", Nucl. Instr . Meth., A299 (1990) 281.

[27] DICKENS, J. K.: "SCINFUL: A Monte Carlo Based Computer Program to Determine a Scintillator Full Energy Response to Neutron Detection for E_n Between 0.1 and 80 MeV: Program Development and Comparisons of Program Predictions with Experimental Data", ORNL-6463 (1988).

[28] CECIL, R. A., et al.: "Improved Predictions of Neutron Detection Efficiency for Hydrocarbon Scintillators from 1 MeV to about 300 MeV", Nucl. Instr. Meth. 161 (1979) 439.

[29] JOHNSON, R. H., WEHRING,B. W.: "The FORIST Unfolding Code", ORNL/RSIC-40 (1976) 33

[30] BRIESMEISTER, J. F., (Ed.): "MCNP4A - A General Monte Carlo N-Particle Transport Code", LA-12625 (1993).

[31] SHIBATA, K., et al.: "Japanese Evaluated Nuclear Data Library", JAERI-1319, (1990).

[32] PEARLSTEIN, S.: "Medium Energy Nuclear Data Libraries: A Case Study, Neutron and Proton Induced Reactions in ^{56}Fe", Astrophys. J., 346 (1989) 1049.

[33] NISHIDA, T., NAKAHARA, Y., TSUTSUI, T.: "Development of a Nuclear Spallation Simulation Code and Calculations of Primary Spallation Products", JAERI-M 86-116 (1986) (in Japanese).

[34] UNO, Y., et al: "Measurement of Neutron Activation Cross Section between 15 and 40 MeV", (Proc. of Symposium, JAERI, 1993) (1993) 247.

[35] UWAMINO, Y., et al.: "Measurement of Activation Cross Sections by Using p-Be Neutrons of Energy up to 40 MeV", (Proc. Int. Conf.,Jülich, 1991) (1991) 726.

[36] BAUER, G. S., et al.: "A Target Development Program for Beamhole Spallation Neutron Sources in the Megawatt Range", (Proc. Int. Conf., Las Vegas, 1994) (1994) (in press).

[37] NIITA, K., et al.: "Unified Description of the Nuclear Reactions by Quantum Molecular Dynamics Plus Statistical Decay Model. I. The Basic Model and Analysis of the (n, xn') Reactions", Phys. Rev. C. (to be published).

[38] VERBINSKII, V. V., et al.: "The Response of Some Organic Scintillators to Fast Neutrons", (Proc. Am. Nucl. Soc., San Francisco 1964) (1964)

D.1.5. DEMONSTRATION EXPERIMENTS AT PNC

S. Tani and H. Nakamura

Power Reactor and Nuclear Fuel Development Corporation

D.1.5.1. MEASUREMENT OF CROSS SECTION

The cross sections of photonuclear reactions are important for estimation of the energy balance of the transmutation system for long-lived FPs, such as Cs-137 and Sr-90. It is known that a giant resonant peak exists in the range of 10-20MeV for most nuclides; however, most cross section data are still missing or their accuracy is not sufficient enough.

PNC is therefore planning to measure the cross sections of photo nuclear reactions precisely using a Compton suppressed Ge(Li) detector surrounding BGO scintillators. The energy resolution will be 10keV and this system will improve the sensitivity of measurements of the cross section.

D.1.5.2. GENERATION OF MONOCHROMATIC GAMMA RAY

To improve the energy balance of transmutation by photonuclear reactions, it is very effective to use monochromatic gamma rays. This makes it possible to select a gamma ray energy corresponding to that of the giant resonant peak.

The basic concept for obtaining intense monochromatic gamma rays has been proposed by K.Imasaki et. al.[1]. Figure 1 shows a schematic diagram of the experiment, which will be conducted as a collaboration between the Institute for Laser Technology, Osaka University and PNC.

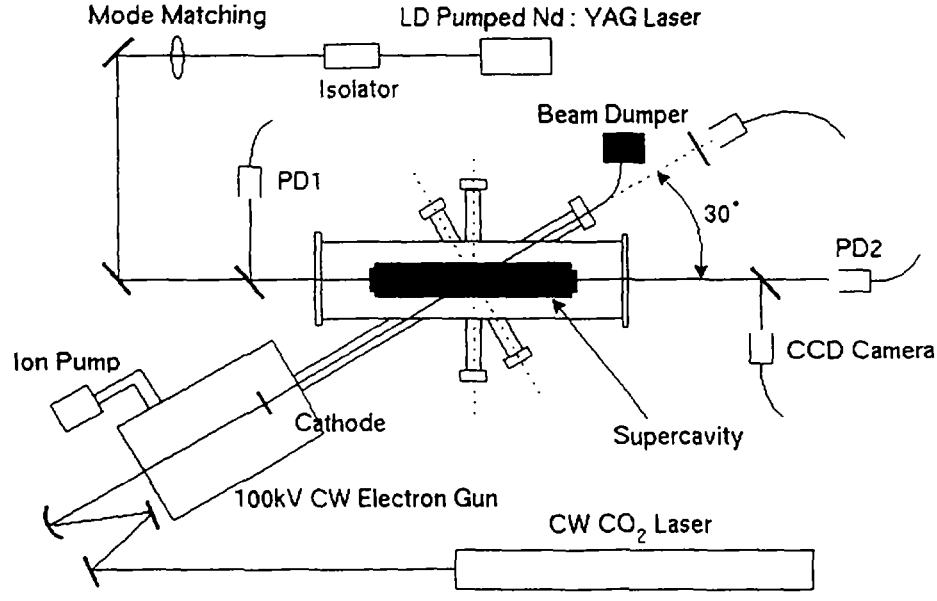

FIG. 1. Schematic diagram for monochromatic gamma ray generation.

Photons generated by an intense laser system are stored by, so called, supercavity mirrors and electrons accelerated by a high power linac are injected into the cavity. This makes the probability of Compton scattering three or four orders higher and intense monochromatic gamma rays are expected.

D.1.5.3. DEMONSTRATION OF FP TRANSMUTATION

Based on the above results, PNC would like to demonstrate FP transmutation by an electron linac. In the first step, the target design will be fixed and its resistance to enormous heat will be examined using a high power electron linac and a non-active target. Next, FP transmutation will be demonstrated using a radioactive target and preferably intense monochromatic gamma rays. Based on the test results, the design of a future transmutation system will become clearer and additional R&D items will be identified.

REFERENCE

[1] K. Imasaki et. al.,"Compact High-Brightness Radiation Sources",The Proceedings of the 16th International Free Electron Laser Conference.

D1.6. PNC - ELECTRON LINAC CONCEPT

S Tani and H Nakamura

Power Reactor and Nuclear Fuel Development Corporation

D 1 6 1 OBJECTIVE

It is quite important to pursue the possibility of transmuting long-lived fission products (FPs), especially ^{137}Cs and ^{90}Sr, because of their extremely high decay heat Significant reduction of these elements would considerably benefit safety and economy of nuclear waste storage

It is difficult to transmute most of these FPs in fission reactors, because of their smaller neutron cross sections The Power Reactor and Nuclear Fuel Development Corporation (PNC) has been studying the possibility to transmute FPs, mostly ^{137}Cs and ^{90}Sr using electron accelerator [1] The basic idea is to apply a photonuclear reaction, using gamma rays produced by the accelerator The advantages of this method are a smaller production of secondary radioactive wastes and a broader base of accelerator technology This work has been conducted as a part of the OMEGA program in JAPAN

Figure 1 shows the electron linacs in the world An extremely high power CW electron linac (e g 100MeV. 1A) will be required in a future transmutation system , because of the high production rate of the target nuclides It is quite difficult to achieve such a high power in one step Thus, an energy of 10MeV and a maximum/average current of 100mA/20mA have been selected as the present objective

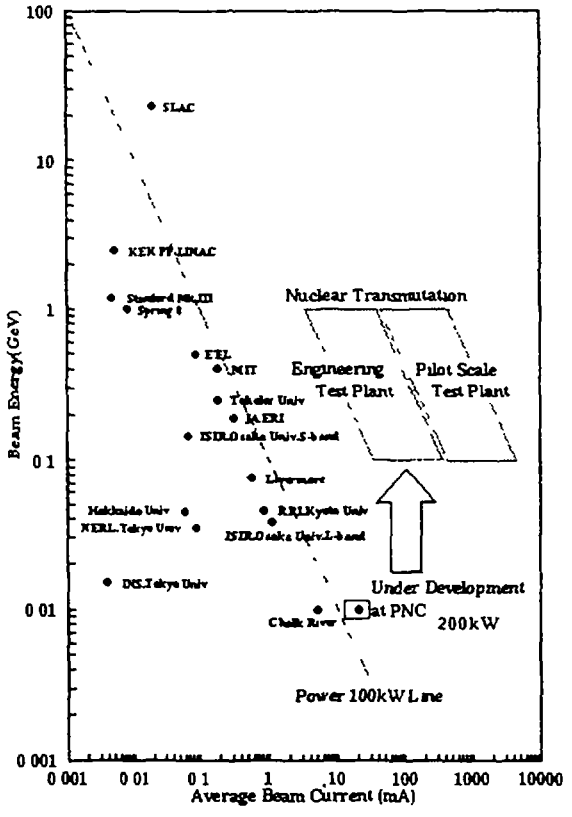

FIG 1 Electron linacs in the world

D 1 6 2 DESIGN OF THE ELECTRON LINAC

The main specification and the basic structure of the linac are shown in Table I and Fig 2, respectively The beam line consists of a 200kV DC gun, an RF chopper, a prebuncher, a buncher, accelerator guides, and a beam dump

The basic common technical challenges for a high power linac are the suppression of BBU(Beam Break Up), the removal of heat generated in the linac and the achievement of high efficiency To overcome these difficulties, various new ideas have been adopted in the design, such as a non-intercepting aperture grid for the high current electron gun, an RF chopper system for low emittance growth, the TWRR (Traveling Wave Resonant Ring) accelerator guides for good maintenance of maximum accelerator performance, a high power solid beam dump and a high power CW L-band klystron using a pill-box type window The details of the design are shown elsewhere [2].

TABLE I. MAIN SPECIFICATION OF PNC ELECTRON LINAC

Max. Beam Energy	10 MeV
Max./Ave Beam Current	100 mA / 20 mA
Pulse Length	4 ms
Beam Repetition	50 Hz
Duty Factor	20 %
Average Beam Power	200 kW
RF Frequency	1.25 GHz
Length of Microwave	24 cm
Mode of Acceleration	$2\pi/3$
Klystron Power	1.2 MW
Total Length of Linac	16 m

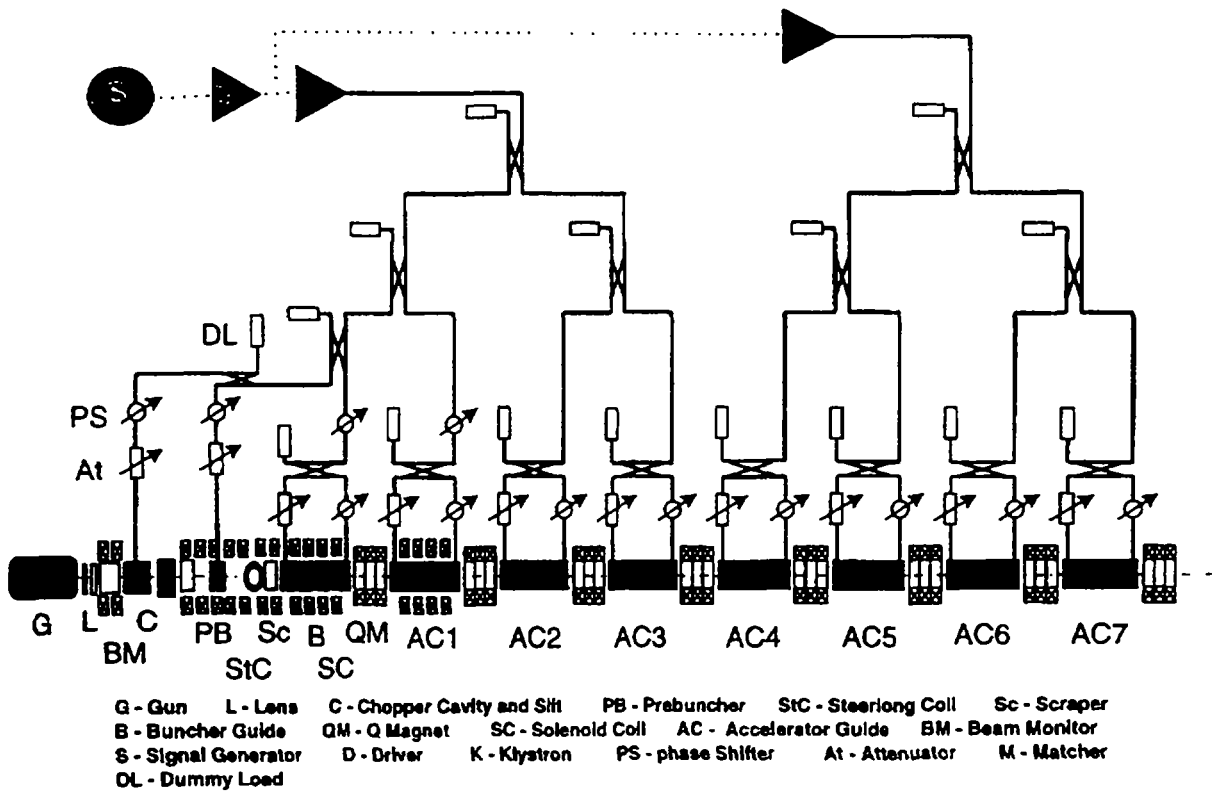

FIG. 2. Scheme of CW Electron Linac in PNC

In addition to the design and analysis, important components such as an accelerator guide and a high power L-band klystron were built and successfully validated many of the design concepts as a collaboration work between PNC and KEK (National Laboratory for High Energy Physics) in 1992. Figures 3 and 4 show the view of the TWRR and the klystron used for the test, respectively.

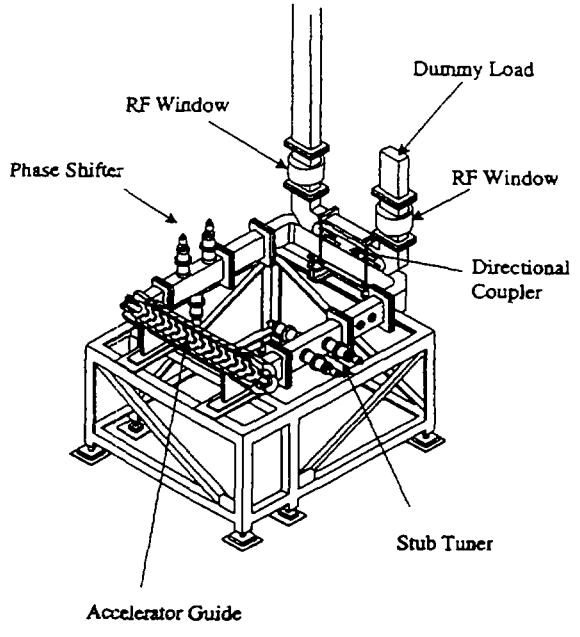

FIG. 3. Layout of traveling wave resonant ring

It was demonstrated that the accelerator guide could endure a power of 800kW, without any electric discharge or thermal deformation. Based on the test results, the klystron window was modified to increase heat resistance. The construction of the high power electron linac is in progress and all the components will be installed by March 1997.

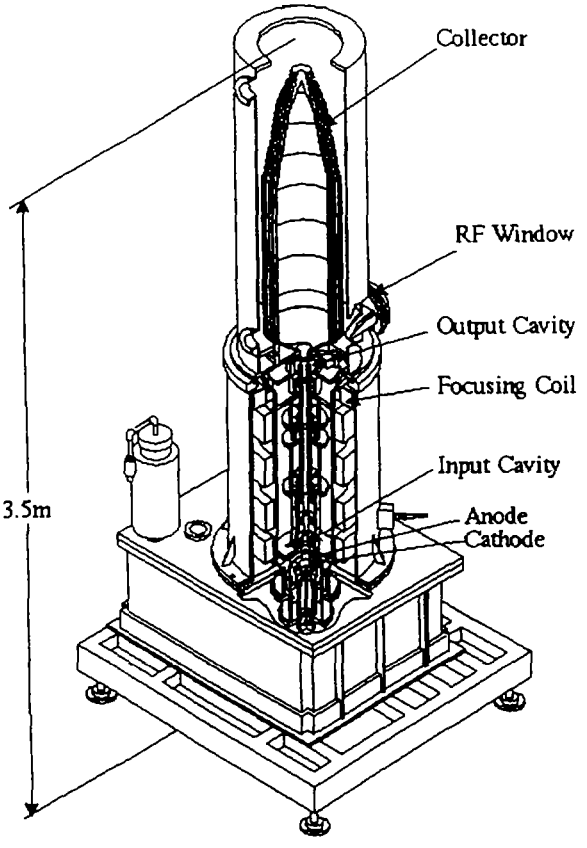

FIG. 4. High power klystron

REFERENCES

[1] H. Nakamura et. al.,"Transmutation of Fission Products through Accelerators", 3rd International Exchange Meeting on Actinide and Fission Product Partitioning and Transmutation.

[2] T. Emoto et. al.,"PNC High Power CW Electron Linac Status", Proceedings of the 1994 International Linac Conference.

D.2. LOS ALAMOS NATIONAL LABORATORY ADS PROJECTS

D.2.1. BASIS AND OBJECTIVES OF THE LOS ALAMOS ACCELERATOR DRIVEN TRANSMUTATION TECHNOLOGY PROJECT

Charles D. Bowman

LER-ADTT, Los Alamos National Laboratory

Los Alamos, NM 87545 USA

The Accelerator-Driven Transmutation Technology (ADTT) Project carries three approaches for dealing with waste from the defense and commercial nuclear energy enterprise. First, the problem of excess weapons Plutonium in the U. S. and Russia originating both from stockpile reductions and from defense production site clean-up is one of significant current and long-term concern. The ADTT technology offers the possibility of almost complete destruction of this Plutonium by fission. The technology might be particularly effective for destruction of the low quality Plutonium from defense site clean-up since the system does not require the fabrication of the waste into fuel assemblies and can tolerate a high level of impurities in the feed stream. Second, the ADTT system also can destroy the Plutonium, other higher actinide, and long-lived fission product from commercial nuclear waste which now can only be dealt with by geologic storage. And finally, and probably most importantly the system can be used for the production of virtually unlimited electric power from Thorium with concurrent destruction of its long-lived waste components so that geologic containment for them is not required. In addition Plutonium is not a significant by product of the power generation so that non-proliferation concerns about nuclear power are almost completely eliminated. All of the ADTT systems operate with an accelerator supplementing the neutrons which in reactors are provided only by the fission process, and therefore the system can be designed to eliminate the possibility of a runaway chain reaction. The means for integration of the accelerator into nuclear power technology in order to make these benefits possible is described including estimates of accelerator operating parameters required for the three objectives.

D.2.1.1. INTRODUCTION

Concerns about waste from the defense and commercial nuclear sectors has grown to such an extent in recent years that it now dominates the nuclear enterprise. The emphasis in the nuclear technology field has moved from its earlier reactor-design focus into clean-up of defense production sites and a resolution of the commercial nuclear waste problem. The development of cleaner and safer systems for nuclear energy generation is almost at a standstill because of growing international concerns about the waste issues. The predominant approach to this problem for the past thirty years has been the geologic storage of waste whether it be from the defense or the commercial sector. Geologic storage offers the prospect of confining nuclear waste by the features of a stable geologic structure rather than relying on long-term containment of the waste in man-made containers. In addition the waste is made much less accessible by its placement deep underground. Therefore many countries are providing significant funding for the development and siting of geologic waste storage facilities. While a number of sites might be under study in a given country, the intent is to provide a single site capable of confining the high level waste.

It has become increasingly difficult to convince a community to become host to a nation's single site for storage of waste which many consider to be the nation's most dangerous. The fact that the waste remains dangerous for many tens of thousands of years exacerbates these concerns. The concern that such repositories can become mines for Plutonium has become of even greater concern as the U. S. has made it known that dangerous nuclear weapons can be made from commercial Plutonium [1]. The natural

transformation of commercial Plutonium into weapons Plutonium by radioactive decay[1] means that eventually many thousands of tons of weapons Plutonium will be stored at many sites around the world. Some are becoming concerned about the possibility of natural or induced supercriticality of fissile material stored underground [2]. As a consequence of these and other concerns remaining to be resolved about geologic storage, no nation is expected to begin emplacement of high level waste in a geologic repository before the year 2010 and the ultimate viability of the geologic storage concept remains to be demonstrated.

The world is therefore in need of an acceptably priced and safe alternative to the geologic storage concept. In the U. S. commercial nuclear waste is accumulating at reactor sites and the defense site clean-up effort is struggling to understand what will happen to the Plutonium and other high-level waste which will be gathered together after the clean-up has been completed. The Los Alamos National Laboratory along with a rapidly developing national and international community has therefore been studying Accelerator-Driven Transmutation Technology (ADTT) as a possible means of destruction of this nuclear waste and of generating nuclear power by systems which do not generate the most dangerous components of this waste and which concurrently destroy their own waste. If the full capability of the ADTT systems can be realized at acceptable cost, geologic storage of defense and commercial waste would not be required.

The main elements and function of an ADTT system are illustrated in Fig. 1 for a system which generates nuclear energy from Thorium, avoids the production of Plutonium and concurrently destroys its long-lived high-level fission product waste. This system is referred to as Accelerator-Driven Energy Production (ADEP). The system starts with benign ^{232}Th and converts it by neutron absorption into the excellent fissile fuel ^{233}U from which electric power is produced. The system consists of a reactor-like component referred to in the figure as the target-blanket which contains the fissile material and the waste to be destroyed. For a reactor each fission on average produces enough neutrons after losses to cause another fission so that the chain of fissions is continuous. For all ADTT systems, the losses are made somewhat larger by the expenditure of neutrons on waste destruction so that there are about 5-10 % fewer neutrons than necessary to maintain the chain. Therefore by itself the system is totally passive and inoperative. However, by making up for the 5-10 % loss of neutrons from an external neutron source, the system would function effectively even though the chain reaction would not be self-sustaining.

The essential conceptual difference between the ADTT system and a reactor is the presence of an accelerator to produce neutrons and the presence of a target inside of the reactor-like component to convert a beam of protons from the accelerator into neutrons. All electric-power-producing reactors presently operating have means for removing the heat from the system, converting it to steam, and driving generators for electric power production. These elements are also shown in Fig. 1 with most of the power being sent into the commercial grid except for 10-15 % being used to power the accelerator. Operation of the system stops when the accelerator stops because the system fission chain is not self-sustaining. For this reason the system can be made safe from a runaway chain reaction such as that which occurred at Chernobyl by entirely different means than that incorporated in other reactors, and many of the safety features required in accelerators such as control rods may be omitted.

To understand the value of the accelerator more clearly, consider a system containing ^{233}U fuel which undergoes fission with 92 % probability upon absorption of one thermal neutron and which releases 200 MeV per fission. Assume further that no neutrons are released in fission. The 100,000 MeV released by 500 such fission events would be converted with 42 % efficiency to 42,000 MeV of electric energy. The accelerator would convert this with 45 % efficiency to 18,900 MeV of proton beam power if all of the electric power were fed back to the accelerator. For a proton energy of 800 MeV, the accelerator would produce 18,900/800 = 23.6 protons. At the conversion rate of 25 neutrons per proton which probably can be achieved, a total of 23.6 × 25 = 590 neutrons per 500 fissions is possible. Upon absorption, 92 % of these neutrons would lead to fission of 543 nuclei of ^{233}U. Comparing this number with the original 500 fission events, we see that an accelerator-linked chain reaction is possible even if no neutrons were emitted

---

[1]The isotope that makes the principle difference between commercial Plutonium and weapons Plutonium is ^{240}Pu which decays with a half life of 6,600 years. After about 13,000 years commercial Plutonium containing about 24 % ^{240}Pu transforms to weapons Plutonium containing about 6 % ^{240}Pu.

from fission[1] Of course instead of no neutrons per fission 2 49 neutrons are produced per fission of a ^{233}U nucleus so that altogether one has 590 + 500 × 2 49 = 1835 neutrons per 500 fissions for an increase in the effective number of neutrons from fission from 2 49 to 3 67 if all of the electric power from the target blanket were fed back to the accelerator This is an increase of more than one neutron per fission and is an enormous increase in the number of neutrons per fission which are available to a nuclear system designer The latter figure is far more neutrons than are required to maintain the fission process and to breed the ^{233}U from the Thorium, so that only a small portion of the electric power must be consumed by the accelerator The possibility to dial the neutron production requirement as desired and to operate effectively a system well away from criticality greatly broadens the parameter space available to the nuclear system designer

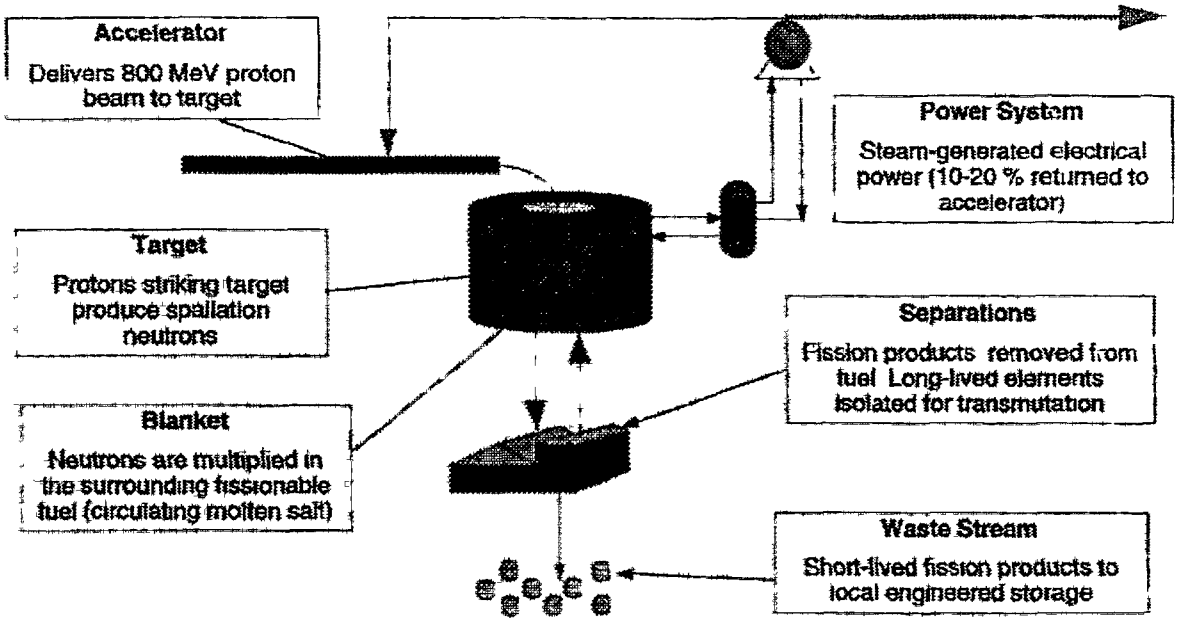

FIG 1 ADTT System Components An accelerator produces 800-MeV proton beam which is directed into a reactor-like assembly consisting of a Lead target for the beam and a surrounding blanket containing fissile material The beam strikes the liquid Lead target and produces about 22 neutrons per proton The neutrons are moderated in the surrounding blanket which consists mostly of graphite and molten salt which carries the fissile fuel as actinide fluoride The system operates at $k_{eff} = 0\ 95$ so that the system multiplies the beam-produced neutrons by about a factor of 20 The blanket contains internal heat exchangers which transfer the heat from the working salt to a secondary external salt stream and then to a steam generator for electric power production Most of the power is fed into the commercial grid but some of it is used to power the accelerator The liquid fuel allows the system to be continuously refueled and allows the waste products from fission to be continuously removed

Owing largely to the enhanced safety of the system one need no longer remain attached to solid fuel assemblies as in ordinary reactors Liquid fuel becomes an option with all of the many advantages it provides In Fig 1 we show at bottom center a loop carrying the liquid fuel outside of the target-blanket in a continuous flow An obvious advantage is that the fuel can be continuously added to the system to make up for that which is burned without shutting down for refueling as in the case of the reactor Of course, the whole process and expense of solid fuel fabrication required for the reactor is avoided as well But there is even greater benefit from the ability to remove the fission products from the liquid fuel on-line without stopping the system for removal of solid fuel assemblies By means which will be described later,

the liquid fuel can be continuously cleansed of the fission products which act as neutron poisons Those long-lived fission products which would ordinarily require geologic storage can be returned to the system to be converted by neutron absorption to stable or short-lived fission product

Since only fission product is removed from the system, there is no actinide waste except for a very small amount which slips through in the fission product separation process Because the long-lived waste is destroyed, the only waste from the system is the short-lived and stable fission product This waste is made up of a number of different species but none of the waste species have half-lives longer than 30 years Containers can be made to confine this remnant waste until the radioactivity has decayed away by a factor of 1,000 or so Geologic confinement of the waste is not required because, as is shown later, the remnant waste can be made to satisfy near surface disposal criteria of the NRC and the EPA If the site of the ADEP system meets the criteria for near-surface disposal, the waste need not leave the site Therefore only benign Thorium need be brought to the site and no waste need be carried away

More will be said later about the Thorium-burning system about weapons Plutonium and commercial waste destruction, and the relationship between the latter two technologies

D 2 1 2 TARGET-BLANKET DESCRIPTION

More detail on the target-blanket system is shown in Fig. 2 The system consists of a stainless steel tank which contains graphite blocks for neutron moderation and reflection and a molten salt carrier for the fertile and fissile fuel which will be described below The graphite and molten salt are known to be compatible with one another from extensive experience at Oak Ridge National Laboratory with the Molten Salt Reactor

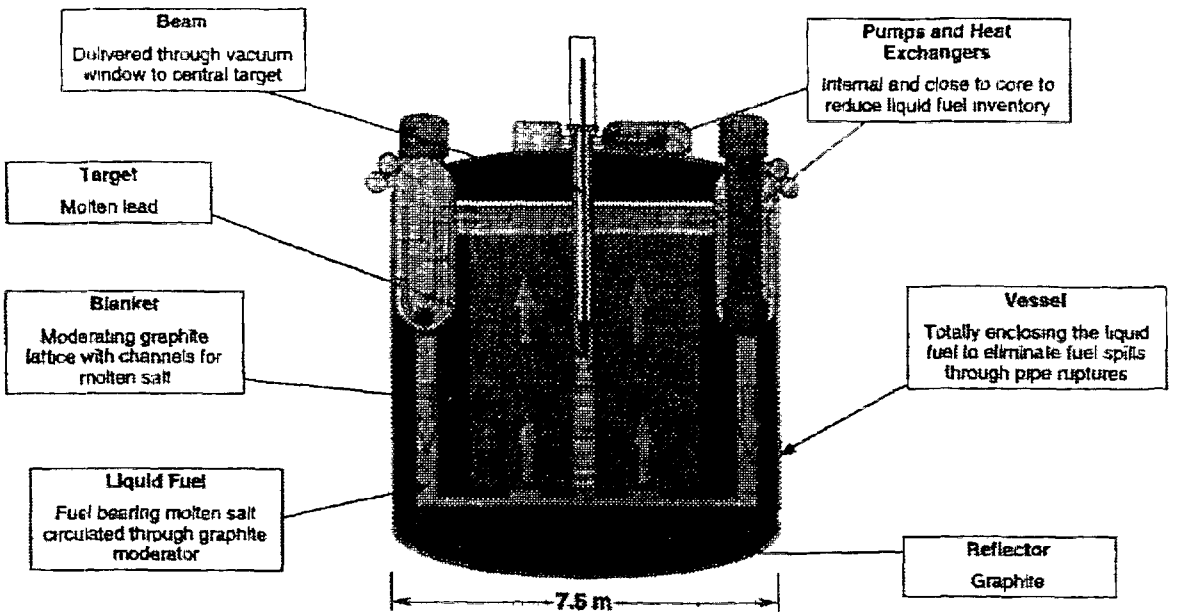

FIG 2 Target blanket function The proton beam enters through a window at the top of the system and strikes a liquid Lead target at the center The Lead is circulated and cooled from above Five layers of graphite blocks are shown which moderate the neutrons The molten salt fuel flows upward through holes in the blocks and to the outside through pumps and heat exchangers and back to the bottom Graphite on all sides serves as a neutron reflector A cover-gas of helium collects the volatile species and carries them away for appropriate separations

Experiment (MSRE) [5]. The molten salt flows upward through holes in the graphite blocks across the top of the system to internal magnetic pumps and heat exchangers and back to the bottom of the system. The heat from fission is transferred in the heat exchangers to an external salt loop which carries the heat to steam generators for electric power production. The molten salt is a $LiF\text{-}BeF_2$ eutectic which melts at about 450 degrees centigrade and operates at between 650 and 720 °C. Almost all elements react as fluorides and can be dissolved in small but adequate amounts into the carrier salt for the transmutation and fission requirements. A cover gas of helium is circulated above the molten salt to collect and remove the noble gas and volatile fluoride fission products from the salt. The molten salt never leaves the tank, except for a small slip-stream for on-line refueling and waste removal, and therefore there is no possibility for spillage of the salt through pipe breaks.

Other liquids such as water could be chosen for the carrier. However the salt has the advantage of being an excellent solvent for almost any of the elements present in the system. It also has a low vapor pressure at high temperature which is a major safety advantage allowing operation without a pressure vessel which would be required for a higher vapor pressure medium such as water. The higher operating temperature allows a thermal-to-electric efficiency which might be as high as 44 %. Also the salt is non-reactive with air, nitrogen, or concrete, in contrast with for example, the liquid sodium coolant on which fast reactor technology is now based.

The neutrons are produced at the center in a liquid Lead target. Protons enter from the top through a window and are stopped in the Lead, with the Lead pump and heat exchanger on top of the tank. The Lead is confined by metal resistant to corrosion by the Lead. Since the corrosion properties of the Lead are different from those of the molten salt, the Lead and salt are separated by an inner container compatible with the Lead and an outer container compatible with the salt. The metal for the salt containment probably will be Hastelloy-N developed for the MSRE and for the Lead it probably will be Inconel.

The system operates at a k_{eff} of about 0.95 compared to $k_{eff} = 1$ for a reactor. The neutrons produced by the accelerator therefore are multiplied by a factor of about 20 for and therefore an ADEP system producing power from Thorium with a fission power of 250 MW_t for an electric power output of 100 MW would require an accelerator capable of producing 6 ma at 800 MeV and consuming 11 MW of electric power. The thermal-to-electric conversion efficiency for such a system would be 44 %. The bussbar-to-beam efficiency would be 45 %.

All systems which produce nuclear power from fission must protect against a potential loss of coolant accident (LOCA) which might occur when the primary coolant system fails and the fission product decay heat builds to dangerous levels. The nuclear reactors now operating have active redundant systems which come into action when the coolant system fails. Newer designs for reactors include passive means to deal with this situation. For example the power density and total power capacity of the reactor might be kept small enough so that the heat can be transferred to the outside of the reactor vessel and from there away from the system into the surroundings by convection or radiant heat loss. The power of such a passive system is usually limited by the rate of heat transfer to the vessel with the components at the center of the reactor being at highest risk.

The ADTT systems are also designed with passive capability for after-heat removal. They have the advantage over water-containing systems that the temperature can be allowed to rise much higher because the ADTT system contains mostly low vapor pressure high melting or vaporization temperature materials such as graphite and molten salt. Therefore much higher temperatures can be tolerated in the ADTT systems without risk of internal damage or dangerously high pressures. In addition to the use of liquid fuel, the incorporation of an internal inside-to-outside flow path and natural convection both contribute to enhanced heat transfer from the inside to the outer wall of the blanket. Therefore ADTT systems can be designed for substantially higher electric power capacity than conventional reactors while still maintaining the passive heat removal capability.

From the beginning of the development of the ADTT program, the discussion has continued as to whether the ADTT system requires a geologic storage facility as back-up for the untransmuted waste. The purpose of this section is to address the question of the requirement for geologic storage of remnant waste after destruction of the actinide and the long lived constituents of the fission products. It will be shown here that near-surface storage of this waste might be made consistent with existing NRC and EPA regulations with an addition to the regulations for storage of Cs, Sr, and Kr for about 200 years until they meet low-level radioactivity levels covered by existing regulations.

D.2.1.3.1. Review of Regulations

To begin the discussion, it is useful to review several aspects of near-surface waste storage. Waste destined for near-surface storage is divided into three classifications as class A, B, and C waste.

Class A waste is the most benign and it can be stored at the surface without stabilization. That is, no special precautions must be made to protect the system from natural dispersion mechanisms such as rainfall, wind, etc. There are of course some restrictions such as exclusion from flood plains and from unstable land. The site must be clearly marked, and monitored for 100 years but no fencing is required. After that time it is assumed that controls are no longer operative and that the site should not be dangerous to an inadvertent intruder. An inadvertent intruder is defined in NRC Regulation 10 CFR 61.2 as;

"a person who might occupy the disposal site after closure and engage in normal activities such as agriculture, dwelling construction, or other pursuits in which the person might be unknowingly exposed to radiation from the waste."

Class B waste must be immobilized or contained by components in the waste site that maintain their "gross physical properties and identity" for 300 years. Surface storage is permitted and institutional control is required for 100 years. Productive use of the land during this 100-year period is possible so long as the "integrity and long-term performance of the site are not disturbed." Therefore the site perhaps might be used as a parking lot. Elsewhere in 10 CFR 61 the use of concrete in such systems is suggested and it is proposed later in this report to use that means for immobilization.

Class C is reserved for waste with even greater radioactivity concentrations. This waste also requires stabilized waste forms or waste containers. This waste must be stored at least five meters below the ground surface such that after 500 years the waste would not be a hazard to an inadvertent intruder or to the public health and safety.

There is no absolute limit on the amount of radioactivity which can be emplaced at one site, whether designated Class A, B, or C. The amount is only limited by the radiation released to the surroundings and risk to an inadvertent intruder. The radiation released from the site "must not result in an annual dose exceeding 25 millirems to the whole body, 75 millirems to the thyroid, and 25 millirems to any other organ of any member of the public." This release criterion for near surface disposal is the same as that for a single geologic storage system built to confine all of the radioactive waste of the nation. The siting criteria for surface storage of waste are specifically stated in 10 CFR 60 and are easily met so that such facilities can be sited almost anywhere except in flood plains, areas of unstable land, etc. Therefore there could be many such sites and almost certainly many more than one in every state. If there were 100 such sites in the U. S., the total radioactivity burden in a single site could be 1/100 of that at a national central repository. If in addition these sites were receiving the remnant waste from an ADTT system which reduces the long lived constituents by a factor of about 1000, the long-lived radioactive waste burden for any single site would be smaller by a factor of 100,000 than that of a single geologic repository without transmutation. It therefore seems likely that the surface storage sites for remnant waste following transmutation could meet the whole body and specific organ dose limits for a much smaller radiation source term even though the confinement capability of the surface site would be less than that from a geologic site. This probably would

have to be demonstrated on a site-by-site basis.

It might be argued that if the waste is distributed over 100 sites instead of a single geologic site, that more people would be endangered. The spirit of the release limit however is that the dose received be too low to risk harm to the surrounding population. Therefore the same release limits apply to each of the many low-level waste sites as apply to a geologic storage site for the nation's entire commercial spent fuel. The number of people exposed is considered not to be a factor because no member of the public is to be subjected to a dangerous dose from any waste site...either high or low level.

The other type of restriction for the inadvertent intruder into the site relates to the concentration of the waste and to whether the waste stream from a transmutation system meets the concentration limits for class A, B, or C waste. Classes B and C waste require stabilization before emplacement. The method of stabilization chosen for this report is mixing with concrete, a material already mentioned in 10 CFR 60 as appropriate for use in surface storage systems. The stabilization before emplacement as required by the regulations will obviously result in the dilution of the waste. There are no statements in the regulations about the degree of the dilution allowable....only limits regarding radiation release to the surroundings and dose to the inadvertent intruder , which depend on dose concentration. Weakly contaminated dirt which is being cleaned up from some of the sites at Los Alamos and elsewhere can be disposed of in surface storage if the contaminated material meets the regulatory limits for radiation release or dose to an inadvertent intruder. For the remnant waste after transmutation from a 3000 MW_t commercial reactor, we assume stabilization with 50 m^3 of concrete per year. Assuming the waste to be Class C, these blocks which might be 1m × 1m × 2 m = $2m^3$ would have to be stored under 5 meters of overburden according to 10 CFR 60. If stacked end-on, one year's remnant waste from a 3000 MW_t system would occupy a surface area of 5m × 5m. The waste from 35 years of operation of the facility would therefore occupy approximately a 30 m by 30 m area. Since the land can be put to some beneficial use, this area would be much smaller than a 3000 MW_t plant's parking lot and could be used as a small part of the plant's parking lot.

It would be correct to argue that stabilization amounts to dilution, but *stabilization is required* for class C storage and *dilution is not forbidden* by the regulations. In fact stabilization, which is required, demands some level of dilution by the stabilization medium. The operating criteria are (1) dose to an inadvertent intruder and (2) leakage of radiation from the site into the surrounding environment.

D.2.1.3.2. Disposition of remnant waste from ADTT systems

For ADTT the issue then is what should happen to the remnant waste stream. This stream may be considered to have three components for the accelerator-driven transmutation of waste system (ATW). We assume here a system designed to deal with the actinide and fission product waste from a single 3000 MW_t LWR thermal reactor destroying the waste at the rate that the waste is being produced in the reactor. The first components of the waste encountered in transmutation are the Uranium, which is the primary constituent of the spent fuel, and the Zirconium cladding. These components probably could be stored for reuse and are discussed later. The liquid fuel system allows the continuous feed of all of the waste left over after Uranium and Zirconium removal including both higher actinide and fission products. The ATW system destroys the higher actinide waste by fission generating an average fission power of about 750 MW_t per 3000 MW_t reactor. The liquid fuel system also allows the continuous removal of fission products. The only actinides which escape are those which contaminate the fission product removal process. We assume that the atom fraction of actinides in the fission product removal stream can be held to 1 part per 10,000 and next compare the actinide loss rate with the Class C criteria for actinides.

This is illustrated in Table I where the first four columns show the isotopes, the annual production rates, the half-lives, and the decay rates. The fifth column shows the decay rate of the 1/10,000 of the actinide escaping from the transmuter through the separations process into the fission product stream. Stabilization of this annually escaping quantity of actinide waste with 50 m^3 of concrete as described above gives the decay rate per gram of column 6. This may be compared with the class C decay rate limits for these actinides given in 10 CFR 61 and shown in column 7. Except for the shorter half-life nuclides ^{238}Pu, ^{241}Am

and ^{244}Cm, the concentrations are about a factor of 10 lower than the limits. For ^{238}Pu we use the limit given in 10 CFR 61.55 for the parent ^{242}Cm. For ^{241}Am we use the limit given for the parent ^{241}Pu. Applying the sum-of-fractions rule for combining the decay rates for several isotopes as given in paragraph (a) (7) of 10 CFR 61.55, the sum is still well below the decay rate limits. Therefore if the separations can be accomplished at the 1/10,000 level, the remnant could be disposed of as Class C waste.

A similar evaluation of fission products is summarized in Table II where those isotopes with half-lives 10 years or greater are listed along with their production rates, half-lives, and decay rates. The isotopes are divided into groups according to the treatment received and each group is discussed below.

1. ^{137}Cs, ^{135}Cs, and ^{90}Sr

These isotopes cannot be handled as near-surface low-level waste and they cannot be transmuted with significant beneficial effect using accelerators. Therefore they must be removed from the waste stream with a separation factor of 10-100. Column 6 shows the decay rate of the isotope left after the separation. Once isolated, the cesium and strontium must be stored until their radioactivity decays by about a factor of 100 or for about 200 years before they can also be disposed of as Class C waste. Containers can be built for containment for this storage period so that geologic storage is not necessary. The cans must be isolated from the public and protected so that they maintain their integrity. They must be stored with passive means for decay heat removal through this storage period. While geologic containment is not required for these relatively short-lived nuclides, they do not qualify for near-surface storage and new regulations must be developed for handling them on the transmutation site or at a central limited period storage site.

2. ^{107}Pd and ^{93}Zr

These nearly noble metals materials are almost benign with long half-lives and weak decay energies. No Class C limit is given explicitly for these in 10 CFR 61.54. However the limit for the semi-noble metal ^{94}Nb is given as 0.2 curies/m^3. It is more chemically active than either Zirconium or palladium and its decay energy is more than a factor of ten higher than both. Therefore we assume that the Class C limit for ^{107}Pd and ^{93}Zr would be at least a factor of ten higher than for ^{94}Nb and use the ^{94}Nb limit increased by a factor of ten to 2 curies/m^3 to estimate the regulatory limit. With this limit no separation of these isotopes from the rest of the fission product waste would be required before storage as Class C waste and transmutation would not be necessary.

3. ^{79}Se and ^{126}Sn

No regulatory limit has been established for these nuclides. We assume their chemical reactivity is comparable to ^{94}Nb as are their decay energies. Therefore we use the Class C limit for ^{94}Nb of 0.2 Curies/m^3. A separation of a factor of ten must be achieved to reach the assumed Class C limit for each of these. These isotopes must be transmuted.

4. ^{99}Tc, and ^{129}I

These nuclides are perhaps the most chemically mobile of the long-lived fission products and regulatory Class C limits exist for them. To reach these limits, the ^{99}Tc must be separated by a factor of 100 and the ^{129}I by a factor of 10. These nuclides must be transmuted.

5. ^{151}Sm

This nuclide exhibits a very weak decay energy and we therefore assume the limit of 2.0 curies/m^3 derived from the established limit for ^{94}Nb. To reach this limit, the separation factor must be about 300. The separated material must then be transmuted.

TABLE I. CHARACTERIZATION OF THE LONG-LIVED FISSION PRODUCT WASTES

Isotope	Annual Production (Atoms/a) $\times 10^{25}$	Halflife (years)	Decay Rate (Curies)	Separation factor and decay rate (Curies)		Concentration After Stabilization[a] (Curies/m^3)	Class C Decay Rate Limit (Curies/m^3)
^{79}Se	0.13	65,000	11.9	10	1.2	0.024	0.2
^{90}Sr	9.0	29.1	1,860,000	10	190,000	3800	7000
^{93}Zr	15	1,500,000	60	1	60	1.2	2.0
^{99}Tc	15	213,000	426	100	4.26	0.85	3.0
^{107}Pd	4.1	6,500,000	3.8	1	3.8	0.076	2.0
^{126}Sn	0.46	100,000	27	10	2.7	0.054	0.2
^{129}I	2.7	15,700,000	1.0	10	0.1	0.002	0.08
^{135}Cs	4.2	2,300,000	8.4	100	0.084	0.0017	0.08
^{137}Cs	14	30.2	2,800,000	100	28,000	560	4600
^{151}Sm	0.16	90	11,000	300	37	0.74	2.0
^{85}Kr	1.0	10.7	560,000	1	560,000		

[a] Stabilized with 50 m^3 of concrete

TABLE II CHARACTERIZATION OF THE LONG-LIVED ACTINIDE WASTES

Isotope	Annual Production (Atoms/a)	Half life (Years)	Decay Rate (Curies)	Reduction by Separation[c] (Curies)	Concentration After Stabilization[d] (Nanocuries/gram)	Class C Decay Rate Limit[a] (Nanocuries/gram)
^{238}Pu	1.13×10^{25}	88	7.5×10^{4}	7.5	68	20,000[b]
^{239}Pu	41.6×10^{25}	24,100	1.0×10^{4}	1.0	9.1	100
^{240}Pu	19.2×10^{25}	6,560	1.7×10^{4}	1.7	15.	100
^{241}Pu	6.4×10^{25}	14.4	2.7×10^{6}	270.0	2454.5	3500
^{242}Pu	3.9×10^{25}	375,000	6.1×10^{1}	.006	0.05	100
^{237}Np	3.7×10^{25}	2,140,000	1.1×10^{1}	.001	0.009	100
^{241}Am	4.1×10^{25}	433	5.5×10^{4}	5.5	50.	3500[b]
^{243}Am	0.73×10^{25}	7,370	5.9×10^{2}	.059	0.54	100

[a] Used decay limits from 10 CFR 61.55

[b] Used decay limit for parent from 10 CFR 61.55

[c] For a separation factor of 10,000

[d] Stabilization with 50 m^3 of concrete

6. ^{85}Kr

This noble gas is difficult to transmute because its cross section is small and gas-containing systems inside a nearly critical system must be avoided for criticality safety reasons. According to regulation, it must therefore be stored in 100 Curie or smaller amounts in separate containers with a volume of about 100 ml. These containers must then be immobilized in the Class C waste in accordance with 10 CFR 61.54. There are no regulatory limits to the number of containers, but 5600 would be required per year. It would therefore probably be preferable to collect the gas in yearly production volumes of about 10 m^3 and store it along with the cesium and strontium. After 200 years the container confining the remnant could be stored as Class C waste according to regulations.

Of the eleven long-lived fission products, two require no action. The other nine must be separated using eight chemical separations and five of these must be transmuted and stored as Class C waste with the other fission product. The remaining three (Kr, Sr and Cs) must be placed in engineered storage for about 200 years. After the 200-year period, the latter four can be stored permanently as Class C waste also. The five isotopes to be transmuted constitute about 6 % of the fission product and will require about 300 moles of neutrons per 3000 MW_t-year of reactor operation. These neutrons may come either from an accelerator or from the excess neutrons produced by the fission of weapons Plutonium or highly enriched Uranium. Once the five long-lived fission products have been destroyed, the remnant fission product waste can be diluted and stored in concrete at the rate of 50 m^3 per year per 3000 MW_t fission power. For the Los Alamos Thorium burner, which transmutes its own fission product and produces 200 MW_e (500 MW_t) for 35 years, the subsurface storage area required for Class C waste immobilized in concrete if stored two meters thick would be about 12 m × 12 m.

The Uranium and Zirconium cladding are nearly benign materials and could be stored in containers at some central site for probable future use. There is no apparent reason now to place them in geologic storage where they would be almost inaccessible by definition.

In summary, with transmutation and separations factors which need not exceed 10,000 and more nearly 1,000 for actinides and about 100 for fission product, remnant waste would not require geologic storage. For the on-site transmutation of the waste from a commercial nuclear power plant, the fission product immobilized in concrete could stay on the reactor site as Class C near-surface waste. The Cs, Sr, and Kr could stay or be moved in accordance with state and local government decisions. Without the need for a central geologic repository, the federal government need not become involved in the siting of waste storage facilities. Its role would be limited to providing the regulatory framework for near-surface storage.

D.2.1.4. WEAPONS PLUTONIUM DESTRUCTION (ABC SUBPROJECT OF ADTT)

This is the first of the three applications which were mentioned at the beginning of this paper and has been pursued under the acronym ABC for Accelerator-Based Conversion. Excess weapons Plutonium (w-Pu) is being made available by major reductions in the U. S. and Russian stockpile of nuclear weapons and by the clean-up of U. S. and Russian w-Pu production sites. Altogether more than 100 tons of this material exists [1] with perhaps 20 % of it being material reclaimed from the production sites. The ultimate disposition of w-Pu has been the subject of recent intensive study in the U. S. Basically three options are considered: (1) burning of the Plutonium to the point where it has roughly the same isotopic composition as commercial Plutonium (c-Pu), referred to as the "spent fuel standard" followed by geologic storage, (2) geologic storage of the w-Pu without burning after vitrification with defense radioactive waste, or (3) complete burn-up of w-Pu.

Since there is about ten times as much c-Pu as w-Pu in the world today and the c-Pu is increasing rapidly, present U. S. policy appears to favor burning the w-Pu to the spent fuel standard. The advantages of this seem to be that the w-Pu then becomes a small increment on the already larger c-Pu inventory, the

w-Pu is less effective as weapons material, the radioactivity of the burned w-Pu is a deterrent to the handling of this material in nuclear weapons fabrication, geologic storage of the burned Plutonium makes it much less accessible than it now is, and the technology to burn the w-Pu to the spent fuel standard exists now. The arguments against the spent fuel standard are that the resulting material is still quite effective for weapons construction, that it probably could be recovered from geologic storage without great difficulty, and that there is very little near-term political advantage because it will probably take 30-50 years to complete the conversion to the spent fuel standard and the placement of the material in geologic storage.

Perhaps most importantly, disposing of the material this way costs money or yields negative value from the w-Pu whereas there are clearly large positive-value uses for this material for start-up of the ADEP system and for ADTT commercial waste destruction. The destruction of commercial nuclear waste requires supplemental external neutrons all of which could be supplied by an accelerator. However the neutrons could also be supplied by fission of weapons material. The weapons materials are valuable for weapons precisely because they are an excellent source of neutrons. Each fission of ^{239}Pu produces 2.88 neutrons of which one per fission must be used to sustain the chain reaction. An additional 0.35 per fission are lost because not all neutron absorptions in ^{239}Pu lead to fission and a total of about 10 % of the neutrons per fission are lost to parasitic capture and leakage. After subtracting off these losses of neutrons, one is left with about 1.2 excess neutrons per fission available for other uses. The number of neutrons from HEU is slightly smaller. In the burning of commercial waste using the ADTT technology, the accelerator supply of neutrons can be reduced by about a factor of two by the use of w-Pu or HEU. Since the accelerator source can be reduced significantly and we know roughly what the cost of the accelerator-produced neutrons is, the price which could be paid for w-Pu and HEU in this application can be estimated from the savings in cost of the accelerator, which are relatively well known. The value for w-Pu is found to be perhaps as high as $250,000 per kilogram[3]. This value is far more than the value of HEU blended down for commercial reactor fuel. An even higher price could be paid for w-Pu and HEU for the one initial load required for the ADEP system without bootstrapping from the commercial grid using the accelerator.

If one compares the present inventory in the U. S. and Russia of w-Pu and HEU to the amount required for destruction of the world's nuclear waste, there is a surprisingly good match, so that all of these materials could be used for commercial waste destruction. It can be argued that the price quoted above is artificially high because HEU can be separated from natural Uranium at a much smaller price and that therefore a major need for either w-Pu or HEU would be satisfied by lower priced newly produced HEU. However continued production of HEU would not be consistent with international agreements to forego the enrichment of Uranium to HEU when much smaller enrichments are quite sufficient for use as fuel in all of the world's commercial nuclear power plants. International political agreements therefore probably would make it difficult or impossible to produce HEU for commercial waste destruction. Nevertheless, a user of HEU or Plutonium would argue effectively against paying the high accelerator-displacement value when it could be produced anew much more cheaply. A value higher by a factor of two than that for new HEU might be paid for existing HEU or w-Pu in which case the 100 tons of w-Pu might be valued at about $50 billion and the ten times larger amount of HEU at about $500 billion. Such high positive values for these weapons materials would be good news from the perspective of weapons material security since we willingly guard our valuables and grudgingly pay to dispose of our waste. Fortunately Russia still considers its weapons material valuable and we can expect that it will be more carefully guarded if the U. S. policy is directed toward maintaining the high value perspective. Furthermore, since the value for the material is not received until the weapons material is sold for the desired purpose, one can expect the desire for converting the book value to real value to drive the sale of the material as soon as the waste destruction facilities are able to use it. The temptation to hold on to the material for weapons purposes is countered by the high value which could be obtained when it is sold.

Quite obviously these arguments for use of the weapons material for high value purposes are inconsistent with w-Pu destruction which is the purpose of the discussion in this section of the paper. None of the three options for near-term negative value w-Pu disposition identified by the National Academy Study [1] would be favored from the perspective of ADTT. This is especially true since the burning of w-Pu (or HEU) produces many more neutrons than are required to sustain a chain reaction so that the main

purpose of the accelerator, which also is to produce surplus neutrons, is superfluous. The accelerator is however useful if high burn-up of the Plutonium is required so that there is virtually no Plutonium in the waste stream and the isotopic composition is incompatible with use of the remnant as weapons material.

Thus the Los Alamos National Laboratory has proposed an accelerator-driven subcritical system [4] in which fission product poisons are allowed to build up they consume not only the excess fission neutrons from w-Pu fission, but also the supplemental neutrons from the accelerator. The system achieves very high burn up without fuel reprocessing or fuel fabrication and refabrication. Also no chemistry for fission product removal is required. The General Atomic Corporation has proposed a program with a similar objective. Its helium-cooled graphite-moderated reactor with w-Pu fuel particles suspended in the graphite has been proposed as the first stage of w-Pu destruction. After the Pu has been burned sufficiently that it will not sustain criticality, the fuel is transferred to an accelerator-driven assembly which continues to destroy the Plutonium using accelerator-generated neutrons until k_{eff} of the system has dropped to about 0.6. The burn-up of the Los Alamos and the General Atomic systems are similar and are the highest of any of the proposed w-Pu-burning systems; neither require fuel reprocessing or fuel refabrication. Present U. S. DOE policy towards w-Pu burning seems to be to burn the Pu only to the spent fuel standard. The Los Alamos ADTT Project Office position is that preferably the w-Pu either should be burned completely or reserved for enhancing commercial spent fuel waste transmutation as described above with the latter choice much preferred.

D.2.1.5. ACCELERATOR-DRIVEN ENERGY PRODUCTION (ADEP SUBPROJECT OF ADTT)

Perhaps the most important element of the ADTT project in the long term is the Accelerator-Driven Energy Production (ADEP) which uses Thorium as a nuclear fuel. The system is based on the Th-U cycle in which ^{232}Th is converted by neutron capture to thermally fissile ^{233}U. This cycle has been studied extensively [5] for use in commercial nuclear reactor power generation. The primary objective of the molten salt reactor experiment was to show that an effective breeder reactor could be built on this cycle which produced more ^{233}U than it consumed. This reactor technology lost out to the fast breeder based on the U-Pu cycle because its breeding ratio was barely larger than unity even when fission products were promptly removed from the fuel. The U-Pu cycle showed much higher breeding ratios at a time when Plutonium was in demand rather than in excess.

A major advantage in the present climate is that the Th-U cycle produces almost no Plutonium. The Th-U cycle development program also focused on a molten salt liquid fuel program with on-line removal of fission products, and the operation of a liquid fuel reactor was demonstrated with the several-year Molten Salt Reactor Experiment (MSRE) at the Oak Ridge National Laboratory. Not only could fission products be continuously removed from this system but the liquid fuel allowed the reactor to be continuously refueled. For this reason the MSRE still holds the world record for the longest continuous chain reaction. A great deal of successful research was done on the materials to contain the salt and all of the ADTT projects rely on the materials work done for the MSRE. While the MSRE had virtually no actinide waste stream, it had the usual fission product waste and its neutron economy did not allow it to breed as much ^{233}U as it burned and still have excess neutrons left for transmutation of its fission products.

By preserving many of the design features of the MSRE and introducing an accelerator into the system, one achieves the capability to produce as much ^{233}U as is burned so that the nearly unlimited energy available in Thorium can be accessed. In addition the extra accelerator-produced neutrons enable the long-lived fission products to be avoided so that there is no long-term high-level waste stream from this system. Because of the subcriticality of the system a runaway chain reaction can be made much smaller than any reactor and perhaps the probability for such an event can be reduced truly to zero. These three features of "unlimited" energy, criticality safety, and absence of high-level waste are the highly touted features of fusion systems which have been heavily studied for the many years. We believe that we can demonstrate these benefits to society during the coming decade by merging established reactor technology with the existing highly developed accelerator technology. The system produces almost no Plutonium and it is has

excellent non-proliferation features. This system has already been described in some detail at the beginning of this report so we will concentrate mostly here on the non-proliferation features which are of vital importance for any new nuclear power system

All existing commercial reactors for production of nuclear power produce Plutonium as a by-product which is seen by many as an asset because of the additional power which can be derived from it. Others see it as a serious liability since it can be used for nuclear weapons and because of radiological concerns. The established means for separating the Plutonium for reuse in reactors produces a stream of "naked" Plutonium. This Plutonium is pure and unmixed with other material which would inhibit its usefulness in nuclear weapons. This material might be diverted in the separation facility, in storage, in transport to fuel fabrication facilities, etc. There is the fear that in some countries it will simply be stockpiled for planned or possible future use in nuclear weapons. Therefore the U. S. has followed a policy of discouraging the reprocessing of commercial spent fuel and the use of Plutonium for energy generation.

Instead the U. S. and Sweden follow a once-through cycle where the spent fuel would go directly from reactor storage to geologic repository storage. Some are concerned about the consistency of U. S. policy if the once-through policy is proposed as a waste management solution, which will promote the much greater use of nuclear power throughout the world. In that case there eventually would be many repositories spread all over the world which could be mined for Plutonium. Furthermore the reactor-grade Plutonium decays into weapons-grade Plutonium. Therefore neither reprocessing, as it is presently performed, nor once through geologic storage are entirely satisfactory solutions. The ADEP program offers the opportunity to have the benefits of nuclear energy without the weapons potential from Plutonium or other material which could be used for nuclear weapons.

The ADEP system is fed ^{232}Th and transforms it to ^{233}U which is then fissioned to obtain the nuclear electric power. After a stable equilibrium is reached, there will always be a fixed amount of ^{233}U in the system which might be accessed for nuclear weapons.

A number of non-proliferation features of the ADEP system will be described below, which limit the amount of ^{233}U available to a much lower amount than ^{239}Pu in current LWRs. They also limit its accessibility, allow simple detection of any diversion attempt, and allow low impact actions to forcefully terminate any diversion which is underway, if necessary.

Limiting the amount of fissile material present

Fast reactor technology which is being pursued in many countries around the world carries a large inventory of Plutonium. The fundamental reason for this is that the fission cross section for ^{239}Pu in the fast neutron spectrum is smaller by about a factor of 100 than that for thermal spectrum fission of ^{239}Pu. Therefore, other things being equal, the inventory for the thermal spectrum system is smaller by about a factor of 100 than for a fast spectrum system. The neutron flux for the thermal system is about a factor of ten smaller so that as a practical matter the thermal system requires about 10-30 times less material than a fast spectrum system. The same situation is true for ^{233}U when fast and thermal spectrum systems are compared. Generally speaking the ADEP system will carry about the same amount of ^{233}U as an LWR has of ^{235}U and ^{239}Pu together if the flux and power level are the same. The primary point here therefore is that the ADEP system carries a much smaller inventory of potential weapons material than the fast reactors under development in other countries.

Isotopic dilution of ^{233}U in ADEP

If the ^{233}U were diluted with ^{238}U to the 20 % level or lower, the ^{233}U would be classified as non-weapons material according to present regulations. A 500-MW_t thermal ADEP system can be brought immediately into power production by a start-up inventory of 10,000 kg of Th and 700 kg of 20 % low enriched Uranium (LEU) where the 20 % is ^{235}U. The original ^{235}U will be burned out over time and replaced with ^{233}U derived from the Thorium. The distribution of isotopes reached after ten years of operation is given in Fig. 3 where the amount is given in grams. At ten years, which is essentially

equilibrium, the Uranium fissile material inventory will be 100 kg of ^{233}U along with 10 kg of ^{235}U for a total fissile content of 110 kg. The amount of ^{238}U present at this time is about 600 kg so that the required isotopic dilution of about 20 % is maintained. However the inclusion of ^{238}U in the systems will result in the production of a small amount of ^{239}Pu. The isotopic distribution of Plutonium as 239, 240, 241, 241, and 242 is present in the amounts of 1.2, 1.2, 0.3, and 2.5 kilograms. The ratio of fissile to total Plutonium is 0.29 so that the Plutonium would be very poor quality weapons material and there would be only 5.2 kg of Plutonium altogether to be accessed.

"Raiding" the ADEP for ^{233}U through ^{233}Pa

The conversion of ^{232}Th to ^{233}U is a three-step process involving neutron capture by ^{232}Th to produce ^{233}Th which decays almost immediately to ^{233}Pa, which itself subsequently decays with a 26-day half-life to ^{233}U. Fig. 3 shows that the inventory of ^{233}Pa in the system is about 22 kilograms. If operation of the ADEP system were interrupted and the molten salt removed, it would be possible in principle to separate the ^{233}Pa before it decayed to ^{233}U from the 8000 kg of other actinide. If such a separation could be completed in about 26 days, about half of the ^{233}Pa could be recovered. When this half decayed to ^{233}U, the 11 kilograms of ^{233}U resulting would be useful weapons material. The separation in question would be a dangerous activity in view of the very high radioactivity of the salt so soon after shut-down. Ordinarily spent reactor fuel is allowed to decay 300 times longer (about 10 years) before separations begin. A further operational factor would be that the value for k_{eff} for the system would have dropped to about 0.85 from the normal value of about 0.95 by the removal of the 11 kg of ^{233}Pa. This may be compared with about 100 kg of Plutonium which could be recovered from the interruption of operation of an LWR operating at the same thermal power level. A fast spectrum reactor of similar power would carry about 1000 kg of accessible Plutonium.

With the removal of the 11 kg of ^{233}Pa, the thermal power level would have decreased by a factor of three and the net electric power into the commercial grid by a factor of about five while the accelerator power would have remained the same. The power level would recover over a period of several months, but the inconsistency between the accelerator power and the electric power output would be readily observed by infrared mapping from satellites or by other means.

Benefits from "lock-up" of ^{233}Pa

There are two disadvantages if the ^{233}Pa is allowed to circulate freely in the salt. The first is that a "raid" on the ^{233}Pa might be started by draining the salt, although the follow on separations would be exceedingly sophisticated and dangerous. The second is that performance degradation through neutron capture on ^{233}Pa limits the flux to about 2×10^{14} n/(cm^{2}s). The gain from internal isolation of the ^{233}Pa during its decay period would offer many benefits in overall system performance.

Start-up without fissile material

There might be nations which could benefit greatly from nuclear power but which are considered to be substantial proliferation risks. In those cases providing non-radioactive LEU at 20% enrichment to start up the system might be considered a proliferation risk in that much of the enrichment towards highly enriched Uranium has already been done. The start-up load might be diverted for enrichment for weapons use instead of being used for its intended purpose. The ADEP system can be brought into operation with no fissile material at all. For a system initially containing only ^{232}Th, the accelerator can be powered off the commercial grid and the neutrons produced used to produce ^{233}U. As the fission of the ^{233}U increases, the neutron flux also increases generating even more ^{233}U so that over a period of six to twelve months the system bootstraps itself to full power. No reactor existing or under development can operate with absolutely no fissile fuel load.

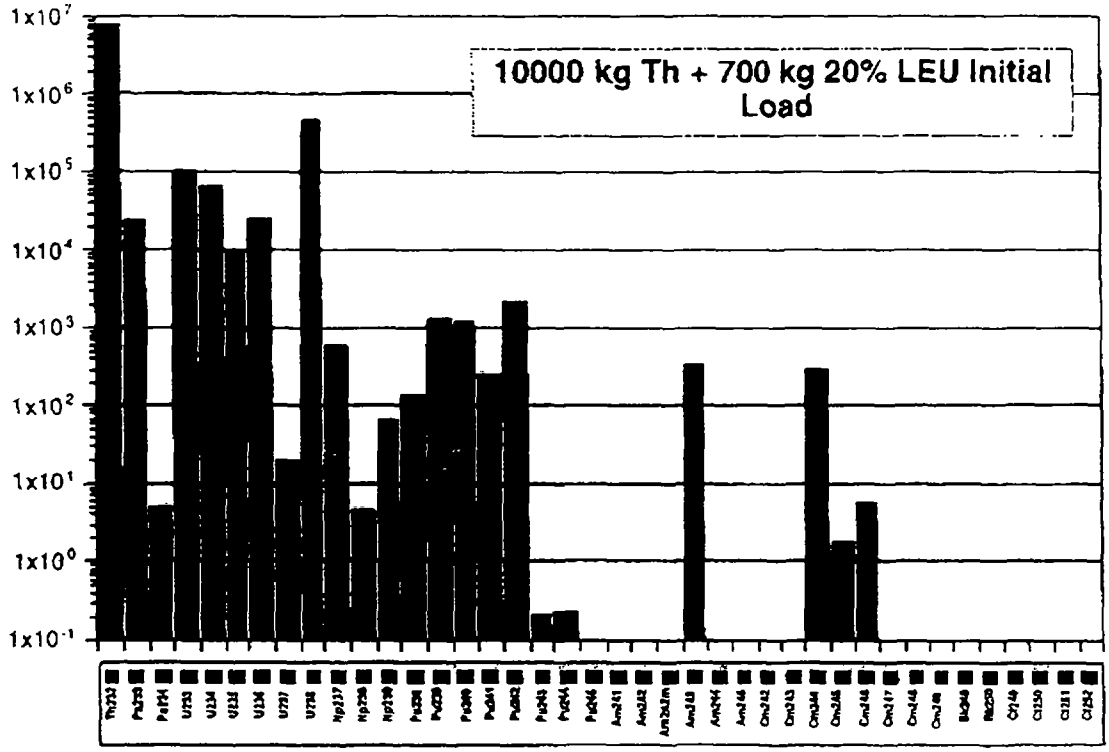

FIG. 3. Actinide isotopic distribution for the ADEP system. The distribution of actinide isotopes for the ADEP system is given ten years after start-up long after the system has reached equilibrium. The fission power level of the system is 500 MW_t. The system was started with 10,000 kg of Thorium and 700 kg of 20 % enriched Uranium. The inventory is given on the ordinate in grams for isotopes from ^{232}Th to ^{246}Cm. The ^{233}U is diluted with ^{238}U such that the ^{233}U is never useful weapons material. The amount of Plutonium in the system is very small and is of a very poor isotopic ratio. The ^{233}Pa decays in 26-days to ^{233}U. As described in the text it might be possible, using heroic measures, to extract a fraction of the 22 kg present. The loss of this material would have a significant effect on k_{eff} and probably could be readily detected remotely.

Remote detection of anomalous operation and possible diversion

All conventional nuclear power systems deployed or under development use solid fuel which must be enriched, fabricated, brought to the site, burned, stored, eventually removed from the site, perhaps reprocessed, returned to the site, and finally placed into a repository. Each of these transfers might require a measurement to confirm the amount of fissile material present in the system. If each measurement could be done to 1 % accuracy and nine were required, the total uncertainty over the fuel cycle for nine independent measurements would be about $9^{1/2} \times 1\% = 3$ %. Since a 3000-MW_t reactor typically burns about 1200 kg of fuel per year, the real uncertainty in the fissile fuel in the system is about 36 kg. About half of this might be Plutonium which could be diverted into nuclear weapons without being missed.

In contrast, no power is generated in ADEP without the operation of the accelerator and all of the fuel is generated internally. No actinide must be removed from the system in the course of normal operation of the system. The accelerator beam power, the fission power, the electric power generated, the electric power consumed by the accelerator and the plant, and the power fed into the external grid must all be internally consistent. If the accelerator power is increased, all of the other power levels must increase in a fixed relationship. If the plant is found to be operating out of balance, for example by power meters at the strategic points or by satellite infrared mapping, it is a signal that material diversion might be

underway. A more detailed study of these anomalous conditions and their dependence on the rate of feed of Thorium and the rate of removal of fission products might provide means to sense remotely when the source of the anomaly is nuclear material diversion.

Limited consequences of extreme measures to control diversion

If an existing operating reactor is suspected or determined to be used for production of nuclear weapon material, the ultimate response by those alarmed could be the destruction of the nuclear reactor. There is a significant possibility that such action could lead to widespread death for the surrounding public and land contamination near the reactor. With such consequences the destruction of a reactor after it has begun operation is probably impractical. The accelerator component of the ADEP system is large and easily damaged into inoperation without significant possibility of damage to the target-blanket itself and the release of radiation. Diversion can therefore be terminated without exposing the surrounding population to significant danger.

D.2.1.6. COMMERCIAL WASTE TRANSMUTATION (ATW SUBPROJECT OF ADTT)

The objective of the Accelerator Transmutation of Waste (ATW) subproject of ADTT is to destroy the actinide and long-lived fission product waste from commercial nuclear reactor spent fuel. If the separations can be done sufficiently well, storage of the remnant waste could be in near-surface sites rather than in geologic storage facilities. The amounts of material requiring transmutation and the selectivity of chemistry separations has already been described in the section of this report entitled, "Geologic Storage and the ADTT System." Separation factors of about 1/100 are shown to be adequate to meet Class C storage criteria for fission product and about 1/10,000 for the Plutonium and other minor actinides.

The ATW system also has means for continuous feed of waste from commercial light water reactors. To many this would appear to require the separation of Plutonium and other components of the waste before feeding them into the system. This is referred to as reprocessing which was forbidden in the U. S. by President Carter by Executive Order. Even though this order expired when he left office, as a practical matter it has continued to govern U. S. internal policy on spent fuel and our foreign policy position has strongly attempted to discourage the reprocessing option for commercial spent fuel. The purpose is to reduce the opportunity for diversion of commercial Plutonium to nuclear weapons purposes and to prevent the accumulation of large inventories of this material which is considered by many to be highly dangerous. Because of the excess neutrons provided by the accelerator, front end reprocessing is not required. The ATW system would require only the removal of the Zirconium cladding and the Uranium. All of the other actinide and all of the fission product can be fed into the blanket, because the capabilities for removal of the fission product already exist in the back-end separations system.

The front-end removal system has not been selected but there are at least two options under consideration. One would involve the crushing of the spent fuel assemblies which contain mostly UO_2 and the oxidation of this to U_3O_8. The volume expansion on the transformation to a higher oxide and the resulting conversion of the spent fuel to fine powder allows the spent fuel to be poured out of the spent fuel assemblies. Separation of the spent fuel from the cladding might approach 99 % for this process, but that might not be adequate and it might be difficult to clean the hulls further. Another means of removing the cladding might be to burn the spent fuel assemblies in a chlorine atmosphere over a plasma torch converting the Zirconium to volatile $ZrCl_4$. The oxide in the cladding however would fall as rubble into the bottom of the chlorination facility and be collected for subsequent fluorination. The bulk of the spent fuel is Uranium and this would be removed as volatile UF_6. All of the other spent fuel material including the fission products, the Plutonium and other higher actinides would be converted to fluorides and fed directly into the ATW system by dissolving them in the molten salt carrier.

In contrast to the aqueous reprocessing system developed long ago and now in common use, the processes described do not produce a pure stream of "naked" Plutonium. The Plutonium is never separated

from the most highly radioactive components of the spent fuel, but only from the relatively benign Zirconium and Uranium. The front-end separation required for the ATW therefore produces a stream which is mostly highly radioactive fission product and separation of the Plutonium from this fission product and from the other actinides would be required before it could be used in weapons. It is also important to mention that the front-end separations for the ATW system would be an integral part of the ATW system so that product stream from the Zr and U removal would be difficult to access.

Commercial nuclear power plants are typically sized at 3000 MW thermal and produce about 300 kg of Plutonium and other higher actinide per year while fissioning 1200 kg of fissile material per year. Therefore an ATW system operating at the same fission power level of the LWRs could burn the waste from four LWRs if its operating life were the same as the LWRs. Destroying the LWR waste arising from the roughly 100 LWRs in the U. S. using ATW systems would require the deployment of about twenty five 3000-MW_t ATW systems if the waste were to be destroyed in about 30 years. Unless the income from electric power sales were sufficient to offset the capital and operating costs of the ATW system, the cost of destroying the waste by this means could be prohibitive. The economic picture for the ATW system will be less favorable than for the ADEP system because the ADEP system need only destroy its own waste and only a modest accelerator is required for the modest neutron supplement. However the ATW system must destroy not only its own waste but also that from the four LWRs. Substantially more accelerator-produced neutrons are required therefore with greater capital cost for the larger accelerator and for the additional power which the accelerator consumes.

There is an attractive way around this. Presently the U. S. and Russia are reducing their weapons stockpiles and freeing up large amounts of highly enriched Uranium and Plutonium. Both are excellent sources of neutrons, which is part of the reason why they are ideal weapons materials. Over the long run it is probably unsafe to store these materials and so they will have to be destroyed almost certainly by fission. If some of these weapons materials are consumed in the ATW system, the excess neutrons can make up for some of the neutrons which otherwise would have to be supplied by the accelerator. Therefore by burning these weapons materials concurrently with the destruction of the commercial nuclear waste, the size of the accelerator probably can be reduced by at least a factor of two. With the resulting benefit to the economic picture for the ATW system, the destruction of the waste using the ATW system might be practical. A comparison between the amount of LWR waste and the amount of excess weapons material available shows that there is a satisfactory match.

There are other practical matters concerned with the practical deployment of the ATW systems. These systems will probably have to be located at government reservations and operated in clusters both because of the sheer size and the use of the weapons material. If four ATWs were located on the same site, the electric power output into the local commercial grid would be about 3-4 GW_{el} from each reservation and there would have to be about three sites if all of the waste was to be burned in 60 years. It is not easy to reliably estimate the U. S. power requirements over the next 30-50 years and how the power will be produced, but having access to a commercial market for the electric power from the ATW systems is an important consideration for this deployment option for the ATW system.

There is a second ATW deployment option for the destruction of the LWR waste which is a hybrid of the ATW and ADEP systems. This would involve the replacement of existing LWRs at the end of their life with an ATW system on the same site feeding the same amount of electric power into the grid. The ATW system would over its life destroy the waste from the LWR and also its own waste stream. About 25 % of its power would be derived from the actinide waste from the LWR and the rest from Thorium. The accelerator requirement would be about the same as that for the other ATW deployment option, but no weapons material would be required. Of course it probably would not be desirable to have these weapons materials being delivered to the approximately 100 ATW systems operating in follow-on to the existing 100 LWRs. An advantage of this deployment scenario is that the waste need not leave the site, some level of radioactivity inventory already exists on the site, and there is probably a clear market for the ATW electric power and an existing distribution system. Under this scenario, the amount of nuclear power would continue to be at least as large as that produced today. The present system would have been replaced with systems which do not produce the waste stream of existing LWRs, which avoid the criticality and after heat

safety concerns of existing reactors, and which nullify the requirement for a nuclear infrastructure of mining, enrichment, fuel fabrication, reactor, fuel storage, reprocessing plants, and fuel refabrication. The requirements for geologic storage of remnant waste would be greatly reduced or perhaps made entirely unnecessary depending on the technical and economic performance of the system.

In summary, the first ATW deployment option carries more of the features which might be associated with a nuclear close-out option. The second option could provide a bridge over the next 30-50 years from the present LWRs with their major infrastructure requirements to the ADEP systems which operate with little infrastructure support .

D.2.1.7. PRESENT STATUS AND SUMMARY

This paper describes a new accelerator-based nuclear technology which offers total destruction of the weapons Plutonium inventory, a solution to the commercial nuclear waste problem which greatly reduces or perhaps eliminates the requirement for geologic waste storage, and a system which generates potentially "unlimited energy from Thorium fuel while destroying its own waste and operating in a new regime of nuclear safety The accelerator technology is already rather mature after 50 years of development and is being driven by other programs. Reactors are also well understood after 50 years of development of many different reactor types. The next essential step in the ADTT program is demonstration of the successful integration of reactor and accelerator technology in an experiment of significant size. Such an experiment has been proposed for the Los Alamos Meson Physics Facility (LAMPF) at Los Alamos and for the Moscow Meson Factory at Troitsk, Russia. For a system operating at a $k_{eff} = 0.96$, LAMPF would drive the system at a power level of 40 MW_t thermal. Of course lower powers are contemplated for the earlier stages of the experiment which might extend over about seven years including both construction and operation. The experiment would be accompanied by research and demonstration, at about the same technical effort as the experiment, on the required separations in the molten salt context. Perhaps seven years hence, an integrated demonstration of the ADTT system could be in operation at the 200 MW_t level, with the deployment of the ADTT system beginning in about fifteen years. This time scale is approximately the same as the earliest planned opening of a geologic repository in the U. S. or elsewhere.

REFERENCES

[1] Maintenance and Disposition of Excess Weapons Plutonium, National Academy of Sciences, Committee on International Security and Arms Control, National Academy Press, Washington, DC 1994

[2] R. W. Benjamin, Savannah River Laboratories, Private communication, 1994; P.J. Sentieri and K. B. Woods, Idaho National Engineering Laboratory, Private Communication, 1994

[3] C. D. Bowman, "High Value use of Weapons Plutonium by Burning in Molten Salt Accelerator-Driven Systems or Reactors," International Seminar on Nuclear War and Planetary Emergencies, 18th Session, pp. 400-411, E. Majorana Center for Scientific Culture, Erice, Italy, 1993

[4] "The Los Alamos Accelerator-Based Conversion Concept for Plutonium Disposition," transparency set prepared for review by the JASON Group in January 1994, available from The ADTT Project Office, Los Alamos National Laboratory, Los Alamos, New Mexico; and C. D. Bowman, "Weapons and Commercial Plutonium Ultimate Disposition Choices...Destroy Completely or Store Forever," in Managing the Plutonium Surplus: Applications and Technical Options, pp 125-138, Kluwer Academic Publishers, Dordrecht, The Netherlands, 1994

[5] Alvin M. Weinberg, "Molten Salt Reactors," in Nuclear Applications and Technology 8, 102-219 (1970)

D.2.2. THE LOS ALAMOS ACCELERATOR DRIVEN TRANSMUTATION OF NUCLEAR WASTE (ATW) CONCEPT DEVELOPMENT OF THE ATW TARGET/BLANKET SYSTEM

F. Venneri, M.A. Williamson, L. Ning

LER-ADTT Project Office

Los Alamos National Laboratory

D.2.2.1. THE ATW OBJECTIVE

The objective of the ATW project is to provide a compelling, proliferation-resistant and economically viable alternative to partial reactor burning and geologic storage in the management of nuclear spent fuel and other plutonium bearing materials.

In the ATW concept, highly efficient and robust waste cleanup procedures produce a feed directly suitable for nearly complete subcritical burning, without significant additional waste generation. ATW technology will significantly reduce waste streams from the nuclear power cycle and essentially eliminate excess fissile materials. Plutonium and other hazardous components of nuclear waste will be destroyed to a high degree and with very low process inventories. Demands on permanent repositories will therefore be greatly reduced, and such repositories (containing no fissile plutonium or highly-mobile long-lived fission products) will become more technically feasible and politically acceptable and economically attractive.

The immediate technical goal is to demonstrate the feasibility of effective treatment of spent fuel and other types of plutonium-bearing materials (including residues and excess weapons plutonium), to eliminate fissile plutonium (utilizing it to produce energy and neutrons) and destroy by transmutation certain fission product nuclides of particular concern to long-term repository performance. Partitioning and isolation of plutonium will not be required to accomplish the project's goal. If ATW is to become the preferred option for nuclear waste management in the US, economic viability of the entire ATW-based fuel cycle must also be demonstrated.

The program will rely on the innovative application of proven technologies with emphasis on safety and anti-proliferation features.

For the past several years researchers at Los Alamos have been studying and analyzing a fundamentally different approach to nuclear power and the elimination of nuclear waste. At Los Alamos this approach is called Accelerator Driven Transmutation Technology (ADTT). We feel that ADTT has the potential for mitigating many of the difficulties inherent in present day nuclear power systems including nuclear waste disposal and the buildup of plutonium inventories [1]. In dealing with the problems of nuclear waste and management of excess plutonium, we believe that ATW has the potential to place nuclear power into a regime with significantly reduced waste streams and no accessible plutonium or highly enriched fissile materials.

ATW-based systems can consume nuclear waste (plutonium, minor actinides and long-lived fission products), burning down existing inventories and producing very little new actinide waste, while generating power and can further use the substantial excess neutrons that they are capable of generating to do useful work, such as transmute long-lived fission products or reconstitute uranium or thorium based nuclear fuel for further use in reactors. ATW comes to the scene with four unique attributes, which are the result of the combination of its subcriticality and use of liquid fuel. These are process robustness, poison insensitivity, neutron efficiency and completeness. The robustness of the ATW system processes allows it to accept a wide range of nuclear waste with significant variability in isotopic assay and chemical contamination, from defense spent fuel and scrap plutonium to commercial spent fuel. Since there is no need to reach and maintain criticality, the ATW systems are relatively insensitive to poisons and burnup fuel variation or poor fuel characterization. Because of the rapid elimination of fission product poison and

the achievement of high neutron fluxes, ATW systems should be able to burn plutonium and most other components of nuclear waste efficiently , with low standing inventories, and to a high degree of completeness, so that the waste load destined for permanent storage in a repository might be reduced, and such repository (containing no significant TRU waste or mobile fission products) would become technically feasible and politically acceptable.

ATW can accept the spent fuel generated by any of the existing and conceivable future types of nuclear reactors. ATW's front-end processes produce a feed of unseparated actinides directly suitable for nearly complete subcritical burning in the actinide burn unit. The unit operates subcritically, driven by a large current LINAC. Power production to offset operational costs is optional.

In ATW, the excess neutrons generated by the accelerator and the fission of the higher actinides are used in a blanket/reflector containing long-lived fission products to be transmuted. The separated uranium is collected and sent to permanent storage. Plutonium and higher actinides are completely eliminated, as well as the most troublesome fission products

The successful implementation of ATW systems will lead to the elimination of plutonium, higher actinides and selected fission products from the nuclear waste stream. With the implementation of ATW systems the efficient (and eventually full) utilization of the existing uranium and thorium energy resources will become possible, with strong proliferation barriers.

D.2.2.2. GENERAL FEATURES OF ATW

Fuel preparation. Spent fuel coming from operating nuclear reactors (LWRs, HTGRs, CANDU, and others) is processed using the "Hydrofluorination+Electrowinning in Molten Fluorides" process conceived at LANL. The process allows the separation of the enriched uranium and/or thorium contained in the spent fuel without plutonium or actinide separation. The role of the fuel preparation part is to prepare the waste feed for use in the target/blanket cell. The process is designed to be relatively insensitive to the composition of the waste feed. A unique feature of ATW is that the system can accept a wide range of feeds with minimal chemical preparation. The use of stable high-temperature molten salts as the primary chemical medium is key to this opportunity.

Actinide and selected fission-product burn. Subsequent to fuel preparation, destruction of plutonium, higher actinides and selected fission products is accomplished in the passively safe, deeply subcritical blanket conceived at LANL. Neutrons to sustain the burn phase are produced in a liquid metal spallation target driven by a large-current proton accelerator operating in the 1- GeV energy range. When a proton beam is injected into the target, over 30 neutrons per incident particle per GeV are generated via spallation reactions. These neutrons are multiplied by fissions in the surrounding subcritical blanket containing the actinides. Electricity may be generated from the heat released by the fission processes, and a fraction of the electric power generated will be available to the commercial grid for distribution. The high-flux, low-inventory burn phase is assisted by the cleanup processes for fission product removal conceived at LANL for use in the ATW burner (sparging, electrowinning and reductive extraction). The burn is nearly complete and only certain fission products are discharged by the process.

At the end of ATW operations, practical processes will be used for removal and recycle of radioactive materials from the salt. The long-lived hazardous fission products, e.g. ^{129}I and ^{99}Tc, will be transmuted into stable isotopes by neutron irradiation. Because there are no significant amounts of actinides and technetium or iodine (the long-term hazards) in the waste stream, the waste need not be guarded for fear of diversion of fissionable material, and its long-term toxicity is greatly reduced. A general layout of the ATW components is illustrated in Fig. 1.

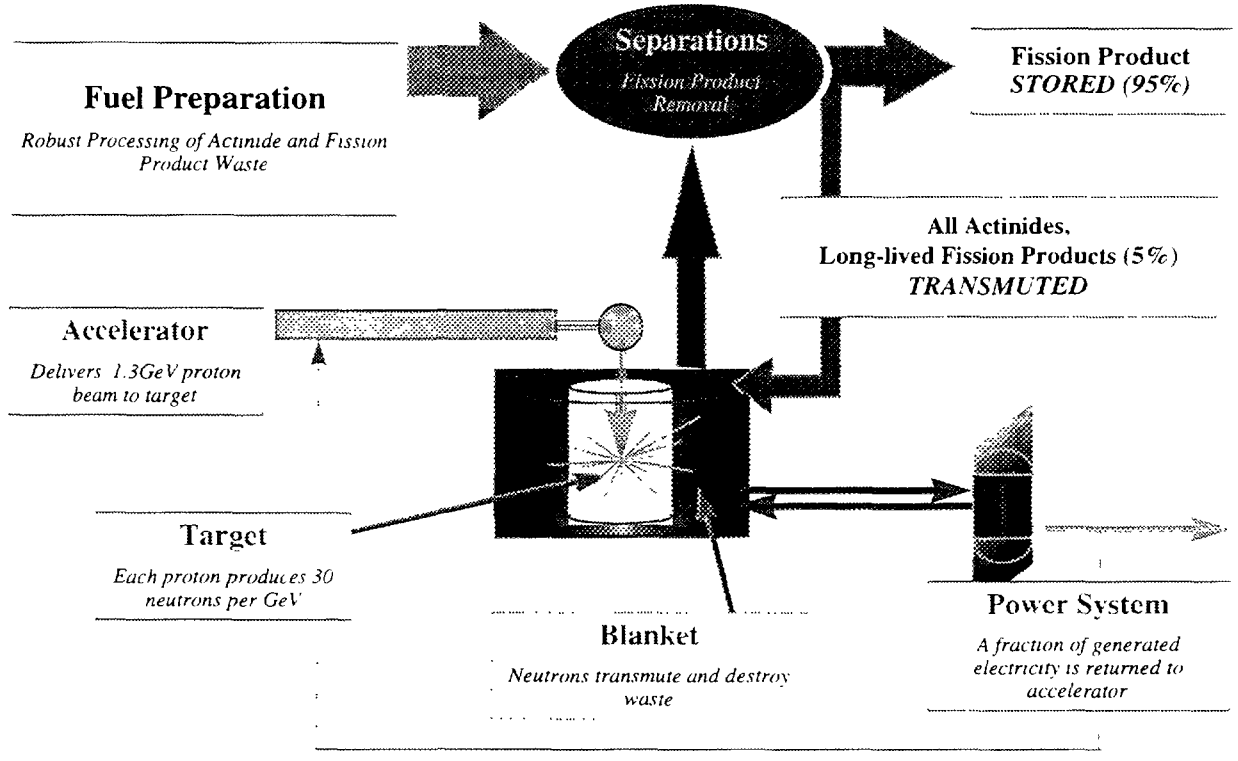

FIG. 1. A general layout of the ATW components

D.2.2.3. THE VALUE OF SUBCRITICALITY

The ATW system is operated in a subcritical mode, thereby precluding a self-sustained chain reaction regardless of whether the accelerator being on or off. From a dynamic standpoint, driving a system with an accelerator decouples the source of neutrons from the fissile fuel: subcritical systems can operate relatively unconstrained by the internal workings of the blanket. Critical systems, on the other hand, are driven by the internally generated delayed neutron "source." Their control mechanism depends on the absorbing properties of the control rods and their influence on the reactivity of the system, and is deeply affected by the internal conditions of the core, e.g. neutron flux and spectrum, and fission-product buildup. Critical reactors are therefore constrained by the flux, spectrum and internal composition tolerated in the core because these parameters determine the effectiveness (reactivity worth) of the control mechanism.

From a static point of view, the accelerator provides a convenient control mechanism for subcritical systems that is much faster than that provided by scram rods in critical reactors. Subcriticality itself adds an extra level of operational safety concerning possible criticality accidents.

Although additional safe-shutdown mechanisms might be required, accelerator-driven subcritical systems can work without control rods, and in principle are insensitive to flux, spectrum, fission-product buildup and core composition changes to a much higher degree than the equivalent critical reactor. The response to reactivity transients is also much less severe and higher neutron fluxes are possible. This inherent robustness allows subcritical systems to accept fuel that would not be acceptable in critical systems, and burn it with minimal processing requirements [2].

A considerably larger excess of neutrons per fission can be produced in deeply subcritical systems than it is possible to generate in critical (reactor) systems. Although these neutrons are not inexpensive, the

substantial progress recently achieved in accelerator design and operation efficiency, allows the effective use of such neutrons for the transmutation of long lived fission products and other tasks.

Neutron economy of subcritical systems.

The basic equation relating source- and fission- generated neutrons and governing the behavior of subcritical systems is the following:

$$k_{eff} = \frac{\eta}{1+\alpha+P+L}$$

where k_{eff} is the reactivity of the system, related to its neutron multiplication M factor by the equation:

$$M = \frac{1}{1-k_{eff}}$$

Critical (self-driven) systems have keff =1 and infinite multiplication

η= average number of neutrons released by each fission

α= ratio of neutron-absorption-to-fission cross section in the active component of the fuel (plutonium and actinides in the case of the ATW burner)

P= number of neutrons parasitically absorbed in the system per fission

L= number of neutron that leave the system (leakage) per fission. These are the "excess neutrons" available for work (waste transmutation and fuel enrichment)

If the ATW burner is operated with a fast neutron spectrum then the values for the parameters are: α=0.6; P=0.2 ; η~3. If the ATW burner is operated with a more thermal spectrum (molten salt reflected by graphite), then the values for the parameters are: α=1.4 ; P=0.4 ; η~3. Values of n significantly larger than 3 may be possible in "hyperfast", deeply subcritical systems directly driven by spallation neutrons generated in the fuel, where a substantial number of fissions are initiated by high energy spallation neutrons instead of the relatively slow fission neutrons. These systems (which could be obtained in liquid lead/bismuth fueled ATW systems) have a spectrum substantially harder than that of fast reactors and offer special advantages in neutron-intensive applications. A schematic view of thermal and fast ATW burner is illustrated in Fig. 2. The number of available neutrons per fission (the L parameter) can be explicitly written as:

$$L = \frac{\eta}{k_{eff}} - (1+\alpha+P)$$

A cursory examination of this relation reveals the existence of two contribution to the number of neutrons available from a given system: the first term is determined by the subcriticality level, the second term by the neutron spectrum. The use of the accelerator drive (systems with lower k_{eff}) will improve the contribution from the first term. The use of fast neutrons will improve the contribution to the total number

of available neutrons per fission from the second term It should be noted that "hyperfast" systems (directly driven by spallation neutrons) could provide also additional neutrons by increasing the value of the parameter n Applying the values for the parameters n, A, and P to the expression for L, it is apparent that more neutrons are available for use in the fast-spectrum system than in the more thermal system for the same value of k_{eff}

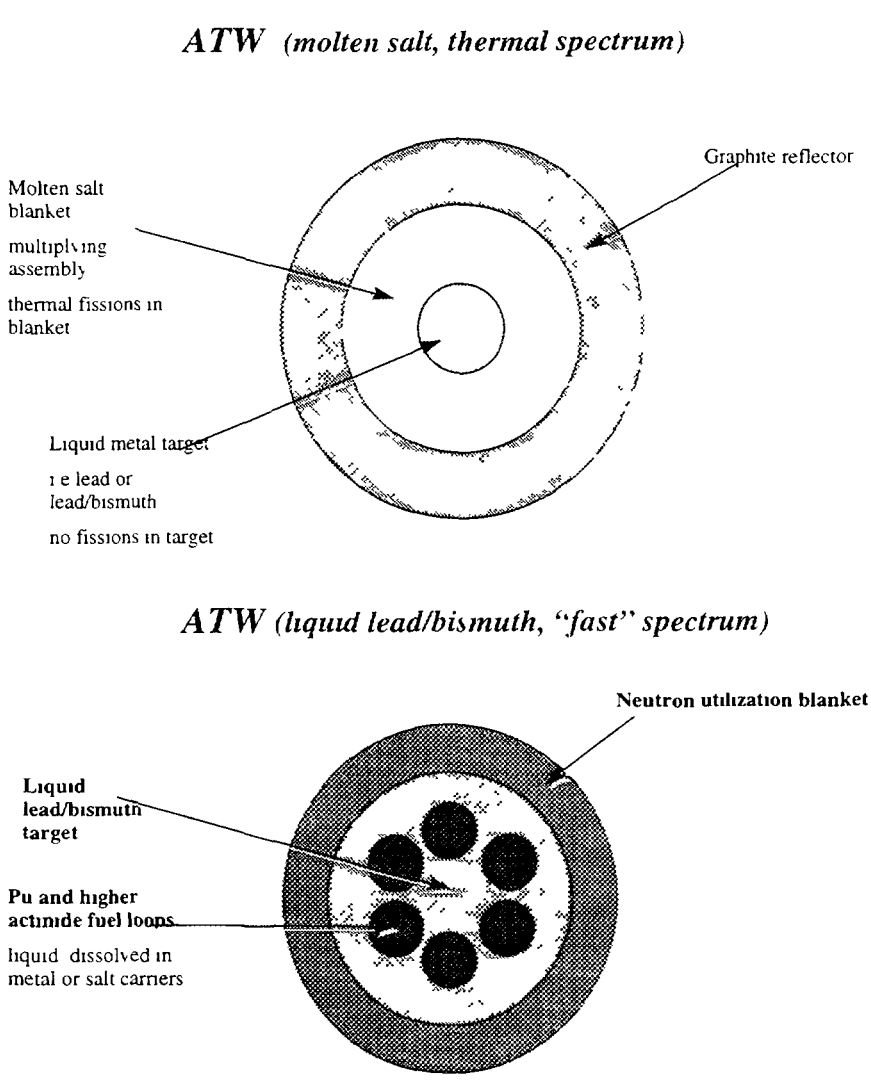

FIG 2 A schematic view of thermal and fast ATW burners

Just how many neutrons per fission are necessary will of course depend on the extent of the work that is required from the ATW system An important task for these systems is the transmutation of fission products Some of the fission products targeted for transmutation remain in the fuel of the ATW burner and their transmutation is accounted for in the fuel capture parameter P Some will have to be transmuted in special loops, by leakage neutrons The number of neutrons per fission needed to destroy the long-lived fission products is directly related to the power produced in the ATW burner The relation depends on the extent of the fission-induced power production in previous operation (fuel burnup), and the type of fuel cycle (whether uranium- or thorium-based) For uranium-based spent fuel, with a burnup of 33,000 MWd/t (typical of a majority of present-day spent fuel), 0 25 extra neutrons per fission in the ATW burner are needed to destroy the long-lived fission products generated during previous and present fission processes This is the number of extra neutrons per fission that is to be made available through leakage in ATW systems where the transmutation of the long-lived fission products is sought in addition to the destruction of the plutonium and higher actinides) In a near-thermal spectrum configuration (molten salt reflected by graphite), a subcritical system (driven by the accelerator), operating at a keff =0 95 will free the additional neutrons to allow 0 25 leakage neutrons per fission to be used for fission product transmutation It is true however that most of the usable leakage neutrons will have to come from the accelerator-driven source A fast-spectrum system will have more than enough neutrons available even in a critical configuration (without accelerator) to perform the required transmutations of fission products Unfortunately a critical system cannot be constructed to operate on pure plutonium and higher actinides, especially in the fast spectrum Therefore some degree of subcriticality (accelerator drive) must be used also in fast spectrum systems, its extent to be determined by safety considerations more than by neutron economy factors More demanding applications, such as spent fuel reconstitution or the transmutation of a larger number of fission

products, will require a larger number of neutrons available per fission. For these applications, fast or "hyperfast" subcritical systems, capable of supplying over 2 available neutrons per fission, are clearly preferable.

In the following discussion we will concentrate on the ATW systems with application to actinide and long-lived fission product burning from spent fuel, and in particular to subcritical systems operating in the thermal neutron spectrum. As we have hinted and will show in more detail, the neutrons introduced into these subcritical systems by the accelerator, the absence of neutron absorbing reactivity control devices, and the possibility of achieving high neutron flux levels can improve the neutron economy to the point that fuels that were considered very difficult to use in the thermal spectrum due to their poor neutron economy, i.e. minor actinides, can be burned subcritically by thermal or near-thermal neutrons [3], with the ensuing advantage of lower inventory.

Liquid-fuel subcritical systems

While it is strictly correct that any type of reactor can be arranged in a subcritical configuration, the attractive features that subcriticality makes possible in ATW (fuel feed flexibility, completeness of burn, low sensitivity to changes in core parameters, relatively high flux, large number of excess neutrons) are best accomplished with liquid-fuel systems, where the burnup is uniform, continuous fueling is available, regular fuel cleanup is possible, and no excess reactivity is required. Furthermore, because of the strongly spatially non-uniform power distribution typical of deep-subcritical systems, fluid fuels are most likely to be used in high-power configurations [4].

Among liquid fuel carriers, both liquid lead and molten fluoride salts, similar to the fuel used in the Oak Ridge National Laboratory (ORNL) experiment [5], offer a good interface for the versatile, proliferation-resistant front-end process identified for the waste plutonium (molten salt hydro-fluorination and electrowinning). Both molten salt and liquid lead, because of their chemical and electrochemical stability, also can provide a natural medium for simplified back-end fuel cleanup processes. Both carriers are low vapor pressure liquids even at high temperatures, and therefore add to the safety and performance of the systems, allowing low-pressure operation of the blanket and high-efficiency power production. The complete absence of water in the primary system also eliminates the possibility of hydrogen generation and the attendant risk of accidental explosions. Designs based on both options are currently under investigation at Los Alamos. In the following chapters, the molten salt fuel carrier option will be explored. The lead-fueled system, which form the basis of the "hyperfast" system currently under investigation at LANL, and other variants where both fast and thermal spectra are used to minimize the required accelerator size, will not be described in this paper.

D.2.2.4. BASIC DESIGN CHOICES FOR THE ATW MOLTEN SALT CONCEPT

Molten salt reactors have been operated and elements of the molten salt fuel cycle were developed and deployed at ORNL during the 1970's. The addition of the accelerator drive and the absence of breeding requirements for the fuel cycle make the ATW system considerably simpler and more forgiving than the critical reactor proposed and carried to a considerable level of design detail in the ORNL work. After a long search through a broad parameter space of options [6, 7, 8, 9 and 10], the Los Alamos molten salt ATW concept has converged on a system reflected by graphite, a liquid lead-bismuth neutron production target, and pyrochemical separation processes.

High-current accelerators and liquid-lead target

The high-power accelerator technology required for ATW has been under continuous development for the past three decades at Los Alamos. Presently, Los Alamos is involved in a major project to develop a large accelerator (100 mA, 1300 MeV) for the production of tritium (APT) for defense applications.

Similar accelerator designs were reviewed by the Energy Research Advisory Board of the U.S. Department of Energy [11] and by the JASONS [12]. These reviews gave general endorsement of the proposed accelerator technology with the provision that appropriate pilot and demonstration steps be made along the way towards the construction of a full scale facility [13]. In October 1995 the DOE committed to the demonstration of the accelerator technology for application to tritium production (APT). The operating parameters of the proton linac envisioned for the APT project will be similar to those needed for the ATW system.

The average power needed for the very largest of systems we propose requires an accelerator power of around 200 MW (100 mA beam at 2000 MeV). This can most readily be achieved with a linear accelerator. At present, the highest-power, linear proton accelerator is at LANSCE (formerly called LAMPF), and operates at around 1 MW (1 mA at 800 MeV). At first, proposing an accelerator 100 times bigger might seem like a very large extrapolation, but it is not as demanding as it appears. First, the LANSCE linac is operated with only every fourth bucket filled with proton beam. Filling every bucket (by use of funneling) or every other bucket (if unfunneled) immediately increases the average power by a factor of four (or two). Also, the LANSCE linac is a pulsed machine operated at 6% duty factor: going to 100% duty factor would produce a factor of 17 increase in power. The charge in each microbunch can be increased by about a factor of four and still stay well within the stable space-charge regime. Therefore, an improvement by a factor of more than 200 (4 x 17 x 4) is possible by the extension of proven proton linac technologies. This should enable operation of 100-mA, 2000-MeV linacs based on current technology. Figure 3 illustrate the possibility of using LANSCE LINAC for ATW applications.

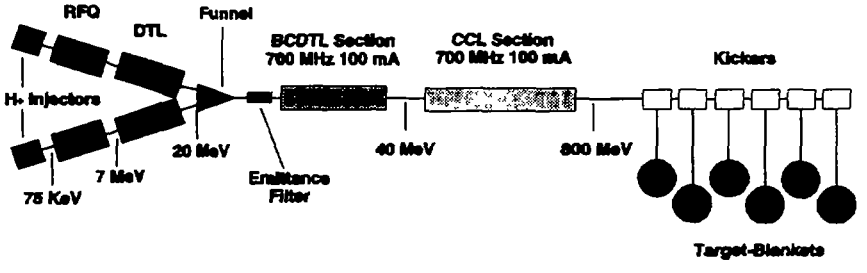

FIG. 3. The ADTT linear accelerator design for multiple targets.

The function of the target in the ATW system is to convert the incident high-energy proton beam to neutrons. Among the requirements for an ATW target are:

1. Compact size to enable good coupling to the surrounding blanket,
2. High power operation, up to 200 MW,
3. High proton-to-neutron conversion efficiency,
4. Reliable and low maintenance operation,
5. Safe operation,
6. Small contribution to the waste stream.

These system requirements are best met by molten lead or lead-bismuth eutectic (LBE). LBE has a melting point of 125°C (200°C lower than for pure lead) and considerable experience exists in the use of LBE in reactor systems. A significant problem with LBE, however, is the production of radioactive and highly mobile polonium from high-energy proton and neutron reactions on bismuth. This becomes a concern in accident scenarios where the polonium contained in the LBE is rapidly released at high temperatures. Irradiation of lead, on the other hand, produces much less polonium, but there is also considerably less experience for pure liquid lead systems in reactor operation.

The use of molten lead or lead-bismuth eutectic in the neutron production target provides the following advantages:

1. High power operation. For compact solid-target systems, the maximum incident beam power is limited by the ability to cool the targets. In liquid metal targets, the medium can be circulated to

external heat exchangers, eliminating the need for coolant in the target production volume.

2. Lead and LBE have good proton-to-neutron conversion efficiency because of their high atomic number, high density and low neutron absorption cross section. The neutron production of large-size lead targets has been measured at LANL to be 22 neutrons per 800-MeV proton, substantially better than any of the other materials tested [15]. The absorption cross sections are about one hundred times lower for thermal neutrons than that of tungsten .
3. Radiation damage and shock issues that exist in solid targets are less of a concern with liquid targets. The fluid container and window are the only parts of the target system which have radiation-induced lifetime limitations. The performance of the liquid part of the target is not affected by irradiation, so that the operational life of the lead or LBE fluid can extend far beyond the lifetime of the container.
4. Lead and LBE are low pressure liquids with boiling points greater than 1600 °C. They are solid at room temperature, reducing the potential for uncontrolled release of radioactive material when the target fluid is removed and cooled.

The beam/target/blanket interface (target structure) is the point where three systems converge and certainly will be the most stressed in the design from the materials point of view. The ATW design for this structure will have to "demonstrate ability to maintain system integrity at the beam/target/ blanket interface" for the anticipated time of operation. In the ATW system, the low pressure of the target and blanket systems and the liquid nature of the target material will be helpful in this regard. The target should be a totally enclosed structure, capable of being rapidly inserted and extracted from the blanket. This structure must be compatible with both the lead and molten-salt liquid interfaces and therefore might suffer from limited resistance to radiation damage due to the properties of the available structural materials. The use of liquid metal targets however, should allow for the softening of the very hard spallation spectrum at the target container walls to levels typical of fast reactor systems. The choice of structural materials can therefore directly extend to the large number of materials tested and satisfactorily used in fast reactors. Proton and neutron damage rates for the window and the rest of the structural parts of the target are not expected to exceed the operational limits established at the Los Alamos Neutron Science Center (LANSCE) [16]. Based on LANSCE experience and extensive experimental studies of materials damage by neutrons (HT-9, Cr-Mo alloys, and Inconel), the lifetimes of the parts of the target most exposed to the neutron flux will be one to two years [16]. These materials have also shown good compatibility and no corrosion problems with LBE as long as the temperature is kept below 400°C [17]. For higher temperature compatibility, the use of carbon based ceramic materials will need to be explored. Figure 4 illustrates a design for the liquid lead target currently under development at Los Alamos.

Experience Base

- ***Solid targets and windows at LAMPF accelerator***
- ***Flowing Pb-Bi technology in Russian reactors***

Development Areas

- ***Adaptation of western and Russian molten metal technologies***
- ***Optimal integration with blanket***

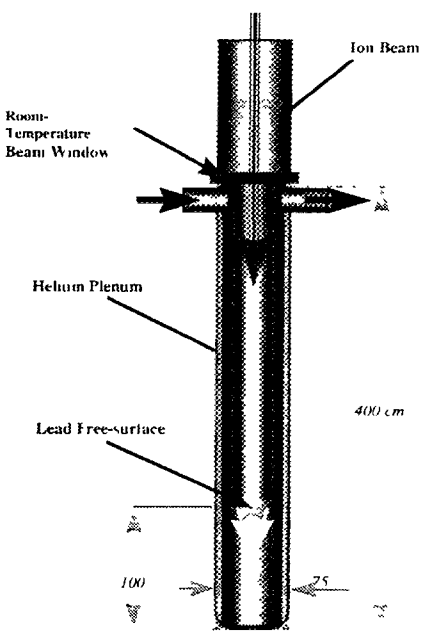

FIG. 4. A design for the liquid lead (lead/bismuth) spallation target

Molten-salt liquid fuel.

In the homogeneous molten salt fuel, as opposed to solid fuels or liquid suspensions (slurries), many fission products are readily dissolved into the liquid medium, and can be extracted readily without processing the fissile component of the fuel. The use of homogeneous molten salt fuel, in fact,

allows the adoption of fuel preparation (front-end) and on-line cleanup (back-end) processes that do not require fuel partitioning and refabrication These processes which will not be detailed in this paper, except for the description contained in Fig 5, do not give rise to extraneous waste streams and provide substantial proliferation and diversion barriers

Process Chemistry Identified for ATW Front-end and Back-end

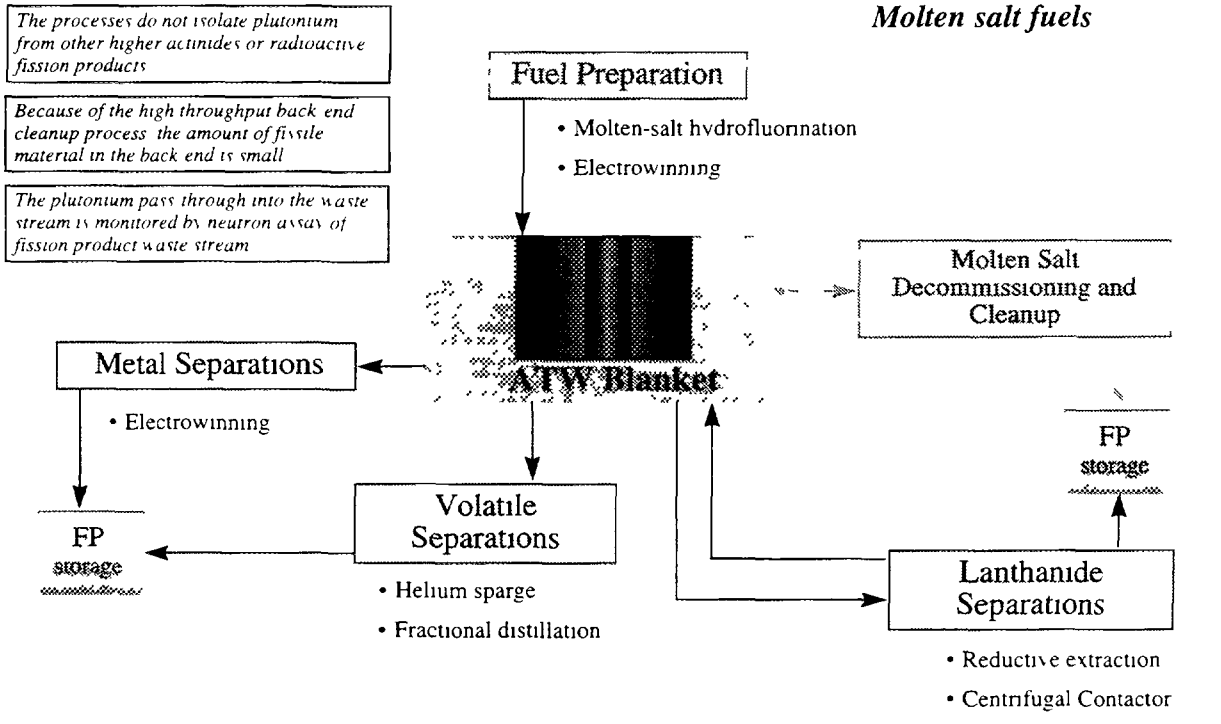

FIG 5 Process chemistry identified for ATW front-end and back-end

The molten salt envisioned for the ATW system is a mixture of lithium fluoride and beryllium fluoride (^{7}LiF-BeF$_2$, 0 67 0 33), with melting point of ~450°C would be used at between 600°C and 700°C Its boiling point is 1700°C, and at 700°C the vapor pressure is only 10 milliTorr Isotopically pure ^{7}LiF would be used because of its lower neutron absorption All elements can be dissolved as fluorides in adequate amounts in the carrier salt which is inert in dry air and nitrogen at all temperatures However, the melting point of ^{7}LiF-BeF$_2$ salt is relatively high, and the presence of lithium in it leads to the production of undesired tritium under neutron irradiation The use of mixtures of other fluoride salts (e g NaF) to mitigate these concerns may be practical [18]

Molten salts as reactor fuels and as coolants have been under study and development for over 40 years, and their chemical, physical, and irradiation properties are well suited to reactor operation The Molten-Salt Reactor Experiment (MSRE) at ORNL, with several years of successful operation, contributed significantly to molten-salt reactor technology This 7 5 MW$_t$ reactor was operated continuously from 1965 to 1969 with no major problems [19] At that time, two industry/utility advisory groups concluded that an adequate molten-salt technology base existed and suggested that the Atomic Energy Commission should proceed with a molten-salt demonstration power plant [20]

The progress of the ORNL molten-salt design study is presented in the entire February 1970 issue of Nuclear Applications and Technology The issue was devoted to a review of molten-salt reactor technology and to a description of a conceptual design for a molten-salt breeder reactor [21] The program at Oak Ridge ended after the Liquid Metal Fast Breeder Reactor (LMFBR) was selected as a superior breeder The successful operation of the MSRE and the substantial amount of research and development

on molten-salt reactor materials and processes at Oak Ridge indicate that with adequate updating of that technology base, a prototype molten-salt ATW plant could be successfully constructed and operated.

Whereas most of the work done at ORNL involved the use of uranium dissolved in the salt, ATW would use primarily plutonium and higher actinides. This would introduce minor modifications to the solutions adopted in the Molten Salt Reactor program, as the oxidation/reduction potential associated with fissions in plutonium fluoride tends to be different than for uranium fluoride. Low molar concentrations of PuF_3 were added to the MSRE as makeup fuel during the latter portion of its operation. Binary and ternary phase behavior data exists for many of the components of interest [22, 23, 24, 25, 26, 27]. Only sparse data exists for quaternary and higher order systems.

Graphite reflector

Due to the presence of large amounts of light isotopes in the salt (lithium, beryllium, fluorine) the neutron spectrum for molten salt systems is always thermalized to a significant extent. To provide optimal moderation and neutron reflection, graphite can be used in the core because of its high-temperature compatibility [28, 5] with the fluoride molten salt fuel. Concerns existed early in the Molten Salt reactor program that seepage of fuel salt into small cracks in the graphite could lead to local overheating and crack propagation. However, there was no evidence that significant salt entrainment took place in the graphite.

In dealing with large amounts of actinides and essentially no resonance absorbers, a well thermalized spectrum will lead to large positive temperature reactivity coefficients. This is due to the presence of low-temperature fission resonances in the cross section of the higher actinides, especially the plutonium isotopes. A less moderated spectrum eliminates the problem in the ATW subcritical liquid fuel system. The ATW burner will use no internal moderation besides that provided by the lithium and beryllium in the base salt. Graphite will be used as a reflector and to protect the nickel-based hastelloy vessel from the damage of neutron flux.

Graphite is subject to neutron damage. With increasing neutron fluence, graphite first contracts, then expands at a fast rate. This rapid growth rate represents a rapid decrease in density and the possible formation of voids and cracks. In this stage, mechanical properties will quickly deteriorate and the graphite might become permeable to the molten salt. A fast neutron fluence above $3x10^{22}$ n/cm^2 in graphite usually produces the onset of the rapid growth phase, with significant dimensional changes and marked degradation of its mechanical properties [29]. The neutron damage to the graphite is caused by the fast component of the neutron flux, which is usually defined as the flux above 50 keV. For a thermal spectrum system, neutrons are quickly moderated so that the neutron damage rate is proportional to the fission rate per cm^3. Therefore the neutron damage rate is proportional to the power density rather than the thermal neutron flux. Because of the significant complications involved with the removal of graphite from molten salt cores, it is highly desirable that the graphite reflector maintain its integrity throughout the plant life.

Because the fuel is kept relatively clean of fission product absorbers, even at the moderate power densities present in the ATW burner, the neutron flux is expected to be in the range $2\text{-}5x10^{15}$ n/s-cm^2 and very strongly peaked This flux could give reasons for concern about the effects of high cross-section fission product poisons, such as xenon, on the stability of the blanket operation. Xenon fixed in position such as by the constraints of solid fuel can cause the onset of spatial power instabilities. In the ATW system however, the fuel is continuously mixed, and therefore local concentrations of xenon in the fuel are not expected. Any unstable behavior would be limited to the amount of xenon that might become constrained by the graphite and would not extend to the bulk of the fuel. Since most of the xenon produced in ATW systems would be removed from the salt through sparging on a very fast time scale (1-2 minutes), and since there is no graphite moderator, but only a reflector, it is highly unlikely that xenon could be a source of unstable behavior. Xenon permeation into the graphite would be more of a waste cleanup problem because of the embedding of radioactive cesium daughter isotopes in the graphite, and should be dealt with accordingly by appropriate surface treatment (i.e. pyrolytic sealing) [28, 18].

Secondary coolant

An intermediate (secondary) coolant loop is required in the ATW system to transfer the heat generated in the molten salt fuel to a power-producing steam cycle. The coolant in this loop must have low vapor pressure at its operating range of 500 to 700 °C. The coolant must be compatible at one end with the fuel salt, and at the other end with the water/steam of the steam generator loop. The coolant must trap tritium produced in the core and keep it from reaching the steam plant. Materials compatibility must be assured and it is also desirable to provide an environment that is essentially free of hydrogenous materials for safety reasons. The coolant selected for the intermediate-loop in the MSBR design was a sodium fluoride/fluoroborate eutectic salt ($NaF-NaBF_4$). This was chosen because of its compatibility with Hastelloy and with the fuel salt, its low cost compared to ^7Li-bearing salts, its adequate thermophysical properties (melting point, viscosity, specific heat and conductivity), its ability to trap tritium and its value in shielding the heat exchangers from delayed neutrons coming from the irradiated salt. No nuclear experience exists with this fluoroborate, but extensive non-nuclear tests were performed on this salt under the MSBR program, and several concerns were uncovered. At high temperature, the fluoroborate decomposes and forms chemically hazardous BF_3. Fluoroborate also decomposes upon contact with fuel salt, and has a limited compatibility with steam, in that its corrosivity is greatly increased by the presence of moisture.

These issues do not rule out the use of the salt. One of the most important reasons for specifying fluoroborate as the secondary coolant salt is its ability to trap tritium. Significant quantities of tritium, in fact, are formed as a result of neutron capture (n, a) in ^6Li, which is always present in the salt because of (n,2n) reactions in ^7LiF, and tritium is also produced by (n,nα) reactions in ^7LiF. This tritium might migrate through the coolant system into the steam system, and from there to the environment. Simulation experiments using the fluoroborate salt, however, showed that the tritium could be effectively trapped by oxygen-bearing species ($Na_2B_2F_6O$) contained in the fluoroborate loop, as sodium hydroxy-fluoroborate ($NaBF_3OT$) [30]. Alternative coolants are also possible, such as lead and lead alloys or low melting point salts.

Structural materials and components

The structural material of choice for the molten salt blanket is Hastelloy-N, that was used at Oak Ridge during the MSRE work [31, 28]. Two problems, however, were discovered during the operation of the MSRE that required further alloy development:

1. Hastelloy-N suffered radiation embrittlement due to the accumulation of helium and, to a lesser degree, hydrogen at the grain boundaries [5]. The helium and hydrogen resulted from thermal (n, a) and (n,p) reactions on the unstable ^{59}Ni produced by thermal neutron absorption in the Hastelloy nickel. Helium was also produced by (n, a) reactions on boron impurities. To achieve a 30-year lifetime for the reactor vessel (made of Hastelloy N), the MSBR design had the inside surface protected by a 76-cm thick graphite reflector to reduce the thermal neutron fluence.
2. Post-operation testing of Hastelloy-N samples from the MSRE system revealed the presence of small cracks on the side exposed to fuel salt [5]. These cracks were later determined to be due to the presence of the fission product tellurium at the grain boundaries [18].

Experimental work following the shutdown of the MSRE laid the basis for eliminating these problems. It was found that modified Hastelloy-N, with fine carbide precipitants (Ti at first, then Nb, Zr and Hf) within the grains, could restrain the helium migration to the boundaries and mitigate the radiation embrittlement problem [32, 29]. Two solutions to the tellurium cracking problem also were investigated: adjustments to the salt oxidation potential to keep the tellurium from attacking the Hastelloy, and slight modification of the Hastelloy-N composition (addition of niobium). The combination of both essentially eliminated the tellurium problem [29]. The above-cited solutions to the problems observed in the MSRE have all been demonstrated in the laboratory environment. In the ATW system, tellurium would also be continually extracted from the salt.

The availability of a suitable structural material in the Molten Salt Reactor program allowed a considerable amount of engineering work to be conducted at Oak Ridge on the design and construction of components suitable for operation in fluoride molten salt fuel. Corrosion-resistant pumps, valves and heat exchangers capable of reliable operation at high temperature [19] were provided for the MSRE.

Pumps. The pumps for molten salt blankets must reliably circulate fluoride salts in the primary and secondary salt systems at temperatures as high as 750°C. The low electrical conductivity of molten fluoride salts hinders the use of electromagnetic pumps. However, centrifugal pumps, albeit of low power, were demonstrated to work very reliably in the MSRE [33]. For full-scale ATW systems, there is yet no experience in constructing and operating the much larger fuel pumps that will be required.

Valves. Valves are required in the ATW primary and secondary systems for isolating portions of loops, directing flow to alternate paths, and providing flow variations during startup, shutdown, and off-normal conditions. The only type of molten salt valve that was operated in the MSRE was the freeze valve. This is a type of valve suitable for on/off operations, such as fuel-salt drain. The fuel-salt drain valve used in the MSRE consisted of a flattened section of a two-inch pipe equipped with external heaters and coolers. It operated reliably. Although a large body of experience exists on several types of valves for operation in liquid metals at comparable temperatures, considerable more work is required for the satisfactory application of these designs to the molten salt environment

Heat Exchangers. The operation of the MSRE heat exchangers was reliable, although the capacity of the heat exchangers was somewhat lower than expected. There was no evidence of scaling or corrosion. The experience base with the proposed NaF-$NaBF_4$ secondary coolant derives from numerous tests for the MSBR design, but not from actual heat-exchanger design and construction. The experience base appears however to be sufficient to justify that the heat exchanger design be based on correlations for normal fluids, once the physical properties are accurately measured.

Overall, the MSRE fuel salt, LiF-BeF_2, its containment system and the associated hardware performed well throughout the life of the project [21, 5]. The ATW project will build on that experience, using the improved materials and techniques available in the 1990's.

D.2.2.5. ELEMENTS OF MOLTEN-SALT NUCLEAR SYSTEM DESIGN

In 1960's, the Molten Salt Reactor Program at ORNL worked on thorium-based molten salt breeding systems. The activity led to the design of the Molten Salt Breeder Reactor (MSBR) and was based on the design and operating experience of the Molten Salt Reactor Experiment (MSRE) and its technology support programs. In the early 1970's, ORNL proposed, with strong backing by industry and utilities, a major technology development program that would have culminated in the construction and operation of a demonstration reactor called the Molten Salt Breeder Experiment [5]. Later, in 1979, the Denatured Molten Salt Reactor (DMSR) was proposed for power generation with enhanced proliferation resistance [18].

Based on the evaluation of those activities, the National Laboratories of Los Alamos and Oak Ridge, within the ADTT program, have recently started to revisit the technology base for the design of molten-salt systems, in a framework stressing safety and reliability and with the different goal of waste and/or plutonium destruction replacing the original one of breeding [34, 35]. As a result of this effort, attractive features of molten salt systems were identified as well as special concerns which need to be addressed in the design of the molten-salt ATW concept.

Low pressure. The very low vapor pressure of molten-salts even at high temperatures and the low pressure-drop design of the primary molten-salt circulation system allow for an overall low operating pressure in the primary system. This enhances passive and engineered safety, for example, through natural-convection flow capability, design simplifications, and increased system component and structure reliability. To fully take advantage of this feature, the pressure should also be kept low in the secondary coolant and care should be taken in the steam generator so that the high pressure of that subsystem remains

isolated from the low pressure systems in the primary and secondary loops. This will require that pressure isolation devices be employed in the loops and that in the steam generator the pressure be kept as low as practical.

Pool design. The "pool" concept, used in the most recent sodium cooled reactor designs, has significant advantages in terms of a large heat sink and containment of coolant leaks, over the more traditional "boiler" type configuration, used in the large Pressurized Water Reactors (PWR). In the classical pool concept the core is located inside a vessel, together with pumps and heat exchangers. Hot coolant outside the core is separated from the cold coolant by an interface that directs the hot coolant to flow through the pump and heat exchangers back into the core inlet region without using piping. Such a configuration is not directly applicable to a liquid fuel reactor because the absence of clear flow paths would significantly increase the system fuel inventory. By the strategic use of graphite in the blanket and clearly identified salt flow paths, the ATW design can utilize a modified form of the pool concept, which preserves the advantages of the pool concept, especially in terms of heat sinks, natural convection and containment of fuel leaks, and does not lead to large fuel inventories.

Natural convection. The ATW system will be designed so that natural convection is enhanced by using up-flow circulation in the core and arranging the thermal centers for core, heat exchanger and steam generator at increasing elevations. A low pressure-drop design with enhanced natural convection flow will allow for easy passive decay-heat removal in case of a loss of flow, without recourse to fuel drainage.

Large heat sinks and passive safety. Under the worst-case accident scenario (complete loss of primary heat removal), no operator action would be required to remove the decay heat and prevent the release of radionuclides. Temperature increases will be slow because of the large heat capacity available in the primary system cell. To safely dissipate the decay-heat, large heat sinks could be provided surrounding the blanket, or built into the salt drainage system. In-situ heat sinks could passively remove the decay-heat generated by moderately-sized molten-salt blankets (up to 1000 MWt). Larger-sized units might have to be gravity-drained through a freeze valve from the primary system into a drain tank where the heat would be passively transferred to a molten salt coolant and from there to water/steam.

The high flux of ATW systems is not reached through high power density, but through low parasitic capture in the fuel because of fission product extraction. As a consequence, the power density in the blanket is likely to be a factor of 10 lower than in LWR systems. We have evaluated systems of up to 1000 MWt which are passively safe in the event of loss of coolant, even without drainage of the fuel. The main reasons for this special ability to handle shutdown heating are: 1) the liquid nature of the fuel allows natural convection in properly designed systems, 2) the heat source is not localized, 3) the graphite reflector has large heat capacity and heat conductivity; 4) the integrity of the blanket can be maintained for peak core temperatures greater than 1500 °C because of the excellent high temperature properties of graphite and Hastelloy and the high boiling point of molten salt, and 5) with continual removal of the volatile fission products, the decay heat source term is substantially lower than for solid-fuel systems in any time scale longer than a few minutes, while the core heatup characteristic time is of the order of hours. In the event of total loss-of-coolant events at higher power levels, i.e. 3000-MWt systems, fail-safe drainage of the fuel with attendant passive decay-heat removal into large heat sinks is possible.

Containment of radionuclides. Radionuclide containment should be provided through the primary system loop, the loop containing the pressure isolation devices and secondary coolant, and the loop containing the steam generator system. All three loops will be designed as closed-cell constructions located within an additional containment structure. Attention will be given to the penetrations from one cell into another to ensure that proper isolation can be maintained.

Reduction of in-core graphite use. The presence of the graphite moderator in the MSBR design provided the well-moderated neutron spectrum which was essential for the effective breeding of thorium. However, the presence of graphite elements introduces problems concerning (1) the neutron damage in graphite and the need for its periodic replacement in high power-density systems, (2) the need to dispose of highly radioactive graphite, and (3) the possibility of flow obstruction by graphite breakage following extensive radiation damage. Because breeding is not desired in the ATW, all these problems can be

reduced by limiting the use of graphite moderator elements in the high power density regions of the core

Design simplicity Because of its liquid form, the molten salt fuel permits a greater level of design simplicity than solid fuel reactors For example, the following items will not be required refueling machines, fuel rods and assemblies, reactivity control systems and their backup, complex shutdown systems and extensive accident-recovery procedures On the other hand, salt cleaning equipment, fission product handling apparatus and remote maintenance devices would be required

Minimization of material problems The achievement of low inventories during waste destruction is related to high neutron fluxes Neutron flux and power density are not necessarily closely correlated The proper selection of operating conditions and sufficient shielding inside the reactor vessel will be required to achieve both low actinides inventories and low radiation damage to blanket components, and to operate at as high a power density as possible to reduce costs Some compromises will have to be found

Spatial separation of primary system components Because all primary system components contain fuel salt, any neutron leakage into components will have to be minimized because it would produce fissions in those regions, with consequent heat generation and fast neutron flux damage and activation

Conservative operating conditions Fuel and salt temperatures, flow rates, power densities, operating pressures in the primary system, intermediate system and steam generator system should be selected based on previous experience with the MSRE, the conceptual design work performed for MSBR, the laboratory experience with molten salt tests, and the experience of other operating reactors, most notably the liquid metal reactors Above all, the selected operating conditions should emphasize safety and reliability

Based on the previous points, Figs 6 and 7 illustrate the current thinking in the ATW conceptual nuclear design The performance of such conceptual design, when coupled with the process chemistry which is being developed at Los Alamos for use in the ATW fuel cycle, should provide very small standing inventories and a limited waste stream Fig 8 based on preliminary neutronics and depletion calculations, illustrate the low inventory feature of the ATW actinide burner

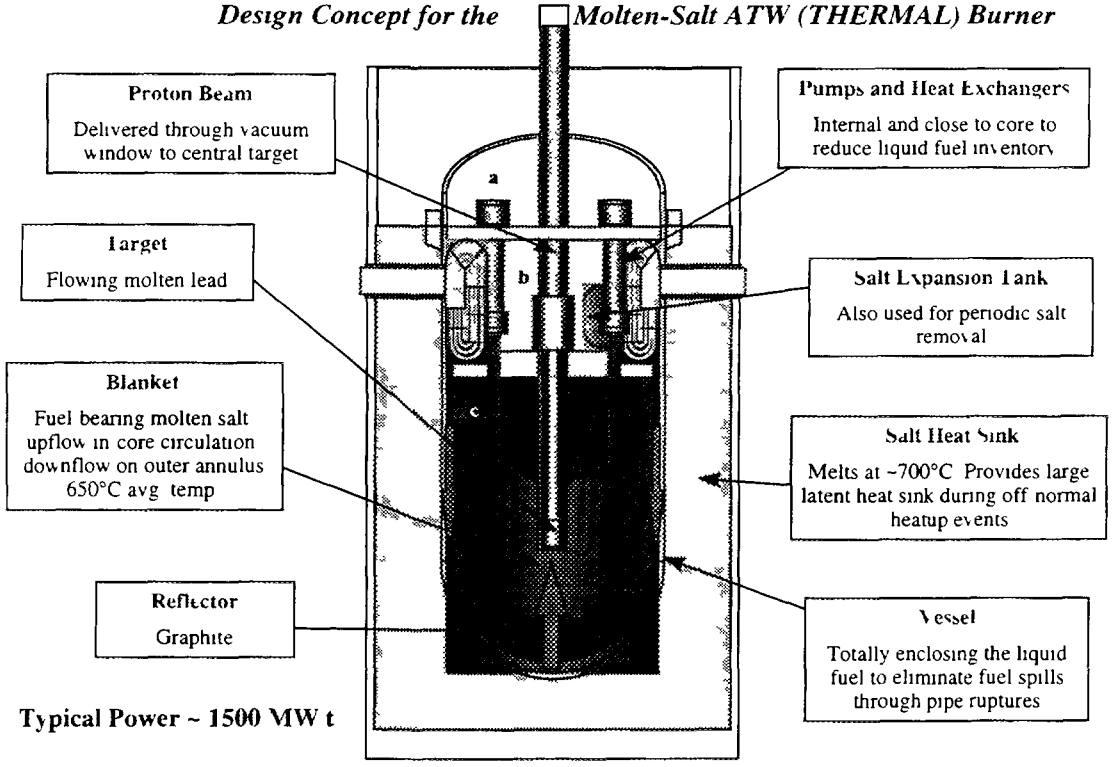

FIG 6 A design concept of thermal ATW burner

Lead Cooled ATW System

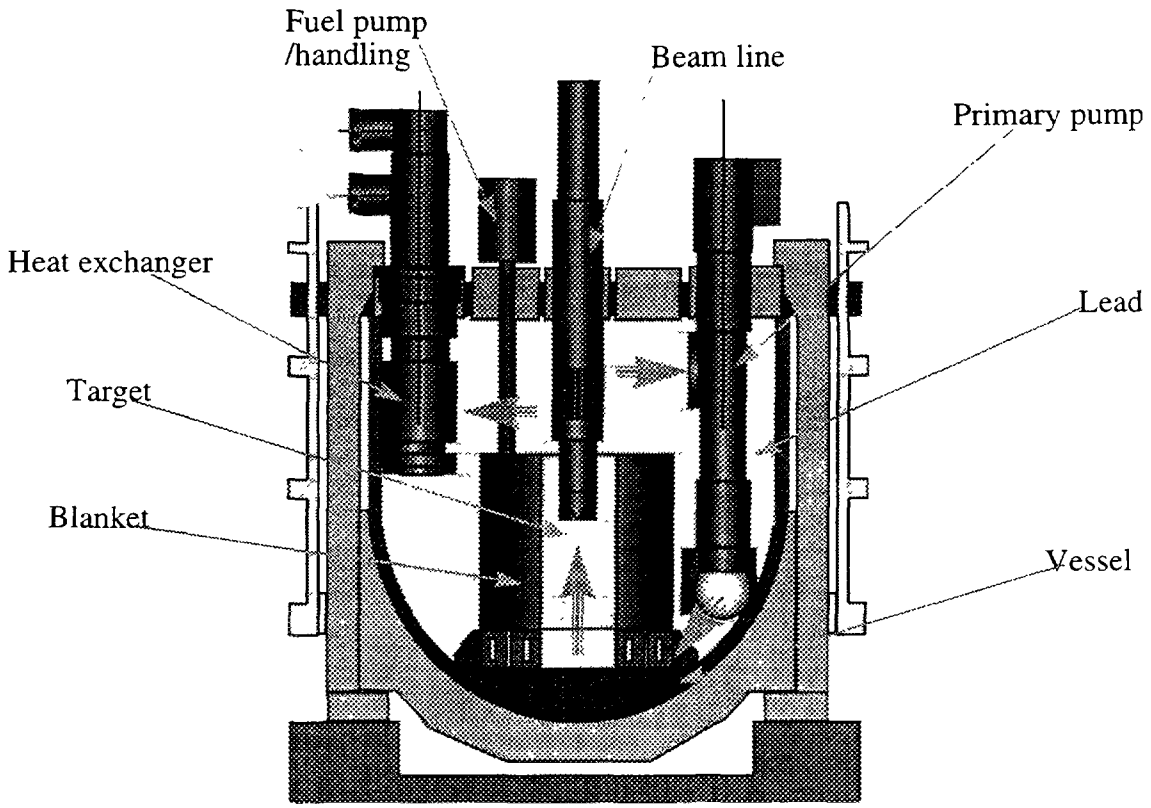

FIG. 7. A design concept view of fast, lead-cooled ATW burner

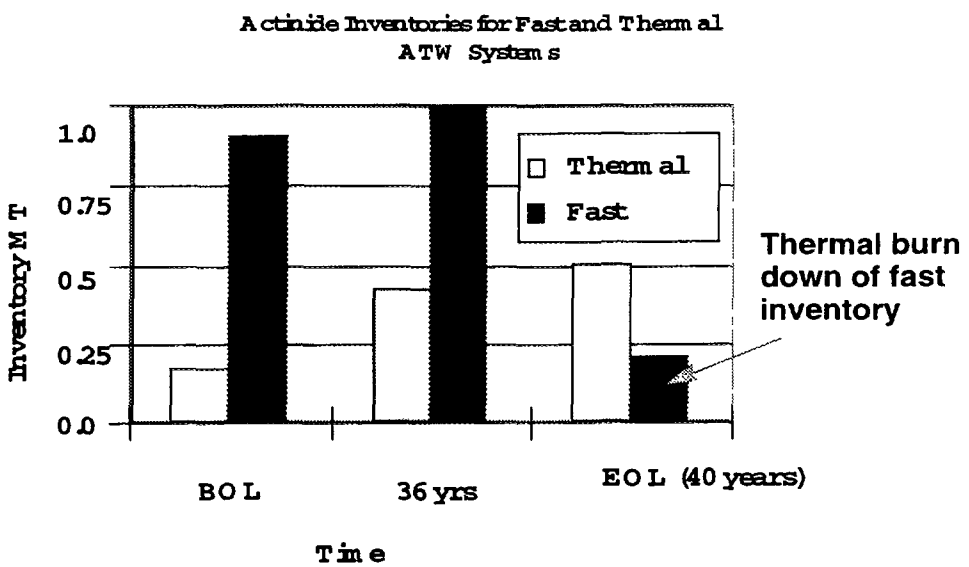

FIG. 8. Life-time actinide inventory for fast and thermal ATW systems

Accelerator-driven subcritical systems involve sustained fission processes that will produce radiation and fission product levels comparable to conventional power reactors. As such, a nuclear safety approach similar to that used for reactors must be employed.

The fundamental nuclear safety objectives applied to the design of fission reactors are [36]: 1) control of fission power, 2) adequate cooling, 3) containment of radioactive materials, 4) prevention of inadvertent criticality and 5) control of personnel and public exposure. Also, for an ATW system to be licensed in the United States, it would need to have characteristics consistent with those delineated by the Nuclear Regulatory Commission (NRC) in its policy statement on regulation of advanced nuclear power plants [37]. These characteristics include: simplicity, slow response, passive system reliability, reduced system interdependencies, reduced severe-accident concerns, assured defense-in-depth barriers, and clarity in safety analyses: these features provide the safety robustness and margins that are desired for advanced systems, which initially will have had little operational history.

Control of fission power

The response of a neutronically critical system to reactivity insertions is highly nonlinear and rapid: the initial response is in fact related to the prompt-neutron generation time and the longer-term response is related to the addition of delayed neutrons from particular decaying fission products. Indeed, it is these delayed neutrons that make reactor control practically feasible. Reactivity control systems must be capable of preventing power levels that exceed specific limits, which are set to ensure fuel stability, cooling sufficiency, and first-barrier integrity.

To obtain a general sense of the responses of critical and subcritical systems to reactivity insertion events, simple point-kinetics calculations have been performed [14] and their results are shown in Fig. 9.

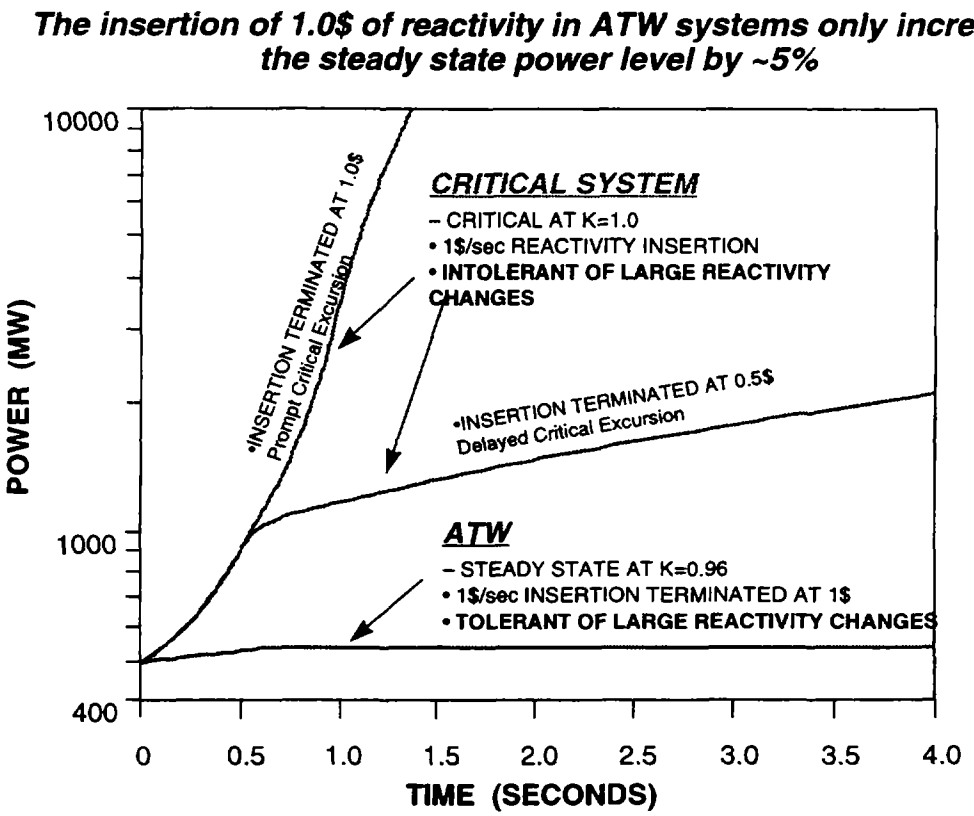

FIG. 9. Kinetics of the critical and subcritical nuclear systems. Responses to reactivity insertion events: 1$/s reactivity insertions.

In these calculations, the reactivity insertion rate was 1 $/s, and its duration was assumed to be either 0.5 sec or 1 sec. For a typical plutonium-fueled molten-salt system, where up to ½ of the delayed neutrons may be released beyond the boundaries of the core in pipes or heat exchangers, a dollar of reactivity is approximately equal to a change in k_{eff} of 0.002. No reactivity feedbacks were assumed in either case to simplify the understanding of the results. The initial multiplication in the subcritical system was assumed to be 0.96, and the initial power for both systems was assumed to be 500 MW. The predicted performance is plotted in figure.

As expected for the critical system, the power rises rapidly and continues to rise after the reactivity insertion is completed. Without negative reactivity insertions from inherent negative feedbacks and/or addition of neutron absorbers, the transients are unterminated. The response of the subcritical system is markedly different in that the power changes very little. The power is inversely proportional to the inverse of the degree of subcriticality of the system (initially 1-0.96 or 0.04). At the end of the 1-sec reactivity insertion transient, one dollar of reactivity was gained, making the final multiplication of the system equal to 0.962 and the degree of subcriticality equal to 0.038. The power change is approximately 5%, and a new steady state is established. A subcritical system appears to be robust in accommodating neutronic upset conditions, because the system's response is predictable and relatively insensitive to the reactivity changes (small power changes for large reactivity changes), as long as the degree of subcriticality is substantial, i.e. large compared to the delayed-neutron worth. Even if the system was assumed to be initially at a multiplication of 0.99 and the same reactivity insertion event occurred, the power would only change by approximately 25%. To put things into perspective, a dollar worth of reactivity insertion would be equivalent to a plutonium feed error of a factor of ten at beginning of life (the most sensitive condition) [38].

Although these large margins and the decoupling of power changes from reactivity changes are attractive in preventing and limiting potential power excursions, and make subcritical systems inherently stable, it is also true that other (desirable) feedbacks, such as those from system temperature changes, only weakly affect the power for subcritical systems. In subcritical systems, power cannot be easily adjusted by means conventionally used in reactors. For example, active control with absorber rods would not be particularly effective in subcritical systems because of the weak coupling between reactivity and power. The obvious power control would be by changing the intensity of the driving neutron source by varying the intensity of the proton beam current.

A second objective for nuclear systems is the highly reliable and rapid termination of the fission process if the control system were to fail or unforeseen reactivity increases were to occur (scram). Normally, reactors have mechanically inserted neutron absorber components (shutdown rods, safety rods, absorber balls, etc.) to provide the scram function. To achieve the required high reliability of inserting these absorbers on demand, redundancy and diversity of components and systems are employed. Because of the delays associated with absorber insertion, the power continues to rise above the scram point: this power over-shoot must be predicted and included in the design of the shutdown system to ensure that safety limits are not exceeded. The design must in turn take into account the reactivity properties of the fuel, moderator and coolant. As a result, fuels containing mainly plutonium and higher actinides, for which there may be little inherent negative reactivity feedback are typically not manageable in critical systems.

If a scram event were to occur in an accelerator-driven subcritical system, the delays would be limited to those associated with detection of the condition, and interruption of the proton beam. The sensing and interruption system could be entirely passive, based for example on fuses for the accelerator beam source, placed in the target/blanket. Once the proton beam is interrupted, the neutron production stops nearly instantaneously and the power in the subcritical system drops with a decay time given by the product of prompt neutron lifetime and multiplication. The shutdown can be accomplished quickly, predictably, and reliably, following detection of abnormal conditions, in milliseconds instead of seconds. The need for in-core neutron absorber insertion with the associated mechanical complications is eliminated. The complexities associated with "managing" the power over-shoot are also eliminated, and inherently unstable fuels like plutonium become acceptable [14].

Analogously, the quick restart of a subcritical system can be performed following a forced shutdown

in virtually any situation. A typical problem in reactor operation following shutdown is the buildup of samarium-149, a large cross-section daughter of the fission product promethium-149, which has a 53-hour half-life. Shutting down a reactor (especially a high flux system) can lead to the growth of such large amounts of ^{149}Sm that it may not be restartable until the ^{149}Sm has been removed. No such constraint exist for subcritical accelerator-driven systems: these systems can always restart and burn the accumulated samarium because they do not need to reach criticality in order to start producing neutrons and destroy the poison.

Adequate cooling

Assuring adequate cooling in all situations is essential for all fission reactors. Because the integrity of the first barrier is a key element in the defense-in-depth strategy for preventing the release of fission products, and because this integrity is strongly linked to its temperature, adequate cooling of the first barrier must be assured for normal power operations and for a variety of accident situations, including off-normal shut-downs with the associated decay heat from the fission products. For conventional solid-fuel reactors fuel cladding is the first barrier, and with high power densities and water coolant, the cladding temperature can rise rapidly if cooling is interrupted locally. For the molten salt system, the first barrier is the vessel. The thermal response of this first barrier is therefore linked to the heat capacity of the entire primary system enclosed by the vessel, which is substantially larger than that of the individual fuel pins or fuel assemblies of an LWR. The rate of temperature rise in molten salt systems, therefore, would be much slower than in solid fuel systems. This slow, system-wide response provides substantially increased opportunities to sense inadequate cooling conditions and to respond appropriately.

The molten salt system also exhibits robustness from the standpoint of heat transport in and out of the core region. Again the point of reference is a solid-fuel, rod-type core. In this system, the heat is generated in the solid fuel material and is transferred out of the fuel, across the fuel-clad gap, through the clad, and to the surrounding coolant. The heat transfer processes include conduction, radiation, and convection. The overall heat-transport process is sensitive to dimensional changes, fuel restructuring, fission gas content in the gap, coolant pressure, coolant subcooling, and coolant velocity. Many of these aspects can change substantially during core life, for different operating modes, and for off-normal and accident conditions. Although the process is complex, it must be known reasonably well to assure adequate cooling and protection of the first barrier. In a molten salt system, on the other hand, the heat is generated directly in the molten salt, which is also the heat-transport medium. Heat-transport is therefore greatly simplified and rapid dissipation is possible in the event of inadequate cooling. This arrangement also appears to have a self-limiting characteristic in that if cooling in the core is inadequate, the coolant/fuel salt overheats, eventually boils and is removed from the core [14].

The final aspect of assured cooling is decay heat removal. The challenge is to get the decay heat to an ultimate heat sink before the increase in temperature can damage the integrity of the core. The heat produced in the compact cores of solid fuel systems must be removed into the primary heat transport system. In the molten salt system, instead, the decay heat is generated throughout the

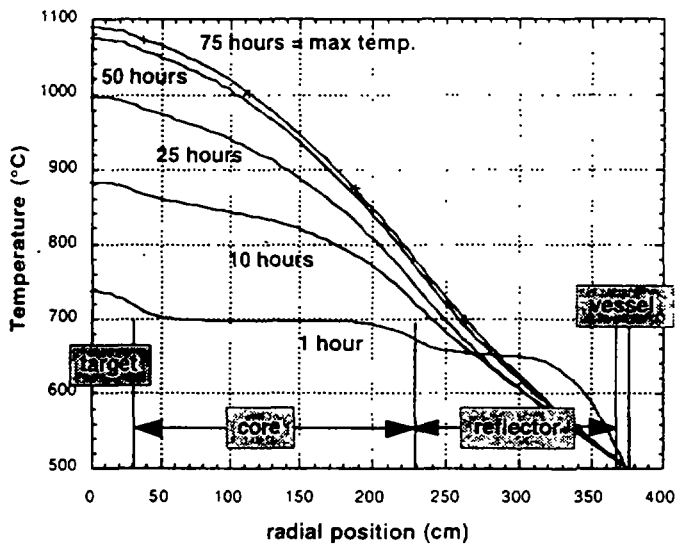

FIG. 10. Temperature rise of a prototype 500 MW$_t$ ADTT blanket in a loss of coolant accident. Assuming only convective cooling and a passive heat removal mechanism, the maximum temperature of 1100 °C is reached in 75 hours.

salt inventory in the primary system. Thus, this system has the possibility for predictable natural convection cooling to the primary system boundary and the possibility of efficient passive heat rejection from the primary system boundary to an external heat sink in emergency situations. The molten salt fuel would then allow the attainment of substantially more powerful "passively safe" units than possible with solid fuels, i.e. able to handle the core heat-up in the event of a cooling system failure unattended and without permanent damage (see Fig.10).

Containment of radioactive materials

The types of fission products retained in the fuel of an ATW-like molten-salt system are different from those in solid fuel systems, and because of the extensive cleanup processes, they are present in much smaller amounts in the liquid fuel. Their release will, nevertheless, constitute a great hazard. Thus, containment of the radioactive materials at all times and for all conditions must be accomplished for the molten salt system.

In conventional reactors, many individual sealed units (fuel pins) are present with limited life requirement (approximately three years before replacement). Thus, if a few of the individual units of the first barrier were to fail for some reason, only a relatively small fraction of the fission product inventory would be released to the next barrier. In contrast, the molten salt system's first barrier (the primary system boundary) must last for the life of the plant, and if it were to fail, a large fraction of the fission product inventory in the salt might well be released to the next barrier.

High reliability in the performance of the primary system boundary must be assured to deal with this challenge, and a highly reliable and effective second barrier. Because the first barrier is not in the core and therefore does not affect the neutronic performance and is generally accessible, design flexibility exists to make the primary system boundary highly robust and to provide inspectability by remote means. Sealed vaults with appropriate heat removal systems, atmosphere control systems, and spill recovery systems could be used as the second barrier. Finally, a surrounding containment or confinement structure would complete the three-barrier strategy to radioactivity release envisioned in the defense-in-depth approach [14].

A special challenge for the accelerator-driven molten-salt system is the integration of the beam transport equipment with the containment barriers. The proton beam can not pass directly through heavy-walled structures without substantial losses and the generation of significant heat and radiation. Some type of redundant thin-window approach is necessary, in order to avoid making the whole accelerator cavity part of the containment enclosure.

Prevention of inadvertent criticality

Prevention of inadvertent criticality in conventional reactors is a relatively straightforward matter because it is a concern only for fuel handling, new fuel storage, and spent fuel storage. Solid fuel segregated into numerous individual assemblies can be handled in a very controlled manner, monitored for structural deterioration, and stored in well characterized and robust structures. In contrast, the molten salt system presents challenges in assuring that the location of all fissile material is known at all times. The potential for precipitation of fissile materials from the molten salt must be considered and taken into account in the design of the various subsystems. The potential for criticality in the fissile material feed system and in the salt cleanup and processing systems will have to be considered. Care will also be required to assure that potential spills and leaks would only accumulate in subcritical configurations. Overall, criticality concerns would be mitigated by the subcritical margin of the accelerator-driven system and by the lower inventories of fissile material.

Radiation exposures to personnel

Limitation of the integrated exposure to the operating staff of a conventional reactor power station

involves equipment reliability and provisions in the design for ease of maintenance, inspections, testing and repairs. In this respect, the ATW system presents a challenge to designers and operators because of four reasons: 1) the fission products distributed throughout the primary system will produce high radiation fields in all areas adjacent to the primary system and potentially high exposures during incident recovery operations. 2) delayed neutrons produced throughout the primary system will activate all primary system equipment resulting in radiation exposure potential even after decontamination. 3) the target system will have limited life and require periodic replacement which could lead to additional personnel exposure. 4) the use of a lithium-based salt will result in the generation of substantial amounts of tritium, which could diffuse through metallic boundaries. All of these exposure potentials will have to be recognized in the design process, and special provisions will have to be included to protect workers during inspections, testing, maintenance, and repairs [14]. A considerable premium will be placed on highly reliable equipment and remote maintenance.

Safety features of the Oak Ridge MSBR design

A conceptual design for the ATW does not exist yet, and therefore a valid safety analysis of this concept cannot be performed. For reference, however, it is useful to look at the safety features of the Molten Salt Breeder Reactor (MSBR), for which a substantially developed conceptual design does exist [5], or the Molten Salt Reactor Experiment (MSRE) [19]. While the safety philosophy of the 1960's and 1970's was different from today's, many of the safety concerns and features would be directly applicable to the ATW system [35].

Passive safety features. The MSRE operation was found to be stable and self-regulating. Responsible for this behavior were the strong negative temperature coefficients of the fuel salt and the large heat sink offered by the graphite moderator. The MSRE was simple to control. In over 14,000 hours of critical operation, nuclear parameters never exceeded the operational limits and a reactor scram was never initiated. The criticality of the reactor was controlled by regulating the feed of fissile material. Similar operational characteristics could have been expected for the MSBR. Both reactors, however, were equipped with control rods, even though the MSRE never used them during operation.

Control rods. The control rods for the MSBR design were movable graphite cylinders, whose withdrawal from the core left an under-moderated region causing a reduction in reactivity. Should any of these control rods have broken, they would have floated out of the core, automatically resulting in decreased reactivity.

Decay-heat removal. Major passive decay-heat removal features were missing from the MSBR design. However, this was not a general limitation, but only specific to the MSBR design. It is reasonable in fact to expect that a properly designed molten salt system will exceed the level of passive decay-heat related safety of all conventional and advanced reactor designs.

Loss of primary coolant. Whereas a primary-system pipe break accident in a solid fuel reactor can lead to loss of coolant with resultant fuel overheating, fuel melting, and eventually fission product release; such a failure in the MSBR would lead directly to the spillage of molten salt fuel. This is equivalent to a partial fuel meltdown with breach of the primary system boundary in a solid fuel reactor. In the MSBR design it was argued that in such an accident situation the fuel would immediately freeze and most likely retain the fission products (especially since the volatiles would have been virtually absent from the fuel) so that cleanup of the contamination, repair and restart of the reactor could follow quickly. This procedure however might not meet modern standards of plant safety.

Steam pressure. The MSBR was designed to operate with a steam pressure of 3800 psig, by far the highest steam pressure found in any nuclear steam generator. The steam generator and power conversion plant were based upon the coal-fired Bull Run Power Plant that produced a net efficiency greater than 44%. Obviously the intent was to capitalize on the large thermal efficiency possible at the high molten salt temperature using the supercritical steam conditions. Pressure relief systems had to be provided in the intermediate loop to prevent over-pressurization in the event of a steam generator tube rupture. Such high

pressures in the steam generator would probably not be acceptable today in a molten salt system even in the presence of pressure relief systems, because of the very low pressure present in both the primary and secondary systems. It may therefore be desirable to consider lower pressure steam systems, i.e. 1000 psi, analogous to those employed in current low-pressure reactor designs such as the Integral Fast Reactor (IFR). While lowering the steam pressure will tend to lower the energy conversion efficiency, the decreased severity of steam line break accidents will facilitate the design of highly reliable heat exchangers and relax the requirements for the design pressure in the containment structure.

Natural convection capability. The MSBR core and heat exchanger, and also the steam generator, were designed to be all at about the same height, with little difference in the elevation of the respective thermal centers. Such a configuration did not encourage natural convection as a means of heat transport in case of a loss of forced flow. A configuration promoting natural convection would be required in the ATW design.

Shutdown capability. Because the MSBR was to operate with only a very small amount of excess reactivity to be compensated by external control, withdrawal of the control rods placed in the core was sufficient to ensure shutdown under all circumstances. Fuel drainage was not relied upon to shut down the reactor.

D.2.2.7. COST ESTIMATES FOR ATW SYSTEMS

Before a new and potentially expensive concept like ATW can be funded for feasibility studies and a demonstration research and development program, one has to be convinced that it does not have excessive intrinsic economical penalties. The extra costs incurred by an accelerator and a chemical processing plant in the ATW systems immediately raise the cost issue to a prominent level.

Lacking a complete conceptual design, costing of ATW systems is obtained by comparison to similar plants. The following analysis is based on the model developed in [39]. It is assumed that the target/blanket system would not cost more than a critical reactor of equivalent thermal power using similar technology (in terms of operating conditions, the IFR/ALMR reactor is the most similar to the molten salt blanket). The accelerator costs were estimated from the LANL-APT concept and the processing system cost was based on existing facilities, such as the LANL plutonium processing facility and on facilities evaluated for the IFR project.

Further details used in our cost estimates are as follows: The accelerator produces 1-GeV protons. 50 mA to drive the ATW burner. Using a liquid lead target, the yield from 1-GeV protons is 30 n/p. Assuming operating $k_{eff} = 0.96$, thermal to electric conversion of 40%, the engineered efficiency is 88% (12% of the electricity generated goes to the accelerator and the auxiliary operation). This ATW system generate 3000 MWt, or 1200 MWe power. Of this amount, 1060 MWe is available to the grid. It can support four 1000-MWe LWRs.

The cost for the chemical plant ($500M) should be lower than previously estimated for aqueous systems [8] and it is based on a comparison with the IFR processing costs [40]. The ATW fuel cycle includes: spent-fuel hydrofluorination, fuel and waste storage at the front end; reduction extraction of lanthanides, off-gas systems and in-blanket electrorefining at the back-end; replacement operation and storage space; waste treatment and end-of-life decommissioning. The ATW system does not require fuel pin (re)fabrication, and the separation requirements are in general lower than in the IFR/ALMR.

The blanket cost is estimated at $300M, which is a conservative estimate based on IFR core costs, augmented to include the target. The other component costs are adapted from [39], with proportional adjustments in turbine machines, miscellaneous equipment and electricity equipment. The result is $1700M. Adding the contingency and interest cost during construction, it amounts to $2590M.

The size of the ATW plant was taken at 3000 MWt, to match it with the standard LWRs to be serviced. One ATW system would process and transmute the spent fuel produced by four identical LWR plants of

equal thermal power.

Using the total cost of $2590M derived for the actinide burner system and standard accounting practices [39], the surcharge on the nominal cost of nuclear-generated electricity (50 mils/kWhr) to destroy plutonium and the higher actinides is calculated to be 3 mils/kWhr. Further surcharges will apply to pay for the destruction of selected long-lived fission products.

This exercise in ATW system costing is not an attempt to put a hard number on costs. It does, however, provide a general indication on the cost issue. It seems reasonable to expect that the ATW systems will cost more than other types of nuclear reactors, and that their introduction in the nuclear energy production infrastructure will increase the cost of nuclear-produced electricity. These extra charges, however, will enable the nuclear industry to deal with the waste problem without depending on geologic storage. It is our belief that such disposal costs are not accurately known for the geologic repository solution at this point, given the uncertainty concerning the feasibility and public acceptance of this option.

It is possible that a centralized geological repository will not be realized, or that permanent nuclear waste storage will become acceptable only in conjunction with a transmutation process that destroys the actinides and the hazardous, long-lived fission products contained in the spent fuel. The increase in electricity rates introduced by transmutation systems might then be properly viewed as the adjustment that needs to be paid in order to take into account the real costs of waste disposal.

D.2.2.8. SUMMARY

In the past several years, the Los Alamos ADTT program has conducted studies of an innovative technology for solving the nuclear waste problem and building a new generation of safer and non-proliferant nuclear power plants.

Based on the LANSCE accelerator experience and the advent of high power accelerator technologies, drawing from the extensive development and operation knowledge bases of the Molten Salt Reactor Experiment at the Oak Ridge National Laboratory, the ALMR/IFR program at the Argonne National Laboratory and plutonium processing experience at Los Alamos, we are developing ATW as a nuclear concept with unique features and capabilities, and we deem it to be technically feasible with a reasonable amount of research and development.

The ATW concept destroys higher actinides, plutonium and selected fission products in a liquid-fuel subcritical assembly. The accelerator provides the extra neutrons and the level of subcriticality needed to perform these operation safely and effectively.

Among the special features of ATW, the following four are especially important:

1. ATW flexibly accepts nuclear spent fuel from any existing type of nuclear reactor using practical and efficient processes
2. Inhibits plutonium accumulation, proliferation and diversion at all levels
3. Effectively destroys plutonium, higher actinides (utilizing them for energy and neutron production), and selected fission products, removing them from the nuclear waste stream
4. Is fully compatible within the existing or foreseeable future nuclear infrastructure of base-load reactors

Admittedly, the ATW system uses technology which is not as developed as present-day commercial nuclear technologies, and actual realization of its objectives will take 15-20 years of hard work and development (see timeline in Fig. 11). No pure actinide burner, subcritical or otherwise, has ever been operated and the experience base for pyroprocessing (molten salt and liquid metal chemistry) is smaller than for more established techniques (i.e. aqueous processing). In the paper we have only hinted at the process chemistry required by ATW. While these processes have been identified and look promising, their full characterization is still far from complete, including the determination of the all-important decontamination factors in the waste streams.

We are clearly just beginning to explore the possibilities of these liquid-fueled accelerator-assisted nuclear systems. However, a molten salt fuel reactor was operated satisfactorily in the past and the liquid lead technology proposed for the neutron target is still well established in Russia. High-power linacs are currently on the drawing board in the US and, through the innovations introduced by the MSR and IFR program, pyroprocessing is now considered a viable alternative to aqueous processing. The ATW system will capitalize on these assets and take advantage of the experience.

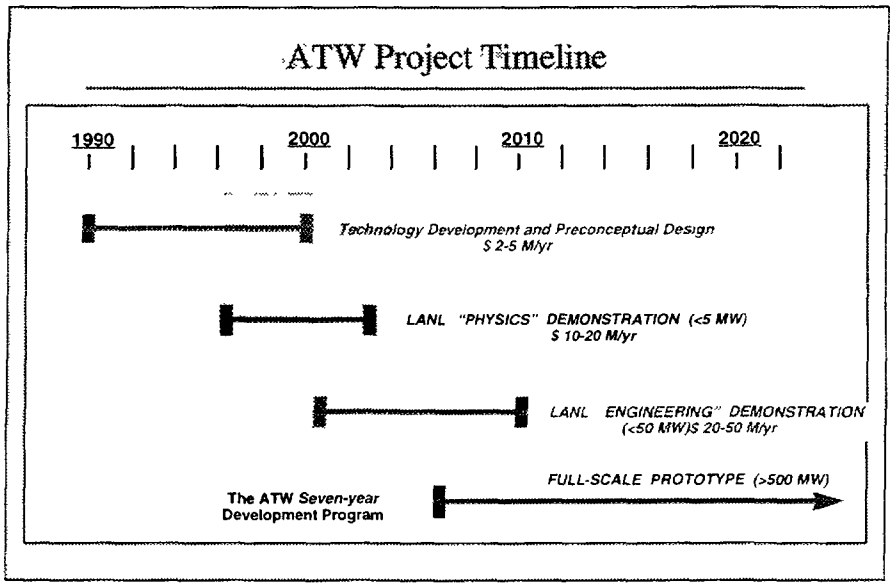

FIG. 11. Anticipated ATW project timeline at LANL.

Acknowledgments:

The help and interest of the following individuals are acknowledged: E.D. Arthur, W. Barthold, T.S. Bathia, C.R. Bell, C.D. Bowman, J.C. Browne, R. Camasssa, B.H. Choi, G.D. Doolen, R. Ecke, M.G. Houts, Y. Hu, B. Newnam, W. Sailor, S. Wender, U. Shin.

REFERENCES

[1] C. D. Bowman, "Basis and Objectives of the Los Alamos Accelerator-Driven Transmutation Technology Project," Proc. Intl. Conf. on Accelerator-Driven Transmutation Technologies and Applications, Las Vegas, NV, 1994, p. 22.

[2] E. D. Arthur, "Enhancements to Transmutation System Performance through Use of an Accelerator/Fluid Fuel Combination," Proc. Intl. Conf. on Evaluation of Emerging Nuclear Fuel Cycle Systems, Versailles, Vol. 1, p. 466, Amer. Nucl. Soc. (1995).

[3] C. D. Bowman et al., "Nuclear Energy Generation and Waste Transmutation Using Accelerator-Driven Intense Thermal Neutron Source," Nucl. Instrum. Methods A230, 336 (1992).

[4] J. Powell et al., "The ADAPT Concept - an Accelerator Driven System for the Rapid and Efficient Disposal of Plutonium," Proc. Intl. Conf. on Accelerator-Driven Transmutation Technologies and Applications, Las Vegas, NV, 1994, p. 151.

[5] R. C. Robertson et al., "Conceptual Design Study of a Single-Fluid Molten-Salt Breeder Reactor," Oak Ridge Natl. Lab. Rept. ORNL-4511, June, 1971.

[6] M. Cappiello et al., "Los Alamos Aqueous Target/Blanket System Design for the Accelerator Transmutation of Waste Concept," Proc. Int. Conf. Future Nuclear Systems: Emerging Cycles and Waste Disposal Options, Seattle,Vol. 1, p. 397, Amer. Nucl. Soc. (1993).

[7] J. Cornwell et al., "Accelerator Based Conversion of Plutonium," JASONS Rept. JSR-94-310, Nov., 1994.

[8] R. A. Krakowski, "Parametric Studies of Aqueous-Slurry Blankets of ATW," Proc. Intl. Conf. Future Nuclear Systems: Emerging Cycles and Waste Disposal Options, Seattle,Vol. 2, p. 781, Amer. Nucl. Soc. (1993).

[9] W. C. Sailor, and C. A. Beard, "Neutronic Analysis for an Accelerator-Based Nuclear Waste Transmuter," Proc. Intl. Conf. Future Nuclear Systems: Emerging Cycles and Waste Disposal Options, Seattle, Vol. 1, p. 369, Amer. Nucl. Soc., (1993).

[10] F. Venneri, C. D. Bowman and R. Jameson, "Accelerators Address Nuclear Waste Problem," Physics World, p. 40, Aug., 1993.

[11] "Accelerator Production of Tritium," Energy Research Advisory Board of the U.S. Dept. of Energy, Washington, DC (1990).

[12] "Accelerator Production of Tritium," JASONS Rept. JSR-92-310, The Mitre Corporation, Mclean, VA (1992).

[13] Accelerator Topical Report, Los Alamos Natl. Lab. Rept. LA-CP-94-48, Mar., 1994.

[14] C. R. Bell, "Safety Features of Subcritical Fluid Fueled Systems," Proc. Intl. Conf. on Accelerator-Driven Transmutation Technologies and Applications, Las Vegas, NV, 1994, p. 167.

[15] G. Morgan et al., "LANL Sunnyside Experiment: Study of Neutron Production in Accelerator-Driven Target," Proc. Intl. Conf. on Accelerator-Driven Transmutation Technologies and Applications, Las Vegas, NV, 1994, p. 682.

[16] J. F. Stubbins et al., "Behavior of Structural and Target Materials Irradiated in Spallation Neutron Environments," Proc. Intl. Conf. on Accelerator-Driven Transmutation Technologies and Applications, Las Vegas, NV, 1994, p. 879.

[17] J. J. Park and J. J. Buksa, "Selection of Flowing Liquid Lead Target Structural Materials for Accelerator Driven Transmutation Applications," Proc. Intl. Conf. on Accelerator-Driven Transmutation Technologies and Applications, Las Vegas, NV, 1994, p. 512.

[18] J. R. Engel et al., "Conceptual Design Characteristics of a Denatured Molten-Salt Reactor with Once-Through Fueling," Oak Ridge Natl. Lab. Rept. ORNL/TM-7207, July, 1980.

[19] P. N. Haubenreich and J. R. Engel, "Experience with Molten-Salt Reactor Experiment," Nucl. Appl. and Tech. 8, p. 119, Feb., 1970.

[20] H. G. McPherson, "The Molten Salt Reactor Adventure," Nucl. Sci. and Eng. 90, 374 (1985).

[21] Nuclear Applications and Technologies, Issue dedicated to the Molten-Salt Reactor Program. Vol. 8, Feb., 1970.

[22] C. J. Barton, "Solubility of Plutonium Trifluoride in Fused-Alkali Fluoride - Beryllium Fluoride Mixtures," J. Chem. Phys. 64, 306 (1960).

[23] C. J. Barton et al., "Phase Equilibria in the Systems BeF_2-CeF_3, LiF-CeF_3, and LiF-BeF_2 - CeF_3," J. Inorg. Nucl. Chem. 36, 1271 (1974).

[24] J.C. Mailen et al., "Solubility of PuF_3 in Molten 2 LiF - BeF_2," J. Chem. Eng. Data 16 (1), 68 (1971).

[25] K.A. Romberger et al., "New Electrochemical Measurements of the Liquidus in the LiF-BeF_2 System. Congruency of Li_2BeF_4," J. Phys. Chem. 76, 1154 (1972).

[26] R.E. Thoma, ed., "Phase Diagrams of Nuclear Reactor Materials," Oak Ridge Natl. Lab. Rept. ORNL-2548 (1959).

[27] R.E. Thoma et al., "Equilibrium Phase Diagram of the Lithium Fluoride -Beryllium Fluoride-Zirconium Fluoride System," J. Nucl. Mater. 27, 166 (1968).

[28] H. E. McCoy et al., "New Developments in Materials for Molten-Salt Reactors," Nucl. Appl. and Tech. 8, 156 (1970).

[29] J. H. DeVan et al., "Materials Considerations for Molten Salt Accelerator-based Plutonium

Conversion Systems," Proc. Intl. Conf. on Accelerator-Driven Transmutation Technologies and Applications, Las Vegas, NV, 1994, p. 476.

[30] G. T. Mays, A. N. Smith, and J. R. Engel, "Distribution and Behavior of Tritium in the Coolant-Salt Technology Facility," Oak Ridge Natl. Lab. Rept. ORNL-TM-5759, Apr., 1977.

[31] H. E. McCoy and J. R. Weir, ASTM STP-457, pp. 290-310, 1969.

[32] D. N. Brasky, and J. M. Leitnaker, "Homogenization of Ti-Hastelloy-N," Metallurgical Transactions A 10A, 427 (1979).

[33] P. G. Smith, "Development of Fuel and Coolant-Salt Centrifugal Pump for MSRE," Oak Ridge Natl. Lab. Rept. ORNL-TM-2987, Oct., 1970.

[34] B. S. Cowell, R. A. Krakowski, et al., "Accelerator-Based Conversion (ABC) of Weapons Plutonium: Plant Layout Study and Related Design Issues," Los Alamos Natl. Lab. Rept. LA-UR-95-1096, 1995.

[35] W. Barthold and Associates, "Preconceptual ABC Definition and System Configuration Layout", Report to LANL ADTT Project Office, 1995.

[36] NUREG-0410, "NRC Program for the Resolution of Generic Issues Related to Nuclear Power Plants", U.S. Nuclear Regulatory Commission, Jan., 1978.

[37] Natl. Res. Council, NRC 10CFR, Part 50: Regulation of Advanced Nuclear Power Plants; Statement of Policy, Federal Register Vol. 51, No. 130, July, 1988.

[38] E. Arthur, J. Buksa, W. Davidson, and D. Poston, "Discriminators for the Accelerator Based Conversion Concept Using a Subcritical. Molten Salt System," Los Alamos Natl. Lab. Rept. LA-12949-MS, May, 1995.

[39] R. A. Krakowski, "Accelerator Transmutation of Waste Economics," Nucl. Tech. 110, 295 (1994).

[40] "ALMR Fuel Cycle Facility. Design Report and Cost Estimate" Burns & Roe Co., for GE Nuclear Energy. BRC-448. UC-87Ta. Mar., 1995.

D.2.3. A SMALL SCALE ACCELERATOR DRIVEN SUBCRITICAL ASSEMBLY DEVELOPMENT AND DEMONSTRATION EXPERIMENT AT LAMPF

S. A. Wender, F. Venneri, C. D. Bowman, E. D. Arthur, E. Heighway
C. A. Beard, R. R. Bracht, J. J. Buksa, W. Chavez, B. G. DeVolder, J. J. Park,
R. B. Parker, C. Pillai, E. Pitcher, R.C. Potter, R. S. Reid, G. J. Russell,
D. A. Trujillo, D. J. Weinacht, W. B. Wilson, K. A. Woloshun

Los Alamos National Laboratory
Los Alamos, NM 87545

A small scale experiment is described that will demonstrate many of the aspects of accelerator-driven transmutation technology. This experiment uses the high-power proton beam from the Los Alamos Meson Physics Facility accelerator and will be located in the Area-A experimental hall. Beam currents of up to 1 mA will be used to produce neutrons with a molten Lead target. The target is surrounded by a molten salt and graphite moderator blanket. Fissionable material can be added to the molten salt to demonstrate Plutonium burning or transmutation of commercial spent fuel or energy production from Thorium. The experiment will be operated at power levels up to 5 MW.

6.2.3.1. INTRODUCTION

The coupling of a neutron producing accelerator with a subcritical fission assembly has been proposed at Los Alamos as a method of addressing several issues of current importance. This type of subcritical system can be operated in a much larger parameter space than an ordinary reactor. Because of this increased flexibility in operating conditions, an accelerator driven subcritical fission system can be used to 1) destroy weapons grade Plutonium with little actinide residue, 2) burn spent fuel from commercial reactors with reduced waste stream and 3) generate power using the Thorium/uranium cycle. Because the fuel does not need to be enriched, it appears that the system can be made more proliferation resistant than other proposed systems that address these issues.

At present the system concept for an accelerator driven transmutation technology (ADTT) system consists of a 500 MW_t module driven with 15 mA of 800 MeV proton beam (12 MW) incident on a neutron production target. The neutron production target is at the center of a $LiF\text{-}BeF_2$ molten salt (MS) and graphite moderator blanket. In the case of Plutonium destruction, Plutonium can be added to the molten salt. Other applications such as energy production (EP) and accelerator transmutation of waste (ATW) will probably use the same basic technology and design philosophy. In these cases Thorium or spent fuel could be added to the molten salt to demonstrate energy production or spent fuel transmutation.

Considerable knowledge and experience in the operation of MS systems exists from the Molten Salt Reactor Experiment (MSRE) that was operated at the Oak Ridge National Laboratory (ORNL) in the 1960's. At the conclusion of the MSRE, the researchers at ORNL felt that they had satisfactorily demonstrated the basic requirements of MS operation. In the design of this experiment we have assumed that the major technical issues have been satisfactorily addressed by this work at ORNL. As we design and fabricate the experiment, we will continuously evaluate the technology and update it where possible or necessary.

As a crucial step towards developing a 500 MW_t prototype module, we are proposing a small scale demonstration experiment. The experiment consists of a phased sequence of development and demonstration activities that begin with the development of a molten-lead target and techniques for molten salt handling. The experiment will culminate in the operation of an integrated accelerator-target/blanket subcritical fission assembly that can operate at power levels of up to 20 MW, although significant progress can be made at lower power levels.

This experiment will demonstrate many of the important aspects of ADTT and will be modeled on the preconceptual design of a single 500 MW_t module. The experiment will take advantage of the high power 800 MeV proton beam from the Los Alamos Neutron Science Centre (LANSCE) accelerator and will be located in experimental Area-A. Proton beam currents of up to 1 mA (800 kW) will be incident on the neutron production target. The experiment has the following ultimate goals:

1. It will demonstrate the integrated operation of a high-power particle beam used to produce neutrons coupled to a subcritical fission assembly. The power levels will be high enough to show significant transmutation processes.
2. It will test the analytical, diagnostic and control instrumentation that will be developed to monitor and operate the system. It will verify predicted system responses, time constants and reactivity behavior of the integrated system.
3. It will demonstrate the operation and performance of the neutron production target both alone and coupled to the molten salt blanket. It will also demonstrate the beam window technology necessary to inject the beam into such a target.
4. It will demonstrate techniques for large scale molten salt handling. It will provide a test bed for gaining safety related experience in molten salt operations.
5. It will demonstrate control of molten salt chemistry, material solubilities, material deposition and plate out problems.
6. It will demonstrate the helium sparging techniques for handling and removing the evolved fission product gases and the containment of tritium.
7. At a reduced flux level, it will verify the integrity of the materials and the design concepts used.
8. It will demonstrate the control of environment, safety and health (ES&H) issues related to the operation of the integrated system.

D.2.3.2. MOLTEN LEAD TARGET

The neutron production target consists of a cylindrical container that holds the molten Lead, a Lead-to-helium heat exchanger that is located above this cylinder and a reservoir below the target volume. A window on the side of the target allows the proton beam to enter the target volume and internal baffling directs the flow of the Lead against the window to ensure proper cooling. A liquid Lead target provides the following advantages:

1. Higher beam powers can be used compared to solid targets. The beam power in solid targets is limited by the ability to cool them. This limits the beam power to approximately 1 MW. Many ADTT concepts as well as spallation targets for material science research involve power levels substantially greater than 1 MW. Development of this technology will have wide and future applications. Similar liquid Lead targets are being developed at PSI for the SINQ spallation source.[1]
2. Because the bulk of the material is liquid, the target is not subject to the same radiation damage issues that are present in solid target designs. Radiation damage concerns are only present in the container and window of the target. In addition, the molten Lead can be removed and reused if the container needs to be replaced.

3. Because a liquid Lead target does not have to be cooled by the salt it can be decoupled from the salt tank and physically isolated from it. This means the target can have its own container and can be removed without having to open up the salt volume that may contain highly radioactive and fissionable material. In addition, removal of the target will be much easier because its volume and mass are only a small part of the salt blanket system. The tank that contains the molten salt does not require a window for the beam.

Two types of molten Lead targets are possible: pure Lead and Lead-bismuth eutectic (LBE). LBE has the advantage of a lower melting point. LBE has a melting point of approximately 125°C which is considerable lower than the 325 °C of pure Lead. This reduced temperature will simplify some of the materials issues in the operation of the target. The major disadvantage of LBE is that the production of radioactive Po is approximately 1000 times greater than that of molten Lead [2]. We are presently evaluating the choice of Lead for this target.

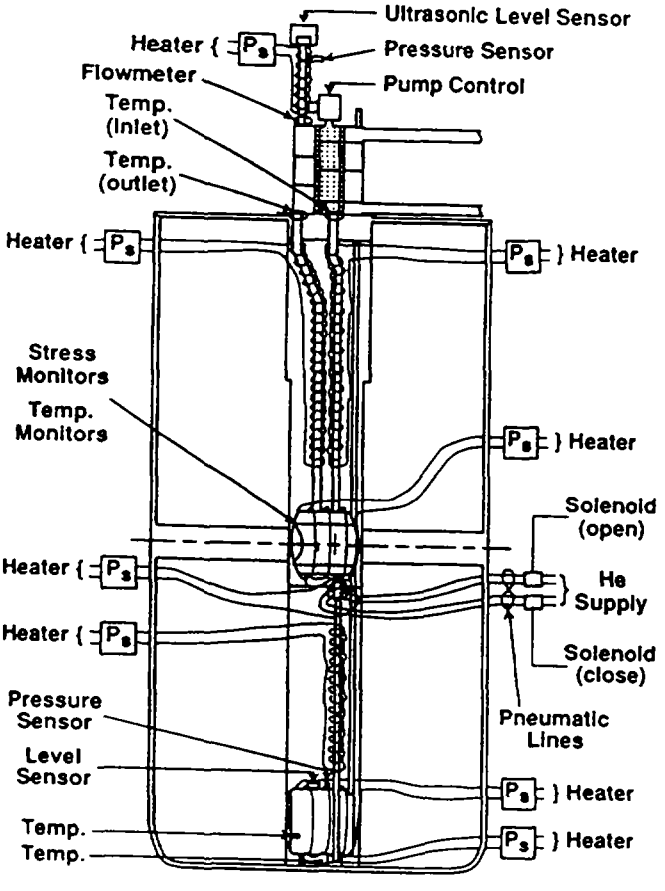

FIG. 1. Drawing of the molten Lead target for the accelerator driven subcritical assembly.

Figure 1 shows a schematic drawing of the liquid Lead target. A detailed description of the target design and operation is given by Beard et. al [3]. The present choice of material for the target container is Nb with 1% Zr. This choice is based on its excellent compatibility with molten Lead and is discussed in a contribution by Park et. al [4].

The Lead is stored in a reservoir below the target volume when not being irradiated. Lead is pumped into the target volume with pressurized argon. During normal operation the valve between the reservoir and the target volume is closed and the Lead circulates between the target volume and the heat exchanger. The Lead is returned to the reservoir to cool and is stored there.

D.2.3.3. SITE SELECTION

We chose to locate the experiment at the LANSCE accelerator because LANSCE presently has the highest beam power of any accelerator in the world and the beam energy is similar to that being proposed for the actual modules. A beam current of 1 mA is about the right intensity to test many of the issues associated with the development of the 500 MW_t module and will not require significant expenditure that going to higher currents will require. The proposed location for the experiment is after the A1 and A2 pion production targets (between the A3 and A4 targets). This location was chosen for the following reasons:

1. The proton beam transport and shielding for up to 1 mA of beam already exists.
2. There is relatively easy access to the proton beamline through stackable shielding, with little or no modification of existing structures necessary.
3. Because this location has never been the site of a production target it is relatively unactivated.
4. There is a large area near the beamline to stage the experiment. This area can be used to set up the experiment prior to its placement in the beam. The support infrastructure such as cooling and electrical power that will be installed for these initial tests can be used in the actual experiment.
5. There is good access to the experimental and setup areas with a large forklift and there is a 30 ton overhead crane in both the setup and the experimental areas.

D.2.3.4. MOLTEN SALT BLANKET

Figure 2 shows a conceptual design of the experimental tank for the experiment. It consists of a 3.6 m diam, 4.2 m high cylinder with a hole in the center for the target cell. The entire tank is fabricated from Hastelloy N and contains the molten LiF-BeF_2 salt and an array of carbon moderators. Hastelloy N has been shown in the MSRE to have excellent compatibility with molten salt. The Lithium in the salt will be enriched to 99.9% in ^7Li to reduce the absorption of neutrons due to the large thermal capture cross section of ^6Li. The beam passes through the tank and enters the molten Lead target cell on the side through a window. The molten salt is heated to a temperature of approximately 600°C and is circulated through the carbon moderators and cooled by heat exchanges located inside the molten salt tank. An external cooling loop, that uses a NaF-LiF molten salt with boron added cools the primary heat exchanger in the tank. The secondary loop is cooled by an independent heat exchanger. Some of the physical properties of the system are listed in TABLE I.

TABLE I. PHYSICAL PROPERTIES OF EXPERIMENT

Volume of salt	1 m^3
Volume of carbon	10 m^3
Operating temperature of salt	600 °C
Lead Target volume	60 l
Operating temperature of target	500°C

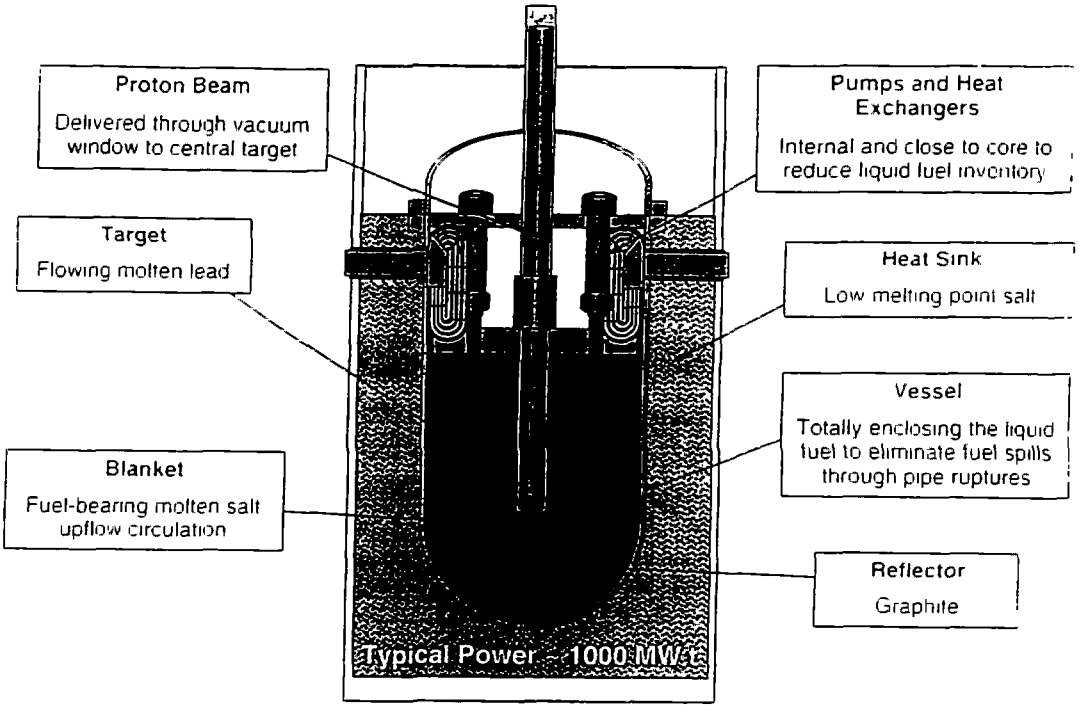

FIG 2 A conceptual system layout of the molten salt blanket for the accelerator driven subcritical assembly

There will be a small pipe installed in the tank to allow the removal of small amounts of salt during the experiment to monitor the oxidation state of the Pu and the build up of fission products (FP) Small amounts of material will be added to the salt blanket to adjust the redox potential of elements in the molten salt blanket The control of the salt flow through this drain pipe will be via freeze plugs that have been used successfully in the MSRE There will be provisions for supplying approximately 1 MW of electrical power to the MS tank to heat the salt during initial setup when there is no power being supplied by the beam

D 2 3 5. EXPERIMENT SCHEDULE

The experiment will proceed in three stages. The first stage involves the development of the molten Lead target In the second stage, the molten salt tank is constructed and the technology for molten salt operation is developed In the final stage, fissionable material is added to the molten salt target/blanket and actual transmutation processes are demonstrated. In this stage, small amounts of fissionable material will be added and the response of the system will be measured. The measurements will be compared to the predicted behavior. If the calculations are verified, more fuel may be added to the blanket and the power increased

At each stage, the systems will be developed first in off-line test stands Following complete testing, each system will be installed in the LANSCE beamline and tested in-beam For the case of the molten Lead target, the radiation testing will occur at the LANSCE beam stop location In the case of the molten salt tank, the testing will occur in the new target area in the location described in section D 2 3 3

We have calculated the performance of a fueled molten salt subcritical target\blanket system based on the conceptual design of this experiment Figures 3 and 4 show calculations of initial blanket power and initial k_{eff} following the addition of ^{239}Pu to the molten salt blanket For these calculations we have assumed 1 mA of proton beam with a neutron production target that produces 21 neutrons /proton For an initial loading of 3 kg of ^{239} Pu, the power in the blanket is calculated to be approximately 4 MW and k_{eff} is approximately 0 7

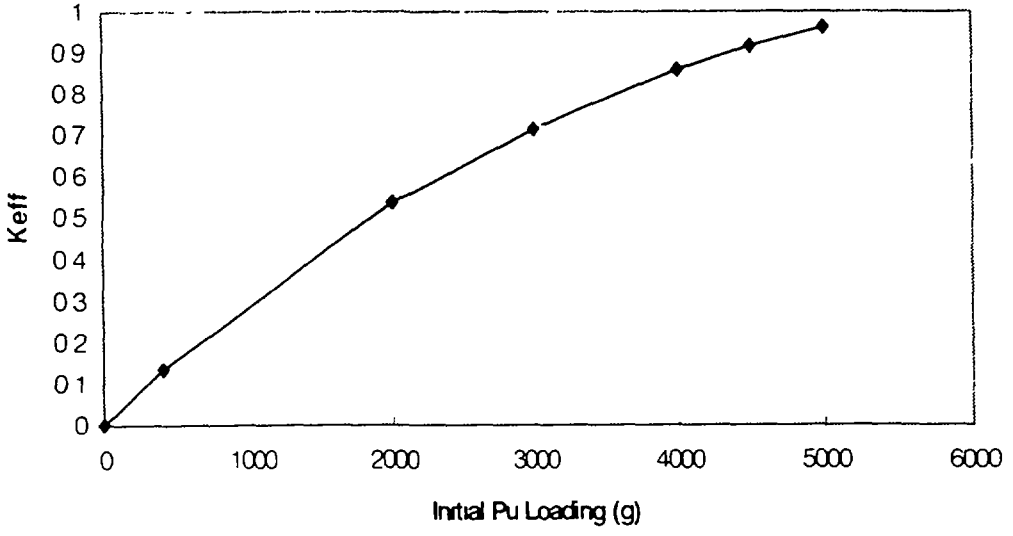

FIG 3 Initial blanket power for various initial plutonium loadings in the molten salt

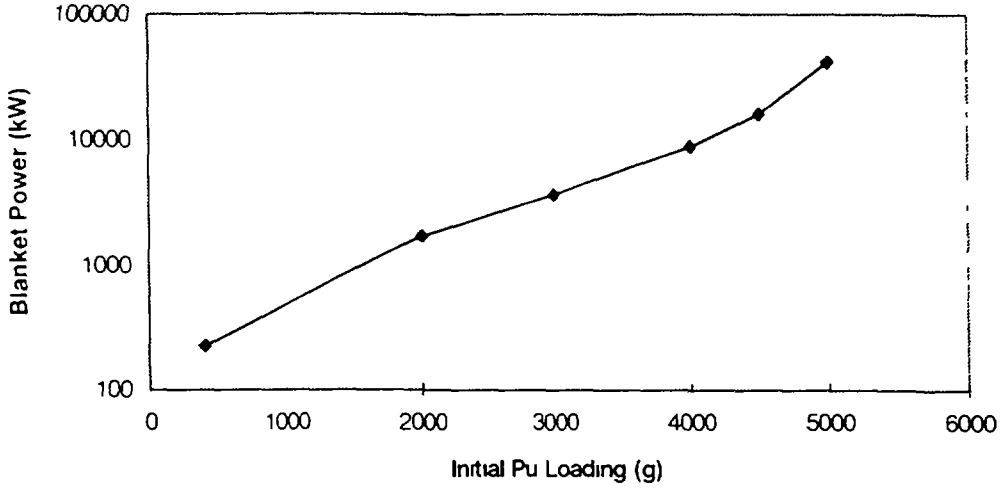

FIG. 4 Initial k_{eff} for different initial plutonium loading in the molten salt blanket

Energy production from Thorium is shown in Fig. 5. The solid squares show the time dependence of the blanket power when the MS blanket is loaded with 1000 kg of Thorium. The open circles show the performance of the system for the case where 2 kg of ^{239}Pu is added to the 1000 kg of Thorium. For comparison, the triangle curve shows the time dependence of the blanket when only 2 kg of pure ^{239}Pu is added. As seen from the figure (squares), the power from the fission of ^{233}U slowly rises when only Thorium is used in the blanket. The power output and the breeding rate of ^{233}U can be increased with the addition of ^{239}Pu . The fact that the curve for Thorium and Plutonium increases above the curve for pure Plutonium is an indication of power generation using the Thorium/uranium breeding cycle.

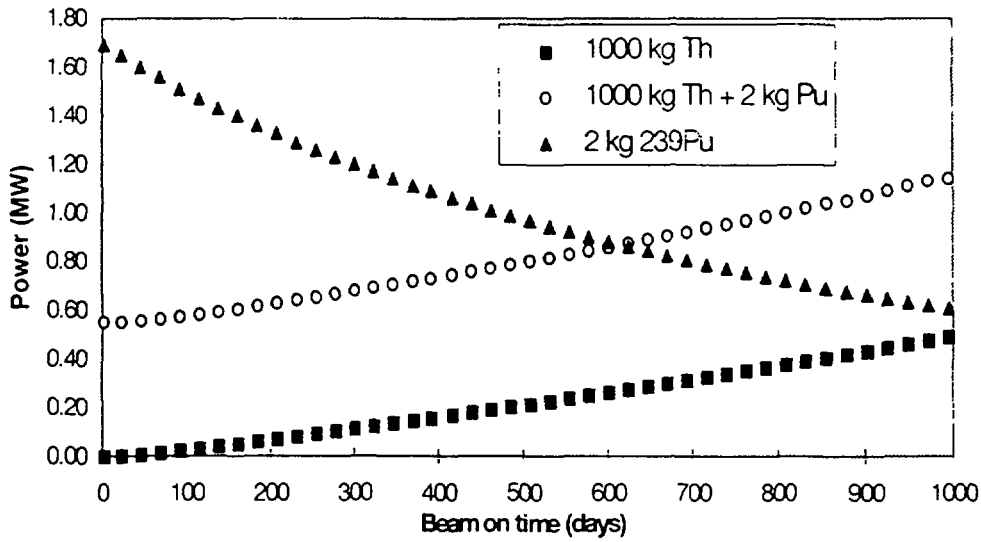

FIG. 5. The blanket power for various initial fuel loadings of the blanket. The solid squares are for an initial loading of 1000 kg of Thorium. The open squares is for an initial loading of 1000 kg of Thorium and 2 kg of ^{239}Pu. For comparison, the triangles show the blanket power for 2 kg of ^{239}Pu alone.

D.2.3.7. CONCLUSION

This small scale demonstration experiment is a crucial step towards the development of a full scale ADTT system. The experiment addresses many key issues in ADTT technology and will demonstrate the following new technologies:

1. Molten Lead neutron production targets
2. Integrated operation of a neutron production target and a subcritical fission blanket assembly.
3. Integral heat exchangers and pumps
4. On-line criticality measurements
5. Helium sparging to remove volatile fission product gases
6. Plutonium burn up
7. Energy production using the Thorium/Uranium breeding cycle.

REFERENCES

[1] Nucl. Sci. and Eng. **113** (1993) 287.

[2] V.T. Gorshkov et. al, "An Accelerator Based Installation of Small Power with the Lead-Bismuth Coolant", International Conference on Accelerator Driven Transmutation Technologies and Applications, Las Vegas, NV, July 25-29 1994.

[3] C. A. Beard et. al, "Flowing Lead Spallation Target Design for Use in an ADTT Experimental Facility Located at LAMPF",International Conference on Accelerator Driven Transmutation Technologies and Applications, Las Vegas, NV, July 25-29 1994.

[4] J. J. Park et. al, "Selection of Flowing Liquid Lead Target Structural Materials for Accelerator Driven Transmutation Applications", International Conference on Accelerator Driven Transmutation Technologies and Applications, Las Vegas, NV, July 25-29 1994.

D.3. CERN-GROUP CONCEPTUAL DESIGN OF A FAST NEUTRON OPERATED HIGH POWER ENERGY AMPLIFIER

C. Rubbia, J.A. Rubio, S. Buono[†], F. Carminati, N. Fiétier[††], J. Galvez, C. Gelès, Y. Kadi, R. Klapisch, P. Mandrillon[††], J.P. Revol and Ch. Roche

European Organization for Nuclear Research, CERN, Geneva, Switzerland

[†] Sincrotrone Trieste, Trieste, Italy

[††] Laboratoire du Cyclotron, Nice, France

The basic concept and the main practical considerations of an Energy Amplifier (EA) have been exhaustively described in Ref. [1]. Here the realisation of the EA is further explored and schemes are described which offer a high gain, a large maximum power density and an extended burn-up, well in excess of 100 GW × d/t corresponding to about five years at full power operation with no intervention on the fuel core. Most of these benefits stem from the use of fast neutrons, as already proposed in Ref. [2].

The EA operates indefinitely in a closed cycle, namely the discharge of a fuel load, with the exception of fission fragments, is re-injected in the sub-critical unit with the addition of natural Thorium to compensate for the burnt fuel. After several cycles an equilibrium is reached, in which the Actinide concentrations are the balance between burning and "incineration". The fuel is used much more efficiently, namely the power obtained from 780 kg of Thorium is roughly the same as the one from 200 tons of native Uranium and a PWR (33 GW × d/t of burn-up). The probability of a criticality accident is suppressed since the device operates at all times far away from it. Spontaneous convective cooling by the surrounding air makes a "melt-down" leak impossible.

An EA module consists of a 1500 MW_t unit with its dedicated 1.0 GeV proton accelerator of 12.5 mA. A compact, highly reliable and modular Cyclotron has been designed. A plant may be made of several such modules. For instance a cluster of three such modular units will produce about 2,000 MW_e of primary electrical power. A relevant feature of our design is that it is based on natural convection to remove the heat generated inside the core. The EA is a large, passive device in which a proton beam is dumped and the heat generated by nuclear cascades is extracted, without other major elements of variability. The delivered power is controlled exclusively by the current of the accelerator. The fuel needs no access during the whole burn-up and it may be kept sealed up as a non-proliferation safeguard measure. Contrary to Fusion, there are no major technological barriers.

After ≈ 700 years the radio-toxicity left is about 20,000 × smaller than the one of an ordinary Pressurised Water Reactor (PWR with an open fuel cycle and reprocessing losses 10^{-4}) for the same energy. Geological storage (10^6 years) is virtually eliminated or at least strongly reduced [≤ 500 Ci/(GW_e × a) after 1000 years]. It could be further reduced (< 35 Ci) "incinerating" some of the nuclides. Radioactivity dose to individuals truncated to 10,000 years and due to operation is about 1/330 of the one of PWR and about 1/33 of Coal burning.

D.3.1. INTRODUCTION

The principle of operation of the Energy Amplifier (EA) has been described in detail in Refs. [1-3]. The present paper is aimed at the demonstration of the practical feasibility of an EA with power and power density which are comparable to the ones of the present generation of large Pressurised Light Water Reactors (PWR). This is only possible with fast neutrons [2].

Greenhouse induced Global Warming concerns related to a massive use of Fossil Fuels may lead to a new call for nuclear revival. But a much larger share of energy produced by conventional Nuclear methods (PWR) will sharpen concerns and enhance many of the problems which must be solved before extending its use. We believe that most of the criteria for a revival of nuclear power are very tough:

(1) Extremely high level of *inherent safety;*

(2) *Minimal production of long lived waste* and elimination of the need of the geologic repositories;

(3) *High resistance to diversion,* since latent proliferation is a major concern.

(4) *More efficient use* of a widely available natural fuel, without the need of isotopic separation.

(5) *Lower cost of the heat* produced and *higher operating temperature* than conventional PWRs in order to permit competitive generation of substitutes to fossil fuels [4]. Substitution fuels are necessary to allow a widespread utilisation of the energy source and to permit retrofitting of existing facilities, now operating with CO_2 producing fuels.

Our design of an EA has these objectives as goals and it is intended as proof that they can be met fully. The primary fuel is natural Thorium which is completely burnt after a number of fuel cycles through the EA. Actinides present in the fuel discharge at the end of a fuel cycle are re-injected in the EA and become the "seeds" for the subsequent cycle. This ensures a very efficient use of the primary fuel element[1]. This objective is identical to the one eventually met by Fast Breeders. Compared to the consumption of natural fuel material, the EA is about 250 times more efficient than the present PWRs based on an open fuel cycle.

Nuclear power has successfully developed the methods of retaining large amounts of radioactivity within the power plant and in isolation with the biosphere. The limited amount of fuel material of the EA and the sealed, passive nature of the device further simplifies the realisation of such a concept. The fractions of radioactivity actually injected in the environment during (1) mining, (2) operation and (3) reprocessing and refuelling are considered first. Preventive measures to eliminate unwanted accidents and their possible consequences on the environment will be considered later on.

The radio-toxicity released by a Thorium driven EA is much smaller than the one of the PWR related throw-away cycle [1] [2]. In the phase of the fuel extraction and preparation, it is about $10^{-3} \div 10^{-4}$ for the same delivered energy, since a much smaller amount of Thorium is required (0.78 ton vs. 200 tons of Uranium for 3 $GW_{th} \times a$) in the first place and which is much less toxic to extract [5]. The toxicity released in form of waste at the back-end of the cycle for Actinides is reduced to the very tiny fraction lost during fuel re-cycling and reprocessing. Among fission fragments, excluding the short lived and stable elements, there are a few elements which are medium lived ($\tau_{1/2} \approx 30$ years, ^{90}Sr-^{90}Y, ^{137}Cs, etc.) and some others (^{99}Tc, ^{135}Cs, ^{129}I, etc.) which are truly long lived. The policy we propose to follow is to store in man-watched, secular repositories for several centuries the medium lived in order to isolate them from the biosphere and to promote a vigorous research and development of methods of incinerating the bulk of the long lived FFs with the help of a fraction of the neutron flux of the EA or with dedicated burners [6]. Therefore, and contrary to the PWR related throw-away cycle, the need for a Geologic Repository is virtually eliminated.

UNSCEAR [7] has estimated collective radioactivity doses to the population associated to various forms of energy production. Coal burning emits radioactivity in fumes and dust, resulting in a typical, *collective radiation exposure* of 20 man Sv $(GW_e\ a)^{-1}$. The practice of using coal ashes for concrete production adds as much as 2.5×10^4 man Sv $(GW_e\ a)^{-1}$. In the case of the PWR throw-away cycle the estimated dose is 200 man Sv $(GW_e\ a)^{-1}$, with the main contribution coming from the mining and preparation of the fuel[2]. Accidents which have plagued some of the present Nuclear Power stations and which are expected to be absent because of the new features of the EA, have added as much as 300 man

[1] The heat produced burning 70.3 kg of Thorium in the EA is equal to the one of 1 million barrels of oil

[2] The main nuclide contributions in the nuclear fuel cycle are Radon from Mill Tailings (150 man Sv/GW/y) and reactor operation and reprocessing (50 man Sv/GW/y). The potential accumulation of collective radiation doses in the far future from the practice of disposing the long lived waste (geologic storage) is not included in the UNSCEAR estimates, since it is subject to major uncertainties.

Sv $(GW_e\ a)^{-1}$, bringing the toll of Nuclear Energy to about 500 man Sv $(GW_e\ a)^{-1}$. Translating the figures of Ref. [7] to the conditions of the EA, we arrive at much smaller collective doses, namely 2.75 man Sv $(GW_e\ y)^{-1}$ for the local and regional dose and 0.44 ÷ 1.42 man Sv $(GW_e\ a)^{-1}$ for the global dose, depending on the type of mineral used. The total radioactivity absorbed by the population *is about one order of magnitude smaller than if the same energy is produced by burning Coal,* even if the ashes are correctly handled. In the case of the Coal option we must add the emissions of pollutants like dust, SO_2 etc. and their toll on the Greenhouse effect.

A novel element of our design is the presence of the proton beam. A recent experiment has specified the required characteristics of such an accelerator [3]. The accelerated particles are protons (there is little or no advantage in using more sophisticated projectiles) preferably of a minimum kinetic energy of the order of 1 GeV. The average accelerated current is in the range of 10 ÷ 15 mA, about one order of magnitude above the present performance[1] of the PSI cyclotron [8]. This current is lower by one order of magnitude than the requirements of most of the accelerator-driven projects based on c-w LINAC [9]. In view of the present developments of high-intensity cyclotrons and the outstanding results obtained at PSI [8], we have chosen a three-stage cyclotron accelerator. In the design particular attention has been given to the need of a high reliability and simplicity of operation. The experience accumulated in the field at CERN, PSI and elsewhere indicates that this goal is perfectly achievable. The expected over-all efficiency, namely the beam power over the mains load is of the order of 40%. The penetration of the beam in the EA vessel is realised through an evacuated tube and a special Tungsten window, which is designed to sustain safely both radiation damage and the thermal stress due to the beam heating. As discussed in more detail later on, the passive safety features of the device can be easily extended to these new elements.

Since the accelerator is relatively small and simple to operate, if more current is needed, several of these units can be used in parallel, with a corresponding increase of the overall reliability of the complex. In this case, the beams are independently brought to interact in the target region of the EA.

For definiteness, in the present conceptual design of the EA we have chosen a nominal unit capacity of 1500 MW_t. This corresponds to about 675 MW of primary electrical power with "state of the art" turbines and an outlet temperature of the order of 550 ÷ 600 °C. The thermodynamical efficiency of ≈ 45% is substantially higher than the one of a PWR and it is primarily due to the present higher temperature of operation. The general concept of the EA is shown in Fig. 1.1.

The nominal energetic gain[2] of the EA is set to G = 120 corresponding to a multiplication coefficient k = 0.98. The nominal beam current for 1500 MW_t is then 12.5 mA × GeV[3]. In practice the proton accelerator must be able to produce eventually up to 20 mA × GeV in order to cope with the inevitable variations of performance during the lifetime of the fuel. Such accelerator performance is essentially optimal for a chain of cascading cyclotrons. A significantly smaller current may not provide the required accelerator energetic efficiency; a higher current will require several machines in parallel. Hence, this size of the module is related, for a given gain, to the state of the art of the accelerator. The electric energy required to operate the accelerator is about 5% of the primary electric energy production. The choice of k is not critical. For instance an EA with k = 0.96 (G = 60) can produce the same thermal energy but with a fraction of re-circulated power about twice as large, namely 10% of the primary electricity, requiring two accelerators in parallel.

An energy generating module consists of a 1500 MW_t unit with its own dedicated 12.5 mA × GeV accelerator. An actual plant may be made of several such modules. For instance a cluster of three such modular units will produce about 2,000 MW of primary electrical power. Beams from the accelerators

---

[1] An improvement programme is on its way to increase the average current to about 6 mA.

[2] The energetic gain G is defined as the thermal energy produced by the EA divided by the energy deposited by the proton beam.

[3] This notation is justified, since the energetic gain of the EA is almost independent of the proton kinetic energy, provided it is larger than about 1 GeV.

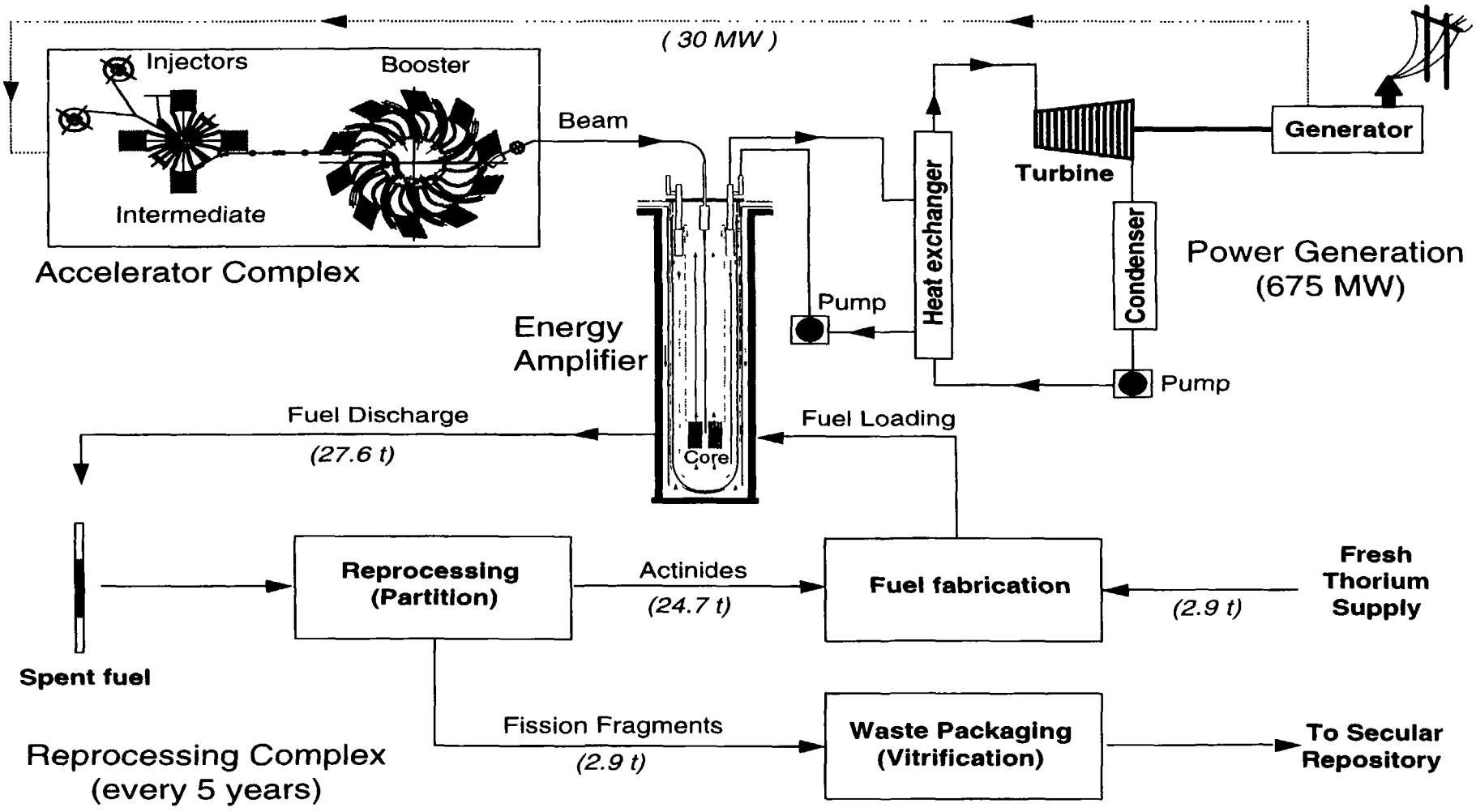

FIG. 1.1 General lay-out of the Energy Amplifier complex. The electric power generated is also used to run the Accelerator (re-circulated power ≤ 5%). At each discharge of the fuel (every 5 years) the fuel is "regenerated". Actinides, mostly Thorium and Uranium are re-injected as new fuel in the EA, topped with fresh Thorium. Fission fragments and the like are packaged and sent to the Secular repository, where after ≈ 1000 years the radioactivity decays to a negligible level (see Figure 1.4). For simplicity the option of incinerating long-lived fragments is not shown.

can be easily transported over the site and switched between units: a fourth, spare, accelerator should be added in order to ensure back-up reliability

The modular approach has been preferred in several recent conceptual designs [10] of Sodium cooled fast reactors in the USA (ALMR, Advanced Liquid Metal Reactor), Japan (MONJU) and in Russia (BMN-170), for reasons of cost, speed of construction and licensing. Such modularity permits the use of the devices in relatively isolated areas. The power plant can be built in a well developed country and transported to the target area. Decommissioning of the device is also simplified. The European approach (EFR, European Fast Reactor) is more conservative and is based on a single, large volume pool for a nominal power in excess of 3,000 MW_t. Such an approach is possible also for the EA. In this case, because of the larger power, the beams from two accelerators will be simultaneously injected in the core of the EA. Both designs are robust, cost-effective and they incorporate many features which are the result of the extensive experience with smaller machines. They are designed for a number of different fuel configurations and they can easily accommodate those appropriate to the EA. We have taken as "model" for our design many of the features of the ALMR. The ALMR was designed to provide high reliability for the key safety, including shutdown heat removal and containment. We intend to follow the same basic design, with, however, the added advantages of (1) sub-critical operation at all times (2) negative void coefficient of molten Lead (3) convection driven primary cooling system and (4) non reactive nature of Lead coolant when compared to Sodium.

The coolant medium is molten natural Lead operated in analogy with our (Sodium cooled) "models" at a maximum temperature of 600 ÷ 700 °C. In view of the high boiling temperature of Lead (1743 °C at n.p.t.) and the negative void coefficient of the EA, even higher temperatures may be considered, provided the fuel and the rest of the hardware are adequately designed. For instance direct Hydrogen generation via the sulphur-iodine method [4] requires an outlet temperature of the order of 800 °C. A higher operating temperature is also advantageous for electricity generation, since it may lead to an even better efficiency of conversion. Evidently, additional research and development work is required in order to safely adapt our present design to an increased operating temperature. In particular the cladding material of the fuel pins may require some changes, especially in view of the increased potential problems from corrosion and reduced structural strength. With these additions the present design should be capable of operating at temperatures well above the present figures.

A most relevant feature of our design is the possibility of using natural convection alone to remove all the heat produced inside the core. Convection cooling has been widely used in "swimming pool" reactors at small power levels. We shall show that an extension of this very safe method to the very large power of the EA is possible because of the unique properties of Lead, namely high density, large dilatation coefficient and large heat capacity. Convection is spontaneously and inevitably driven by (any) temperature difference. Elimination of all pumps in the primary loop is an important simplification and a contribution towards safety, since unlike pumps, convection cannot fail. In the convective mode, a very large mass of liquid Lead (≈ 10,000 tons), with an associated exceedingly large heat capacity[1] moves very slowly (≤ 2.0 m/s inside the core, about 1/3 of such speed elsewhere) transferring the heat from the top of the core to the heat exchangers located some 20 metres above and returning at a lower temperature ($\Delta T \approx -200$ °C) from the heat exchangers to the bottom of the core.

The geometry of the EA main vessel is therefore relatively slim (6.0 m diameter) and very tall (30 m). The vessels, head enclosure and permanent internal structures are fabricated in a factory and shipped as an assembled unit to the site[2]. The relatively slender geometry enhances the uniformity of the flow of the liquid Lead and of the natural circulation for heat removal. The structure of the vessel must withstand the large

---

[1] The heat capacity of liquid Lead at constant pressure is about 0.14 J/g/°C. For an effective mass of $\approx 10^4$ tons = 10^{10} grams and a power of 1.5 GW (full EA power), the temperature rise is of the order of 1.0°C/s. The mass flowing through the core for $\Delta T \approx 200$°C is 53.6 t/s, corresponding to some 1.5 minutes of full power to heat up the half of the coolant in the "cold" loop, in case the heat exchangers were to fail completely.

[2] The shipping weight is about 1500 tons. Removable internal equipment is shipped separately and installed through the top head.

weight of the liquid Lead There are four 375 MW_t heat exchangers to transfer the heat from the primary Lead to the intermediate heat transport system They are located above the core in an annular region between the support cylinder and the walls of the vessel

The vessel is housed below floor level in an extraordinarily robust cylindrical silo geometry lined with thick concrete which acts also as ultimate container for the liquid Lead in case of the highly hypothetical rupture of the main vessel In the space between the main vessel and the concrete wall the Reactor Vessel Air Cooling System (RVACS) is inserted This system [11], largely inspired from the ALMR design, is completely passive and based on convection and radiation heat transfer The whole vessel is supported at the top by anti-seismic absorbers Even in the case of an intense earthquake the large mass of the EA will remain essentially still and the movement taken up by the absorbers

The fuel is made of mixed oxides, for which considerable experience exists More advanced designs have suggested the use of metallic fuels or of carbides [12] These fuels are obviously possible also for an EA We remark that the use of Zirconium alloys is not recommended since irradiation leads to transmutations into the isotope ^{93}Zr, which has a long half-life and which is impossible to incinerate without separating it isotopically from the bulk of the Zirconium metal The choice of the chemical composition of the fuel is strongly related to the one of the fuel reprocessing method A relative novelty of our machine when compared to ordinary PWRs is the large concentration of ThO_2 in the fuel and the corresponding production of a small but relevant amount of Protactinium A liquid separation method called THOREX has been developed and tested on small irradiated ThO_2 fuel samples [13] The extrapolation from the widely used PUREX process to THOREX is rather straightforward and this is why we have chosen it, at least at this stage Methods based on pyro-electric techniques [14], which imply preference to metallic fuels, are most interesting, but they require substantial research and development work Since the destination of the Actinides is now well defined i e to be finally burnt in the EA, the leakage of Actinides in the Fission Fragment stream must be more carefully controlled, since they are the only Actinides in the "Waste" We have assumed that a "leaked" fraction of 10^{-4} is possible for Uranium The recycled fuel has a significant radio-activity We have checked that the dose at contact is similar to the one of MOX fuels made of Uranium and Plutonium, already used in the Nuclear Industry

The average power density in the fuel has been conservatively set to be $\rho = 55$ *W/g–oxide*, namely about 1/2 the customary level of LMFBR[1] (ALMR, MONJU, and EFR) The nominal power of 1500 MW_t requires then 27 3 tons of mixed fuel oxide The fuel dwelling time is set to be 5 years equivalent at full power The average fuel burn-up is then 100 GW d/ton-oxide Since the fissile fuel is internally regenerated inside the bulk of the Thorium fuel, the properties of the fuel are far more constant than say in the case of a PWR As shown later on, one can compensate to a first order the captures due to fission fragments, operating initially with a breeding ratio below equilibrium All along the burn-up, the growth of the fissile fuel concentration counterbalances the poisoning due to fission fragments *Therefore neither re-fuelling nor fuel shuffling appear necessary for the specified duration of the burn-up*

No intervention is therefore foreseen on the fuel during the five years of operation, at the end of which it is fully replaced and reprocessed Likewise in the "all-convective" approach there are no moving parts which require maintenance or surveillance In short the *EA is a large, passive device in which a proton beam is dumped and the generated heat is extracted, without other major elements of variability*

Safety and nuclear proliferation are universal concerns In the case of conventional Nuclear Power, accidents have considerably increased the radioactivity exposure of individuals and the population [7] The total nuclear power generated, 2000 GW × a, is estimated to have committed an effective dose of 400,000 man Sv from normal operation Accidents at Windscale, TMI and Chernobyl have added 2000, 40 and 600,000 man Sv respectively These types of accidents are no longer possible with the EA concept Chernobyl is a criticality accident, impossible in a sub-critical device and TMI, a melt-down accident, is made impossible by the "intrinsic" safety of the EA

[1] This choice is motivated by the relative novelty of the "all-convective" approach and the relative scarce experience with ThO_2, when compared with UO_2

A thermal run-off is the precursory sign of a number of potentially serious accidents. The present conceptual design is based on a swimming pool geometry where the heat generated by the nuclear cascade is extracted from the core by convection cooling, completely passive and occurring inevitably because of temperature differences.Thermal run-off is prevented, since a significant temperature rise due for instance to an insufficiency of the secondary cooling loop and of the ordinary controls will inevitably produce a corresponding dilatation of the liquid Lead. Because of the slim geometry of the vessel, the level of the swimming pool will rise by a significant amount (≈ 27 cm/100 °C), filling (through a siphon) additional volumes with molten Lead, namely :

(1) The Emergency Beam Dump Volume (EBDV), a liquid Lead "beam stopper" sufficiently massive as to completely absorb the beam some 20 metres away from the core and hence bring the EA safely to a stop. In the unlikely event that the beam window would accidentally break, molten Lead will also rise, so as to fill completely the pipe and the EBDV, thus removing the incoming proton beam from the core.

(2) A narrow gap normally containing thermally insulating Helium gas, located between the coolant and the outer wall of the vessel, which in this way becomes thermally connected to the coolant main convection loop. The outer wall of the EA will heat up and bleed the decay heat passively through natural convection and radiation to the environment (RVACS) [11]. This heat removal relies exclusively on natural convection heat transfer and natural draught on the air side.

(3) A scram device based on B_4C absorbers which are pushed into the core by the liquid Lead descending narrow tubes. These absorbers anchor the device firmly away from criticality.

These passive safety features are provided as a backup in case of failure of the active systems, namely of the main feed-back loop which adjusts the current in order to maintain constant the temperature at the exit of the primary cooling loop. Multiply backed-up but simple systems based on current transformers and physical limitations in the accelerator (available RF power in the cavities, space charge forces, etc.) sharply limit the maximum current increase that the accelerator can deliver. Were these methods all to fail, the corresponding increase of temperature will dilate significantly the Lead, activating the ultimate shut-off of the proton beam from the accelerator, the emergency cooling and the scram devices, before any limit is exceeded in the EA.

Normally the EA is well away from criticality at all times, there are no control bars (except the scram devices) and the power produced is directly controlled by the injected beam current. However in some unforeseen circumstances the EA may become critical. In itself, this is not an unacceptable though exceptional operation mode, provided the amount of power produced does not exceed the ratings of the EA. Indeed even a quite large reactivity insertion is strongly moderated by the large negative temperature coefficient (Doppler) of the fuel. Since the operating temperature of the fuel is relatively low, even a rapid increase of the instantaneous power will increase the temperature of the fuel within limits, large enough, however, to introduce a substantial reduction of k as to exit from criticality. The safety of multiplying systems depends to a large extent on fast transients. A kinetic model dealing with fast transients due to accidental reactivity insertions and unexpected changes of the intensity of the external proton beam shows that the EA responds much more benignly to a sudden reactivity insertion than a critical Reactor. Indeed, no power excursions leading to damaging power levels are observed for positive reactivity additions which are of the order of the sub-criticality gap. Even if the spallation source is still active (the accelerator is not shut-off), the power changes induced are passively controlled by means of the increase of the natural convection alone (massive coolant response) thus excluding any meltdown of the sub-critical core.

Any very intense neutron source (≥ 10^{13} n/s) could in principle be used to produce bomb grade Plutonium by extensive irradiation of some easily available depleted Uranium. This is true both for fission and fusion energy generating devices. We propose to prevent this possibility by "sealing off" the main vessel of the EA to all except a specialised team, for instance authorised by IAEA. This is realistic for a number of reasons. The energetic gain of the EA is almost constant over the lifetime of the fuel, though it changes significantly after a power level variation. Convection cooling is completely passive and occurring inevitably because of temperature differences. There are no active elements (pumps, valves etc.) which may fail or need direct access to the interior of the main vessel. In addition the fuel requires no significant

change in conditions over its long lifetime of five years, since the fissile material is continuously generated from the bulk of Thorium. The only two maintenance interventions to be performed are the periodic replacement of the beam window about once a year and the possible replacement of some failing fuel elements, performed remotely with the pantograph. Both activities can be carried out without extracting the fuel from the vessel. We can therefore envisage conditions in which the EA is a sort of "off limits black-box" accessed very rarely and only by a specialised team, for instance authorised by IAEA. The ordinary user (and owner) of the EA will have no access to the high neutron flux region and to the irradiated fuel, a necessary step towards any diversion which may lead to proliferation or misuse of the device.

Proliferating uses of the fuel are further prevented by the fact that the fissile Uranium mixture in the core is heavily contaminated by strong γ-emitter ^{208}Tl which is part of the decay chain of ^{232}U and by the fact that the EA produces a negligible amount of Plutonium. As shown later on, a rudimentary bomb built starting with EA fuel, in absence of isotopic separation, will be most impractical and essentially impossible to use or to hide.

The EA can operate with a variety of different fuels. Several options will be discussed in detail in the subsequent sections. A specialised filling can transform Plutonium waste into useful ^{233}U, for instance, in order to accumulate the stockpile required at the start-up of the EA. More generally one could envisage a combined strategy with ordinary PWRs. Presently operating PWRs represent an investment in excess of 1.0 Tera dollars. It is important to make every possible effort in order to minimise their impact on the environment and to increase their public acceptability. A specially designed EA could be used to (1) transform Plutonium waste into useful ^{233}U and (2) reduce the stockpile of "dirty" Plutonium waste. The EA will be initially loaded with a mixture of Actinide waste and native Thorium, in the approximate ratio 0.16 to 0.84 by weight. Other Actinides, like Americium, Neptunium and so on can also be added. The mixture is sub-critical and the EA can be operated with k = 0.96-0.98.

During operation, the unwanted actinides are burnt, while ^{233}U is progressively produced. The freshly bred ^{233}U compensates the drop of criticality due to the diminishing and deteriorating Actinide mixture and the one due to the build-up of Fission Fragments. A balanced operation over a very long burn-up of up to 200 GW d/t is thus possible without loss of criticality, corresponding to 5-10 years of operation without external intervention. The fuel of the EA is then reprocessed, the ^{233}U is extracted for further use. FFs are disposed with the standard procedure of the EA. The remainders of Plutonium[1] and the like, could either be sent to the Geological Repository to which they were destined or further burnt in the EA, topped with fresh Thorium. This combination of a PWR and an EA has several advantages:

1) It eliminates permanently some of the Actinide waste of the PWR reducing the amount to be stored in a Geological Repository.

2) It produces additional power through the EA, thus increasing by about 50% the energetic yield of the installation.

3) The amount of fissile Uranium, which is by weight about 80% of the incinerated Plutonium is a valuable asset. It can be used either to start a new, Thorium operated, EA or it can be mixed with depleted Uranium to produce more fuel for PWRs. As is well known, ^{233}U is an almost perfect substitute for ^{235}U in a ratio very close to 1. The yearly Plutonium and higher Actinides discharge of a typical ≈ 1 GW_e PWR operated 80% of the time is of the order of 300 kg, thus producing via the EA 240 kg of ^{233}U, which in turn can be used to manufacture ≈ 8 tons of fresh fuel from depleted U with 0.3% ^{235}U and 3.0 % ^{233}U. This is ≈ 1/3 of the supply of enriched Uranium fuel for the operation of the PWR.

We have also considered as an alternative a fast neutron driven EA operated on Plutonium only, namely without Thorium. Similar schemes, though mostly operated with thermal neutrons are under consideration

[1] The discharge after ≈ 150 GW × d/t contains about 50% of the initial Pu, but is highly depleted of ^{239}Pu (1/5) and ^{241}Pu (1/4), while other Pu isotopes are essentially unchanged. Am and Cm isotopes stockpiles are essentially unchanged. Note that the Plutonium is "denatured" of the highly fissile isotopes, making it worthless for military diversions.

at Los Alamos [15], JAERI [16] and elsewhere [17]. Such potential devices require frequent refills and manipulations of the fuel, since the reactivity of the Plutonium is quickly deteriorated by the burning and choked by the emergence of a large relative concentration of FF's. At the limit one is lead to the "chemistry on line" proposed by the Los Alamos Group [15]. Adding a large amount of fertile Thorium greatly alleviates such problems and the device can burn Plutonium and the like for very many years without intervention or manipulation of the fuel, since the bred ^{233}U is an effective substitute to Plutonium to maintain a viable and constant criticality. In addition FFs are diffused in a much larger fuel mass. Finally the ^{233}U recovered at the end of the cycle constitutes a valuable product.

In principle our method of a Th-Pu mixture could be extended to the operation of a Fast Breeder used as incinerator [18], however, probably at a much higher cost and complexity due to the higher degree of safety involved.

We have indicated Thorium as main fuel for the EA since the radio-toxicity accumulated is much smaller than Uranium and it offers an easier operation of the EA in a closed cycle. But there are also reasons of availability. Thorium is relatively abundant on earth crust, about 12 g/ton, three times the value of Uranium [19]. It ranks 35-th by abundance, just after Lead [20]. It is well spread over the surface of the planet. In spite of its negligible demand ($\approx$ 400 t/y) the known reserves in the WOCA[1] countries are estimated [21] to about 4×10^6 tons (Table I.1). Adding a guessed estimate from the USSR, China and so on, we reach the estimate of perhaps 6×10^6 tons, which can produce 15,000 TW $\times$ a of energy, if burnt in EAs, namely about a factor 100 larger than the known reserves of Oil or Gas and a factor 10 larger than Coal. This corresponds to 12.5 centuries at the present world's total power consumption (10 TW).

There are reasons to assume that this figure is largely underestimated. Firstly the demand is now very low and there has been very little incentive to date to search for Thorium "per se". Additional resources of any mineral have always been found if and when demand spurs a more active prospection. The presently exploited Thorium ores are richer, by a factor 10 $\div$ 100, than the ones which are exploitable at a price acceptable by market conditions applicable to the case of Uranium. In view of the small contribution of the primary Thorium to the energy cost, one may try to estimate how the recoverable resources would grow if exploitation is extended to ores which have a content for instance an order of magnitude smaller, i.e. similar to the best Uranium ores. Such analysis has been performed for Uranium [22], assuming that the distribution in the crust follows a "log-normal" (Figure 1.2) distribution. Other metals for which a better mining history is known, show a similar trend, though the slope parameter may be different in each case (Figure 1.3). In the case of Thorium, in absence of better information, we may assume the same slope as in the case of Uranium. Then, a tenfold decrease in the concentration of the economically "recoverable" ores[2] would boost reserves of Thorium by a factor of 300, still a small fraction (3×10^{-5}) of what lies in the Earth crust. Reserves of Thorium energy would then be stretched to 4.5 million TW $\times$ a, *corresponding to $\approx$ 2200 centuries at twice the present world consumption level which can be considered truly infinite on the time scale of human civilisation* [3].

Several other projects have sought the realisation of a "clean" Nuclear Energy. The project CAPRA [23] focuses on the incineration of Plutonium in a Fast Breeder. On a longer time scale, Fusion holds the promise of a "cleaner" energy. Amongst the various projects, Inertial Fusion offers the largest flexibility in design of the combustion chamber and hence the best potentials of reduction of the activation effects due to neutrons [24]. But neither inertial nor magnetic fusion have so far achieved ignition[4]. We have compared

---

[1] This stands for World Outside Centrally Planned Activities.

[2] We remark that even this 10-fold decrease would make these minerals somewhat more concentrated than the 2000 ppm "high content ores" used today for Uranium.

[3] In order to estimate the magnitude of the error in such a "prediction", we note that the somehow extreme cases of Tungsten and of Copper have boost factors of 500,000 and 40 respectively. But even the lower limit of Copper predicts $\geq$ 300 centuries at twice the today's world consumption.

[4] The project ITER is aimed at demonstrating Ignition in magnetically confined fusion, presumably 2005. The new large megajoule range optical LASERs in development at Livermore and in France have the potential for ignition with inertial fusion.

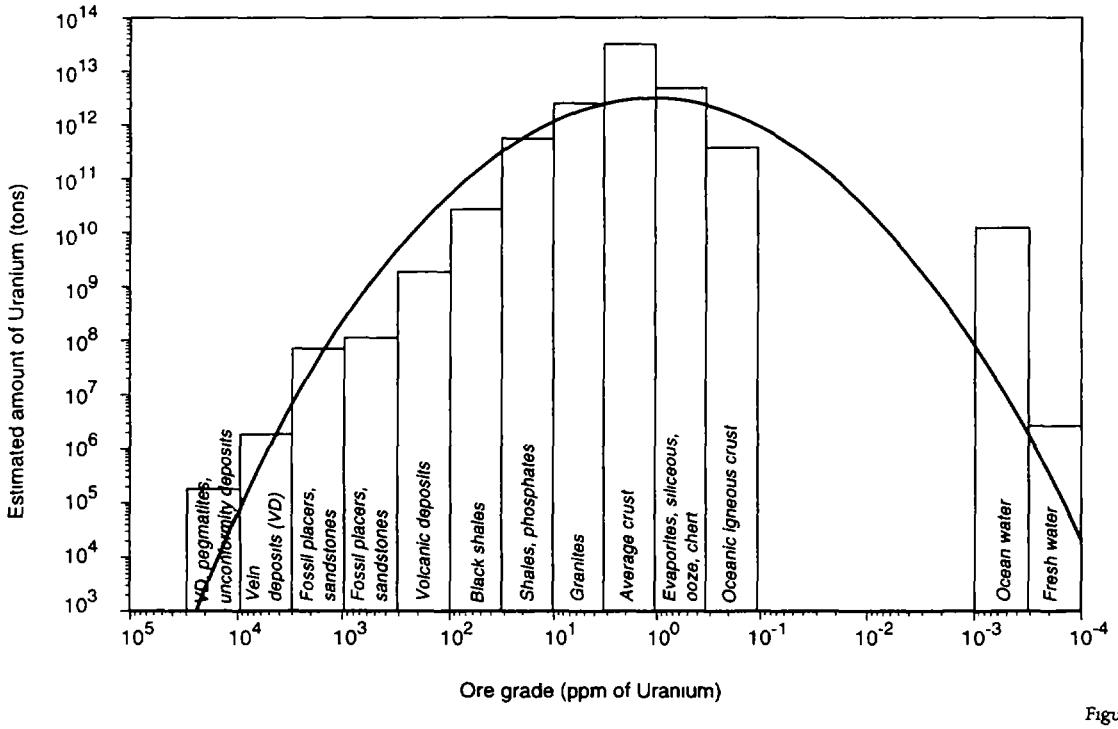

Figure 1 2

Fig. 1.2 Estimated amount of Uranium mined as a function of the concentration of metal in the ores

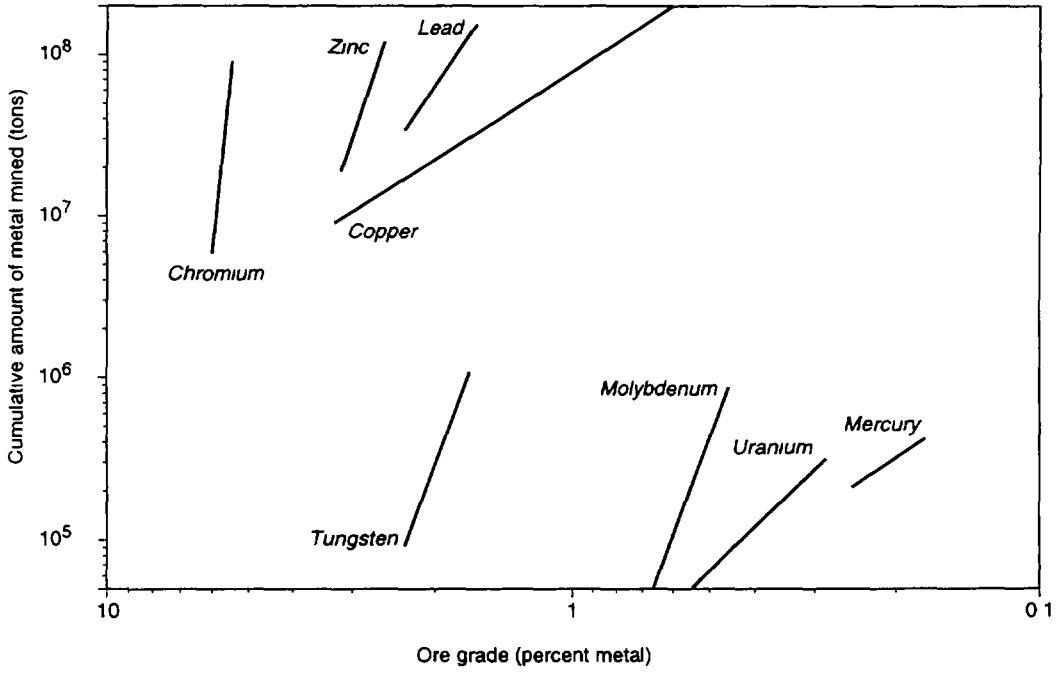

Fig. 1 3 Cumulative amount of metal mined for different metals as a function of the ore concentration of metal.

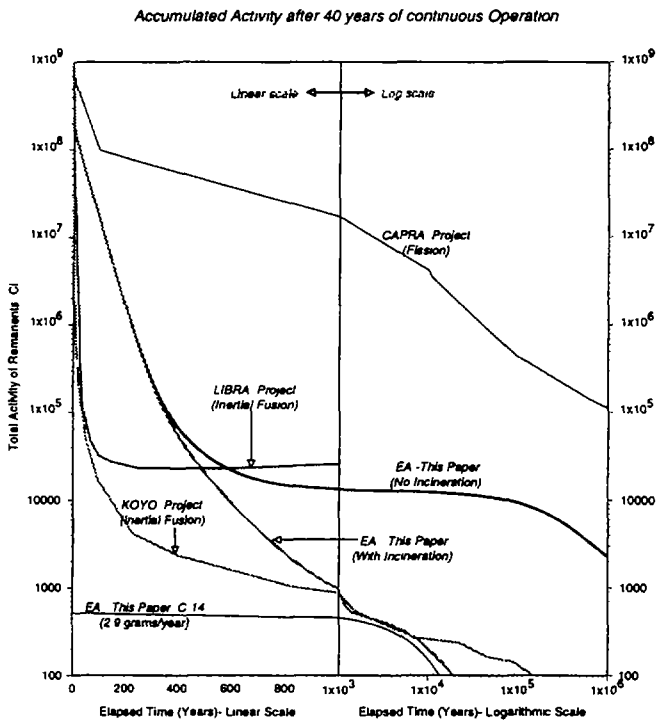

FIG. 1.4 Accumulated activity of Remnants as a function of the time elapsed after shutdown for a number of conceptual projects aiming at minimising the radio-active waste. CAPRA [23] is based on Fast-Breeders similar to Super-Phenix. LIBRA [25] and KOYO [26] are Inertial Fusion devices (ICF). The EA concept with and without incineration of long-lived FFs can reach a level of "cleanliness" which is well in the range of the best Fusion conceptual designs. Activities in Ci are given for 40 years of operation. According to Ref. [24] Magnetically confined Fusion in general produces activation which are up to three order of magnitude larger than ICF.

the activity of the remnants (Ci) of the EA with the one of the CAPRA project and of two of the Inertial Fusion concepts, namely LIBRA [25] and KOYO [26] in which the greatest care has been exercised to reduce activation. In order to make the comparison meaningful we have to take into account that the published values of activation for fusion are given in Ci after shut-down and 40 years of operation. Therefore the activities quoted for the fission case (CAPRA, EA) have been normalised to the same scenario, namely counting the total activity of remnants (sum of all fuel cycles, in the case of EA excluding recycled fuel) after 40 years of continued, uninterrupted operation. Activities have been normalised 1 GW of electric power produced (Figure 1.4).

After the cool-down period in the secular repository ($\approx$ 1000 years) the activity of the remnants (40 years of operation) stabilises at levels which are: 1.7×10^7 Ci for CAPRA, 2.35×10^4 Ci for LIBRA, 900 Ci for KOYO and 1.3×10^4 Ci for the EA without incineration. With incineration we reach the level of 950 Ci, out of which about one half is due to ^{14}C. The activation for unit delivered power of the EA without incineration is comparable to the one of LIBRA concept whilst with incineration we reach a level which is close to the one of KOYO concept based on second generation design of the combustion chamber. The expected doses after 1000 years of cool-down from Magnetically Confined Fusion are typically three order of magnitude larger than the quoted values for Inertial confinement due to substantial differences in the neutron spectra. This improvement is mainly due to the moderation of neutrons in the blanket consisting of LiPb liquid circulating through SiC tubes, before they hit the first wall [24]. *Therefore we conclude that the EA concept can reach a level of "cleanliness" which is well in the range of the best Fusion conceptual designs.*

From the point of view of cleanliness, as well as for the other major goals — namely non-criticality, non-proliferation and inexhaustible fuel resources — the EA matches fully the expectations of Fusion. But like CAPRA — which however is about 1000 times less effective in eliminating radioactive remnants — the EA has no major technological barriers, while in the case of Fusion, major problems have to be solved.

TABLE I.1. THORIUM RESOURCES (IN UNITS OF 1000 TONS) IN WOCA (WORLD OUTSIDE CENTRALLY PLANNED ACTIVITIES)[1] [21]

	Reasonably Assured	Additional Resources	Total
Europe			
Finland		60	60
Greenland	54	32	86
Norway	132	132	264
Turkey	380	500	880
Europe Total	566	724	1290
America			
Argentina	1		1
Brazil	606	700	1306
Canada	45	128	173
Uruguay	1	2	3
USA	137	295	432
America total	790	1125	1915
Africa			
Egypt	15	280	295
Kenya	no estimates	no estimates	8
Liberia	1		1
Madagascar	2	20	22
Malawi		9	9
Nigeria	no estimates	no estimates	29
South Africa	18	no estimates	115
Africa total	36	309	479
Asia			
India	319		319
Iran		30	30
Korea	6	no estimates	22
Malaysia	18		18
Sri Lanka	no estimates	no estimates	4
Thailand	no estimates	no estimates	10
Asia total	343	30	403
Australia	19		19
Total WOCA	*1754*	*2188*	*4106*

[1]This compilation does not take into account USSR, China and Eastern Europe. Out of 23 listed countries, six (Brazil, USA, India, Egypt, Turkey and Norway) accumulate 80% of resources. Brazil has the largest share followed by Turkey and the United States.

D.3.2. PHYSICS CONSIDERATIONS AND PARAMETER DEFINITION

D.3.2.1. SPATIAL NEUTRON DISTRIBUTION

While the neutron distribution inside a Reactor is determined primarily by the boundary conditions, in the EA the geometry of the initial high energy cascade is dominant. The two spatial distributions are expected to differ substantially. The flux distribution is of fundamental importance in order to determine the generated power distribution and the uniformity of the burning of the fuel, both of major relevance when designing a practical device.

We shall consider first, in analogy to a Reactor a simple, uniform fuel-moderator medium operated away from criticality [27]. It turns out that in such "reactor like" geometry, the neutron flux non uniformity associated to sub-critical regime[1] may be so large as to hinder the realisation of a practical device. A radically different geometry, described in paragraph D.3.2.2, can be used to solve this problem.

We neglect the fine structure of the sub-critical assembly and consider a fictitious material with uniform properties. We assume no reflector and therefore the EA is a uniform block of specified size. The high energy beam interacts directly with the fuel material. The basic diffusion equation for the neutron flux for mono-energetic or thermal neutrons in a steady state is

$$D\,\nabla^2\phi - \Sigma_a\phi + S = 0$$

where S is the source term, namely the rate of production of neutrons per cm^3 per second, $D=\Sigma_s/3\,\Sigma^2$ is the diffusion coefficient and Σ, Σ_s and Σ_a respectively the macroscopic total, elastic and absorption cross sections, all homogenised over the fuel-moderator mixture. This formula is strictly applicable only to mono-energetic neutrons of velocity v and then only at distances greater than two or three mean free paths from boundaries.

Let k_∞ be the number of neutrons produced at each absorption in the fuel-moderator mixture. The source term is decomposed in two parts, namely $S=k_\infty\Sigma_a\phi+C$ where the first term is due to fission multiplication in the fuel and the second is the inflow of neutrons (per cm^3 and second) emitted by the high energy cascade. Upon dividing by D and rearranging terms the diffusion equation becomes

$$\nabla^2\phi - \frac{1-k_\infty}{L_c^2}\phi + \frac{C}{D} = 0 \qquad (1)$$

where L_c^2 is equal to D/Σ_a. Boundary conditions are determinant. The neutron density at the outer boundary of the medium is quite small. It cannot be exactly zero because neutrons diffuse out of the medium. In analogy with Reactor theory [27] we shall use the boundary condition that at the extrapolated distance $d = 2/3\Sigma_s$ from the boundaries of the medium the flux must vanish, $\phi = 0$.

In order to solve Eq. (1) we find it useful to introduce a new function $\psi(\vec{x})$ where $\vec{x}\equiv(x,y,z)$ which is defined by the following differential equation, in which only the geometry of the device is relevant:

$$\nabla^2\psi(\vec{x}) + B^2\psi(\vec{x}) = 0 \qquad (2)$$

---

[1] As shown later on, a subcritical device far from criticality has a neutron flux distribution which is exponentially falling from the target region, while a critical reactor has the well known cos-like distribution. The exponential is obviously falling very fast and the burn-up is therefore highly non uniform and concentrated around the beam area.

The boundary conditions $\psi(\vec{x})=0$ at the extrapolated edges introduce a quantization in the eigen-values of B^2 and the corresponding eigen-functions $\psi(\vec{x})$. Therefore we have a numerable infinity of solutions.

For instance in the case of rectangular geometry, namely a parallelepiped with dimensions a, b, c and origin at one edge, such as $\psi(\vec{x})=0$ for the planes x = a, x = 0, y = b, y = 0, and z = c, z = 0, we find

$$\psi_{l,m,n}(\vec{x}) = \sqrt{\frac{8}{abc}} \sin\left(l\frac{\pi x}{a}\right) \sin\left(m\frac{\pi y}{b}\right) \sin\left(n\frac{\pi z}{c}\right)$$

$$B^2_{l,m,n} = \pi^2\left(\frac{l^2}{a^2}+\frac{m^2}{b^2}+\frac{n^2}{c^2}\right)$$

Analogue expressions can be given for different geometries. The eigen-functions $\psi(\vec{x})$ are normalised to one and constitute a complete ortho-normal set. Hence it is possible to express any function as the appropriate series of such eigen-functions, provided the boundary conditions are the same. In particular the high energy neutron source $C(\vec{x})$ produced by the beam interactions (zero outside, in order to satisfy boundary conditions) is expanded to

$$C(\vec{x}) = D\sum_{l,m,n} c_{l,m,n}\,\psi_{l,m,n}(\vec{x}) \quad \text{where} \qquad c_{l,m,n} = \frac{1}{D}\int_{volume} \psi_{l,m,n}(\vec{x})\; C(\vec{x})dV$$

It is then possible to express the neutron flux as a series expansion with the help of Eq. (1) and of Eq. (2):

$$\phi(\vec{x}) = \sum_{l,m,n} \frac{c_{l,m,n}}{B^2_{l,m,n} + \Gamma}\psi_{l,m,n}(\vec{x}) \quad \text{where} \quad \Gamma = \frac{1-k_\infty}{L_c^2} \tag{3}$$

Note that the only parameter which is not geometry related is Γ. The criticality condition can be defined as a non zero flux for the limit of $c_{l,m,n}\to 0$. Therefore one of the denominators $B^2_{l,m,n}+\Gamma$ of Eq. (3) must vanish, which of course implies $\Gamma<0$ or equivalently $k_\infty>1$. The smallest value of $B^2_{l,m,n}$ and therefore the smallest value of k_∞ which makes the system critical occurs for l = m = n = 1, namely the fundamental mode of Eq. (2). This result exhibits the well known sinusoidal distribution of the neutron flux of a Reactor and the classic condition for criticality, $k_\infty - 1 = B_0^2 L_c^2$, where B_0^2 is the "buckling" parameter.

The significance of $B^2_{l,m,n}$ is further illustrated if one considers the neutron absorption and escape rates or probabilities for the mode $i\equiv(l,m,n)$, $P^{(i)}_{abs}$ and $P^{(i)}_{esc}$ respectively. Let us consider a case in which the i-th eigen-mode of the wave function is dominant. It is easy to show that

$$P^{(i)}_{esc} = P^{(i)}_{abs}\frac{D}{\Sigma_a}B_i^2 = P^{(i)}_{abs}L_c^2 B_i^2$$

where L_c is the (already defined) diffusion length. The (small) escape probability for each mode $P^{(i)}_{esc}$ is then simply equal to B_i^2 in units of the inverse of the square of the diffusion length. Note that since B_i^2 is a rapid rising function of the mode i, higher modes escape much more easily from the volume. Therefore the containment of the cascade is improved if the source geometry is such as to minimise the excitation of the higher eigen-modes.

This interpretation of B_i^2 makes also more transparent the classic condition for criticality of a Reactor, $k_\infty - 1 = B_0^2 L_c^2$. Evidently in order to have criticality, the number of neutrons produced at each absorption k_∞ must exceed 1 precisely by $P_{esc} \approx L_c^2 B_0^2$, the fraction of neutrons escaping the active volume. To extend this formula to the EA it is then natural to introduce the mode dependent multiplication coefficient $k_i = k_\infty - L_c^2 B_i^2$, in which the escape probability has been taken into account. In the case of the fundamental mode, the corresponding k-value has the classic significance of the Reactor Theory. This makes even more transparent the significance of the denominator of Eq. (3), which becomes

$$B_i^2 + \Gamma = \frac{1}{L_c^2}\left(L_c^2 B_i^2 + 1 - k_\infty\right) = \frac{1}{L_c^2}(1 - k_i)$$

We can then re-write Eq. (3) as

$$\phi(\vec{x}) = L_c^2 \sum_{l,m,n} \frac{c_{l,m,n}}{1 - k_{l,m,n}} \psi_{l,m,n}(\vec{x})$$

where the "(1-k) enhancement" of each mode is further emphasised. The formula can be used to readily calculate the neutron flux distribution in the uniform EA starting from the known initial cascade distribution.

In contrast with the case of the critical reactor in which only the fundamental mode is active, any reasonable source configuration in an EA will excite a large number of different modes, each with its different criticality coefficient k_i. The neutron distribution will be wider than the source distribution only because $B_{l,m,n}^2$ grows with increasing order and therefore expansion coefficients are indeed different from $c_{l,m,n}$. In general the distribution of neutrons inside a uniform medium operated as an EA reasonably far from criticality will remain strongly non uniform. One can show that far from the source it decays approximately exponentially rather than having the characteristic cos-like shape of a Reactor.

Since the neutron inventory is very critical, the neutron containment inside the EA must be as complete as possible. Inevitably this implies a large fraction of the volume with a low neutron flux and hence with a small specific energy production. An EA made of a uniform volume of fuel with the beam interacting in the central region will therefore be highly impractical.

D.3.2.2. EA UNIFORMISATION WITH A DIFFUSIVE MEDIUM

One can overcome this difficulty by embedding discrete fuel elements in a large, diffusing medium of high neutron transparency. In Figure 2.1 we show the capture cross sections at the typical energy of the neutrons in the EA as a function of the element number. One can remark very pronounced dips, which are due to the occurrence of closed shell in the nuclei. This is why their "nuclear reactivity" is minimal. These dips are somehow the equivalent of the Noble Gases in the atomic shell structure. The unique properties of the Lead and Bismuth are evident. The uniformisation of the fuel burn up is then ensured by the long migration length of the diffusing medium. Since the present design of the EA is based on fast neutrons, the medium must have also a very small lethargy, i.e. a high atomic number. Two elements appear particularly suited: Lead and Bismuth. In general Lead will be preferable because of its lower cost, smaller toxicity and smaller induced radioactivity. Both elements have the added advantage that the neutron yield of the high energy beam is large: the same medium can therefore be the high energy target and the diffuser at the same time.

While ^{209}Bi is a single isotope, natural Lead is made of ^{204}Pb (1.4 %), ^{206}Pb (24.1%), ^{207}Pb (22.1 %) and ^{208}Pb (52.4 %), which have quite different cross sections. Isotopically enriched ^{208}Pb would be very attractive because of its smaller capture cross sections. However, we shall limit our considerations to the use of natural Lead.

Assume a large, uniform volume made of Lead, initially without fuel elements. The proton beam is arranged to interact in the centre, producing a relatively small, localised source of spallation neutrons. The solution of the diffusion equation (Eq. (2) in the case of an infinite diffusing medium and a small source of strength Q(n/s) is given by [27]:

$$\phi(r) = \frac{Q}{4\pi D}\frac{e^{-\kappa r}}{r} = \frac{Q\kappa}{4\pi D}\frac{e^{-\kappa r}}{\kappa r}$$

where D is the diffusion coefficient and κ The reciprocal of the diffusion length with $\kappa^2=\Sigma_{abs}/D$. In the case of Lead, D is very small ($D\approx\lambda_s/3\approx1.12$ cm) and 1/κ very large, about 1 metre, the exact values depending on the energy dependent cross sections. Neutrons will then fill a very large volume of few 1/κ units and they will execute a brownian motion, stochastically "stored" in the medium by the very large number of diffusing collisions.

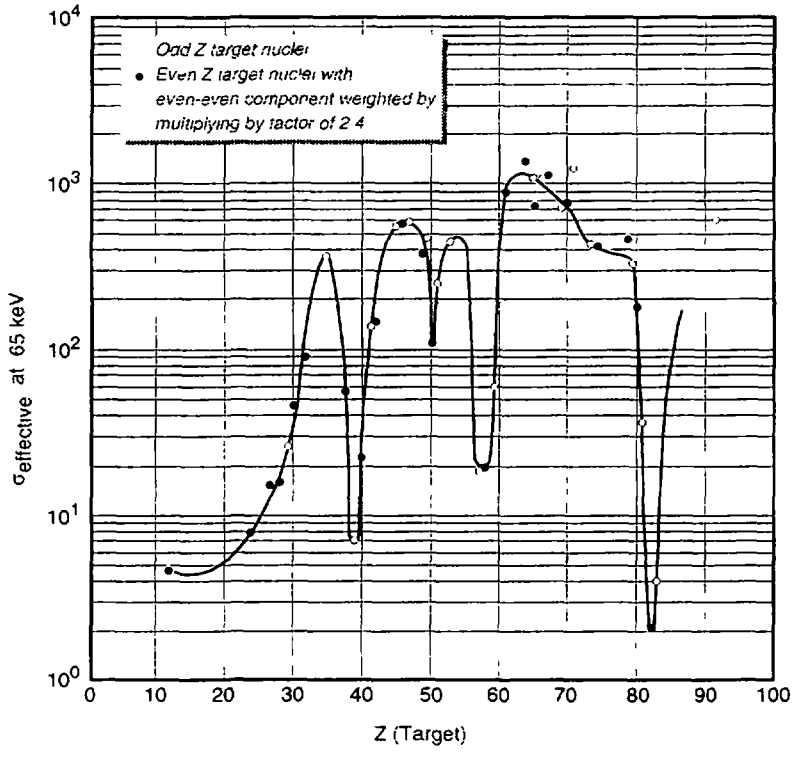

Fig. 2.1 Capture cross sections at 65 keV, as a function of the element number.

Spallation neutrons above a few MeV are rapidly slowed down because of the large (n,n') cross section. Once below threshold (≈ 1 MeV), the well known slowing-down mechanism related to elastic collisions takes over. The logarithmic average energy decrement for Pb and Bi is very small $\xi = 9.54\times 10^{-3}$ and the mean number of collisions to slow down the neutron for instance from 1 MeV to 0.025 eV (thermal energies) is very large, $n_{coll} = \ln(1\text{ MeV}/0.025\text{ eV})/\xi = 1.8 \times 10^3$ The elastic cross section, away from resonances is about constant, around 10 b corresponding to a scattering mean free path of $\lambda_s = 3.38$ cm (700 °C). The total path to accumulate n_{coll} is then the enormous path of 62 metres! The actual average drift distance travelled is of course much smaller, of the order of 1 metre, since the process is diffusive.

During adiabatic moderation, the neutron will cross in tiny energy steps a resonance region, located both for Pb and Bi in the region from several hundred keV to few keV. We introduce the survival probability $P_s(E_1, E_2)$, defined as the probability that the neutron moderated through the energy interval E_1 - E_2 is not captured. The probability that a neutron does *not* get captured while in the energy interval between E and E + dE is $[1 - (\sum_{abs}/(\sum_{abs}+\sum_{sc}))\ (dE/E\xi)]$ where $\sum_{sc}$ and $\sum_{abs}$ are the macroscopic elastic scattering and absorption cross sections. Evidently such probability is defined for a large number of neutrons in which the actual succession of energies is averaged. Combining the (*independent*) probabilities that it survives capture in each of the infinitesimal intervals, $P_s(E_1, E_2)$ is equal to the product over the energy range:

$$P_s(E_1,E_2)\cong\prod_{E_1}^{E_2}\left(1-\frac{\Sigma_{abs}}{\Sigma_{sc}+\Sigma_{abs}}\frac{dE}{\xi E}\right)=\exp\left[-\frac{1}{\xi}\int_{E_2}^{E_1}\frac{\Sigma_{abs}}{\Sigma_{sc}+\Sigma_{abs}}\frac{dE}{E}\right]=\exp\left(-\frac{I_{res}}{\xi}\right)$$

where the resonance integral I_{res} is defined as

$$I_{res} = \int_{E_2}^{E_1} \frac{\Sigma_{abs}}{\Sigma_{sc}+\Sigma_{abs}} \frac{dE}{E}$$

If the cross sections are constant, the integral is easily evaluated

$$P_s(E_1,E_2) = \exp\left| -\frac{\Sigma_{abs}}{\Sigma_{sc}+\Sigma_{abs}} \frac{1}{\xi} \ln\left(\frac{E_1}{E_2}\right) \right|$$

which evidences the large enhancement factor due to the slow adiabatic process, $\ln(E_1/E_2)/\xi=104.8\ \ln(E_1/E_2)$ with respect to a single scattering. For instance, if $E_1/E_2=50$, the effective value of the absorption cross section Σ_{abs} is increased by a factor 410. The values of the resonance integral I_{res} for the Lead isotopes are given in Table II.1 for E_1= 1.0 MeV and several final energies E_2.

TABLE II.1. RESONANCE INTEGRAL AND SURVIVAL PROBABILITY FOR LEAD AND BISMUTH (E_1 = 1 MeV, T = 20 °C)

Element	^{204}Pb	^{206}Pb	^{207}Pb	^{208}Pb	Nat Pb	^{209}Bi
Integral I_{res}						
E_2=1 eV	0.0781	.00787	.0272	.000685	.00974	.00621
E_2=10 eV	0.0649	.00728	.0125	.000676	.00626	.0054
E_2=100 eV	0.0607	.0071	.00783	.000673	.00516	.00512
E_2=1 keV	0.0568	.00706	.00635	.000672	.00475	.00331
E_2=10 keV	0.0287	.0065	0.005	.000671	.00283	.00223
E_2=100 keV	0.0124	.00435	.00395	.000636	.0018	.00195
Surv.prob., $P_s(E_1, E_2)$						
E_2=1 eV	0.000278	0.438	0.0578	0.930	0.360	0.521
E_2=10 eV	0.00111	0.466	0.269	0.931	0.519	0.567
E_2=100 eV	0.0017	0.475	0.440	0.931	0.582	0.584
E_2=1 keV	0.0026	0.477	0.514	0.931	0.607	0.706
E_2=10 keV	0.0494	0.506	0.582	0.932	0.743	0.791
E_2=100 keV	0.272	0.633	0.661	0.935	0.828	0.815

Natural Lead and Bismuth have similar properties, while a pure ^{208}Pb will be vastly superior. The temperature coefficient of the survival probabilities is (slightly) negative, since Doppler broadening increases the extent of the resonances. About 20% of the fission neutrons are absorbed in pure diffusing medium before they reach an energy of 100 keV, which is the typical energy in a practical EA. In reality the presence of a substantial amount of fuel in the EA will reduce such a loss: typically one expects that about 5% of the neutrons will end up captured in the diffusing medium.

Let us assume that a localised, strongly absorbing fuel element is introduced in the diffusing medium. The effects on the flux due to its presence will extend over a volume of the order of the migration length, as one can easily see describing the localised absorption as a "negative source". Hence one can in a good approximation use averaged properties for a diffuser-fuel region.

In a fuel-diffuser mixture with a relatively small concentration η of fissile material, $\Sigma_{sc} \approx \Sigma_{sc}^{diff}$ whilst $\Sigma_{abs} \approx \eta \Sigma_{abs}^{fuel} = \eta(\Sigma_{n,\gamma}^{fuel} + \Sigma_{fiss}^{fuel}) \gg \Sigma_{abs}^{diff}$. The survival probability is therefore strongly reduced, namely due to the large probability of absorption in the fuel. Adding fuel elements in the otherwise "transparent" medium makes it "cloudy". Evidently a large fraction of the absorptions will occur in the fuel even if in relatively small amounts, because of the very high transparency of the pure medium.

Once the capture in the added materials becomes dominant, a larger fuel concentration with respect to the diffuser concentration implies an earlier neutron capture and hence a higher average neutron energy. This leaves a large freedom in the quantity of fuel to be used, depending on the power required for the application. An analytical analysis of such a composite system is necessarily approximate, lengthy and outside the scope of the present paper. For more details we refer to Ref. [28]. (The actual behaviour of some specific designs will be derived with the help of numerical calculations).

The conceptual design of the diffuser driven EA consists of a large volume of diffusing medium in which one can visualise a series of concentric regions around the centre, where the proton beam is brought to interact (Figure 2.2):

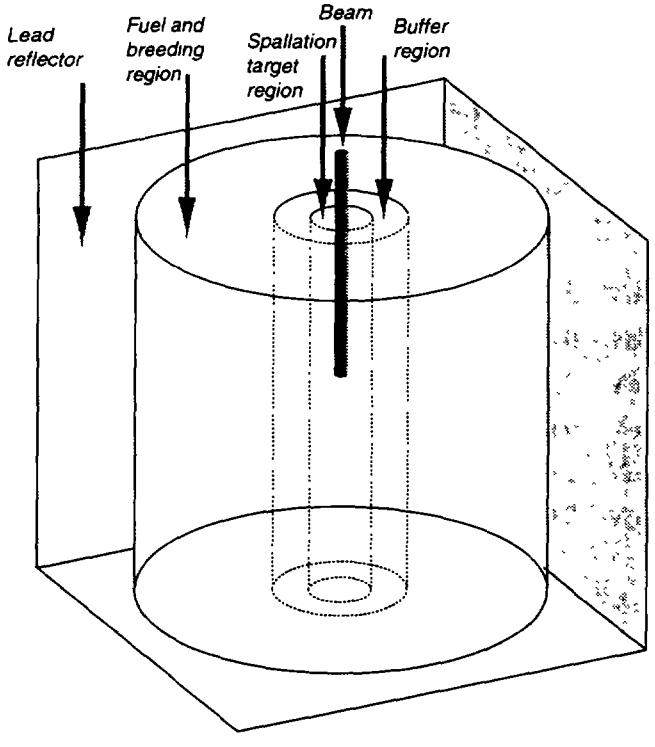

FIG. 2.2 Conceptual design of the diffuser driven EA.

i) A *spallation target* region, in which neutrons are produced by the high energy cascade initiated by the proton beam. This region is made of pure diffuser. The proton beam is brought in through an evacuated pipe and a thin window.

ii) A *buffer* region, again of pure diffuser in which neutrons are migrated and the energy spectrum is softened by the (n,n') reactions. This ensures that the structural elements (fuel assembly) is not exposed to high energy neutrons from the proton beam which may produce an excessive radiation damage.

iii) A *fuel* region in which a series of discrete fuel elements are widely interspersed in the diffusing medium. The outer part of the fuel region can be loaded with non-fissile materials to be bred (breeder region).

vi) A *reflector* region made of pure diffuser, with eventually an outer retaining shield, which closes the system, ensuring durable containment of neutrons.

In order to ensure appropriate containment, the Lead or Bismuth volume must be of the order of 2000÷3000 tons, arranged in a sort of cylinder or cube of some 6 m each side. Since the neutron containment is essential, this order of magnitude of diffuser volume is required in all circumstances. The amount of fuel to ensure dominance of the capture process needs instead to be much smaller. A realistic EA is already possible with 6-7 tons of fuel, corresponding to a ratio fuel/diffuser $\eta \geq 2.5\ 10^{-3}$. On the other hand larger fuel amounts are possible for large power applications. From the point of view of the neutronics, $\eta \leq 0.01$ is ideal. The neutron leakage out of the diffuser is then typically less than 1% and the fraction of captures in the Lead nuclei of the order of 4 ÷ 6%, i.e. much smaller than in the case of a pure diffuser.

D.3.2.3. NUMERICAL EXAMPLE OF SPATIAL DISTRIBUTIONS

In order to evaluate the actual neutron flux distribution in practical cases, analytic calculations are either too approximate or too cumbersome. It is preferable to use the Montecarlo computer method described in paragraph D.3.2.6. The burn-up radial distribution for three different values of k and a typical EA geometry[1] of Figure 2.2 has been calculated with the full Montecarlo method (see paragraph D.3.2.6) and it is shown in Figure 2.3. The value of k has been varied changing the pitch of the hexagonal fuel lattice and hence the fuel density. One can see clearly how the neutron flux distribution changes from exponential for k = 0.95 (pitch 1.40 cm) to an almost perfect cos-like distribution for k = 0.99 (pitch 1.138 cm), indicating the emerging dominance of the fundamental mode. At k = 0.98 (pitch 1.243 cm) which is the chosen working point for our conceptual design, one is somehow in a transitory region. The concavity of the curve passes through a zero and a linear fit is a good approximation.

A number of different machine geometries have been explored in order to assess the effects of higher modes in a more general way. In general one can say that lowering the k produces a faster decay in the exponential mode, in agreement to what is found in the elementary theory. The actual transition value of k from pure exponential to linear and eventually to cos-like depends on the geometry of the spallation source and of the core. A geometry with several spallation sources (beams) or a widely diffused source can be beneficial in order to improve the uniformity, especially if the source distribution follows a symmetry pattern such as to cancel the contribution of the most offending higher modes.

D.3.2.4. FUEL BREEDING

For many reasons illustrated for instance in Ref. [1], the by far preferred fertile material is ^{232}Th, although applications based on other Actinides are of interest for burning Plutonium, depleted Uranium and similar surpluses. Neutron captures in the fertile element lead to production of fissile material. The main chain of events for ^{232}Th is then

---

[1] The outer radii are as follows: Spallation Target and Buffer: 40 cm, Main core and Breeder : 1.67 m. The height of the core is 1.5 m and the containment box a cylinder of 6 m diameter and 6 m high. The fuel is a compact hexagonal lattice with fuel pins as described in Table IV.4. The fuel is made of ThO_2 with 10% by weight of $^{233}UO_2$. The cladding is made of HT-9, low activity steel.

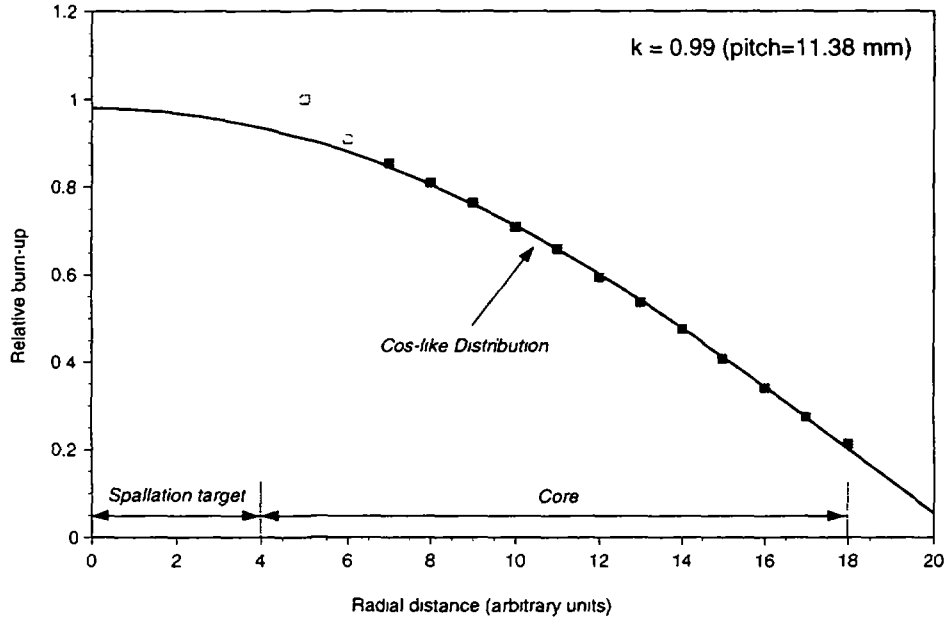

FIG. 2.3a The burn-up radial distribution for different criticality coefficients, namely for (a) for k=0.99, (b) for k=0.975 and (c) for k=0.950. Open points have not been included in the fits.

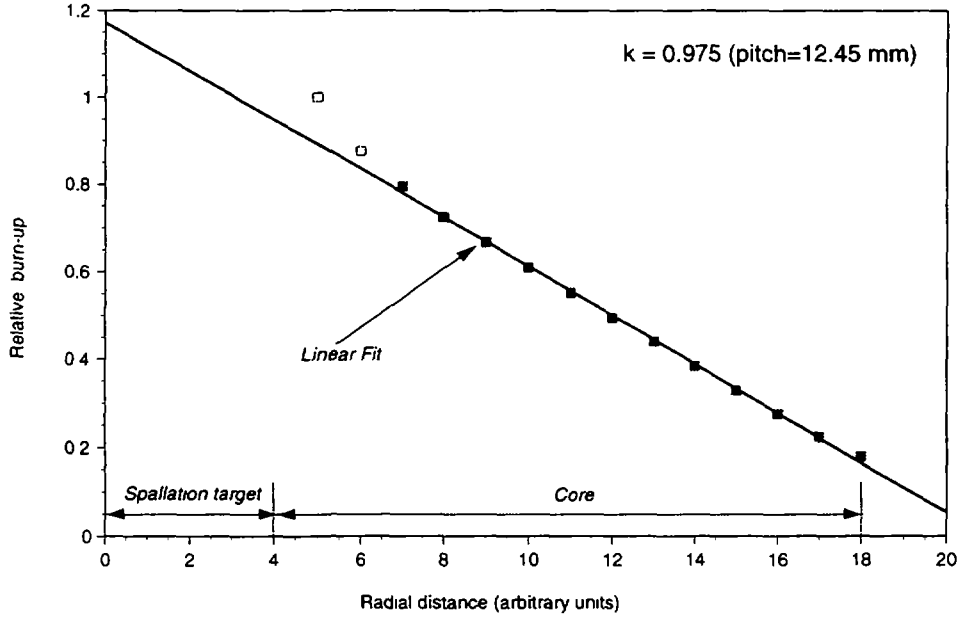

FIG. 2.3b k=0.975 - see caption for Fig. 2.3 a.

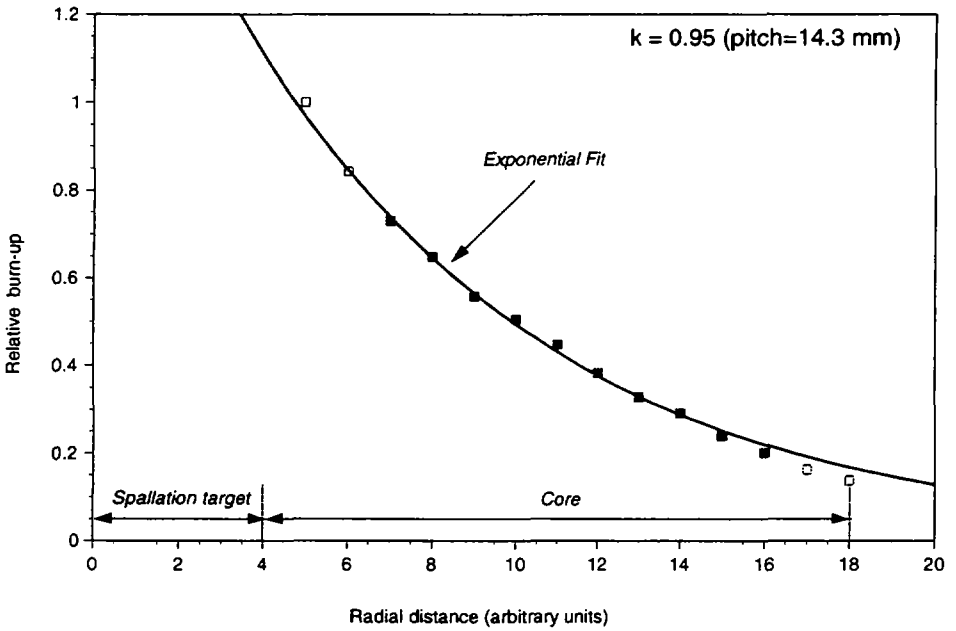

FIG. 2.3c k=0.950 - see caption for Fig. 2.3 a

$$^{232}Th + n \xrightarrow{\gamma} {}^{233}Th \xrightarrow{\beta^-,\ 22\ min} {}^{233}Pa \xrightarrow{\beta^-,\ 27.0\ days} {}^{233}U$$

In steady neutron flux conditions, the chain will tend to an equilibrium, namely in a situation in which each fissioned ^{233}U nucleus is replaced by a newly bred fuel nucleus. To a first order, the equilibrium condition can be summarised by the equations:

$$N(^{232}Th)\sigma_{\gamma}(^{232}Th)\phi = N(^{233}Pa)/\tau(^{233}Pa \rightarrow {}^{233}U) = N(^{233}U)\sigma_{fiss+\gamma}(^{233}U)\phi$$

where cross sections are averaged over the neutron spectrum of integrated flux ϕ. Such a "breeding" equilibrium is naturally attained with a specific value of the fuel/breeder concentration ratio determined solely by the ratio of cross sections

$$\xi = \frac{N(^{233}U)}{N(^{232}Th)} = \frac{\sigma_{\gamma}(^{232}Th)}{\sigma_{fiss+\gamma}(^{233}U)}$$

This equation assumes no alternatives besides the main chain, justified as long as the rate of neutron captures by ^{233}Pa competing with natural decay is kept negligible with a sufficiently low neutron flux. This is the "decay dominated" regime [1] in contrast with the high flux, "capture dominated" regime investigated by Bowman et al [15] where the ^{233}Pa must be quickly extracted to avoid capture.

The breeding ratio at equilibrium is about $\xi = 1.35 \times 10^{-2}$ for thermal energies and it rises to $\xi = 0.126$ for fast neutrons and cross sections of Table II.2. An EA based on fast neutrons (F–EA) will then require a fuel concentration which is about nine times the one of a device based on fully thermalised neutrons (T–EA). However, it can operate with much higher burn-up rates and hence the total mass of fuel is correspondingly reduced: for the same *output power*, the stockpiles of ^{233}U are in general comparable.

During the actual burn-up of the fuel following an initial fuelling, the equilibrium equation above is only approximately attained, since the concentration of the bulk, fertile material is decreasing with time. Solving the related Bateman equations with an initial breeding material exposed to a constant neutron flux shows that correction terms have to be introduced to the asymptotic value of the breeding ratio[1]:

$$\xi_{lowflux} = \frac{N(^{233}U)}{N(^{232}Th)} = \frac{\sigma_\gamma(^{232}Th)}{\sigma_{fiss+\gamma}(^{233}U)}\left(1+\frac{\sigma_\gamma(^{232}Th)}{\sigma_{fiss+\gamma}(^{233}U)}\right)$$

$$\xi = \frac{N(^{233}U)}{N(^{232}Th)} = \xi_{lowflux}\left(1+\phi\sigma_\gamma(^{232}Th)\,\tau(^{233}Pa\rightarrow^{233}U)\right)$$

The first correction is negligible for a T-EA, but it increases significantly (by 10%) the breeding equilibrium of the F-EA. The second, flux dependent term is smaller but not negligible ($\Delta\xi = 0.31 \times 10^{-3}$ for a burn-up rate ρ = 60 W/g and cross sections of Table II.2) and it compensates partially the flux dependent losses due to captures of the intermediate state ^{233}Pa.

The energetic gain *G*, namely the energy produced in the EA relative to the energy dissipated by the high energy proton beam is given by the expression [1]

$$G = \frac{G_0}{1-k} = \frac{2G_0}{2-\bar{\eta}(1-L)}$$

where G_0 is the gain proportionality constant, typically 2.4 ÷ 2.5 for a well designed EA; *k* is the fission-driven multiplication coefficient $k = \bar{\eta}(1-L)/2$; *L* is the sum of fractional losses of neutrons (absorbed in a variety of ways, like captures in structures and coolant, in fission-product poisons, diffused outside the EA and so on); $\bar{\eta}$ is the (spectrum averaged) number of fission neutrons produced by a neutron absorbed in the fissile isotope[2]. The parameter $\eta(E)$ has a rather complicated neutron energy dependence, with a somewhat lower value in some parts of the resonant region, before rising to larger values for fast neutrons.

As is well known, in order to achieve criticality the denominator must become zero, $\bar{\eta} = 2(1-L)$. More precisely, criticality is achieved when neutron losses are reduced to the value $L_{crit} = 1 - 2/\bar{\eta}$. Note that since L > 0 in order to reach criticality $\bar{\eta} > 2$, one neutron being required to maintain the chain reaction and the second being absorbed by the fertile material.

The F-EA has the advantage, when compared to a T-EA that it operates in a region where $\bar{\eta}$ is significantly larger. In addition because of the higher energies, additional neutrons are produced at each generation by different processes, like for instance fast fissions in the fertile material ^{232}Th and (n,2n) reactions in the fuel and the moderator. In order to take into account these contributions it is customary to replace the parameter $\bar{\eta}$ with $\bar{\eta}\varepsilon$ where ε (fast fission factor) is the ratio of all neutrons produced to the ones from the main fission reaction. For a F–EA we expect $\bar{\eta}\varepsilon \approx 2.4 \div 2.5$, conveniently and significantly larger than 2 and larger than $\bar{\eta}\varepsilon \approx 2.1 \div 2.2$ [2] appropriate for a T-EA. The larger allowance for losses (f.i. $L_{crit} = 1 - 2/\bar{\eta}\varepsilon = 0.167 \div 0.200$ vs. $L_{crit} = 0.048 \div 0.091$) is an important asset of the F-EA, even if operation is always with $L > L_{crit}$. As discussed in more detail later on, these extra neutrons do not necessarily have to be thrown away: they may for instance be used to breed additional fuel or to eliminate radiotoxic sub-

[1] In our treatment we do not include the captures in ^{233}Pa, which of course are also a rate dependent effect. These losses are instead counted in L.

[2] This equation is easily worked out realising that *at the breeding equilibrium* the number of neutron captures in ^{233}U and in ^{232}Th at each generation must be the same and normalised to 1 neutron are equal to (1–L)/2, since, by neutron conservation, [captures in ^{233}U] + [captures in ^{232}Th] + [Losses]= 1 = (1–L)/2+(1–L)/2+L = 1. As the number of next generation neutrons $\eta(1-L)/2$ generated by ^{233}U fissions is also, by definition, the multiplication coefficient k, we conclude that $k = \eta(1-L)/2$.

TABLE II.2. AVERAGED CROSS SECTIONS (BARN) OF ACTINIDES RELEVANT TO THE FAST EA.

Element	Capture	Fission	Elastic	(n->2n)	(n->n')	Total
^{230}Th	0.198672	0.018918	14.060925	0.000598	0.989135	15.268245
^{232}Th	0.386855	0.005966	10.923501	0.000560	0.699221	12.016131
^{231}Pa	3.309176	0.179791	9.133289	0.000398	1.110933	13.733619
^{233}Pa	1.121638	0.038989	8.093003	0.000162	1.754808	11.008615
^{232}U	0.731903	2.096317	9.368297	0.000281	0.433875	12.630690
^{233}U	0.289003	2.783923	8.919141	0.000211	0.280445	12.272738
^{234}U	0.615564	0.248950	10.031339	0.000054	0.718069	11.613976
^{235}U	0.574071	1.972008	8.858968	0.000457	0.640860	12.046378
^{236}U	0.490142	0.068786	11.125422	0.000294	0.855951	12.540620
^{237}U	0.492199	0.610042	9.189025	0.000920	0.491900	10.784104
^{238}U	0.428265	0.025351	11.254804	0.000529	0.832077	12.541045
^{237}Np	1.674921	0.233176	9.157094	0.000115	0.759934	11.825250
^{238}Np	0.089278	0.595202	10.439487	0.000000	0.000000	11.123966
^{239}Np	2.083201	0.353837	9.184162	0.000135	0.865835	12.487206
^{238}Pu	0.756840	1.025175	11.046388	0.000152	0.342888	13.171463
^{239}Pu	0.557041	1.780516	9.156214	0.000237	0.770227	12.264245
^{240}Pu	0.667103	0.288079	10.331735	0.000083	0.573045	11.860045
^{241}Pu	0.425030	2.577470	8.104389	0.000880	0.801986	11.909761
^{242}Pu	0.535288	0.190578	11.024648	0.000229	0.667679	12.418422
^{243}Pu	0.403097	0.810772	9.283313	0.002254	0.623218	11.122661
^{244}Pu	0.236048	0.157011	10.805879	0.000808	0.813081	12.012833
^{241}Am	1.963967	0.190469	9.580900	0.000004	0.565741	12.301095
^{242}Am	0.079728	0.530819	10.233513	0.000462	0.073528	10.844059
^{243}Am	1.582431	0.146245	10.003948	0.000028	0.935282	12.667938
^{242}Cm	0.372092	0.105767	10.362508	0.000007	0.724242	11.564615
^{243}Cm	0.265210	2.655223	10.012800	0.000456	1.005476	13.939172
^{244}Cm	0.909153	0.318102	10.515990	0.000135	0.540912	12.284297
^{245}Cm	0.335178	2.475036	8.750109	0.000831	0.862513	12.423669
^{246}Cm	0.230261	0.181669	10.844025	0.000174	0.780190	12.036336
^{247}Cm	0.348536	1.926754	9.117731	0.001353	0.372127	11.766518
^{248}Cm	0.265514	0.218438	11.295776	0.000234	0.813142	12.593122
^{249}Bk	1.447988	0.113146	10.220059	0.000052	1.186927	12.968192
^{249}Cf	0.667223	2.707975	9.064980	0.000189	0.425589	12.865973
^{250}Cf	0.614795	0.944213	8.927651	0.000406	0.468860	10.955943
^{251}Cf	0.368920	2.488528	8.815815	0.001573	0.417832	12.092679
^{252}Cf	0.320039	0.573875	11.865360	0.000335	0.414425	13.174031
^{253}Cf	0.180410	0.716114	9.940411	0.000000	0.000000	10.836935

stances [6]. It is also convenient to start operation of a F-EA with a ^{233}U concentration smaller than the one corresponding to the breeding equilibrium. During operation, the increase of criticality due to the build-up of the ^{233}U relative concentration can be used to compensate growing neutron losses due to captures by fission fragments, thus ensuring a more uniform gain during a longer period of operation without interventions.

D.3.2.5. FLUX DEPENDENT EFFECTS

It has been pointed out [1] that there are sharp limitations to the neutron flux at which an EA can operate in acceptable conditions. The power produced is directly proportional to the neutron flux. We define with ρ the specific power, in units of thermal Watt produced by one gram of Thorium in fuel[1]. At the breeding equilibrium the fluxes for thermal and fast neutrons are given by

$$\phi_{thermal} = 1.80\times10^{12}\times\left[\frac{\rho}{W/g}\right] cm^{-2}s^{-1} \; ; \; \phi_{fast} = 3.88\times10^{13}\times\left[\frac{\rho}{W/g}\right] cm^{-2}s^{-1}$$

where for the latter we have used the cross sections of Table II.2. Let us estimate some orders of magnitude. For thermal neutrons (E = 0.025 eV), a power of $\rho = 15.0$ W/g corresponds to a flux $\phi = 2.7 \times 10^{13}$ cm^{-2} s^{-1}, which is considered optimal for a T-EA [1]. In practice the flux in a T-EA will depend somewhat on the energy spectrum of the neutrons, which in turn depends on the operating temperature of the device and on the choice of the moderator. For the same power yield, the neutron flux in a F-EA is approximately 20 times larger. As is well known, it simply reflects the fact that at higher energies cross sections are generally smaller. A practical burn-up rate of a F-EA is about $\rho = 60$ W/g : the flux will then be $\phi = 2.33 \times 10^{15}$ cm^{-2} s^{-1}, about 80 times larger than the one optimal for a T-EA.

There are several flux dependent effects which have a direct influence on the value and the stability during operation of the multiplication factor k, and hence on the gain:

1) Neutron capture by the intermediate elements of the breeding process and specifically by the ^{233}Pa which destroys a nascent ^{233}U atom at the price of an extra neutron. Such a loss involves a competition between neutron capture and radioactive decay, and it is proportional to the total flux ϕ through the parameter $\Delta\lambda_l = \sigma_a(^{233}Pa) \times \tau(^{233}Pa \rightarrow ^{233}U) \times \phi << 1$ where τ is the mean life. The absorption cross section $\sigma_a(^{233}Pa)$ is about 43 b at thermal energies, it has a resonance integral of 850 b and it is equal to 1.12 b for fast neutrons (Table II.2). The corresponding value for a T–EA is $\Delta\lambda_l \approx 1.45\times10^{-16}\phi$, corresponding to a contribution to L of $\Delta L = (1-L)\bar{\eta}\varepsilon\Delta\lambda_l/2 \approx 3.78\times10^{-3}$ for the typical flux of 2.7×10^{13} cm^{-2} s^{-1}. For fast neutrons the cross section is much smaller but the flux is correspondingly larger: for a given burn-up rate ρ, $\Delta\lambda_l$ is 0.56 times the value for thermal neutrons. Note however that the allowance for neutron losses is much greater for the F-EA and therefore larger burn-up rates are practical: for ρ = 60 W/g, $\Delta\lambda_l = 8.81 \times 10^{-3}$ which is quite acceptable.

2) A consequence of the relatively long mean life of ^{233}Pa (1/e decay after τ = 39 days) is that a significant reactivity increase occurs during an extended EA shut-down. Conversely, any prolonged increase in burn-up rate produces a temporary reduction of reactivity until the ^{233}Pa inventory has been re-established. The magnitude of such a reactivity change following a shut-down need not be a problem, but appropriate measures would be required to correct its effects. The density of ^{233}Pa is given by

$$N(^{233}Pa) = \tau\,(^{233}Pa \rightarrow ^{233}U)\overline{\sigma_{\gamma+fiss}(^{233}U)}\,N(^{233}U)\phi = \\ = (1+\alpha)\tau\,(^{233}Pa \rightarrow ^{233}U)\times\left[N(^{233}U)\overline{\sigma_{fiss}}(^{233}U)\phi\right]$$

where α is the ratio of the non-fission (n,γ) to fission reactions and the last term $N(^{233}U)\overline{\sigma_{fiss}}(^{233}U)\phi$

[1] *In this chapter we define the power density with reference to the main Thorium content, unlike the rest of the paper where we have taken as reference the unit weight of the actual chemical mixture of the fuel.*

is directly proportional to the ^{233}U burn-up rate, ρ. If the accelerator beam is shut down, following the characteristic decay lifetime $\tau(^{233}Pa \rightarrow ^{233}U)$, the concentration of ^{233}U will increase by an amount asymptotically equal to $N(^{233}Pa)$, essentially independent of the mode of operation of the EA for a given equilibrium burn–up rate. However since in the case of the F-EA the equilibrium concentration ξ of ^{233}U is about nine times larger, its effect on reactivity max(Δk/k) = N(^{233}Pa)/N(^{233}U) will be only 1/9 of the one for a T-EA. For the chosen examples of burn-up rates, $\max(\Delta k/k) \approx 5.2 \times 10^{-2}$ for the T-EA and only $\max(\Delta k/k) \approx 2.08 \times 10^{-2}$ for the F-EA, in spite of the factor four in ρ in favour of the present option.

3) Neutron losses due to the high cross section fission product ^{135}Xe are well known [29]. The Xenon poison fraction is neutron flux dependent, since it relates, like in the case of ^{233}Pa to an equilibrium between captures and decays. For thermal neutrons and at the breeding equilibrium, the fraction of neutrons captured by ^{135}Xe is given by $\Delta\lambda_3 \approx 0.9\times10^{-19}\phi / (2.1\times10^{-5}+3.5\times10^{-18}\phi)$ which tends to an asymptotic value $\Delta\lambda_3 \approx 0.021$ for a flux $\phi \approx 2.7 \times 10^{13}$ cm^{-2} s^{-1}. Following a reactor shutdown or reduction in power, the Xenon poisoning temporarily increases even further [29] because decays producing Xe continue to occur, passing through a maximum 10 to 12 hours after the shutdown. The magnitude of this transient additional poisoning is also dependent on the neutron flux. Although the temporary loss is not significant, a reactivity reserve, if normally compensated by control rods, would represent a permanent loss of neutrons. The Xenon type poisoning effect is essentially absent in the case of F-EA, since there is no fission fragment nucleus which has the required features in the energy domain of importance.

As one can see in a F-EA the importance of these effects is much smaller. The estimated effects at the burn-up rate ρ = 60 W/g are given in Table II.3.

TABLE II.3. NEUTRON FLUX DEPENDENT EFFECTS IN THE F-EA BASED ON THE ^{232}Th CYCLE. THE PARAMETER ρ IS THE POWER DENSITY PRODUCED PER UNIT FUEL MASS AT BREEDING EQUILIBRIUM.

Quantity		Values for ρ = 60 W/g
Ratio N(^{233}Pa)/N(^{233}U)		0.0208
Variation of the breeding ratio, ξ	$\Delta\xi$	$+ 0.388 \times 10^{-3}$
Neutron Flux cm^{-2} s^{-1}	ϕ	2.33×10^{15}
Effects of ^{135}Xe, ^{149}Sm, etc.	$Max(\Delta k)$	$< 10^{-4}$
Breeding loss due to premature capt. in ^{233}Pa	Δk	− 0.00480
Criticality rise after 10 days shut-down (^{233}Pa)	Δk	+ 0.00413
Criticality rise after infinite shut-down (^{233}Pa)	$Max(\Delta k)$	+ 0.0203

The reactivity increase due to ^{233}Pa decays is quoted for a 10 day cooling period, since such a time is largely sufficient to overcome any imaginable technical problem, assuming that the "scram" system fails in blocking the reactivity. The most direct consequence of this fact is that a larger value of k is operationally conceivable, with a consequently higher energetic gain, (see paragraph D.3.2.6). As discussed further on, the temperature coefficient of criticality is negative, corresponding to $\Delta k = +0.01$ for a temperature drop of 700 °C. Adding linearily the effect of such a large temperature swing to the 10 day intervention limit suggests that the largest, practical maximum value of operational reactivity of a subcritical F-EA is about $k \leq 0.98$. It should be noted however that already for $k = 0.96$ the recirculation power through the accelerator is less than 10% of the delivered, useful electric power.

The exact definition of the parameters of the F-EA implies an appropriate account of the resonance or otherwise complex energy behaviour of the cross sections of the many elements which intervene in the cascade reactions.

As in Ref. [1] we have adopted a Montecarlo method in which a large number of individual neutrons are followed from their birth to absorption. We make use of the concept of neutron generation and introduce the effective multiplication coefficient k_{eff}, the fraction of neutrons which are regenerated at each generation. Both fissions and (n, 2n) reactions are considered. Cross sections are finely interpolated from the most complete sets of cross section data available today [30] and include all main channels, like for instance inelastic (n,n') scattering. Thermal movement of the target nuclei (Doppler broadening) is included in the simulation.

The elementary structure of the EA is subdivided in a number of different regions, which reflect the geometrical properties of the device. The composition of each of these regions is allowed to change as a function of time taking into account the changes in concentrations of the newly produced elements due to (1) the nuclear transformations and (2) the spontaneous decay chain. A complete database of all known elements with their decay modes and rates is used [31] and new elements are introduced to the list whenever a decay or a reaction channel justifies it.

Particular attention has been given to fissions, since they are the dominant, driving process for the multiplication. The energy dependence of the neutron multiplicity has been parametrized from existing data [30].

One important feature of the programme is the one of calculating the evolution of the (poisoning) fission fragments. In order to do so effectively many hundreds of different elements must be followed during the calculations. This very complete method of simulation has been made possible only recently due to the availability of more powerful computers. It is still somewhat limited in the statistical accuracy due to lack of computing power [32].

In practice, the computer programme requires that one defines the different geometrical regions, their initial composition and their operating temperatures. One has to define then the scale of time and of reaction activity. The programme then calculates the time evolution of the system — based of course on a much smaller random neutron population but with changes of concentrations scaled to the actual flux — and calls on further elements whenever required. The calculation can be coupled with a Montecarlo programme which simulates the high energy cascade. Hence the Montecarlo emulates the whole process initiated by an incoming beam of specified characteristics. More often it is used as a stand-alone module to determine the multiplication coefficient k_{eff}, starting from an initial spectrum due to fission neutrons.

The Montecarlo method has the advantage over other methods that in principle it provides a very realistic evolution of the system. However the computing time is long and the results affected by statistical errors. Therefore it has been coupled with another, simpler evolution programme, which permits a faster exploration of the main features of an EA. This programme makes use of some of the information from the full Montecarlo, namely

1) the averaged cross sections for all relevant elements are extracted as the average over the energy and the fuel volume of the flux as computed by the Montecarlo. Since (see paragraph D.3.2.2) the flux is rather uniform over the fuel elements, the spatial average is a good approximation. The averaging over energy may introduce some approximations in presence of strong resonances, where the flux may be locally affected. The extent of this approximation has been checked comparing true Montecarlo with the evolution programme and found acceptable for our purposes.

2) the parameter L, namely the sum of fractional losses of neutrons (absorbed in a variety of ways, like captures in structures and coolant, diffused outside the EA and so on) is divided into two components, namely a term which is constant, but geometry dependent and another (mainly due to fission-product poisons, spallation and activation nuclei etc.) which is linear in the burn up.

This parametrization is in excellent agreement with the Montecarlo results. Actual values to be used in the evolution programme are fitted from the Montecarlo simulation. Hence they take into account all burn-up dependent neutron losses.

The time evolution in a slab of material subject to a neutron flux and with spontaneous decays cannot be calculated following the classic Bateman evolution equations [33]. This is due to the fact that the Bateman's description assumes an open, successive chain of decay nuclei, eventually leading to the final stable isotopes, namely a specific path in the (A,Z) plane. Under the simultaneous action of neutrons and decays, nuclei can both rise (neutron induced reactions) and fall in the atomic A, Z number (spontaneous decays). Hence the decay paths in the (A,Z) plane perform loops which may bring back the same nucleus an arbitrary number of times and imply products of an infinite number of terms, although with a decreasing probability. For this reason our time evolution programme is based on numerical step-wise methods. In our analysis both programmes are used and give consistent results. Furthermore the neutron flux and criticality predicted by the Montecarlo programme is in good agreement with the results of standard, non evolutionary programmes [34].

D.3.2.7. CUMULATIVE FISSION FRAGMENT POISONING

One of the most serious limitations in the T-EA comes from the losses of neutrons due to slowly saturating or non saturating fission fragments (FFs). In contrast to ^{135}Xe and ^{149}Sm, which have a very large neutron cross section and therefore reach saturation in a short time, the majority of the fission products have cross sections which are comparable or smaller than the one of the fuel itself. Hence the aggregate poisoning effect of such fission products is roughly proportional to the fractional burn-up of the fuel. The accumulated effect depends significantly on the past history of the fuel. Computer calculations have been used to analyse the poisoning as a function of the integrated burn-up for a variety of different conditions.

One important result is that losses due to fission fragment poisoning are much less important for a F-EA, when compared to a T-EA (Figure 2.4). In both cases however the build up of FFs implies a progressive reduction of criticality.

An important feature of the F-EA is that it is possible to operate the device for a long time (several years) without intervention on the fuel. In order to enhance such a feature we have investigated the possibility of starting with a ^{233}U concentration smaller than at the breeding equilibrium ξ and thus compensate as much as possible the drop of criticality due to fission fragment poisoning with the help of the increasing fraction of bred ^{233}U.

In Figure 2.5 we have considered with the help of the evolution programme the criticality coefficient k for the EA device described in paragraph D.3.2.3 as a function of burn-up for a constant neutron flux and given initial ^{233}U concentration. Since the neutron flux will in practice depend on time, the criticality coefficient will be slightly affected also by the dependence of the ^{233}Pa concentration with flux. The initial criticality coefficient is adjusted "ad hoc" to $k = 0.965$ by slightly increasing the neutron losses L. The initial filling of ^{233}U is set to $\xi = 0.117$, significantly lower than the breeding ratio at equilibrium. The graph shows three different fluxes and hence power yields, ρ. The general behaviour of the curves shows an initial drop related to ^{233}Pa production, followed by a rise due to the increment of ξ due to breeding. Fission fragment captures eventually become important and bring down k. A higher ρ gives lower k values since early captures in ^{233}Pa reduce the breeding yield. Curves without fission fragment poisoning are alsoshown.One can conclude that (1) a very smooth running is possible up to a burn up of the order of 150 GW d/t, essentially without intervention and (2) a power yield of the order of $\rho \approx 100$ W/g is perfectly acceptable[1]. An extended shut-down will move to the curve for $\rho \to 0$, still sufficiently far away from criticality. Of course, as already pointed out, in view of the long ^{233}Pa lifetime, there is plenty of time to introduce corrective measures.

[1] Note that in the present design, we have conservatively set the power density to about one half of this value.

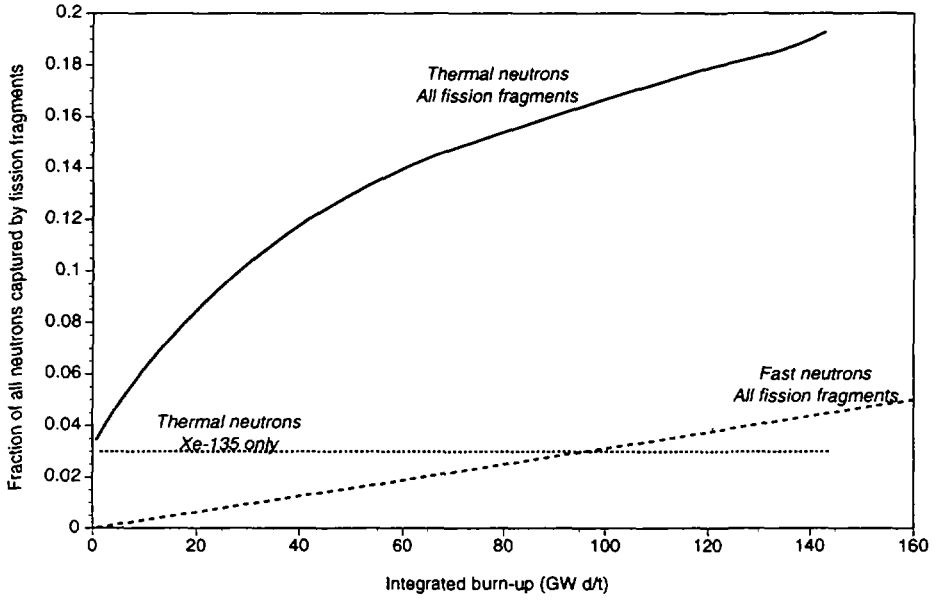

FIG. 2.4 Fraction of neutrons capture by the fission fragments as a function of the integrated burn-up, for thermal and fast EA.

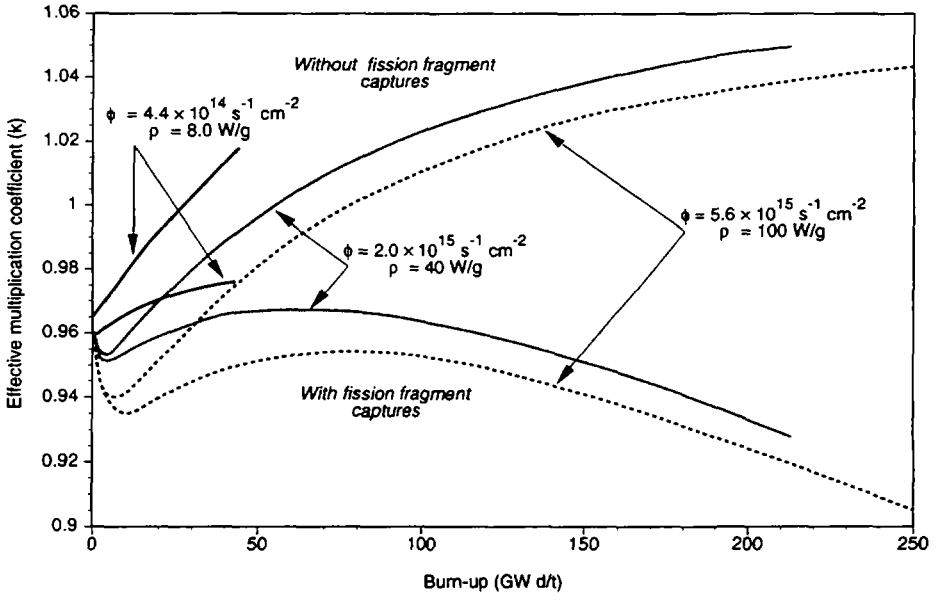

FIG. 2.5 Criticality coefficient k as a function of the integrated burn-up for different power yields. The effect on k due to the neutron captures by the fission fragments is also shown.

For a fixed beam power the flux is time dependent, and will vary proportionally to gain. Since gain is related to the ^{233}Pa concentration and in turn to its capture probability, the dependence of k as a function of burn up is even smoother. In Figure 2.6 we show the typical k behaviour for a somewhat larger initial

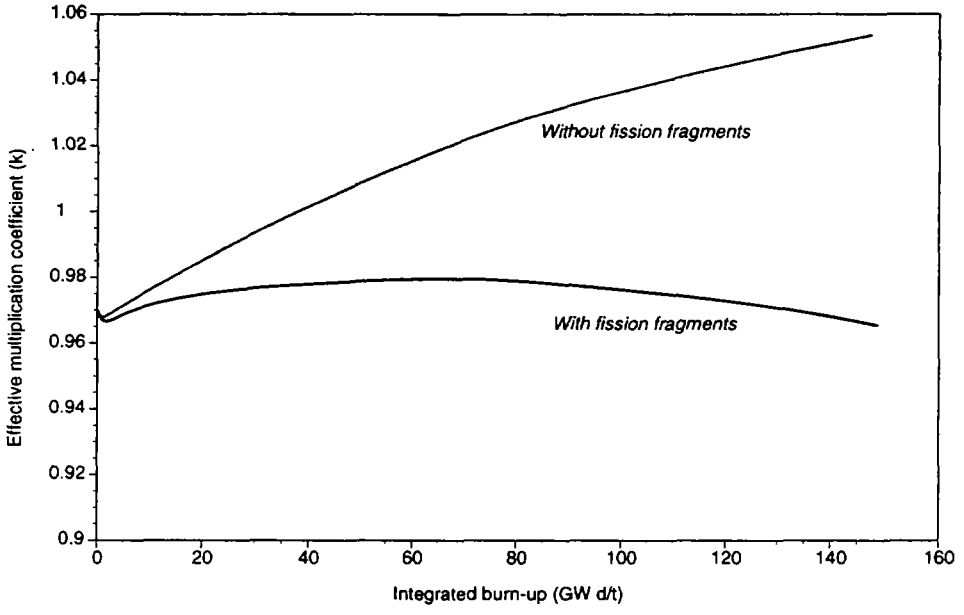

FIG. 2.6 Behaviour of k as a function of the integrated burn-up.

value of *k*. Almost constant conditions can be ensured without intervention over a burn up of 100 ÷ 150 GW d/t, namely over several years.

D.3.2.8. HIGHER URANIUM ISOTOPES AND OTHER ACTINIDES

Higher Uranium isotopes and higher Actinides are produced by successive neutron captures. The time evolution of an initially "pure" ^{232}Th and ^{233}U fuel mixture can be easily calculated and is given in Ref. [1] for a T-EA. The build-up of the several isotopes introduces more captures and some fissions. Hence in principle the multiplication coefficient k is also modified. It was shown in Ref. [2] that the asymptotic mixture preserves an acceptable value of *k* for initial ^{232}Th both in thermal and fast neutron-conditions, while for initial ^{238}U only fast neutrons preserve an acceptable gain.

In the EA the initial fuel is *completely* burnt in a closed, indefinite cyclic chain in which Actinides of the spent fuel become the "seeds" of the next fuel cycle [1]. At each discharge an appropriate amount of fresh fuel is added to compensate for the burn-up and the accumulated nuclear species, products of the fission (fission fragments, FFs) are removed. The initial fuel nuclei (either Th^{232} or U^{238} or eventually a mixture of both) undergo a series of transformations induced by neutron captures and spontaneous decays, until they achieve ultimate fission. The first of these transformations is the initial "breeding" reactions which continue to be the dominant source of fissions (^{233}U or ^{239}Pu respectively) even after a long burn-up. However a rich hierarchy of secondary processes builds up at all orders. These secondary processes become essential in determining the atomic concentration vector $c_{(A,Z)}$ of Actinides and hence the neutron economy of the cascade. For stationary conditions the atomic concentration vector $c_{(A,Z)}(\phi)$ tends asymptotically, (i.e. after long burn-ups) to a limiting equilibrium value.

In order to estimate the actual evolution of $c_{(A,Z)}(\phi)$ we have studied the time evolution of some fuel exposed to the average flux of an F-EA with the help of the evolution programme and using the cross sections of Table II.2. Results have been checked with the full Montecarlo programme. The chain of many successive re-fillings has been simulated. Although the results are widely independent of the power density, for definiteness the value ρ = 100 W/g has been used. After a pre-assigned burn-up of 150 GW d/t, Actinides are discharged and the fuel topped-up with fresh ^{232}Th. Since the amount of fuel burnt is not

negligible the stockpile of ^{233}U is affected by the over-all reduction of the fuel mass, even if the relative concentration with respect to ^{232}Th has remained constant (at the breeding equilibrium) or significantly increased (if initially below the breeding equilibrium). It is therefore necessary in general to add to the renewed fuel an amount of ^{233}U which is larger than what is recovered at the discharge. For this reason a small breeder section has to be added to the EA: initially made of pure Thorium, it is designed to supply such a needed difference. The total ^{233}U stockpile as a function of burn up has been calculated with the full Montecarlo for the geometry given in paragraph D.3.2.3 and shown in Figure 2.7. With the help of such an extra breeding, it is realistic to expect that the initial volume of ^{233}U can be made available at the end of the cycle. Therefore in our simulation of the evolution of $c_{(A,Z)}(\phi)$ we assume that both ^{232}Th and ^{233}U are topped up to the initial values at each filling. The new fuel will contain in addition all the remaining Actinides produced by the previous combustion.

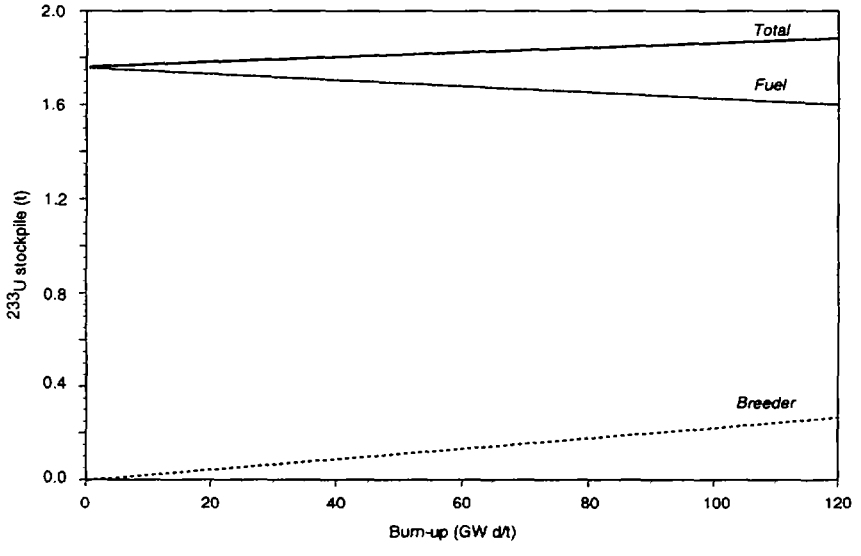

FIG. 2.7 ^{233}U stockpile as a function of the integrated burn-up.

In Figures 2.8a, 2.8b and 2.8c we show the Actinide distribution at discharge, as a function of the discharge number. The relative concentrations are listed in Table II.4. All elements clearly reach an asymptotic concentration, in which production and incineration are in equilibrium. Concentrations of higher actinides tend to a stable equilibrium condition which is a fast decreasing function of A and Z. This is due to the fact that almost at each step of the neutron induced evolution ladder, fissions subtract a significant fraction of nuclei. The most offending isotopes, because of their amount and their radio-toxicity, namely ^{231}Pa and ^{232}U are practically close to the asymptotic values of 1.06×10^{-4} and 1.30×10^{-4} already at the first discharge. Note also the large concentration of ^{234}U which quickly reaches an asymptotic concentration which is about 38% of ^{233}U. The Uranium composition at (asymptotic) discharge is therefore 9.354×10^{-4} of ^{232}U, 63.88 % of ^{233}U, 24.12 % of ^{234}U, 5.870 % of ^{235}U, 6.01 % of ^{236}U and 1.03×10^{-4} of ^{238}U, which constitutes about 14% of the spent fuel mass. Likewise the Neptunium and Plutonium, produced in negligible amounts during the first fillings grow to asymptotic values of 0.2% and 0.1 % respectively. Plutonium is dominated by the isotope ^{238}Pu which has the short half life of 87.7 years and therefore has no practical military application. Higher Actinides, Americium and Curium, never reach concentrations of significance. Note that for instance after 20 refilling the fuel seeds have produced an integrated burn up of the order of 3000 GW d/t and therefore these contaminating amounts, once normalised to the produced energy are totally negligible. For instance the Plutonium concentration at the discharge of an ordinary PWR is about 1.1% for 33.0 GW d/t. The amount of transuranic Actinides produced per unit of energy delivered is about three orders of magnitude less than in an ordinary PWR.

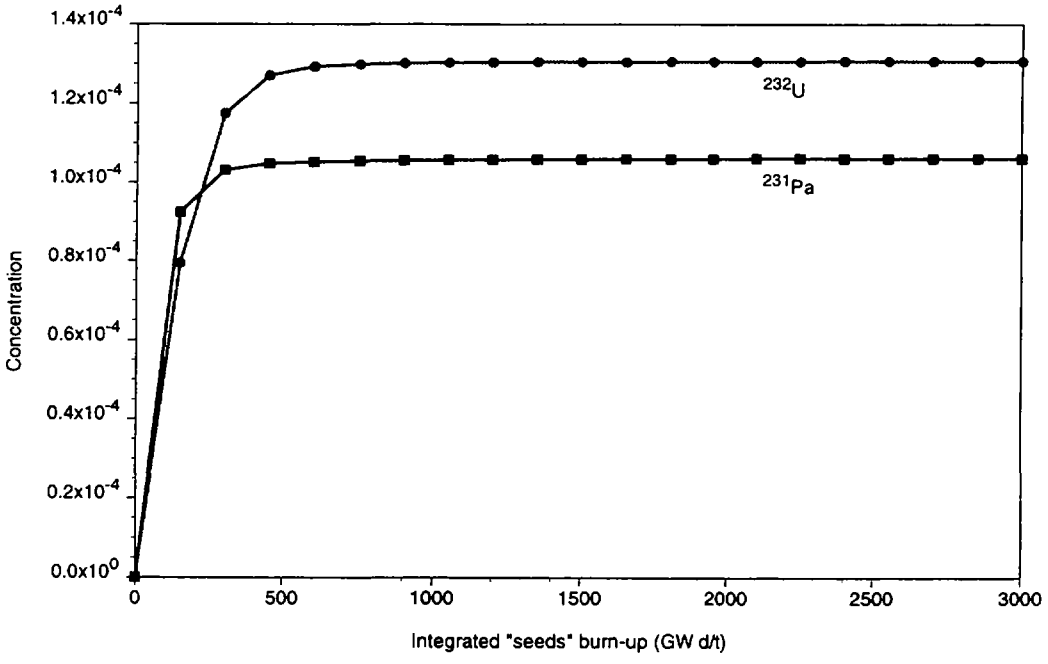

FIG. 2.8a ^{231}Pa and ^{232}U stockpile as a function of the discharge number (integrated seeds burn-up).

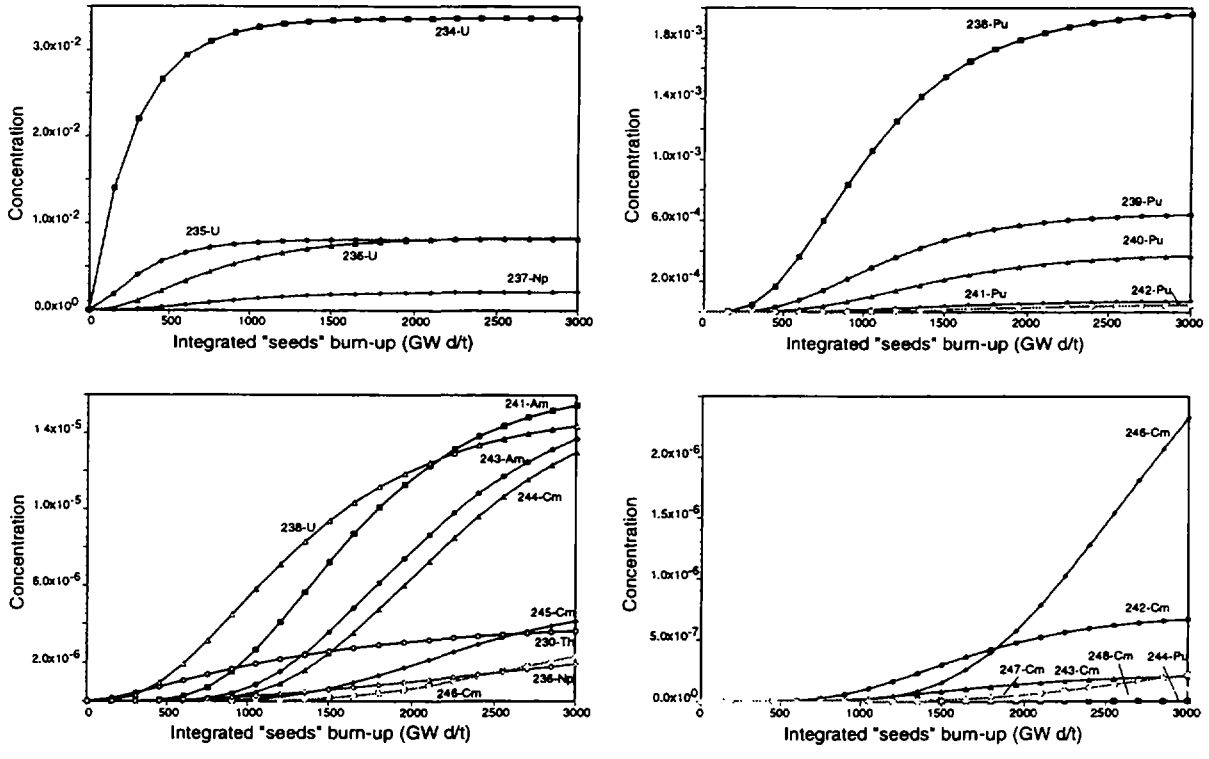

FIG. 2.8b Other actinides stockpile as a function of the discharge number (integrated seeds burn-up).

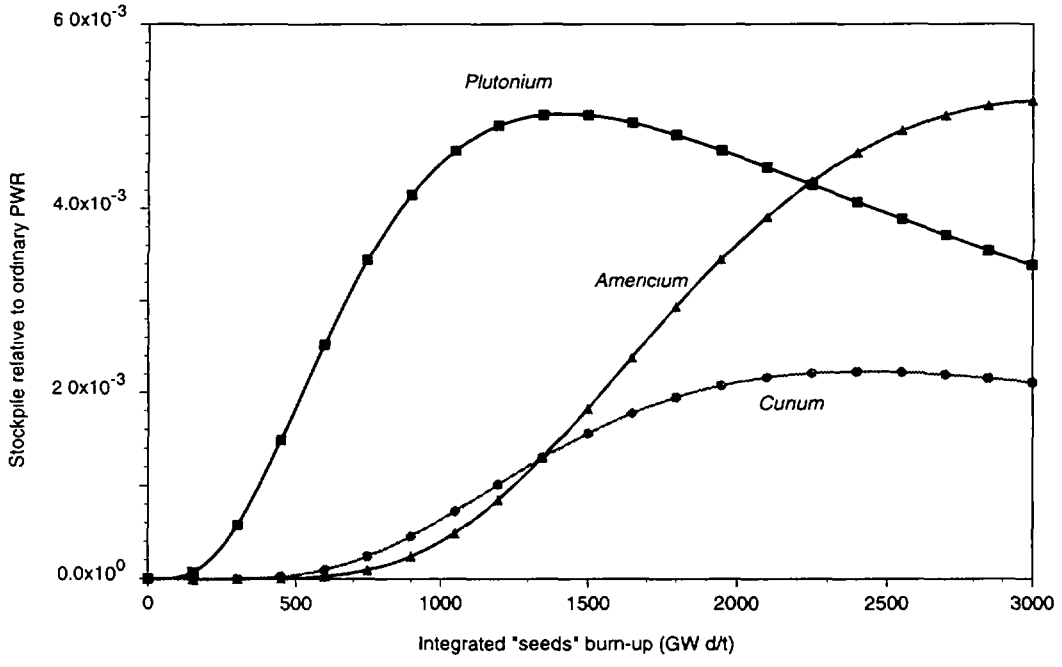

FIG. 2.8c Trans-uranic production/unit energy relative to ordinary PWR as a function of the discharge number (integrated seeds burn-up).

We have compared the evolution of k as a function of burn-up obtained with the simple evolution programme and the "exact" calculations of the Montecarlo programme. As shown in Figure 2.9, the agreement is excellent.

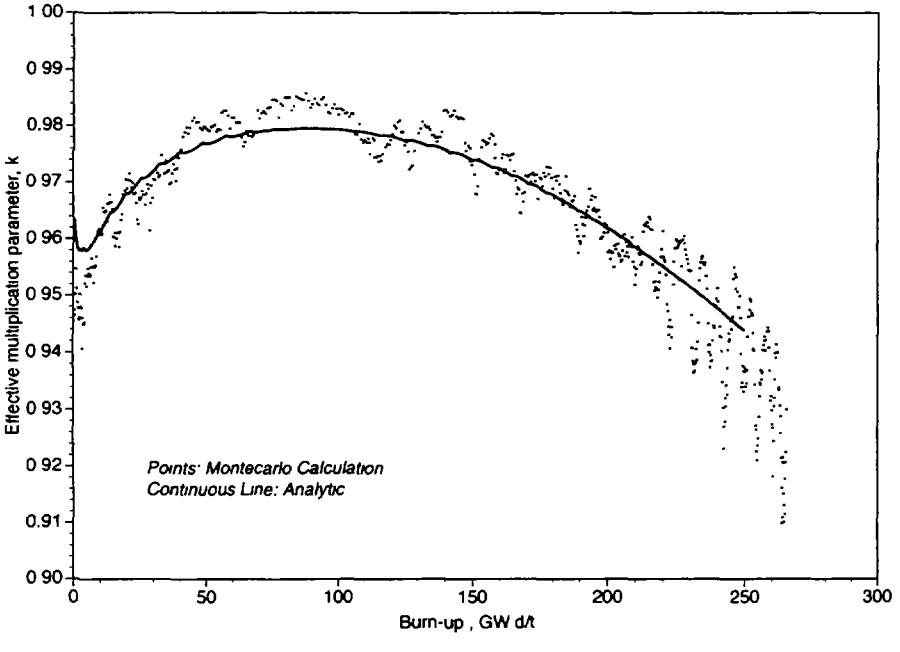

FIG. 2.9 Comparison of k_{eff} calculated analytically and by Montecarlo.

TABLE II.4. RELATIVE CONCENTRATIONS OF ACTINIDES AT THE DISCHARGE AFTER 150 GW d/t OF BURN UP. THE POWER DENSITY WAS ρ = 100 W/g, CORRESPONDING TO A CYCLE OF ABOUT 5 YEARS. CONCENTRATIONS ARE NORMALISED TO THE FUEL MASS WHICH IS MADE OF CORRESPONDING OXIDES.

Element	First discharge	5th discharge	10th discharge	15th discharge	Asymptotic limit
^{230}Th	1.408 E-7	1.378 E-6	2.586 E-6	3.271 E-6	3.642 E-6
^{232}Th	7.637 E-1	7.637 E-1	7.637 E-1	7.637 E-1	7.637 E-1
^{231}Pa	9.246 E-5	1.055 E-4	1.059 E-4	1.061 E-4	1.061 E-4
^{232}U	7.942 E-5	1.298 E-4	1.304 E-4	1.305 E-4	1.306 E-4
^{233}U	8.919 E-2	8.919 E-2	8.919 E-2	8.919 E-2	8.919 E-2
^{234}U	1.403 E-2	3.102 E-2	3.340 E-2	3.365 E-2	3.368 E-2
^{235}U	1.851 E-3	7.242 E-3	8.101 E-3	8.185 E-3	8.196 E-3
^{236}U	2.420 E-4	4.475 E-3	7.428 E-3	8.214 E-3	8.395 E-3
^{238}U	3.239 E-8	3.145 E-6	9.390 E-6	1.296 E-5	1.440 E-5
^{236}Np	2.626 E-10	1.047 E-7	5.787 E-7	1.228 E-6	1.924 E-6
^{237}Np	1.669 E-5	9.127 E-4	1.832 E-3	2.104 E-3	2.168 E-3
^{238}Pu	3.163 E-6	5.975 E-4	1.545 E-3	1.875 E-3	1.958 E-3
^{239}Pu	2.274 E-7	1.422 E-4	4.706 E-4	6.029 E-4	6.374 E-4
^{240}Pu	1.172 E-8	3.709 E-5	2.144 E-4	3.307 E-4	3.703 E-4
^{241}Pu	5.192 E-10	5.084 E-6	3.756 E-5	6.172 E-5	7.034 E-5
^{242}Pu	1.694 E-11	9.800 E-7	1.536 E-5	3.508 E-5	4.572 E-5
^{244}Pu	2.494 E-17	8.631 E-12	3.155 E-10	1.163 E-9	1.999 E-9
^{241}Am	2.924 E-11	7.003 E-7	7.218 E-6	1.316 E-5	1.547 E-5
^{243}Am	5.577 E-13	1.406 E-7	3.575 E-6	9.807 E-6	1.372 E-5
^{243}Cm	1.647 E-14	4.741 E-9	7.930 E-8	1.646 E-7	2.010 E-7
^{244}Cm	4.859 E-14	5.683 E-8	2.479 E-6	8.489 E-6	1.303 E-5
^{245}Cm	2.185 E-15	9.850 E-9	6.417 E-7	2.550 E-6	4.158 E-6
^{246}Cm	3.693 E-17	9.783 E-10	1.519 E-7	1.023 E-6	2.329 E-6
^{247}Cm	3.660 E-19	4.102 E-11	1.038 E-8	8.604 E-8	2.166 E-7
^{248}Cm	5.510 E-21	3.492 E-12	2.011 E-9	2.743 E-8	9.618 E-8

The behaviour of the multiplication coefficient k as a function of the burn-up during successive refills is given in Figure 2.10. One can see that in spite of the significant change of the fuel composition, the value of k remains remarkably constant.

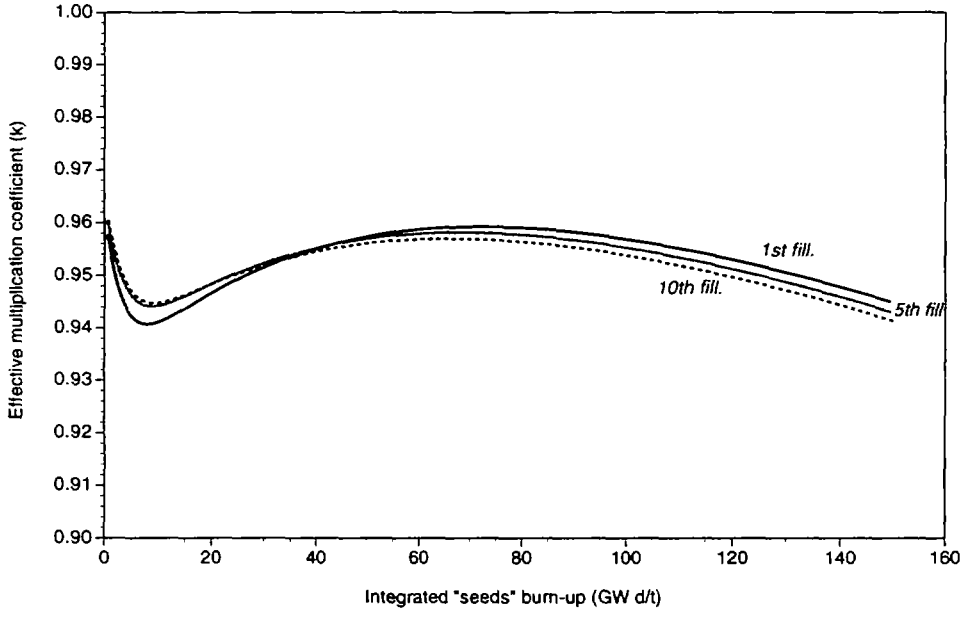

FIG. 2.10 Behaviour of k as a function of the burn-up for different fillings.

We conclude that the fuel can be indefinitely used in an open ended chain of cycles. Indeed the fuel can survive the lifetime of the installation and be re-used as long as there is demand for EAs, with very small or no loss of performance. In contrast with an ordinary reactor the EA produces no "Actinide Waste" to speak of, but only valuable "Seeds" for further use and once the asymptotic concentrations have been reached, there is no significant increase with operation of the radio-toxicity of the Actinide stockpile (see next paragraph).

D.3.2.9. ELEMENTARY, ANALYTIC FORMULATION OF ACTINIDE EVOLUTION

A number of simplifying assumptions permits calculating analytically the essential features of the evolution of the concentration vector $c_{(A,Z)}(\phi)$. We ignore the discontinuity of the refills and assume a constant inflow of the father element and neglect the (n,2n) and other channels which may introduce "loops" in the (A,Z) evolution plane, as already mentioned. We assume that in the presence of the neutron flux ϕ, for all elements there is only one transformation channel (either with neutron capture averaged cross section $\sigma^{(i)}_{capt}$ or radioactive decay with decay rate $\lambda^{(i)}$ whichever is dominant) and a dissipative, fission channel with spectrum averaged cross section $\sigma^{(i)}_{fiss}$. For very high values of A spontaneous fission and other forms of nuclear instability will contribute to such dissipative terms. The rate of transformation in a neutron flux ϕ is $\phi\sigma$ and the total rate $\mu^{(i)}=\phi(\sigma^{(i)}_{capt}+\sigma^{(i)}_{fiss})$ or $\mu^{(i)}=\phi\,\sigma^{(i)}_{fiss}+\lambda^{(i)}$ if the transformation is decay dominated. The survival, chaining coefficient, which represents the probability of continuation to the next step of the evolution chain is defined as $\alpha^{(i)}=\sigma^{(i)}_{capt}/(\sigma^{(i)}_{capt}+\sigma^{(i)}_{fiss})$ or $\alpha^{(i)}=\lambda^{(i)}/(\lambda^{(i)}+\sigma^{(i)}_{fiss}\times\phi)$ respectively. The procedure is schematically shown below:

Chain	$P \rightarrow N_1 \rightarrow$ /	$N_2 \rightarrow$ /	$N_3 \rightarrow$ /	$N_i \rightarrow$ /
Initial amount	$N_1(0)$	0	0	0
Removal rate	$\phi\sigma_{fiss}^{(1)}$	$\phi\sigma_{fiss}^{(2)}$	$\phi\sigma_{fiss}^{(3)}$	$\phi\sigma_{fiss}^{(i)}$
Transfer rate	$\phi\sigma_{capt}^{(1)}, [\lambda^{(1)}]$	$\phi\sigma_{capt}^{(2)}, [\lambda^{(2)}]$	$\phi\sigma_{capt}^{(3)}, [\lambda^{(3)}]$	$\phi\sigma_{capt}^{(i)}, [\lambda^{(i)}]$
Survival coeff. $\alpha^{(i)}$	$\frac{\sigma_{capt}^{(1)}}{\sigma_{capt}^{(1)} + \sigma_{fiss}^{(1)}}$	$\frac{\sigma_{capt}^{(2)}}{\sigma_{capt}^{(2)} + \sigma_{fiss}^{(2)}}$	$\frac{\sigma_{capt}^{(3)}}{\sigma_{capt}^{(3)} + \sigma_{fiss}^{(3)}}$	$\frac{\sigma_{capt}^{(i)}}{\sigma_{capt}^{(i)} + \sigma_{fiss}^{(i)}}$
Total rate $\mu^{(i)}$	$\phi\sigma^{(1)_{fiss}} + \lambda^{(1)}$	$\phi\sigma^{(2)_{fiss}} + \lambda^{(2)}$	$\phi\sigma^{(3)_{fiss}} + \lambda^{(3)}$	$\phi\sigma^{(i)_{fiss}} + \lambda^{(i)}$

Assuming first no refill (P = 0) and an initial number of nuclei $N_1(0)$ the time evolution is given according to the Bateman equation (i >1):

$$N^{(i)}(t) = N^{(0)}(t)\left(\prod_{j=1}^{j=i-1}\alpha^{(j)}\right)\times\left[\left(\prod_{j=1}^{j=i-1}\mu^{(j)}\right)\times\sum_{j=1}^{j=i}\frac{\exp(-\mu^{(j)}t)}{\prod_{k=1,k\neq j}^{k=i}(\mu^{(k)}-\mu^{(j)})}\right]$$

If alternatively, there is refill at the constant rate P per unit time and no initial nuclear sample, i.e. $N_1(0) = 0$, the formula becomes (i > 1)

$$N^{(i)}(t) = P\left(\prod_{j=1}^{j=i-1}\alpha^{(j)}\right)\times\left[\left(\prod_{j=1}^{j=i-1}\mu^{(j)}\right)\times\sum_{j=1}^{j=i}\frac{1-\exp(-\mu^{(j)}t)}{\mu^{(j)}\prod_{k=1,k\neq j}^{k=i}(\mu^{(k)}-\mu^{(j)})}\right]$$

In practice, both refilling and initial nuclei are present and the actual number of nuclei will be simply the sum of the two above terms. Note that for $\rho \approx 100$ W/g, $\phi \approx 5 \times 10^{15}$ cm^{-2} s^{-1} and that the sum of cross sections is of the order of magnitude of $\approx 2 \times 10^{-24}$ cm^2, leading to an evolution time constant $1/\mu^{(i)}$ of the order of ≈ 3 years.

The asymptotic distribution is reached at the limit $t \rightarrow \infty$. At this stage the process is dominated by the refill term P and one can easily calculate the equilibrium amounts:

$$N^{(i)}(t\rightarrow\infty) = P\frac{\left(\prod_{j=1}^{j=i-1}\alpha^{(j)}\right)}{\mu^{(i)}} = N^{(1)}(t\rightarrow\infty)\frac{\mu^{(1)}}{\mu^{(i)}}\left(\prod_{j=1}^{j=i-1}\alpha^{(j)}\right)$$

The time required by $N^{(i)}$ to grow to $N^{(i)}(t\rightarrow\infty)(1-1/e)$ is approximately given by $\Sigma 1/\mu^{(i)}$ where the sum is extended up to i. Since the order of magnitude of the time constant is typically 3 years, equilibrium is reached after ≈ 3 (i-1) years where we have used i-1 to take into account that the step through the ^{233}Pa is fast. The fast decrease of $N^{(i)}(t\rightarrow\infty)$ with the rank in the chain is due to the product of the $\alpha << 1$ terms. To a fast decreasing degree of concentrations, the whole table of elements is eventually involved. As already pointed out, in practice the chain is not open-ended since spontaneous fissions and other instabilities ensure very small α–values toward the end.

D.3.2.10. PRACTICAL CONSIDERATIONS

Strictly speaking, continuing operation of the EA requires merely the recycling of the Uranium isotopes. However at each refill of the fuel, inevitably, individual Actinides are separated during the reprocessing. Furthermore their relative incineration rate is independent of the concentration. Therefore, although their elimination requires permanence in the EA for a long time, it is not mandatory to dilute these extra products in every fuel refill of each EA. They can be accumulated and inserted instead in a dedicated device. Whichever strategy is chosen, the already calculated evolution of the trans-uranic stockpile as a function of the integrated burn up (Figures 2.8a-c) remains valid.

In order to positively destroy such trans-uranic Actinides, the exposure time is long, extending over many refilling steps. Since their relative amount is very small it is possible to concentrate them in a few, dedicated fuel bars, to be inserted somewhere in the bundles of ordinary fuel, which is then made of Uranium and Thorium only. After irradiation, such dedicated bundles do not need further reprocessing, since even if the local Fission Fragment concentration becomes very high, it will not affect the over-all criticality of the device which is not appreciably different than if they were generally distributed. Therefore it may be sufficient at each refill of the main fuel to bleed the gaseous fragments produced and to add a new protecting sleeve or otherwise ensure the continuing mechanical strength of such specialised fuel bars: it will make sense not to reprocess them any more, until all actinides are positively transformed into fission fragments and their incineration completed.

Therefore a practical scenario will consist in (1) reprocessing of the bulk of the spent fuel at each refill, with separation of Thorium and Uranium which are to be used to fabricate the next fuel refill and (2) separation at each reprocessing stage of the trans-uranic Actinides and of Protactinium in a small stockpile which is then introduced in the neutron flux of the EA once and for all and up to its total incineration, with gas bleeding and strengthening of the cladding at each refill.

The amount of elements at the discharge depends critically on the concentration of ^{236}U, which acts as the gateway to ^{237}Np. Therefore we have considered the production of trans-uranic elements after 150 GW d/t, starting from the asymptotic mixture of Uranium in the fuel. Much smaller amounts will be produced during the early fillings, as seen from Figures 2.8a-2.8c. Results are listed in Table II.5. The discharge consists primarily of ^{237}Np (66.0 %), ^{231}Pa (4.24 %), medium lived ^{238}Pu (26.1 %, half-life of 87.7 years) and ^{239}Pu (3.3%) and it is ridiculously small, namely 276 g/t of fuel, or 4.14 kg for a 15 t discharge. The radioactive heat of this discharge is $\approx$ 600 W, primarily due to ^{238}Pu, and quite manageable.

The relative radiotoxicity of such trans-uranic products is also very modest, when normalised to the produced energy. The volume is only a few percent of the production of a PWR for the same energy. As already pointed out, once inserted in an appropriate fuel containment rod, they will not be handled again until fully incinerated. In view of the simplicity of such a procedure, geologic storage of trans-uranic waste from an EA is unnecessary. Clearly the best place to put the unwanted long lived waste is the EA itself, where an incineration lifetime of years is at hand.

D.3.2.11. PROLIFERATION ISSUES

A great concern about Nuclear Power is that military diversions may occur with the spent fuel. The present EA scheme offers much better guarantees against such a potential risk. We assume that the procedure of fuel loading and reprocessing is the one described in the previous section. Critical Masses (CM) and other relevant parameters for bare spheres of pure metal are listed in Table II.6. The addition of a neutron reflector, a few inches thick may be used to reduce the CM by a factor two or so. One can see that three chemical elements of the discharge, namely the asymptotic Uranium Mixture, Neptunium and Plutonium exhibit potential nuclear explosive features. However several other features limit the feasibility of an actual explosive device. We consider them in turn, following the arguments given in Ref. [35]:

1) Decay heat produced by the α-decays of the material in some instances is much larger than the

eight Watts emitted from the approximately three kilograms of weapon grade plutonium which is suggested to be in a modern nuclear warhead. Since the high-explosive (HE) around the fuel would have insulating properties (≈ 0.4 W m °C^{-1}), only 10 cm of HE could result in an equilibrium temperature of about 190 °C for 100 W of heat. Apparently the breakdown rate of many types of HE becomes significant above about 100 °C. Although methods could be envisaged to add heat sinks to the device, we assume that α-heat yield much larger than 1000 W will not be acceptable.

TABLE II.5. TRANS-URANIC AND PROTACTINIUM FROM DISCHARGE FOR ASYMPTOTIC FUEL CONCENTRATION. INTEGRATED BURN UP IS 150 GW d/t

Element		Partial density (g/cm^3)
^{231}Pa		0.9179 E-04
	Total Pa	0.9179 E-04
^{236}Np		0.5469 E-07
^{237}Np		0.1428 E-02
	Total Np	0.1428 E-02
^{238}Pu		0.5640 E-03
^{239}Pu		0.7141 E-04
^{240}Pu		0.6185 E-05
^{241}Pu		0.3924 E-06
^{242}Pu		0.1887 E-07
	Total Pu	0.6420 E-03
^{241}Am		0.2638 E-07
^{243}Am		0.8461 E-09
	Total Am	0.2722 E-07
^{242}Cm		0.4182 E-09
	Total Cm	0.5500 E-09
	Total discharge	2.1618 E-03

TABLE II.6. SOME PROPERTIES OF ACTINIDES FROM EA DISCHARGE HAVING RELEVANCE TO POSSIBLE MILITARY DIVERSIONS OF FUEL.

Element from EA	Uranium Mix	Neptunium	Plutonium
Critical mass (CM), kg	28.0	56.5	10.4
Decay Heat for CM, W	24.3	1.13	4400
Gamma Activity, Ci/CM	790	small	small
Neutron Yield, n g^{-1} s^{-1}	very small	2.1 10^5	2.6 10^3

2) Gamma activity from some of the decay products of the chain are making the handling of the device during construction and deployment very risky and eventually impossible. In particular the hard γ-ray emitted by ^{208}Tl is very hazardous. The corresponding dose rate of 30 kg of Uranium mixture with 10^3 ppm of ^{232}U contamination is asymptotic after 10^3 days [36] and is about 3.6×10^4

mSv/hour which corresponds to a 50% lethal dose after 10 minutes exposure to the bare mass.

3) Spontaneous fissions produce neutrons which could cause the pre-initiation of the chain reaction and thus dramatically reduce the potential yield of the device. Gun-type implosion systems, which are the easiest to realise, are particularly sensitive to pre-ignition. This effect for instance discourages the use of such simple systems in the case of weapon grade Plutonium, which has a yield of 66 n g^{-1} s^{-1}, where high power explosives providing an implosion speed of one order of magnitude larger must be used. We assume therefore that fuels with a neutron yield much larger than 1000 n $g^{-1}s^{-1}$ are not practical, leading to a too small "fizzle yield", namely the smallest possible yield resulting from pre-initiation.

As already mentioned, the total discharge of Neptunium and Plutonium is of the order of 4 ÷ 5 kilograms after a long burn-up (5 years of operation) of a typical EA. Hence in order to accumulate the amount of explosive to reach a single CM the full discharges of many decades of operation, and the result of the reprocessing of hundreds of tons of spent fuel must be used. Note that according to our scenario, this is impossible since the spent fuel is re-injected in the EA right after reprocessing and completely incinerated. Clearly the accumulation of a CM demands suspending such a procedure for decades. In addition it will be a very poor explosive, since as one can see from Table II.6, both cases will have a very small "fizzle yield" which will require HE ignition. This effect is particularly large in the case of Neptunium, since the CM will produce 10^{10} n/s! In the case of Plutonium, this effect is also large, but the ignition method will be heavily hampered by the large heat production of the short-lived (half-life 87.7 a) ^{238}Pu isotope, 4.4 kW for the CM.

Therefore the main concern stems from the possible diversion of the Uranium Mixture, which is abundantly produced. It has been suggested to denature the Uranium adding a significant amount of ^{238}U. In our view such a method is not foolproof since the ^{238}U will quickly produce ample amounts of ^{239}Pu which is a well proven, widely used explosive and which could be extracted maliciously during reprocessing, as is the case of ordinary PWRs. Instead we believe that the very strong γ-radiation from the ^{208}Tl contaminant constitutes a strong deterrent and an excellent way to "denature" the fuel. A new technology in constructing, assembling and handling the weapon must be developed, which we believe is highly self-discouraging, with respect to other ways of achieving such a goal.

D.3.2.12. BURNING OF DIFFERENT FUELS

As one can see from Table II.2 the majority of Actinides have a large cross section for fission. Therefore the required level of sub-criticality can be attained with a very large variety of different fuels. Clearly the choice is application dependent and an almost infinite number of alternatives are possible. In this report we shall limit ourselves to a number of specific cases.

1) Fuel based on ^{238}U, in which the fissile element bred is Plutonium, which might be of interest in view of the huge amount of unused depleted Uranium. The main draw-back of this fuel, when compared with Thorium is the large amount of Plutonium and higher Actinides produced. However they are eventually incinerated and the stockpile remains constant, just as in the case of the previous example based on Thorium.

2) Initial mixture of Thorium and "dirty" Plutonium from the large amount (≥ 1000 t) of the surplus Plutonium stockpile, presently destined to the geologic storage. In this way one can actually "transform" Plutonium into ^{233}U with about 85% efficiency, to be used for instance to start-up other EAs, besides incinerating the unwanted ashes and producing a considerable amount of useful energy.

We shall briefly review the basic properties of the breeding cycle based on ^{238}U, $^{238}U + n \xrightarrow{(n,\gamma)} {}^{239}U \xrightarrow{\beta^-,\ 23\ min} {}^{239}Np \xrightarrow{\beta^-,\ 2.3\ days} {}^{239}Pu$. Such a burning cycle is of interest in view of the huge amount of surplus of depleted Uranium, but it implies a major concern in view of the larger radio-toxicity of the spent fuel and of the possible military diversion of the large amounts of Plutonium.

It has been shown in Ref. [1] that the thermal EA cannot use this fuel, since the asymptotic fuel has a reactivity k_∞ which is smaller than the one of Thorium. With fast neutrons, however, this cycle has "per se" some advantages over the Thorium cycle, namely an even higher reactivity k_∞ which in principle could permit envisaging even a critical device and a shorter half-life (2.12 days) of the intermediate ^{239}Np which considerably reduces the reactivity changes with power, as shown in Table II.7.

Cross sections have been integrated over the neutron spectrum calculated with Montecarlo methods on a realistic model (see paragraph D.3.2.6). The breeding ratio ξ is somewhat larger than the one for Thorium, while the amount of intermediate state ^{239}Np is much smaller, mainly because of its shorter lifetime. The main consequence is that the variation $Max(\Delta k)$ subsequent to an extended shutdown and the breeding loss due to premature captures in ^{239}Np are much smaller. Note that the value of k_∞ at breeding equilibrium is for the binary mixture ^{238}U – ^{239}Pu. As we shall see the Plutonium mixture will rapidly evolve in a mixture of several isotopes, which reduce the value of k_∞ at the asymptotic limit. Notwithstanding, as already

TABLE II.7. NEUTRON FLUX DEPENDENT EFFECTS IN THE F-EA BASE ON ^{238}U CYCLE. THE PARAMETER ρ IS THE POWER DENSITY PRODUCED PER UNIT FUEL MASS AT BREEDING EQUILIBRIUM.

Quantity		Values for ρ = 120 W/g
Neutron Flux cm^{-2} s^{-1}	ϕ	5.967×10^{15}
Breeding ratio, zero flux $N(^{239}Pu)/N(^{238}U)$	ξ	0.190
Rate variation of the breeding ratio, ξ	$\Delta\xi$	-6.00×10^{-4}
Ratio $N(^{239}Np)/N(^{239}Pu)$		3.66×10^{-3}
Fuel intrinsic mult. factor at breeding equil.	k_∞	1.250
Effects of ^{135}Xe, ^{149}Sm, etc.	$Max(\Delta k)$	$< 10^{-4}$
Breeding loss due to premature capt. in ^{239}Np	Δk	-3.816×10^{-3}
Criticality rise after infinite shut-down (^{239}Np)	$Max(\Delta k)$	3.256×10^{-3}

pointed out in the introduction, the large value of k_∞ at first sight would indicate that for instance a traditional Fast Breeder might suffice to exploit the fuel cycle [37][18]. But in the case of an EA the excess criticality could be used to extend the burn up, typically in excess of 200 GW d/t, in presence of fission fragments, starting the EA with a mixture well below the breeding equilibrium. The radiation damage of the fuel sleeves and the gas pressure built up have to be periodically taken into account, for instance by a periodic renewal of the fuel encapsulation and gas bleeding. These procedures are much simpler than a full reprocessing and in principle do not have to be exposed to the full radio-toxicity of the fuel.

Reprocessing and in general the fuel handling strategy implies that several components of the spent fuel are assembled into a renovated fuel, eventually with the external supply of additional fuel (i.e. "dirty" Plutonium) and/or with additional fissile material produced in the breeder section. A simplified, elementary method of estimating the relevant multiplication coefficient can be formulated assuming that the neutron spectrum in the EA is not appreciably affected by the variations in the mixture. This is only approximately valid in the case of strong resonances which may produce "screening", namely local "dips" in the spectrum. Also large variations of fuel concentration will affect the spectrum and hence the performance of the system since the fraction of captures and the lethargy effects in the Lead diffuser will change. Notwithstanding, such a treatment could be very useful to understand at least qualitatively the general evolution during burn-up and refills. The multiplication coefficient k_∞ of a small amount of element mixture of two components exposed to an "external" neutron flux $\phi(E)$ is given by

where $\nu^{(i)}$ is the spectrum averaged neutron multiplicity due to fissions and the multiplication coefficients for the two media are, as obvious

$$k_\infty^{(1)} = \frac{\sum_1^k N_i \sigma_{fiss}^{(i)} \nu^{(i)}}{\sum_1^k N_i(\sigma_{fiss}^{(i)} + \sigma_{capt}^{(i)})} \quad and \quad k_\infty^{(2)} = \frac{\sum_{k+1}^n N_i \sigma_{fiss}^{(i)} \nu^{(i)}}{\sum_{k+1}^n N_i(\sigma_{fiss}^{(i)} + \sigma_{capt}^{(i)})}$$

The weights are given simply by the relative absorption rates (per unit time) in the two media

In order to simplify the algebra we have limited our consideration to the dominant contribution due to fission. The discussion can be easily extended to other processes, like (n,2n) and so on. Generalising, the multiplication coefficient of a mixture of n-elements is simply given by the "stoichiometric" weight of the coefficients of the components. In particular, after n cycles with refills of fuel with no external additions (each after a predetermined flux exposure $\beta = \int \phi \, dt$) the multiplication coefficient can be easily estimated as stoichiometric sum of the same fuel which is subject to a series of successive exposures corresponding to If at each cycle some fresh amount of fuel is added or eventually some component is removed, its contribution must obviously be added or subtracted stoichiometrically.

Linearization of the problem permits using simple "chemistry" considerations which are very useful for instance in defining the strategy of the refills. The definition of the elements of the mixture is of course dependent on the problem one wants to solve. They can be either the refill mixture or even single isotopes. Each of the elements will then independently evolve inside the fuel i.e. N_i will change with time. In our approximation the total number of nuclei ΣN_i will decrease because of fissions. Clearly the gain G is not a linearized quantity and it must be estimated with the help of the parameter k. In order to calculate k, one has to introduce the effect of the losses L as discussed in the previous paragraphs, starting from the value of k_∞.

The total burn up of the fuel is the sum of the burn-ups of the elements, since the power produced is the sum of the power delivered by each of the elements, $\rho = \Sigma\rho^{(i)} = \phi \varepsilon_{fiss} \Sigma N_i \sigma_{fiss}^{(i)}$, where $\varepsilon_{fiss} = 3.2 \times 10^{-11}$ *joules* is the energy produced by each fission.

We have estimated the evolution of some of the primary ingredients of the fuel strategy. Spectra are taken from the exemplificative designs of section D.3.2.3. They should be a good representation of the actual situation, with the above mentioned provision. We have considered sub-fuel elements made of pure ^{232}Th, ^{233}U, ^{235}U, ^{239}Pu and the typical trans-uranic discharge of a PWR after 33 GW d/t of burn-up, in which Np, Pu, Am and Cm isotopes have been included. In Figure 2.11 we have plotted k_∞ as a function of the days of exposure to a flux $\phi = 4.0 \times 10^{15}$ n cm^{-2} s^{-1}. One can distinguish the difference between the fissile elements which have a k_∞ decreasing with the isotopic evolution of the mixture and the breeder elements in which k_∞ starts very small (some fission is present even for pure elements) and grows because of the progressive breeding of fissionable elements.

In order to estimate the value of k_∞ for a mixture of such elements as a function of the burn-up one has to introduce the stoichiometric weights n_i. In Figure 2.12 we plot $r_{abs}^{(i)}$ the relative absorption rates (per unit time) for 1 initial gr/cm^3 of each element, which must then be multiplied by the actual initial concentration of each element d_i to compute n_i. Likewise the power produced for 1 gram of the mixture by the flux ϕ is easily calculated with the help of Figure 2.13, in which ρ_i the power/g of each element is given as a function of the integrated flux. The irradiation dependence and the power/g of the mixture are then

Note that in practice one might prefer to set the more relevant parameter ρ and derive the consequent flux, which is trivially done with the above formula. Finally in Figure 2.14 we give the disappearance rate of nuclei due to fissions as a function of the integrated flux. Note that the burn-up for full disappearance is about 950 GW d/t and therefore the burn-up for a given integrated exposure can be calculated with the appropriate weights directly from the Figure 2.14, rather than integrating ρ. Fission fragment captures must be evaluated in order to calculate k from k_∞. An approximate formula has been derived from the full Monte-

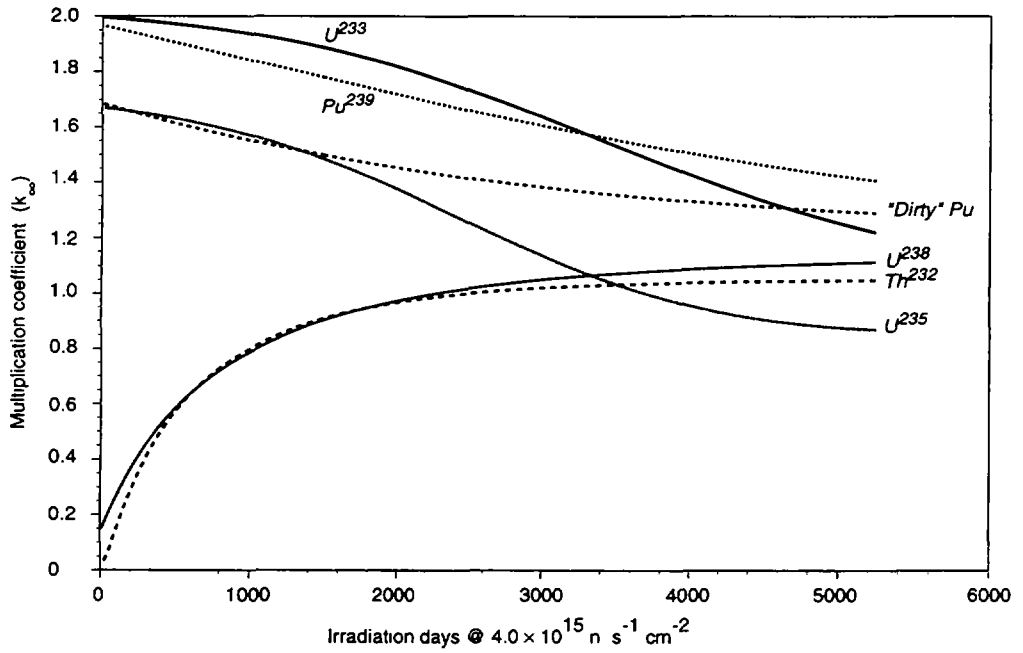

FIG. 2.11 Behaviour of k_∞ as a function of the irradiation time at a constant flux of 4.0×10^{15} n s^{-1} cm^{-2}.

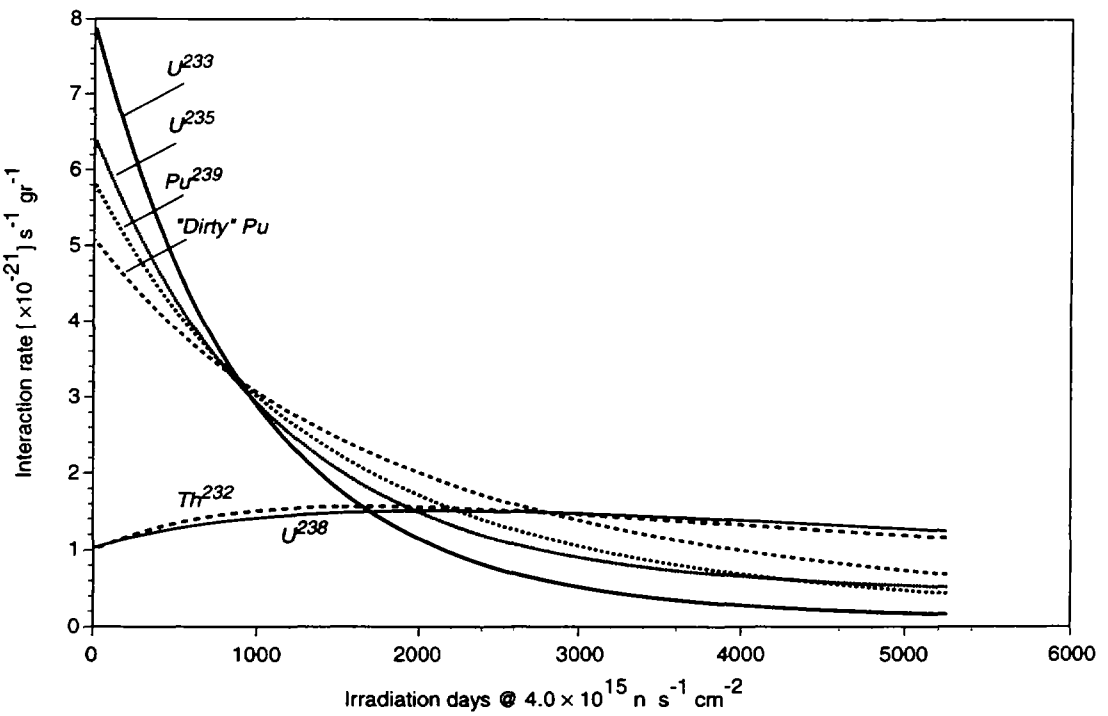

FIG. 2.12 Relative absorption rates for different isotopes as a function of the irradiation time at a constant flux of 4.0×10^{15} n s^{-1} cm^{-2}.

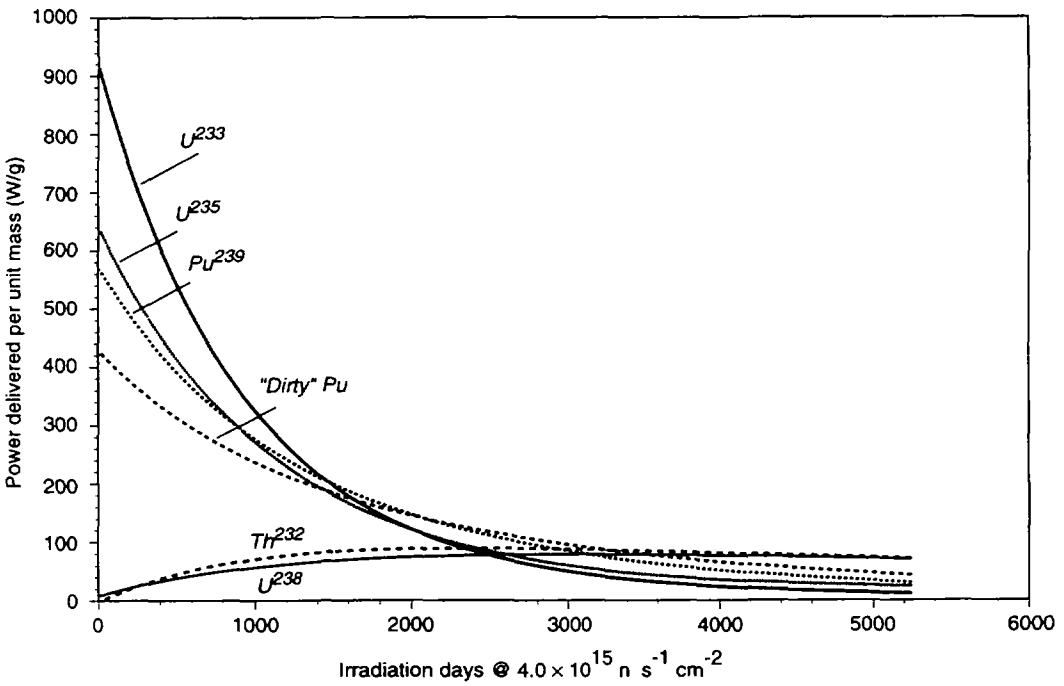

FIG. 2.13 Power delivered per gram of different isotopes as a function of the irradiation time at a constant flux of 4.0×10^{15} *n* s^{-1} cm^{-2}.

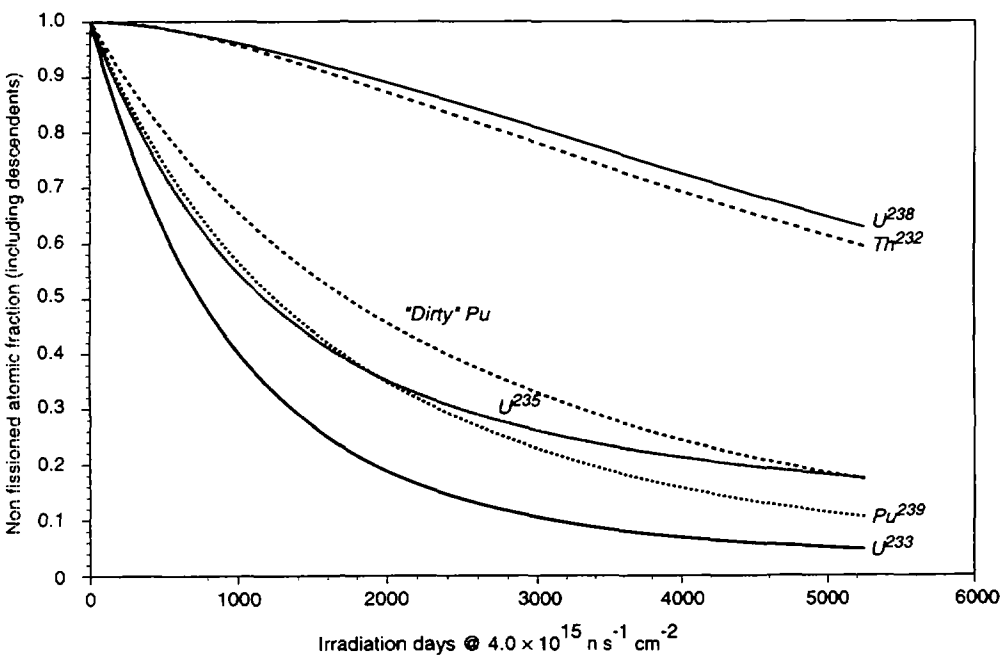

FIG. 2.14 Rate of disappearance of different isotopes as a function of irradiation time at a constant flux of 4.0×10^{15} *n* s^{-1} cm^{-2}.

carlo calculation and gives a linear dependence of the fraction of neutrons vs. burn-up, with $L = 0.065$ for 100 GW d/t.

As one can see from Figure 2.11 to Figure 2.14, the features amongst the various fissionable elementson one hand and of the two main breeding materials on the other are surprisingly similar. This means that a large flexibility exists in substituting a fissionable material for another or in building a convenient mixture of them: a wide spectrum of choices is possible, depending on the availability of fuels and on the application. The same EA can be used (even simultaneously) (1) to produce energy (2) to transform fuels, like for instance Plutonium discharge into ^{233}U and (3) to incinerate unwanted Actinides. In general using mixtures other than $^{232}Th/^{233}U$ would, however, produce fuel discharges with a much greater radio-toxicity.

D.3.2.13. CONCLUSIONS

In order to ensure a practical utilisation of the fuel, the neutron distribution in an EA must be sufficiently uniform. This in turn requires abandoning the classic homogeneous fuel-moderator mixture geometry of an ordinary reactor and instead inserting sparse fuel elements in a strongly diffusive medium. Lead or Bismuth appear to be ideal materials for such purposes, at least for a F-EA. Other media with similar properties, like for instance Graphite or Heavy Water could be used for a T-EA.

The energetic gain of a T-EA, as discussed in Ref. [1] is of the order of $G = 30 \div 50$. In practice this is realised operating the EA at an effective multiplication k in the range $0.92 < k < 0.95$. Fission poisoning limits the burn-up of the T-EA to some 30-50 GW d/t. There are other reasons which suggest operation of the T-EA with relatively small values of k, namely its relatively large variations due to decay mechanisms after shut-down or power variations (^{233}Pa and ^{135}Xe) so as to leave enough margin from risk of criticality.

The same type of considerations would however suggest a much greater gain for a F–EA [2], for which an operating point in the vicinity of $k = 0.98$ is an optimal operating point, corresponding to an energetic gain in the interval $G = 100 \div 150$. A first reason for this choice stems from the much larger value of $\overline{\varepsilon\eta} \approx 2.5$, which implies $k_\infty \geq 1.20$ and $\Delta L = 8.6\ 10^{-3}$ for $k = 0.980$. On the other hand the fission poisoning is much smaller and linearly growing with the burn-up, amounting to about $\Delta L = 0.05$ after 100 GW d/t. The flux dependent ^{135}Xe effect is absent and the time dependent k variation due to ^{233}Pa decays is much smaller for a given power density. All these considerations suggest $k \approx 0.98$ as quite appropriate for a F-EA.

The multiplication factor k_∞ is such as to permit to reach such a k value with a ^{233}U concentration below the breeding equilibrium, thus permitting to compensate the growth due to fission fragment captures during operation with the increase of k_∞. In this way, very long burn-ups are possible without intervention and in exceptionally stable conditions.

At the end of each of these very long cycles, reprocessing is necessary in order to remove Fission Fragments and replace the burnt fuel mass with fresh Thorium. Uranium isotopes are chemically recovered and reused as seeds for the next fuel load. The rest of the trans-uranic Actinides are of modest amount (few kilograms) and they should be stored indefinitely in the EA where they are progressively incinerated. Thus, Geological Storage of Actinides is unnecessary.

Although the optimal performance of the EA is ensured with the Thorium cycle, a variable amount of other isotopes could be used instead, with very little or no change in performance. For instance depleted Uranium (^{238}U) of which vast amount of surplus exists, could be used to replace ^{232}Th. The fissionable ^{233}U could be replaced in part or totally with ^{235}U, ^{239}Pu or even the trans-uranic discharge mix of a PWR. Burning such unwanted "ashes" of the present PWR power plants is not only providing a very large amount of extra energy from an otherwise useless waste destined to geologic storage, but also helps to eliminate permanently materials that nobody wants.

D.3.3. THE ACCELERATOR COMPLEX

D.3.3.1. A THREE-STAGE CYCLOTRON FACILITY

The accelerator has to provide a proton beam of 10 ÷ 15 mA, one order of magnitude lower than the one of most of the accelerator-driven incineration projects based on continuous-wave (c-w) LINAC [9]. The relatively modest requirement of the present application, primarily related to the high gain of the F-EA, allows alternative and much simpler solutions based on circular machines producing a continuous beam, such as ring cyclotrons [38] [39] which have a lower cost and a much smaller size.

Taking into account the recent development of high-intensity cyclotrons and the outstanding results obtained at PSI [8], we have chosen a scheme based on a three-stage cyclotron accelerator (Figure 3.1), namely in succession: (1) the injector, made of two 10 MeV, Compact Isochronous Cyclotrons (CIC). Beams are merged with the help of negative ion stripping; (2) the intermediate stage, a cyclotron with four separated sectors (ISSC) bringing the beam up to 120 MeV; (3) the final booster with ten separated sectors and six cavities (BSSC), raising the kinetic energy up to about 1 GeV.

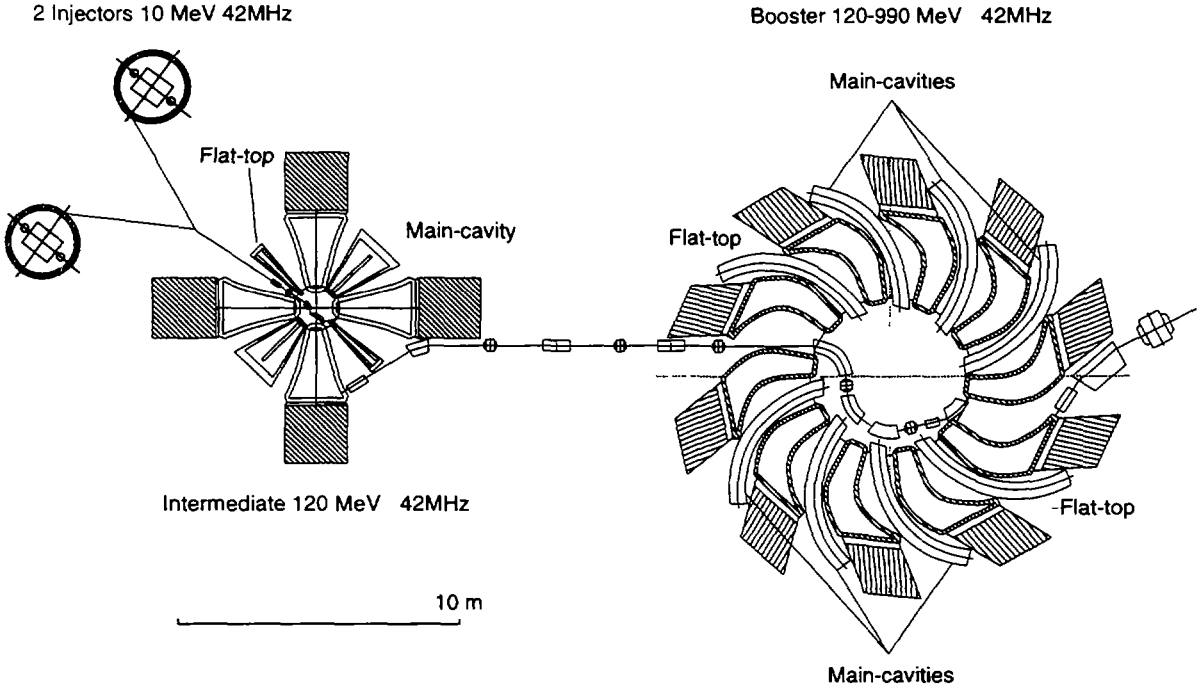

Fig. 3.1 General lay-out of the accelerator complex.

The main novelty of our design, besides the about tenfold increase of the accelerated current, well within the expectations of the present knowledge of space charge effects and beam instabilities, is the increased power efficiency. This extrapolation can be made with confidence and relies primarily on the performance of the RF cavities, which is confirmed by specific model studies that we have made. In particular we believe that the increased beam loading can be adequately handled. This conclusion has been confirmed by a similar study of the PSI Group [8].

The main parameters of the two separated sector cyclotrons are given in Table III.1. An essential aspect of the accelerator complex is the overall efficiency which depends mainly on the RF performances. Power

estimates have been made assuming a 70 % yield of the RF power amplifiers and taking into account measurements on cavity models for the RF losses. Further optimisations of the cavity shape which are in progress show that a global efficiency slightly greater than 40 % is within the reach.

TABLE III.1. MAIN PARAMETERS OF THE TWO RING CYCLOTRONS

Accelerator	ISSC	BSSC
External diameter	10.5 m	16 m
Magnet iron weight	1000 tons	3170 tons
Magnet power	0.6 MW	2.7 MW
RF power	1.54 MW	12.5 MW

An important aspect of the Accelerator complex when used in conjunction with the EA is the high level of reliability required. Based on previous experience with similar machines and possible improvements within reach we believe that the unscheduled down-time of the accelerator can be kept to the level of 3÷5 %.

D.3.3.2. OVERALL DESIGN CONSIDERATIONS

Acceleration of intense beams requires a very efficient extraction. To this effect, the main parameters of the accelerators should follow several design criteria:

1) Injection energy should be high enough in order to reduce the longitudinal space charge effects especially during the first turns after injection in the intermediate stage.
2) Separated sectors magnets with small gap (5 cm) to obtain good vertical focusing and to provide plenty of free space between sectors for accelerating structures, injection and extraction devices. A high energy gain per turn is important in order to reduce the number of turns to reach the extraction radius. The number of sectors is mainly determined by engineering considerations (number of RF cavities as well as extraction channel problems).
3) Flat-topping RF cavities: in order to decrease the energy spread flat-topping accelerating cavities are added, namely, two additional RF resonators working on a harmonic of the main RF cavity frequency in order to obtain an "as flat as possible" accelerating voltage wave form. These cavities operate on a third (or fifth) harmonic mode with a peak voltage between 12 and 14% (or 4 and 5%) of the main RF cavities.
4) Single turn extraction: in order to get a high extraction efficiency, it is necessary to achieve a large radial separation of the last turns. In turn this requires choosing a large extraction radius, i.e. a low average field and a high energy gain per turn. The effective turn separation depends somewhat also on the phase width of the beam; for 20 ° (30 °) it is 12.9 mm (12.4 mm) in the intermediate (ISSC) cyclotron and 9.0 mm (8.4 mm) for the final booster (BSSC).
5) Matching the three stages: in order to avoid any beam loss, matching conditions must be satisfied between the different stages. To simplify the overall design of the RF system, a good choice is to operate all three machines at the same frequency, i.e. 42 MHz in the proposed design, and to accelerate protons on the same harmonic number at least in the ISSC and BSSC, since at the same time the magnetic fields can be kept sufficiently far away from saturation.

The main parameters of the Accelerator complex for the RF option at 42 MHz are given in Table III.2. Equilibrium orbits and related properties have been calculated numerically using realistic magnetic field

maps.

D.3.3.3. THE INJECTOR CYCLOTRON

It consists of a four sector isochronous cyclotron capable of delivering 5 mA in the acceptable phase width of the intermediate stage. The beams of two such injectors working at the same frequency are then merged before injecting them into the intermediate stage (ISSC) and the final booster. Commercial compact cyclotrons accelerating negatively-charged H^- ions [40] operate routinely with an internal ion source (i.e. an injection at low energy, about 30 KeV) at about 2 mA intensities. In our case a higher current is required

TABLE III.2. MAIN PARAMETERS FOR THE 42 MHz DESIGN

Accelerator type	*Injector*	*Intermediate*	*Booster*
Injection	100 keV	10 MeV	120 MeV
Extraction	10 MeV	120 MeV	990 MeV
Frequency	42 MHz	42 MHz	42 MHz
Harmonic	4	6	6
Magnet gap	6 cm	5 cm	5 cm
Nb. sectors	4	4	10
Sector angle (inj/ext)	15 /34 deg	26/31 deg	10/20 deg
Sector spiral extraction	0 deg	0 deg	12 deg
Nb. cavities	2	2	6
Type of cavity	delta	delta	single gap
Gap Peak Voltage injec.	110 kVolt	170 kVolt	550 kVolt
Gap Peak Voltage extrac.	110 kVolt	340 kVolt	1100 kVolt
Radial gain per turn ext.	16 mm	12 mm	10 mm

and therefore the injection energy must be increased to about 100 keV in order to avoid space charge limitations in the source-puller gap. Taking into account the possibility to inject large currents from an external source at high voltage [41], we have chosen an axial injection system at about 100 kV for various reasons:

1) A high extraction voltage for the source.
2) A multicusp ion source for the production of negatively charged ions. This source is cumbersome and therefore it could not be installed in the central region of the cyclotron.
3) A high brightness beam accelerated by the cyclotron requires a careful 6D matching (the two transversal and the longitudinal phase space); in particular, it is necessary to use a buncher in a way to avoid too strong effects of the space charge.
4) Increasing the reliability of the cyclotron: the absence of an internal source assures a better vacuum in the cyclotron, which allows higher RF peak voltages.

5) Refined 3-D computations of the magnetic field have been carried out, in particular in the injection and extraction regions. As opposed to the intermediate and booster cyclotrons, a closed magnet configuration with a return yoke is used in order to make the cyclotron more compact.

6) The RF system consists of two accelerating and two flat-topping cavities. The fourth harmonic of the particle frequency has been chosen to make the cyclotron rather compact. In order not to worsen space-charge effects by phase compression, a constant voltage distribution along the cavity gaps is desired.

Table III.3 summarises the main parameters of the injector cyclotrons. A general view of the injector cyclotron is visible in Figure 3.2. Bunches of the two 5 mA beams produced by each of the two injectors are merged in order to obtain a single 10 mA beam to be injected in the ISSC. Both injectors operate with negative ions (H^-). A H^+ beam extracted by stripping H^- ions and an H^- beam, extracted by a conventional channel, are synchronised so that bunches are superposed (in phase space) in a straight portion of the ISSC injection line. A stripper is installed at the end of the injection line, before the beam enters the ISSC magnetic field to convert the H^- beam into a H^+ beam. As a result the particle density in the phase space injected in the ISSC is about doubled, leading to an injected current of 10 mA at no increase of the single beam emittance. The method can be easily extrapolated to the merging of currents of even a larger number of injector cyclotrons.

TABLE III.3. MAIN PARAMETERS OF THE INJECTOR CYCLOTRONS

Injection energy	100 keV
Extraction energy	10 MeV
Number of sectors	4
Pole radius	0.75 m
Total yoke height	1.2 m
Maximal field in the sectors	1.5 T
Number of main RF cavities	2
RF frequency	42 MHz
Harmonic number	4
Peak Voltage	113 kV
Losses per cavity	17 kW
Number of flat-top cavities	2
RF frequency of flat-top cavities	126 MHz
Peak Voltage of flat-top cavities	13 kV
Axial Deflector field	15 kV/cm

D.3.3.4. THE INTERMEDIATE SEPARATED-SECTOR CYCLOTRON (ISSC)

The general view of the ISSC is given in Figure 3.3. A four-separated-sector cyclotron has been chosen as the intermediate stage because of the following reasons :

1) the acceleration to a sufficiently-high injection energy for the booster can be achieved in about 100 turns due to the possibility to install, between the sectors, cavities providing a high accelerating voltage without prohibitive losses.

2) the flat-topping of the RF voltage is easy to achieve.

3) the strong magnetic focusing provided by the four identical C-shaped sector magnets with a constant small magnetic gap (5 cm).

4) the possibility to install an efficient extraction channel in the field-free valleys.

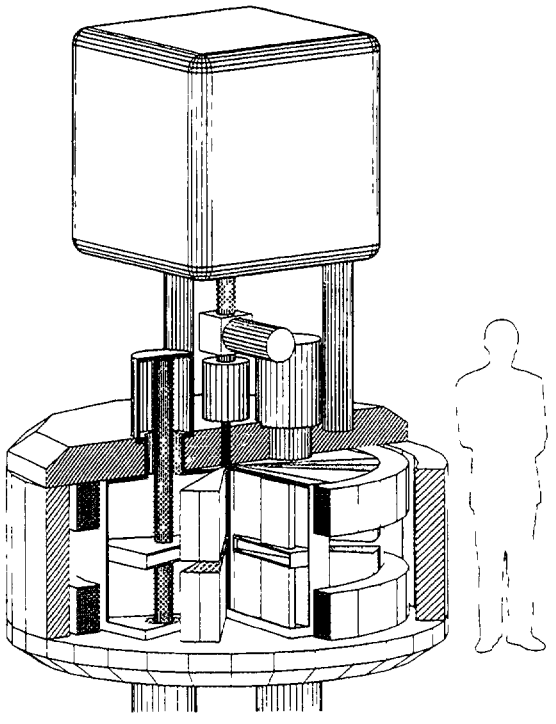

FIG. 3.2 General view of the injector.

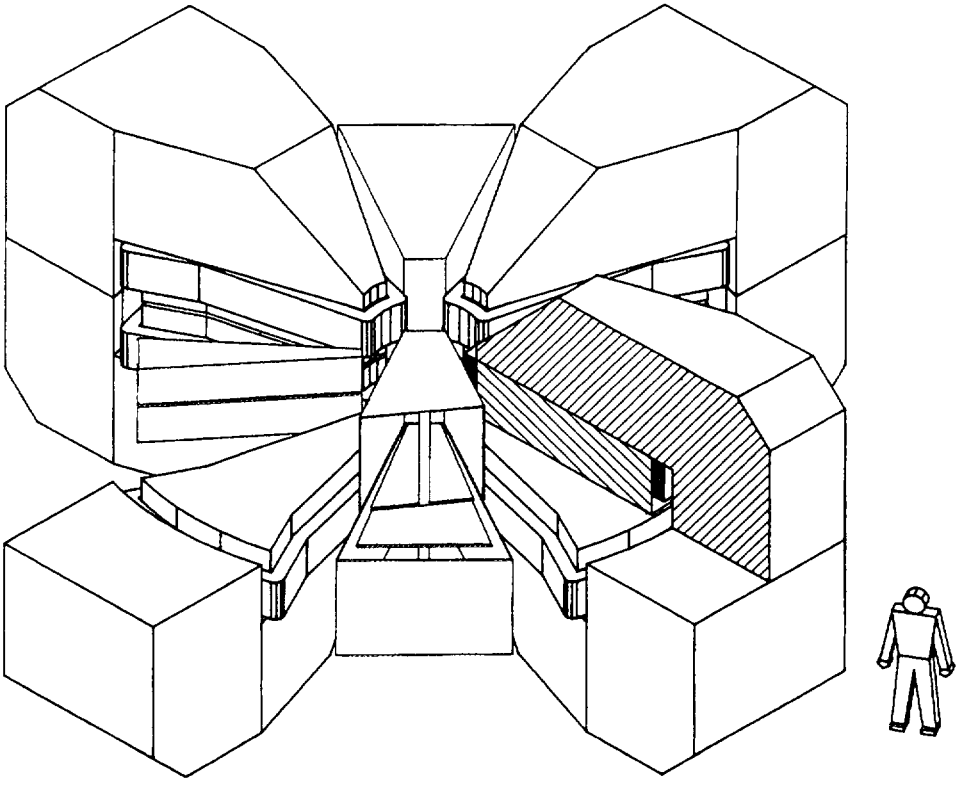

FIG. 3.3 General view of the ISSC.

The choice of the injection energy into the ISSC is certainly one of the most important parameters which influences the overall performances of the cyclotron complex. The space charge effects are strong at low energy. They are present in both transversal and longitudinal directions of the beam. Figure 3.4 shows the simulation of the evolution of the accelerated beam in the radial-longitudinal plane during the first 16 turns under the following conditions: intensity 20 mA, injection energy 10 MeV, energy spread 0.05 MeV, normalised emittances π mm.mrad in both radial and vertical directions. Flat-topping with a third harmonic voltage and a shift in phase (-10 RF deg.) with respect to the accelerating voltage have been used in order to compensate the linear effects of the space charge and increase the longitudinal acceptance ($\pm$ 15 RF deg.) of the bunch. It has been observed that the beam shape in the r-ϕ plane seems to stabilize after a certain number of turns (cf. Figure 3.4). The beam radial spread is about $\pm$ 15 mm in the extraction region. The result of these simulations is that a nominal 10 mA beam can be handled at an injection energy of the order of 10 MeV.

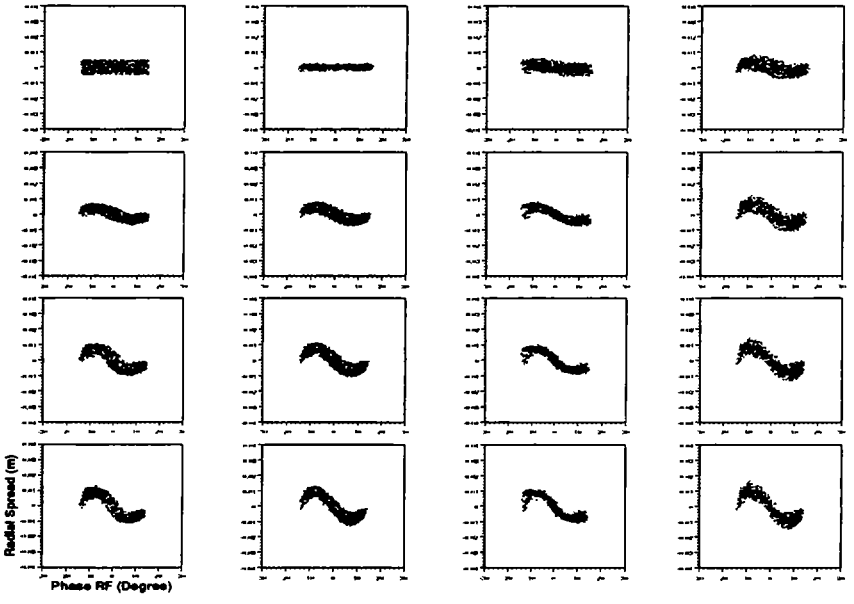

FIG. 3.4 Beam evolution in the r-ϕ plane for the first 16 turns.

Acceleration of the beam is provided by two main resonators located in opposite valleys giving an energy gain per turn of 0.6 MeV at injection and 1.2 MeV at extraction, increasing the beam energy from 10 MeV to 120 MeV. The RF frequency of the accelerating (main) cavities has been chosen equal to 42 MHz, which corresponds to the sixth harmonic of the particle revolution frequency in the cyclotron. Due to the large (30 RF deg.) beam phase width, flat-topping cavities would operate on the third harmonic of the main cavities i.e. on the eighteenth harmonic of the revolution frequency.

Double-gap cavities have been selected (as opposed to single-gap) because their radial extension is much smaller, thus leaving more space in the centre of the machine for the bending and injection magnets and the beam diagnostics. A voltage (or phase compression) ratio of 2.0 is used between injection and extraction. In order to reduce the number of turns in the cyclotron and to have sufficient turn separation, accelerating voltages of 170 kV and 340 kV are required at injection and extraction. The main characteristics of the RF cavities are given in Table III.4.

The shape of the cavities has been defined with the help of the 3D electromagnetic code MAFIA [42]. Models of the main and flat-top cavities have been respectively built at 1:3 and 1:1 scales in order to check

the computations with MAFIA. These models are of the low-power type and are mainly made of wood and copper. Photographs of the accelerating and flat-topping cavity model during assembling and measurements are shown in Figure 3.5.

For a current of 10 mA, the power to be delivered to each main cavity of the ring cyclotron is estimated to be about 770 kW (550 kW beam power and 220 kW cavity loss), which correspond to about 1.1 MW electrical power load (assuming a 70% DC to RF conversion efficiency). The beam power to be absorbed by each cavity is 65 kW, which is about seven times the power dissipated in the walls (9 kW).

The injection channel of the ISSC cyclotron brings the beam from outside the cyclotron to the first RF cavity gap where it is accelerated. It starts after the stripper which is located at the end of the beam line that transports the combined H^+/H^- beam from the injectors. The stripped H^+ beam is injected in the cyclotron through a valley along a flat-top RF cavity as shown in Figure 3.6. When it reaches a radius lower than the injection radius it is deflected in a first bending magnet BMI1 in the clockwise direction (seen

TABLE III.4. MAIN CHARACTERISTICS OF THE ISSC CYCLOTRON RF CAVITIES

	Main cavities	Flat-top cavities
Number of cavities	2	2
Type of cavity	λ/2, double-gap, tapered walls	λ/2, double-gap, tapered walls
Frequency	42.0 MHz	126.0 MHz (h=3)
Cavity height	2.6 m	1.0 m
Cavity length	2.6 m	2.45m
Voltage at injection	2×170 kV	2×20 kV
Voltage at extraction	2×340 kV	2×40 kV
Quality factor	13000	11000
Losses/cavity	220 kW	9 kW
Beam power/cavity	550 kW	65 kW
Total power/cavity	770 kW	56 kW
Total electric power/cavity (70% efficiency)	1.1 MW	13 kW

from above). It is then deflected counter-clockwise, first by a second bending magnet BMI2 and by a electromagnetic channel EMDI located in one of the cyclotron sector gap so that it reaches the first RF cavity gap where beam acceleration starts. Injecting at 10 MeV allows to take benefit of enough room to locate the deflecting magnets and use a simple set of deflecting elements with moderate magnetic field requirements. The main parameters of the injection channel are given in Table III.5. The location of the injection and extraction channel elements of the ISSC are given in Figure 3.6.

TABLE III.5. ISSC INJECTION CHANNEL CHARACTERISTICS

Element	Length (m)	Magnetic field DB (T)
BMI1	0.4	0.4
BMI2	0.6	1.0
EMDI	0.8	0.25

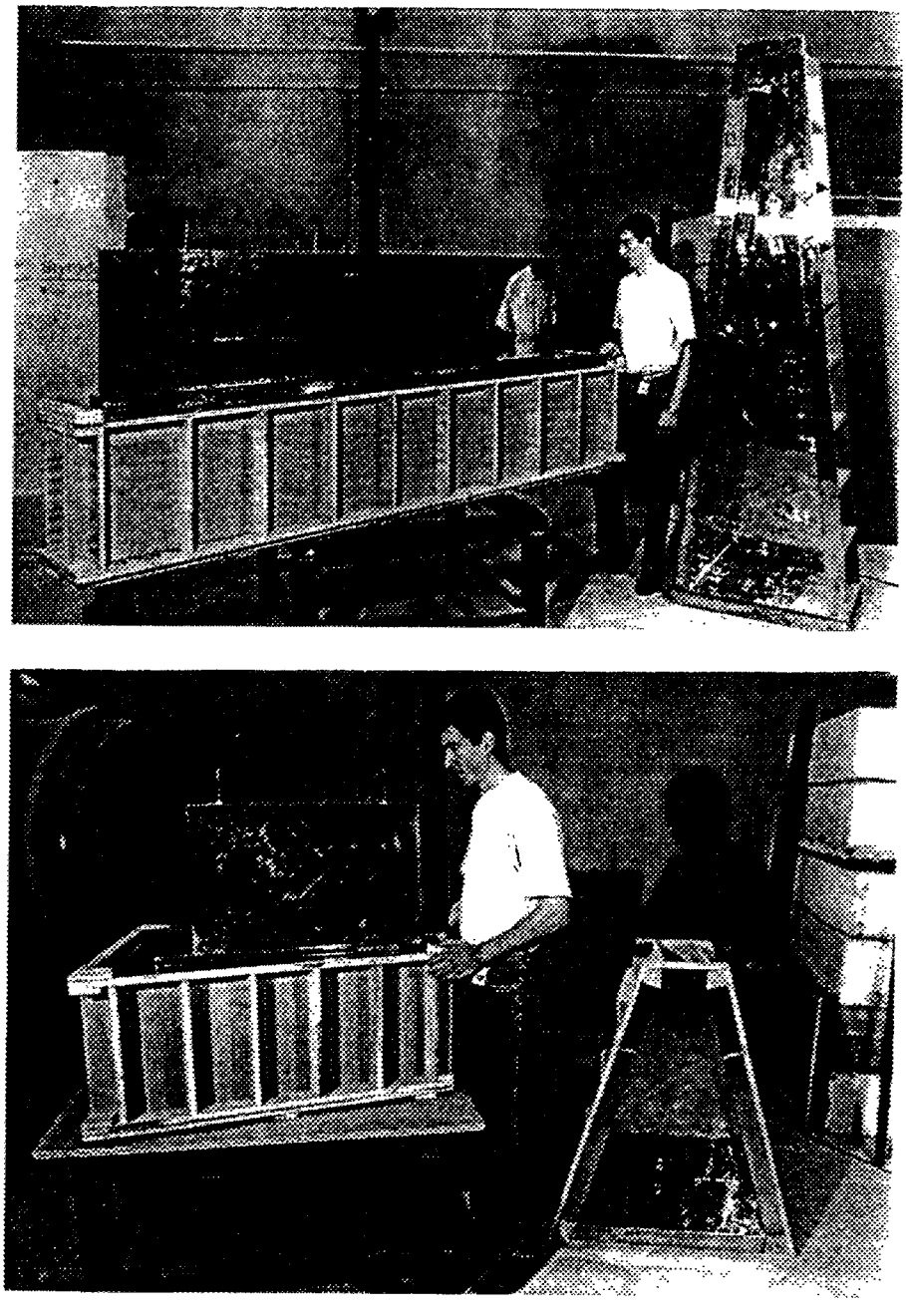

FIG. 3.5 Photographs of the cavity models (top: main cavity during assembling, bottom: flat-topping cavity during assembling.

The extraction channel allows deflecting the accelerated beam outside the cyclotron. In order to achieve an extraction efficiency of nearly 100% so as to reduce induced radioactivity, the extracted orbit at the channel entrance should be fully separated from the last internal orbit. It consists of an electrostatic deflector (ESDE), an electromagnetic deflector (EMDE) and a bending magnet (BME). The three channel components are located in two successive valleys. After the beam is kicked outwards from the last internal orbit, by the electrostatic deflector located at the exit of a main RF-cavity it passes through the magnet sector. It is then further deflected to the entrance of the next valley by the electromagnetic deflector. The last section is a conventional bending magnet which is located in the valley behind the RF flat topping cavity as shown on Figure 3.6. Table III.6 gives the main parameters of the extraction channel.

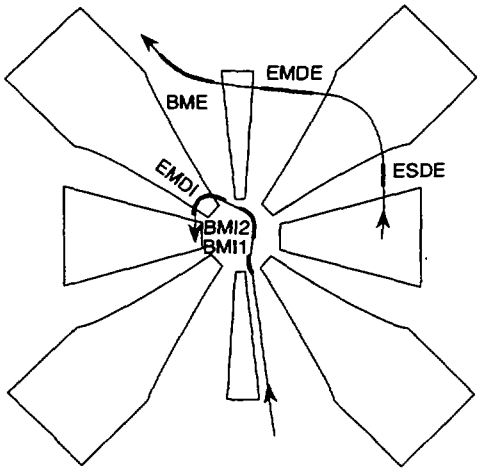

FIG. 3.6 Location of the injection and extraction channel elements of the ISSC.

TABLE III.6. ISSC CHARACTERISTICS OF THE EXTRACTION CHANNEL ELEMENTS

Element	Length (m)	Electric field (kV/cm)	Magnetic field DB (T)
ESDE	0.4	80	0
EMDE	0.9	0	0.25
BME	1.2	0	1.0

D.3.3.5. THE SEPARATED-SECTOR BOOSTER CYCLOTRON (BSSC)

A general view of the booster can be seen in Figure 3.7. The magnet of the final booster consists of 10 identical C-shaped sector magnets with a strong spiral needed in order to obtain sufficient vertical focusing at high energies. Each sector is made of a pair of spiral pole tips whose angular aperture is increasing with the radius. The width of the sector at low energies fixes the magnetic field level Bs needed in the magnet for isochronism and the value of the vertical focusing frequency ν_z. The sector width should not be too large so that devices like the RF cavities and the extraction channel elements can be installed in the valleys. All these considerations have led us to select a 10 degree sector angle width at low radii. The corresponding values of the vertical focusing frequency and sector field are respectively 1.2 T (without space-charge) and 1.8 T. As in the ISSC cyclotron design, no trimming coils are used for generating the radial magnetic field increase required by isochronism. This effect is obtained by increasing the sector width with radius. The characteristics of the magnet are presented in Table III.7.

Acceleration of the beam is provided by 6 main resonators located in the valleys. They should provide an energy gain per turn of 3.0 MeV at injection and 6.0 MeV at extraction, increasing the beam energy from 120 MeV to 990 MeV. In order to compensate the effects of the space charge forces, two flat-topping cavities are needed. The RF frequency of the accelerating (main) cavities has been fixed equal to 42 MHz, which corresponds to the sixth harmonic of the particle revolution frequency in the cyclotron. Since the

beam phase width can be reduced to 15 degrees at the intermediate cyclotron exit, fifth harmonic operation has been selected for the flat-top cavities. This enables to decrease the flat-top cavity power compared to operation on the third harmonic. Single-gap cavities are the most suitable candidates because azimuthal space is restricted and they have high quality factors. This type would be used for both accelerating and flat-topping cavities. A voltage (or phase compression) ratio of 2.0 is used between injection and extraction in order to reduce the number of turns in the cyclotron and to have sufficient turn separation at extraction. The main characteristics of the accelerating cavities are given in Table III.8. Measurements on the accelerating cavity model (1:3 scale) which can be seen on Figure 3.8 where the upper part has been removed, have been carried out in order to check and determine precisely the cavity characteristics. A very good agreement has been found between theoretical calculations and experimental results.

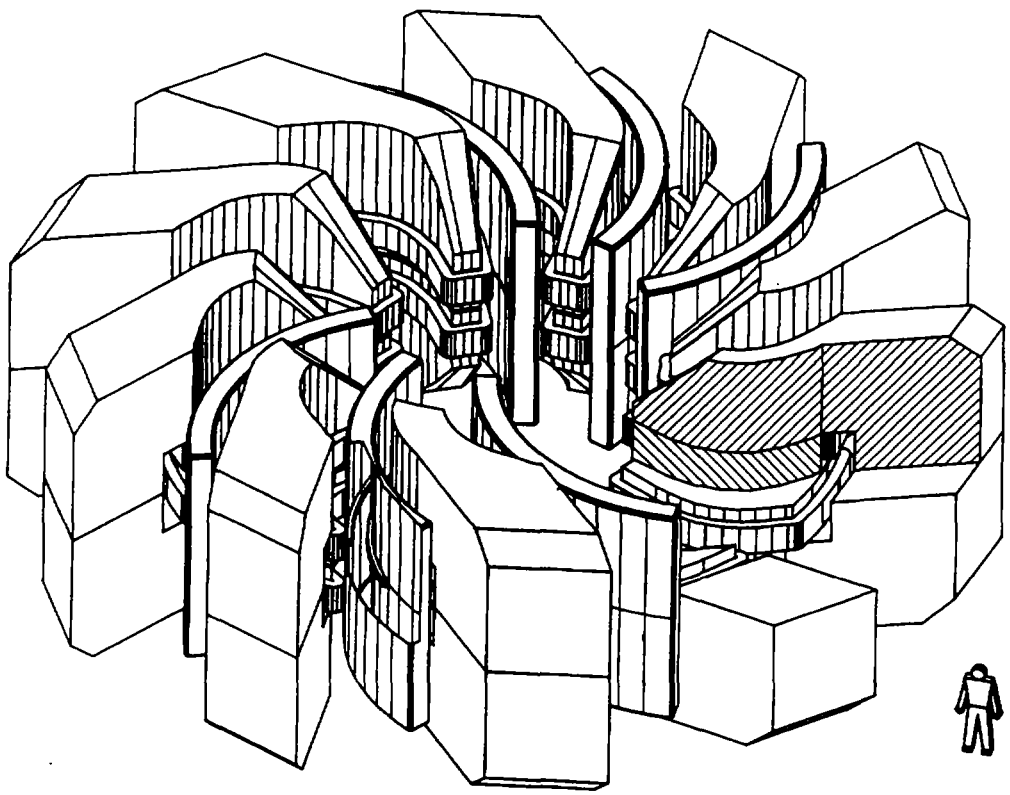

FIG. 3.7 General view of the booster ring cyclotron.

TABLE III.7. MAIN CHARACTERISTICS OF THE BOOSTER MAGNETS

Number of sectors	10
Angular aperture at injection	10 deg
Angular aperture at extraction	20 deg
Spiral angle at extraction	12.0 deg
Magnetic gap in the sector	50 mm
Overall external diameter	15.8 m
Total iron weight	3170 tons
Maximum field in the sector	1.8 T
Total electric power	2.7 MW

The power to be delivered to each main cavity of the ring cyclotron is estimated to be about 2.05 MW (1.45 MW beam power and 0.60 MW cavity loss), which corresponds to about 2.9 MW electrical power (assuming a 70% DC to RF conversion efficiency). The beam power to be absorbed by each flat-top cavity is 220 kW, which is about 20 times the power dissipated in the walls (10 kW). Operating on the fifth harmonic allows to reduce the power absorption in flat-top cavities by a factor slightly larger than 2. All the figures above are given for a current of 10 mA.

The injection channel of the BSSC cyclotron is the system that allows to bring the beam from outside the cyclotron to the first RF cavity gap where it is accelerated. Its layout can be seen in Figure 3.9, where both injection and extraction channel components are visible. The main parameters of the injection channel are given in Table III.9. The main parameters of the extraction channel are given in Table III.10.

TABLE III.8. MAIN CHARACTERISTICS OF THE BOOSTER CYCLOTRON ACCELERATING CAVITIES

Frequency (MHz)	42.0
Number of cavities	6
Type of cavity	$\lambda/2$, double-gap, curved walls
Voltage at injection	550 kV
Voltage at extraction	1100 kV
Quality factor	31000
Losses (estimated)	600 kW

TABLE III.9. BSSC INJECTION CHANNEL CHARACTERISTICS

Element	Length (m)	Field drop DB (T)
BMI1	0.90	1.70
BMI2	0.50	1.30
BMI3	0.50	1.70
BMI4	0.50	1.70
BMI5	0.50	1.30
EMDI	0.90	0.25

TABLE III.10. BSSC EXTRACTION CHANNEL CHARACTERISTICS

Element	Length (m)	B-Field drop (T)	E-Field (kV/cm)
ESDE	0.80	-	55
EMDE	0.30	0.16 T	-
BME	1.30	1.0 T	-

D.3.3.6. BEAM TRANSPORT TO THE EA

The beam extracted from the cyclotron complex has a typical transverse invariant emittance of $\varepsilon_{inv} = 2\ \pi\ 10^{-6}$ rad m (the true emittance is $\varepsilon = \varepsilon_{inv} / \beta\gamma$ where $\beta\gamma$ is the usual relativistic factor), and a momentum spread of the order of a few 10^{-4}. The current density is roughly uniform in the transverse phase-space, leading to an approximately parabolic current density in a focal point. It is not difficult to transport such

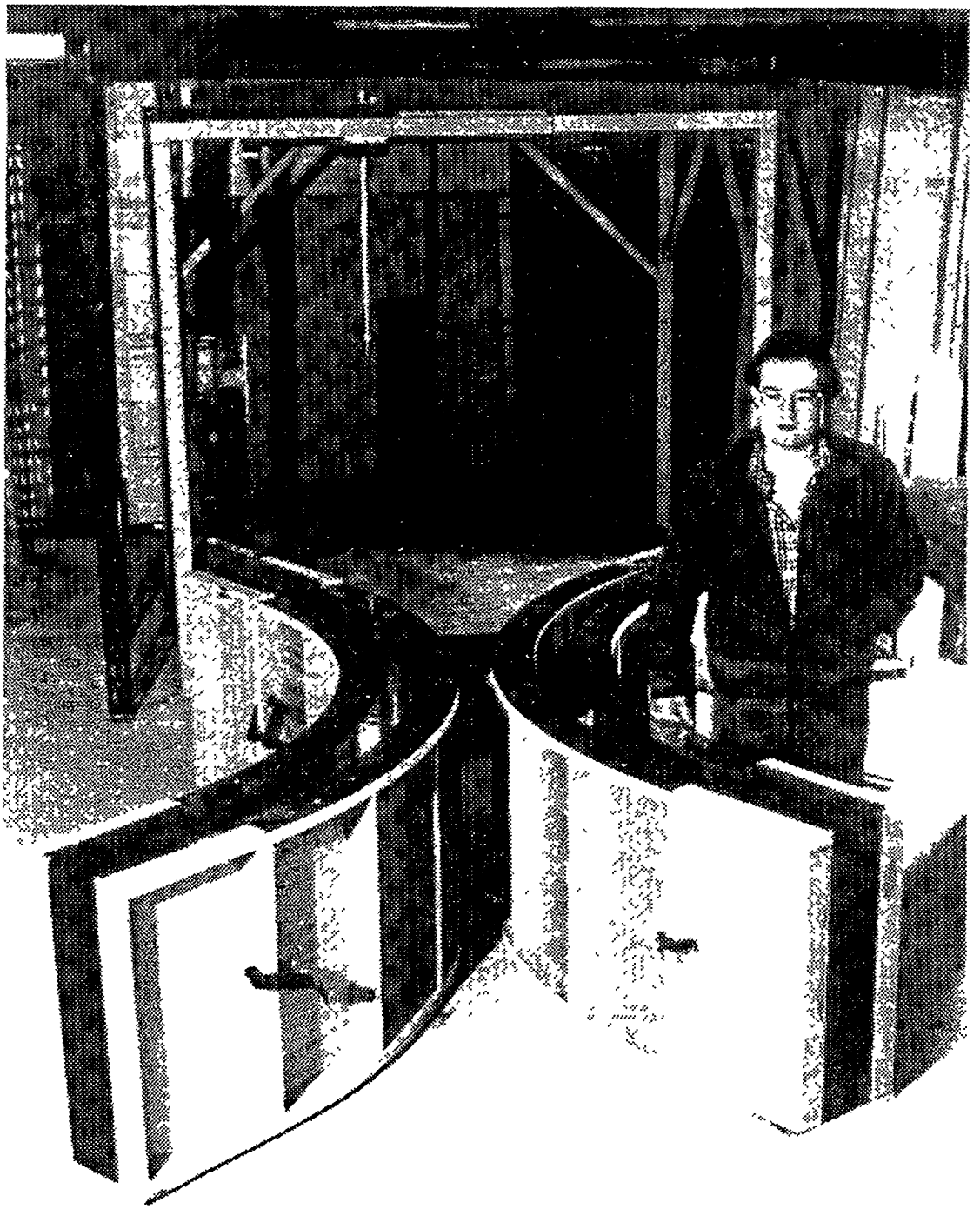

FIG 3 8 Photograph of the model of the accelerating cavity of the booster

a beam over significant distances and to the EA This can be accomplished with the help of standard bending magnets and quadrupoles The momentum of a 1 0 GeV kinetic energy protons is 1 696 GeV/c corresponding to a magnetic curvature radius of 3 77 metres in a field of 1 5 Tesla and to $\beta\gamma = 1\ 807$ In particular the "goose neck" required to bend the beam from horizontal to vertical into the EA requires a total bending strength of 8.88 Tesla × metre This magnet is also used to separate the beam transport from the neutrons escaping the EA through the beam pipe An appropriate beam catcher is used to remove them far away from the proton beam path

As is well known, the beam transverse radial dimensions in each plane are determined by the so-called

betatron function $\Delta x(z) = \sqrt{(\beta(z)\varepsilon/\pi)}$. Over the beam transport channel, typically $\beta(z) \approx 20$ m and the beam radius is $\Delta x \approx 5.0$ mm. At the EA beam window we want $\Delta x \approx 7.5$ *cm* and therefore $\beta(z) \approx 4000$ m. This is realised by creating a focal point some $L = 30$ metres away from the window and letting the beam spread-out naturally because of its emittance. In absence of magnetic fields, the evolution of the β-function at a distance L from the focal point is given by the well known formula $\beta(z) = \beta(0) + L^2/\beta(0) \approx L^2/\beta(0)$. Setting $\beta(z) = 4000$ m we find $\beta(0) \approx L^2/\beta(z) = 0.225$ m, which is within reach with the help of an ordinary quadrupole triplet[1]. The beam radius at the focal point is very small, $\Delta x(0) = \sqrt{(\beta(0)\varepsilon/\pi)} = 0.70$ mm. In short the idea is the one of enhancing the angular divergence of the beam by making a very tiny focal spot[2]. A long drift space following such a focal point will traduce this angular divergence into a large spot.

An appropriate collimator is limiting the aperture available to the beam in this point to about 10 times its nominal radial size, large enough in order to let the beam through with no loss in ordinary conditions. In case of the accidental mis-steering of the beam or of a malfunctioning of the focusing lenses, the spot will grow in size and the beam will be absorbed by the collimator. In this way the beam window can be protected against accidental "hot spots" caused by the wrong handling of the beam. It has been verified that the defocusing forces due to the beam current do not appreciably affect the beam optics[3].

The beam must be transported under a reasonable level of vacuum. In our design the last part of the beam tube is filled with Pb vapour at the pressure of about 5×10^{-4} Torr, the vapour tension of the coolant at the operating temperature. Differential pumping and a cold trap will remove these vapours which may be radioactive before they reach the accelerator. There are no appreciable effects of this residual pressure on the beam propagation. The need of clearing electrodes will be further studied, but it appears unnecessary at this level.

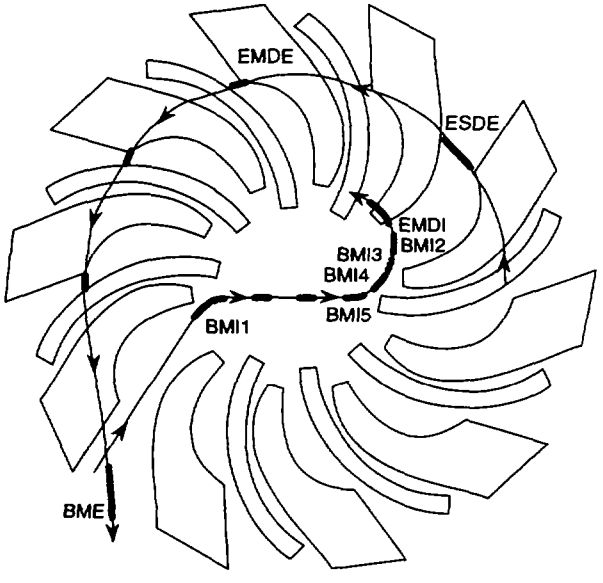

FIG. 3.9 Location of the injection and extraction channel elements of the booster ring cyclotron.

The extracted beam current and positions are carefully monitored with non-destructive probes, beam profile monitors and pick-up electrodes. In case of a malfunctioning of the beam, the accelerator current can be cut-off very easily on the axial injection line of the injectors in times of the order of microseconds (the transition time from the ion source to the final focus), thus avoiding any damage of the hardware due to beam mis-steering. An alternate beam dump should be provided to which the beam could be dumped during accelerator tuning

[1] It may not seem entirely obvious to obtain such a low beta value with a beam transport if the actual emittance from the accelerator were less than what is quoted. If so, one could easily increase the emittance of the beam through the beam transport with the help of multiple scattering or with a pair of orthogonal small steering magnets operated at high frequencies (Lissajous pattern).

[2] From phase-space conservation in fact through the beam transport the product of the beam size and angular divergence is a constant.

[3] For instance the CERN-PS Booster routinely handles and transports peak currents of the order of 100 mA, about one order of magnitude larger than the present case.

and the like.

D.3.3.7. CONCLUSIONS

The above preliminary studies have shown that a 3-stage Cyclotron facility could provide a solution for a ≈ 10 GeV × mA beam to drive the Energy Amplifier. Detailed design studies are now being undertaken in order to clarify the following points in beam dynamics:

1) detailed calculations on the beam dynamics in the injectors in order to assess the intensity limits of this kind of injector.
2) more refined calculations of the merging of the 2 beams (H^+ and H^-) coming out of the injectors in order to define the beam characteristics at injection in the ISSC.
3) detailed beam dynamics in the ISSC with space charge effects taking into account the particle distribution after stripping.

Besides this, technical design studies on the three accelerators have to be started, in particular mechanical design studies (vacuum chamber of the large SSCs, optimisation of the shape of the main cavities of the SSCs, etc.). Finally, a conceptual study aiming at increasing the final energy towards 1200 MeV is in progress.

D.3.4. THE ENERGY AMPLIFIER UNIT

D.3.4.1. INTRODUCTION

The general layout of the EA unit is shown in Figure 4.1a-b. The main design parameters are given in Table IV.1. In short it consists of a main vessel, about 6 m in diameter and 30 m tall, filled with molten Lead. The vessels, head enclosure and permanent internal structures are fabricated and shipped as an assembled unit to the site. The shipping weight is then about 1500 tons. Removable internal equipment is shipped separately and installed through the top head. The relatively slender geometry enhances the uniformity of the flow of the molten Lead and of the natural circulation for heat removal.

A high energy beam is injected through the top and made to interact in the Lead near the core. The heat produced by the nuclear cascade is extracted by the Heat Exchangers. Most of the inside of the vessel is free of obstructions, in order to permit a healthy circulation of the cooling liquid. The circulation of the

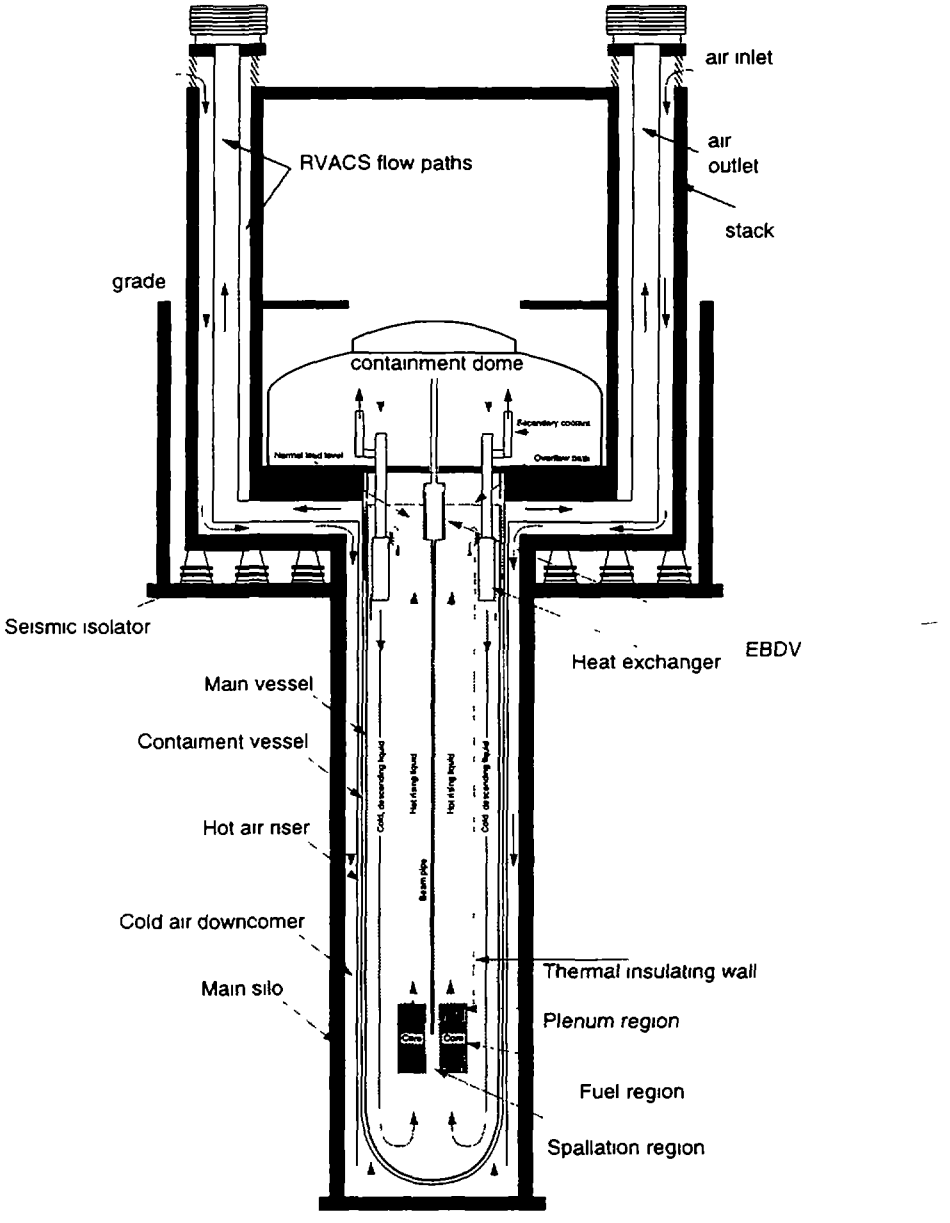

FIG. 4.1a General layout of the Energy Amplifier unit.

Lead in the vessel is ensured exclusively by natural convection. There are four 375 MW_t heat exchangers to transfer the heat from the primary Lead to the intermediate heat transport system. They must be designed in such a way as to introduce a small pressure drop in order not to slow down too much the convective cooling flow. The liquid once cooled by the heat exchangers, descends along the periphery and feeds the lower part of the core and the target region. A thermally insulating wall separates the two flows. In order to have an effective circulation at the chosen power level (1500 MW_t), the temperature gradient across the Core must be of the order of 250 °C. Consequently the volume inside the vessel can be ideally divided in three separate regions, namely (1) the target/core/breeder region, (2) the convection draft generating region and (3) the heat exchangers region. A remotely controlled pantograph transfer machine is used to transfer fuel between the core, storage racks located in the convection generating region and the transfer station, where they can be inserted or removed from the EA vessel by a transfer cask[1]. The fuel storage region can be used also as a cooling down region for spent fuel. Fuel bundles can be extracted or introduced into the vessel with the help of appropriate tooling through the top cover of the vessel[2]. According to previous experience with such pantographs, widely used in existing Fast Reactors, the refuelling time may require of the order of 1-2 weeks. As described in the text, it is to be performed about once every five years or so.

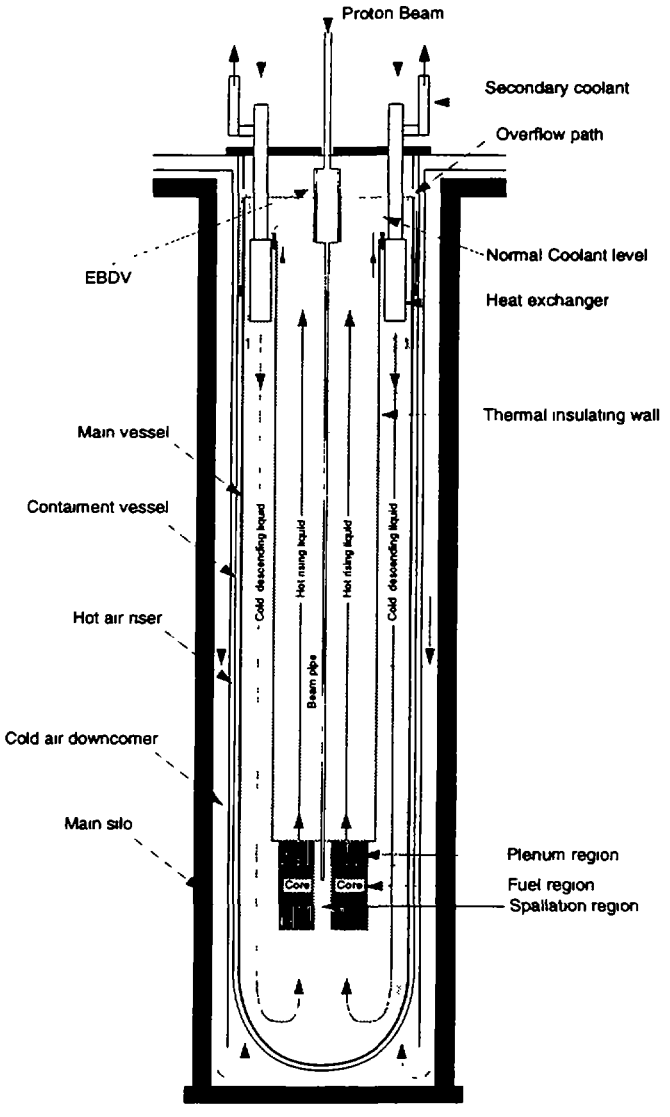

FIG. 4.1b The energy producing unit, side view.

The proton beam enters the vessel through a long cylindrical evacuated tube of about 30 cm diameter, which restricts to 20 cm before entering the core region. The beam diameter at the window is about 15 cm. The life expectancy of the beam penetration window is estimated to be about 1 year, namely it requires periodic replacement, performed extracting the full beam tube. The window is cooled by the main Lead circulation in the vessel. Accidental breaking of the window will fill the beam tube with molten Lead. This will bring the Energy Amplifier to a halt, since the injected lead will act as a beam stopper. The design of the beam penetration channel is more amply discussed further on.

---

[1] Refuelling machines of this type have been applied in the UK's PFR, Italy's PEC and Japan's MONJU. The conceptual design for the ALMR transfer machine was provided by Ansaldo (Italy).

[2] As already pointed out, in order to reduce the proliferation risk, the fuel extraction or injection operation may be restricted to the user (owner) of the plant and allowed only to specialized team. This is possible since refuelling occurs only once about every 5 years and there are no major, active elements which need access during operation.

TABLE IV.1. MAIN PARAMETERS OF THE ENERGY AMPLIFIER

Gross Thermal Power/unit	1500	MW
Primary Electric Power	625	MW
Type of plant	Pool	
Coolant	Molten Lead	
Sub-criticality factor k, (nominal)	0.98	
Doppler Reactivity Coefficient, ($\Delta k/\Delta T$)	-1.37×10^{-5}	
Void coefficient (coolant) $\Delta k/(\Delta \rho / \rho)$	+ 0.127	
Nominal energetic Gain	120	
Accelerator re-circulated Power	30	MW
Fraction Electric Power recirculated in Accel.	0.0465	
Control Bars	none	
Scram systems(3)	CB_4 rods	
Seismic Platform	yes	
Main Vessel		
Gross height	30	m
Diameter	6 m	m
Material	HT-9	
Walls thickness	70	mm
Weight (excluding cover plug)	2000	t
Double Liner	yes	
Proton Beam and Spallation Target		
Accelerator type	Cyclotron	
Number of beams	1	
Accelerator overall efficiency[1]	43%	
Kinetic energy	1.0	GeV
Nominal current	12.5	mA
Nominal beam Power	12.5	MW
Maximum current	20	mA
Spallation Target material	Molten Lead	
Beam radius at spallation target	7.5	cm
Beam window	Tungsten, 3.0 (1.5)	mm
Max. power density in window	113	W/cm^2
Max. Temp. increase in window	137	°C
Window expected lifetime	≥ 1	year

[1] Beam power/Mains Load

TABLE IV.1 (CONT.)

Fuel Core				
Initial fuel mixture	$ThO_2 + 0.1^{233}UO_2$			
Initial fuel mass	28.41			t
Cladding material	low act. HT-9			
Specific power	52.8			W/g
Power density	523			W/cm^3
Average Fuel Temperature	908			°C
Maximum Clad Temperature	707			°C
Dwelling time (eq. @ full power)	5			years
Average Burn-up	100			GW d/t
Breeder Core				
Initial fuel mixture	ThO_2			
Initial fuel mass	5.6			t
Cladding material	low act. HT-9			
U^{233} stockpile at discharge	242.7			kg
Power density at end cycle	3.0			W/g
Primary cooling system				
Approximate weight of the coolant	10,000			t
Pumping method	Nat. Convection			
Height convection column	25			m
Convection generated primary pressure	0.637			bar
Heat exchangers	4 x 375			MW
Decay heat removal	RVACS			
Inlet temperature, Core	400			°C
Outlet temperature, Core	600			°C
Coolant Flow in Core	53.6			t/s
Coolant speed in Core, average	1.5			m/s
Decay Heat Passive Cooling (RVACS)				
Riser channel gap width		18		cm
Downcomer channel gap width		57		cm
Trigger Temperature	500	600	700	°C
EA Coolant max Temperature rise	110	83.5	64.5	°C
Time to max.Temperature rise	17.5	11.2	9.5	hours
Outlet air Temperature (@ max. temp.)	273	302	334.3	°C
Outlet air Speed (@ max. temp.)	13.4	14.2	15.2	m/s
Air flow Rate (@ max. temp.)	52.8	56.1	60	m^3/s
Extracted Heat (@ max. temp.)	8.57	9.65	10.84	MW

There are no control bars and the power produced is controlled with the beam current. A feed-back system ensures that the inlet temperature of the heat exchangers is maintained to the specified value. For further safety however the ultimate shut down assembly which drops CB_4 by gravity, is retained, following the ALMR design, but slightly modified since the buoyancy of the Lead is much greater than the one of Sodium. This simple scram system is however used to anchor the EA solidly away from criticality when not operating. In contrast with an ordinary Reactor, in the EA there are no main elements of variability in the neutronics of the device.

Accidental thermal run-off is ultimately prevented using the natural expansion of the coolant. In case of an overheating of the EA, its lead level rises at the rate of 27 cm/100 °C. Such a level rise (see Figure 4.1b) is used to activate an overflow path which

(1) fills through a siphon a cavity located about 25 m above the Core, in which the proton beam is safely absorbed. Natural convection is sufficient to remove the residual power of the proton beam, which represents about 1/6 of the amount of the initial decay heat.

(2) fills with molten Lead the narrow gap between the vessel liner and the containment vessel, ordinarily filled with Helium[1] gas at normal pressure (Figure 4.1b). The thermal conductivity increases from the 0.03 W/m/K of Helium at 1 bar pressure to 16 W/m/K for Pb. This allows the surplus heat to be dissipated away into the environment through air convection and radiation (RVACS),

(3) scrams the EA to a low *k*-value. Safety is also enhanced by the strong negative void coefficient and the negative temperature coefficient (Doppler) of the fuel which operates at relatively low temperatures.

These passive safety features are provided as a backup in case of failure of the active systems, based on the ultimate shut-off of the proton beam from the accelerator, which brings to an immediate stop the fission generated power of the Amplifier. These functions are achieved by passive means without operator action. The key processes underlying these functions are governed by thermal expansion, natural circulation of molten Lead, natural air circulation on the outer containment surface, and thermal radiation heat transfer which becomes very effective at elevated temperatures. Our design integrates all these effects into an efficient passive safety system which can accommodate primary coolant flow loss and loss of heat removal of secondary transport system with benign consequences on the Core, which can survive with no damage.

The various main components constituting the EA will be separately discussed.

D.3.4.2. MOLTEN LEAD AS SPALLATION TARGET AND COOLANT

Lead constitutes an ideal spallation target, since its neutron yield is high, and it is very transparent to neutrons of energies below 1 MeV. It has also excellent thermodynamical properties which make it easy to dissipate the intense heat produced by the beam. As illustrated in the previous sections, Lead has also the required properties in terms of small lethargy and small absorption cross sections to perform the function of main coolant. Its very high density and good expansion coefficient make convection sufficient even for large power production. Finally it is an excellent shielding material and most of the radiation produced by the EA core is readily and promptly absorbed. There is no need to add additional internal shields or reflectors like in the case of Liquid Sodium to protect structurally important elements inside the vessel. The radiation dose transmitted to the outer Main vessel is very small. Hence, unlike for instance in PWRs, its active life is very long since the neutron fluence is about 10^{20} n/cm^2/year its radiation damage is negligibly small (see Table V.5).

Molten Lead when compared to Sodium, has considerable advantages on safety. The void coefficient

[1] The choice of helium gas is justified by the fact that the more commonly used Argon will mix with the radio-active nuclide ^{42}Ar produced by the spallation cascade.

of Sodium is notoriously positive, namely creation of bubbles increases the reactivity. In Lead the void coefficient is negative. The absence of void coefficient problem allows for instance a less flattened shape of the fuel core. Hence the fuel pins in our design are substantially longer. The boiling point of Lead (1743 °C) is also much higher than the one of Sodium (880 °C) and it does not react like Sodium in contact with air. Thermodynamic properties of both molten metals are given in Table IV.2. Saturation vapour pressure and evaporation rate against vacuum are shown in Figure 4.2. Since these quantities are very small (respectively 5×10^{-4} Torr and 10^{-5} g cm^{-2} s^{-1}) it is possible to keep molten Lead in an evacuated region: this feature is very important to ensure safety for the proton beam. In general, in order to have the same pressure and temperature changes through the core for a given specific power production, the speed of circulating Lead must be about 0.38 times the one of Sodium and the pitch in the fuel lattice must be enlarged in order to provide a flow area which is 1.8 times larger. The flow speed of Lead in the core is typically of the order of few m/s. The mass flow through the core is approximately doubled with respect to Sodium. Once these changes are easily implemented the two fluids become essentially equivalent.

Notwithstanding there is little or no experience in the use of Lead as a coolant in Reactors, with the exception of Military applications in the former USSR. For instance the use of molten Lead requires further studies to overcome corrosion. As discussed further on, such a problem appears fully manageable.

TABLE IV.2. MAIN PROPERTIES OF MOLTEN SODIUM AND LEAD.

	Sodium	**Lead**	
Melting Temperature	98	328	°C
Boiling Temperature	880	1743	°C
Values at 600 °C			
Vapour pressure	24.13	5×10^{-4}	Torr
Density	0.81	10.33	g/cm^3
Heat capacity (by mass)	1.30	0.15	J/g °C
Heat capacity (by volume)	1.053	1.5495	J/cm^3 °C
Volumic dilatation coeff. ($\times 10^4$)	3.1938	1.3935	°C^{-1}
Therm. conductivity	62.24	16.45	W/m °C
Heat transfer coeff ($\times 10^4$)	3.6	2.3	W/m^2 °C
Dynamic viscosity ($\times 10^{-3}$)	0.206	1.55	N s/m^2
Surface tension ($\times 10^{-3}$)	146	431	N/m
Electric conductivity (e.m. pumps)		9.4×10^{-7}	Ω m

Natural Lead exposed to an intense neutron flux in the EA will become activated. Since the Lead is circulating in the EA this activity will spread from the core to the rest of the device. Fortunately the main activation channels are benign. Natural Lead is made of several isotopes, ^{208}Pb (52.4%), ^{206}Pb (24.1%), ^{207}Pb (22.1%) and ^{204}Pb(1.4%). If the target is ideally made of pure ^{208}Pb, a neutron capture will produce ^{209}Pb, which quickly ($t_{1/2}$ = 3.25 h) decays into the stable ^{209}Bi (with a β^- decay of 645 keV end point and no γ-ray emission) which will remain as eutectic mixture with the target material. Reactions of type (n, 2n) occur at a level which is few percent of captures and create ^{207}Pb, also stable. Both daughter nuclei are stable elements and excellent target material themselves. A target with natural Lead will produce an appreciable amount of ^{205}Pb from captures of ^{204}Pb and to a smaller level from (n, 2n) of ^{206}Pb. This element is long lived ($t_{1/2}$ = 1.52 10^7 a) and decays into stable ^{205}Tl by electron capture (i.e. by neutrino emission) and no γ-ray emission. The Q of the decay is only 51 keV. Therefore its presence is relatively harmless. Neutron capture properties of ^{205}Pb are unknown and therefore it is impossible to estimate the possibility of further transformations. However it is likely that the main channel will be neutron capture, leading to

the stable ^{206}Pb. Finally ^{203}Pb from (n, 2n) of ^{204}Pb is short lived ($t_{1/2}$ = 51.8 h) and decays into stable ^{203}Tl by electron capture and γ-ray emission. Reactions of the type (n,p) which are very rare since they occur only for high energy neutrons, transform Pb isotopes into the corresponding Thallium isotopes (^{208}Tl, ^{207}Tl, ^{206}Tl and ^{204}Tl) which all β-decay quickly into Pb nuclei again.

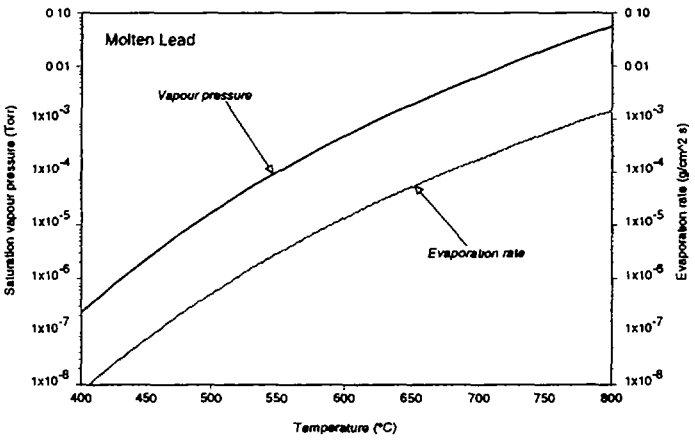

FIG. 4.2 Saturation vapour pressure and evaporation rate against vacuum for molten Lead.

The situation is more complex in the case of a Bismuth target. Neutron captures lead to short lived ^{210}Bi which decays ($t_{1/2}$ = 5.0 d) in ^{210}Po which, in turn, decays with $t_{1/2}$ = 138 days to stable ^{206}Pb. There is a long lived ($t_{1/2} = 3\times10^6$ a) isomeric state ^{210m}Bi, also excited by neutron capture, which decays by α-decay to short lived ^{206}Tl (RaE), which in turn β-decays in stable ^{206}Pb. Reactions of the (n,2n) type would produce the long lived ($t_{1/2} = 3.68\ 10^5$ a) ^{208}Bi, which ends up to stable ^{208}Pb via internal conversion. Therefore a Bismuth moderator may present significant problems of radio-toxicity which must be further examined before seriously considering such material as target. Consequently the use of Bismuth or of Bismuth-Lead eutectic mixtures is not considered as main coolant, since Bismuth via the leading single neutron capture produces sizeable amounts of Polonium which is radio-toxic and volatile at the temperatures considered for the present study. However such mixture is envisaged for secondary cooling loops because of its lower melting point (125 °C).

Additional fragments are produced by the spallation processes due to the high energy beam (see Table V.10). The toxicity problem is investigated later on, although there is expectation that no major problems should arise, provided the appropriate precautions are taken.

D.3.4.3. CORROSION EFFECTS DUE TO MOLTEN LEAD

Molten lead has a significant solubility for many metals (Ni and Mn > 100 ppm; Fe, Cr, Mo, 1 ÷ 10 ppm at 600 °C), which is a rising function of temperature (Figure 4.3). As a consequence, after prolonged immersion some metals and alloys exhibit a significant deterioration. This is a relevant problem and it must be mastered. Some experience on the use of Lead and Bismuth coolants in Nuclear Reactors exists in the former Soviet Union. Extensive studies of corrosion of Lead-Lithium mixtures have been carried out in the context of Fusion, where a neutron multiplying, Tritium breeding blanket is necessary. For instance a steel type HT-9 immersed in liquid Lead for 50,000 hours exhibits a corrosion loss of about 80 μm at about 500 °C [43]. In general Ferritic steels are moderately corroded by lead and in particular they do not exhibit inter granular damage (typically 30 μ after some 3000 hours at 575 °C for EM 12). The effect is more pronounced for austenitic steels (typically 120 μ after the same period at 700 °C for 800 H, where also mass transfer from the hot to cold regions is observed). Several successful methods have been devised and demonstrated effective in order to suppress corrosion due to prolonged hot Lead Immersion:

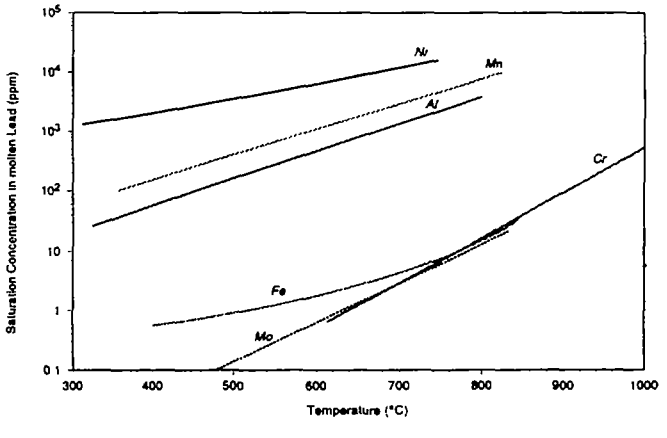

FIG.4.3 Solubility of different metals in molten Lead.

1) *Purification and additives to the liquid metal.* When a de-oxidant (225 ppm Mg) is added to lead, no corrosion (0 μ) is observed [44] for 15 CD 9-10 loops after 28000 hours (3.2 years) of tests at 550 °C. In comparison, the same conditions and no additive would result in a corrosion in excess of 300 μ. Similar results are obtained with Titanium or Zirconium additions to the liquid Lead, where no corrosion is observed after 750 hours at 950 °C [45], in contrast to a 400 μ for an uncoated steel. Their beneficial effect is probably related to the formation of nitrides at the interface Steel/Lead. The Nitrogen is contained in the Steel, if not treated beforehand. If the Zirconium is maintained constantly the film is self-healing and its long term effectiveness is preserved.

2) *Coating materials.* Amongst all the coated materials which have been tested, some seem to give the best results (i) 15 CD 9-10 low chromium steel coated with plasma sprayed Molybdenum [46][47], where no cracking or dissolution is observed after 1500 hours at 720 °C; (ii) Aluminium on low Chromium steel [46] where no evolution of the specimen is observed after 1500 hours at 750 °C. The coated material is prepared by heating the specimen in contact with a mixture of aluminium oxide and Aluminium. The coating probably reacts with traces of Oxygen to form a self-healing protective Alumina film; (iii) Z6 CN 91-9 coated with ZrN: this coating is self-healing if Zirconium is added to Lead. These last two possibilities are considered the most promising in view of to their self-healing capacity.

A small amount of embrittlement may also occur for some alloys (45 CD 4 and 35 CD 7) mostly around the melting point of Lead. Liquid metal embrittlement is a reduction of the fracture strength of a metal stressed in tension while in contact to a surface active liquid metal. This effect is enhanced when some elements such as Sn, Sb and Zn are added to the Lead. As for 15 CD 9-10, no significant embrittlement effect has been evidenced, even in the 320-350 °C temperature range. Hence specifications on the maximum concentration of certain elements in Lead must be established.

In conclusion there is no doubt that some type of additives and/or coating can effectively stop corrosion in the domain of interest [37]. *But an important experimental work has to be done (non isothermal experiments, effects of cyclic load and so on).*

D.3.4.4. THE PROTON BEAM

The proton beam (≈ 10 mA) after acceleration and beam transport is brought to the Amplifier by conventional beam transport and a 90 degrees bending on top of the vessel. The amount of power of the beam is comparable to the one envisaged in Neutron Spallation sources under design [48]. The magnetic bending helps also in separating leakage neutrons, which are absorbed in an appropriate beam dump. By switching off the bending magnets of the last bending, the beam can be safely diverted to an appropriate beam dump. An appropriate but conventional design of the beam channel allows to perform the switch to the beam dump in a time of the order of 1 millisecond, which is extremely short in view of the thermal inertia of the Amplifier. The beam, focused by conventional quadrupoles, traverses the whole beam penetration tube and enters in the lead coolant and target through a window made of Tungsten ≈ 3 mm thick. The material has been chosen for its high melting temperature (3410 °C), its excellent thermal conductivity, its high mechanical strength[1] and acceptable activation properties. In addition it exhibits a negligible corrosion by molten Lead [49].

The beam spot size is determined by the physical distance from the focal point (≈ 30 m), where a narrow collimator has been installed (see paragraph D.3.3.6). This arrangement ensures that the beam size at the window cannot become abnormally small, for instance as the result of a miss-steering or a failure of

[1] The use, for example, of alloys like Tungsten-Rhenium can further enhance the mechanical resistance of the window and its weldability. In particular such an alloy has a higher re-crystallisation Temperature (1650 °C vs. 1350 °C for pure Tungsten). However it has a considerable disadvantage, namely the thermal conductivity is about a factor 2 lower. Note that the operating temperature of the window is about 540 °C and the incipient re-crystallisation temperature is considerably higher (1150 °C).

the beam transport. The proton beam window has a spherically curved profile and it is cooled by the bulk of the Lead coolant circulating in the target region at a speed of the order of a few m/sec. At the window the proton beam spot size has a parabolic profile, $2I_p/\pi r_o^2[1-r^2/r_o^2]$ with $2r_o$=15 *cm* corresponding to a peak current density of 113.2 μA/cm^2 for I_o= 10 mA. Montecarlo calculations show that the beam deposits about 1% of its kinetic energy in passing through the window, mostly due to ionisation losses, namely ≈ 95 kW, with a peak power density in the centre of 113 W/cm^2, which is comparable to the peak power density of the fuel rods. The same Montecarlo calcula-tions, in excellent agreement with experimental data [50] have been used in conjunction with a fluid-dynamic code to predict the temperature and flow of the coolant and the conditions of the window[1]. The maximum tem-perature rise for the Tungsten and the surrounding Lead is respectively ΔT = 137 °C and ΔT = 107 °C. Thermal stresses associated with beam intensity variation have been estimated and found largely within the limits set by the properties of the material[2]. We have reduced such thermal stresses by reducing the thickness of the window from 3 mm in the welding of the pipe to 1.5 mm in the centre of the hemisphere, along the beam axis and were most of the energy is released (see Figure 4.4). More generally the energy deposited by the beam predicted by the Montecarlo calculations is pictured in Figure 4.5. The temperature profiles of the window and of the surrounding Lead are shown in Figure 4.6 for a local Lead speed of 5 m/s. The main parameters of the final beam transport in the Vessel are listed in Table IV.3.

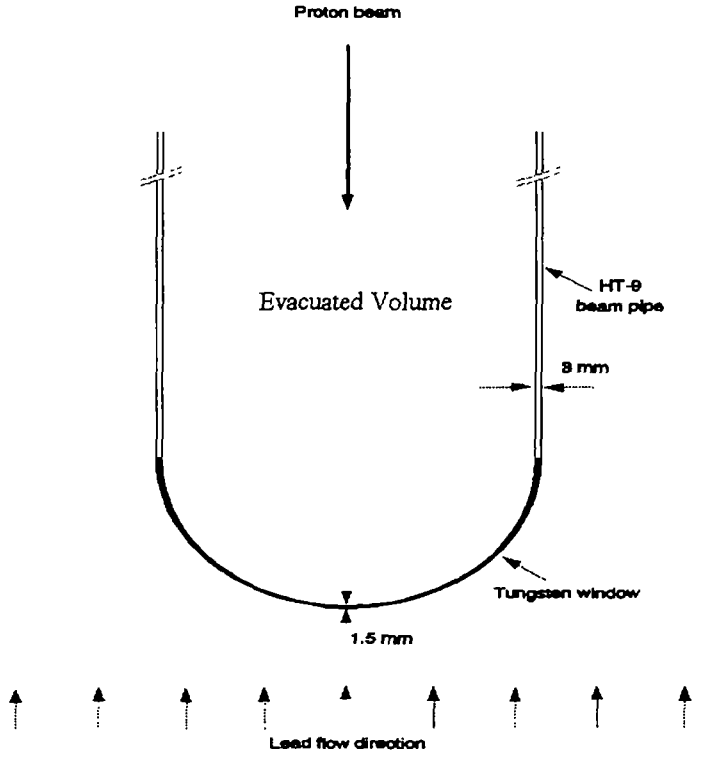

Fig. 4.4 Layout of the beam window

The window should safely withstand accidental power densities which are more than one order of magnitude larger than the design value. The expected peak radiation damage in the window after 6000 hours at full beam intensity is of 171.1 d.p.a. and the associated gas production are of 1.1 × 10^4 He (appm) and 9.97 × 10^4 H (appm). These values are reasonable but suggest that the window should be periodically replaced. A high quality vacuum (≤ 10^{-4} Torr) in the final beam transport and in the Accelerator is easily ensured by differential pumping and a Cold Trap in which Lead vapour will condense. The low Lead vapour pressure in the last part of the beam transport (≈ 5 × 10^{-4} Torr at 600 °C) has no appreciable influence on the proton beam which has a high rigidity and penetrating power.

In the unlikely possibility that the proton beam will persist even for instance if the main cooling system of the Amplifier would fail, a totally passive system (Figure 4.7), driven by the thermal dilatation of the Lead coolant will ensure that an enlarged volume region, sufficiently massive to stop the proton beam will be automatically filled with liquid Lead, the Emergency Beam Dump Volume (EBDV). A shut-off valve

[1] The thermal hydraulic model has been built using the code STAR-CD [51] and describes at the same time, the thermal behaviour of the lead (liquid) and of the beam window (solid).

[2] The static structural analysis of the window has been performed using the code ANSYS [52]. The model developed used detailed pressure and temperature maps coming from the thermal hydraulic calculations.

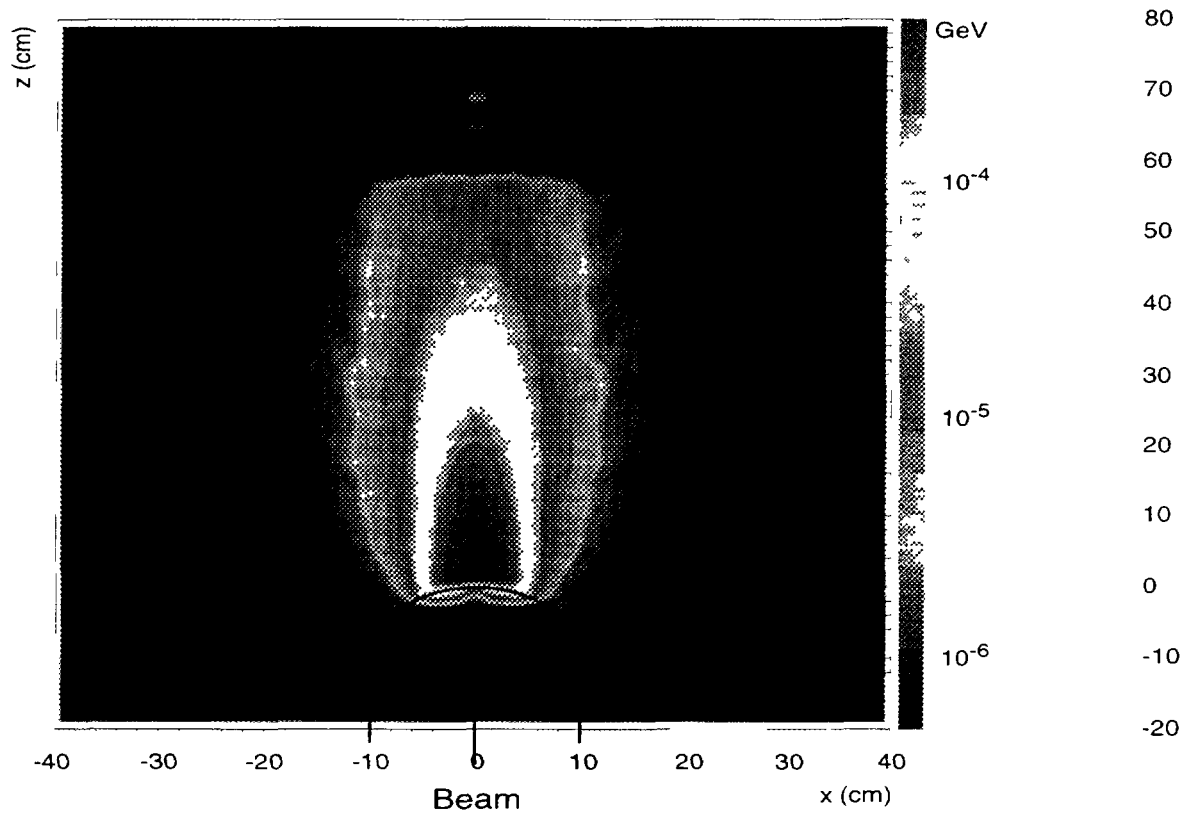

FIG 4 5 Contour Map of the Energy Deposit of a 1 GeV Proton into the F-EA Target

at the bottom of the volume ensures that the whole beam pipe is not filled with Lead This measure has no character of necessity, but only of convenience Indeed in the unlikely case that the Tungsten window would break, liquid Lead will rise, such as to fill completely the pipe and the Emergency Beam Dump Volume, though at a slightly lower level, but still sufficient to kill the beam and bring the Amplifier safely to a halt It has been verified that convection cooling can safely transfer the heat produced in the EBDV (10 MW) to the main Lead coolant This method is applicable because of the high density (10 55 g/cm^3) and the low vapour pressure ($\approx 5 \times 10^{-4}$ Torr at 600 °C) of the molten Lead (Table IV 2)

D 3 4 5 FUEL DESIGN AND BURN-UP GOALS

Fuel and Breeder elements are loaded in the form of thin rods (pins) Pins are clustered in sub-assemblies, each with a pre-determined number of pins, arranged at constant pitch roughly in an hexagonal configuration Pins are made of small oxide pellets inserted in a robust steel cladding Each pin has two extended void regions, called "plenums", one at each end, intended to accumulate the gaseous fission fragments The pins are kept separate by a wire wrapped around the pin, which also improves the coolantflow The main parameters of the fuel assemblies are listed in Table IV 4 They are quite similar

TABLE IV.3. MAIN PARAMETERS OF THE FINAL BEAM TRANSPORT TO THE VESSEL

Beam pipe material	HT9	
Beam pipe shape	cylindrical	
Beam pipe length	~ 30	m
Beam pipe external diameter	20	cm
Beam pipe thickness	3	mm
Window material	Tungsten	
Window shape	hemispherical	
Window external diameter	20	cm
Window thickness (edge,centre)	3.0, 1.5	mm
Beam radius at spallation target	7.5	cm
Values for 1 GeV, 10 mA beam		
Lead coolant nominal speed	5.0	m/s
Heat deposition in the lead	6.97	MW
Max. Temperature increase of Lead	107	°C
Heat deposition in the window	95	kW
Max. Temperature increase of window	137	°C
Max. power density in window	113	W/cm^2
Max. thermal window stress[1] (britt, duct)	48.2, 82.2	MPa

to the ones used in Fast Breeders (FB).

But in order to adapt these well proven designs to our case we must (1) modify the pitch between pins to the different thermo-dynamical properties of the Lead coolant when compared to Sodium and (2) reduce the coolant pressure losses through the plenum region. The temperature and pressure drop across the core must be adjusted to the requirements of convective cooling. We have chosen two different subassemblies with different pitches: a wider pitch is used in the central part of the core where the specific power is larger.

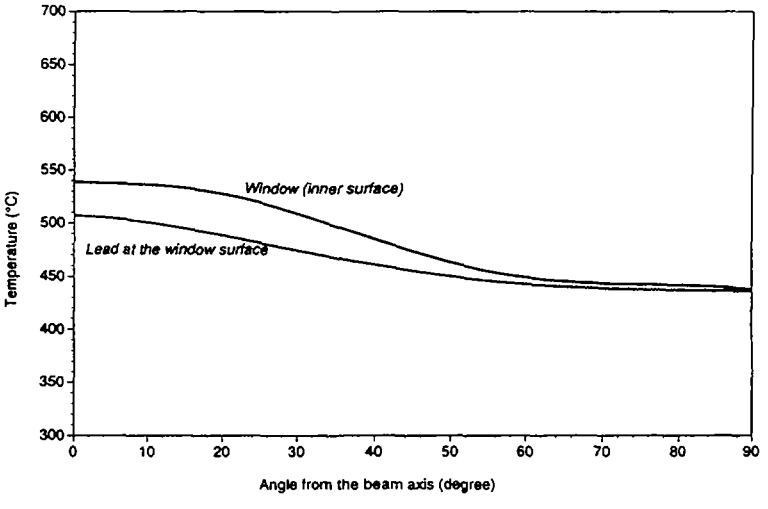

FIG. 4.6 Temperature profiles of the beam window and the surrounding Lead.

The flat to flat distance is the same for all sub-assemblies but the number of pins is slightly different to accommodate the two different pitches.

The burn-up of an ordinary reactor varies from the 7 GW × d/t of a natural Uranium fuel of CANDU reactors to the 30 ÷ 50 GW × d/t of enriched Uranium in PWRs. The fuel burn-up of the EA is of the order

[1] Tensile strength of Tungsten at 550 °C: 380 MPa

of 100 GW × d/t, averaged over the fuel volume. The most exposed pins, if no intermediate shuffling is performed will accumulate about 200 GW × d/t. The practical final burn-up is determined

TABLE IV.4. MAIN DESIGN PARAMETERS OF THE FUEL-BREEDER ASSEMBLIES

Pins	FFTF	EFR	Monju	F-EA	
Outer diameter	5.84	8.2;	6.5	8.2	mm
Cladding thickness	0.38	0.52; 0.6[1]	0.47	0.35	mm
Wrapper wire thickness	1.42	1.75	1.75		mm
Cladding material	HT-9	many	SUS316	HT-9	
Active length	91 (+?)	100 (+24)	93 (+65)	150	cm
Void length (total)	162	120		180	cm
Void outer diameter	5.84	8.2	6.5	5.0	mm
Void cladding thickness	0.38	0.52	0.47	0.35	mm
Max. clad temperature	700		675	692	°C
Average power/met. fuel	100		121	60	W/g
Max. radiation damage		≈ 120	≈ 100	≈ 34	dpa/y

Sub-Assemblies	FFTF	EFR	Monju	F-EA		
Configuration	Hexag.	Hexag.	Hexag.	Hexag (IC)[2].	Hexag (OC)[3]	
No hexagonal rounds	8	10		10	11	
No of pins	217	3,311,69[1]		331	397	
Total length	4.7	4.8		5.3		m
Flat to Flat	120	188		234		mm
Pitch between pins	7.26	9.95	8.25	12.43	11.38	mm
No units-fuel(IC+OC)	192	387		120		
No units-breeder		78		42		

not only by the losses of fuel quality due to FF captures, but also by (1) radiation damage of the supporting structures; and (2) pressure build-up of gaseous fission fragments. These two effects are briefly reviewed:

1) Radiation damage of the pins. Note that for a given power yield, the flux in the case of ^{233}U is smaller than the one of ^{239}Pu in a FB by a factor 0.64 due to the difference in cross sections. Therefore 150 GW × d/t for a Thorium based EA produce an integrated neutron fluence through the cladding $\int \phi\, dt$ equals to the one after about 96 GW × d/t in a FB. Considerable experience exists in burn-up tests for fuel pins in FB. Based on this extensive experience, a limit of about 100 ÷ 120 GW × d/t is a current goal value for most of these designs. A reasonable goal for the radiation damage in the Amplifier will then be 160 ÷ 180 GW × d/t for the most exposed pins. A burn-up of 100 GW × d/t in our case corresponds to an integrated neutron fluence through the cladding of $\int \phi\, dt = 3.3 \times 10^{23}$ n/cm^2. The most exposed pins will accumulate about twice such a fluence. The effects on the properties of the HT-9 steel used have been exami-ned [53]. The conclusion is that we expect ≈ 34 d.p.a./year for the most exposed pins. A reasonable ultimate limit

[1] The two values correspond to the fuel and breeder resp.

[2] Inner core

[3] Outer core

applicable to this material is 225 d.p.a. A five year lifetime is therefore reasonable. Likewise other effects, namely He production and embrittlement appear fully acceptable.

2) The fuel material in form of (mixed) Oxides will undergo considerable damage and structural changes in view of the considerable fraction which is burnt and transformed into FFs. The behaviour of ThO_2 is not as well known as the one of the UO_2 which is presently universally used. However, the thermal conductivity, the expected mechanical properties and the melting point of ThO_2 are more favourable than in the case of UO_2 and we do not anticipate any major problem For these reasons we have chosen at least at this stage the rather conservative average power density of $\rho = 55$ W/g[1]. The most exposed pins will operate at $\rho = 110$ W/g. The temperature of the fuel averaged over the core is then 908 °C. The average temperature of the most exposed pins is then 1210 °C and its corresponding hottest point 2350 °C, well below the melting point of ThO_2 which is 3220 °C

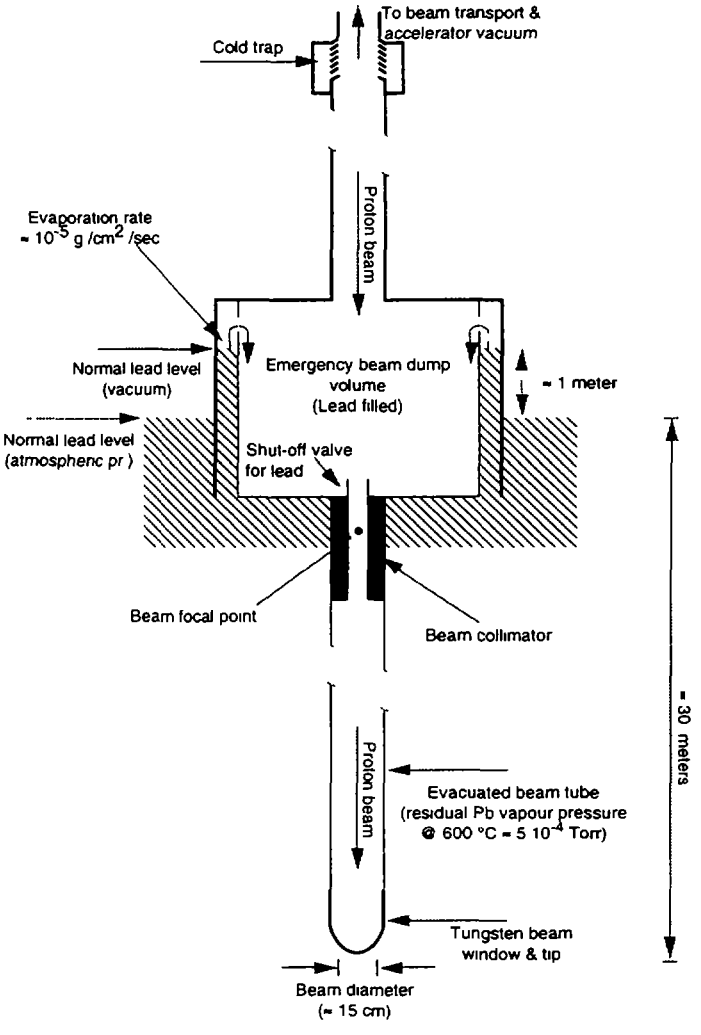

FIG. 4.7 The Emergency Beam Dump Volume (EBDV).

3) Some space must be provided for the fission fragments, which have in general a significant mobility, especially at high temperatures. The pressure build-up is not very different for different fissionable fuels and therefore the volume of the plenum for the gases due to FFs has been calculated taking into account the mechanical properties of the cladding under a specified pressure increase, assuming that all gaseous products escape the fuel. The plenum fractional volume turns out to be essentially the same as the one of the conventional pin designs for Fast Breeders (ALMR, EFR etc.). The hottest point of the cladding is 707 °C, well below the structural limits of the steel of the cladding[2]. Note also that, when compared to Sodium cooled pins, we are dealing with a single phase coolant with negative void coefficient.

We have therefore taken as reference parameters for our design pins (Figure 4.8) which are essentially the same as those used in our "FB-models" designs with, however, the following changes

(1) longer fuel pins to improve neutron containment in the core (1.5 m);

[1] This value is about one half of what is currently used in SuperPhenix and Monju

[2] The corresponding value for Monju is 675 °C

(2) a larger, variable pitch to accomodate the differences in hydraulics of molten Lead in a convective regime. Two different pitches have been used, a wider one for the Inner Core and a tighter one for the Outer Core;

(3) an appropriate "plenum" to ensure the required burn-up, but with smaller diameter and correspondingly more elongated in order to reduce the pressure drop through the core;

(4) cladding made of steel with low activation and small corrosion rate by molten lead (HT-9). More research work is still required to ensure an effective protection against corrosion (see paragraph D.3.4.3).

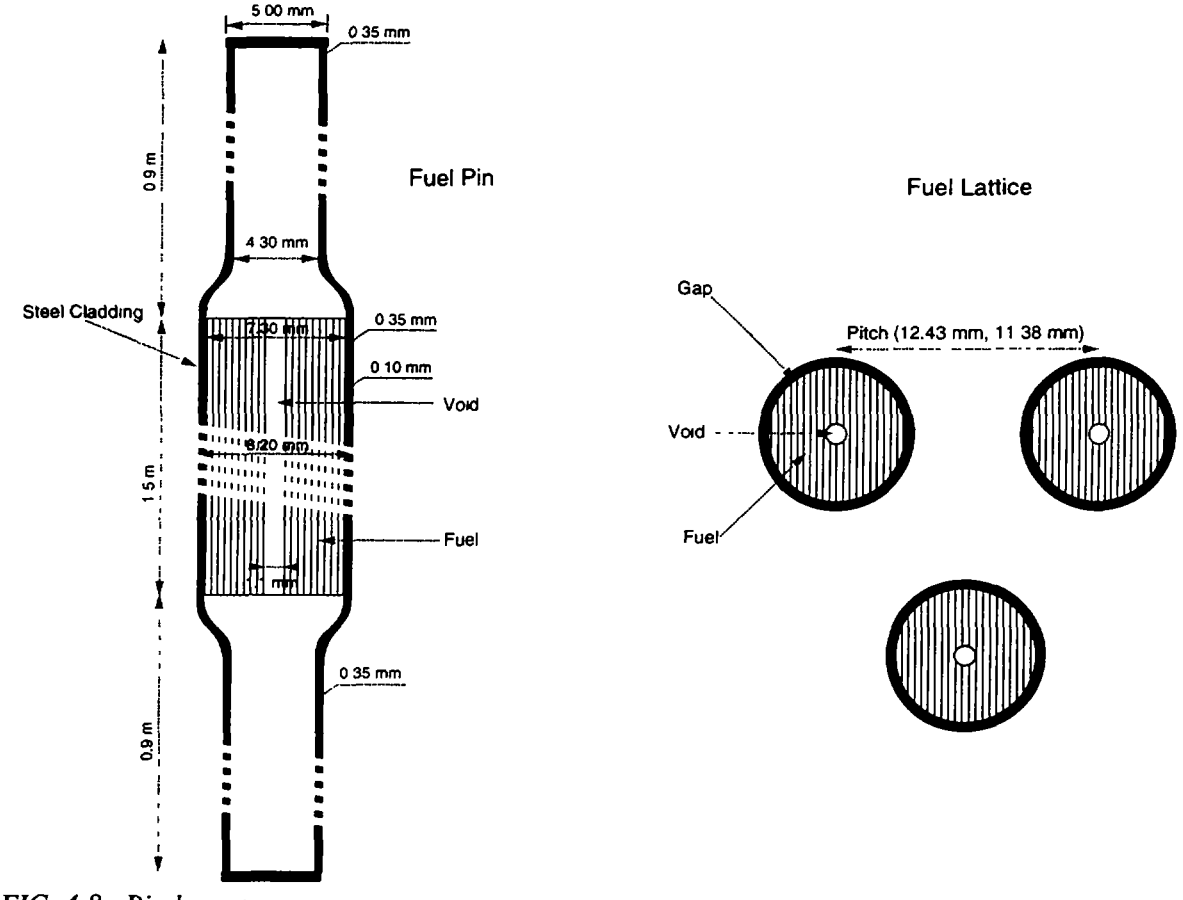

FIG. 4.8 Pin layout.

The general layout of the two fuel subassemblies is shown in Figure 4.9. Many of these subassemblies which have all the same flat to flat dimensions are arranged in a continuous, quasi circular geometry with an empty central region for the Spallation Target assembly and the molten Lead diffusing region. A few hexagonal elements are left empty for the scram device and other control functions.

The Breeder is designed to compensate for the reduction of the ^{233}U stockpile during the long burn-up and the inevitable losses due to reprocessing. Especially if the EA is started well below the breeding equilibrium, such an additional amount is small. Hence the breeder mass is typically some 20% of the total fuel mass. For simplicity, the pin and subassembly geometry have been taken to be the same as in the case of the Fuel elements. Toward the end of the fuel cycle, some significant power is produced also by the Breeder (ρ = 3.0 W/g), though much smaller than in the Fuel.

During successive fuel cycles, the isotopic composition of the Uranium changes, especially due to the production of a substantial amount of ^{234}U. In order to accomodate the extra mass some additional 20 cm of the fuel pin are left initially empty and progressively filled. Hence for asymptotic fuel composition, the active length of the fuel pins may be increased to as much as 1.70 m.

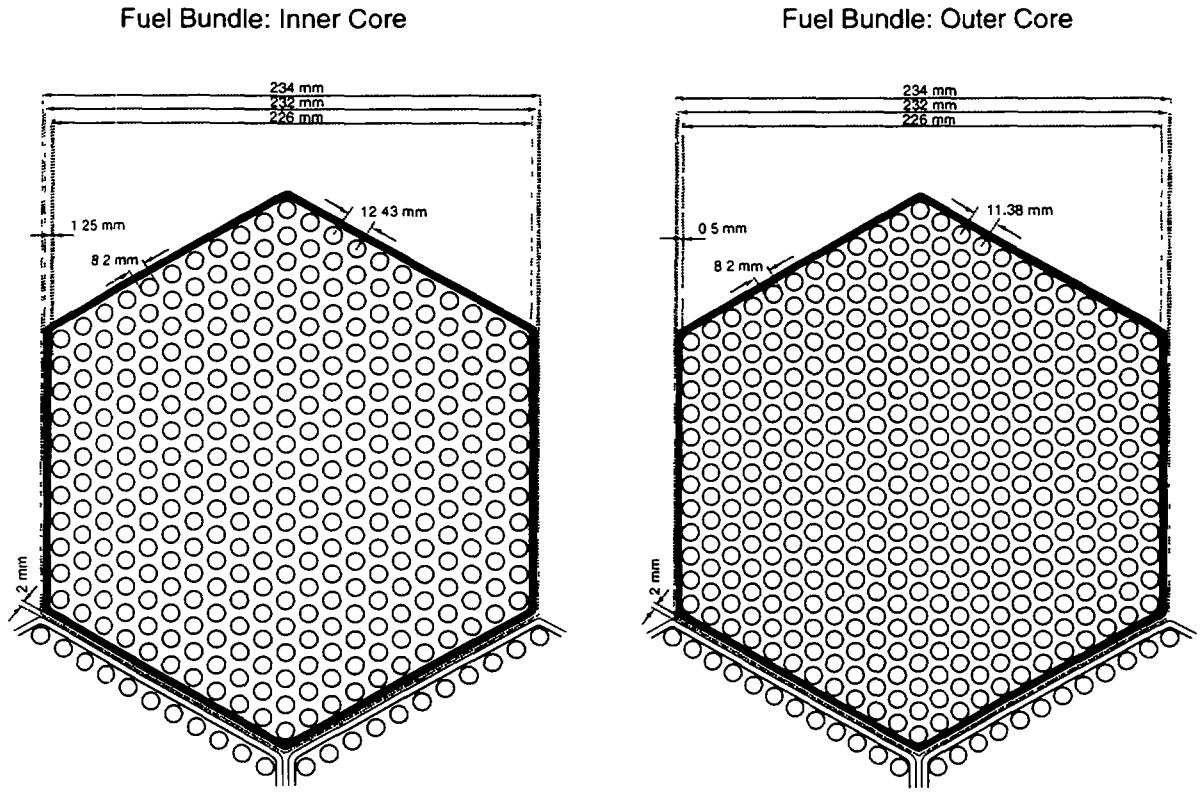

FIG. 4.9 General layout of a fuel sub-assembly.

Small amounts of Trans-uranic elements (Np, Pu and Am) and long lived ^{231}Pa are separated out during each reprocessing and re-injected in the EA for final incineration. It is convenient to insert these materials in special "incineration" pins which undergo no successive periodic reprocessing at least until a major fraction of the isotopes is incinerated. These pins have a much shorter fuel section and a much larger "plenum" section, to allow build-up of fission fragments. The lifetime of the cladding is limited by radiation damage. We have already estimated that the ordinary fuel exposure accumulates ≈ 34 d.p.a./year. Assuming an ultimate cladding lifetime of 250 d.p.a. these pins may last 7/8 years. After this time they must be reinforced with a second, fresh cladding or equipped with a new one. In order to ensure the fastest incineration these pins must be located where the flux is the highest, namely near to the target region.

The operating temperature of the plant is application dependent. In our basic design we have retained the choices of the reference design, which calls for a fuel outlet temperature of about 600 °C. It must be noted however that in principle the Lead coolant could permit a somewhat higher operating temperature, which is advantageous to increase the efficiency of the conversion into electricity and eventually to produce synthetic Hydrogen [4]. Evidently additional research and development work is required in order to safely adapt our present design to an increased operating temperature. In particular the cladding material of the fuel pins may require some changes, especially in view of the increased potential problems from corrosion and reduced structural strength[1].

[1] Titanium based alloys have been studied for the Fast Breeder and may be an interesting development for our application. In particular the corrosion of molten Lead on Titanium is very low.

The EA is based on a highly diffusive structure (molten Lead) in which a number of fuel elements are inserted. In absence of fuel, spallation neutrons produced roughly in the centre of the device will diffuse and loose adiabatically energy until either they are captured or they escape. If fuel is inserted gradually in the molten Lead medium, both the captured fraction in Lead and the escape probability will decrease. The fuel properties will gradually influence the neutronics. We consider as reasonable design parameter an escape probability ≤ 1% and captures in the Lead moderator of the order of 5-6% (Table IV.5). Note that

TABLE IV.5. TYPICAL NEUTRON CAPTURE INVENTORY OF A EA.

Zone-Wise			Fraction
Core			0.8879
Blanket			0.0456
Plenum			0.0277
Diffuser			0.0309
Beam Tube + Window			0.0005
Main Vessel			0.0073
Leakage			0.0012
Material-Wise			**Fraction**
Fuel (Th + U)			0.8493
Breeder (Th)			0.0427
Lead of which	percentage	Abs. Fraction	
Diffuser	(48.75 %)	0.0305175	
Plenum	(12.11 %)	0.00758086	
Core	(37.13 %)	0.02324338	
Blanket	(2.01 %)	0.00125826	
Lead Total			0.0626
Structures of which	percentage	Abs. Fraction	
Cladding	(83.28 %)	0.03780912	
Window	(1.03 %)	0.0004676	
Main Vessel	(15.69 %)	0.00712326	
Structures Total			0.0454
Leakage			0.0012

in an EA the neutron inventory is of primary importance and that these losses must be as small as possible. While in an ordinary PWR losses can be easily compensated with a more enriched fuel, the necessity of full breeding does not offer much degrees of freedom in an EA. On the other hand the void coefficient for molten Lead is negative and therefore the rather awkward measures ordinarily taken in a Sodium cooled device are no longer necessary. In particular one does not need to make the shape of the fuel core "pancake" like. A more spherical profile improves the neutron containment and hence the losses in the moderator.

Because of the long migration length in the Lead medium, these parameters are largely independent on the detailed geometry of the fuel and depend primarily on the fuel and diffuser masses. The core can be ideally divided into three concentric regions. The first region (the *Spallation Target*) has no fuel and it is

naturally filled by the molten lead. In this volume beam particles interact to produce primary neutrons. The radial size of such a volume has to be sufficiently ample in order to ensure that the neutron spectrum is made softer by the occurrence of (n,n') inelastic interactions in Lead. In this way the spectrum at the first fuel element is softened sufficiently as to ensure a minimal radiation damage to the structural materials and to uniformise by diffusion the vertical illumination of the fuel pins. We have chosen a radial distance of the order of ≥ 40 cm. With this choice, the calculated spectrum at the edge of the target region is not appreciably different from the one in the core. The second region is the *Main Fuel* region, in which a variety of fuels can be inserted (generally subdivided in two parts, the Inner Core and the Outer Core with different pitches), followed by a third region, the *Breeder* region, initially loaded with pure ThO_2 breeding material.

The nominal power of 1500 MW_t requires 27.3 tons of mixed fuel oxide at the average power density of 55 W/g. The duration of the fuel is set to be 5 years equivalent at full power. The average fuel burn-up is then 100 GW d/t-oxide. The main parameters of the Fuel/Breeder core are listed in Table IV.4. As already pointed out the breeding equilibrium concentration of ^{233}U, referred to ^{232}Th is $\xi = 0.126$. With such a high concentration there is obviously no problem in setting the wanted value of k and eventually even of reaching criticality. However with continued burn-up the fraction of captures due to FFs, ΔL_{ff} will grow linearly with time, absorbing for instance about 6% of all neutrons at 100 GW × d/t and causing a corresponding reduction in the criticality. The reduction of the multiplication coefficient $\Delta k_{ff} = -(\bar{\eta}\epsilon/2)\ \Delta L_{ff}$ will be very large. For instance, if initially we have $k = 0.98$ and $G = 120$, after 100 GW × d/t, $k = 0.908$ and $G = 26.0$. Such fivefold decrease of gain would be completely catastrophic. It is therefore preferable to start with a ^{233}U concentration lower than the breeding equilibrium and let it grow toward such a limit during burn-up. As already pointed out in paragraph D.3.2.7 one can realise a first order cancellation between the approximately linear rise of the FF captures and the exponentially approaching breading equilibrium. This leads to a much smaller initial ^{233}U concentration, $\chi = 0.105$.

D.3.4.7. CONVECTIVE PUMPING

Convection pumping is realised with the help of a sufficiently tall Lead column in which the warm coolant from the Core rises as a result of the large value of the Lead expansion coefficient, 1.32 kg m^{-3} K^{-1}. The coolant returns to the Core after being cooled down to the initial temperature by the heat exchangers. The pressure difference generated in the loop by the convective pumping action is given by $\Delta P = K\Delta T h g$, where ΔT is the temperature change, K is the coolant expansion coefficient, h is the height of the column and g the gravity acceleration constant. Typically for $\Delta T = 200$ °C, $h = 25$ m, we find $\Delta P = 0.637$ bars! Such a pressure difference is spent in order to put into movement the coolant and in stationary conditions it is equal to the sum of the pressure drops in the loop, primarily the pressure drops across the Core and the Heat exchangers. The pumping power required to move a volume V = 10 m^3/s of coolant with a pressure difference ΔP across the Core is $W_{pump} = V\Delta P = 0.647\ MW$. Such power must evidently be produced by the convective pump.

In order to dissipate a power q produced by nuclear reactions in the pin with a resulting temperature difference ΔT, the coolant must traverse the core with a speed v given by

$$v = \frac{q}{f_a \Delta T \rho c_p}$$

where f_a is the flow area and ρ and are c_p respectively the density and specific heat of the coolant. For cylindrical pins of radius $r \equiv [r_f, r_p]$ of the fuel and the plenum respectively arranged in an infinite hexagonal lattice of pitch p, the flow area is $f_a = \sqrt{3}p^2/2 - \pi r^2$ Neglecting end effects and the temperature dependence of the parameters, the pressure drop through the core ΔP consequent of a given flow speed v in the fuel which the pump must supply is given by

$$\Delta P = \frac{2\chi\eta l\rho v^2}{d_e}; \quad \eta = 0.079\times\left(\frac{\rho v d_e}{\mu}\right)^{-0.25}; \quad d_e = \frac{4f_a}{2\pi r}; \quad \chi = \frac{l_f}{l}+\frac{l_p}{l}\left(\frac{d_{e,f}}{d_{e,p}}\right)^{1.25}\left(\frac{f_f}{f_p}\right)^{1.75}$$

where χ is a geometry dependent factor, $l = l_f + l_p$ the pin length, divided in the fuel section and the plenum section; η is the friction factor, function of the Reynolds number, which in turn depends on the viscosity μ; $d_e \equiv [d_{e,f}, d_{e,p}]$ is the effective diameter of the fuel and the plenum and, function of the coolant flow area $f_a \equiv [f_f, f_p]$ and of the so-called wetted perimeter. Additional corrections which typically amount to a maximum of 8% are due to the abrupt changes of the coolant flow area:

$$\Delta P = \frac{2\chi\eta l\rho v^2}{d_e}+\frac{\rho v^2}{4}\left[\left(1-\frac{f_p}{f_o}\right)\left(\frac{f_f}{f_p}\right)^2+\left(1-\frac{f_f}{f_p}\right)+2\left(1-\frac{f_p}{f_f}\right)^2+2\left(1-\frac{f_o}{f_p}\right)^2\left(\frac{f_f}{f_p}\right)^2\right]$$

where f_o is the free flow area. With these corrections, the results of the formula [54] are in excellent agreement with the full hydrodynamic code COBRA [55].

In practice we take the temperature difference ΔT as an input design parameter, which determines the primary pressure difference ΔP_{pump} for a given convective pump column of length L. Such pressure difference must get the coolant through the Core, the heat exchangers and the full loop (> $2L$ long) at a sufficiently high speed as to transfer the large amount of heat produced from the Core to the secondary loop. In order to provide sufficient margin for the other pressure drops, somewhat arbitrarily we have set the pressure drop across the core to 0.7 ΔP_{pump}, setting in this way the pressure and the temperature differences across the core. The pitch size of the lattice can be adjusted next in order to set the coolant speed v through the core to the value required by the actual power density and by ΔT. The resulting pitch and coolant speed as a function of the power density in the pins is given in Figure 4.10a and Figure 4.10b for L= 25 m and different temperature differences in the range 150 °C to 250 °C. They appear quite acceptable.

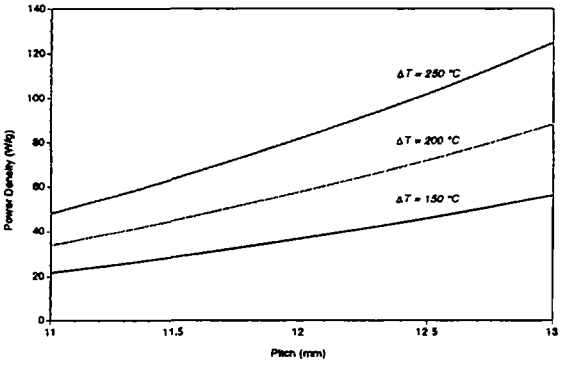

FIG. 4.10a Power density in the pins as a function of pitch.

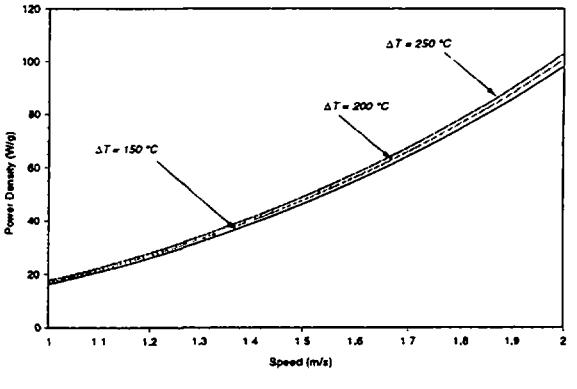

FIG. 4.10b Power density in the pins as a function of coolant speed.

Since the power density produced in the fuel rods is falling about linearly with the inverse of the radius, the resulting pitch will be a smooth function of the core radial co-ordinate, leading to a pitch size decreasing with radius. In practice and in order to permit the same flat to flat dimensions for the fuel bundles across the core and a given fuel pin radius, we have actually quantified the pitch into discrete values corresponding to different number of integer rounds of hexagonal shape. This leads to some residual radial dependence of ΔT, which is partially absorbed by natural mixing along the convective column and it should be compensated restricting the flow for instance at the entry of the fuel bundles. Evidently a radial pitch variation affects also the neutronics of the core, which in turn has effects onto the power density. Hence, all these parameters have to be recurrently adjusted to their optimal values.

The motion of the warm coolant in the convective column is the key to the convective pumping and it has been carefully simulated with help of the full hydrodynamic code. The actual temperature and speed distributions at the exit of the core have been used as input in a simulation of the rising liquid.

The speed and temperature of the coolant gently homogenise along the path through the column as shown in Figure 5.12 in the following section. The programme described in paragraph 5.5 to which we refer for more details reproduces the main results of our simpler analysis.

The previous calculations are made for the nominal power of the EA and stationary conditions. It has been verified that correct cooling conditions persist over the full range of conceivable powers, including decay heat and major transients. In general, convective cooling has "self-healing" features, namely the pumping action is directly related to the amount of power to be transported.

In stationary conditions and at the nominal power, the ≈ 10,000 tons of coolant will flow through the core at the rate of some 52 t/s, corresponding to a turn-around time of the order of 200 seconds for a total length of the loop of the order of 50 metres. In view of the large mass of the coolant, a considerable momentum is stored in the coolant during normal operation and it has considerable effect in (fast) changes of conditions.

D.3.4.8. SEISMIC PROTECTION

As already pointed out in order to reduce capital costs and increase flexibility large portions of the EA plant should be standardised. Furthermore, to gain public acceptance, the plant must be reliable and should have passive inherent features. Seismic design can play a major role in achieving a standardised design which could accommodate a range of seismic conditions. One approach to standardisation would be to design a plant using traditional methods for a Safe Shutdown Earthquake (SSE) which envelopes the responses of 90 percent of existing nuclear sites in the USA. This is the present licensing seismic basis (RC 1.60) and it calls for a maximum horizontal and vertical acceleration (PGA) of 0.30 g.

This approach, however, would lead to high seismic loads, especially in components and equipment, and would still exclude for instance California sites and limit the export potential of these plants to high seismic countries such as in the Pacific Rim region. Liquid Metal designs which consist of thin walled vessels designed to accommodate large thermal transients under low operating pressures are more sensitive to seismic loads and thus the EA would be particularly penalised by this approach. An appropriate design of a modular EA requires to be able to accommodate a variety of seismic conditions expected at a wide range of sites, from deep soil sites with a minimum shear wave velocity to stiff rock sites.

The alternative is to seismically isolate the plant. Several studies performed in Japan have shown that it would not be possible to design large LMR plants which are economical in areas of high seismicity without incorporating seismic isolation [56]. In an isolated plant, the design and qualification of equipment and piping and their supports become a simpler task than it is today and the impact of seismic design on preferred equipment layouts is minimised. Since the response of isolated structures is highly predictable, the risk of accidents due to uncertainties in the input motions is reduced, safety margin is increased, and plant investment protection is enhanced. Additionally, if seismic design criteria are upwardly revised, for example due to the discovery of unexpected geo-tectonic conditions, the standard plant design would probably not have to be altered and only the isolation system would need to be upgraded.

Seismic isolation is a significant development in earthquake engineering that is gaining rapid world-wide acceptance in the commercial field [57]. This approach introduces a damped flexible mechanism between the building foundation and the ground to decouple the structure from the harmful components of earthquake induced ground motion, thus resulting in significant reductions in seismic loads on the structure and more significantly on equipment within the structure. In recent years, seismic isolation of nuclear structures has been receiving increased attention. To date, six nuclear power plant units in France and South Africa have been isolated. It is expected that seismic isolation will play a major role in the design of the advanced nuclear plants of the future in the US as well as in Japan and Europe.

Several technological advancements are responsible for making seismic isolation a practical alternative. These include the development of highly reliable elastomeric compounds used in seismic bearings which are capable of supporting large loads and accommodating large horizontal deformations during the earthquake without becoming unstable. Additionally, the development of high damping elastomers and other mechanical energy dissipators has provided the means to limit the resulting displacements in the isolators to manageable levels. Other factors include the availability of verified computer programmes, the compilation of reliable test results of individual seismic isolators under extreme loads, shake table tests for evaluating system response, and validation of computer programmes and confirmation of the response of isolated buildings during earthquakes [58].

Seismic isolation has been included in the EFR and in the ALMR designs. Most of this work is relevant also to our case. The ALMR design calls for a seismically isolated platform which supports the reactor module, containment, the reactor vessel auxiliary cooling system and the safety related reactor shut-down and coast-down equipment. The total mass to be insulated is of the order of 25,000 tons. The fragility of components appears greatly improved by insulation [59]. Some model tests have confirmed the results of these estimates [60]. Our present design can include most of the features of the ALMR design.

D.3.4.9. DECAY HEAT REMOVAL BY NATURAL AIR CONVECTION

Nuclear industry has developed a number of passive natural convection air cooling systems to remove decay heat in the unlikely event that all active cooling systems of a reactor fail [11] [61]. We have applied the design made for the ALMR (RVACS) to the EA, in order to study the behaviour of our system in caseof such an event[1].

The application of the RVACS to the Fast Energy Amplifier is illustrated in Figure 4.1b.

In the unlikely case of a scram event in which all the active cooling systems fail to operate, the heat produced by the fission products decay in the core increases the average temperature of the lead contained in the vessel. Lead expands (the level rising at the rate of 27 cm/100 °C) and when its temperature exceeds a determined safety margin, it overflows into a narrow gap between the main vessel and the containment vessel. This gap is normally filled with Helium which ensures a reasonable thermal isolation during normal operations.

The containment vessel is in contact with ambient air entering the system through a cooling channel. Air reaches the bottom of the vessel through a downcomer channel which is thermally isolated from a riser channel, in direct contact with the vessel.

When the lead fills the gap, a good thermal contact is established between the main and the containment vessels, and heat can be transferred to the air in the riser channel. Air temperature increases, and a natural circulation starts. Air draft is enhanced if a long chimney (about 30 m) is added at the end of the riser channel. The downcomer and riser channels consist of two annular regions around the vessel of respectively 18 and 57 cm thickness. In such conditions, for a vessel temperature of 500 °C, the air velocity attained in the hot channel is of the order of 10 m/s, corresponding to a flow rate of 53 m^3/s. The

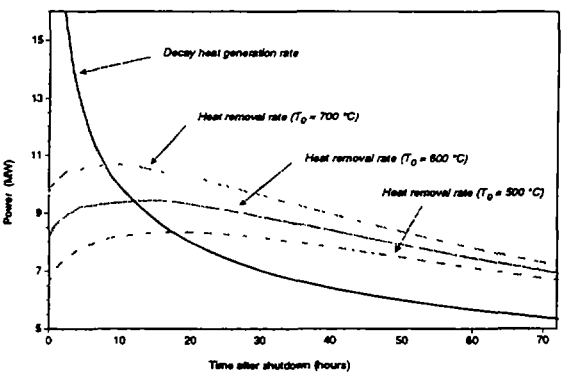

FIG. 4.11 Decay heat generation and heat removal rates during a scram event.

[1] We built a thermal-hydraulic model using the code STAR-CD [51]. The numerical model simulates the natural convection of air in the system, by taking into account convective and radiative heat transfer from the surface of the vessel to the air cooling channel.

average outlet temperature of the air is about 177 °C and the heat removal rate of the order of 6.5 MW, which is linearly dependent on the vessel temperature.

Decay heat is therefore extracted by a simultaneous process of internal (lead) and external (air) natural convection, conduction (through the steel of the vessels) and radiation (from the external vessel into the riser channel).

The core decay heat generation and the RVACS heat removal rates during a scram event are shown in Figure 4.11. At the beginning the decay heat generation is at a much higher rate than the heat removal. Consequently, the lead heats up very slowly, thanks to the large thermal capacitance of the F-EA. The RVACS heat removal rate increases slowly with the gradual increase in the reactor vessel temperature. When the decay heat generation rate and the heat removal rate are equal, the system reaches its highest temperature. From then on, the removal rate exceeds the decay heat generation rate, and the average temperature of the vessel slowly decreases.

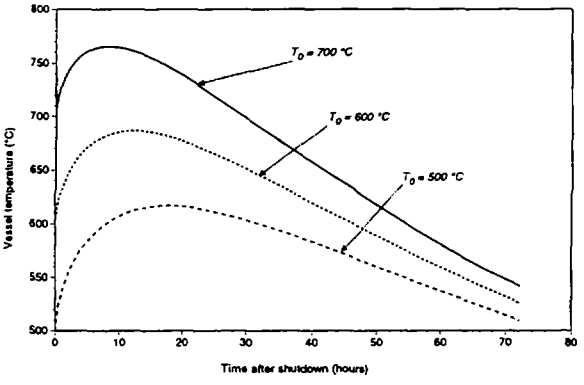

FIG. 4.12 Evolution of the vessel temperature during a scram event.

The thermal transient experienced by the F-EA vessel for different starting temperatures is shown in Figure 4.12. It consists of a slow increase over many hours to a peak temperature followed by a gradual cool down. The peak temperature is reached much earlier (and has a lower value compared to the starting temperature) in the case of higher starting temperatures, since the heat removal rate is higher.

The RVACS is based on the natural mechanism of lead dilatation and air convection. It is therefore completely independent on active components or operator actions, and insensitive to human errors.

D.3.4.10. MISCELLANEA

The on-line, continuous determination of the multiplication coefficient k is essential in order to monitor the correct operation of the EA. The method we propose is based on the lifetime of the fast neutrons after a sudden shut-off of the proton beam (source). This is easily performed gating-off the ion source for a period of time of the order of a few hundred microseconds. The effects on the RF-cavities of suddenly removing the beam load is still being investigated, but it should be manageable by the control system. The time of the neutron activity is roughly exponential, with a time constant proportional to 1/(1-k). Monitoring of the k-value can be performed continuously as a part of the standard operation mode of the Accelerator.

Scram devices are used to anchor the k of the EA to a sufficiently low value during shutdowns, emergencies, etc. This is performed with the help of a series of blocks of CB_4, conveniently located throughout the Core. This material is very effective: about 20 kg of CB_4 diffused uniformly throughout the core produce a reactivity change $\Delta k = -0.04$. There are three types of such devices: (1) ordinary scram, performed with an appropriate, fast-moving mechanical device, (2) emergency scram, based on the design of the ALMR "ultimate shut-off" in which many small spheres of CB_4 are dropped by gravity inside an evacuated tube which descends to the Core, and (3) the Molten Lead Activated Scram (MLAS), associated with the siphon overflow triggered by the excessive expansion of the Lead and consequent level increase in the vessel. As already amply discussed, this trigger activates also the RVACS to convey the extra heat to the surrounding air and blocks the proton beam from entering in the core region, filling with Lead the emergency beam dump volume (EBDV).

The conceptual design of the MLAS is shown in Figure 4.13. If the molten Lead is penetrating through the siphon, RVACS dedicated volume etc., a small fraction fills the long thin tube descending down to well below the core region. At this depth the pressure of the liquid will be of the order of 30 atm, which is amply

sufficient to push upwards the CB_4 blocks well inside the core. A second tube is used to exhaust the neutral gas (Helium) which is normally filling the tubes. The CB_4 blocks, in presence of Lead, will be held firmly in place by the buoyancy of the liquid.

A lead purification unit is needed to remove impurities from the liquid and to ensure that the required additives against corrosion are effective. The detailed parameter list of this device is for the moment largely unknown, pending the results of the corrosion studies (see paragraph D.3.4.3). Some way as to heat-up the Lead whenever appropriate is also necessary.

The heat exchangers are relatively conventional, except that they must be designed in order to introduce a small pressure drop across the primary circuit in order not to hamper natural convective cooling. At this stage we have assumed that the pressure drop is about 1/3 of the one across the main Core. We have verified that this choice is not critical to the performance of the convective cooling. We have indicated that the primary coolant should not contain an appreciable amount of Bismuth because of activation problems. This precaution does not apply of course to the secondary loop which can be filled with a Lead-Bismuth eutectic mixture. The Pb-Bi eutectic mixture has a melting point in the vicinity of 125 °C and it has been chosen to avoid freezing of the coolant in the transmission line.

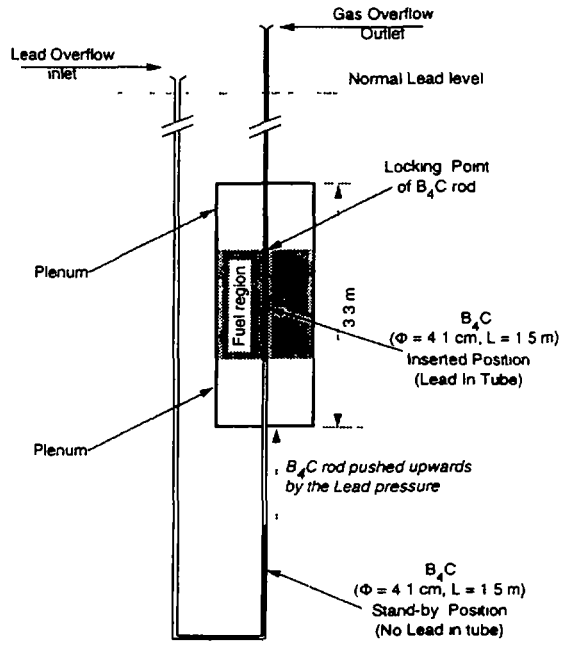

FIG. 4.13 Conceptual Design of MLAS.

The EFR design has foreseen a convection driven cooling loop which performs a function similar to the RVACS. If considered necessary it could be added also to our design, although it is introducing a duplication which may be redundant. It could be considered as an alternative to the RVACS system. In the EFR design the decay heat is extracted by six additional heat exchangers of 15 MW each which reject excess heat directly in the environment. These Direct Cooling Systems (DCS) consist each of a (Lead-Bismuth eutectic mixture) filled loops. These loops extract heat from the hot pool of the primary molten metal by immersed Pb/Pb-Bi heat exchangers and reject the heat to the environment with Pb-Bi/air heat exchangers located well above the pool level. One of these DRC units relies exclusively on natural convection heat transfer and natural draught on the air side. The other is normally operated with forced flow. Each loop is equipped with an electromagnetic pump and two fans in parallel on the air side. These active loops possess passive heat removal, if pumps and fans are off to about 2/3 of that of the active flow mode. A special Pb-Bi heat exchanger freezing protection insures that the temperature in individual pipes cannot fall below 140 °C.

A large number of monitoring devices are required to follow the radiation monitoring, neutronics, the hydraulics (speed and temperatures) and the potential corrosions due to molten Lead.

D.3.4.11. CONCLUSIONS

In this section, we have presented the conceptual design of an EA with a power rating (1500 MW_t, 675 MW_e) that is of direct relevance to the modules presently considered by nuclear industry to meet the needs of utilities. Such a machine represents in our view a real breakthrough in the prospects of nuclear energy in setting the highest standards for safe and economical operation, coupled with realistic solutions for waste disposal and non-proliferation issues.

The machine is always subcritical. There are no control bars and in normal operation, the level of power is controlled entirely by the accelerator beam via a feed-back loop. The separation between the accelerator vacuum and the active medium (a "frequently asked question") appears entirely solved by a specially designed window that would be routinely changed once a year. Even if the window broke, which is unlikely, there would be no serious consequence and the EA would be brought to a safe halt, even without human intervention.

Conspicuous in our design is the absence of coolant pumps: the heat is evacuated by convection alone and transferred to the outside world through heat exchangers via a secondary cooling loop. Convection cooling is a unique feature for such a large power, and is only made possible by the use of molten Lead as coolant. The absence of pumps has advantages from the safety and maintenance point of view (no moving parts). In fact the whole vessel could be sealed during the long interval (five years) between refuelling as the owner utility has no valid reason to intervene inside. Obviously this offers an extra means of monitoring, by the controlling bodies of non-diversion of fissile material. The economical aspect is also important. Suppressing the pumping system is a substantial simplification in construction as well as a sizeable economy in capital costs.

The burn-up of the fuel is a key parameter in the economic performance of the EA. The EA achieves an average burn-up of 100 GW × d/t, whilst maintaining during that time a practically constant gain at the nominal value of G=120, corresponding to k = 0.98 with no external control devices. This is possible because one can compensate the loss of reactivity due to FF accumulation by starting the EA with less ^{233}U than the amount which would correspond to breeding equilibrium. Such a burn-up is matched to the radiation damage and the pressure build-up of fission product gases of the fuel pins. The average power density has been set to the conservative value of 55 W/g which is one half the value considered in Fast Breeders. This necessitates of course having a larger fuel load (for the nominal power of 1500 MW_t one requires a 27.3 tons load of mixed fuel oxide) which has no serious consequence since the fuel is inexpensive. On the other hand, the low burn-up rate translates into a rather long time between refuelling (5 years). This long time between access to the fuel has the important consequence of minimising the radiation dose absorbed by workers. There is no need to have a permanent crew on site devoted to fuel changes and this could probably be the task of travelling crews of specialists, conceivably under some kind of international supervision to insure no possibility of fuel diversion.

A machine designed today should put strong emphasis on safety issues. This has been a prime consideration during our design. First of all, the machine is safely subcritical, since any reactivity excursion leading to an increase in power output, will be immediately corrected by a strong negative temperature effect. The main difference with a Sodium based FB here is the absence of a positive void coefficient which could cause the latter to become prompt critical. Then, in the unlikely case of an accident that would not be corrected by human intervention or electronic feedbacks, passive measure would be implemented relying on basic properties such as thermal expansion of Lead, gravity, natural convection in molten Lead, circulation of air, and radiation. The result would be to bring the machine quickly to a halt and safely bleed the radioactive decay heat to the environment. At no point could a temperature increase occur that would cause the core to melt or otherwise lead to a radioactive release in the environment.

Molten Lead has in our view considerable advantages over Sodium, and its choice has been essential to us, not only in the physical principle of a Fast Neutron EA, but also for the inherent safety features which we have just discussed. Objections against the use of Lead have often been raised in the past on the grounds of its supposedly corrosive action on steel. We believe that up to the 550 °C - 600 °C region, on which we have based the present model, there is enough experience (or reasonable extension of known facts) to plan safely on using a known material such as HT-9 for fuel cladding. However, we believe it would be desirable in the future to go to higher temperatures (800 °C), for processes such as Hydrogen production or in order to increase the efficiency of electricity production. For that temperature range, further R&D would be needed.

D.3.5. COMPUTER SIMULATED OPERATION

D.3.5.1. SIMULATION METHODS

Many classic programmes [34] exist which can calculate the neutronic behaviour of a sub-critical system. However such programmes have major limitations, namely (i) they operate on a given concentration of isotopes, while in our Amplifier the concentration of elements varies dynamically during burn-up or (ii) they are based on multi-group calculation methods and therefore take only approximately into account the narrow resonances in the Lead Moderator and in the Fuel. Finally the proton initiated cascade involves many reactions (spallation etc.) which have important effects on the composition of materials, especially at discharge. Therefore, appropriate Montecarlo methods have been developed in which the full evolution with time of the Amplifier is simulated.

The high energy cascade has been simulated with the help of the programme FLUKA [50] which is known to give a very realistic representation of the many processes in the energy interval of interest. The spallation neutron yield predicted by FLUKA has been compared with experimental data collected at CERN, where a proton beam of different kinetic energies in the interval of interest has been made to interact with Lead targets of different dimensions [3]. The neutron flux emitted has been measured after thermalization in water. The results show an excellent agreement between the experimental results and the predictions of FLUKA [62]. The agreement is typically better than a few percent.

The FLUKA cascade development is, however, still insufficiently accurate to emulate the complex neutronic behaviour below a few MeV. A second programme has been written, based on the ENDF-6 cross sections [30], which follows with Montecarlo technique the fate of neutrons in the Amplifier and the corresponding evolution of the local composition of the fuel elements. The volume of the Amplifier is segmented in a large number of separate regions with independently evolving concentrations and an accurate model of the geometry has been used. The validity of our calculations has been cross-verified with more classic programmes [34]. However all programmes rely on the same cross section data.

While the basic Nuclear Data used in the calculations on the $^{238}U/^{239}Pu$ cycle have been repeatedly checked and improved over the years, some uncertainties have persisted on the cross section data required to predict the Thorium based cycle. Fortunately a rather precise integral experiment has been carried out in the PSI zero-power reactor facility, PROTEUS [63]. These results indicate that the breeding characteristics of heterogeneous ^{232}Th-containing fast reactor cores are predictable to an accuracy comparable to that of ^{238}U-containing systems. Measured and calculated spectra appear in general agreement with calculations based on cross section data [30]. We believe that the underlying physics information is sufficiently well known and verified to predict the behaviour of the EA.

Neutrons spend a considerable fraction of their life span in molten Lead. Lead cross sections have been well measured, but very little experience exists to date on the behaviour of neutrons in a Lead Moderator/Reflector. An experiment in which a spallation neutron source is imbedded in a large Lead block is in progress at CERN in order to compare predictions and experimental data [6].

The Montecarlo simulation starts with a proton beam of specified geometry and a given initial composition of elements in the Amplifier. The geometry of the EA is realistically represented. Various geometrical components are segmented in smaller units that we denominate as "pixels", in order to be able to record the differences in composition as a function of the location during burn-up. In the case of mixing liquids, like for instance the molten Lead, a common concentration table is used. The continuous proton beam is replaced with a limited number of protons which enter the EA at a specified event rate $f_p = 1/t_p$. The fate of these protons is initially determined by FLUKA in a phase in which a number of spallation neutrons are generated. These neutrons are subsequently followed inside the EA to their final destiny by our dedicated programme. Each particle is given a "weight" w in order to scale up the event rate to the number of protons actually introduced by the Accelerator, namely $w = i\ t_p/e$, where obviously i is the proton current and e its elementary charge. Wherever available, a set of 35 possible reaction channels [30], which include inelastic processes like n-n', n-2n, n-p, n-α and so on, are used to construct the development

of the cascade. Secondary neutrons produced by these reactions become the source of additional cascades.

As a consequence of the cascade produced by each proton, the chemical composition of the target pixels is significantly affected. We therefore change the composition of each relevant pixel according to the nature of the interaction, replacing the initial nucleus with the fragments of the reaction and in the case of fission with the appropriate fission fragments, but with a weight w, namely as if all the protons over the time t_p had produced the same reaction. Clearly this approximation will vanish over a large number of events. Spallation products generated by FLUKA are also included.

After the full cascade of a given proton has been followed to its finish line and all pixel concentrations have been changed accordingly, concentrations of all pixels are evolved over the time interval t_p with the help of a full Bateman formalism, in preparation for the next proton shot. In particular the complete decay chain for each element is followed up to the stable elements with the corresponding concentrations in the pixels of the relevant new elements, whenever appropriate. The decay schemes for all known elements, including all possible branching ratios is provided by an appropriate database [31].

Typically the programme will operate with some 1200 different nuclear species (mostly fission and spallation fragments) and up to 256 different pixels of a variety of shapes and sizes. The computing speed on an ALPHA computer is of 50 neutron histories/sec. About one week of computer time is needed in order to obtain adequate statistics on a typical burn-up of 100 GW × d/t, corresponding to about 3×10^6 neutron histories.

The Montecarlo technique and the evolutive nature of the programme permits to introduce quite realistic simulations of the operation of the EA. For instance it is possible to adjust the beam current in order to ensure a specified power output or to simulate power variations and transients. The relevant parameters of the neutronics, (multiplication coefficient k, neutron spectrum, fission fragment poisoning, fuel/breeder ratio and so on) are in this way accurately followed over a specified burn-up. Periodically, the fuel pin location may be shuffled to improve uniformization of burning. At the end of the calculation, the complete list of elements in the various parts of the Amplifier is provided and used to study reprocessing and refuelling. The refuelling can also be simulated, introducing appropriate changes in the pixel concentrations. The asymptotic concentrations after many refuelling and the overall performance of the device can be realistically simulated. The activation of the various parts of the EA can be accurately studied.

We have verified that the values of the main parameters of a sub-critical device obtained with our programme are in excellent agreement with the results of more classic programmes [34]. In particular the value of the multiplication coefficient k in the two methods typically agree to better than a fraction of a percent.

D.3.5.2. SIMULATION OF THE STANDARD OPERATING CONDITIONS

We consider first the simulation of an initial load of fuel made of ^{232}Th-oxide with an initial concentration of pure ^{233}U-oxide, chosen to ensure the wanted initial value of the multiplication coefficient k_o. The initial choice of the multiplication parameter is set high enough in order to make the best possible use of the current of the Accelerator, but low enough as to avoid that the machine in some circumstance may become critical. The main parameters of the EA are the ones listed in Table IV.1. Note that a real life situation may be slightly different since the Uranium fuel bred, for instance starting with spent fuel from a PWR (see section D.3.5.3) or coming from a previous cycle, will contain also some other isotopes, like ^{232}U, ^{234}U etc. As amply discussed in paragraph D.3.2.8, they are not such as to modify the general features of the results, which become more transparent by our simplifying assumption.

In order to simulate as closely as possible the real operating conditions of the EA, the programme can, during execution, change the current of the accelerator in order to ensure a constant power output. This is done introducing a sort of "software feedback" in which the beam current is adjusted for instance every 100 incident protons in such a way as to maintain constant the output power. The typical computer run covers

of the order of some 2000 days of operation or a burn-up in excess of 100 GW × d/t. The integrated burn-up versus simulated time of operation is shown in Figure 5.1. The proton beam feed-back is the only control mechanism and control rods are absent.

In Figure 5.2a we display the accelerator current chosen by the programme as a function of the burn-up in order to produce a constant power of 1500 MW (Figure 5.2b). The variations of the current reflect the variation of the gain G (Figure 5.3), which in turn is primarily determined by the value of the multiplication coefficient *k* (Figure 5.4).

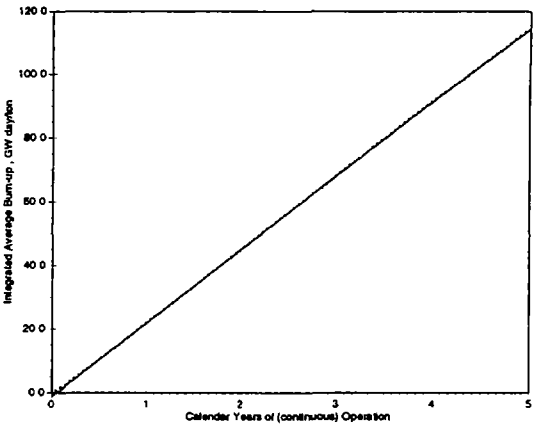

FIG. 5.1 Integrated burn-up versus simulated time of operation for an initial ^{233}U filling and pre-set regime at k ≈ 0.98. Related parameters of the EA are given in Table IV.1.

TABLE V.1. POWER DENSITY DISTRIBUTION, IN UNITS OF AVERAGED POWER, OVER THE CORE. DATA ARE FOR AN AVERAGE POWER DENSITY ρ = 52.76 W/g OF MIXED FUEL OXIDE.

Radial	(Bottom)	--		Segmentation along fuel pins					--	(Top)	Average
↓Segm.↓	1	2	3	4	5	6	7	8	9	10	over pin
Fuel section											
5	1.42	1.74	2.15	2.43	2.62	2.62	2.41	2.1	1.7	1.4	2.06
6	1.28	1.58	1.88	2.18	2.35	2.33	2.14	1.88	1.54	1.24	1.84
7	1.2	1.47	1.77	1.99	2.12	2.11	1.99	1 74	1.45	1.16	1.7
8	1.12	1.36	1.66	1.84	1.97	1.97	1.86	1.63	1.35	1.1	1.59
9	1.05	1.29	1.52	1.71	1.79	1.81	1.7	1.54	1.28	1.02	1.47
10	0.97	1.2	1.45	1.58	1.67	1.69	1.57	1.43	1.18	0.96	1.37
11	0.91	1.12	1.32	1.47	1.53	1.54	1.46	1.3	1.1	0.9	1.27
12	0.82	1.01	1.19	1.33	1.4	1.42	1.32	1.2	1.01	0.82	1.15
13	0.74	0.91	1.07	1.19	1.26	1.25	1.2	1.08	0.91	0.74	1.04
14	0.66	0.82	0.97	1.07	1.11	1.12	1.06	0.95	0.8	0.66	0.92
15	0.6	0.71	0.83	0.92	0.95	0.96	0.92	0.84	0.69	0.58	0.8
16	0.51	0.6	0.7	0.77	0.81	0.8	0.78	0.7	0.59	0.5	0.68
17	0.44	0.49	0.56	0.62	0.65	0.66	0.63	0.57	0.49	0.42	0.55
18	0.38	0.4	0.46	0.5	0.52	0.52	0.51	0.46	0.4	0.37	0.45
Breeder section: Power proportional to burn-up. Values for 100 GW × d/t											
19.00	0.07	0.07	0.09	0.10	0.11	0.11	0.09	0.09	0.07	0.07	0.09
20.00	0.07	0.08	0.07	0.08	0.09	0.09	0.09	0.08	0.07	0.07	0.08

The other two most relevant quantities are the (atomic) concentration of ^{233}U, normalised to ^{232}Th, averaged over the core (Figure 5.5) and the ^{233}Pa (breeding) concentration, normalised to ^{233}U (Figure 5.6). As is well known, this last concentration is closely proportional to the power density. By inspection of these figures,during burn-up we can distinguish two phases.

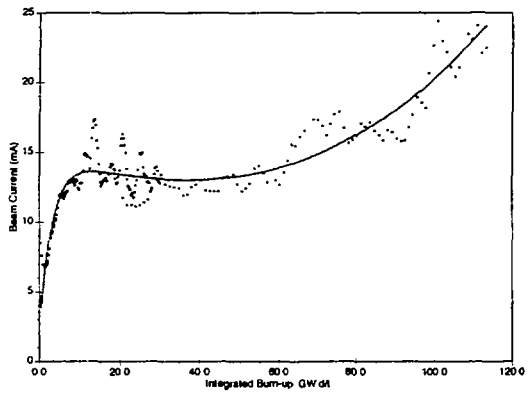

FIG. 5.2a Accelerator current chosen by the programme as a function of the burn-up in order to produce a constant power of 1500 MW. Related parameters of the EA are given in Table IV.1.

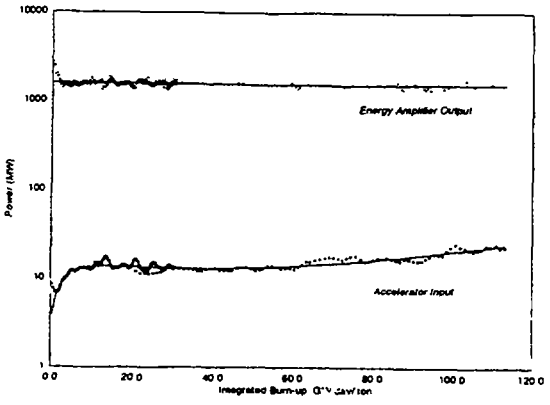

FIG. 5.2b Resulting EA power output as a function of burn-up with appropriate variation of accelerator.

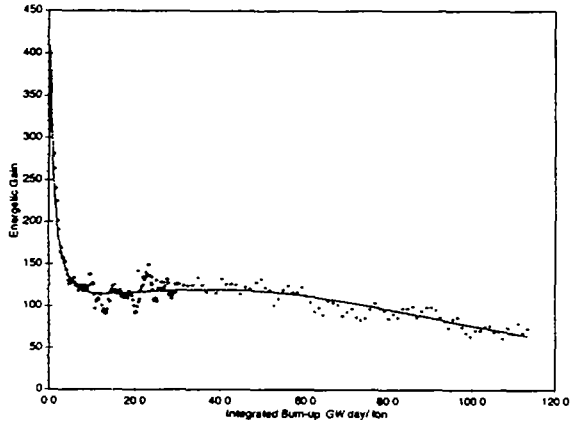

FIG. 5.3 Energetic gain G of the EA as a function of the burn-up. Same conditions as Figure 5.1.

A first, relatively short initial phase in which a fraction of the initial ^{233}U is burnt and the breeding process based on the ^{233}Pa is setting on. During this period the multiplication coefficient, and hence the gain, is dropping typically by $\Delta k = -0.01$. This is normally handled by modulating the proton beam current automatically through the feed-back control system. Since the regime value of $k = 0.98$ has been set (see Table IV.1) the initial value of k at the cold initial start-up will be correspondingly higher, namely about $k_o \approx 0.99$. In real life and provided such a number would be considered as too high, one can during this initial phase introduce for instance some small amounts of neutron absorbing, "burnable poison" materials which are quickly transmuted and keep the value of k within the specified range. Alternatively the fuelling can be done in phases, installing inside the core a small fraction of fuel elements only after an initial period ($\approx$ 10 GW x d/t) with the help of the refuelling machine. Note that storage space is provided inside the vessel for such elements.

This initial phase is followed by a regime phase in which the ^{233}U and the other isotopes tend exponentially to the breeding equilibrium and in which the Fission Fragments (FF) captures[1] grow roughly linearly with burn-up (Figure 5.7) and their effect on k is almost compensated by the increase in concentration of ^{233}U tending to the breeding equilibrium (Figure 2.5). One can adjust such a compensation numerology in such a way as to achieve an almost perfect cancellation over a long burn-up with a remarkably constant value of k and hence of the gain. But towards the end of the chosen burn-up the exponential growth of the ^{233}U concentration flattens out, while the FF growth remains essentially linear, thus causing a drop of the gain and a corresponding increase of the proton beam current required to maintain a constant power output. The maximum available current is set by the parameters of Table IV.1 and hence it determines the ultimate burn-up of the system without refuelling. This effect can be attenuated with more elaborate multiple refuelling schemes. In analogy to standard techniques of PWRs fresh batches

[1] Of course only those elements for which cross sections are known are accounted for. We believe that the correction for the other elements is not very large.

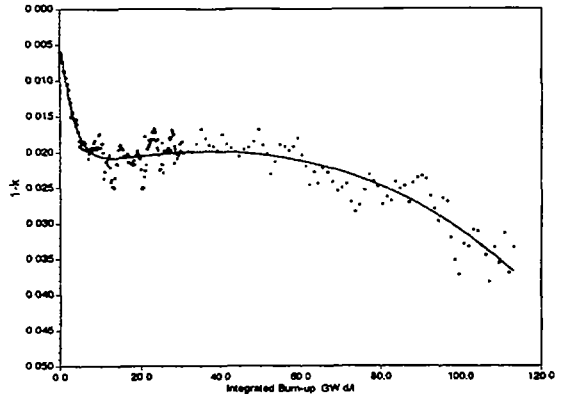

FIG. 5.4a Multiplication coefficient k of the EA as a function of the burn-up: linear time scale. Same conditions as Figure 5.1.

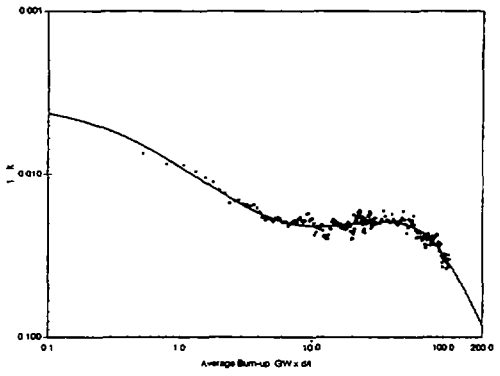

FIG. 5.4b Multiplication coefficient k of the EA as a function of the burn-up: logarithmic time scale. Same conditions as Figure 5.1.

of fuel are periodically introduced. Such schemes do not seem necessary in our case, since the single burn-up is long enough to reach the expected limit of the fuel elements due to radiation damage and gas pressure build-up.

The burn-up is not constant over the volume of the Core. Even if periodic, partial refuelling is not necessary, it may seem appropriate to shuffle the fuel elements locations every maybe ≈ 20 GW × d/t, namely about once a year, in order to uniformise the burn-up of the fuel load. This procedure can be performed without extracting fuel elements from the tank, using the fuel storage facility as a buffer location. If performed fast enough (for instance ≤ 10 days) as not to let a major fraction of the ^{233}Pa decay, it produces negligible effects on k. We have simulated this with our programme and found no real benefit for instance in extending the burn-up of the fuel. Consequently at this stage, we have concluded that this represents an additional complication with little or no advantage and we have therefore not applied this procedure to our simulations.

The relative power density distribution over the Core for unit fuel mass is shown in Table V.1. Its radial (r) dependence is roughly linear, as expected because of the value of k (see Figure 2.3b). The (z,r)-dependence is easily parametrized using as a universal parameter $(r^2 + z^2)^{1/2}$ the distance from the approximate centre of the source ($r = z = 0$). This is why the z-dependence flattens out at larger radii. Likewise the concentration of ^{233}Pa in the various pixels of the core is directly proportional to the power density distribution. We have verified that the power distribution does not change appreciably during burn-

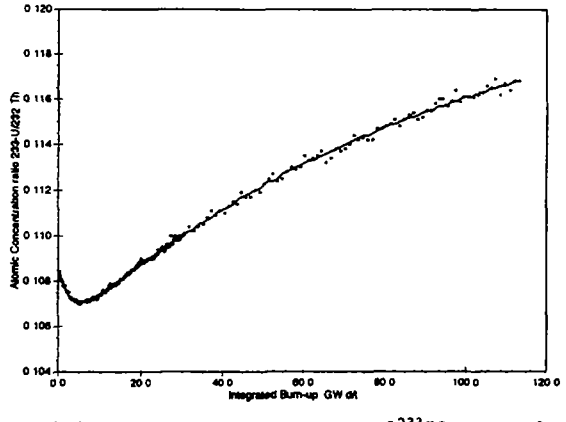

FIG. 5.5 Atomic concentration of ^{233}U, normalised to ^{232}Th, averaged over the core (Breeding Ratio) as a function of the burn-up. Same conditions as Figure 5.1.

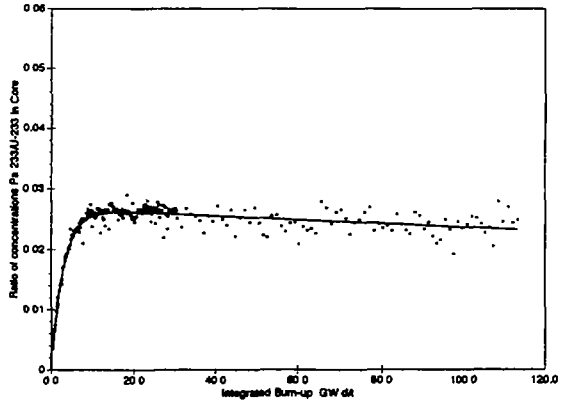

FIG. 5.6 Atomic concentration of ^{233}Pa, normalised to ^{233}U, averaged over the core as a function of the burn-up. Same conditions as Figure 5.1.

up in the specified range, namely≤ 100 GWxd/t

Similar distributions can be generated for the Breeder The concentration of bred ^{233}U rises approximately linearly with time As already pointed out, such a Breeder is necessary since although the relative concentration of ^{233}U is growing with burn-up, its stockpile is in fact reduced because of the

TABLE V 2 (DIRTY) PLUTONIUM INTO ^{233}U CONVERSION STOCKPILES AT START-UP AND AT DISCHARGE THE PLUTONIUM ISOTOPIC CONCENTRATIONS CORRESPOND TO THE DISCHARGE AFTER 33 GW x d/t OF A STANDARD PWR WITH INITIAL ^{235}U ENRICHMENT TO 3 3%

Nuclide	Mass at start-up	Mass at discharge (kg)	Difference
^{238}Pu	67 98	39 49	-28 49
^{239}Pu	1,636	323	-1,313
^{240}Pu	671 6	527	-144 6
^{241}Pu	314 9	78 3	-236 6
^{242}Pu	109 9	105 4	-4 5
All Plutonium's	2,800.38	1,073 1	-1,727 19
^{233}U	0	1,809	+1809

significant fraction of ^{232}Th which is burnt The stockpiles of ^{233}U are shown in Figure 5 8 The total amount of ^{233}U is at the end of the burn-up slightly larger than at start-up Note that the full amount of ^{233}Pa during fuel cool down will also transform itself into ^{233}U Consequently, there is enough fissile material to start a new cycle at a convenient value of k_o

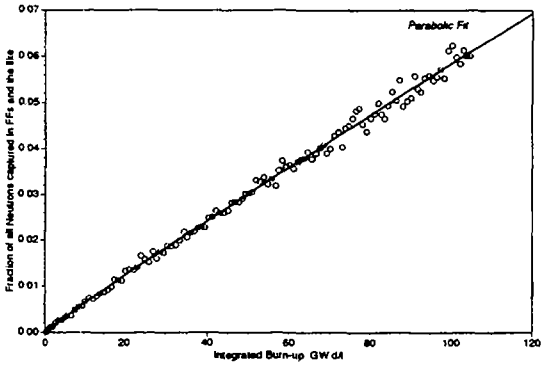

FIG 5 7 Fraction of all neutrons captured by Fission Fragment products, as a function of the burn-up Same conditions as Figure 5 1

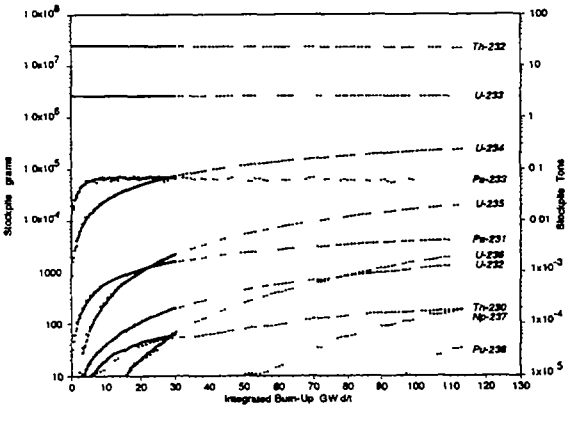

FIG 5 8 Concentration of the main Actinides as a function of the burn-up Same conditions as Figure 5 1

The concentration of the main Actinides as a function of the burn-up is given in Figure 5 8 They are in good qualitative agreement with the simpler analytical calculations of Section D 3.2

The simulation programme has been used to explore successive fuel cycles The simulated procedure is the following After 100 GWxd/t the fuel is extracted from the Amplifier and chemically reprocessed Uranium and Thorium isotopes are extracted and after a cool-down period of some 200 days to let primarily the ^{233}Pa decay into ^{233}U, these are used to manufacture new fuel elements, topped up with additional Thorium Although some 12% of the ^{232}Th has been burnt, the stockpile of ^{233}U in the fuel has only slightly changed We have reloaded in the EA exactly the initial concentration of ^{233}U Since the separation is

chemical, the new Uranium fuel will be made of several isotopes. The tiny quantities of ^{231}Pa (4.68 kg), of ^{237}Np (400 g) and of Plutonium [^{238}Pu (62 g) and ^{239}Pu (4.6 g)] are separated out and inserted again in the EA for an indefinite period of time until they are essentially incinerated.

The initial multiplication factor k_0 of the renewed fuel is extremely close to the initial one and persists to be so over several fuel cycles, in agreement with the analytic description of Section D.3.2.

Finally we have simulated the effects of power variations. As is well known, any major change of power requires that the ^{233}Pa can adjust itself to the new conditions. If the power output is suddenly increased (decreased) the value of k decreases (increases) with the characteristic decay time of the ^{233}Pa (39 days). It has been verified that the magnitude of this effect is in good agreement with the predictions of Section D.3.2.

D.3.5.3. START-UP FUEL CYCLE WITH "DIRTY" PLUTONIUM

There are many ways to initiate the sub-critical operation of an EA. The most naive approach, but most impractical would consist in starting with a pure ThO_2 fuel. This method is most inefficient, since initially the multiplication factor k is hopelessly low and the power of the accelerator will be correspondingly huge. Fortunately large amounts of readily fissile material exist in the form of enriched ^{235}U or of a "waste" trans-uranic elements from ordinary PWRs and either of them can be used as initial substitute for the ^{233}U.

We propose to use for the first fill a mixture of ThO_2 spiked with about 14% of "dirty Plutonium" from the discharge from a PWR, normally destined to geologic Storage. Our scheme permits to start-up the EA at the nominal power and gain right from the beginning and smoothly evolve from the initial to the regime conditions essentially in one fuel cycle. At the end of the first cycle, most of the ^{239}Pu is burnt, converted with a high efficiency into ^{233}U. The higher actinides can then either follow their initial destiny of geologic storage, with a significant reduction in toxicity and reduced military proliferation risk or can be continuously incinerated in the successive cycles until they ultimately fission inside the EA.

The simulation programme has been used in order to simulate the burn up of the initial mixture of "dirty" Plutonium and of Thorium. The fuel is — as previously — made of mixed oxides. The concentrations at start-up and at the discharge are given in Table V.2. Americium and Neptunium can be freely added to the mixture with little effects on the over-all performance. The concentration of Plutonium is chosen such as to produce a reasonable value of initial k_0. During operation, a large amount of breeding interactions occur in ^{232}Th with rapid production of ^{233}U, while the Plutonium isotopes are progressively burnt. We are witnessing a genuine transformation of Plutonium into ^{233}U (Figure 5.9). The multiplication coefficient k (Figure 2.9) and therefore the EA gain is now the resultant of mutual interplay amongst three main processes, namely (1) disappearance of the Plutonium and higher Actinides (2) the formation of ^{233}U and (3) the emergence of captures due to FFs. It is a fortunate circumstance that these three effects combined produce a value of the multiplication coefficient k which is almost constant, in spite of the large changes in concentrations,

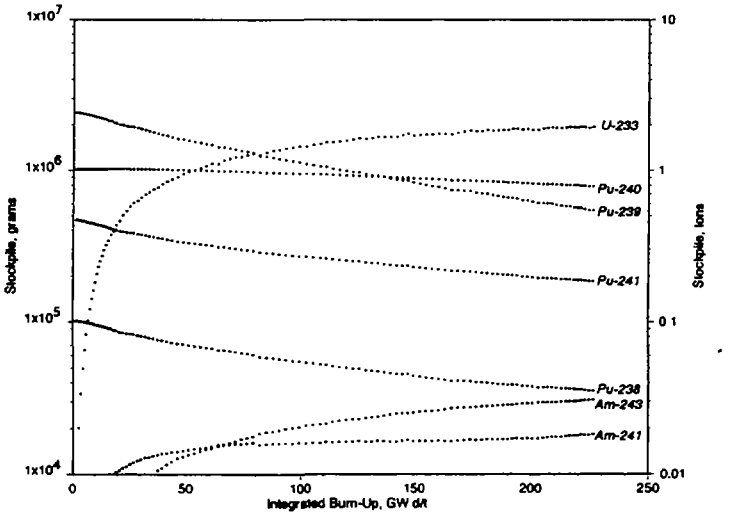

FIG. 5.9 Stockpile of Plutonium and Americium isotopes as a function of the burn-up, for an initial fuel made of "dirty" Plutonium (see Table V.2) and native Thorium. The concentration of produced ^{233}U is also shown.

although not as constant as in the case of an EA operated with Th-U mixture. Note also that the fast drop of k during the early life of the cycle, due in the case of the Th-U mixture to the formation of the ^{233}Pa is essentially absent in our case, since the initial operation is dominated by the Plutonium. The variations of k are now sufficiently large to justify some compensatory measure, justified by the exceptional nature of the initial EA fuel generation and start-up. The easiest way is to play with the refuelling machine and introduce the fuel assemblies progressively in the EA.

Because of the "external" contribution of the Plutonium, the burn-up of this fuel load can be extended well beyond the one of the normal cycles and a value in the vicinity of 150÷200 GW × d/t is appropriate. In order to reach such a long burn-up, it may be necessary to exchange the fuel assemblies during operation, in order to uniformise the radiation damage on the pins. As already mentioned this operation is easily performed in a short time.

D.3.5.4. NEUTRON SPECTRA AND ESTIMATES OF THE RADIATION DAMAGE

Neutron flux distribution can be easily calculated by the Montecarlo programme by adding the path length inside each "pixel". Its energy dependence is easily obtained by binning the accumulated path length according to energy. The results have been cross checked by a less accurate method in which a standard multi-group (reactor-like) calculation has been performed on the structure. The latter method does not take into complete account the sub-critical nature of the device, like for instance spallation neutrons. Since it is not an evolutionary programme, it does not take into account of the variations of the chemical composition during burn-up. As anticipated, the high energy component of the spectrum due to the high energy beam is quickly attenuated by the (n,n') inelastic collisions in Lead (Figure 5.10). By the time the neutrons reach the closest structural element of the Fuel the spectrum has softened to the point of becoming similar to the one of Liquid Metal Fast Reactors[1] (LMFBRs) for which a considerable experience exists already. For instance the flux ≥ 100 keV (≥ 1.0 MeV) is in both cases 55% (10%) of the whole flux. Neutron damage for LMFBRs [64] has been studied in the past theoretically and experimentally, and a large experience up to high fluences has been accumulated. Testing and development of materials for such reactors has arrived at fluences well within the range of the present design (see section D.3.4.5).

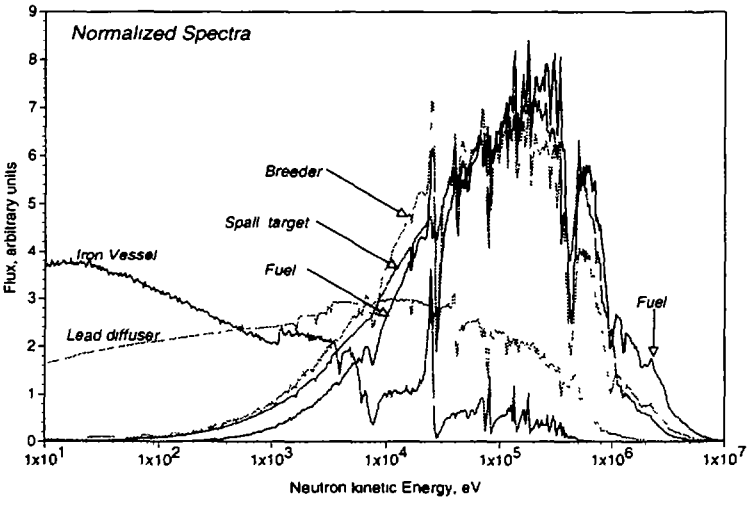

FIG. 5.10 Neutron flux spectrum in the different material regions of the F-EA. The breeder and the Fuel have similar distributions with fine resolution due to the resonant structure of the material cross sections.

Neutron irradiation in structural materials is an important design parameter and it determines their rate of replacement. The main physical and mechanical effects of the irradiation of metals are summarised in Table V.3 [65]. In the case of fast neutrons, for fluences $\int \phi dt \leq 10^{22}$ cm^{-2} changes are usually undetectable. Structural modifications start to appear at larger fluences, eventually approaching saturation for very large irradiation. Effects on metals are relevant to our case and they are generally smaller at higher temperatures since recovery (annealing) of the Frenkel defects produced by irradiation is facilitated. After irradiation one

[1] SuperPhénix (inner core)

generally observes an increase of the yield strength and, to a smaller extent, of the ultimate tensile strength. Hence, irradiation results in a decrease in ductility and an increase in the temperature characterising the transition from ductile to brittle fracture (NDT). This is an important effect in nuclear power systems.

There are several mechanisms by which irradiation may cause modifications besides direct heating. We shall mention two of them, namely creation of defects in the lattice and gas production. Particles of significant energy traversing the material collide both with electrons and nuclei, which in turn recoil inside the lattice generating lattice defects. The magnitude of the corresponding effects on properties such as elasticity, can be described in terms of an empirical parameter, the number of displaced atoms (DPA). Such DPA depends in turn on the total energy spent to cause displacements, E_a, and the (average) energy required to displace an atom from its lattice position, E_d:

$$DPA \propto \frac{E_a}{2E_d} \tag{1}$$

TABLE V.3. GENERAL EFFECTS OF NEUTRON IRRADIATION ON METALS

Irradiation increases	Irradiation decreases
Length (growth)	Ductility
Volume (swelling)	Stress-rupture strength
Yield strength (usually)	Density
Ultimate tensile strength	Fracture toughness
NDT temperature	Thermal conductivity
Hardness	Yield strength
Creep rate	Corrosion resistance
	Strain hardening rate

The denominator E_d is a purely empirical but universal parameter of the material and of which a wide range of values are available in the literature [66] [67]. The energy E_a depends on the spectrum and nature of the incident radiation and on the energy partition between electronic excitations and atomic recoils. We have used in our computer simulations the module HEATR of the nuclear data processing code system NJOY [68]. The partition function used was given by Robinson [69] based on the electronic screening theory of Lindhard [70]. HEATR calculates the damage energy production cross section, $\langle \sigma E_a \rangle$ (barn-keV). An estimate of the number of displacements per second in the metal is given by:

$$S\left[\frac{dpa}{s}\right] = \frac{\langle \sigma E_a \rangle}{\frac{2E_d}{\eta}} \phi \cdot 10^{-21} \tag{2}$$

where η=0.8 is the collision efficiency factor and ϕ the particle flux ($cm^{-2}s^{-1}$).

Helium, Hydrogen and other light gases are produced in structural materials by nuclear reactions process with α, p, T and so on in the final state. In the case of fast neutrons (n,α) and (n,p) reactions have significant cross sections. In conditions of large fluence, these locally generated gases may be in sufficient amount as to have a pronounced effect on the mechanical and dimensional properties of components, like for instance:

- The radiation induced swelling due to vacancy agglomeration (voids), in which the internally produced gas acts as a nucleating agent for voids, promoting their growth and stabilising them once they are formed.
- The high temperature embrittlement due to inert gas bubbles.
- The low temperature embrittlement due to defect clusters-vacancy or interstitial clusters.

- The "in-pile-creep" producing dimensional changes like swelling.

Swelling and "in-pile-creep" may cause some dimensional changes of the core components which may even affect the dynamics of the energy amplification.

We consider next in more detail the radiation damage in two main structural components namely (1) the beam window and (2) structure and cladding of the Fuel Core. Note that molten Lead is not a "structural material" and it is continuously recirculated from a very large mass. Paradoxically, radiation damage in the highest flux by the highest energy particles can be neglected, evidently with the exception of the beam window! Molten Lead acts as a "filter", moderating the most radiation damaging components of the spallation spectrum.

The rate of radiation damage in the beam window is comparable to the one in high-yield spallation sources under design and construction (see for instance SINQ [71]). The most severe effect is produced by the incoming proton beam. Effects due to the secondary neutrons produced by the cascade are small in comparison with the high energy charged particles. According to Eq. (2), the damage rate is given by:

$$S\left[\frac{dpa}{s}\right] = 3.18\times10^{-6}\frac{\langle\sigma E_a\rangle}{\frac{2E_d}{\eta}D^2}\ I\ (mA)$$

where D is the beam diameter. Production yields of He and H can be obtained from cross sections and incident flux (current density):

$$P\left[\frac{appm}{s}\right] = 7.95\times10^{-3}\frac{\sigma}{D^2}\ I\ (mA)$$

Parameters for a proton energy of 800 MeV and several relevant materials are given in Table V.4. Since cross sections change only very slowly with energy, these values are applicable to a wide interval of proton energies and in particular to our design. The relevant parameters after 7000 hours at the nominal (see section D.3.4.4) peak current density of 113 $\mu A/cm^2$ are about 200 dpa, 13150 He (appm), and 116,350 H (appm). With these numbers, because of embrittlement and swelling, in order to guarantee safety, the window should be replaced after about one year [53]. The periodic replacement of the proton window can be easily accomplished as a routine maintenance task.

TABLE V.4. PARAMETERS RELEVANT TO A PROTON ENERGY OF 800 MEV (EXTRACTED FROM REFERENCE [71])

Material	(σE_a) [*barn-keV*]	E_d [*eV*]	σ_{He}[*barn*]	σ_H[*barn*]
Al	63	40	0.21	0.86
Steel	300	40	0.32	2.52
Cu	330	30	0.40	2.58
Mo	900	58	0.58	4.00
W	1430	65	0.58	5.13

It is however evident that some experimental work is required in order to ensure safe conditions of operation of this relatively new component which is the beam window. In particular we remark that the peak beam current density is inversely proportional to the square of the beam diameter. If required by these

additional investigations, the beam size could be enlarged without major consequences in the rest of the system.

The irradiation effects on the Fuel Core region have been already mentioned. They must not limit the maximum burn-up due to FFs poisoning which has been set to be of the order of 100 GW × d/t . This corresponds to an integrated neutron fluence through the cladding of $\int \phi dt = 3.3 \times 10^{23}$ n/cm^2, averaged over the core. The most exposed pins will accumulate about twice such a fluence. Two structural components deserve consideration namely (1) the Fuel itself, a mixture of ceramic oxides and (2) the steel cladding of the fuel pins and other structural materials holding the pins together.

If Thorium is mixed with Uranium using Thorium-Uranium oxides, the irradiation experience available for these components indicates a small incidence on fuel swelling. However, more data needs to be collected to attain a high degree of confidence for long-term performance [53].

It is expected that our cladding material will experience conditions similar to those of an LMFBR at 600 ÷ 700 °C and neutron fluences above 0.1 MeV of about 10^{23} cm^{-2}. As already mentioned we must consider four major effects: (1) radiation hardening, (2) irradiation creep, (3) embrittlement and (4) swelling. Different alloys have been proposed and studied as cladding in these neutron environments: (i) stainless steels (304, 316, 321, 347, Incoloy 800); (ii) Nickel based alloys (Inconel 600, Inconel X750, Hastelloy X, Inconel 718, Inconel 625). Type 316 is the reference material for many LMFBR in-core cladding and structural applications.

In the design of the EA there are the added requirements of corrosion in molten Lead (see section D.3.4.3) and the necessity of keeping the activation stockpile to a minimum at long times. For these reasons we prefer to use instead low-activation HT-9 steel [72]. Ferritic steels (e.g. HT-9) have demonstrated a high swelling resistance, a good stress-corrosion resistance, and a particularly high temperature strength which could increase significantly the fuel element lifetime. The rates of displacements and gas production in different material zones of interest are given in Table V.5. Combining these with the data of ref. [72] it is expected a swell fraction of ≈ 1 % and a shift in the temperature characterising the transition from ductile to brittle fracture (DBTT) of about 30 °C at design fluence. Under these conditions, our design lifetime of approximately 5 years corresponds to an acceptable radiation damage level for the fuel cladding.

TABLE V.5. DISPLACEMENTS AND GAS PRODUCTION RATES IN THE ENERGY AMPLIFIER

Region	Fluence/y	dpa/y	He [appm]/y	H [appm]/y
Inner Core	1.1×10^{23}	25	2.0	40
Outer Core	6.5×10^{22}	15	1.5	27
Breeder	2.3×10^{22}	3.5	0.2	3
Plenum	2.5×10^{22}	2.5	0.1	1
Main Vessel	9.7×10^{19}	0.001	--	--

D.3.5.5. TEMPERATURE DISTRIBUTIONS AND COOLANT FLOW

The temperatures reached by the different elements of the core are important parameters related with the safety of the EA. In particular, a safe operation requires the cladding and fuel temperatures to be well below the structural limits of the constituent materials.

The lead temperature distribution along any cooling pin channel can be estimated on the basis of the pin axial power density distribution. The internal temperature of the pin cladding can be calculated adding to the lead temperature the temperature increases from the lead to the outer part of the cladding and from there to the inner part. The fuel temperature is then obtained by adding to the internal cladding temperature

the increment inside the fuel.

For the EA the linear power density axial distribution *(q')* can be expressed as:

$$q'(z) = q'_{\max}[1 - b(z - z_{mid})^2] \qquad (q' \equiv W/m) \tag{1}$$

where z is the axial coordinate, q'_{max} is the maximum linear power density, reached in the middle of the pin ($z = z'_{mid}$), and b is a parameter given by the power distribution shape. Both q' and b are function of the pin radial position in the core. The temperature distribution of lead can be calculated by using the expression

$$\frac{dT(z)}{dz} = \frac{q'(z)}{f_a \upsilon \rho C_p} \tag{2}$$

where T is the lead temperature and f_a, υ, ρ and C_p are the lead flow area, velocity, density and specific heat respectively. In the approximation in which these quantities are kept constant (as an averaged value) the lead axial temperature through the channel distribution is given by

$$T_{Lead}(z) = T_{Lead,in} + \frac{q'_{\max}}{f_a \upsilon \rho C_p}\left[z - \frac{b}{3}(z - z_{mid})^3 - \frac{b}{3} z_{mid}^3\right] \tag{3}$$

The heat flow between the cladding and the lead surface is described by the Newton law of convection

$$T_{out\ clad}(z) = T_{Lead}(z) + \frac{q''(z)}{h}$$

where q'' is the surface power density distribution and h is the local heat transfer coefficient which can be calculated as a function of the Nusselt number

$$Nu = 4.82 + 0.0185 \times \left(\frac{\upsilon \rho C_p d_e}{k_L}\right)^{0.827} \qquad ; \qquad h = \frac{Nu \cdot k_L}{d_e}$$

d_e is the effective diameter, defined in section D.3.4.7, and k_L is the lead thermal conductivity. By using for the surface power density *(q'')* the same z behaviour for the linear power density, the temperature increase between the lead and the outer surface of the cladding can be obtained,

$$T_{out\ clad}(z) = T_{Lead,in} + \frac{q'_{\max}}{f_a \upsilon \rho C_p}\left[z - \frac{b}{3}(z - z_{mid})^3 - \frac{b}{3} z_{mid}^3\right] + \frac{q''_{\max}[1 - b(z - z_{mid})^2]}{h} \tag{4}$$

A similar calculation allows to get the temperature difference between the outer and inner part of the cladding, which depends on the HT-9 thermal conductivity k_c and the cladding thickness e, according to the following expression

$$T_{inn\ clad}(z) = T_{out\ clad}(z) + \frac{e}{k_c} q''_{\max}\left[1 - b(z - z_{mid})^2\right]$$

The temperature increase inside the fuel, without considering the axial pin heat transfer, can be written as a function of the radius and the fuel length:

$$T_{inn\ fuel}(r,z) = T_{out\ fuel}(z) + \frac{q'''(z)}{4\bar{k}_{ThO_2}}\left(r_1^2 - r^2\right) \qquad r_2 \le r \le r_1$$

Where $q'''(z) = W\rho_{ThO_2}(W/m^3)$

$$T_{out\ fuel}(z) = T_{inn\ clad}(z) + \frac{q''_{\max}}{\bar{k}_{ThO_2}}\left[1 - b(z - z_{mid})^2\right]$$

r being the radial position and r_1, r_2 the fuel pellet radius and the inner void radius respectively. $\bar{k}_{ThO_2}$ is the temperature averaged thorium oxide thermal conductivity.

The calculations were performed with a simulation programme [73]. The results, which are in excellent agreement with the full thermal-hydraulic code COBRA [55], give a maximum cladding and fuel temperature of 707 °C and 2250 °C, well below 1470 °C and 3220 °C, which are the HT-9 and ThO_2 melting temperatures respectively.

As described in section D.3.4.7 the EA cooling is achieved by convective pumping. The pressure difference generated in the lead loop is sufficient to extract the heat from the core. For a fixed ΔT in the core, a variable pitch value is used in order to adjust the coolant speed through the core to the pin power density. In practice, however, the pitch value is quantified and there is a residual radial dependence of ΔT. This effect is particularly important if the breeder is to be included in the same coolant loop and if its pitch value is not drastically different from that of the fuel, since its power density is very low. A simple method of cancelling this residual dependence is to decrease the pressure at the entry of the bundles such as to get the same ΔT than for the hottest channel, for which the pressure decrease is set to zero. For the other channels this extra pressure drop increases when the power density decreases. This implies a tuning of the coolant flow rate as

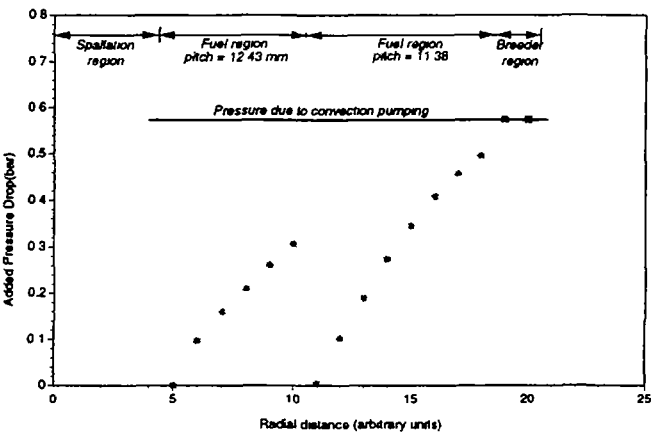

FIG.5.11a Pressure drop inserted as a function of the radial position. As a reference the total pressure drop due to the Lead column is also displayed.

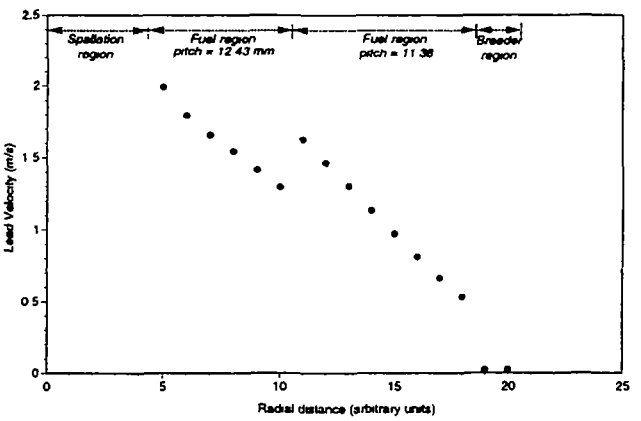

FIG. 5.11b Lead velocity distribution as a function of the radial position.

implies a tuning of the coolant flow rate as a function of the bundle radial position.

The calculations were done by a simulation programme using the expressions already described in sect. D.3.4.7. The results, pressure drop inserted and lead velocity distribution, are shown in Figures 5.11a and b. Finally, the speed map at the exit of the core has been used as input in a simulation of the coolant flow. As observed in Figure 5.12, the speed gently homogenises along the path through the lead column.

The convection start-up has been simulated using a computational model based on the following expression

$$l_f \rho \frac{\partial v}{\partial t} = \Delta P_{Column} + \Delta P_{Core} - \sum \Delta P_i$$

where l_f is the fuel length, ΔP_{Column}, ΔP_{Core} are the pressure induced by the lead in the column and in the core and ΔP_i are the pressure terms losses due to friction and changes in flow area, as defined in section D.3.4.7.

The lead outlet core temperature T_{out} has been obtained as:

$$T_{out} = T_{in} + \frac{q}{\rho f_a v C_p}$$

where T_{in} is the lead inlet core temperature.

The equation was solved by time steps and for each time ΔP_{Column} and ΔP_{Core} have been estimated by averaging, with the appropriate weights, the temperatures of the lead in the column and in the core with the temperatures of the lead leaving and entering the core respectively. In the model the time of heating the fuel has been neglected and the heat transmission to lead was supposed instantaneous.

TABLE V.6. SIMULATION OF CONVECTION START-UP AND SHUT-DOWN (HOTTEST FUEL CHANNEL)

Steady conditions:		
q^{st}		102 W/g
T^{st}_{in}		400 °C
T^{st}_{out}		649 °C
v^{st}		2.02 m/s
Start-up [1]: Power Density, quadratic for ($0 < t < at_1^2$), exponential for $at_1 < t < t_1$, constant = q^{st} for $t_1 < t$		
T_{max}	$649 + 439\, e^{-0.051 t_1}$	$10 < t_1 < 120$
T_{max}	≈ 649	$t_1 > 120$
Time in which the Lead T_{max} is reached, in seconds:		
$t(T_{max})$	$0.43\, t_1$	$10 < t_1 < 120$
$t(T_{max})$	$\approx t_1$	$t_1 > 120$
Shut-down: *Power Density for $t < 0$, $q = q^{st}$; for $t > 0$, $q = q^{st}$*		
$v(t)$ (m/s)		$v(t) = \frac{v^{st}}{(1+0.2t^{0.725})}$
$T_{out}(t)$(°C)		$T_{out}(t) = T^{st}_{in} + \frac{(T^{st}_{out} - T^{st}_{in})}{(1+0.4t^{0.76})}$

[1] Steady conditions reached at $t=t_1$, in seconds

[2] The results are for a=0.35 but they do not change significantly for other values giving a smooth time dependence.

The results show that it is possible to reach the operating power conditions in a few minutes without overheating the Lead leaving the core beyond the nominal operating temperatures (Table V.6). For start-up times below 2 minutes the lead is overheated, for instance by about ≈ 20 °C if the start-up is done in 1 minute or by ≈ 100 °C if it is done in 30 s. Also, after an instantaneous shut down and without considering the residual heating, the inertia of the coolant is such as to maintain the lead speed in ≈ 8% of its steady state value after 5 minutes, and ≈ 3% after 15 minutes.

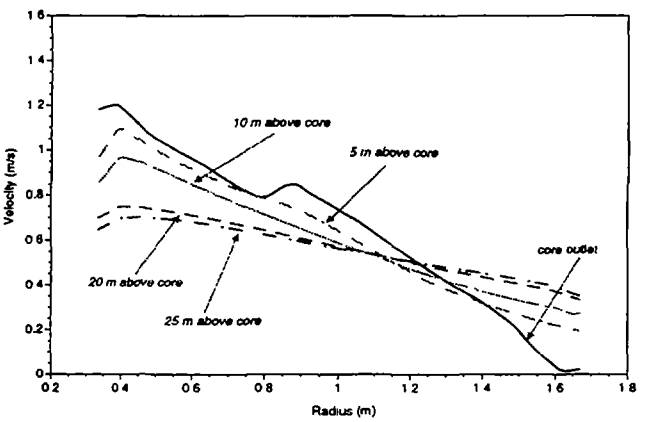

FIG. 5.12 Velocity map of Lead in the column above the Core.

D.3.5.6. SAFETY AND CONTROL OF FAST TRANSIENTS

The safety of multiplying systems depends to a large extent on fast transients caused by accidental reactivity insertions. To study the power changes in accelerator driven systems a kinetic model dealing with fast transients as a function of reactivity insertion, Doppler feedback and the intensity of an external neutron source, was developed and programmed.

A kinetic model is given by the diffusion equation, in one energy group. This equation relates the change in time of the neutron density with the physical constants of the system, specially the reactivity, and has to consider the prompt and delayed neutron production rates [74]:

$$\frac{\partial N}{\partial t} = \left(\frac{1-\beta}{1-\rho(\$)\beta} - 1 \right) \frac{N}{\Lambda} + \sum_{i=1}^{6} \lambda_i C_i + S(t) \tag{1}$$

$$\frac{\partial C_i}{\partial t} = \frac{\beta_i}{1-\rho(\$)\beta} \frac{N}{\Lambda} - \lambda_i C_i \tag{2}$$

where N is the neutron density, β_i, β are the delayed neutron fraction of the i-th delayed precursor group and the total delayed neutron fraction respectively, λ_i and C_i are the decay constant and the concentration of the i-th delayed precursor group respectively, $\rho(\$)$ is the total reactivity, expressed in dollars, Λ is the averaged prompt-neutron lifetime and $S(t)$ is the external source term.

For a sub-critical device, fed by a spallation neutron source, the source term may be expressed as [75]:

$$S(t) = -\frac{\rho_0 n_{sp}}{\Lambda} \tag{3}$$

where $\rho_0 < 0$ is the total reactivity in the steady state and n_{sp} is the number of spallation neutrons density per source proton. At the steady state the external source term is kept constant. Establishing the k_0 effective multiplication factor, at this steady state, the n_{sp} value is expressed as:

$$n_{sp} = \frac{1}{1-\rho_0(\$)\beta} N_0$$

$$S(t) = (1-k_0)\frac{N_0}{\Lambda}$$

Here N_0 is the neutron density at the steady state.

The coupled equations (1) and (2) are solved by a numerical method described later. The general features of the program include time dependence of the total reactivity, prompt neutron generation time and time size step, and a maximum of six delayed neutron precursors groups. In addition, the total stored energy is also calculated by integrating the reactor power from $t = 0$ to the time of interest.

The total reactivity of the sub critical device is then a sum of four terms:

$$\rho(t) = \rho_0 + \rho_{ext} + \rho_{Doppler}(t) + \rho_{Mod.density}(t) \tag{4}$$

$$\rho_{Doppler} = \frac{\alpha(\$/^0C)}{c_p} \times P(t) \times t$$

$$\rho_{Mod.density} = \alpha'(\$/g\ cm^{-3}) \times (Dens.(T_{\mathrm{mod}}(t)) - Dens_{\mathrm{mod.},0})$$

where $\rho_{ext}(t)$ is the external reactivity inserted, simulating an accident. It is time dependent, usually represented by a linear or quadratic ramp; $\rho_{Doppler}$ is the reactivity decrease due to the fuel temperature increase ($\alpha < 0$) and P(t) is the power density. The reference fuel temperature is the one at the steady state. This effect is very fast, it is therefore the main stability feedback of an external reactivity insertion accident which would rise at high speed. The rapid fuel answer is due to the direct relationship between the power density change with the reactivity increase and the fuel temperature variation, $\rho_{Mod\ density}$ is the reactivity decrease ($\alpha' < 0$) due to the moderator density change, which is a moderator temperature function. This negative reactivity evolves at a lower speed because of the thermal inertia of the moderator. Hence, this effect is less important than the one mentioned above.

The last equations, necessary to complete the cycle, are the power density and neutron density relationships, and the temperature changes due to a power density variation. The first one is given as

$$P(t)\ (W/g) = \frac{\varepsilon \Sigma_f N(t) v}{Fuel\ density}$$

where $\varepsilon = 3.044 \cdot 10^{-11}$ *J (190 MeV/fission)*, v is the averaged neutron speed. Once the averaged power density at the steady state is known (P_0) and also the neutron density (N_0) is fixed, it is not necessary to calculate the neutron group constants (Σ_f, ν)

$$P(t) = P_0 \frac{N(t)}{N_0} \tag{5}$$

The reactivity reduction by the Doppler coefficient is calculated as a heat generation coefficient [74]. Let ρ_0 represent the initial reactivity increase resulting from a step change. If $\alpha = -d\rho/dT$ is the negative of the temperature coefficient of reactivity, i.e. α is a positive quantity, the reactivity resulting from a temperature increase T is given by

$$\rho = \rho_0 - \alpha T$$

Suppose the time scale of the power excursion is such that the heat loss from the system is insignificant. The increase in thermal energy E will then be related to T by

$$E = CT$$

where C is the heat capacity, i.e., mass × specific heat, of the system. Hence,

$$\rho = \rho_0 - \frac{\alpha}{C}E = \rho_0 - \gamma E \tag{6}$$

where $\gamma = \alpha/C = -d\rho/dE$ is the negative of the energy coefficient of reactivity. The reactor power P is equal to the time rate of energy change, i.e., dE/dt; it is obtained by differentiating equation (6) with respect to time, so that

$$P = \frac{dE}{dt} = -\frac{1}{\gamma}\frac{d\rho}{dt}$$

It follows, therefore, that

$$\frac{d\rho}{dt} = -\gamma P. \tag{7}$$

The coupled equations (1) and (2) were integrated by discrete time steps. It is important to note that the time step has to be of the same order of magnitude as the prompt-neutron average lifetime. Three types of unprotected reactivity accidents have been considered.

- A slow reactivity ramp insertion: the reactivity increases at a rate of *170 $/s* for a period of *15 ms* (this corresponds to a control rod withdrawal speed of *0.55 cm/ms* in the case of a reactor). After this time the reactivity is kept constant.
- A fast reactivity ramp insertion: the reactivity increases at a rate of *250 $/s* for a period of *15 ms* (*0.81 cm/ms*).
- A thermal run-off of the accelerator, due to a variation in the proton beam intensity. The new source term is:

$$S'(t) = S(t)\frac{I_{new}}{I_0}$$

where I_0 is the nominal beam intensity and I_{new} is the accidental new proton current, increased by a factor 2.

The analysis of this problem allows a comparison with transient calculations obtained for a critical reactor (Figure 5.13). It gives a first indication of the mitigating effect of using a sub critical accelerator driven system. The parameters used for the Energy Amplifier transient study, extracted from references [76] [77], are indicated in Table V.7. Figures 5.14(a-d) show the power, fuel average temperature and reactivity change in a critical reactor (lead cooled) and in the Fast Energy Amplifier subjected to a slow reactivity insertion. The important reactivity effects all occur within one second.

- The power excursion curve which corresponds to a critical reactor oscillates and has two distinct peaks in a short time interval. Super prompt criticality produces these peaks (Figure 5.14b). The power rises rapidly during the period of super prompt criticality and reaches

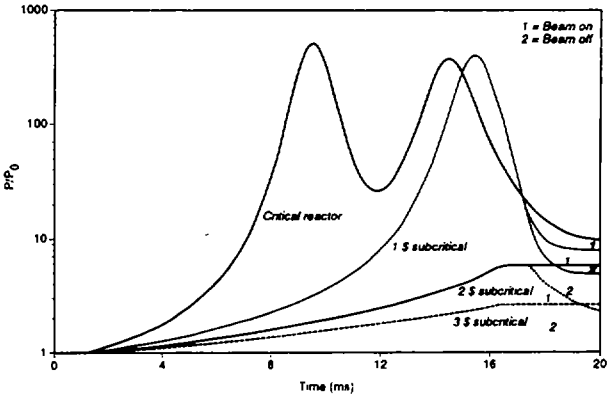

FIG. 5.13 LMFBR power excursion benchmark (as defined in a comparative NEACRP exercise) assuming a rod ejection accident

its peak, *100* times nominal after *7 ms*, atthe time when the Doppler effect reduces the reactivity to values below super prompt limit. However, the fuel average temperature continues to rise rapidly during *15 ms* (due to the thermal inertia of the fuel), until the Doppler counter-reactivity has fully established itself. By this time, the average temperature of the fuel has increased by *50 %* ($T_{fuel} \approx$ 1250°C), assuming that the heat loss from the fuel is insignificant during the power excursion. The integrated power, after *20 ms*, measured from the start of the ramp is ≈ 0.8 full power seconds.

- In the case of the Fast Energy Amplifier operated at $k = 0.98$, the power increases only by *42 %* after *15 ms* and after *20 ms* the power decreases almost proportionally with the neutron source strength. If on the other hand the neutron source is maintained (the accelerator is not shut-off), the power remains almost constant in this time range. The total energy released during the excursion is much less than for a critical reactor (*0.025* full power seconds after *20 ms*). The average temperature of the fuel rises gradually but at a much lower rate. After *20 ms*, the fuel average temperature has increased by *8%*. Note, that in this case the Doppler reactivity feedback is almost negligible and very much delayed (appears only after *23 ms*). The long time constant of the response implies that the heat loss from the fuel cannot be neglected anymore. In fact, there is sufficient time (of the order of a few seconds, as estimated by the convection studies described in *section D.3.5.5*) for the natural convection mechanism to safely adapt itself to the new operating conditions without occurring any fuel damage.

TABLE V.7. MAIN KINETIC PARAMETERS USED FOR THE ENERGY AMPLIFIER TRANSIENT STUDY

Prompt neutron lifetime:	
$\Lambda =$	2.9×10^{-8}s
Doppler effect coefficient:	
$\left(\frac{\Delta k}{\Delta T}\right)_{fuel}$	-1.38×10^{-5} °C^{-1}
$\left(\frac{\Delta \rho}{\Delta T}\right)_{fuel} = \frac{1}{k_0^2}\left(\frac{\Delta k}{\Delta T}\right)_{fuel}$	-1.44×10^{-7} °C^{-1}
Moderator density change coefficient:	
$\left(\frac{\Delta k}{\Delta Dens}\right)_{lead}$	9.68×10^{-5}m^{3}kg^{-1}
$\left(\frac{\Delta \rho}{\Delta Dens}\right)_{lead} = \frac{1}{k_0^2}\left(\frac{\Delta k}{\Delta Dens}\right)_{lead}$	1.01×10^{-6}m^{3}kg^{-1}
$Dens_{lead}$(kg/m^3)	$11149.7442-1.3595\times T_{lead}$ (°C)
	$T_{lead} \in$ [400 °C, 900 °C]
$\left(\frac{\Delta \rho}{\Delta T}\right)_{lead} = \left(\frac{\Delta \rho}{\Delta Dens}\right)_{lead}\left(\frac{\Delta Dens}{\Delta T}\right)_{lead}$	-1.37×10^{-6} °C^{-1}

The next examples illustrated in Figures 5.15(a-d) and 5.16(a-d) deal with a fast reactivity ramp insertion and a thermal run-off of the accelerator, respectively. Compared to the previous case, the power peak values are higher. The power and temperature changes are faster, and so is the response (fuel Doppler reactivity feedback). The integrated power, i.e. the total energy released during the excursion, is slightly larger.

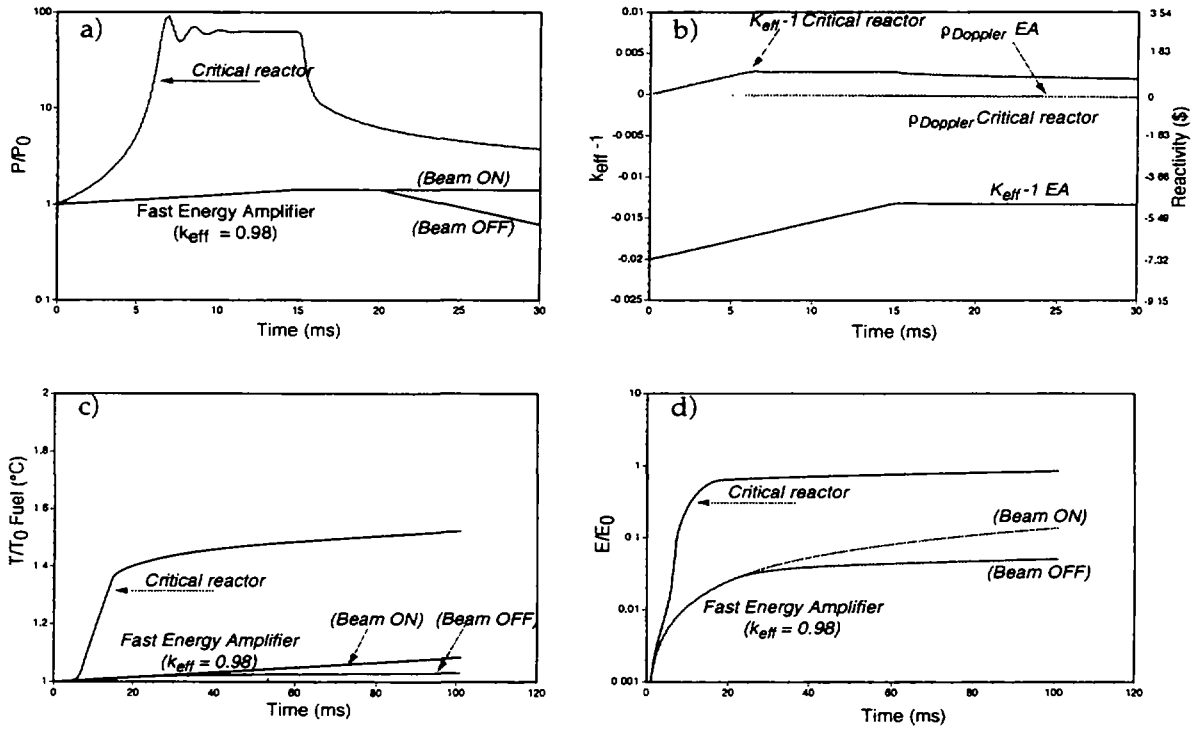

FIG. 5.14 Comparison of power excursions in a critical reactor (lead cooled) with the Fast Energy Amplifier for an accidental reactivity insertion of 170 $/s for 15 ms.

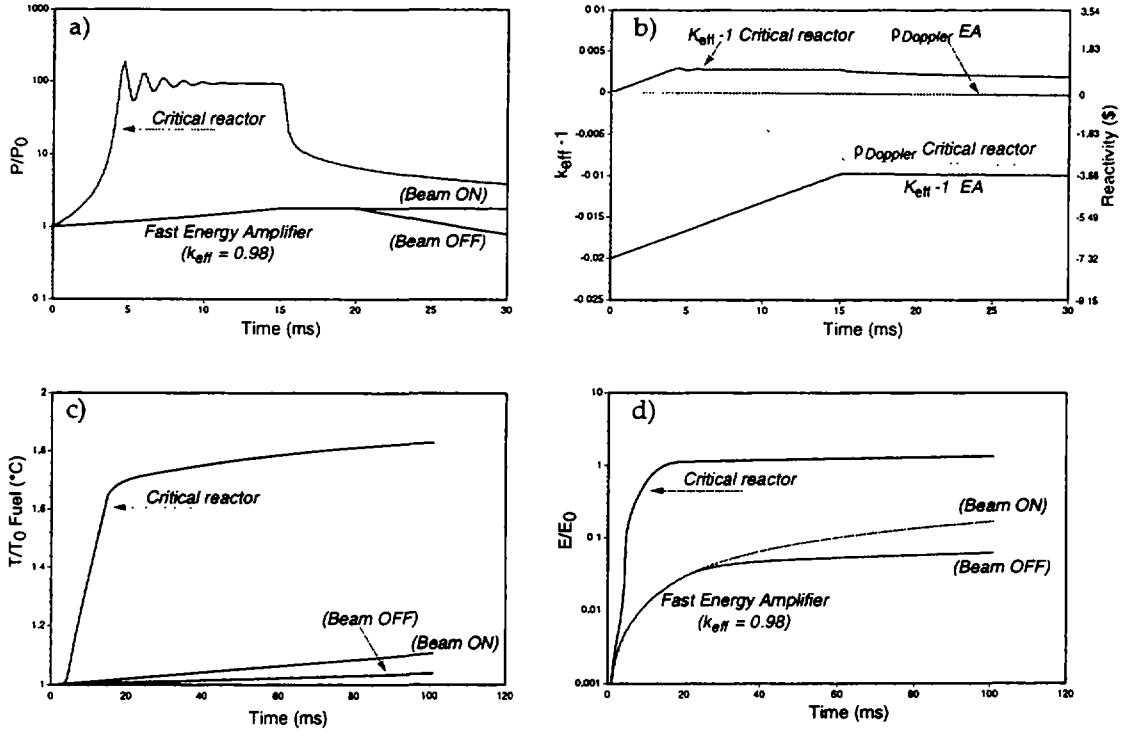

FIG. 5.15 Comparison of power excursions in a critical reactor (lead cooled) with the Fast Energy Amplifier for an accidental reactivity insertion of 255 $/s for 15 ms.

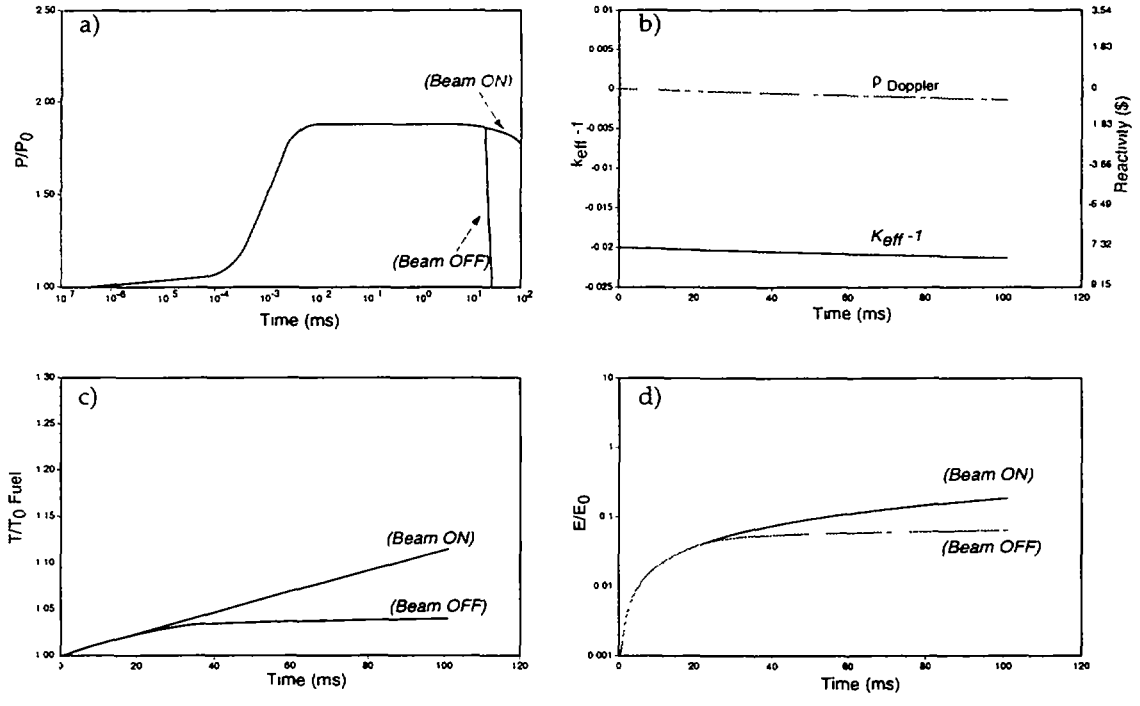

FIG. 5.16 Power excursion and reactivity behaviour during a beam run-off in the Fast Energy Amplifier

An interesting result of this analysis is the fact that the Fast Energy Amplifier responds much more benignly to a sudden reactivity insertion than a critical reactor. Indeed, no power excursions leading to high power levels are possible for positive reactivity additions which are of the order of the sub criticality and similarly for a thermal run-off of the accelerator. More importantly, even if the spallation source is still active (the accelerator is not shut-off), the relative slow power changes induced could be passively controlled by means of natural convection alone (massive coolant response) thus avoiding any meltdownofthe sub-critical core.

D.3.5.7. COMPOSITIONS AT DISCHARGE

The evolution programme computes the full composition of the elements of the EA during operation. The composition at discharge is therefore directly obtained, with the proviso however that the beam is made of discrete pulses separated in time. Appropriate corrections have to be introduced if short-lived components, with lifetime shorter than the proton repetition rate (typically $5\times10^{3}\div3\times10^{4}$ s) have to be exactly estimated. In the case of the Fuel discharge also an appropriated, averaged mixture of elements substitutes the actual fine structure of the fuel pins and of the lead coolant. Therefore, the discharge composition will include also the small amount of new elements produced in the closely surrounding Lead.

The discharge composition of the Fuel after 110 GW x d/t corresponding to approximately 5 years in the standard operating conditions are listed in Table V.8. We have listed only those elements which have a 1/e lifetime longer than 10 days and an amount larger then 100 mg. The relative scarcity of trans-uranic elements reflects the conditions of the first Fuel cycle. The evolution of the Actinide with fuel cycle has been amply discussed in section 2.9 to which we refer for further details. The FF mass composition is substantially different from the one of an ordinary PWR for two main reasons, namely (1) the fission yields for ^{233}U and ^{235}U are quite different and (2) incineration of some of the FFs is quite strong for thermal

spectrum and it is quite small in our case. We have listed in Table V.8 the ratio of mass yields for the same thermal energy produced by the EA and a PWR after 33 GW × d/t and initial enrichment of the ^{235}U to 3.3%. Some of the elements show a ratio very different than 1.

The activation of the Fuel cladding material (HT-9) leads mainly to about 0.2 kg of ^{54}Mn (1.24 a), 1.72 kg of ^{55}Fe (3.95 a), 0.234 kg of ^{185}W (108.6 d) and 2.52 kg of ^{187}Re (6.30×10^{10} a), the last two elements due to the very small content of just 162.6 kg of W in the steel alloy. Other radioactive elements like ^{60}Co, ^{51}Cr, ^{59}Fe etc. are present in traces at the level of ≤ 1g.

The Lead coolant within the core volume accumulates over 5 years of operation about 20.3 kg of rather inoffensive ^{205}Pb (2.2×10^7 a, K-capture at 0.065 MeV, no γ i.e ν-emission), some 45 g of ^{202}Pb (7.5×10^4 a) and very small traces of ^{194}Hg (751.9 a),^{204}Tl (5.47 a),^{208}Bi (5.32×10^5a) and ^{210}Po (200 d). The very small amount of ^{194}Hg is in contrast with the much larger production rate of the same isotope in the Spallation target (see next paragraph). Its absence evidences the sharp confinement of the spallation processes in the target region, away from the fuel core. Radioactive isotopes in the coolant are rapidly mixed in the bulk of the coolant, about 10^4 tons, leading to very small relative concentrations[1], in many instances measured in units of parts per billion. The fate of these impurities is to a major extent unpredictable and specific experiments are required.

The discharge from the Breeder has to a major extent the same general features as the one from the Fuel, with the exception of the much smaller number of FFs and the smaller neutron flux.

The Lead coolant surrounding the Core and Breeder volumes, with the exception of the spallation region which will be discussed separately, is relatively unaffected by the neutron flux (paragraph D.3.4.2). Two unstable Lead isotopes are present, the long lived ^{205}Pb with 43.71 kg and the short lived (4.7 h) ^{209}Pb with traces at the level of 1 g. Its modest activation is related to the lower energy and flux in the region immediately surrounding the core. Even smaller is the activation of the containment vessel, dominated by ^{55}Fe (3.95 a) and ^{59}Fe (64.35 d), with 400 g and 1 g respectively.

The Actinide composition is also radically different from the one for instance of a PWR and its consequences need some consideration. The main differences are:

(1) the presence of several Protactinium isotopes. At the design power level, the stockpiles of ^{233}Pa is of 53.25 kg in the Core and of 5.60 kg in the Breeder. This relatively short lived element is the source of a substantial amount of decay heat, 2.99 MW (2.70 MW in the Fuel Core) immediately after shut-off and decaying with the characteristic 1/e time of 38.99 days. Since the ^{233}Pa concentration is proportional to the power produced during steady operation, its decay heat represents a constant fraction of this last quantity, initially 0.2 % of the design power. In view of its relatively long decay constant, the contribution of ^{233}Pa is comparable to the decay heat produced by the FFs and it must be taken into account (Figure 5.17). The breeding transformation is accompanied by intense γ-emission. More specifically we have calculated the time dependence of the γ-spectra produced by Actinides of Table V.8. In Figure 5.18 we give the time

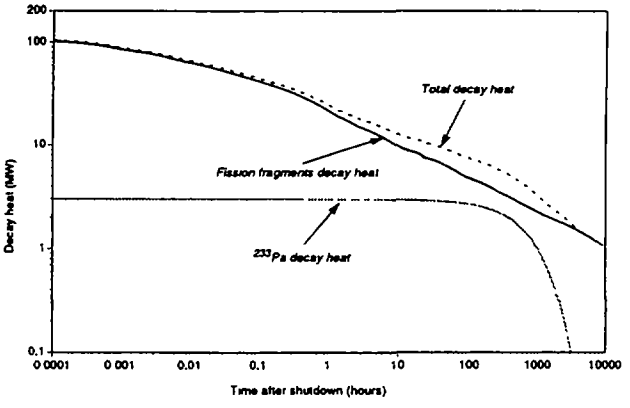

FIG. 5.17 Effect of ^{233}Pa on the decay heat of the Fast Energy Amplifier.

[1] 1 kg of dissolved material corresponds to 0.1 ppm in relative mass. Many radioactive impurities which amount typically to ≈ 1 g, once diluted in the bulk of the coolant, reprresent a concentration of 10^{-10} by weight in the coolant.

dependence of the γ-activity of the Fuel weighted proportionally to energy over the spectrum, namely the number of 1 MeV equivalent γ's produced per second. As one can see, the dominant contribution comes from ^{233}Pa, at least during the early times. A corresponding cooling time of about one year is strongly recommended, which also insures that the major fraction of ^{233}Pa has decayed into useful ^{233}U. With these provisos, the presence of ^{233}Pa should not introduce additional, specific problems. Other Protactinium Isotopes are some 4.47 kg (including the 0.15 kg in the Breeder) of the long-lived ^{231}Pa (4.74×10^4a), amply discussed in paragraphs D.3.2.8 ÷ D.3.2.10 and traces (≤ 1 g) of the short-lived ^{232}Pa (1.89 d) and ^{234}Pa (9.69 h). The long-lived isotope ^{231}Pa primarily produced by fast neutrons through the (n,2n) reaction on the main element ^{232}Th followed by ß-decay, constitutes a considerable source of radio-toxicity and it must be incinerated, re-injecting it inside the subsequent Fuel Loads, as discussed in paragraph D.3.2.10. Fortunately the cross section for neutron capture, leading to ^{232}U is quite large and equilibrium between production and decay is reached already at the end of the first cycle. This means that a net stockpile of the order of 5 kg of ^{231}Pa will persist during the whole lifetime of the EA plant as balance between production and incineration.

(2) The presence of a specific composition of Uranium isotopes, evolving toward an asymptotic distribution. A relative novelty is the presence of a substantial amount (1.46 kg) of the long lived isotope ^{232}U (99.6 a) produced by fast neutrons and the (n,2n) reaction on the main fissile material ^{233}U. As in the case of ^{231}Pa, the concentration of ^{232}U reaches practically its asymptotic limit already at the end of the first fuel cycle. As already pointed out, the presence of such an isotope, which has a decay chain prolific of high energy γ-rays is a major inconvenience if some of the Uranium fuel were to be diverted to military applications. The γ-ray activity of the Fuel is of primary importance also during reprocessing and new fuel preparation. We show in Figure 5.18 the number of 1 MeV equivalent γ's produced per second by the discharge fuel of an EA and compared with the one of an ordinary PWR. This last curve has been normalised to the same electric energy produced in the EA. *As one can see, after the cooling down period of about one year needed to transform the ^{233}Pa, the γ-doses of the spent fuel of an EA are not substantially different than the one of an ordinary PWR.*

(3) The isotopic composition of the Uranium is a rapidly decreasing function of the atomic number. There is essentially no ^{238}U produced, since the previous element, ^{237}U is short lived (9.76 d) and it β-decays into ^{237}Np, which is the main gateway to the trans-uranic elements.

(4) A remarkable scarcity of trans-Uranic elements. Concentrations are fuel cycle dependent and values of Table V.8. refer to the most favourable case of the first fuel cycle. The main production mechanism is neutron capture of the long-lived ^{237}Np producing ^{238}Np, which then quickly (3.06 d) decays into ^{238}Pu (127 a). The family of Plutonium isotopes with A ≥ 239 becomes accessible by successive neutron captures. Even asymptotically, as shown in detail in paragraph D.3.2.9, concentrations decrease rapidly with growing A, because of the competing fission channel at each step. Asymptotic concentrations are also many orders of magnitude lower than for instance in the case of a Uranium driven Reactor. Seven neutrons are needed for instance to transform ^{232}Th into ^{239}Pu, while a single neutron capture can achieve the same result starting from ^{238}U.

Amongst the unstable elements which require special consideration in the Table V.8, there is a significant amount (14.5 g) of ^{14}C (8286 a) produced by n-capture reaction on the isotope ^{17}O, present in small amounts (1.84 kg) in the natural Oxygen of the ThO_2 and UO_2 in the Fuel and in the Breeder. The production of this isotope is however of importance since it is one of the main contributors to the radio-toxicity emitted in the environment during reprocessing. It is difficult to separate out such a small amount of Carbon with the methods proposed to reprocess the Fuel (see paragraph D.3.6.2). The relevant neutron capture cross section for the process ^{17}O(n,α) (averaged over the Fuel spectrum) is the relatively large value of 23.3 mbarn. An additional source of ^{14}C in the EA, not included in Table V.8 could be due to the presence of N_2 impurities in the fuel, typically of the order of 10 ppm by weight (0.3 kg). The cross section for the relevant process ^{14}N(n,p) is of the order of 2 mbarn and its contribution for the integrated neutron fluence $\int \Phi dt = 3.3 \times 10^{23}$ n/cm^2 is then only 0.198 grams. Note that the total amount of chemical Carbon

produced in the Fuel is 0.587 kg, mostly of ^{13}C. It is expected to be almost completely oxidised at the fuel operating temperatures and therefore be mostly in the form of CO_2 at the time of reprocessing.

TABLE V.8. DISCHARGE OF CORE VOLUME AT THE END OF THE FIRST FUEL CYCLE.

	Mass (kg)	EA/ PWR	1/e Lifetime
^{14}C	0.0145	—	8286. a
^{49}V	0.0003	—	1.339 a
^{51}Cr	0.0078	—	40.06 d
^{53}Mn	0.004	—	0.540E+07 a
^{54}Mn	0.2019	—	1.237 a
^{55}Fe	1.717	—	3.948 a
^{59}Fe	0.0033	—	64.35 d
^{60}Co	0.0006	—	7.622 a
^{70}Zn	0.006	—	0.723E+15 a
^{79}Se	0.9983	1.916	0.94E+06 a
^{85}Kr	21.64	10.160	15.55 a
^{86}Rb	0.0088	4.261	26.94 d
^{87}Rb	46.52	2.157	0.687E+11 a
^{89}Sr	2.402	1.127	73.07 d
^{90}Sr	74.76	1.578	41.62 a
^{88}Y	0.0006	—	154.2 d
^{91}Y	3.313	0.991	84.61 d
^{93}Zr	88.34	1.387	0.221E+07 a
^{95}Zr	3.537	0.623	92.57 d
^{94}Nb	0.0011	—	0.293E+05 a
^{95}Nb	2.026	0.649	50.57 d
^{97}Tc	0.0003	—	0.376E+07 a
^{98}Tc	0.0014	—	0.607E+07 a
^{99}Tc	56.08	0.827	0.305E+06 a
^{103}Ru	0.708	0.176	56.77 d
^{106}Ru	1.147	0.074	1.480 a
^{102}Rh	0.0007	_	299.3 d
^{107}Pd	1.926	0.096	0.939E+07 a
^{111}Ag	0.0063	0.152	10.77 d
^{123}Sn	0.1047	2.645	186.8 d
^{125}Sn	0.0149	1.435	13.94 d
^{126}Sn	4.236	1.734	0.144E+06 a
^{124}Sb	0.0084	1.087	87.05 d
^{125}Sb	1.127	0.889	3.988 a
^{126}Sb	0.0026	2.253	18.02 d
^{129}I	27.28	1.722	0.227E+08 a
^{131}I	0.2924	0.458	11.63 d
^{134}Cs	6.062	0.546	2.982 a
^{135}Cs	115.9	4.505	0.332E+07 a
^{136}Cs	0.1134	2.103	19.03 d
^{137}Cs	118.5	1.109	43.52 a
^{140}Ba	0.8585	0.470	18.44 d
^{137}La	0.0135	—	0.867E+05 a
^{138}La	0.0040	—	0.151E+12 a
^{139}Ce	0.0023	—	199.0 d
^{141}Ce	2.5330	0.575	47.00 d
^{144}Ce	17.300	0.515	1.129 a
^{143}Pr	0.9254	0.547	19.62 d
^{147}Nd	0.2539	0.401	15.88 d
^{146}Pm	0.0010	—	7.996 a
^{147}Pm	15.410	1.315	3.793 a
^{147}Sm	12.010	2.551	0.153E+12 a
^{151}Sm	4.7700	0.568	130.1 a

TABLE V.8 (CONT.). DISCHARGE OF CORE VOLUME AT THE END OF THE FIRST FUEL CYCLE.

	Mass (kg)	EA/ PWR	1/e Lifetime		Mass (kg)	EA/ PWR	1/e Lifetime
^{152}Eu	0.0324	12.843	19.58 . a	^{194}Hg	0.0026	—	751.9 a
^{154}Eu	0.6074	0.164	12.43 a	^{203}Hg	0.0001	—	67.40 d
^{155}Eu	0.4376	0.290	6.767 a				
^{156}Eu	0.0046	0.012	21.96 d	^{204}Tl	0.0049	—	5.466 a
^{160}Tb	0.0028	0.300	104.5 d	^{202}Pb	0.0455	—	0.759E+05 a
				^{205}Pb	20.300	—	0.221E+08 a
^{185}W	0.2344	—	108.6 d				
				^{208}Bi	0.0011	—	0.532E+06 a
^{187}Re	2.5220	—	0.629E+11 a				
				^{210}Po	0.0055	—	200.1 d

TABLE V.8(CONT.). ACTINIDES OF CORE VOLUME AT THE END OF THE FIRST FUEL CYCLE.

Element	Mass (kg)	1/e Lifetime	Element	Mass (kg)	1/e Lifetime
^{228}Th	0.0213	2.766 a	^{232}U	1.4270	99.63 a
^{230}Th	0.2352	0.1090E+06 a	^{233}U	2,463	0.2302E+06 a
^{232}Th	20,850 [1]	0.2032E+11 a	^{234}U	260.40	0.3543E+06 a
^{234}Th	0.0059	34.85 d	^{235}U	24.0800	0.1018E+10 a
			^{236}U	2.7860	0.3387E+08 a
^{231}Pa	4.3120	0.4737E+05 a			
^{233}Pa	53.2500	38.99 d	^{237}Np	0.2889	0.3094E+07 a
			^{238}Pu	0.0712	126.9 a
			^{239}Pu	0.0003	0.3486E+05 a

D.3.5.8. SPALLATION PRODUCTS

The spallation process produces a large amount of fragments. These fragments, which are generated primarily by high energy particles, have been properly taken into account in the FLUKA part of the simulation programme. The mass spectrum of the spallation fragments is strongly energy dependent. At low proton energies ($\leq$ 40 MeV), the mass (A,Z) spectrum is peaked close to the father nucleus. At intermediate energies ($\approx$ 400 MeV) a splitting similar to fission occurs, in which two fragments of roughly similar mass are formed. At very high energies, the spallation spectrum changes again and all (A,Z) are produced in a roughly flat distribution. This complex phenomenology is only approximately represented by FLUKA and the mass yield could be uncertain to up to a factor two.

In order to evidence them the spallation target region, namely the Lead volume to which the core is concentric has been considered as a different material. In our design however the whole coolant is mixed

[1] Initially 24.230 Kg. Difference due to burn-up.

during operation. Hence in reality spallation products will diffuse inside the whole EA volume.

As shown in Figure 5.18, the overall γ-activity of the spallation products is many orders of magnitude smaller then the one of the Fuel. Still it is sizeable and it must be considered carefully. We give in Table V.9 the list of unstable elements with lifetime larger than 10 days. As already mentioned this corresponds to very small concentrations (1 g = 0.1 ppb) and therefore it is difficult to predict what will be their actual fate without additional experiments.

Qualitatively we can say that several elements will come out in the form of gas or vapours and accumulate in the (inert) gas inside the vessel[1]. This is definitely the case of (1) some Tritium and the noble gases ^{39}Ar (389 a), ^{42}Ar (47.6 a),^{81}Kr (3.3 × 10^6 a), ^{85}Kr (15.5 a),^{127}Xe (52.6 d), which are produced at the modest total rate of about few g/a, (2) traces (≤ 1 g) of some elements which have a significant vapour tension at the operating temperature of the EA, namely ^{36}Cl (4.3 × 10^6 a), ^{73}As (116 d), ^{125}Sb(4.0 a), ^{125}I (86 d), ^{134}Cs (2.98 a) and the main elements which are 15.25 g of ^{202}Tl (17.68 d), 386 g of ^{204}Tl (5.5 a), 415.9 g of ^{194}Hg (751.9 a) and 6.2 g of ^{203}Hg (67 d).

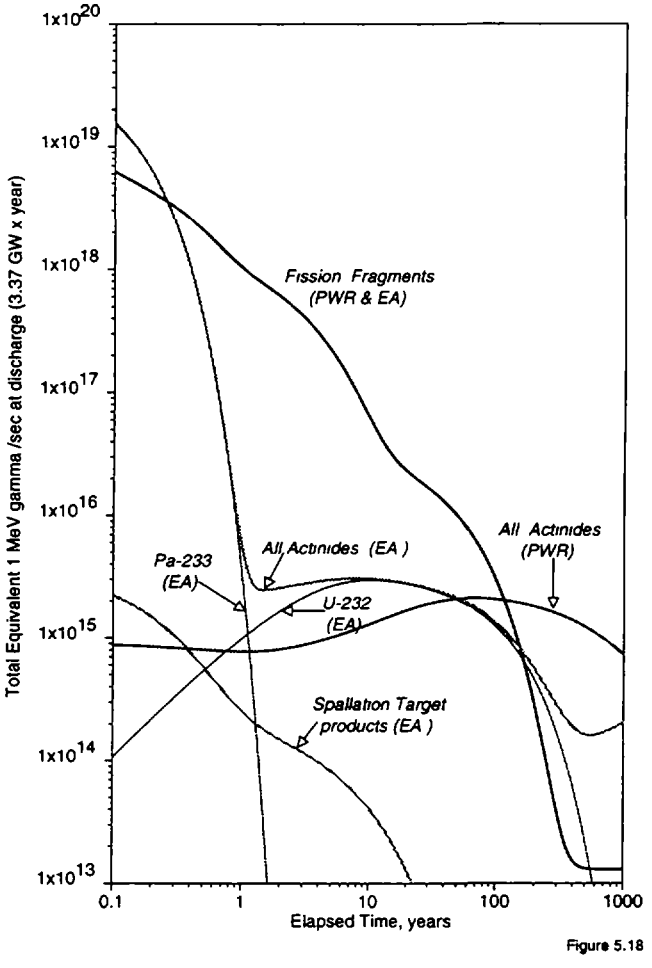

FIG. 5.18 Time Evolution of the γ-activity of the fuel after discharge of the EA. The number of γ-rays is normalized according to their energy in MeV. The curve for the PWR has been calculated for the same energy delivered and a burn-up of 33 GW × d/t.

Others will remain in solution inside the coolant. There is a large number of elements which will form with Lead inter-metallic compounds. Some elements will combine chemically with Lead (S, Se and Te) and remain dissolved. We note that ^{210}Po (200 d) belongs to the same series but its precise chemistry is unknown. There are several elements which will remain metallic but have a large solubility in Lead and therefore should be retained. Finally some elements have a very high melting point and presumably will also remain trapped inside the coolant.

During operation some of the spallation products may be "incinerated" by the neutron bombardment. The programme records the secondary interactions of all the materials of the spallation target and therefore the effect is taken into account in Table V.9. The effects of these secondary interactions are negligibly small, since the concentrations are insufficient to produce a sizeable interaction probability.

[1] Note that the quoted values for the masses are the values at dicharge after 5 years of continuous operation. If continuously extracted, the total amount of the short-lived elements is correspondingly larger.

TABLE V.9. PRODUCTS AT DISCHARGE PRODUCED IN THE SPALLATION TARGET VOLUME.

	Mass	1/e	Vapour [boil. T]
^{3}H	1.435	17.83 a	*Gaseous* [-252°C]
^{35}S	0.009	126.5 d	*Gaseous* [445 °C]
^{36}Cl	0.204	0.435E+6 a	*Bound* +) [- 34°C]
^{39}Ar	0.336	389.0 a	*Gaseous*
^{42}Ar	0.336	47.57 a	*Gaseous* [-186°C]
^{45}Ca	0.007	236.9 d	*Intermet* 0.2 Torr
^{49}V	0.072	1.339 a	*Solid* [3409°C]
^{53}Mn	0.387	0.540E+7 a	*Solid(*)* 10^{-5} Torr
^{59}Fe	0.049	64.35 d	*Solid(*)*
^{60}Fe	0.586	0.216E+7 a	*Solid(*)* [2862°C]
^{56}Co	0.029	111.7 d	*Solid(*)*
^{57}Co	0.065	1.077 a	*Solid(*)*
^{58}Co	0.002	102.4 d	*Solid(*)*
^{60}Co	1.084	7.622 a	*Solid(*)* [2928°C]
^{59}Ni	0.253	0.109E+6 a	*Solid(*)*
^{63}Ni	2.134	144.7 a	*Solid(*)* [2914°C]
^{65}Zn	0.004	353.2 d	*Volatile*
^{70}Zn	2.424	0.723E+15a	*Volatile* 40 Torr
^{68}Ge	0.032	1.073 a	*Solid*
^{71}Ge	0.079	16.53 d	*Solid* [2834°C]
^{73}As	0.329	116.1 d	*Gaseous* [615 °C]
^{75}Se	0.184	173.2 d	*Intermet*
^{79}Se	2.03	0.939E+6 a	*Intermet* [685 °C]
^{81}Kr	5.777	0.331E+6 a	*Gaseous*
^{85}Kr	4.326	15.55 a	*Gaseous* [-153 °C]

	Mass	1/e	Vapour [boil. T]
^{83}Rb	0.036	124.6 d	*Gaseous*
^{86}Rb	0.181	26.94 d	*Gaseous* [688 °C]
^{85}Sr	0.264	93.76 d	*Intermet*
^{89}Sr	0.21	73.07 d	*Intermet*
^{90}Sr	3.88	41.62 a	*Intermet* 0.40 Torr
^{88}Y	0.247	154.2 d	*Solid*
^{91}Y	0.318	84.61 d	*Solid* [3338°C]
^{88}Zr	0.581	120.6 d	*Solid(*)*
^{93}Zr	6.426	0.221E+7 a	*Solid(*)*
^{95}Zr	0.46	92.57 d	*Solid(*)* [4409°C]
^{91}Nb	4.139	983.3 a	*Solid*
^{92}Nb	0.496	0.501E+8 a	*Solid*
^{94}Nb	1.13	0.293E+5 a	*Solid*
^{95}Nb	1.187	50.57 d	*Solid* [4744°C]
^{93}Mo	4.726	5784. a	*Solid* [4639°C]
^{97}Tc	1.896	0.376E+7 a	*Solid*
^{99}Tc	8.333	0.305E+6 a	*Solid* [4265°C]
^{103}Ru	0.182	56.77 d	*Solid*
^{106}Ru	1.069	1.480 a	*Solid* [4150°C]
^{101}Rh	4.32	4.772 a	*Solid*
^{102}Rh	0.244	299.3 d	*Solid* [3697°C]
^{107}Pd	5.207	0.939E+7 a	*Solid* [2964°C]
^{105}Ag	0.108	59.71 d	*Solid ?* 5 10^{-6} To
^{109}Cd	1.627	1.833 a	*Volatile* 200 Torr
^{113}Sn	0.427	166.4 d	*Solid(*)*
^{123}Sn	0.206	186.8 d	*Solid(*)*
^{126}Sn	0.622	0.144E+6 a	*Solid(*)* 3 10^{-8} To

+) Lead Cloride, $PbCl_2$, b.p. 950 °C (*) Dissolved in the Molten Lead

TABLE V.9 (CONT.). PRODUCTS AT DISCHARGE PRODUCED IN THE SPALLATION TARGET VOLUME.

	Mass	1/e	Vapour [boil. T]
^{124}Sb	0.043	87.05 d	*Volatile*
^{125}Sb	0.404	3.988 a	*Volatile*
		[1585°C]	0.5 Torr
^{121}Te	0.008	24.26 d	*Intermet* -)
^{125}I	0.014	85.90 d	*Gaseous*
			[184°C]
^{127}Xe	0.37	52.63 d	*Gaseous*
			[-108°C]
^{131}Cs	0.003	14.01 d	*Gaseous*
^{134}Cs	0.282	2.982 a	*Gaseous*
			[671°C]
^{131}Ba	0.001	17.06 d	*Intermet*
^{133}Ba	0.396	15.21 a	*Intermet*
			2 10^{-2} To
^{137}La	2.653	0.867E+5 a	*Solid*
			[3464°C]
^{139}Ce	0.722	199.0 d	*Solid*
^{141}Ce	0.002	47.00 d	*Solid*
			[3443°C]
^{143}Pm	1.1	1.050 a	*Solid*
^{145}Pm	0.419	25.59 a	*Solid*
^{146}Pm	0.205	7.996 a	*Solid*
			[3520°C]
^{145}Sm	1.064	1.347 a	*Intermet*
^{146}Sm	0.406	0.148E+9 a	*Intermet*
^{151}Sm	2.492	130.1 a	*Intermet*
			2 10^{-4} To
^{149}Eu	0.001	134.6 d	*Intermet*
^{150}Eu	0.76	51.77 a	*Intermet*
^{154}Eu	0.932	12.43 a	*Intermet*
			8 10^{-3} To
^{151}Gd	0.05	179.3 d	*Solid*
			[3273°C]
^{160}Tb	0.214	104.5 d	*Solid*
			[3230°C]
^{159}Dy	0.021	208.8 d	*Solid*
			[2587°C]

	Mass	1/e	Vapour [boil. T]
^{173}Lu	0.908	1.981 a	*Solid*
			[3402°C]
^{172}Hf	0.288	2.704 a	*Solid*
^{175}Hf	0.029	101.2 d	*Solid*
			[4603°C]
^{179}Ta	2.467	2.588 a	*Solid*
^{182}Ta	1.025	165.5 d	*Solid*
			[5458°C]
^{181}W	1.621	175.3 d	*Solid*
			[5555°C]
^{183}Re	3.267	101.2 d	*Solid*
^{187}Re	1.829	0.629E+11a	*Solid*
			[5596°C]
^{185}Os	8.957	135.3 d	*Solid*
			[5012°C]
^{189}Ir	3.362	19.09 d	*Solid*
			[4428°C]
^{188}Pt	1.515	14.75 d	*Solid*
^{190}Pt	196.2	0.94E+12 a	*Solid*
^{193}Pt	307.4	72.30 a	*Solid*
			[3827°C]
^{195}Au	109.5	269.1 d	*Solid*
			[2857°C]
^{194}Hg	415.9	751.9 a	*Gaseous*
^{203}Hg	6.252	67.40 d	*Gaseous*
			[357°C]
^{202}Tl	15.25	17.68 d	*Volatile ?*
^{204}Tl	386	5.466 a	*Volatile ?*
			6 10^{-2} To
^{202}Pb	2,071	0.759E+5 a	*Dissolved*
^{205}Pb	11,960	0.221E+8 a	*Dissolved*
			30 Torr
^{205}Bi	4.299	22.14 d	*Eutectic*
^{207}Bi	69.79	45.62 a	*Eutectic*
^{208}Bi	14.63	0.532E+6 a	*Eutectic*
^{210}Po	0.995	200.1 d (boils at	*Volatile* 254 °C)

-) Lead Telluride, PbTe, m.p. 917 °C

D.3.6. CLOSING THE FUEL CYCLE

D.3.6.1. GENERAL CONSIDERATIONS

There are significant, conceptual differences between what one means by "reprocessing" in the case of a PWR and an EA. In the case of a PWR, the primary purpose of reprocessing — if one excludes recovery of Plutonium for military applications — is the one of preparing for a more orderly, definitive repository of the radio-toxic products, separating for instance Actinides from FFs. Many conceptual designs have been proposed for the purpose of further healing the strong radio-toxicity of such individual products with nuclear transformations with the help of neutrons from Accelerators and Reactors. We shall mention as our reference case the project CAPRA [23] in which one intends to reduce the radio-toxicity of the Plutonium from spent fuels by about a factor 30 with the help of Fast-Breeders similar to SuperPhénix. In addition to producing a large amount of electric energy, one such device could process Plutonium and eventually Americium produced by about five ordinary PWRs.

In the case of the EA, at "replacement" time the fuel itself (Actinides) is still perfectly sound and it could continue to burn much further if it were not for the neutron absorption due to the accumulated FFs. Hence after a "reprocessing", which is in fact basically a "FF separation and disposal", the fuel can and should be used again. This is a fundamental difference with a PWR, where spent fuel is hardly more than waste material and for which reprocessing is arguable. In the case of an EA, fuel reprocessing could be better described as fuel regeneration. The purpose of such a procedure is

(1) to remove the poisoning FFs;

(2) to add the fraction of the Thorium fuel which has been burnt;

(3) to re-establish mechanical solidity to the fuel and the cladding which has been affected by the strong neutron flux.

In nuclear power generation, radioactive materials must be isolated at all times from the environment with an appropriate, multiple containment. The residual radio-toxicity is defined as the toxicity of products extracted from such a closed environment. Since the bulk of the Actinides are recycled inside the core for further use, the relevant toxicity is basically the one which is spilled out during the fuel regeneration process and the one of the elements which are deliberately removed, like for instance the one of the FFs which are not incinerated and of the sleeves which contain the fuel which are not reused. This is in contrast with an ordinary PWR — at least if no incineration is performed — in which the totality of the radio-toxicity of the spent fuel constitutes "Waste" and it must be isolated from the environment by a Geologic Repository over millions of years.

D.3.6.2. STRATEGY FOR THE SPENT FUEL

The main requirement of the reprocessing of the fuel from the EA is the one of generating a new fuel free of FFs. Therefore reprocessing is inevitable in our conception of the EA. In practice one must separate the Fuel into two different stock piles, the first destined to the next fuel load and the remainder which is usually called the high activity stream (HLW). The bulk of the Actinides are to be recycled into new fuel and they belong to the former stockpile. There is no need to worry about their long lasting consequences, since they will be burnt in the successive, cycles. The latter stockpile will contain all fission fragments and activity in the cladding plus the tiny fraction f of Actinides which is not separated by the reprocessing. They represent a considerable radio-toxicity, which will be handled either with natural decay or with active incineration of some specific radio-nuclides. Figure. 6.1 gives the ingestive radio-toxicity [31] of such a high activity stream assuming $f = 1.0 \times 10^{-4}$ (the choice of such a value will be clearer later on). The total radio-toxicity of a PWR initially loaded with 3.3% enriched Uranium and without reprocessing is also shown for comparison. Data are given for the fuel discharge after the first fill and for asymptotic fuel

composition. The two distributions are very similar, since the fuel remaining radio-toxicity at long times is dominated by the ^{233}U contamination which is the same for all fillings. After a large drop over the first ≈ 500 years due to the decay of medium lifetime FFs (^{90}Sr-^{90}Y, ^{137}Cs), the ingestive radio-toxicity stabilises to a roughly constant level, dominated by the truly long lived FFs (^{129}I, ^{99}Tc, ^{126}Sn, ^{135}Cs, ^{93}Zr and ^{79}Se) and to a lower extent by the residual fraction *f* of Actinides. After such a cooling-off time the residual radio-toxicity is comparable to the one of the ^{232}Th in the EA and about 5×10^{-5} times smaller than the one of a throw-away PWR of equivalent yield. The α-activity is very modest since it is dominated by the leaked fraction *f* of Actinides.

Inspection of Figure 6.1 suggests that the HLW should be stored for about 500 ÷ 700 years in what we call the "Secular Repository". Beyond such period, the residual radio-toxicity is considerably reduced as shown in Figure 6.2. The specific FFs contributing to radio-toxicity after 1000 years are listed in Table VI.1. It is possible to consider at this point the surviving radiation as Class A (10 CFR 61) for surface storage material even if the waste material will remain buried and provided it is diluted in ≥ 1000 $m^3/(GW_e \times a)$.

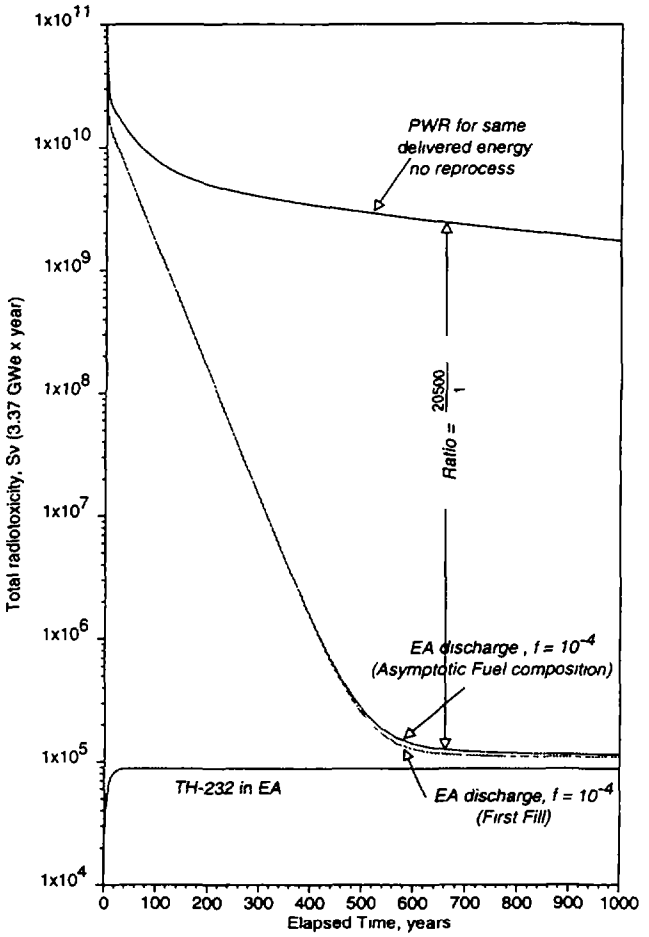

FIG. 6.1 Evolution of the ingestive radio-toxicity of High Level Waste (HLW) during Secular Repository period.

It is possible to further reduce the activity of the residual waste by extracting some or all the sensitive elements of Table VI.1 and "incinerating" them with neutrons in the EA. A more detailed paper on incineration is in preparation [78] and an experiment is in preparation at CERN [6], since most of the relevant cross sections are poorly known. Here we shall limit our considerations to the ones on general strategy. Three possible further steps are possible:

1) Technetium and Iodine are chemically extracted and incinerated. The first is a pure ^{99}Tc isotope and the second besides ^{129}I contains about 33% of stable isotopes which are kept in the incineration stream. The total mass to be incinerated is about 19 $kg/(GW_e \times a)$, which is modest. The ingestive radio-toxicity of the remainder after 1000 years is reduced from 63.4 kSv to 16.2 kSv and the Class A dilution volume from 1194 $m^3/(GW_e \times a)$ to 68 $m^3/(GW_e \times a)$.

2) Procedure as point 1) but also Caesium is chemically extracted. The amount of Caesium is much larger, ≈ 100 $kg/(GW_e \times a)$. In addition isotopic separation is necessary in order to separate the 34 $kg/(GW_e \times a)$ of ^{135}Cs from the very radio-toxic (3.92×10^6 Sv) but shorter lived ^{137}Cs. This may be difficult, although a feasibility study has been carried out [79]. After incineration of ^{135}Cs, the ingestive radio-toxicity after 1000 years of the remainder is reduced to 6.3 kSv and the Class A dilution volume to 29 $m^3/(GW_e \times a)$.

3) Procedure as point 2) but also Zirconium and Tin are chemically extracted. Both elements require isotopic separation. One of the other isotopes of Tin is radioactive and slightly toxic. In this way the only known long lived isotope left in the discharge is ^{79}Se (0.3 kg) which represents 0.745 kSv

and the ridiculously small Class A dilution volume of 0.6 $m^3/(GW_e \times a)$.

These procedures (Figure 6.3) will ensure that the radio-toxicity of the FFs in the "Secular Repository" is exhausted in less than 1000 years, which is a sufficiently short time to be absolutely confident that current technologies of vitrification and of containment can make the storage totally safe.

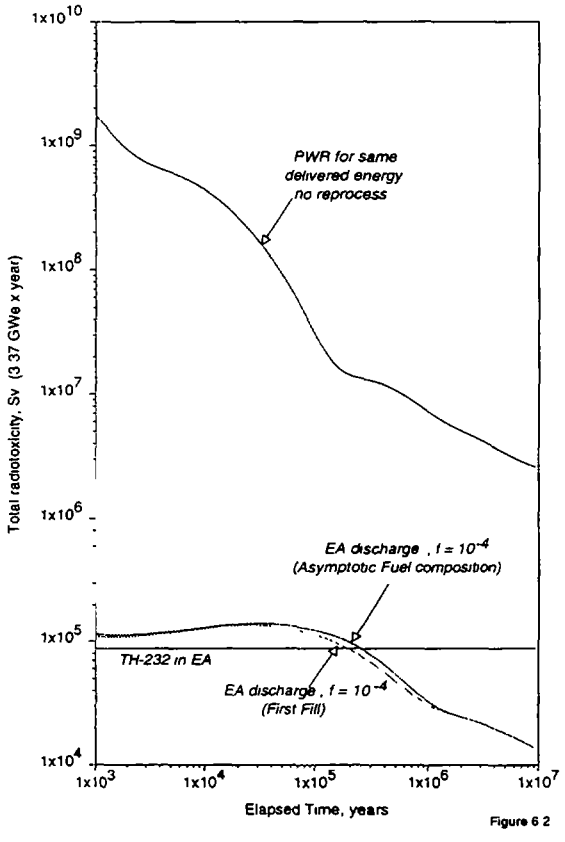

FIG. 6.2 Evolution of the ingestive radio-toxicity of HLW beyond the "Secular Repository" period.

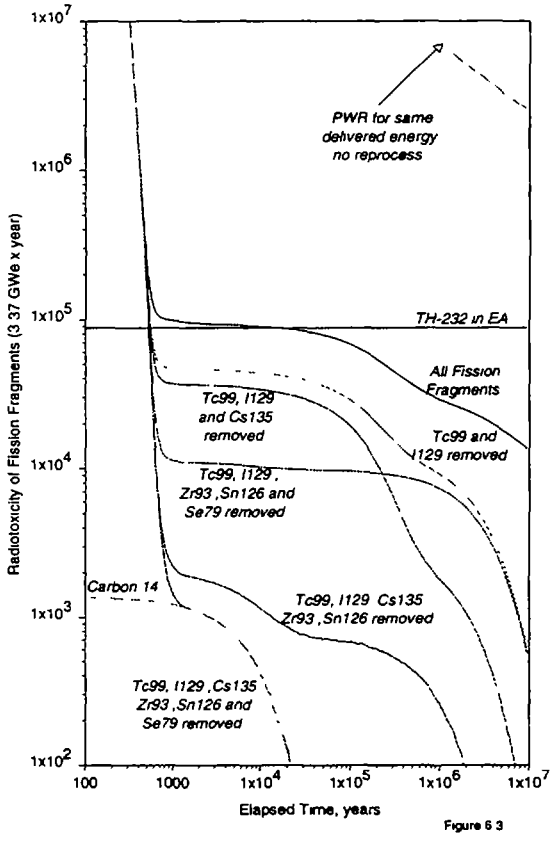

FIG. 6.3 Evolution of the ingestive radio-toxicity of the FFs for different incineration procedures.

In addition to the FFs, in the High Level Stream there will be leaks of Actinides due to the imperfections of the reprocessing. These radio-nuclides are more worrisome since some of them are important α-emitters. The radio-toxicity and the α-activity in Ci for leaked fractions $f = 10^{-4}$ and $f = 2 \times 10^{-6}$ are displayed in Figure 6.4 and in Figure 6.5 respectively. The radio-toxicity has two maxima or "bumps", the first roughly for time span of the secular repository and a second for very long times, namely $10^5 \div 10^6$ years. The second maximum is due to ^{233}U and its descendants. The first bump in the toxicity in the early fillings is due to ^{232}U and it grows substantially in the later fillings and in the asymptotic fuel composition because of the increased presence of ^{238}Pu and its descendants. The α-activity is instead always determined by the ^{232}U and its descendants at short times and by ^{233}U and its descendants at long times. The total α-activity of Actinides is about 10^5 Ci, for a fuel mass of the order of 22 tons, which corresponds to an average activity of about 5 mCi/g. Note that the activity of Thorium which is the largest mass is very small and that if Uranium's are separated out they will have a specific activity which is about ten times larger than the bulk of the spent fuel.

D.3.6.3. FUEL REPROCESSING METHODS

In our case production of the lighter Neptunium and Plutonium isotopes is very low and higher actinides are nearly absent. However the (n,2n) reactions, more probable at high energies, increase the

amount of highly toxic ^{231}Pa and ^{232}U.

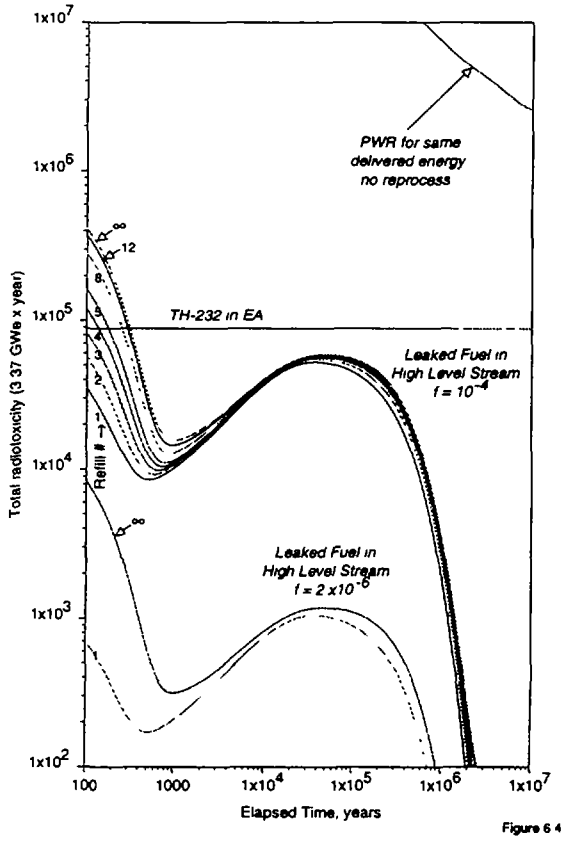

FIG. 6.4 Radio-toxicity of the residual Actinide waste stream for different leak fractions.

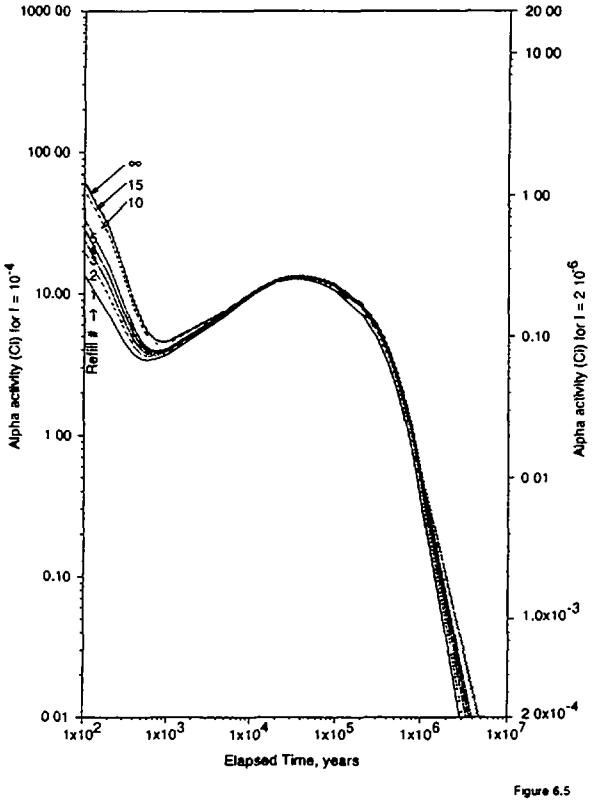

FIG. 6.5 α - activity of the residual Actinide waste stream for different leak fractions.

The EA requires the recovery of the Uranium (^{233}U). However, it offers the opportunity of destroying the other Actinides by concentrating them, after each discharge, in a few dedicated fuel bars (targets) inserted somewhere in the bundles of ordinary fuel, where an incineration lifetime of years is at hand. The amount of leaking Actinides in the High activity Waste stream destined to the Secular repository must be a small fraction $f \leq 10^{-4}$ of the produced amount. If incineration of the long lived FFs is performed to alleviate the radio-toxicity of the stored products after 500 years, an even higher performance in separating power is advisable, $f \leq 2.0 \times 10^{-6}$. The efforts in order to attain such a figure is justified by the considerable benefit attained by the practical elimination of the "Geologic times Repository". We remark that such an incentive has been so far absent.

Two methods have been considered and appear suitable to our application: (1) aqueous methods, presently in use and (2) the newly developed pyro-electric method. We shall review both of them in succession.

Aqueous reprocessing methods have proven to be efficient, particularly for the separation of U and Th (99.5% and higher). The best known example is the THOREX process, based on solvent extraction through the use of tributyl phosphate (TBP), which extracts and separates the Thorium and Uranium. Other Actinides can also be extracted although their concentrations are so low that the extraction efficiency will be lower.

Figure 6.6 describes schematically the overall fuel cycle. The fuel rods should be stored for cooling at least for one year, to allow the ^{233}Pa to decay to ^{233}U. Fuel rods are then sheared and chopped. The gaseous fission products will be accumulated, with in particular attention for the ^{85}Kr and $^{14}CO_2$ which are destined to the secular repository. Dissolution should be made with a mixture of nitric acid (HNO_3) and hydrofluoric acid (HF) since ThO_2 is a very refractory ceramic material. The HF concentration should not be higher than

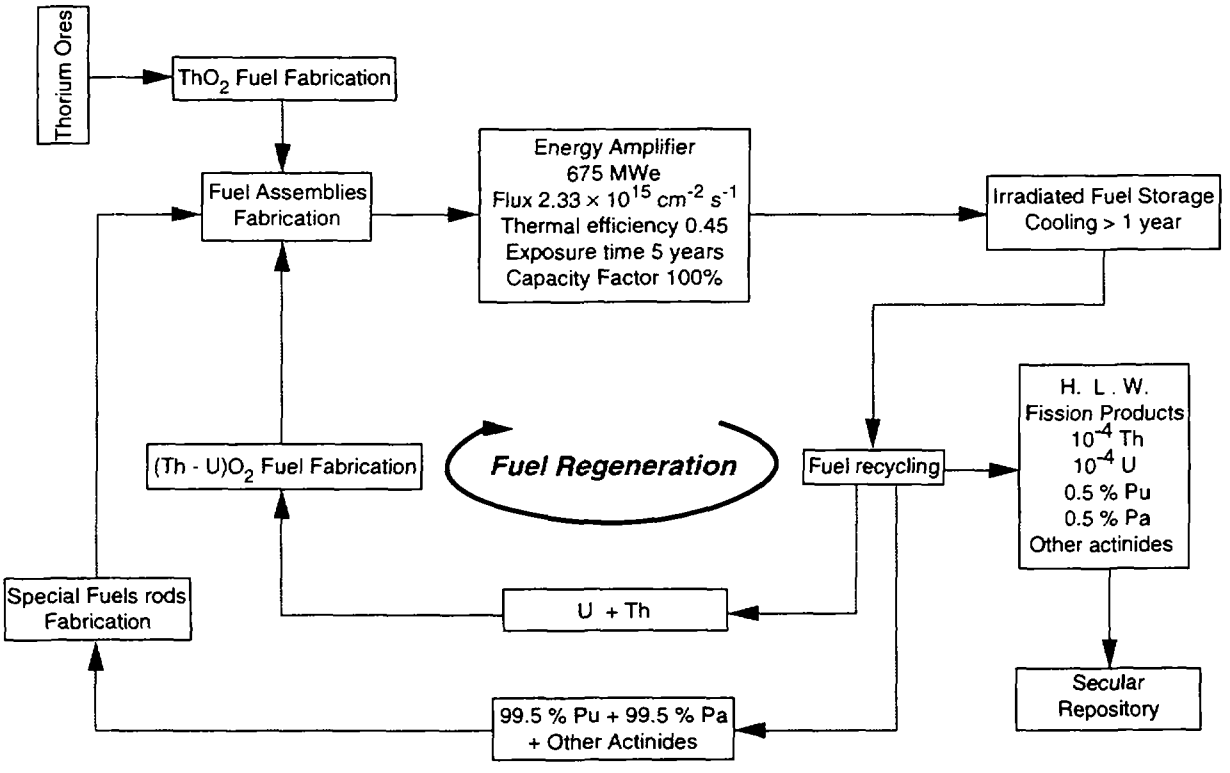

FIG. 6.6 Flow diagram of the partitioning process of spent fuel.

0.1 M and the addition of aluminium nitrate $Al(NO_3)_3$ as reagent could be needed in order to avoid corrosion of the stainless steel dissolver. Before carrying out the solvent extraction process from the obtained liquids they should be cleared of the remaining solids. The main components of the liquid will then be Thorium, Uranium, Fission Products, Protactinium and other trans-uranic Actinides.

The classic process to carry out the separation of Th and U from fission fragments is the acid THOREX. It uses TBP 30% v/v diluted with an organic solvent like dodecane. The partition of U from Th is done by washing the organic phase with diluted nitric acid. The U stream will also contain the very small amount of Pu and some contamination of Th and FF. The contamination of the Thorium stream will be mainly FF. The high active liquid waste stream will mainly contain FF, trans-uranic Actinides (^{231}Pa, ^{237}Np) and some residual contamination of Th and U. Further cycles for purification of Uranium and Thorium should be applied using TBP as extractant.

There is little information on the recovery of Pa and it will possibly require some additional studies. Tests carried out at Oak Ridge have shown [80] that Pa could be absorbed from solutions with high content of nitric acid by using various absorbents like unfired Vycor glass, silica gel or Zirconium phosphate. Its extraction should be done from the high level waste stream. Relative to the other Actinides its extraction will be less efficient since their concentration in the Highly Radioactive liquid Waste stream, although it can and should be increased, will nevertheless be very low.

The performance quoted in Figure 6.6 is above the current values according to standard experience on the THOREX process [13], [81], but appropriate tuning of the chemical parameters should allow higher efficiencies. The minimisation and ultimate disposal of High-Level radioactive Waste (HLW) generated from the reprocessing of spent fuel (THOREX) is an important part of the global nuclear fuel recycling strategy proposed in the framework of the Energy Amplifier Concept, as an alternative to classical disposal methods. The goal is twofold, (i) to recover from the insoluble residue useful metals such us Ru, Rh and

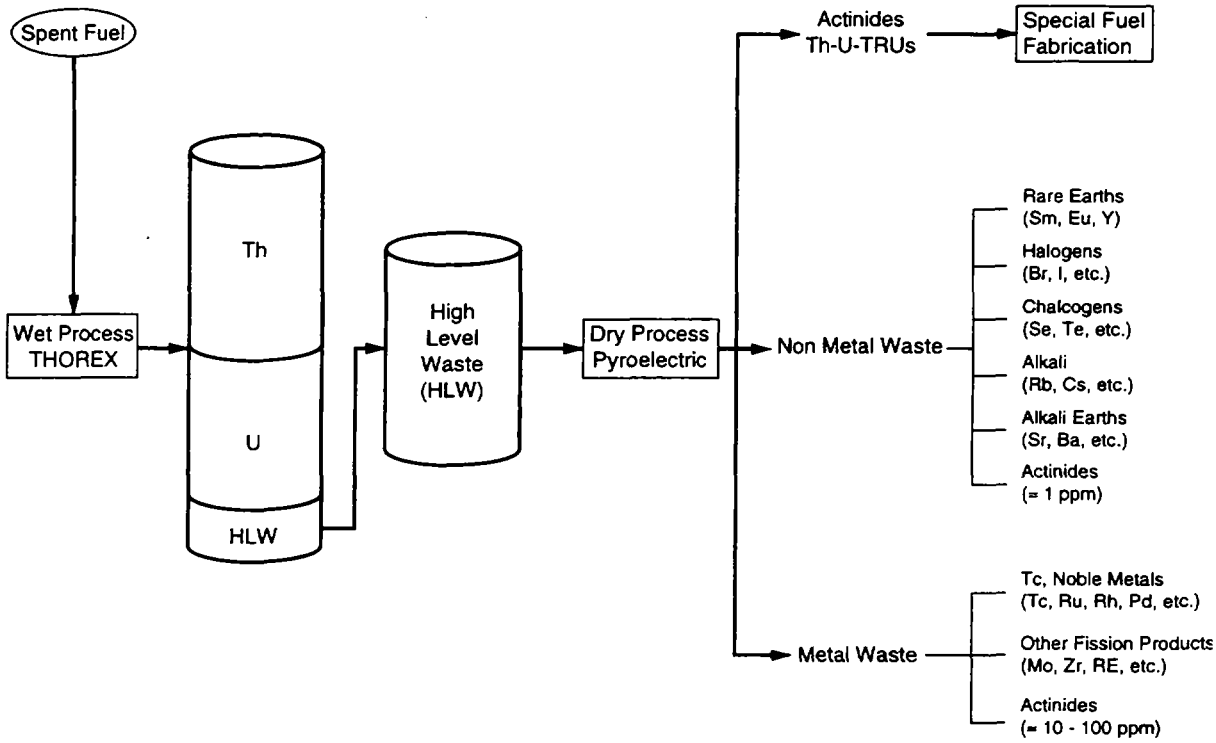

FIG. 6.7 High-Level Waste (HLW) reprocessing scheme.

Pd; (ii) and to separate Actinides[1] and some of the LLFPs (Long-Lived Fission Products) for their further use (incineration) or disposal. We believe this can best be achieved with the method developed in the context of the IFR (Integral Fast Reactor) programme [82], where it is proposed to separate actinides[2] and FPs from HLW by dry process with pyro-chemical (or pyro-metallurgical) methods (Figure 6.7). However, the only process that has reached an industrial scale is, at least for the moment, the PUREX process (aqueous method) which has already been described in the previous paragraphs. All the other methods are still in the technical or laboratory development phase.

Figure 6.8 shows the flow diagram of the dry process for partitioning of Actinides [83]. This process consists of (i) denitration to obtain oxides, (ii) chlorination to oxide to chlorides, (iii) reductive extraction to reduce Actinides from molten chlorides in liquid cadmium by using lithium as reductant, and (iv) electro-refining to increase the purity of Actinides recovered. Both denitration and chlorination steps are pre-treatment processes prior to the application of the pyro-metallurgical process.

The principle of the reductive extraction with the subsequent step of electro-refining is schematically drawn in Figure 6.9. The electro-refiner is a steel vessel that is maintained at *775 K (500 °C)*. Liquid LiCl-KCl electrolyte in the electro-refiner contains about *2 mol%* of the Actinide chlorides. The Actinide solution (in liquid cadmium) is inserted into the electrolyte and connected to the positive pole of a dc power source (anode). The negative pole of the power source is connected to a cathode immersed in the same electrolyte. The cathodes are simple steel rods. About *80%* of the Actinide metals is electro-transported from the anode to the cathode rods, where it deposits as nearly pure metal along with a relatively small

[1] In the F-EA, the Actinide residue consists mainly of Thorium, Protactinium, Uranium and a very small amount of TRUs, whereas in a PWR it is mostly TRUs.

[2] We expect this method can be extended to the extraction of Thorium and Protactinium.

amount of rare earth fission products[1]. All the products are retorted to remove salt (and Cadmium from the Cadmium electrode). Ingots from the retort are blended to appropriate composition, and recast into special fuel pins. The fission products, with the exception of Tritium, Krypton and Xenon, accumulate in the electro-refiner during processing, and some noble metal fission products are removed with the anode after each batch of fuel has been processed. The three gases are released into the process cell which has an argon atmosphere. They are recovered at high concentrations by the cell gas purification system.

Several dozen batches of fuel are processed in a "campaign". At the end of a campaign, the salt in the electro-refiner is treated by a series of steps to remove active metal fission products, particulate noble metals, and any oxide or carbide impurities for incorporation in high-level waste forms. The salt and its associated Actinide chlorides are returned to the electro-refiner. The Actinide inventory in the electro-refiner amounts to about *20%* of the Actinide elements fed; this must be recovered to achieve more than *99.9%* overall Actinide recovery. A non-metal and a metal waste form will accommodate all of the high-level wastes. The non-metal waste form will contain Samarium, Europium and Yttrium; the halogens and chalcogens; the alkali, and alkaline earth fission products; and a small amount of excess salt generated in the process. The Actinide content of that waste form will be exceptionally low (less than 1 part in 10^6 of the Actinides in the fuel that is processed). The only significant long-lived activity in this waste will be Se-79, I-129 and Cs-135: the total alpha activity should be less than *10 nCi* g^{-1}. Metal wastes from the electro-refiner - noble metals, cladding hulls and salt filter elements - will be combined with any process scrap such as broken electrodes and the rare earths from the salt purification process in the metal waste form. The metal waste form will have a very low Actinide content, because of the effective Actinide recovery in the pyro-metallurgical process, but its Actinide level will not be quite as low as that of the non-metal waste form. This whole process can be made continuous, and thus can take place in a matter of only a few hours.

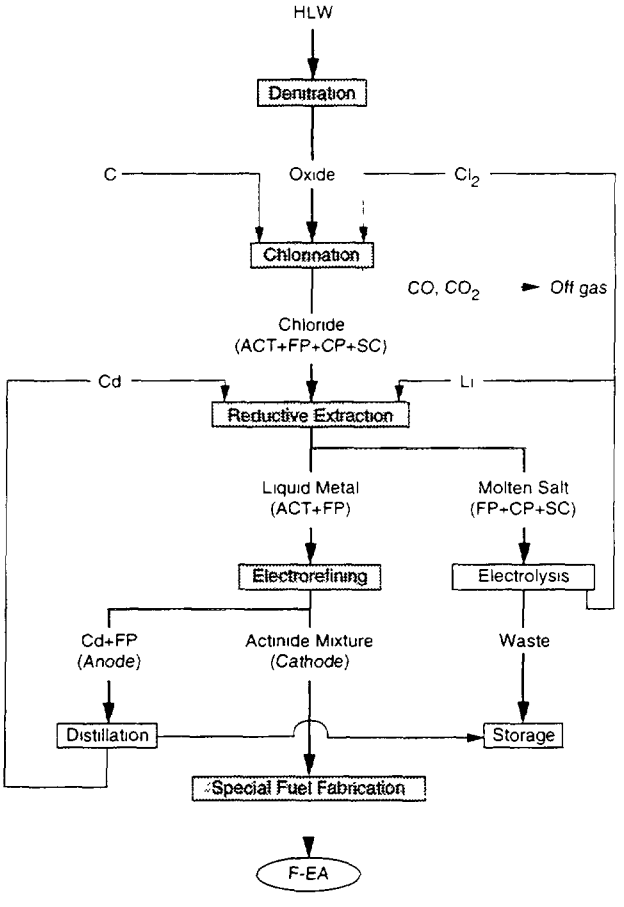

Figure 6.8

FIG. 6.8 Flow diagram of the pyro-metallurgical process for partitioning of the residual Actinides from HLW.

Pyro-processing offers a simple, compact means for closure of the fuel cycle, with anticipated high decontamination factor *(> 99.9%)*, minimal production of high-level radioactive waste, and significant reductions in fuel cycle costs. In addition, mainly from the weapons proliferation viewpoint, it offers an advantage over the PUREX and/or TRUEX methods, in that there is only partial removal of the fission products. Even though the process is based on the use of a metallic fuel alloy with nominal composition U-20Pu-10Zr, we believe it can be readily adapted to the EA fuel cycle without much efforts.

[1] In reprocessing F-EA fuel, the complete removal of fission products may not be necessary since their effect on the neutron economy is much less in a fast neutron spectrum than it is in a thermal spectrum.

The final content of the HLW stream coming from the EA fuel reprocessing is mainly FFs, with only traces of Actinides. The volume generated is about 5 m^3 per ton of fuel. The following step is to concentrate the aqueous raffinate and to transfer it to an intermediate storage of the reprocessing plant. The volume of the concentrate will be about 1 m^3/t. of fuel and the usual intermediate storage are tanks of suitable stainless steel such as to minimise the acid waste corrosion. To prevent the highly active liquid from boiling a redundant cooling system is required. Then, the concentrate is cooled for a period of about 10 years in order to reduce the heat generation by more than an order of magnitude before proceeding to waste solidification. Among the fission fragments, excluding the short lived and stable elements, there are a few elements which are medium lived (30 years, ^{90}Sr, ^{90}Y, ^{137}Cs, etc.) and some others (^{99}Tc, ^{135}Cs, ^{129}I, etc.) which are long lived (Table VI.1). Since Actinides are essentially absent from the HLW concentrates the policy we proposed to follow is to store in man-watched, secular repositories for several centuries the medium lived, in order to isolate them from the biosphere and to promote a vigorous research and development of methods for incinerating the bulk of the long lived FFs. The EA is an efficient tool to incinerate these wastes at the price of fraction of the neutron flux [6], but alternatively dedicated burners can be used.

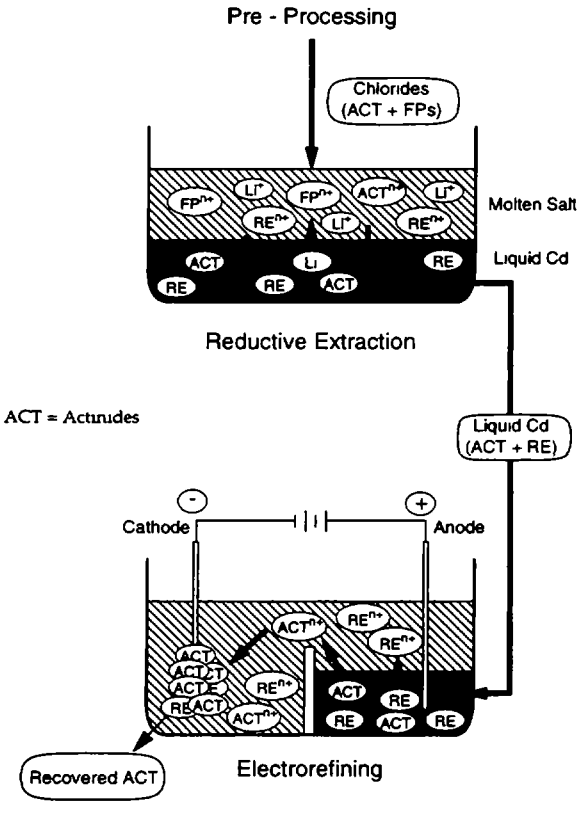

Figure 6 9

FIG. 6.9 Schematic illustration of the pyro-metallurgical partitioning process.

In parallel with the R&D on incinerators, development on solvent extraction methods of long lived FF, which in some cases may additionally require isotopic separation, should be promoted, the goal being to virtually eliminate the need for Geological Repositories.

After the concentrates will be cooled down for the 10 years period and the long-lived FF extraction applied for later incineration the wastes will be solidified by using well known techniques. For instance by calcination and vitrification. The first step allows to get waste oxides and in the second step glasses are obtained by melting the waste oxides together with additives such as SiO_2, B_2O_3, Al_2O_3, P_2O_5, Na_2O, and CaO. Borosilicate glass is the most studied solidification product but others like phosphate glass, glass ceramic, etc. are also used. When the solidification process is finished the wastes are ready for disposal in the appropriate secular repositories.

D.3.6.4. SPALLATION INDUCED RADIO-NUCLIDES

In addition to the radioactive waste produced in the Fuel and in a minor extent in the Breeder, substantial amounts of radio-nuclides are produced by the spallation target. As pointed out they divide roughly into two batches, those which remain inside the molten Lead and those which are either gases or volatile and which can be found in the neutral filling gas of the main vessel.

TABLE VI.1. FISSION FRAGMENTS' ACTIVITY AFTER 1000 YEARS OF COOL-DOWN IN THE SECULAR REPOSITORY. VALUES ARE GIVEN FOR 1 GWe x year.

Radio-Isotope	1/e Life	Mass	Other Isotopes (kg)	Activity @ 1000 a (Ci)	Ingestive Toxicity (Sv) x 10^3	Dilution Class A (m^3)
^{129}I	2.27E+7	8.09	3.48	1.43	19.58	178.47
^{99}Tc	3.05E+5	16.61	—	284.29	27.67	947.65
^{126}Sn	1.44E+5	1.187	1.783	33.79	3.2	9.65
^{135}Cs	3.32E+6	34.12	66.77	39.32	9.87	39.32
^{93}Zr	2.21E+6	26.11	99.11	65.64	2.38	18.75
^{79}Se	9.40E+5	0.3	3.02	2.06	0.745	0.59

These last compounds are collected from the gas and stored in an appropriate way in order to avoid leaks in the biosphere (paragraph D.3.5.8). The relative ingestive radio-toxicity of the various components of the Spallation target are given in Figure 6.10. Following Table V.9 spallation products at 700 °C can be broadly divided into three different categories namely (1) gases or vapours in which the contribution of ^{194}Hg (751.9 a, 123 g/(GW_e × a)) is largely dominant in size and duration; (2) volatiles which, after a few years, are essentially dominated by to ^{204}Tl (5.466a, 114 g/(GW_e × a)), (3) inter-metallic combinations (alloys) with the molten Lead which at short times, shows a leading contribution from ^{90}Sr and, at longer times by ^{202}Pb (7.59×10^4 a, 614 g/(GW_e × a)). The radio-toxicity of the spallation products is by no mean negligible: at early times it is about 10^{-3} of the total radio-toxicity produced. At the end of the Secular repository time for FFs, the effects of ^{194}Hg exceed all other contributions until about 2,000 years. There is no major difficulty in extending safely and economically the storage of about 2.3 kg/(GW_e × a) of Mercury collected as vapours from the top main Vessel up to about 2000 years. Note that at least in the present design, the molten Lead of the Target region is directly mixed with the big volume (≈ 1000 m^3) which constitute the main coolant. Therefore at least the elements which remain inside the liquid are largely dispersed. They will follow the fate of the Lead at the time of final decommissioning of the installation.

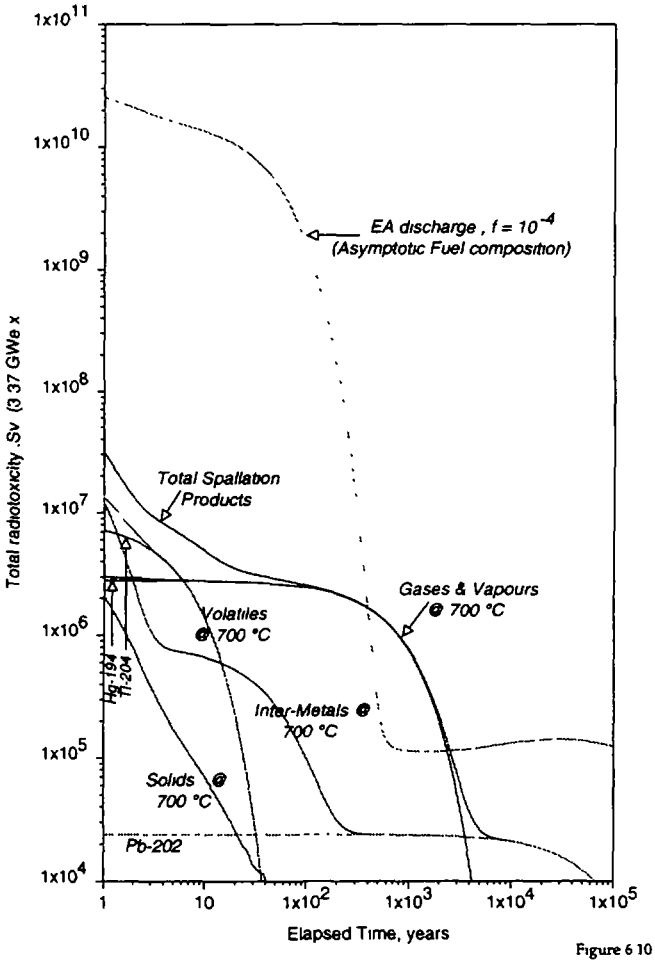

FIG. 6.10 Relative ingestive radio-toxicity of the spallation target products.

We finally remark the existence of another lead isotope, ^{205}Pb (2.21×10^7a) which is abundantly produced by neutron capture of ^{204}Pb, namely 3.54 kg/(GW_e × a) in the target region and 23.15 kg/(GW_e

× a) in total, and fortunately it is also rather inoffensive, since it is very long lived and it decays by K-conversion with an energy release of 51 keV mostly in the form of neutrinos.

D.3.6.5. RADIO-TOXICITY EMITTED IN THE ENVIRONMENT

Nuclear power production is based on the concept that pollutants and toxic materials are retained within the plant and in total isolation from the biosphere. The limited mass of such products makes it possible to achieve such a goal. Mining process however cannot retain all products and a significant amount of radiation is emitted in the biosphere during preparation of the fuel. Likewise in the reprocessing of the spent fuel some radioactive elements are currently re-emitted in the biosphere. Finally the ultimate storage of such materials (geologic repository) have raised some question on the ability of isolating them from the biosphere for times which largely exceed what can be considered an experience based retention. The EA concept strongly reduces such environmental impacts, when compared to the present reactor technology. We examine these points in turn.

(1) *Mining*. Thorium is largely present in the Earth's crust, but in small concentrations. In addition several minerals exist, which have an excellent concentration of Thorium and which can be exploited economically. The primary choice is the monazite, which is a phosphate of Cerium and other lantanides, containing a variable amount of Thorium and Uranium in a solid mixture. Usually the Thorium concentration is of the order of 10% but some mineral may reach as much as 20% by weight. Uranium minerals are usually much less rich, its concentration being in the best cases of the order of 0.2%. Incidentally one can remark that the solubility of Thorium is 1000 times smaller than the one of Uranium. Taking into account that Thorium burnt in the EA has an energetic yield which is 250 times larger than one of natural Uranium destined to PWRs, we conclude that the relative mining effort is reduced by a factor of the order 250 × 50 = 12500 times for a given produced energy. Starting with mineral containing 10% of Thorium by weight we need to dig only 70 tons of mineral to produce GW_e × a. For comparison and for the same energy produced the standard PWR methodology would require 0.875 10^6 ton of mineral. In the case of Coal, the mass of fuel (TEC) is 4.24 10^6 ton.

A pure Thorium mineral out of which the totality of Thorium is extracted will produce tailings with a negligible radio-toxicity after some sixty years, since all descendants of ^{232}Th have short decay lifetimes. Their evolution is governed by the 5.7 year half-life of ^{228}Ra. Furthermore there will be no risk associated to Radon, since ^{220}Rn has a half-life of 55.6 seconds and it decays before escaping the minerals. As pointed out by Schapira [5] the situation in reality is somewhat more complex, mainly because the monazite, which is the primary source of Thorium is generally mixed with some Uranium contamination. Such a contamination is strongly source dependent, as shown in Table VI.2, taken from Ref. [5]. Assuming somewhat pessimistically that the Uranium content is about 10% of the one of Thorium and that the long lived toxicity and Radon contamination are primarily due to Uranium, we conclude that the radio-toxicity produced at the mine is in the case of an EA about 250 / (10%) = 2500 times smaller than the one of today's PWR for a given energy produced.

The UNSCEAR report [7] has estimated that the level of exposure of individuals to mining for today's PWRs amounts to about 1.5 man Sv $(GW\ y)^{-1}$ as local and regional component and to 150 man Sv $(GW\ y)^{-1}$ as global component. We remark that according to the same report the production of electricity from Coal is estimated to result in a global collective dose of 20 man Sv $(GW\ y)^{-1}$. The practice of using coal ashes for production of concrete will add as much as 20,000 man Sv $(GW\ y)^{-1}$. Values relative to Thorium and its use in the EA for some possible mineral sources are listed in Table VI.2. We conclude that the typical radiation exposure to public with the EA due to mineral mining for the same energy produced are much smaller than today's PWRs and also Coal burning, even if solid ashes are correctly handled.

TABLE VI.2. URANIUM AND THORIUM CONTENT IN PERCENT [5] AND LEVELS OF POPULATION EXPOSURE FOR TYPICAL ORES [7].

Source	UO_2	ThO_2	Ratio U/Th	Local	Global
Italy	15.64	11.34	1.38	8.28×10^{-3}	0.828
Sri Lanka	0.1	14.32	0.007	4.20×10^{-5}	4.2×10^{-3}
California	6.95	4.22	1.64	9.84×10^{-3}	0.984
India	0.29	9.80	0.029	1.74×10^{-4}	0.0174

The same report estimates the collective dose due to initial Uranium enrichment and fuel fabrication to as little as 0.003 man Sv $(GW\ y)^{-1}$. In the case of the EA it is expected to be at least 1/4 of such a number, since the burn-up is four times longer and there is no isotopic separation. The collective doses are negligible in both cases.

(2) *EA Operation.* During the EA operation the fuel and the spallation target volumes are kept strictly sealed. Indeed also for proliferation protective measures it is recommended that such volume be opened only in occurrence with the re-fuelling, namely once every about five years and only by a specialised team. While the fuel is safely sealed, the Lead coolant produces a significant amount of radioactive products, some of which remain in the liquid phase, but others are either gaseous or volatile and are found in the neutral gas (Helium) with which the main Vessel is filled. These volatile compounds are summarised in Table VI.3, extracted from Table V.9. Some of these are noble gases and Tritium which remain gaseous at room temperature.Other, mostly Mercury and Thallium can be condensed and preserved in the solid state. Some other elements will be collected by the Lead purifier. In view of its small amount involved we believe that the gaseous elements can be released in the atmosphere. The collective effective dose per unit energy release is given by the UNSCEAR report [7] and summarised in Table VI.4. It is assumed that gases are released every 6 months, without cool-down period. A short cool-down will dramatically reduce the effects of ^{127}Xe (52.63 d) and it is recommended. The total local and regional doses are 0.42 man Sv $(GW\ y)^{-1}$. The global doses, integrated over 10,000 years, following the convention of Ref. [7] are of 0.18 man Sv $(GW\ y)^{-1}$. Both values are dominated by the effects of Tritium. The rest of the solid high activity waste from the spallation products (dominated by Mercury and Thallium) has a substantial ingestive radio-toxicity (Figure 6.10) and it should be carefully accumulated and destined to the repository.

(3) *Fuel reprocessing* has to deal with the very large radioactivity of the spent fuel. Since the techniques are not different that those generally in use, we can make direct use of the estimated collective doses of Ref. [7] (Table VI.5), taking into account the differences in stockpile of the radio-nuclides produced (see Table V.8). It is however assumed that both ^{14}C and ^{85}Kr are extracted during reprocessing and sent to the repository for cool-down. Separation of ^{85}Kr can be performed cryogenically according to a well documented procedure [84]. Also ^{14}C once reduced in the form of CO_2 can be extracted on the same time by the same method.

The total doses to members of the public are summarised in Table VI.6. Total global dose truncated at 10,000 years is 0.6 man Sv $(GWa)^{-1}$, namely for the same energy produced about 0.003 of the one of an ordinary Reactors [7] — without counting occurred criticality and melt-down accidental releases, avoided by the EA, ($\approx$ 300 man Sv $(GW\ y)^{-1}$) — and about 0.03 of the alternative of Coal burning, even if solid ashes are correctly handled.

TABLE VI.3. RADIO-NUCLIDES EMITTED IN THE NEUTRAL GAS INSIDE THE VESSEL BY THE SPALLATION TARGET AND THE MOLTEN LEAD COOLANT (≈ 700 °C).

Gas at Room Temperature				Solid at Room Temperature			
	Mass	1/e	Boils at °C		Mass	1/e	Boils at °C
^{3}H	1.435	17.83 a	-252	^{35}S	0.009	126.5 d	445
^{39}Ar	0.336	389.0 a	-186	^{65}Zn	0.004	353.2 d	907
^{42}Ar	0.336	47.57 a	-186	^{70}Zn	2.424	0.723E+15y	907
^{81}Kr	5.777	0.331E+6a	-153	^{73}As	0.329	116.1 d	615
^{85}Kr	4.326	15.55 a	-153				615
				^{83}Rb	0.036	124.6 d	688
^{127}Xe	0.37 (675)[1]	52.63 d	-108	^{86}Rb	0.181	26.94 d	688
				^{109}Cd	1.627	1.833 a	767
				^{125}I	0.014	85.90 d	184
				^{124}Sb	0.043	87.05 d	1,585
				^{125}Sb	0.404	3.988 a	1,585
				^{131}Cs	0.003	14.01 d	671
				^{134}Cs	0.282	2.982 a	671
				^{194}Hg	415.9	751.9 a	357
				^{203}Hg	6.252	67.40 d	357
				^{202}Tl	15.25	17.68 d	1,473
				^{204}Tl	386	5.466 a	1,473
				^{210}Po	0.995	200.1 d	254

[1] Total integrated production, without decay over 5 years.

TABLE VI.4. NORMALISED, COLLECTIVE EFFECTIVE DOSE FROM LOCALLY, REGIONALLY AND GLOBALLY DISPERSED RADIO-NUCLEI DURING OPERATION OVER A PERIOD OF 10,000 YEARS.

	Normalised release (TBq)	Collective dose per unit release (man SvTBq^{-1})[7]		Normalised collective Dose (man Sv (GW a)$^{-1}$)	
		Local & Regional [1]	Global [2]	Local & Regional	Global
^{3}H	521	0.0027	0.0012	0.418	0.185
^{14}C	—	0.4	85	—	—
^{39}Ar	0.43	$7.4\ 10^{-6}$	$5.0\ 10^{-4}$	$9.4\ 10^{-7}$	$6.38\ 10^{-5}$
^{42}Ar	3.268	$7.4\ 10^{-6}$	$6.1\ 10^{-5}$	$7.2\ 10^{-6}$	$5.91\ 10^{-5}$
^{81}Kr	0.004	$7.4\ 10^{-6}$	$1.8\ 10^{-2}$	$9.2\ 10^{-9}$	$2.24\ 10^{-5}$
^{85}Kr	63.6	$7.4\ 10^{-6}$	$2.0\ 10^{-5}$	$1.4\ 10^{-4}$	$3.77\ 10^{-4}$
^{127}Xe	3,718 [3]	$7.4\ 10^{-6}$	$1.05\ 10^{-7}$	$8.2\ 10^{-3}$	$1.16\ 10^{-4}$
Totals	*4,307*			*0.42*	*0.186*

TABLE VI.5. NORMALISED RELEASED DOSE OF AIRBORNE AND LIQUID EFFLUENTS OF RADIO-NUCLIDES DURING REPROCESSING OF FUEL. VALUES HAVE BEEN NORMALISED TO CURRENT PRACTICES [7].

	Process (kg)	EA/ PWR	Normalised collective Dose (man Sv (GWa)$^{-1}$)		Comments
			Airborne Effluents	Liquid Effluents	
^{3}H	—	10	0.11	0.0012	assumed same as PWR
^{14}C	0.0145	9.2	(7.45)	—	Retained
^{85}Kr	21.64	10.16	(0.924)	—	Retained
^{129}I	27.28	1.722	0.43	—	Standard practices
^{131}I	0.2924	0.458	1.37×10^{-4}	—	" "
^{137}I	118.5	1.109	0.0188	1.22	" "
^{90}Sr	74.76	1.578	—	0.205	" "
^{106}Ru	1.147	0.074	—	0.207	" "
Totals			*0.6*	*1.63*	

[1] For noble gases, values are taken to be the same as ^{85}Kr.

[2] For noble gases, values are taken the same ones as ^{85}Kr, for decay over 10,000 years.

[3] Periodic (every 6 months) release, without cool-down.

D.3.6.6. CONCLUSIONS

Realistic schemes are possible in which the spent Fuel from the EA is "regenerated" for further uses. Separation of the fuel materials into two streams is performed, the Actinide stream destined to the fuel fabrication and the FFs stream which is destined to the Secular repository. After 500 years the radio-toxicity for unit energy produced of the EA is about 20,000 smaller than the one of a PWR with a "throw-away" cycle. Incineration with the help of neutrons of some of the critical, long lived radio-nuclides can strongly reduce the radio-toxicity of the waste beyond 500 years. If sufficiently diluted it could be also let "die away" without incineration since it can be made to satisfy the requirements for Class A repository. Note also that at that time the residual ingestive radio-toxicity is comparable with the one of the Thorium metal burnt in the EA.

TABLE VI.6. SUMMARY OF NORMALISED, COLLECTIVE DOSES TO MEMBERS OF THE PUBLIC FROM RADIO-NUCLIDES RELEASED FROM THE EA.

Source	Local and regional Doses (manSv(GW a)$^{-1}$)	Global Doses (manSv (GW a)$^{-1}$)
Mining [1], Milling, Fuel fabrication	$4.2\ 10^{-5} \div 9.8\ 10^{-3}$	$0.0042 \div 0.984$
EA operation	0.42	0.188
Reprocessing (Atmospheric)	0.60	0.1
Reprocessing (Aquatic)	1.63	0.1
Miscellanea [2]	0.1	0.05
Totals (variation over mining range)	*2.75 ÷ 2.76*	*0.44 ÷ 1.42*

An essential element in the clean disposal of the spent fuel is the small leakage of Actinides (mainly Uranium) into the FFs stream. A level of 100 ppm. or better is required. We believe that it is within the state of the art, eventually with a few improvements.

An important source of radio-toxicity are the spallation products due to the proton beam interacting with the molten Lead target. A specific element of concern is ^{194}Hg which is the main surviving source of toxicity of the EA in the period of time between 500 and 2000 years. It can either be preserved far from the biosphere that long or, alternatively, incinerated, following the fate of the Actinides inside the EA. Unfortunately the relevant cross sections are only poorly known but they should be measured soon [6].

An experimental test of the feasibility of incineration with neutrons in a Lead diffuser [6] is in preparation at CERN. Would it be successful it could offer the right technique in order to eliminate also the modest amount of long lived radio-toxic elements produced.

Likewise important is the total radioactivity doses to members of the public due to operation. Total global dose of the EA truncated at 10,000 years is estimated to be 0.6 man Sv (GW a)$^{-1}$, namely about 1/330 of the one of an ordinary Reactors for the same energy produced (200 man Sv (GW a)$^{-1}$)— without counting occurred criticality and melt-down accidental releases, avoided by the EA (≈300 manSv (GW a)$^{-1}$) — and about 1/33 of the alternative of burning Coal (≈ 20 man Sv (GW a)$^{-1}$), even if solid ashes are correctly handled.

[1] The dose range depends on the Uranium content in the Thorium mineral. We have taken extreme values of Table VI.1.

[2]This includes mainly Transportation, Fuel fabbrication, Solid Waste disposal. Figures are taken from Ref. [7].

ACKNOWLEDGEMENTS

We would like to acknowledge the superb and dedicated work of Susan Maio and F. Saldaña, without whom this paper could not have become a reality. We would like to thank many of our CERN colleagues for frequent discussions of various aspects of the project and for their continuing and enthusiastic support. Stress analysis and hydrodynamic calculations have been performed with the help of M. Battistin and A. Catinaccio. I. Goulas has helped with programming. M. Cobo, M. Embid and R. Fernandez have diligently helped during their stay as summer students at CERN.

We have profited from (too) short, but illuminating visits of E. Greenspan (Univ. California at Berkeley), V. Orlov (RDIPE, Moscow), H. Branover (Ben Gurion University, Israel) and K. Mileikowski.

Many experts have helped us in different fields. We would like to thank in particular: A. Ferrari and P. Sala (University of Milan) for the code FLUKA; J.P. Schapira and R. Meunier (IN2P3) for their contributions to radio-toxicity and end-of-cycle aspects; E. Gonzalez and A. Uriarte (CIEMAT, Madrid); R. Caro and A. Alonso (Consejo de Seguridad Nuclear, Madrid); M. Perlado, J.L. Sanz, E. Gallego and P. Trueba (Universidad Politecnica, Madrid) and A. Perez-Navarro (Alfonso X El Sabio) for numerous and extended contributions pertinent to safety, radiation damage and end of cycle aspects; H. Rief (JRC, Ispra) for contributions to the question of reactivity insertions; P. Gerontopoulos, J. Magill, M. Matzke, C. O'Carrol, K. Richter and J. Van Geel (JRC Karlsruhe) for proliferation aspects; D. Finon and Ph. Menanteau (Institut d'Economie et de Politique de l'Energie, Grenoble), M. Gigliarelli-Fiumi (INFN, Frascati) and M.A. Rodriguez-Borra (SERCOBE, Madrid) for the economic and industrial aspects; E. Sartori (NEA), The International Dosimetry and Computation Group of NRPP (UK); C. Dunford and S. Ganessan (IAEA) and G. Audi, (CSNSM, Orsay), for their invaluable assistance in facilitating our access to relevant Data Banks.

The design of the accelerator has been made possible with the help of Laboratoire du Cyclotron, Centre Antoine Lacassagne. We thank its Director, F. Demard, and wish to acknowledge J.M. Bergerot, A. Giusto, P. Montalant, J.F. Di Carlo, V. Rossin. We had helpful discussions with W. Joho, U. Schryber and P. Sigg (PSI, Zurich) and J. Pamela (CEN, Cadarache). Last but not least, we would like to acknowledge the continuing support of the CERN Management (in particular of H. Wenninger), of the Sincrotrone Trieste (in particular G. Viani), and the DGXII of the European Commission, in particular its Director General, P. Fasella and H.J. Allgeier, G.C. Caratti and W. Baltz.

REFERENCES

[1] F. CARMINATI, C. GELÈS, R. KLAPISCH, J.P. REVOL, CH. ROCHE, J.A. RUBIO AND C. RUBBIA, "An Energy Amplifier for Cleaner and Inexhaustible Nuclear Energy Production Driven by a Particle Beam Accelerator", CERN/AT/93-47 (ET) (1993).

[2] C. RUBBIA ET AL., "A High Gain Energy Amplifier Operated with Fast Neutrons", Contribution to the Las Vegas Conference on Accelerator Driven Transmutation Technologies and Applications, 25-29 July 1994, to be published.

[3] S. ANDRIAMONJE ET AL., Physics Letters B 348 (1995) 697-709.

[4] C. RUBBIA, "On the Feasibility of Fission Driven Hydrogen Production as Substitute for Natural Gas", CERN/AT/95-12 (ET) (1995).

I.T. ÖZTÜRK, A HAMMACHE AND E. BILGEN, Trans. IChemE, 241, 72A, (1994). and reference therein. The original □process has been described in J.H. Norman et al. General Atomic Company Report, GA-A16713, 1982.

S. SHIMIZU ET AL. "Iodine-Sulphur Process for Thermochemical Hydrogen Production", Proceedings of ICENES '93, H. Yashuda Editor, World Scientific, 1993.

[5] S. MENARD AND J.P. SCHAPIRA, "Impact Radiologique à long terme de l'extraction du Thorium", IPNO-DRE 95-07, Orsay, France.

[6] S. ANDRIAMONJE ET AL., "Experimental Study of the Phenomology of Spallation Neutrons in a Large Lead Block", Proposal to the SPSLC, SPSLC/P291, May 1995.

[7] "Sources And Effects Of Ionising Radiation", United Nations Scientific Committee on the Effects of Atomic Radiation, UNSCEAR 1993 Report to the General Assembly, with Scientific Annexes, New York, 1993.

[8] TH. STAMMBACH ET AL., "Potential of Cyclotron Based Accelerators for Energy Production and Transmutation", Contribution to the Las Vegas Conference on Accelerator Driven Transmutation Technologies and Applications, 25-29 July 1994, to be published.

[9] R.A. JAMESON ET AL., "Accelerator-driven transmutation technology for energy-production and nuclear-waste treatment", 3rd EPAC, Berlin 1992, pp. 230-234.

[10] For a comprehensive description of these Projects, see for instance "Status of liquid metal fast reactor development", IAEA-TECDOC-791, March 1995.

[11] See for instance H. ALTER, p. 2 in "Specialists' Meeting on Decay Heat removal and Natural Convection in LMFBRs", BNL (1985) and additional information in the same Proceedings.

[12] D. GEITHOFF, G. MÜHLING AND K. RICHTER, "Performance of a Mixed Carbide Fuel Sub-Assembly in KNK II", in Proceedings of Global '93, 12-17 September, 1993, published by the American Nuclear Society, Inc., Vol. 2, p. 1173.

[13] L. KUECHLER, L. SCHÄFER, B. WOJTECH, "The Thorex Two-Stage Process for Re-Processing Thorium Reactor Fuel with High Burn-Up", Farbwerke Hoechst AG, Kerntechnik 13. No. 78, pp. 319-322 (1971).

[14] J.J. LAIDER ET AL, "Development of IFR Pyroprocessing Technology", in Proceedings of Global '93, 12-17 September, 1993, published by the American Nuclear Society, Inc., Vol. 2, p.1061 and also McPheeters et al, "Pyrochemical Methods for Actinide Recovery from LWR Spent Fuel", Vol. 2, p. 1094.

[15] C. BOWMAN ET AL., Nucl. Instr. Methods, A320, 336 (1992). More recent developments are to be found in the Proceedings of the International Conference on Accelerator-Driven Transmutation Technologies and Applications, Las Vegas, 25-29 July 1994.

[16] T. TAKIZUKA ET AL., Specialist Meeting on Accelerator-driven Transmutation for Radwaste and other Applications (Stockholm, 24-28 June 1991).

[17] G. VAN TUYLE ET AL., BNL Report 52279 (1991);

H. TAKAHASHI, Fusion Technology 20 (1991) 657.

V.D. KAZARITSKY ET AL., in Accelerators Applied to Nuclear Waste, 8th Journées Saturne, Report LNS/Ph/94-12.

[18] H. TAKANO ET AL, "A concept on self-completed fuel cycle based on Lead-cooled Nitride-fuel Fast Reactors", in Proceedings of ICENES-93, World Scientific.

[19] PROCEEDINGS OF THE FIRST INTERNATIONAL CONFERENCE ON PEACEFUL USES OF ATOMIC ENERGY (Geneva 1955) Vol 4.

[20] CRC HANDBOOK OF CHEMISTRY AND PHYSICS, D.R. Lide Editor, CRC Press, 73rd Edition p. 4-29.

[21] F.H. BARTHEL AND F.J. DAHLKAMP, "Thorium Deposits and their Availability", IAEA TECDOC-650, Vienna, 1992, pp 104-115.

[22] K.S. DEFFEYES AND I.D. MACGREGOR, "World Uranium Resources", Scientific American, January 1980, pp. 50-66.

[23] J. ROUAULT ET AL., "Physics of Pu burning in Fast Reactors: Impact on Burner core design", Proc. ANS Topical Meeting on Advances in Reactor Physics, Knoxville, 11-15 April (1994).

[24] J. SANZ, J.M. PERLADO, A.S. PEREZ AND D. GUERRA, J. of Nucl. Materials, 191-194, (1992), 1450.

[25] J. PERLADO AND J. SANZ, "Irradiation Effects and Activation in Structural Material", in "Nuclear Fusion by Inertial Confinement", edited by G. Verlarde, Y. Ronen and J.M. Martinez-Val, CRC Press (1993).

[26] J. PERLADO, Private Communication.

[27] C RUBBIA, "An analytic approach to the Energy Amplifier", Internal Note CERN/AT/ET/Internal Note 94-036.

J.P. REVOL, "Analytical Study of the Energy Amplifier Microscopic Physics", internal Note CERN/AT/ET/Internal Note 95-025.

[28] C. RUBBIA, paper in preparation.

[29] S. GLASSTONE, Principles of Nuclear Reactor Engineering (D. Van Nostrand, New York, 1955).

[30] F. CARMINATI, "EET Code Collection User Guide", Internal Note, CERN/AT/ET/Internal Note 95-027, 16 March 1995.

[31] I. GOULAS, J.P. REVOL, "Further Update of Nuclear Data for the EET Group", Internal Note CERN/AT/ET/Internal Note 95-012, 26 April 1995 and "Corrections to the EET Nuclear Data Base", Internal Note CERN/AT/ET/Internal Note 95-026, 19 June 1995.

[32] F. CARMINATI, I. GOULAS, Y. KADI, "Proposal for transforming the evolution and MC program into a general purpose code", Internal Note CERN/AT/ET/Internal Note 95-020, 9 June 1995.

[33] H. BATEMAN, "The Solution of a System of Differential Equations Occurring in the Theory of Radioactive Transformations", Proc. Cambridge Phil. Soc. Vol. 15, p. 423, 1910.

[34] 1) MCNP: Judith F. Briesmeister, "MCNP™ - A General Montecarlo N-particle Transport Code", Los Alamos National Laboratory Report, LA-12625-M, November 1993.

2) TWODANT: R.E. Alcouffe, F.W. Brinkley Jr., D.R. Marr and R.D. O'Dell, "User's Guide for TWODANT: A Code Package for Two-Dimensional, Diffusion-Accelerated, Neutral-Particle Transport", Los Alamos National Laboratory Report, LA-10049-M, February 1990.

[35] J. CARSON MARK, "Explosive Properties of Reactor-Grade Plutonium", Science & Global Security, 1993, Volume 4, pp. 111-128.

[36] J. MAGILL, C. O'CAROLL, P. GERONTOPOULOS, K. RICHTER, J. VAN GEEL, "Advantages and Limitations of Thorium Fuelled Energy Amplifiers", Contribution to the Nuclear Society 5th Annual Conference on Nuclear Power and Industry, Obninsk, 7-11 November 1994.

[37] V. ORLOV, Private Communication, November 1994.

[38] P. BONNAURE, P. MANDRILLON, H. RIEF, H. TAKAHASHI, Actinide Transmutation by Spallation in the Light of Recent Cyclotron Development, ICENES 86, Madrid, July 1986.

[39] C. RUBBIA, P. MANDRILLON, N. FIÉTIER, "A High Intensity Accelerator for Driving the Energy Amplifier for Nuclear Energy Production", 4th EPAC, London 1994, pp. 270-272.

[40] Y. JONGEN ET AL., "Extremely high intensity cyclotrons for radio-isotope production", Proc. of EPAC 1994, London.

[41] P. MANDRILLON, "Injection into Cyclotrons", CERN Accelerator School, La Hulpe, Belgium, 2-6 May 1994.

[42] "MAFIA, A Three-Dimensional Electromagnetic CAD System for Magnets, RF Structures and Transient Wake-Field Calculations", The MAFIA Collaboration, T. Weiland et al., Technische Hochschule Fachbereich 18, Fachgebiet Theorie Elecktromagnetischer Felder, 6100 Darmstadt, Germany.

[43] E. BRANOVER, Private Communication.

[44] A.J. ROMANO, C.J. KLAMUT, D.H. GURINSKY, B.N.L. 811 (T 313), (1963).

[45] U.K. BIERMAN, B. LINCH, W.M. VAN DE WIJGERT, Patent No. 2516296, Neth., (1974).

[46] R.C. ASHER, D. DAVIES, S.A. BEETHAM, Corrosion Science, 17, (1977), 545-557.

[47] F.R. BLOCK, V. SCHWICH, Mater.Behav.Phys.Chem.Liq.Met.Syst., (1982), 253-264.

[48] H. LENGELER, "Proposal for Spallation Sources in Europe", EPAC '94, Proc. 4th European Particle Accelerator Conference, Vol. I, p. 249, 1994.

[49] SHUNK, "Constitution of Binary Alloys", McGraw-Hill, 1969.

[50] A. FASSÓ ET AL, in "Intermediate Energy Nuclear Data: Models and Codes", Proceedings of a Specialists' Meeting, Issy les Moulineaux (France) 30 May-1-June 1994, p. 271, published by OECD, 1994, and references therein.

A. FASSÓ, A. FERRARI, J. RANFT, P.R. SALA, G.R. STEVENSON AND J.M. ZAZULA, Nuclear Instruments and Methods A, 332, 459 (1993), also, CERN Divisional Report CERN/TIS-RP/93-2/PP (1993).

[51] AA.VV., "STAR-CD Version 2.2 Manuals", Computational Dynamics.

[52] AA.VV., "ANSYS User's Manual, Version 5.0", Vol. I, II, III, IV, Swanson Analysis System, Inc. Huston.

[53] We Would Like To Acknowledge The Contribution From J.M. PERLADO AND J. SANZ. A part of their work is included in "Radiation Damage in Structural Materials", J.M. PERLADO, J. SANZ, Instituto de Fusion Nuclear, Universidad Politecnica de Madrid (1995).

[54] S. BUONO ET AL., "An Energy Amplifier System cooled by natural convection", Internal Note CERN/AT/ET/Internal Note 95-022, 21 August 1995.

[55] C.L. WHEELER, C.W. STEWART, R.J. CENA, D.S. ROWE AND A.M. SUTEY, "COBRA-IV-I: An Interim Version of COBRA for Thermal-Hydraulic Analysis of Rod Bundle Nuclear Fuel Elements and Cores", Battelle Pacific Northwest Laboratories Report, BNWL-1962, March 1976.

[56] H. SHIBATA ET AL., "On Problems to be solved for utilizing shock isolation system to NPP", Proc. SMIRT-10, Vol. E, Anaheim, August 1989.

[57] J.M. KELLY, "Aseismic Base Isolation: Review and Bibliography", Soil Dynamics and Earthquake Engineering, Vol. 5, No. 3, 1986.

[58] F.F. TAJIRIAN, J.M. KELLY, I.D. AIKEN, "Seismic Isolation for Advanced Nuclear Power Stations", to appear in Earthquake Spectra, Earthquake Engineering Research Institute (EERI), May 1990.

[59] F.F. TAJIRIAN, M.R. PATEL, "Response of Seismic Isolated Facilities: A Parametric Study of The ALMR", submitted to SMIRT 12, Stuttgart, Germany, August 1993.

[60] O. GOKCEK ET AL., "Seismic Risk Reduction through Seismic Isolation", Proc. ANP '92, Tokyo, October 1992.

[61] J.M. BERKOE, "Modelling Passive Decay Heat Removal in Modular High Temperature Gas-cooled Reactor", Proceedings of the 5th FIDAP Users Conference, Chicago, Il, May 2-4, 1993.

[62] F. CARMINATI ET AL. "Analysis of 4th Week Data", Internal Note CERN/AT/ET/Internal Note 95-003, 17 January 1995.

[63] R. CHAWLA ET AL., "Fast Reactor Experiments with Thorium at the PROTEUS Facility, Paul Scherrer Institute Report, EIR-Bericht Nr. 444, November 1981.

[64] A.E. WALTAR, AND A.B. REYNOLDS, "Fast Breeder Reactors", Pergamon Press (1981).

[65] S. GLASSTONE, AND A. SESONSKE, in Nuclear Reactor Engineering: Reactor Design Basics. Vol. 1, Chapter 7, p. 242, Chapman & Hall, Fourth Edition (1994).

[66] T.A. GABRIEL, J.D. AMBURGY, AND N.M. GREENE, "Radiation Damage Calculations: Primary Knock-On Atom Spectra, Displacement Rates, and Gas Production Rates", Nucl. Sci. Eng. 61, 21 (1976).

[67] D.G. DORAN, "Neutron Displacement Cross Sections for Stainless Steel and Tantalum Based on a Lindhard Model", Nucl. Sci. Eng. 49, 130 (1972).

[68] R.E. MACFARLANE, D.W. MUIR, AND R.M. BOICOURT, "The NJOY Nuclear Data Processing System, Volume I: User's Manual", Los Alamos National Laboratory Report, LA-9303-M (ENDF-324) (1982).

[69] M.T. ROBINSON, in Nuclear Fusion Reactors (British Nuclear Energy Society, London, 1970).

[70] J. LINDHARD ET AL., Mat-Fys. Medd. 33 (1963).

[71] W.E. FISHER, "Target System Materials and Engineering Problems", in ICANS X, LA–UR-89-2920 (1988).

[72] J.M. PERLADO ET AL., "Radiation Damage and Activation in the HT-9 Structure of ICF Reactors Using INPORT Protection", Ninth Topical Meeting on the Technology of Fusion Energy, Oak Brook (USA), October 1990. Fusion Technology, Vol. 19, 3, Part. 2A, 709 (1991).

[73] M. COBO, M. EMBID, R. FERNÁNDEZ, J. GÁLVEZ, C. RUBBIA, J. A. RUBIO, "Study of the maximum cladding temperature reached in the Energy Amplifier", Internal Note, CERN AT/EET 95-023, 21 August 1995.

[74] SAMUEL GLASSTONE & ALEXANDER SESONSKE, Nuclear Reactor Engineering. Reactor Design Basics. Vol. I, Chapter 5, p. 238-321 Chapman & Hall, Fourth Edition.

[75] H. RIEF & H. TAKAHASHI. "Safety and Control of Accelerator-Driven Subcritical Systems".

[76] FEDERICO GODED & VICENTE SERRADELL, Teoria de Reactores y Elementos de Ingenieria Nuclear. Tomo I. Publicaciones Cientificas de la Junta de Energia Nuclear. Tercera Edicion, 1975.

[77] REACTOR PHYSICS CONSTANTS, Argonne National Laboratory, United States Atomic Energy Commission, 1963.

[78] C. RUBBIA, paper in preparation.

[79] R. MEUNIER, "Faisabilité et Evaluation Exploratoires d'un Projet pour la Séparation Isotopique du Cesium Issu de la Fission", CSNSM, IN2P3-CNRS, Orsay, October 1994.

[80] A. URIARTE, "The Energy Amplifier, Considerations about the back-end of the Fuel Cycle", CIEMAT ITN/TR-05/II-95 and ITN/TR-13/II-95, 1995 (and references therein).

[81] J.T. LONG, "Engineering for Nuclear Fuel Reprocessing", Gordon and Breach Science Publishers, 1967 (and references therein).

[82] J.P. ACKERMAN AND T.R. JOHNSON, "New High-Level Waste Management Technology for the IFR Pyroprocessing Wastes", in Proceedings of Global '93, published by the American Nuclear Society, Inc., Vol. 2, p. 969.

[83] T. HIJIKATA ET AL., "Development of Pyrometallurgical Partitioning of Actinides from High-Level Radioactive Waste", in Proceedings of Global '93, published by the American Nuclear Society, Inc., Vol. 2, p. 1074.

[84] A. VAN DALEN ET AL., "Sea Disposal of Radioactive Krypton", European Applied and Research Reports, Nuclear Science and Technology Section, Vol. 4, 111-190, 1982

D.4. ADS PROGRAM IN RUSSIA

D.4.1. WEAPON PLUTONIUM IN ACCELERATOR DRIVEN POWER SYSTEM

Shvedov O.V. (ITEP), Murin B.P. (MRTI)., Kochurov B.P. (ITEP), Shubin Yu.N. (IPPE), Volk V.I. (VNIINM), Bogdanov P.V.(MNP)

with participation of:

Azshnin E.I. - SSC DBMB
Belygin V.M. - MRTI RAS
Blokhin A.I. - SSC PhPI
Bondarev B.I. - MRTI RAS
Durkin A.M. - MRTI RAS
Fedotov A.P. - MRTI RAS
Gay E.V. - SSC PhPI
Vassiliev V.V. - SSC ITEP
Ivanov Yu.D. - MRTI RAS
Ignatyuk A.V. - SSC PhPI
Igumnov M.M.- SSC ITEP
Kvartsakheli A.Yu. - SSC ITEP
Kozodaev A.M.- SSC ITEP
Konev V.N. - SSC ITEP
Konobeev A.Yu.- SSC PhPI
Lasarev N.V. - SSC ITEP
Lunev V.P. - SSC PhPI
Malygina H.U.- SSC DBMB
Petrunin V.V. - SSC DBMB
Rabotnov N.S.- SSC PhPI
Selivanova N.N.- SSC ITEP
Sobolev A.M. - SSC DBMB
Strahov E.B. - SSC ITEP
Shumakov I.V. - MRTI RAS
Uksusov N.I. - MRTI RAS
Vasiliev V.V. - SSC ITEP
Zavadsky I.M.- RPIPT

D.4.1.1. INTRODUCTION.

D.4.1.1.1 Introductory comments

Completion of cold war between the former USSR and the countries of NATO and USA has called global reducing of nuclear weapon. Use (or destruction) of several dozens of tons of weapon-

grade Plutonium (W-Pu) is a many-sided problem, including various aspects, such as W-Pu use in existing nuclear reactors or creation of Nuclear Power (NP) installations of a new generation. Among them the main places take the projects of Accelerator Driven Systems (ADS), development of methods of long-duration safe storage of W-Pu, maintenance of its physical safety and the problem of non-proliferation.

This report is devoted to the substantiation of advantages of W-Pu use in ADS power installation.

The problems are determined:

- area of research - W-Pu use in ADS power installations;

- purpose and problems of research - creation of safe and reliable ADS installation for processing of ~ 50 t of W-Pu in 30 years on the basis of a linear accelerator of proton with energies 0,8-1,2 GeV and a current 10-30 mA; melt-down Pb-Bi eutectic targets; partitioned fast - thermal blanket with Plutonium fuel. Thorium is used as reproducing materials; actinides formed being incinerated in fast zone of blanket;

- objects of research - linear accelerator with beam transport systems, neutron-producing target, partitioned blanket, monitoring and controlling system fuel cycle, electro-nuclear neutron generator;

- modern status of objects in consideration.

Method of W-Pu utilisation is substantiated. It consists on understanding of unconditional priority of safety of ADS power installation over economic considerations and, accordingly, priority of subcritical systems over critical, which are cheaper but have not a sufficient level of safety on condition that Pu and actinides are used as fission materials.

Choice of accelerator with superconducting accelerating structures is justified. At a current of protons 10 mA and higher common efficiency of accelerator will be not below 60 %. The large stocks on throughput provide losses of proton beam not more than 10^{-5}, that guarantees radiation cleanliness of accelerator, hand-operated service, and opportunity of accelerator burial during its removing from operation without use of special storage.

Consumed capacity and cost of operation for superconducting linear accelerator is essentially reduced, the reliability is increased, length is not less than 2 times decreased.

In the offered report the description of a variant of ADS installation, the most acceptable for Russia from the point of view of opportunity of its realization in reasonable terms (7-10 years) on the base of feasible technologies is given. For main elements of installation alternative variants and existent prototypes in Russia and abroad are considered. Evaluations of possible experimental and calculational support of chosen installation variant are given.

Techniques of calculation of main parameters of installation, including processes of fuel burn- up in blanket and optimum library of neutron constants are chosen.

With the use of existent analogues the cost of ADS installation as well as the cost of its operation during a scheduled period and removing from operation on the basis of cost valuations of various kinds of activity, characteristic for Russia, is determined.

The decision of W-Pu utilization problem in ADS installation is based on the following main principles:

- Pu (weapon and energetic grade) is national riches of Russia and is a subject of only rational utilization in NP installation (immediately or after some period of storage).

- Pu utilization should not result in diminishing nuclear and radiation safety of NP installation. The refusal from critical NP installation in favour of ADS installation having a powerful external source of neutrons is one of the most effective means of increasing safety of NP installation.

- At preservation of necessary level of safety of ADS installation with Pu and effective working-out of electric power, it should use excess fission neutrons for producing new perspective fission materials (for instance, ^{233} U) with their partial burning-up (it increases efficiency of working-out of

electric power per unit of initial fission material), radionuclides of various purposes, transmutation of a number radionuclides (^{99}Tc, ^{129}I) not requiring large neutron fluxes.

- For maintenance of technical realization of ADS installation and technical reliability at the stage of formation of active zone, blanket elements should be used the serviceability of which are checked on operating critical NP installation or in special loop resource experiments.

- For fuel elements and fuel compositions the worked out and operating (or have to be put in operation to a certain term) radiochemical technologies must exist.

- Complete refusal from conventional reactor control system leads to diminishing of nuclear safety and work efficiency of blanket, that requires conservation of useful elements of a system. Creation of control system for ADS installation - a new, yet by nobody investigated problem.

- Justifying impossibility of restoration of W-Pu after its use in blanket of ADS installation, it should note that nuclear fuel of ADS installation is better protected from thefts or switching it on manufacturing of weapon in comparison with the fuel of critical systems, since the opportunity to work in subcritical mode reduces the requirements to fuel composition, enabling including in it high active or high absorbing components.

- The problems of maintenance of physical protection of W- Pu in ADS installation do not differ in essence from appropriate problems for critical NP installation.

-The fitness of ADS installation is stipulated by the fact that acceptability of nuclear power for the population is impossible within the framework of conventional nuclear technologies with critical NP installation.

- ADS installation - in essence a new approach, completely excluding reactivity failure at the expense of deep subcriticality of blanket, failure caused by melting of blanket because of impossibility essentially to increase current of accelerator, as well as at the expense of guaranteed switching-off for a time ~1 ms with any given probability.

- The level of thermal neutrons flux in blanket with W-Pu in a mode of ^{232} Th-^{233}U production from Th does not exceed ~ 10^{14} n/ cm^2 s therefore such type of active zone have relatively low specific power.

- Thermal neutrons flux of a necessary level in blanket is provided by a linear proton accelerator with technically realizable parameters on the basis of worked-out technologies as well as by justified effective neutron-multiplication factor in blanket.

- Including of actinides for transmutation and fission products into blanket should not result in diminishing safety below limit characteristic for critical NP installation.

- At formation of blanket scheme the partitioned approach with the best use of neutron properties of multiplicating lattices with various spectrum of neutrons is necessary. For this purpose the fast neutron multiplication zone with coolant coincided with target material should be arranged around superfast neutron source target.

By choice of parameters of multiplicating zones of blanket unique experience of creation fast reactors in Russia and other countries as well as heavy-water reactors of various types and purposes and the most perspective type of NP installation on thermal neutrons from the point of view of economies of neutrons and maintenance of internal safety properties is to be used.

Chemical technology defines reliability, technical safety and economy of ADS power plant in many respects. Significance of chemical technology is conditioned by using of heavy water, that is tied, besides problems of water preparation, special water purifying and degassing, with conditioning of initial heavy water, its detritization, deprotization, with necessity of deuterization and dedeuterizatio of used ion exchange materials and so on.

The decision of a problem of ADS installation on W-Pu will essentially speed up creation in the nearest years ADS installation small power on the basis of already operating accelerators and multiplicating systems.

Support experiments for heavy water blanket zone physics could be realized on zero power heavy water reactor MAKET ITEP.

- In parts of the report, relating to various elements of ADS installation, the information on the programs and neutron constant maintenance of calculation of installation elements is given. The list of experiments for project support, testing of programs and libraries of constants made for creation ADS installation is defined.

D.4.1.1.2. Comparison of circular and linear accelerators for intensive proton beam production

The circular and linear accelerators of intensive proton beams, being machines of different classes, have own areas of effective application. The region where a sharp competition between these classes of installations is possible, is rather narrow.

The main attractive quality of cyclic accelerators - repeated use of an accelerating field and, as a consequence, their compactness. The external diameter of terminal cyclotron BSSC of an accelerating complex on energy 990 MeV, suggested by C. Rubbia for "the energy amplifier" [1], is equal only 16 m. However current limit, which authors rely on, makes only 10 - 12,5 mA. Note, that on today highest current, received on cyclotron SIN, is equal only 1,5 mA. If in opportunity of easy progress in current from 1,5 up to 10 mÀ one makes doubt because of plenty of resonances, an achievement of substantially large currents is not assumed even by the authors of the project.

Another situation is in linear accelerators. Here, efficiency of the accelerator rises with beam current growth. Today, a structure of high efficiency linear accelerators on current 300-500 mA and more is real. The area of average currents from several units up to few tens of milliamperes is covered at high efficiency with use of superconductivity or pulsing mode. There is no doubt in principle possibility of current acceleration up to several hundreds of milliamperes, since the stage is for a long time covered in pulsing mode.

At natural extraction of particles along straight line, particle losses in a linac are less. For instance, relative losses are 10^{-4} on the whole length of the accelerator LAMPF, while only in extracting node of SIN, they are equal $2 \cdot 10^{-4}$ locally.

Large length of linear accelerators is sometimes considered like a disadvantage. The machine on energy 1 GeV in "warm" variant has length about 1 km. However, for intensive beam production it is rather plus, than minus. On large length of the accelerator it is easier to solve problems to feed RF power, making tens-hundreds MW, and heat removal, and at the same time a distributed level of a radiation field is less, that facilitates service.

Complete efficiency of C. Rubbia's accelerating complex is estimated as 40-42 %. For linear accelerator in "warm" variant (continuous or pulsing mode) this parameter lays in the range of 40-60 % (depending on beam current), and in superconducting variant - 60-70 %.

Application of superconductivity in linear accelerators permits to increase rate of acceleration as well as to reduce length of resonators and building. Use of superconductivity in cyclotrons is probably complicated, in particular, because of presence of a magnetic field destroying superconductivity, which, to the point, is the essential consumer of the electric power, and which is not present in linear machines.

For production of currents more than 10 mA, the supporters of cyclic machines offer to use several complexes, similar mentioned above. We compare (see Tab. I) variants of production of required 30 mA beam current at energy 1 GeV in case of offered in present project LPA and in variant of several complexes of cyclic accelerators [1.2.1]. The items of information on cyclotron complex dimensions have rough character, since they were estimated on schemes and drawings. However common insight can give the following comparison:

From Table I one can see, that in cyclotron variant capital expenses on building construction and operational expenses on service for 3 independent accelerating complexes will be essentially more, as soon as reliability (at least, of the vacuum system) - is much lower, than in case of linear accelerator.

Besides, LPA efficiency is by the factor of 1,5 higher. Therefore multicomplex cyclotron variant cannot compete linac variant.

Summarizing stated above, but not applying on categorical resume, it is possible to make the following conclusions.

TABLE I. COMPARISON OF CYCLOTRON WITH LINAC ACCELERATOR

		C. Rubbia proposal (with cyclotrons)	Alternative proposal (with SC linac)
Amount of accelerating facilities		3	
Efficiency	(%)	40-42	65
Vacuum cavity volume	(m^3)	486	30
Building for accelerators (without technology system)	(m^3)	27000	6000

In the range of proton beam currents from small values up to about 10 mA depending on specific conditions the use both cyclic and linear accelerators may be considered as effective variants (last - in superconducting or pulsing modes). In region of currents, more than 10 mA there are no another variants except use of linear accelerators. And in range 10 - 70 mA (approximately) - by use superconducting or pulsing mode, and at much large currents - by continuous regime with "warm" resonators.

D.4.1.2. LINEAR ACCELERATOR OF PROTONS AND NEGATIVE IONS OF HYDROGEN FOR ADS POWER INDUSTRY.

D.4.1.2.1. Introduction

Solution of the tasks of conversion of weapon-grade Plutonium and of nuclear-power tasks ("power amplifiers" [2]) requires proton beams with energy 1 GeV and average current 10 - 30 mA. The most expedient way of obtaining of such proton beams is acceleration in linear accelerators with superconducting accelerating structures. As it is shown in this technical proposal total efficiency of such accelerator under acceleration of beam 10 mA and more will be not lower than 60%. High margin of acceptance in the considered version of linear accelerator allows to expect that losses of the beam in the process of acceleration will not exceed 10^{-5}. Modern level of technique and of technology allows to realize the proposed project of linear accelerator. The accelerator will be radiation clean [3]: it may be serviced without manipulators (hand-operated); elements of the accelerator do not require any specific processing and burying after decommissioning of the installation.

Superconducting linear accelerator of protons [4] possesses a number of decisive advantages in comparison with "room" temperature accelerators in the region of average beam currents of tens of milliamperes: consumed RF power is significantly decreasing and as a consequence the cost of construction and of routine operation are going down, reliability rises and not less than twice the length of the accelerator decreases.

Some publications consider possibilities of production of proton beams with similar parameters by installations consisting of a cascade of isochronous cyclotrons [2] or by a cyclotron with separated orbits [5]. It is not difficult to show that even in the case of realization of these projects their technical

parameters - efficiency and losses - will be lower than of a superconducting linear accelerator. Efficiency of cascade cyclotrons [2] will be not higher than 40%.

Description and the characteristics of the accelerator of protons and negative ions of hydrogen are presented in this work. Energy of accelerated particles is 1 GeV, current - up to 30 mA. Accelerating structures are superconducting. The base of the work is taken from [6].

D.4.1.2.2. Principal scheme of the linear accelerator. The main parameters

The proposed scheme of the CW proton linear accelerator to energy 1 GeV and current 10 - 30 mA with superconducting accelerating resonators [6] is shown in the Fig.2.1.

The injector produces a beam of protons with energy 60 keV. Further the protons are accelerated in the initial part of the linear accelerator (IPA) - an accelerator with space-uniform quadrupole focusing (RQF). A four-chamber H-resonator excited with the wave TE_{211} of 425 MHz accelerates protons to energy 3 MeV.

The first part of the linear accelerator consists of short four-gap resonators with drift tubes excited at the frequency 425 MHz. Energy of protons in this part of the accelerator rises to 50 MeV (this figure will be corrected after detailed investigations). Separation of the accelerating structure to short resonators is dictated by necessity to place between them quadrupole focusing lenses of permanent magnets. The structure of the period of focusing is FODO. Total number of resonators - 28.

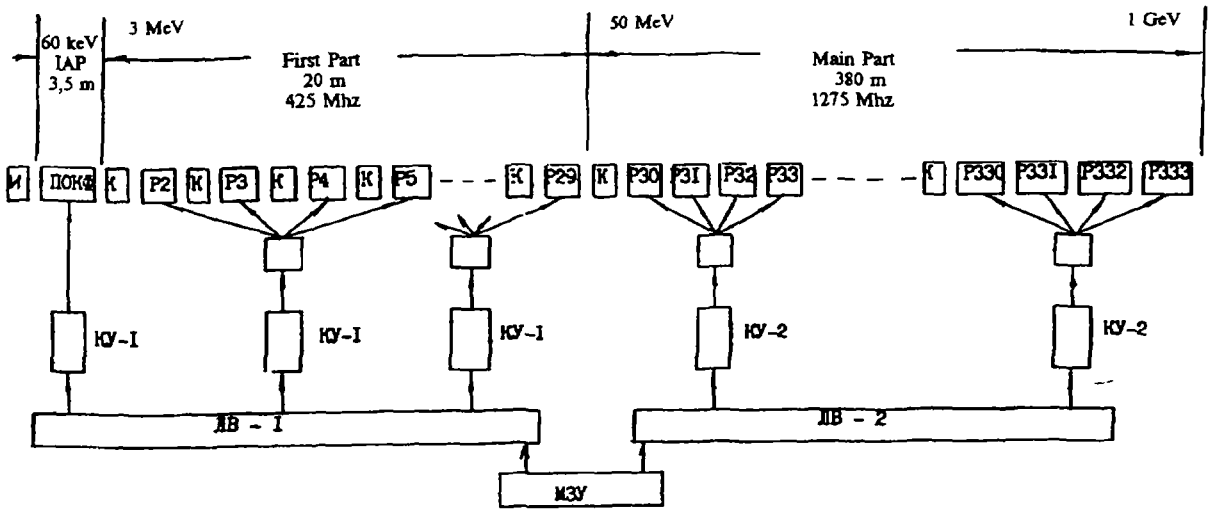

*FIG. 2.1. Scheme of superconducting proton linear accelerator with the energy of 1 GeV and the current of 10-30 mA: **И** - injector; RFQ - initial part of accelerator; P2-P333 - resonators; K - permanent magnet quadrupoles; KY-1 - HF amplification channel at 425 MHz; KY-2 - HF amplification channel at 1275 MHz; **МЗУ** - powerful master device.*

The second (main) part of the linear accelerator provides acceleration of protons to energy 1 GeV. Accelerating structure consists of 304 nine-cell axially symmetric resonators with cells of elliptical shape excited at the frequency 1275 MHz. Odd ratio the frequencies of the first and the second parts of the linear accelerator is equal 3 and this allows in case of necessity to accelerate simultaneously protons and negative ions of hydrogen. Acceleration rate at the "pure" length of the resona-

tors is 5 MeV/m. Averaged along the whole length of the accelerator rate of acceleration is 2.5 MeV/m.

HF system and the system of automatic control are proposed as classic for proton linear accelerator scheme.

The main parameters of the linear accelerator are presented in the Table II. Value of power for acceleration of the beam is given for the current 10 mA. For higher intensity beams of protons this figure should be proportionally increased. Losses taken by Helium do not change. The parameters of the acceleration will not change for the case of acceleration a beam of negative ions of Hydrogen.

In order to provide superconductivity the resonators, operating surface of which is covered with Niobium layer, are cooled by liquid Helium. Adopted temperature 2K corresponds to minimum of capital investments and the cost of routine operation. The version of the cryogenic system consisting of typical cryomodules is chosen in these technical proposals. A cryomodule consists of a cryostat with several resonators together with adjacent devices inside of it. Different versions of cryomodules were considered. As an example a cryomodule of the main part of the linear accelerator is shown in the Fig.2.2. it consists of two accelerating resonators: 1 - a quadrupole lens, 2 - resonators, 3 - Helium vessel, 4 - magnetic and nitrogen shield, 5 - vacuum housing, 6 - superinsulation, 7 - tubes for liquid Helium, 8 - can-type RF window, 9 - waveguide, 10 - mechanical drive, 11 - a mechanism for adjusting of the resonators, 12 - a load to suppress higher modes, 13 - 14 - supports, 15 - a frame with adjusting devices.

The following ideology linked with quantitative characteristics of heat removal by Helium is adopted. Total power of losses for Helium in the resonators of the linear accelerator is approximately 4000 W (TableII). Acceptable losses by Helium due to losses of the beam in the linear accelerator with hand controlling are 380 W or approximately 10% of the losses in the resonators. The same value is taken for acceptable heat flux from the external space through the cryostat. It defines the requirements to thermal insulation of the cryostat. So the total thermal power (P_{He}) removed by Helium is 4700 - 5000 W.

One of the main characteristics of particle accelerators for the considered nuclear-power utilization is the value of total efficiency defining efficiency of utilization of electric power put to the accelerator. Estimation of the efficiency for the proposed linear accelerator is given later [7].

Full efficiency of a superconducting linear accelerator

$$\eta = P_b/(P_e + P_{eke}),$$

where P_b is HF power for acceleration of the proton beam, P_e and P_{eke} - powers of electric feeding of the HF system and of cryogenic system of the accelerator. Let us introduce notations for efficiency of HF system $\eta_{rf} = P_{rf} / P_e$ and $\eta_k = P_{He}/P_{eke}$. Then

$$\eta = P_b/[(P_b + P_{rf.c})\cdot\eta_{rf}^{-1} + P_{He}\cdot\eta_k^{-1}],$$

Where $P_{rf.c}$ is power of HF losses in the walls of the resonators.

$$\text{As } P_b >> P_{rf.c} \quad \text{then} \quad \eta = P_b/(P_b\cdot\eta_{rf}^{-1} + P_{he}\cdot\eta_k^{-1}),$$

The efficiency of cryogenic system may be estimated from the relationship [8]

$$\eta_k = 0.3\, T_2/(T_1 - T_2)$$

For T_1 = 300 K and T_2 = 2K we have $\eta_k = 2\cdot10^{-3}$. Accepting for estimation η_{rf} = 0.7 and P_{He} = 5 kW we shall obtain expression for calculation of efficiency of superconducting accelerator as a function of P_b:

$$\eta = P_b/(1.41\cdot P_b + 2.5\cdot10^6)$$

Under beam current 10 mA $P_b = 10^7$ W efficiency of the accelerator is equal 60%. For beam current 30 mA we have η = 65%.

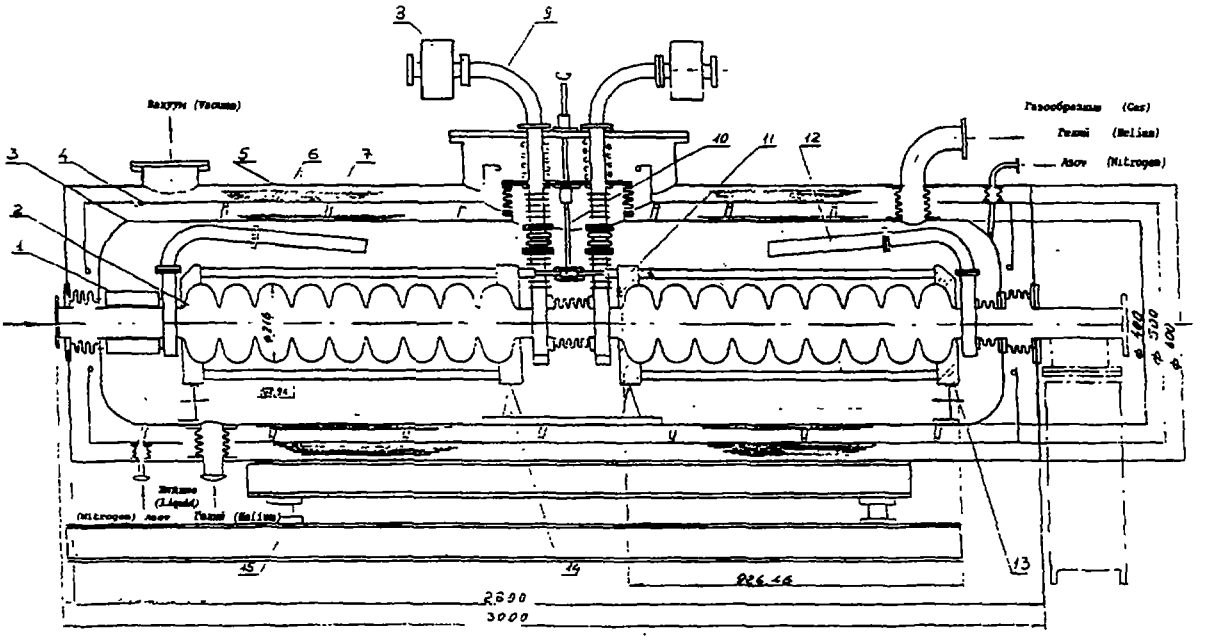

FIG. 2.2. Cryomodules

D.4.1.2.3. Beam dynamics

D.4.1.2.3.1. Initial part of the accelerator (RFQ accelerator)

Calculations and investigation of beam dynamics allowed to define main parameters of RFQ section which is the initial part of the accelerator (Table II). Voltage between the electrodes is 60 kV.

A matching fun of $3\beta\lambda$ length is placed to match the beam at the input of the accelerator.

Variation of the main parameters along the channel is shown in the Fig. 2.3 where the curves of variation of average radius of the beam R, coefficient of electrodes modulation m, equilibrium phase FS, efficiency of acceleration T, voltage between the electrodes U are presented. All curves are presented in three scales: in dependence of the distance to the beginning of the accelerator Z, particle energy W, number of a period N (length of a period - $\beta\lambda$).

Figs 2.4 and 2.5 show behaviour of phase and radial trajectories of the beam; the last are presented at the background of the aperture of the channel: upper line corresponds to the largest aperture at a period, the lowest - to minimal, medium - to medium radius of the aperture. Trajectories show that the beam may pass through the accelerating-focusing channel practically without losses.

Results of calculations allow to shows: a) phase width of output beam is rather small in order to start acceleration in the following sections with equilibrium phase -45^0 (with some margin); b) coefficient of rising of the emittance due to dependence of the phase portrait of the beam upon phase of leaving at RF-period is 1.5 - 2; this was the reason why under calculation of the following part of the accelerator emittance of input beam was supposed to be 0.1 π cm·mrad (with some margin).

D.41.2.3.2. The first part of the accelerator.

The first part of the accelerator consists of short resonators containing 4 similar single-gap cells. The length of a cell - $\beta\lambda$. Calculations and investigations of particles dynamics allowed to define the main characteristics of the accelerator which are presented in the Table II. Structure of focusing period is FODO. Maximal length a lens - 5 cm, maximal gradient of magnetic field is 7-8 kGs/cm.

Calculations and investigations showed that the intervals between the resonators from 6 cm at the beginning to 20 cm at the end of the accelerator are acceptable.

TABLE II. MAIN PARAMETERS OF SUPERCONDUCTING LINEAR ACCELERATOR FOR ENERGY 1 GEV AND CURRENT 10 mA

Parameter	Initial Part	First Part	Part Second
Type of accelerator, resonator	RFQ	4-gap resonator with drift tubes	9-cell resonators
Injection energy, MeV	0.06	3	50
Output energy, MeV	3	50	1000
Frequency of accelerating field, MHz	425	425	1275
Number of resonators	1	28	304
Period of focusing, m	0.007-0.056	0.6-2.0	2.0-4.0
Acceptance, specified, π cm·mrad	0.07-0.25	0.2-0.35	0.5-0.7
Effective emittance, specified, π cm mrad	0.04-0.08	0.08-0.12	0.12-0.2
Equilibrium phase, deg	-(90-45)	-(45-30)	-30
Phase width, deg	360-40	40-15	45-40
Pulse spread at output, %	0.4	0.08	0.025
Resonator length, m	3.2	0.25-0.85	0.35-0.93
Diameter of resonator, cm	15.6	49-45	24-21,6
Aperture diameter, mm	3-6	15-20	30-40
Accelerator length, m	3.5	25	380
Power for beam, kW	30	470	9500
Losses removed by Helium per a part of accelerator, W	50	580	3400

The Figs.2.6 and 2.7 show longitudinal acceptance of the first part and the phase portrait of the beam at the output. Comparison of the acceptance of the first part presented in the Fig.2.6 with phase portrait of the beam at the output of the RFQ section show that passage of the beam from the initial part into the first one may be realized without losses of particles.

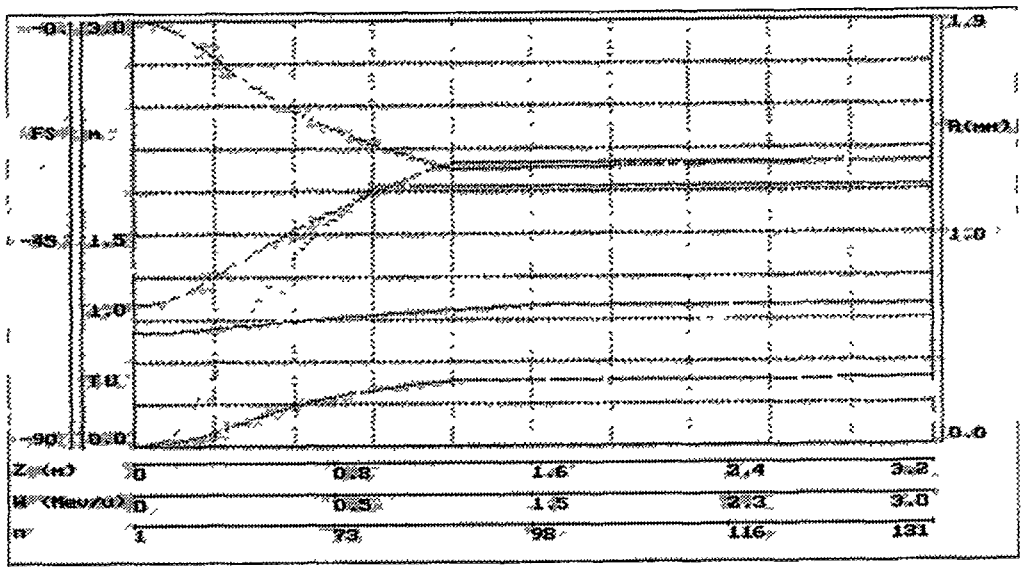

FIG 2 3 Parameters of RFQ section with energy of 0 06 - 3 MeV R - minimal aperture radius , m-electrode modulation factor, FS- equilibrium phase U- voltage between electrodes (relative units), T-acceleration efficiency

In order to define conditions of passage from the first part into the main accelerator and also from the initial part into the first additional investigations were carried out As it is seen from the Fig 2 7 phase length of 50-MeV beam at the output of the first part does not exceed 20° i e it is possible to think that acceleration by three times higher frequency under equilibrium phase -30 has foundation As it will be shown later transverse matching of the beam also does not create any difficulties

D 4 1 2 3 3 Main part of the accelerator

Main part of the accelerator consists of a sequence of nine-cell resonators Length of a cell is $\beta\lambda/2$ Resonators operate with three times higher frequency

Matching of the beam under passage from the first part into the main is simpler as the lengths of the periods of focusing in both parts less differ In this case period of the first part is 10 $\beta\lambda$ and in the main - 30 $\beta\lambda$ i e in optimal case the period contains 60 cells The period of FODO containing 4 nine-cell resonators is of approximately similar to the finite number of focusing in the first part That is the reason why it is expedient to choose the structure of the FODO period with lenses placed between the resonators (pairs)

The characteristics of the main part of the accelerator obtained as result of calculation of particle dynamics are presented in the Table II We notice that acceptance far exceeds beam emittance at the input of this accelerator part

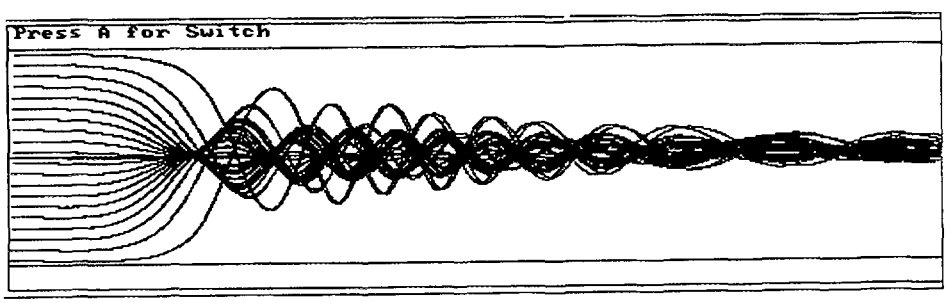

FIG. 2.4. Beam phase trajectories in RFQ section.

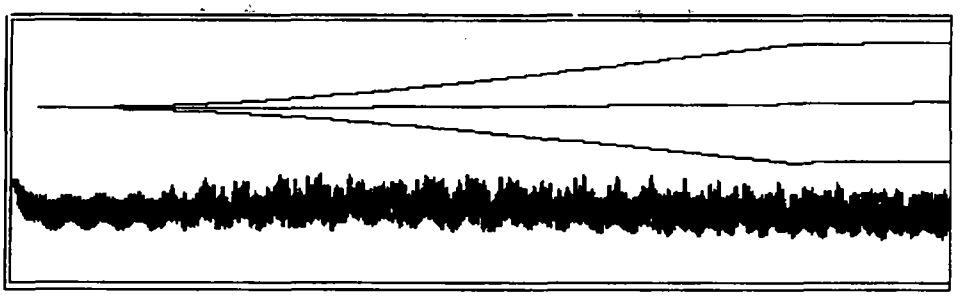

FIG. 2.5. Beam radial trajectories in RFQ section.

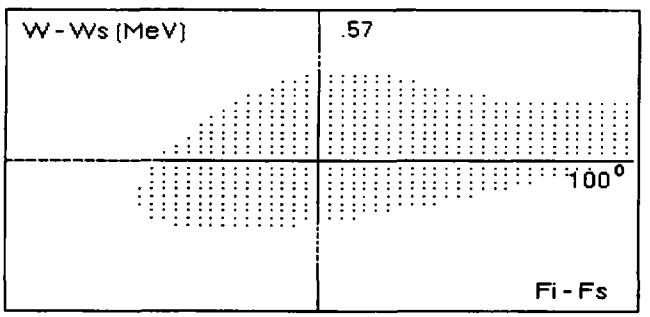

FIG. 2.6. Accelerating channel acceptance of the first accelerator part.

D.4.1.2.4. Superconducting accelerating structure

D.4.1.2.4.1. Initial part of the accelerator. Superconducting H - resonator

A four-chamber H - resonator with space-uniform focusing (RFQ) will be used in the initial part of the accelerator (0.06 MeV - 3 MeV). Operating mode is H_{211}. Oscillation of H type creates quadrupole focusing field and modulation of the tops of the electrodes introduces local variation adequate to appearance of longitudinal accelerating field.

As a design the four-chamber H - resonator is a cylinder loaded with V - shaped plane plates (electrodes) symmetrically fixed to the cylindrical wall. The tops of the plates are modulated along their length. The plates have their edges at some distance from the bottom walls of the cylinder. The four-chamber H - resonator is relatively simple for fabrication, mechanical adjusting and cooling. Utilisation of the resonator in the pointed limits of energies for "room" accelerators became traditional.

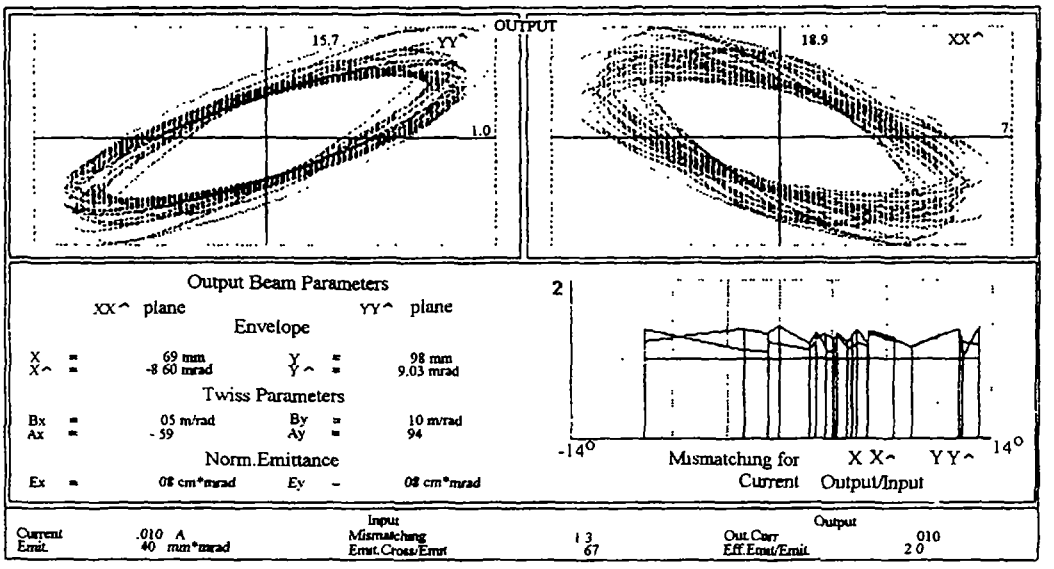

FIG. 2.7 Beam transverse characteristics at the output of RFG section.

Now, in a number of scientific centers abroad investigations on creation of superconducing resonators with RFQ are being carried. Argonne National Laboratory develops H - resonator for acceleration of heavy ions (operating frequency 194 MHz, initial velocity 0.02 [9]. Los-Alamos National Laboratory develops a four-chamber H - resonator for protons acceleration (frequency 425 MHz) [10].

Theoretically obtained length of the H - resonator of our project is 3.25 m. This is the reason why the resonator will be fabricated as several short sections connected through Indium sealing. Diameter of the resonator equal 0.156 m was calculated with the aid of the code ISFEL3D for calculation of electromagnetic fields and of parameters of SHF devices of arbitrary shape of ideally conducting surface [11]. The electrodes will be fabricated as plane plates. Losses per unit length equal approximately 15 W/m were calculated by expressions [12]. The main parameters of the resonator with RFQ are presented in the Table III.

Technology of fabricating Niobium resonators is well experienced in several accelerator centers of the world.

ITEP obtained good results on development of technology of superconducting resonators on the base of Niobium covering by the method of magnetron spraying to copper surface without welding joints. These results give possibility to expect relatively quick development of Russian technological base. A method of fabrication of copper matrixes without welding joints of practically any shape and dimensions for resonators from 0.55 GHz to 14 GHz with the aid of halvanoplastics [13; 14] is developed in the institute. H - resonator will be fabricated by this technique.

Input of power into the resonator will be provided with the aid of a coupling loop from the side of cylindrical wall.

Design developed in Argonne National Laboratory will be taken as a prototype of design of the external shell of the resonator. Niobium resonator in this design (or of copper with sprayed to operating surface Niobium) has a shell of stainless steel. Liquid Helium will circulate in the gap between the resonator and the shell (Fig.2.8).

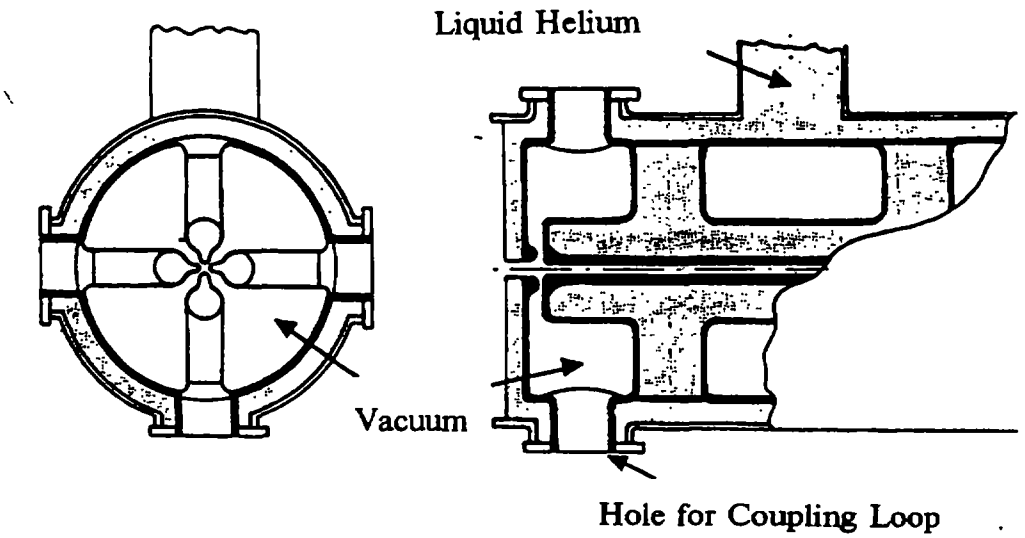

FIG. 2.8. Superconducting resonator with RFQ

D.4.1.2.4.2. The first part of the accelerator. Superconducting four-gap resonators with drift tubes

Superconducting four-gap resonators with drift tubes without lenses will be used for acceleration of protons from energy 3 MeV to energy 50 MeV.

Theoretical value of the quality factor of resonator with Niobium cover under temperature 2K will be approximately (2 - 3) 10^9. Acceleration rate at the length of resonators rises from 2 MeV/m to 4 MeV/m.

The main parameters of the first and the last resonators are presented in the Table II.

The resonators with drift tubes will be fabricated with the pointed IHEP technology. Drift tubes and bars will be empty inside for circulation of liquid Helium. Preliminary adjusting will be accomplished due to mechanical deformation of the resonator from the sides of the bottoms, exact tuning - by a piezoelectric tuner.

Input of power will be accomplished with the aid of a coupling loop from the side of cylindrical wall in the middle of the resonator. The loop will not enter into the resonator.

D.4.1.2.4.3. The second (main) part of the accelerator. Superconducting nine-cell resonators

Accelerating structure consisting of axially symmetrical coupled with each other through aperture holes resonators with elliptic boundaries proposed in Cornell university, USA, 1982 will be used in the main part of the accelerator for acceleration of protons from energy 50 MeV. The design of the

structure is the most suitable from the point of view of simplicity of fabrication and possibility to obtain the highest possible accelerating field. π - mode wave is the operating wave of the structure. The period of the structure is consequently $\beta\lambda_{oper}/2$, where β is relative velocity of particles, λ_{oper} - operating wavelength which is equal 23.53 cm.

This structure is used in several electron accelerators abroad [12]. These are - accelerator CEBAF (USA), accelerating complex LEP (CERN), laboratory SACLAY (France), accelerating complex on Darmstadt (Germany), accelerator LISA (Italy). Large experience on development and creation of the structure is accumulated.

A nine-cell resonator is chosen for the main part of the supposed accelerator. Total number of resonators is 304. Accelerating-focusing modules of the main part consists of two resonators and of one quadrupole with permanent magnets. Design of such modules is presented in the Fig.2.2.2. Input of HF power is accomplished outside of the cells of the resonator through a travel tube.

On the base of the data obtained from calculations of particles dynamics (diameter of the aperture hole, longitudinal dimensions, amplitude of accelerating wave) with the aid of the codes AZIMUTH [15], ISFEL3D [11] and of service (auxiliary) codes allowing to simplify description of the starting data for these codes geometrical dimensions and parameters of two resonators - of the first to energy 50 MeV and of the last for energy 1000 MeV were defined. Intervals of drift tubes with the length 50 mm at the beginning and at the end of the resonators necessary under large aperture hole to suppress irradiation of waves were taken into account in calculations. Final (exact) calculation of geometry of every of the resonators and their parameters will require sequential correlation with calculations of beam dynamics (taking into account the real fields) and also to take into account variation of frequency under cooling of resonators and under vacuum pumping.

The cells of the first and of the last resonators of the main part of the accelerator are shown in the Figs.2.9. The parameters of these resonators are presented in the Table III.

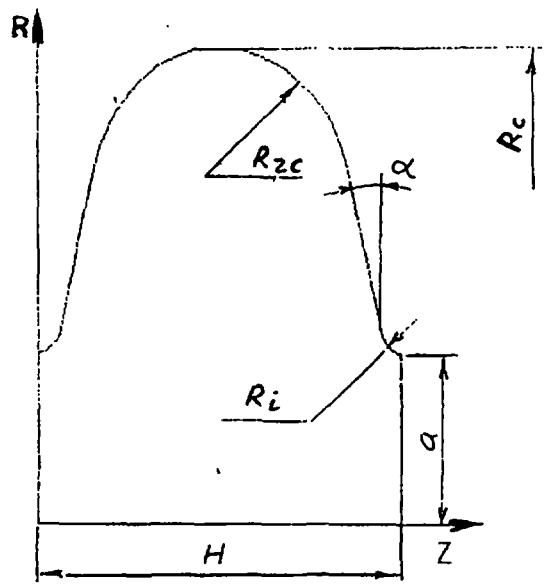

FIG. 2.9 Sketch of the cell of the .last resonator of the main part of the accelerator.

D.4.1.2.4.4. Focusing quadrupoles with permanent magnets

Focusing of protons in the linear accelerator is implemented by permanent magnet quadrupoles (except the initial part where RFQ is used). There are 28 quadrupoles in the first part and 152 - in the second. The structure of focusing period in the both parts - FODO. Quadrupoles of the second part should have gradient of magnetic field 1 - 2 kGs/cm under diameter of the aperture 30 - 40 mm. The length of a quadrupole lens is 10 - 20 cm.

TABLE III. PARAMETERS OF THE FIRST AND OF THE LAST RESONATORS OF THE MAIN PART OF THE ACCELERATOR.

Energy, MeV	50	1000
β	0.325	0.87
Period of accelerating structure H, mm	38.4	102.
Diameter of the aperture, 2a, mm	77.4	77.4
Radius of rounding if the iris, R_i, mm	3	6
Radius of rounding of the cell, R_{rc}, mm	6	37
Radius of cell, R_c, mm	119.7	107.
Angle of wall slope, a, grad	8	15
Length of nine cells of the resonator, cm	36.4	92.6
Coupling coefficient K_{cpl}, %	8.87	3.52
Losses in Helium, W/m	17.5	11.8
Losses in BKSh, W/m	0.4	0.4
Anomal losses, W/m	8.4	2.7
Statistic losses, W/m	8.7	8.7
Losses in Helium in resonators, W	6.1	10.9

Necessity to make short interresonator gaps providing optimal beam dynamics and a wish to simplify the cryostats lead to relatively longer cryostats - not less than 5 - 10 meters. Magnetic quadrupoles turn out to be put into liquid Helium.

Alloy Samarium-Cobalt is supposed to be used as magnetic material. It possesses high volume density of magnetic energy $(BH)_{max}$, comparatively high temperature stability and strictly fixed position of magnetization vectors. This alloy may operate under Helium temperature [16].

The gradient of the field may be calculated for a sector lens (8 sectors in a lens) by the following expression

$$G = [2\ Sin(3p/8)/(3p/8)]\ M(1/r_0 - 1/r)$$

Here G is gradient of the field in kGs/cm, M - magnetization in kGs, r_0, r internal and external radii of a lens in cm.

For the alloy "Samarium-Cobalt" M = 10 kGs. In order to obtain G = 2 kGs/cm under r_0 = 2 cm the external radius of the lens should be equal 2.8 cm.

D.4.1.2.5. High frequency system and system of automatic control

D.4.1.2.5.1. Peculiarities of the system

Principal scheme of the linear accelerator (Fig.2.1) contains a system of high frequency feeding of the initial and first parts with operating frequency 425 MHz and a system of feeding the resonators of the main part with operating frequency 1275 MHz. Synchronous excitation of these systems is realized from a powerful master device through excitation lines and of reference phase LB-1 and LB-2. Master device contains a modules of stabilization of the phases of HF oscillations inter outputs of 425 and 1275 MHz.

Taking into account necessity to provide high reliability of operation of the linear accelerator and accepting into consideration Russian and world experience of development of similar by parameters HF systems it was supposed to use amplifying klystrons in the output cascades of HF channels. Suitable by the parameters klystrons of continuous way of operation are produced by different Russian and foreign firms [17].

Creation of a multichannel HF system for superconducting linear accelerator with proton current 10 - 30 mA is linked with solution of a number of specific technical tasks arising in particular due to high loading of the superconducting resonators by beam current and due to high quality factor of these resonators. So there are some additional requirements to the channels of HF system:

- possibility of smooth controlling of HF power;
- stable operation of HF channel under conditions of significant variations of load;
- high electric stability of feeding system;
- provision of stability of HF field in resonators at levels of accuracy approximately 1% of amplitude and 1 degree by phases under significant variation of load and output power of HF generator;
- quick shut up of HF power in case of loss of accelerated proton beam.

Meeting to these requirements is simplified due to utilization of continuous way of operation of the linear accelerator and under utilization of decoupling devices between the klystrons and resonators providing mode of operation of klystrons to matched load. Calculations showed that reverse attenuation should be not less 15 - 20 db. Circulators produced in Russia meet these requirements. These devices will also stabilize frequency characteristics of the system "HF generator - feeding line - resonator" that will simplify operation of the systems of amplitudes and phases stabilization and of automatic tuning of the resonators.

Coupling of feeding lines and the resonators is usually taken in the HF systems of linear accelerators with strong load by the beam on condition of matching of the feeding lines under acceleration of nominal value of beam current. In dependence of used system of automatic tuning of resonant frequency of resonators the following two versions of operation are possible:

- resonator is tuned exactly in resonance with exciting frequency;
- resonator is detuned to such extent that its input impedance together with beam loading is purely active.

Comparison of these versions allows to make the following conclusions:

1. In both versions under acceleration of the beam power of HF generator must be increased by the factor of four times in comparison with zero value of beam current. In these conditions in the first version HF generator must generate higher power than in the second version by the value of HF power reflected by resonator.

2. Under utilization of the second version of tuning in dependence of the value of the beam current it is necessary to retune the resonator.

3. Under decreasing of synchronous phase difference of these modes of operation decreases.

Any mode of operation may be realised in a HF system. If to choose the average length of resonator of the main part of the linear accelerator equal 0.6 m (see Table II) and acceleration rate 5 MeV/m then HF power necessary for acceleration of beam 10 and 30 mA will be correspondingly 30 and 90 kW. Routine power of generator in a channel of HF system of such resonator must be 40 kW for current 10 mA and 120 kW for current 30 mA. Limits of variation of output power of HF generator in the process of tuning of the accelerator to acceleration of normal current should be provided by controlling systems in the ranges 10 - 40 kW and 30 - 120 kW correspondingly.

Construction of systems of automatic control of amplitude (ACA), of phase (ACP) and tuning of resonators (ACF) are of traditional type and they are described in [18, 19]. Principles of construction are described briefly in the next section.

D.4.1.2.5.2. HF system and system of automatic controlling

The system of HF feeding and the system of automatic control may be designed on classical principles adopted for high current linear accelerators where every accelerating resonator is excited by a separate HF channel with system of ACA, ACP and ACF. But in order to rise reliability of HF system and of automation systems and to lower the costs it is desirable to decrease number of HF channels due to excitation of a group of resonators by one HF generator. At the facility LEP-2 [20], for example, one HF channel of amplification operating with frequency 352 MHz and of 1300 kW output power excites 16 resonators.

The main part of the accelerator consists of 304 resonators operating with frequency 1274 MHz. In a group of four sequentially placed resonators these resonators consume approximately equal HF powers (even without optimization this difference does not exceed 1%). That is the reason why it is possible to excite such groups by one generator (Fig.2.10). System of distribution of HF power to the resonators is constructed with the aid of bridge-type devices [21] proposed for decoupling of two loads and division of HF power to equal parts, Split-type of double T-shape bridges may be used as prototypes of such devices. Amplifying klystrons with output power approximately 500 kW for acceleration of 30 mA beam and 150 - 200 kW under beam current 10 mA will be needed for excitation of a group of four resonators.

Systems of ACA and of ACP are constructed by traditional for linear accelerators schemes [19]. Control signals are extracted from each resonator as it is shown in the Fig.2.10. Systems of ACF are applied to each resonator. Adjusting of phases of HF fields in resonators is carried out with the aid of phase-controllers Ô placed at the outputs of the bridges M_2 and M_3. Adjusting of phases is accomplished with the aid of phase-controllers Ô at the inputs of amplification channels and in the line of reference phase φ_{ref}.

HF system of initial part and of the first part of the accelerator provides excitation of one resonator of RFQ type and 28 short resonators with drift tubes. RFQ resonator requires approximately 90 kW of HF power for acceleration of current 30 mA and 30 kW for acceleration of 10 mA. Resonators with drift tubes require 45 - 108 kW and 15 - 36 kW for acceleration of 30 and 10 mA correspondingly. HF power rises with rising of the number of resonators. Due to the fact that under constant along the whole length of the accelerator rate of acceleration and different levels of power in separate resonators here a "classical" scheme with individual excitation of every resonator by a separate klystron generator might turn to be expedient. In this case a circulator should be installed in the feeding line between the klystron and resonator. The resonators with corresponding HF channels are covered with systems of stabilization of amplitudes, phases and resonant frequencies. Klystrons of equal power - 130 kW -are supposed to be used for unification of the devices for acceleration of beams to 30 mA. For current 10 mA the required HF power is three times less. Under corresponding optimization of the accelerating channel the version of excitation of two or four resonators of the first part of the linear accelerator becomes possible (see Fig.2.5.1).

D.4.2.6. Characteristics of the alternative technical decisions.

The intensive supercounducting linear accelerator is technically feasible and should ensure extreme high performance on economic and power efficiency. The reason on realization proposal is possible to support, having specified on opportunity of reception of enough high parameters by use of new ideas in traditional techniques of warm resonators.

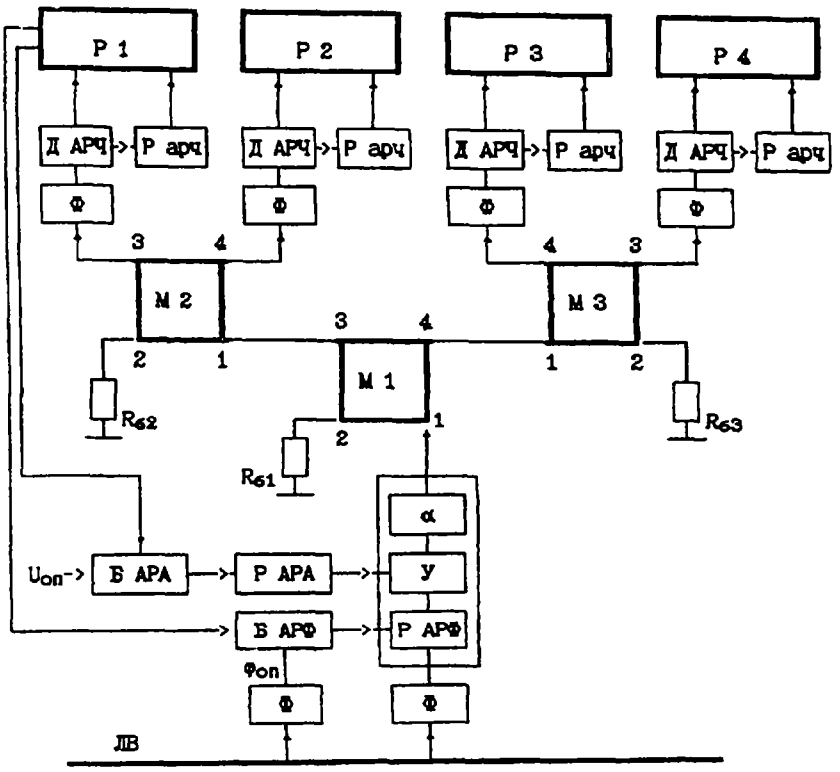

FIG.2.10 Scheme of excitation of 4 resonators by one channel of amplification with system for controlling the parameters of HF field. P1...P4 are accelerating resonators; M1, M2, M3 bridges for distribution of HF power; R_{b1}, R_{b2}, R_{b3} - balasting loads; a - circulator; Y - amplifier of HF power; ËÂ - line of reference phase excitation; B-APA - a set for processing of the error signal in the system ACA; P APA - executing mechanism of ACA system; B-AP Ф - a set for processing of the error signal in the system ACP; P APФ - exacuting mechanism of ACP system; Д - a probe of ACF system; P AP Ч - executing mechanism of ACF system; T - phasecontroller.

So, as spare variant to use of superconductivity at higher temperature it is useful to consider also pulsing mode of operations of warm resonators, when the high meaning efficiency of acceleration of large beam currents is transformed to area of smaller currents and is supported high irrespective of value of an average current of a beam, which is defined by frequency of pulse repetition rate [22]. Calculations show, that the efficiency of resonators in pulsing mode can come near to 90 % in whole range of average currents 10 - 30 mA of the offered accelerator, that will ensure general efficiency (from ac network to beam) about 50 %.

Pulsing mode is rather effective, if a current in pulse in 2 and more time exceeds necessary average meaning, and duration of pulses more than 500 ms. The natural pauses between pulses of a beam current thus can be used in this case for switch on and off deflecting of the output beam at it distribu-

tion on several directions, that would be economically expedient in case to work of a target on lowered power or functioning of several targets.

Restriction of relative losses of particles by value smaller, than 10^{-5} is determined by necessity of a level of induced radioactivity reduction with the purpose of reception of access to accelerator through small time after switch off the beam and maintenance of radiating cleanness of linac units in case of their dismantle. The reduction stipulated in the present proposal of radiating fields (at the excess value of the channel acceptance and reduction of losses of particles) can be considerably strengthened, if to provide accommodation along accelerating channel of graphite proton absorbers [23], dropping out from mode of resonant acceleration. Thus on 1-2 order (up to 10^{-4}) the requirements to limit of allowable losses are reduced, that is a reached a stage on working linear accelerators [24]. Thus, one of main problems of acceleration of intensive beams - problem of reduction of radiation up to acceptable level in the linac can be confidently resolved.

Reliability of rather expensive installation, which is the high-current the accelerator, requires of the special attention. In heaviest degree it depends on reliability of RF system.

Calculations show, that supplying of 1-5 cells from individual RF of channels of rather small power (as it is already done on SC resonators of heavy ions post - accelerators) and having increased total number of cells (or intensity of a field in their gaps) only on 1-2 %, it is possible to ensure trouble-free RF excitation of cells necessary for nominal acceleration [26]. In case of the RF channel failure all elements of the given section, including cells of section, pass in category of switched off, and compensating influence on a beam is provided at the expense of automatic increase of RF field intensity and updating of its phase in operating sections. The failed channel after repair comes back in work, and the intensity of the field in all sections is automatically lowered.

The additional rather valuable quality of the recommended circuit is that the failure of a section (or some their amount) does not cause a stop of the accelerator and does not require immediate replacement or repair (if, certainly, it is not connected with loss of high vacuum or occurrence of a mechanical obstacle to flight of beam bunches). Failure of a section is compensated by work of staying in operating conditions, and the elimination of malfunction can be postponed on long time before scheduled preventive maintenance.

ITEP has a unique opportunity prior to the beginning creation of electronuclear installation to check up experimentally number of principally important questions on prototype of full - scale electronuclear installation - the subcritical neutron generator [27], which is constructed on the basis of the proton linear accelerator ISTRA-36 and equipment of shut-down heavy-water reactor HWR. The general scheme of the generator is shown on Fig. 9.1 and section D.4.1.9. Now this installation consists of the accelerator - driver and subcritical blanket is the most advanced ones. The generator will serve range for study and improvement:

- Principles of a beam dosage of the accelerator - driver,
- Formation of optimum distribution of density of a proton flux on target,
- Safe for resonators and RF system of the accelerator at beam manipulations,
- Uninterrupting beam diagnostics ,
- Reliable way of measurement of proton flux on target.

D.4.1.3. Pb-Bi TARGET AND PARTITIONED SUBCRITICAL BLANKET

Subcritical blanket with fast and thermal zones (Fig.3.1) consists of the following components:- proton beam transport duct;

- fast spectrum blanket zone;
- thermal spectrum blanket zone;

- coolant and moderator circulation loops;

The fast spectrum blanket zone is a separate cylindrical vessel which encloses:

- vertical section of a proton beam transport duct ending with a window which separates a vacuum plenum of the accelerator from the internal space of the vessel with Pb-Bi coolant.

- a vessel separating coolant flows in downcomer and riser sections;

- a zone with fuel assemblies;

Steam generators providing heat removal from liquid metal coolant and generation of steam with specified parameters are arranged at the top part of the vessel at a boundary between the riser and downcomer sections.

The separating vessel above the zone with fuel assembles consists of two concentric shells with a vacuum plenum between, which provides thermal insulation between the downcomer and riser sections of coolant flow path to eliminate heat losses.

Natural circulation of liquid-metal coolant is provided in the vessel.

The fast spectrum blanket zone is installed into a cylindrical central plenum of the thermal spectrum blanket zone and is supported by a removable cover of the thermal zone.

The fast zone of the blanket (Fig. 3.1) comprises 18 fuel assemblies (Fig.3.2), each consisting of 311 fuel pins with nuclear fuel made of oxide weapon-grade Plutonium and Thorium (Fig.3.3). Eutectic alloy 45% Pb + 55% Bi has been selected as a coolant. It serves also as a neutron-absorbing target located in a center of the fast-spectrum zone. Proton beam reaches the central plenum with the eutectic alloy via an ion-transport duct which ends by a spherical window made of Titanium.

A steam generator installed in the upper part of the fast-spectrum blanket 'zone vessel is intended for heat removal from liquid-metal coolant. It represents a straight-tube heat exchanger comprising 4180 tubes of 16x2.5 mm diameter and 8m length. Pb-Bi coolant flows downwards in an inter-tube space by natural convection, while secondary coolant (water) circulates upwards inside the tubes. The tubes are united in separate sections which can be isolated in a water side, if necessary. Further, after design optimization of the breeding zone and SG's elements a possibility may appears to reduce both sizes of the components and length of a section between them.

The thermal-spectrum blanket (Fig.3.4) zone is arranged around the fast-spectrum one and consists of a vessel made from two cylindrical shells one of which is installed inside another. The shells are connected in their lower part by a welded semitorous bottom, while in its upper part they are connected by a removable cover made as a flat ring-shaped plate with orifices through which technological channels (Fig.3.5) containing the fuel assemblies, as well as instrumentation and control channels (if necessary) are penetrated.

The channels upper end fittings are attached hermetically to the removable cover of the blanket's vessel.

A plenum of the vessel between the cylindrical shells is filled with heavy water moderator. A special circuit with feed and discharge portions of pipelines, a heat exchanger, pumps and isolation valves is provided for cooling the moderator.

The technological channels (Fig. 3.2) installed in the heavy water thermal blanket zone are provided with their own high-temperature cooling circuit with D_2O coolant. For this aim the channels are made as Field-type tubes (tube-in-tube structure). Coolant flows downward through an annular gap between the tubes, then it moves upward along the inner tube cooling a column of fuel assemblies arranged in it. To organize coolant circulation through the channels they are provided with individual feed and discharge tubes connected to in the region above the blanket vessel removable cover (Fig.3.6). Beyond the blanket these tubes are united in collectors. Control valves are installed in the tubes to provide flowrate shaping through the channels.

Taking into account a substantial difference of temperatures between moderator in interchannel space and coolant in the channels they are mutually insulated with the aid of a gas layer formed by a

plenum between a channel's pressure tube and a guard jacket around it. Leak-tightness of the technological channels may be monitored by moisture and pressure control in this plenum.

The core of thermal blanket (Fig.3.2) comprises 684 fuel assemblies of a Field-tube type, arranged in a triangular lattice with 280 mm pitch and surrounded by inner and outer heavy water reflectors. Each of the assemblies includes 36 fuel rods made of anixed oxides of weapon-grade Plutonium and Thorium (Fig.3.6). Up to 36 control rods can be arranged in the thermal-spectrum blanket, if necessary.

The choice of liquid-metal coolant. Lead - bismuth alloy (in 45:55 by weight) taken as liquid-metal coolant for the fast-spectrum blanket zone is eutectic with melting temperature appr.125°C. Low melting temperature of the alloy is main advantage of this coolant type in comparison with pure lead (melting temperature of ~327°C).

Lower melting temperature of the coolant allows maintenance operations for replacement of in-vessel equipment during planned outage with a higher safety and lower consumption of energy to maintain coolant in melted state. At present, technology for this alloy handling has been developed, which takes into account many-years experience in practical utilization of Pb-Bi coolant. Application of special additives together with protective coatings on structural materials enables to minimize negative effect of such processes as erosion, corrosion and mass transfer.

Furthermore, application of Pb-Bi alloy as coolant and a target material simultaneously provides the same level of primary neutrons born in spallation reactions as for lead target. The advantage of mother lead in lower induced activity under neutron irradiation at spallation reaction disappears since the main contribution to long lived activity ($T_{1/2}$>100-days) for both target materials is caused not by Po-210, but by various isotopes of Bi, Te, Hg and Au accumulated due to (p, xn) and (n, xn) reactions in high-energy part of proton and neutron spectra .

TABLE IV. THE MAIN PARAMETERS OF SUBCRITICAL BLANKET WITH FAST-THERMAL ZONES.

Parameters	Units	Fast zone	Thermal zone
Gross thermal power	MW	300	2000
Main vessel			
height	m	27	9
outer diameter	m	2	9
Coolant target spallation material		molten lead and Pb-Bi	heavy water
moderator			
Coolant mass	t	400	
Pumping method		natural convection	circulation pumps
Coolant flow in core	kg/s	7560	13890
Coolant pressure	MPa		110
Height of convection column	m	25	
Spallation target power	MW	10	
Coolant flow in target	kg/s	502	
Full coolant flow in exchanger -			

TABLE IV (Cont.)

steam generator	kg/s	8062	
Water flow in steam generator	kg/s	1376	
Height of steam generator	m	8	
Fuel core: number of fuel assemblies		18	684
number of fuel pins		331	36
number of control rods			24
Max. coolant speed in fuel assembly	m/s	1,48	7,4
Height of active core	m	1,5	6,0
Radial power flattening factor		1,4	2,2
Axial power flattening factor		1,6	
Maximum fuel pin power	kW	112,9	178
Maximum fuel power density	kW/m^3	$1,42 .10^6$	$4,6.10^5$
Maximum fuel temperature	°C	1609	494
Clad temperature	°C	760	336
Maximum outlet coolant temperature	°C	628	310
Volume water in coolant loop	m^3		45,9
Surface of stainless steel	m^2		3000
Volume of moderator in tank	m^3		80
Total volume of moderator	m^3		160
Temperature of moderator	k		340
Pressure in moderator loop	MPa		0,1
Surface of stainless steel	m^2		350

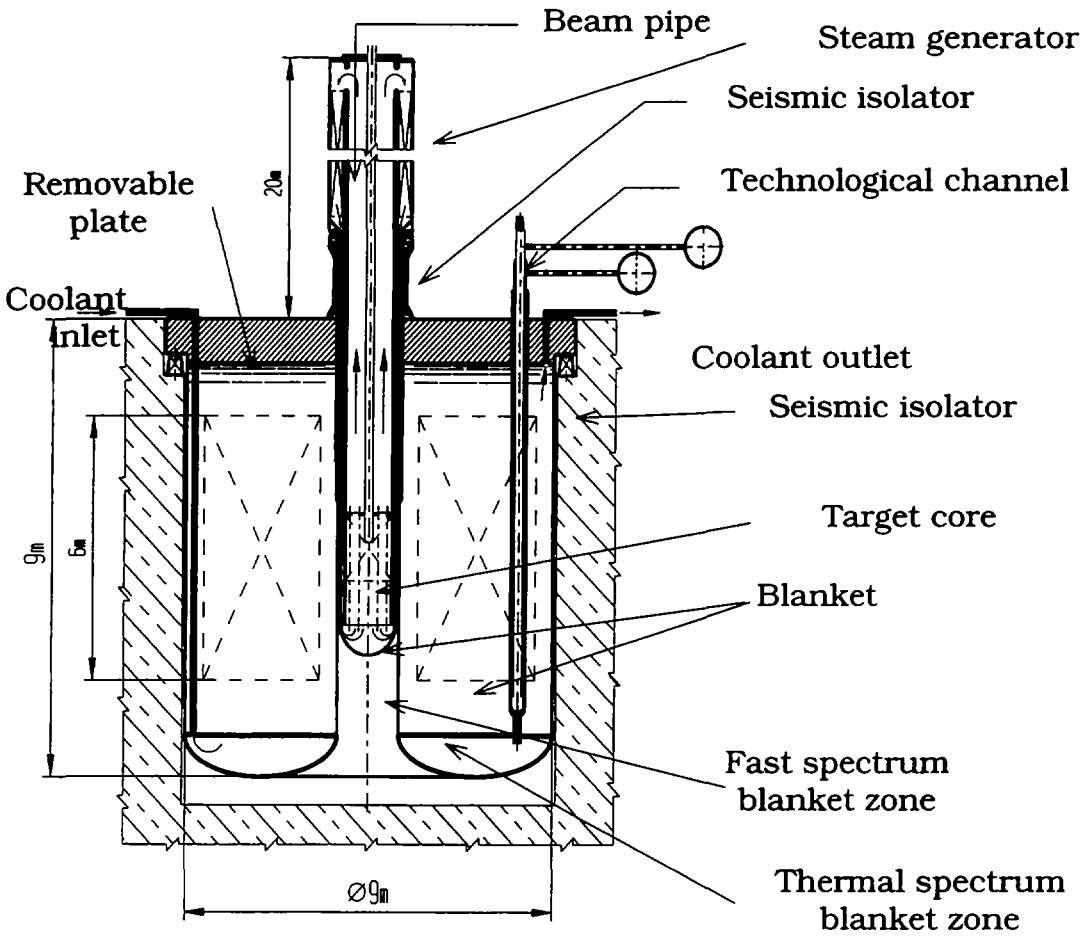

Fig. 3.1 Layout of the subcritical blanket with fast and thermal zones.

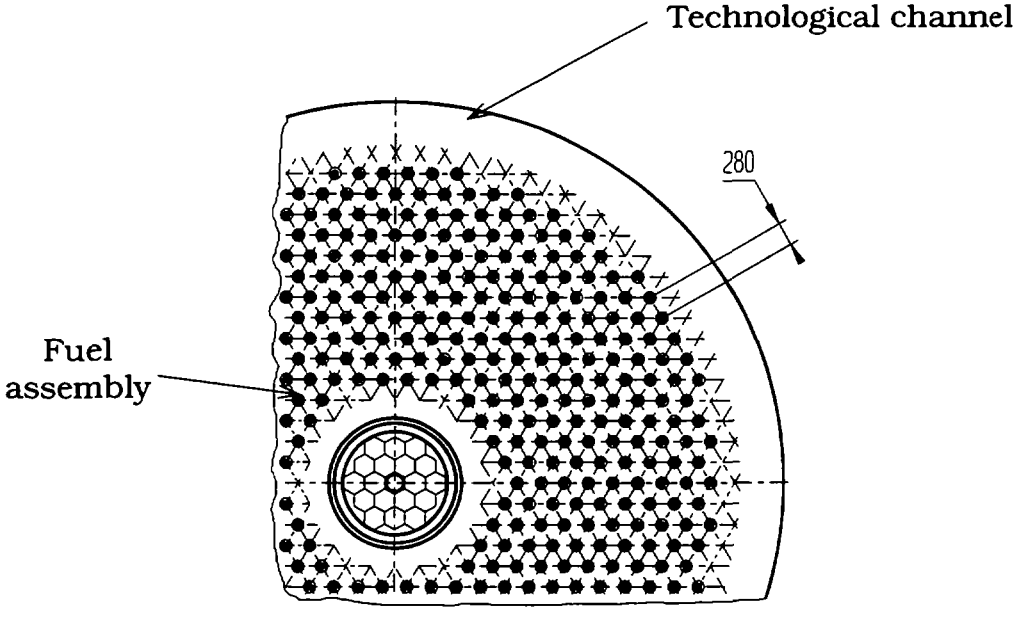

Fig. 3.2 The fuel assembly of the fast zone

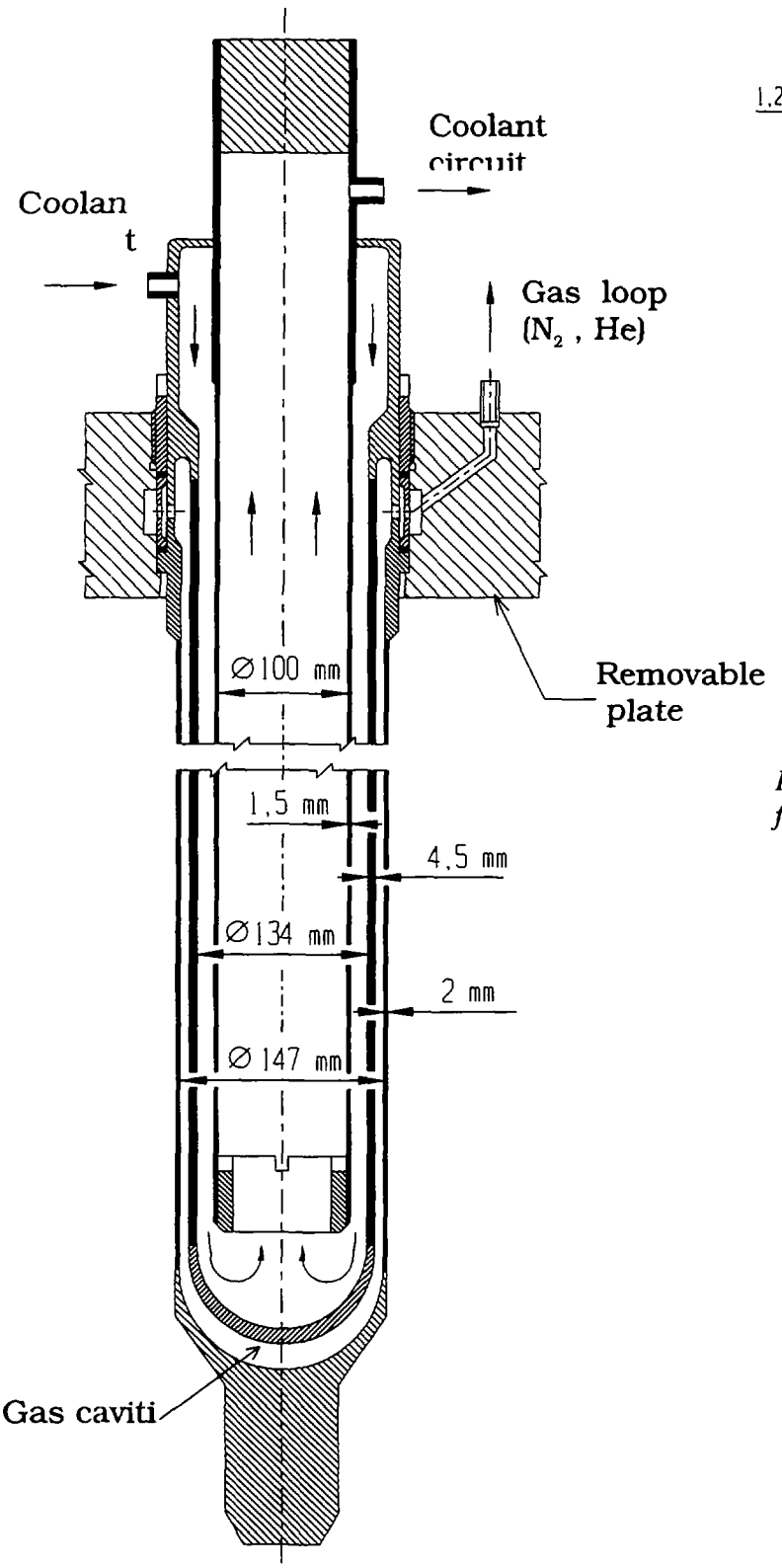

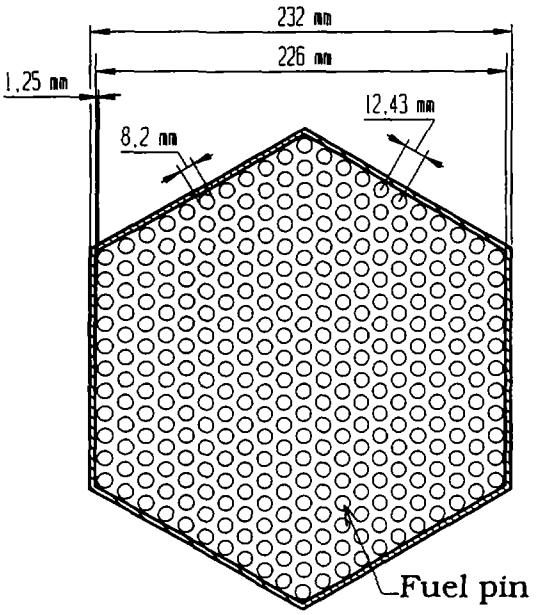

Fig.3.3 The fuel asembly of the fast spectrum sone

Fig.3.4 Layout of the thermal spectrum blanket

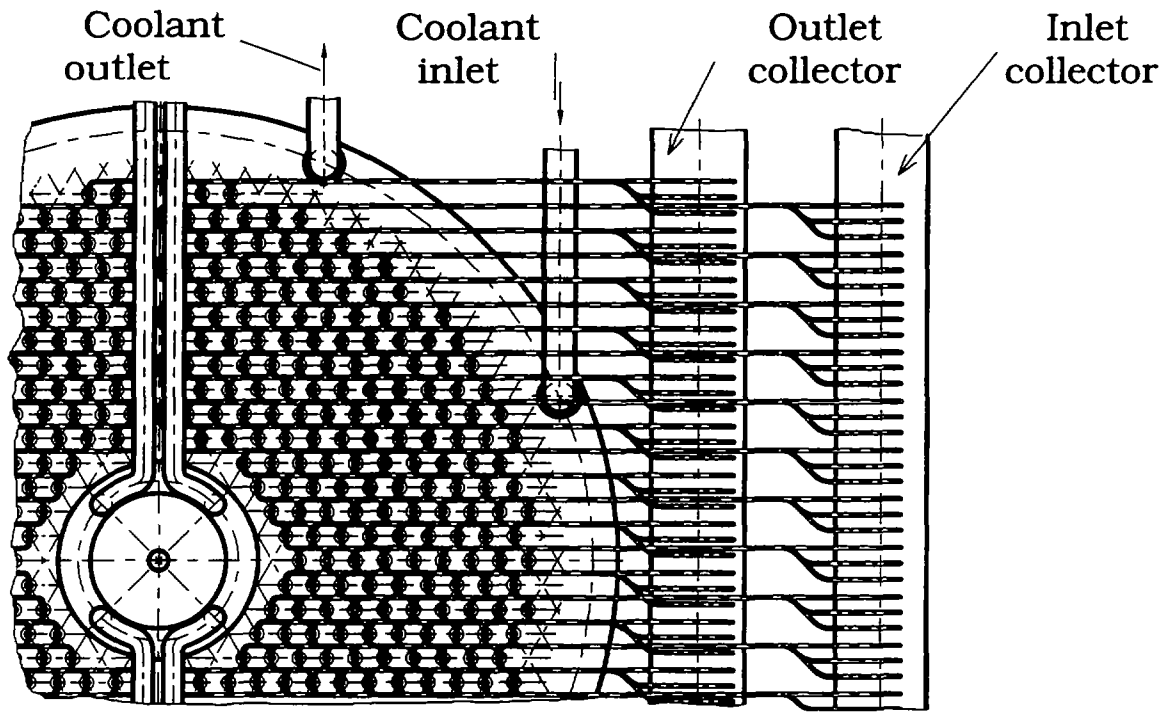

Fig. 3.5 Thermal spectrum blanket - a part of the vessel containing fuel assemblies

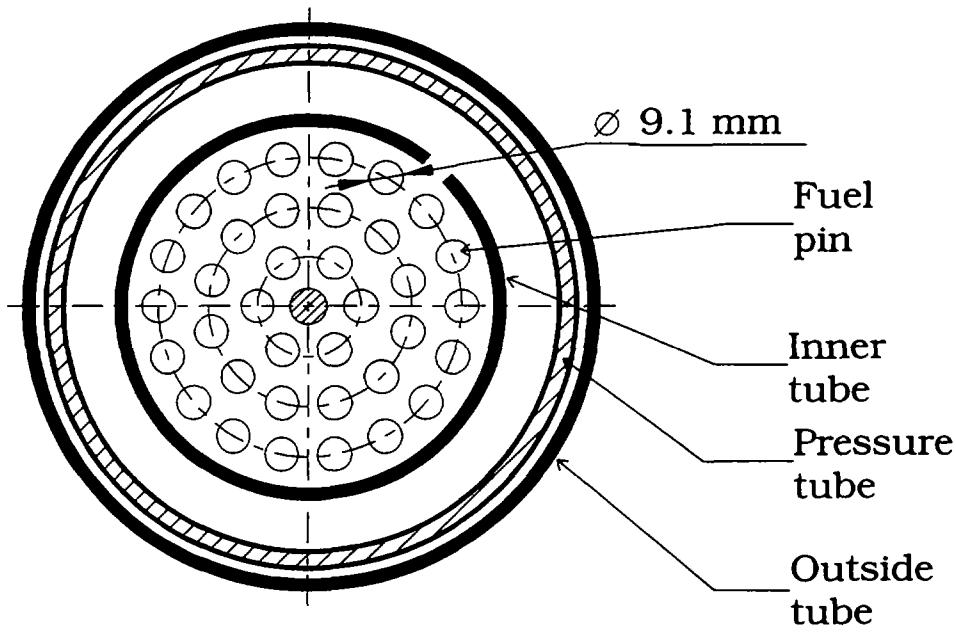

Fig. 3.6 Pressurize tube containing fuel rods.

D.4.1.4. INTERACTION OF PROTONS AND IONGUIDES AND ACCUMULATION OF LONG-LIVED ACTIVITY IN IRRADIATED TARGETS.

Energy release and attenuation of beam in the window

Main power production in thin windows fabricated of stainless steel or titanium of 2 -5 mm of thickness is due to ionization losses of the beam. Using well known tables of ionization losses [28] we can obtain the values of power production in the window (Tab. V):

TABLE V. POWER GENERATION IN THE WINDOW

Beam		Stainless steel		Titanium	
E, MeV	Current, mA	dE/dx, MeV/mm	Power production kW/mm	dE/dx, MeV/mm	Power production kW/mm
800	30	1.34	40.20	0.77	23.10
1600	60	1.20	72.00	0.69	41.40

Losses of intensity of the beam due to nuclear collisions are defined by cross-sections of inelastic interactions which are well known for 800 MeV protons with rather high accuracy: 775 mb for steel (iron) and 695 mb for titanium [29]. Attenuation of beam intensity per one centimetre of target 6.5% for steel and 3.9% for titanium corresponds to these sections. Transfer energy of nuclei and of light charged particles leads to 10 -12% rise of full power production relative to ionization power production. Carried out analysis shows that replacing of stainless steel by titanium decreases power production in the window approximately by a factor of 1.7 under the same thickness of the window.

Radiation damages of the target window

Experimental data on radiation stability of the target window under passage through it of high energy protons are compiled and discussed in [30]. On the base of these data conclusion is made that replacing of a window in the project of the transmutation installation will be necessary only in a half of a year (if it will necessary at all).

The results of estimations on the base of the codes NMTC/JAERY, LAHET and HTAPE and also of [31-34] contradict each other and this makes it necessary to continue the works on comparison of approaches and programs and also to carry on experiments at proton accelerators.

Analysis of long-lived activity of targets

Analysis of accumulation of radioactive nuclei in the target showed [30,35,36] that long-lived activity normalised to similar conditions of irradiation may differ by several orders of the values. Estimations of activity of dominating isotope ^{210}Po ($T_{1/2}$ = 138 days) given in [36] for lead-bismuth target are more than 10^3 times higher than estimations of other authors. It is obvious that so serious discrepancies in the estimations are defined by discrepancies in the used values of sections of corresponding channels of accumulation of the isotopes. It was found that the discrepancy is defined by the fact that the section (n,γ) for reaction ^{209}Bi was taken approximately 10^3 times higher. This is the reason why it is very important to use only reliably tested libraries of activation data in

calculations of induced activities from one hand and to find out the reasons of contradictions of calculations of accumulation of radioactive nuclei in the targets from the other hand.

Calculations for a lead and a lead-bismuth targets irradiated by a 800 MeV 30 mA proton beam for one year are presented in the Figures 4.1 and 4.2 and also in the Tables VI and VII.

Total and partial activities (Ci/kg) in Lead target (Tab.4.1) and Lead-Bismuth (Tab.4.2) for primary proton beam energy 800 MeV and Current 30 mA after a year of irradiation for different cooling times

TABLE VI. ACTIVITY OF THE LEAD TARGET AFTER ONE YEAR IRRADIATION

Cooling time	180 days	2 years	20 years	100 years
Total activity	$1.0\ 10^{2}$	$2.7\ 10^{1}$	2.0	$6.0\ 10^{-1}$
Po-210	$6.0\ 10^{-4}$	$3.9\ 10^{-5}$	$2.8\ 10^{-7}$	$2.3\ 10^{-8}$
Bi-207	$1.7\ 10^{-1}$	$1.6\ 10^{-1}$	$1.2\ 10^{-1}$	$2.7\ 10^{-2}$
Pb-202	$5.4\ 10^{-3}$	$5.4\ 10^{-3}$	$5.4\ 10^{-3}$	$5.3\ 10^{-3}$
Tl-204	$1.9\ 10^{1}$	$1.5\ 10^{1}$	$5.9\ 10^{-1}$	-
Hg-194	$1.3\ 10^{-1}$	$1.3\ 10^{-1}$	$1.3\ 10^{-1}$	$1.1\ 10^{-1}$
Au-194	$1.3\ 10^{-1}$	$1.3\ 10^{-1}$	$1.3\ 10^{-1}$	$1.1\ 10^{-1}$
Pt-193	1.3	1.3	$9.9\ 10^{-1}$	$3.3\ 10^{-1}$

TABLE VII. ACTIVITY OF THE LEAD/BISMUTH TARGET AFTER ONE YEAR IRRADIATION

Cooling time	180 days	2 years	20 years	100 years
Total activity	$1.1\ 10^{2}$	$3.4\ 10^{1}$	$1.2\ 10^{1}$	3.0
Po-210	$1.1\ 10^{1}$	$7.1\ 10^{-1}$	$9.3\ 10^{-6}$	$7.8\ 10^{-7}$
Po-208	1.6	1.1	$1.5\ 10^{-2}$	$7.6\ 10^{-11}$
Bi-207	$1.6\ 10^{1}$	$1.5\ 10^{1}$	$1.1\ 10^{1}$	2.7
Tl-204	9.2	7.0	$2.8\ 10^{-1}$	$1.8\ 10^{-7}$
Hg-203	$2.2\ 10^{-1}$	$6.2\ 10^{-5}$	-	-
Hg-194	$1.1\ 10^{-1}$	$1.0\ 10^{-1}$	$1.0\ 10^{-1}$	$9.3\ 10^{-2}$
Au-195	$4.8\ 10^{1}$	6.2	$1.0\ 10^{-1}$	-
Pt-193	1.1	1.1	$8.4\ 10^{-1}$	$2.8\ 10^{-1}$

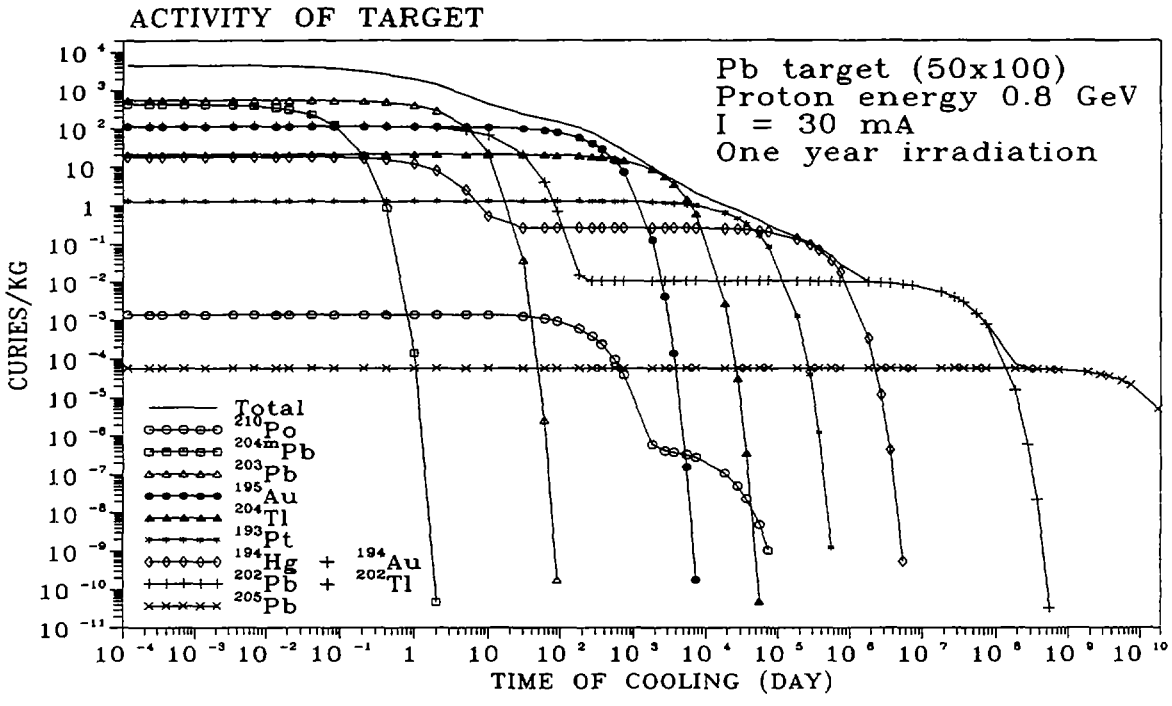

FIG. 4.1 . Total and partial activities of Lead target as a function of cooling time.

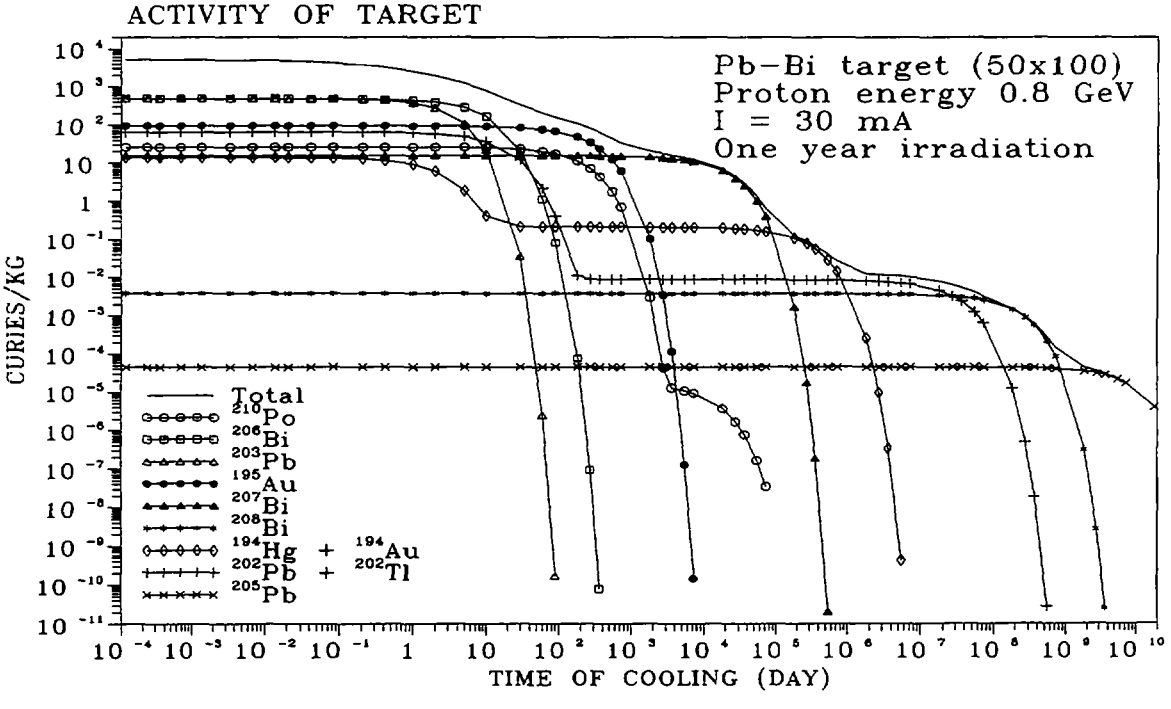

FIG. 4.2. The same as in Fig.4.1 for Lead-Bismuth target

D.4.1.5. PHYSICAL PROPERTIES OF SUBCRITICAL SYSTEM WITH FAST -THERMAL ONE-DIRECTION COUPLED BLANKET ZONE.

D.4.1.5.1. General description

General concept of ABC system with two blanket regions - inner fast spectrum blanket (F-blanket) and outer - thermal spectrum blanket (T-blanket) is presented (tables 5.1.1, 5.1.2, 5.1.3). Liquid Pb-Bi with natural convection pumping is used as target material and coolant in F-blanket. Outer T-blanket is a vessel with heavy water moderator and CANDU-type pressure tubes. Fuel pins are made of mixed W-Pu -Th oxides clad in stainless steel for F-blanket and Zirconium alloy for T-blanket. Stainless steel wall of F-blanket and inner wall of T-blanket present a fast neutron reflector for F-blanket and a structural component (together with an inner heavy water reflector) providing one-direction neutron coupling. Due to the latter property total system can operate at low level of sub-criticality (multiplication factor K 0.99) resulting in a low proton beam current (10 mA for protons with energy 1 GeV) at safety conditions corresponding to much higher sub-criticality of the main - thermal part of blanket (K 0.95). Due to increased non-uniformity of radial power distribution in T-blanket compared to CANDU reactor, mean power output from fuel assemblies is twice lower and their number is two times higher than in CANDU reactor.

TABLE VII. MAIN PARAMETERS OF ABC F-T INSTALLATION

	F-blanket	T-blanket
Gross Thermal Power/unit	300 MW	2000MW
Primary Electric Power	120 MW	580 MW
Type of plant	Pool	Pressure tubes in heavy water vessel
Coolant	Liquid Pb-Bi	Heavy water
Multiplication factor K of total system	0.99	
Reactivity control and protection system	Control rods+Tc- 99 dissolved in heavy water	

TABLE VIII. FAST SPECTRUM BLANKET ZONE (F-BLANKET)

Height of fuel	3.0 m
Inner/Outer diameter	0.246 /1.071 m
Coolant	liquid Pb-Bi
Fuel assemblies	
Number of units	18 (36)
Configuration	hexagonal
Number of hexagonal rounds	2 (3)
Number of pins/unit	331
Flat to Flat	0.234 m
pitch between pins	1.243 cm
Volume of fuel per 1cm of length	174.8 cm**3
Total volume of fuel	471965 cm**3
Density of mixed oxides	10 g/cm**3
Downward section for liquid Pb-Bi coolant the wall of F-blanket vessel, inner/thickness diameter	1.247 m / 4 cm

TABLE IX. THERMAL SPECTRUM BLANKET ZONE(T-BLANKET)

Heavy water vessel	
inner diameter	132.7 cm
thickness of inner wall	4 cm
Inner heavy water reflector - thickness	44.4 cm
Heavy water core - inner/ outer diameter	2.295 / 8.025 m
height	6 m
Heavy water reflector - thickness	0.5 m
Number of fuel assemblies	684
Lattice (hexagonal) pitch	0.28 m
Fuel assembly	
Tube, (Zr - 2.5%) Nb , inner diameter / thickness	10.0 / 0.15 cm
(Downward section for cold coolant)	
Pressure tube - inner diameter / thickness	13.4 / 0.45 cm
Gap	0.2 cm
Calandria tube(Zr- 2% Nb), inner diameter	14.7 cm
thickness	0.2 cm
pellet diameter	1.2154 cm
mean density (effective)	7.9 g/cm**3
clad, outer diameter	1.308 cm
Number of fuel pins	36
element to element spacing	0.155 cm
element to pressure tube spacing	0.102 cm
diameters of centres	2.977, 5.751, 8.661
Volume of fuel per 1 cm of length	41.808 cm**3
Total volume of fuel	17.16 m**3

D.4.1.5.2. The results of fuel cycles simulation

Calculations have been performed by modification of computer code TRIFON [37] for the case of sub-critical systems with external sources and zero flux boundary conditions. An option for support of a constant level of sub-criticality (and consequently constant total power) by continual removal of reactivity control element was used. For this purpose ^{99}Tc was supposed to be dissolved in heavy water moderator of T-blanket. The amount of ^{99}Tc is limited by the value 9.5 g/l in heavy water moderator, as it is estimated below (these values provide negative or zero reactivity effect caused by moderator density decrease). Burn-able poisons (supposed to be added into outer row of fuel pins in T-blanket) - Gd and Am isotopes (simultaneously transmuted) - may be used for decrease of ^{99}Tc concentration.

Several cases were considered:

1. ^{99}Tc as control reactivity element, F-blanket power 300 MW (18 fuel assemblies);

2. ^{99}Tc as control reactivity element, F-blanket power 600 MW (36 fuel assemblies);

3. ^{99}Tc as control reactivity element , F-blanket power 300 MW. U-Th fuel cycle in thermal blanket;

4. 2nd cycle with Pu , Am and Cm nuclides from T-blanket after 1st cycle re-loaded into F-blanket, T-blanket composition the came as in Case 1.

D.4.1.5.2.1. Burn-up calculations in a cell of T-blanket.

The model of multi-layer cylindrical cell was used with fuel pin material and clad material smeared separately inside concentric cylindrical regions in correspondence with 3 fuel pin rows (Tables X and XI).

Typical neutron balance and mean concentrations of nuclides in the cell for beginning of a cycle are presented in Table XII .

TABLE X. COMPOSITION OF CELL IN T-BLANKET - DIMENSIONS AND TYPES OF REGIONS.

Zone	thick., cm	Rmin, cm	Rmax, cm	Volume, cm^3 *	Type
1	.50	.00	.50	7.854E-01	void
2	.15	.50	.65	5.583E-01	clad
3	.40	.65	1.06	2.169E+00	coolant
4	.06	1.06	1.12	4.020E-01	clad
5	.74	1.12	1.86	6.961E+00	fuel
6	.06	1.86	1.92	6.991E-01	clad
7	.51	1.92	2.43	6.964E+00	coolant
8	.06	2.43	2.49	9.419E-01	clad
9	.77	2.49	3.26	1.392E+01	fuel
10	.06	3.26	3.32	1.260E+00	clad
11	.56	3.32	3.89	1.278E+01	coolant
12	.06	3.89	3.95	1.497E+00	clad
13	.77	3.95	4.71	2.088E+01	fuel
14	.06	4.71	4.78	1.813E+00	clad
15	.22	4.78	5.00	6.907E+00	coolant
16	.15	5.00	5.15	4.783E+00	tube
17	1.55	5.15	6.70	5.770E+01	coolant
18	.85	6.70	7.55	3.805E+01	tube
19	7.15	7.55	14.70	4.999E+02	moderator

- per 1 cm of height of fuel assembly

TABLE XI. INITIAL ISOTOPIC COMPOSITION OF MATERIALS, NUCLEAR DENSITIES (CM^{-3}, 10^{24}). FUEL (T=900 K), CLAD(TUBE) (T=570 K/ 550 K/ 340 K), COOLANT (T=550 K), MODERATOR (T=340 K).

Material	Nuclide	Nucl. Density
void	O	1.000E-04
clad (tube)	Zr	4.144E-02
	Nb	1.062E-03
	D	5.117E-02
coolant	O	2.571E-02
	H	2.570E-04
	O	3.600E-02
	Th232	2.056E-02
fuel	Pu239	9.480E-04
	Pu240	6.085E-05
	Pu241	5.064E-06
	D	6.592E-02
moderator*	O	3.313E-02
	H	3.310E-04

*) Some amount of ^{99}Tc may be assumed to be dissolved for compensation of reactivity.

TABLE XII. NEUTRON BALANCE IN THE CELL OF T-BLANKET. TOTAL NEUTRON ABSORPTION IS NORMALISED TO 1.

Cell composition		Epithermal		Thermal	
Element	Conc. *	Capture	Fission	Capture	Fission
O	2.988E-02	3.093E-03	0.	2.408E-04	0.
Zr	2.496E-03	6.137E-03	0.	1.382E-02	0.
Nb	6.398E-05	4.869E-03	0.	2.203E-03	0.
D	5.506E-02	1.811E-05	0.	1.331E-03	0.
H	2.764E-04	1.950E-04	0.	4.438E-03	0.
Th232	1.054E-03	2.290E-02	3.628E-03	4.620E-02	0.
RZTh232 **	1.054E-03	6.125E-02	0.	0.	0.
Pu239	4.860E-05	2.456E-02	4.827E-02	1.353E-01	2.858E-01
Pu240	3.119E-06	1.653E-03	2.716E-04	5.848E-03	0.
RZPu240**	3.119E-06	1.944E-02	0.	0.	0.
Pu241	2.596E-07	1.496E-04	6.266E-04	6.074E-04	1.863E-03
Gd157	1.304E-08	5.760E-05	0.	2.504E-02	0.
Gd155	1.230E-08	1.195E-04	0.	5.257E-03	0.
^{99}Tc	1.399E-04	1.391E-01	0.	1.376E-01	0.

*- mean value of nuclear density (cm, 10^{24}) in the cell

**- RZTh232 and RzPu240 present neutron capture and fission by resonance levels.

Since the mean value of mixed oxides (7.9 g/cm**3) used in fuel pins of T-blanket is less than its natural density (10 g/cm**3) non-uniform initial fuel density distribution in fuel assembly - 20% higher compared to mean value in the 1st and 2nd rings of fuel pins (18 pins) and decreased by the same value in the 3rd ring (18 pins) - may be used for flattening of power distribution. The results of burn-up calculations are presented in Fig. 5.1.

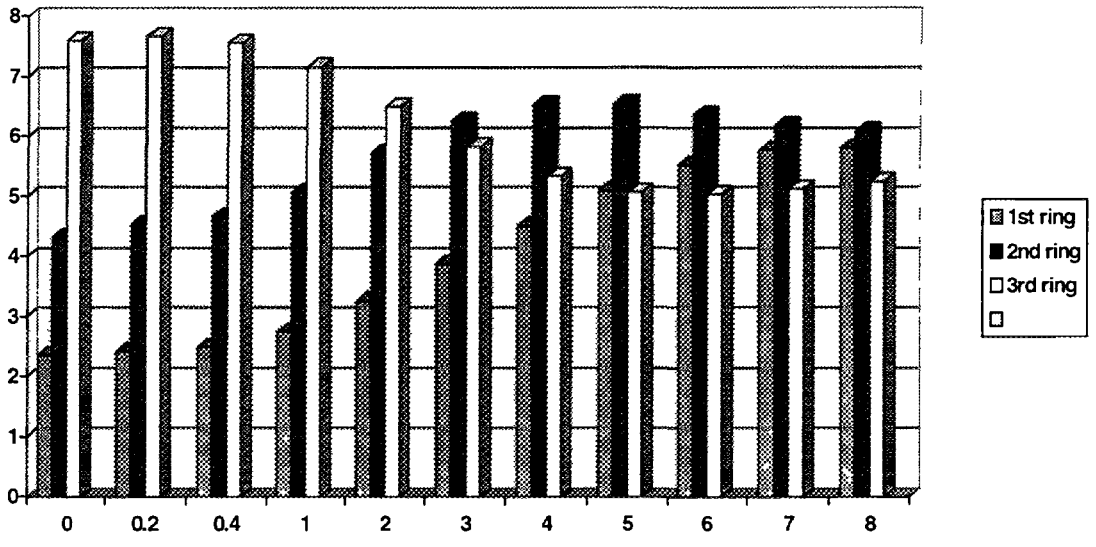

FIG. 5.1 Power distribution across 3 rings of pins in fuel assembly of T-blanket depending on time (years)

Burn-able poison (Gd or Eu) and transmuted isotopes of Am may be added to fuel material in the 3rd ring to improve power distribution within the first period of time (1 year).

D.4.1.5.2.2. Case 2.Simulation of burn-up in the 1st cycle during 5.8 years with Tc99 as control reactivity element.

F-blanket power 300 MW; Total power = 2400 MW.

Total mass of heavy nuclides = 130662 kg.

The results of calculations - power dependence of time in F- and T- blankets (with total power constant) and time dependence of isotopes masses in F- , T - blankets and total in the system - are presented in Tables XIII - XIV and Figs 5.2 - 5..11.

During 30 years period of operation at full power 27 t of Pu239 is destroyed and 28 t of W-Pu incinerated - converted into Pu of different composition , other heavy nuclides and fission fragments. 11 t of Th are involved into fuel cycle with of 7 t of U233 accumulated and 4 t spent in the installation for power production.

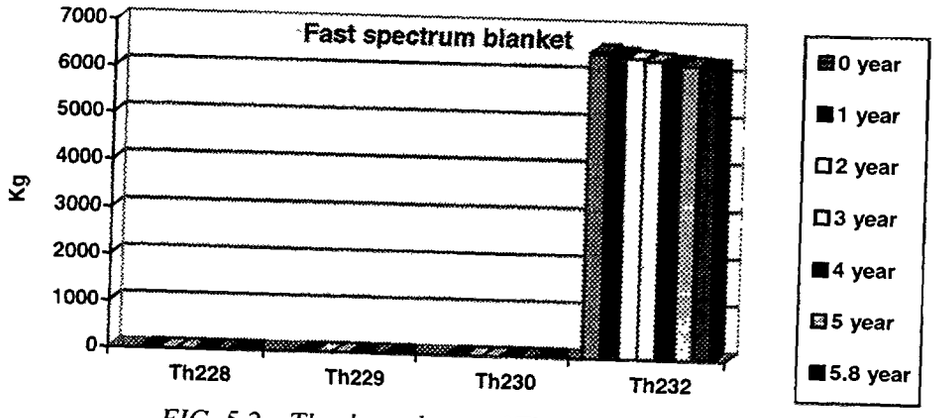

FIG. 5.2. The dependence of Th isotopes masses (kg) on time.

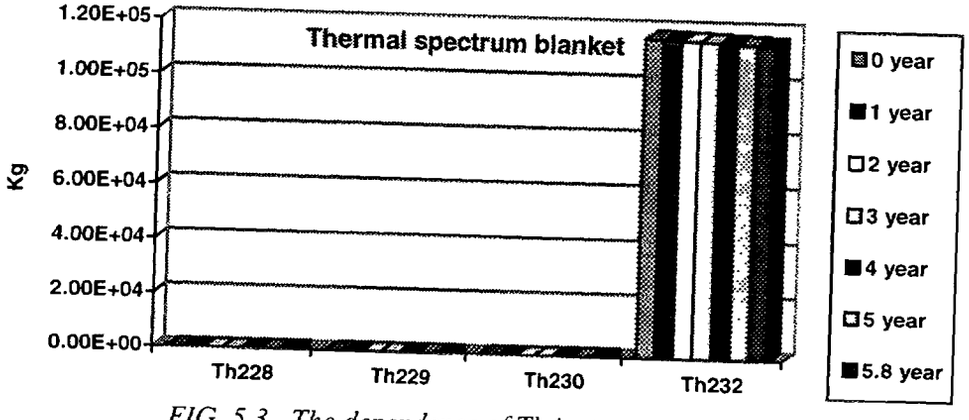

FIG. 5.3. The dependence of Th isotopes masses (kg) on time

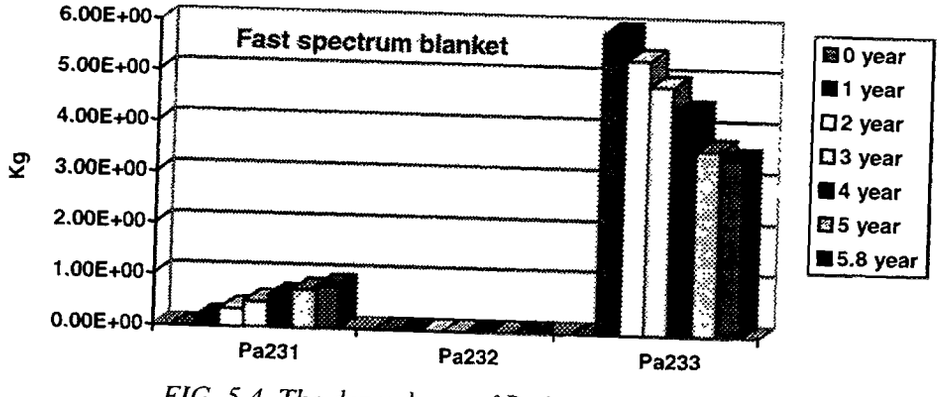

FIG. 5.4 The dependence of Pa isotopes masses (kg) on time.

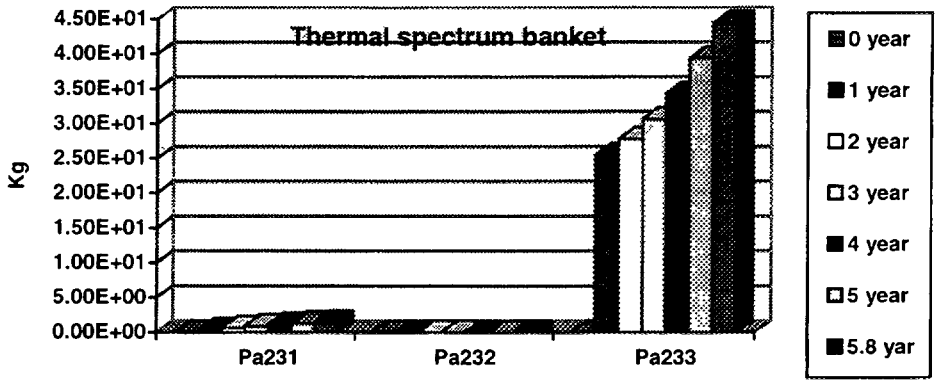

FIG 5.5 The depenence of Pa isotopes masses (kg) on time.

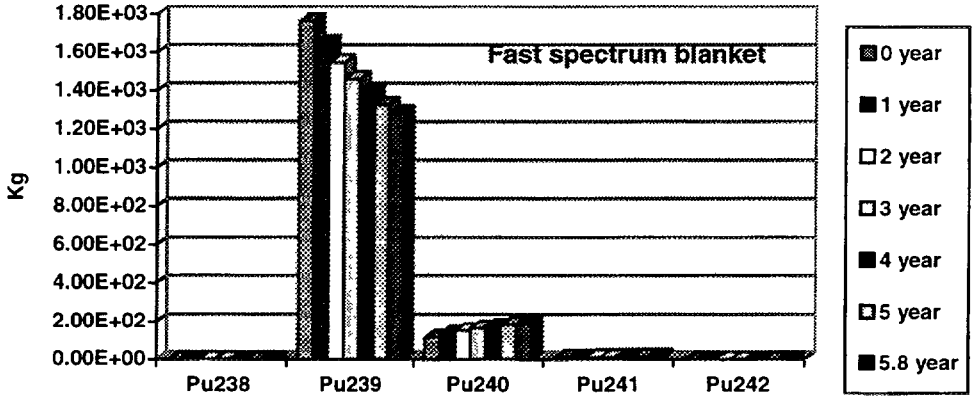

FIG. 5.6 The dependence of Pu isotopes masses (kg) on time.

TABLE XIII. ISOTOPES MASSES (KG) DEPENDENCE ON TIME IN F-BLANKET, T-BLANKET AND TOTAL IN THE SYSTEM

Time (y)	0.0		2.0		4.0		5.8	
	F-bl	T-bl	F-bl	T-bl	F-bl	T-bl	F-bl	T-bl
Th228	0.0	0.0	9.58-6	2.76-4	4.03-5	1.78-3	8.70-5	4.54-3
Th229	0.0	0.0	4.04-04	1.62-03	1.50-3	6.33-3	2.89-3	1.25-2
Th230	0.0	0.0	9.28-06	6.91-05	6.08-05	5.82-04	1.49-4	1.84-3
Th232	6.50+3	1.16+5	6.38+3	1.16+5	6.29+3	1.15+5	6.23+3	1.15+5
Pa231	0.0	0.0	3.44-1	6.24-01	6.24-1	1.12+0	8.18-1	1.42+0
Pa232	0.0	0.0	2.75-5	3.18-4	4.17-5	7.45-4	4.25-5	1.23-3
Pa233	0.0	0.0	5.38+0	2.78+1	4.40+0	3.43+1	3.47+0	4.45+1
U232	0.0	0.0	7.15-3	5.80-2	2.36-2	2.46-1	4.05-2	5.41-1
U233	0.0	0.0	9.65+1	4.10+2	1.69+2	8.05+2	2.15+2	1.11+3
U234	0.0	0.0	9.94-1	8.29+0	2.79+0	3.17+1	4.45+0	7.00+1
U235	0.0	0.0	1.29-2	3.22-1	6.29-2	2.54+0	1.30-1	8.24+0
U236	0.0	0.0	1.02-4	3.43-3	9.03-4	6.32-2	2.45-3	3.66-1
U237	0.0	0.0	3.60-8	2.30-06	2.69-07	5.00-5	5.87-7	3.31-4
U238	0.0	0.0	9.36-9	9.41-7	2.70-7	7.67-5	1.26-6	1.05-3
Np237	0.0	0.0	6.26-7	3.32-5	1.03-5	1.28-3	3.68-5	1.07-2
Np239	0.0	0.0	6.82-13	1.22-10	1.65-11	1.13-08	6.08-11	1.72-7
Pu238	0.0	0.0	2.31-2	9.95-1	1.08-1	1.00+1	2.19-01	3.14+1
Pu239	1.76+3	5.53+3	1.55+3	3.46+3	1.39+3	1.74+03	1.28+3	6.83+2
Pu240	1.16+2	3.56+2	1.51+2	7.48+2	1.75+2	8.40+2	1.89+2	6.81+2
Pu241	9.49	2.98+1	1.13+1	2.98+2	1.29+1	5.11+2	1.39+1	5.27+2
Pu242	0.0	0.0	2.30-1	1.76+1	4.44-1	7.88+1	6.07-1	1.78+2
Am241	0.0	0.0	9.52-1	1.32+1	1.99+0	3.84+1	2.99+0	5.11+1
Am242	0.0	0.0	7.45-3	8.19-3	2.55-2	3.36-2	4.58-2	4.63-2
Am243	0.0	0.0	4.33-3	8.87-1	1.41-2	7.60+0	2.43-2	2.46+1
Cm242	0.0	0.0	1.88-2	1.14+0	3.95-2	5.96+0	4.98-2	1.30+1
Cm243	0.0	0.0	1.55-4	8.29-3	6.22-4	8.98-2	1.08-3	3.01-1
Cm244	0.0	0.0	9.14-5	7.23-2	5.12-4	1.25+0	1.10-3	6.29+0
Cm245	0.0	0.0	1.05-6	1.18-03	1.06-5	3.72-2	2.99-5	2.34-1
Cm246	0.0	0.0	3.68-9	1.63-05	6.84-8	1.42-3	2.56-7	1.91-2
Cm247	0.0	0.0	0.0	5.21-8	0.0	8.88-6	2.16-9	1.72-4
Cm248	0.0	0.0	0.0	0.0	0.0	1.45-7	0.0	4.70-6

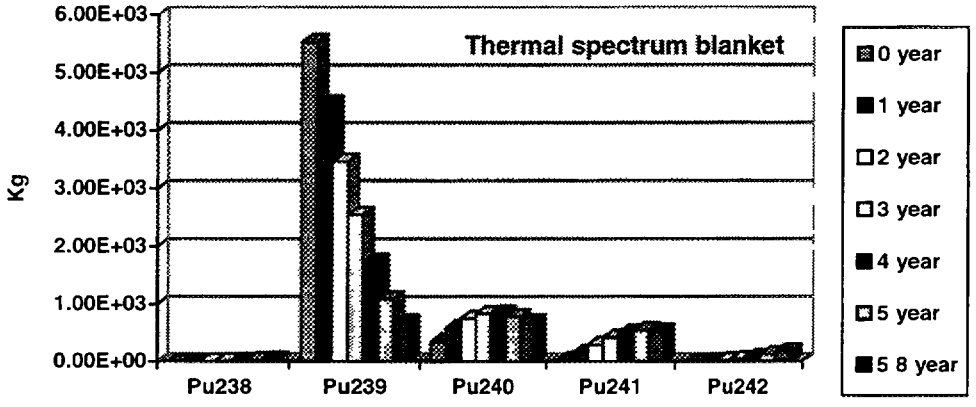

FIG 5 7 The dependence of Pu isotopes masses (kg) on time

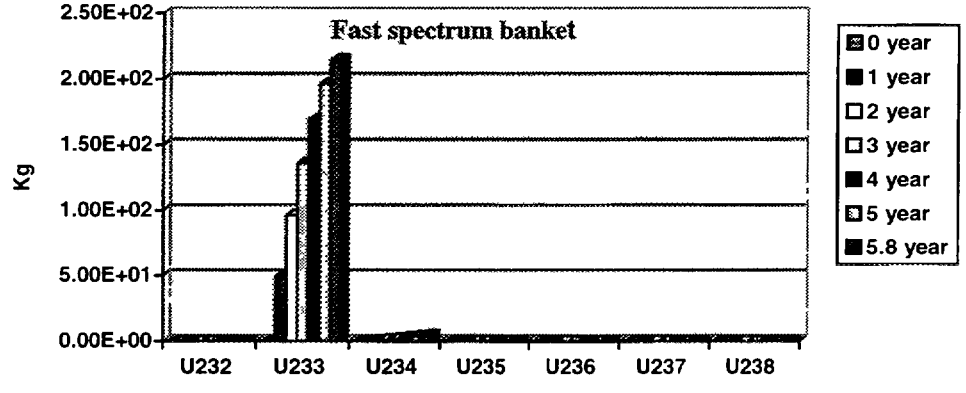

FIG 5 8 The dependence of U isotopes masses (kg) on time

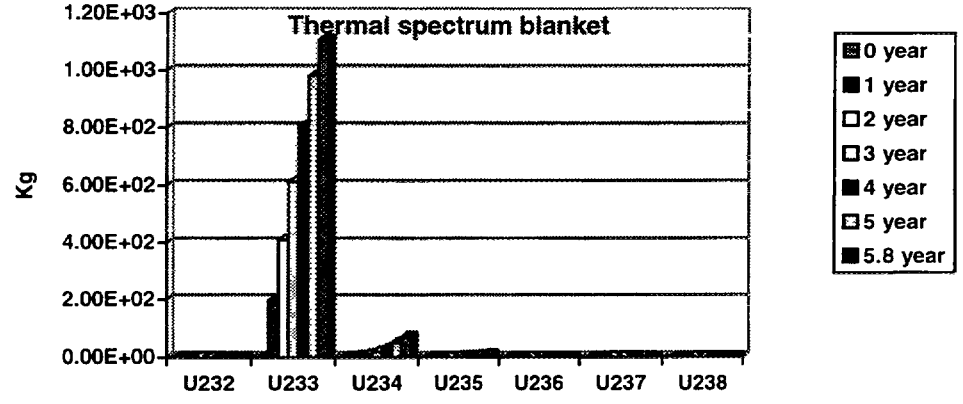

FIG 5 9 The dependence of U isotopes masses (kg) on time

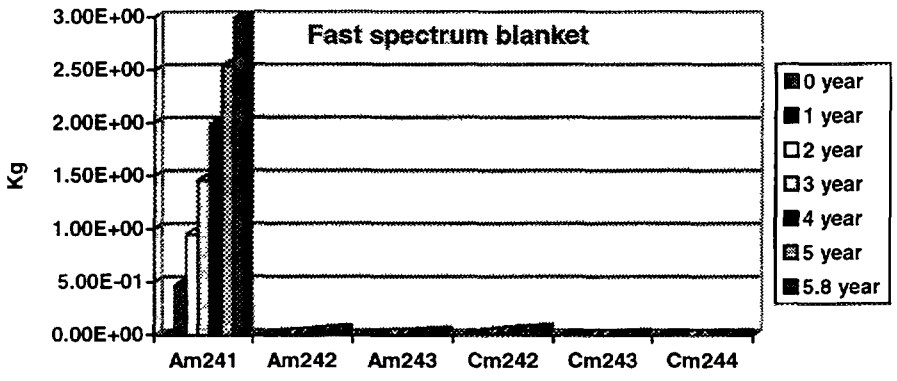

FIG. 5.10 The dependence of Am and Cm isotopes masses (kg) on time.

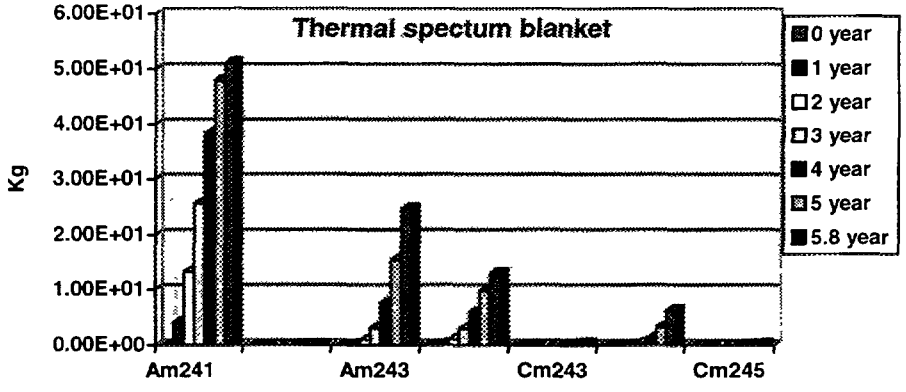

FIG. 5.11 The dependence of Am and Cm isotopes masses (kg) on time.

TABLE XIV. INITIAL AND FINAL ISOTOPES MASSES (KG) FOR 5.8 YEARS BURN-UP PERIOD

	Initial		Final		Difference		
	F-bl.	T-bl.	F-bl.	T-bl.	F-bl.	T-bl.	Total
PU238	0	0	0.22	31.4	0.22	31.4	31.62
PU239	1727	5528.5	1283.1	683.1	-478.3	-4845	-323.7
PU240	111	356.4	189.4	680.7	72.63	324.3	396.9 .
PU241	9.3	29.8	13.9	527.4	4.42	497.6	502.
PU242	0	0	0.61	177.6	0.61	177.6	178.2
Th232	6497	116400	6226.2	114650	-270.7	-1750	-2020.7
Pa233			3.5	44.5	3.5	44.5	48
U232			4.05-2	0.5	4.05-2	0.5	0.5
U233			214.4	1106.6	214.4	1106.6	1321
U234			4.5	70.0	4.5	70.0	74.5
U235			0.13	8.24	0.13	8.24	8.4
U236			2.5-3	0.37	2.5-3	0.37	0.37
U237			5.9-7	3.3-4	5.9-7	3.3-4	3.3-4

TABLE XIV (Cont.)

U238	1.3-6	1.1-3	.3-6	1.1-3	1.1-3
Np7	3.7-5	1.1-2	3.7-5	1.1-2	1.1-2
Np9	6.1-11	1.7-7	6.1-11	1.7-7	1.7-7
Am1	2.99	51.1	2.99	51.1	54.1
Am3	2.4-2	2.6	2.4-2	2.6	2.6
Cm3	1.1-3	0.30	1.1-3	0.30	0.3
Cm4	1.1-3	6.3	1.1-3	6.3	6.3
Cm5	3.0-5	0.2	3.0-5	0.2	0.2
Cm6	2.6-7	0.02	2.6-7	0.02	0.02
Cm7	2.2-9	1.7-4	2.2-9	1.7-4	1.7-4
Cm8	1.7-11	4.7-6	1.7-11	4.7-6	4.7-6

D.4.1.5.2.3. Case 2. Simulation of burn-up during 5.5 years, with Tc99 as control reactivity element, F-blanket size and power increased twice - 600 MW (36 fuel assemblies).

Total mass of heavy nuclides : 127430 kg.

Main results are presented in Table XV and Fig. 5. 12

TABLE XV. INITIAL AND FINAL ISOTOPES MASSES (KG) FOR 5.5YEARS BURN-UP PERIOD

	Initial		Final		Difference	
	F-bl.	T-bl.	F-bl.	T-bl.	F-bl.	T-bl.
Pu238	0	0	0.5	29.2	0.5	29.2
Pu239	2748.3	5520.6	1817.9	732.7	-930.4	-4787.9
Pu240	177.0	355.7	332.3	678.2	155.3	322.5
Pu241	1.5	29.8	26.5	540.4	25.0	510.6
Pu242	0	0	1.5	172.3	1.5	172.3
Th232	13023	116230	12297	114520	-726.	-1710
Pa233			10.6	45.3	10.6	45.3
U232			0.01	0.5	0.01	0.5
U233			541.8	1092.5	541.8	1092.5
U234			15.5	68.3	15.5	68.3
U235			0. 6	8.1	0. 6	8.1
U236			0.02	0.3	0.02	0.3
U237			6.0-06	3.3-04	6.0-06	3.3-04
U238			1.6-05	1.0-04	1.6-05	1.0-04
Np237			3.3-04	1.0E-02	3.3-04	1.0E-02
Np239			1.3-09	1.8-07	1.3-09	1.8-07
Am241			4.9	59.9	4.9	59.9
Am243			6.9-02	23.9	6.9-02	23.9
Cm243			3.3-03	0.3	3.3-03	0.3
Cm244			4.2-03	6.1	4.2-03	6.1
Cm245			1.5-04	0.2	1.5-04	0.2
Cm246			1.8-06	1.8-02	1.8-06	1.8-02
Cm247			2.0-08	1.6-04	2.0-08	1.6-04
Cm248			2.3-10	4.4-06	2.3-10	4.4-06

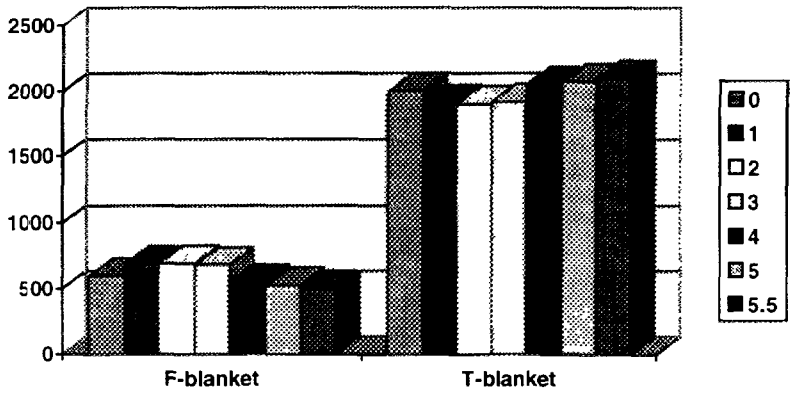

FIG. 5.12 Time dependence of power in F- and T-blankets (total power 2600 MW).

During 30 years period of operation at full power 31.2 t of Pu239 is destroyed and 32.8 t of WG Pu incinerated - converted into Pu of different composition , other heavy nuclides and fission fragments; 13.3 of Th are involved into fuel cycle with of 9.2 t of U233 accumulated and 7.9 t spent in the installation for power production.

D.4.1.5.2.4. Case 3. U-Th fuel cycle in thermal blanket (fuel cycle 1.5 years)

U233 accumulated in Pu-Th-U fuel cycle (about 4 t total during 30 years) may be used in the same installation for power production in U233-Th fuel cycle with low consumption of fissile material. The results of calculations for lower enrichment (1.46%) are presented in Table XVI.

TABLE XVI. INITIAL AND FINAL ISOTOPES MASSES (KG) FOR 1.5 YEARS BURN-UP PERIOD, CASE 3.

	Initial		Final		Difference	
	F-blanket	T-blanket	F-blanket	T-blanket	T-blanket	F-blanket
Th228			4.9-06	4.0-04	4.9-06	4.0-04
Th229			2.4-04	1.1-02	2.4-04	1.1-02
Th230			4.4-06	1.1-03	4.4-06	1.1-03
Th232	6497.4	128800	6406.9	127530	-90.7	- 1270
Pa231			0.3	4.5-01	0.3	4.5-01
Pa232			2.2-05	6.9-04	2.2-05	6.9-04
Pa233			5.9	90.9	5.9	90.9
U232			4.1-03	0.1	4.1-03	0.1
U233		1903.7	77.0	1787.2	77.0	-116.5
U234			0.7	127.5	0.7	127.5
U235			6.9-03	10.2	6.9-03	10.2
U236			4.4-05	0.4	4.4-05	0.4
U237			1.7-08	3.8-04	1.7-08	3.8-04

TABLE XVI (Cont.)

Np237		2.1-07	5.1-03	2.1-07	5.1-03
Np239		2.0-13	6.2-08	2.0-13	6.2-08
Pu238		1.12-02	3.3-12	1.12-02	3.3-12
Pu239	1726.7	1558.3	1.3-06	-168.4	1.3-06
Pu240	111.2	138.7	1.2-07	27.5	1.2-07
Pu241	9.3	10.6	1.7-08	1.3	1.7-08
Pu242		0.2	1.0-09	0.2	1.0-09
Am241		0.7	1.2-10	0.7	1.2-10
Am242		4.4-03	4.5-14	4.4-03	4.5-14
Am243		2.4-03	1.8-11	2.4-03	1.8-11
Cm242		1.3-02	1.5-11	1.3-02	1.5-11
Cm243		8.3-05	5.7-14	8.3-05	5.7-14
Cm244		3.8-05	6.6-13	3.8-05	6.6-13
Cm245		3.5-07	4.4-15	3.5-07	4.4-15
Cm246		9.5-10	1.3-16	9.5-10	1.3-16
Cm247		2.7-12	1.9-19	2.7-12	1.9-19
Cm248		7.0-15	1.7-21	7.0-15	1.7-21
Bk249		1.2-17	1.0-23	1.2-17	1.0-23
Cf250		3.6-20	1.3-23	3.6-20	1.3-23
Cf251		1.2-22	7.2-24	1.2-22	7.2-24
Cf252		1.7-24	1.5-22	1.7-24	1.5-22

The results for 2 enrichments U233/(U233+Th232) % : time of cycle, burn-up (GWt-d/t), breeding ratio BR and conversion ratio CR:

BR =[U233+U235+(Pa233→U233)] (EOC)/ U233 (BOC)

CR= BR+ ΔTc99/ U233 (BOC)

ΔTc99 - the number of nuclei of Tc99 transmuted, together with consumption (-) and accumulation (+) of nuclides (kg) during 30 years of operation are presented in Table XVII. For lower enrichment 1.46% and rather short burn-up (8.6 GWt, 1.5 years) the installation (T-blanket) is close to Th breeder. For higher enrichment 1.74% and higher burn-up (16.7 GWt-d/t, 2.5 years) the consumption of U233 is an order lower (about 3 t) than is necessary for the production of power during 30 years.

TABLE XVII. MAIN PARAMETERS FOR TH-U233 FUEL CYCLE; ACCUMULATION (+) AND DESTRUCTION (-) OF MAIN ISOTOPES (KG) DURING 30 YEARS OF OPERATION

Enrichment %	1.46	1.74
Time of cycle , a	1.5	2.5
Burn-up, GWt-d/t	8.6	16.7
CR	1.025	0.93
BR	0.992	0.88
Th232	-25000	-21480
U232	2	2.4
U233	-186	-2800
U234	2516	2255

TABLE XVII(Cont.)

U234	2516	2255
U235	201	270
U236	8.3	20.4
Np237	0.1	0.4
Tc99	-535	-540

D.4.1.5.2.5.Case 4. 2nd cycle with Pu , Am and Cm nuclides from T-blanket of after 1st cycle re-loaded into F-blanket, T-blanket composition the came as in Case 1.

Total mass of heavy nuclides =127200 kg. The results are presented in Table XVIII and Fig. 5.13

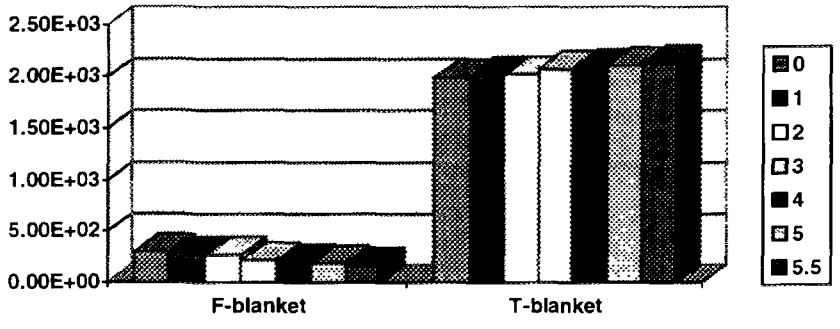

FIG. 5.13 Power dependence on time in F-blanket and T-blanket (total 2300 MW).

TABLE XVIII. INITIAL AND FINAL ISOTOPES MASSES (KG) FOR 5.5 YEARS BURN-UP PERIOD, CASE 4.

	Initial		Final		Difference	
	F-bl.	T-bl.	F-bl.	T-bl.	F-bl.	T-bl.
Th228			4.3-05	4.4-03	4.3-05	4.4-03
Th229			1.3-03	1.2-02	1.3-03	1.2-02
Th230			7.8-05	1.8-03	7.8-05	1.8-03
Th232	2958.2	116400	2839.0	114660	-119.2	-1740
Pa231			3.4-01	1.4	3.4-01	1.4
Pa232			1.89-5	1.3-03	1.89-05	1.3-03
Pa233			1.4	45.1	1.4	45.1
U232	0		1.7-02	5.4-01	1.7-02	5.4-01
U233	0		95.2	1102.7	95.2	1102.7
U234	0		3.7	69.7	3.7	69.7
U235	0		1.1-01	8.2	1.1-01	8.2
U236	0		2.2-03	3.6-01	2.2-03	3.6-01
U237	0		4.7-07	3.3-04	4.7-07	3.3-04
U238	0		1.2-06	1.0-03	1.2-06	1.0-03
Np237			3.3-05	1.1-02	3.3-05	1.1-02
Np239			5.4-11	1.7-07	5.4-11	1.7-07
Pu238	31.4		49.2	30.1	17.8	30.1

TABLE XVIII (Cont)

Pu239	682.9	5528.5	505.7	694.1	-177.2	-4834.4
Pu240	680.0	356.4	637.6	685.1	-42.4	328.7
Pu241	527.2	29.8	310.8	529.7	-216.5	499.9
Pu242	177.5		182.6	177.3	5.1	177.3
Am241	51.1		136.3	49.9	85.2	49.9
Am242			2.8	4.5-02	2.8	4.5-02
Am243	24.6		30.9	23.3	6.3	23.3
Cm242	13.0		2.4	12.8	-10.8	12.8
Cm243			1.5-01	3.0-01	1.5-01	3.0-01
Cm244	6.3		7.5	5.9	1.2	5.9
Cm245			6.3-01	2.2-01	6.3-01	2.2-01
Cm246			1.3-02	1.8-02	1.3-02	1.8-02
Cm247			2.0-04	1.6-04	2.0-04	1.6-04
Cm248			2.8-06	4.4-06	2.8-06	4.4-06
Bk249			1.2-08	3.8-08	1.2-08	3.8-08
Cf250			1.6-10	7.5-09	1.6-10	7.5-09
Cf251			2.3-12	2.4-09	2.3-12	2.4-09
Cf252			1.9-14	9.0-10	1.9-14	9.0-10

D.4.1.5.3 Comparison of 4 Cases (for fuel cycles 5.8 years, 5.5 years, 1.5 years and 5.5 years).

Comparison of results for build-up or destruction of materials -in Figs 5.14 - 5.21

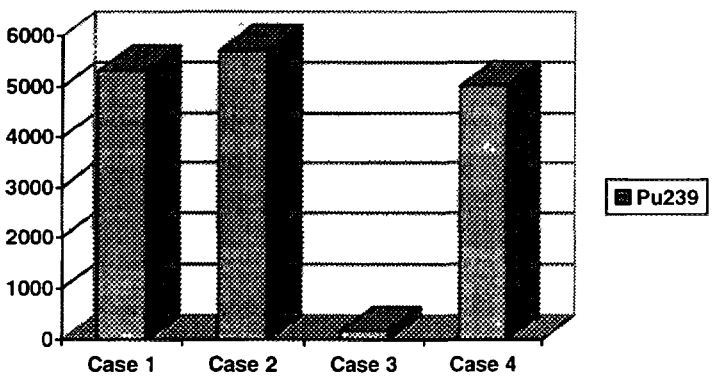

FIG. 5.14 Masses (kg) of eliminated Pu239 for 4 cases

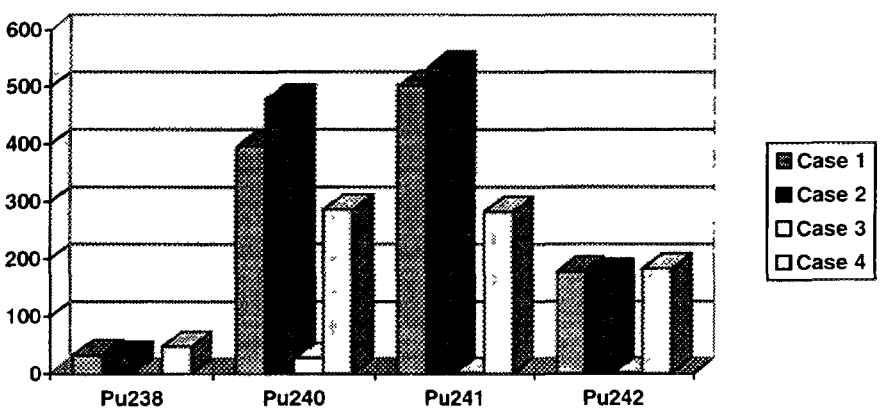

FIG. 5.15 Masses of other Pu isotopes accumulated or eliminated for 4 cases

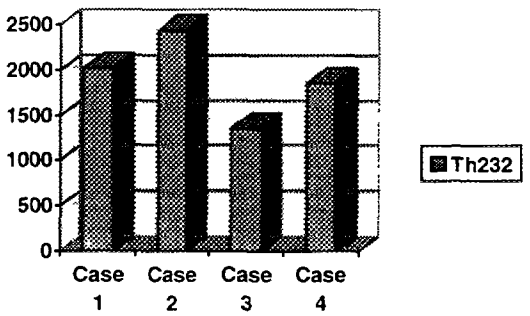

FIG. 5.16 Masses of Th232, converted to Pa and U isotopes

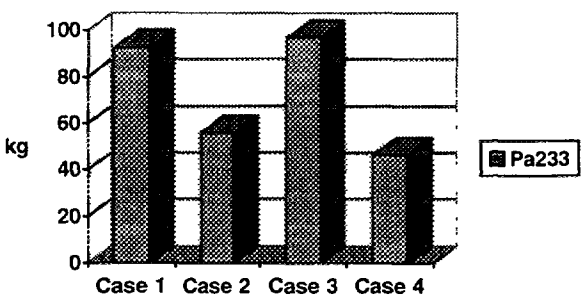

FIG 5.17 Build up (kg) of Pa233 (decays into U233 after unloading)

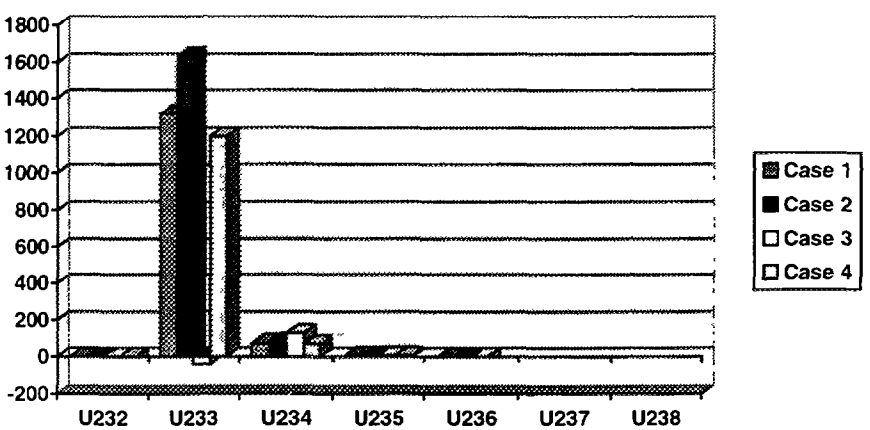

FIG. 5.18 Masses of U isotopes (kg) produced in 4 cases.

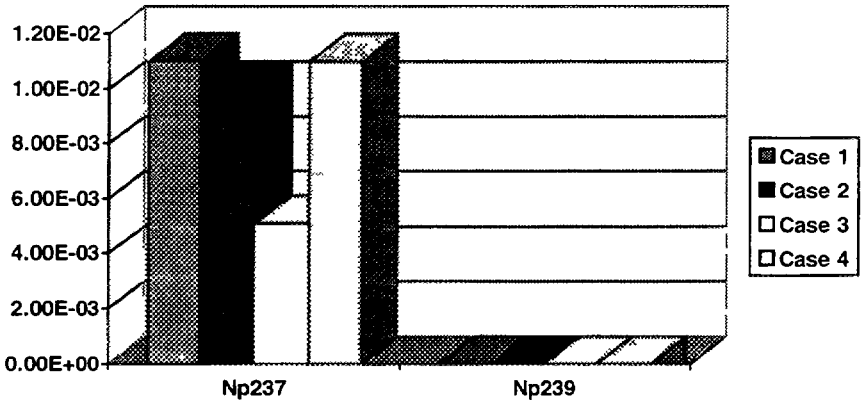

FIG 5 19 Masses of Np isotopes produced in 4 cases

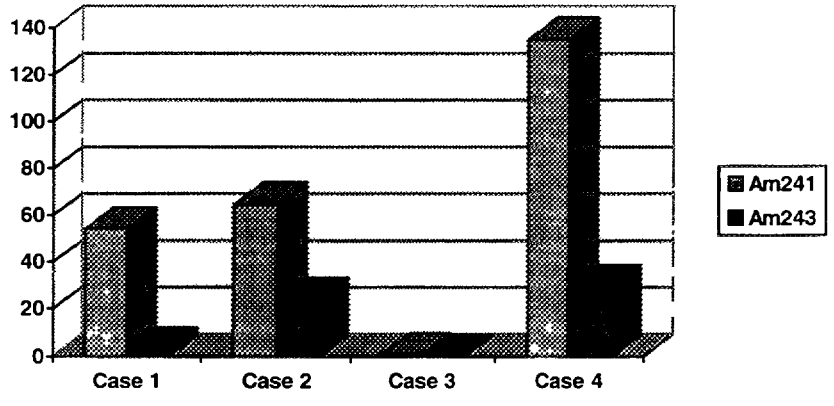

FIG 5 20 Production (kg) of Am isotopes for 4 cases

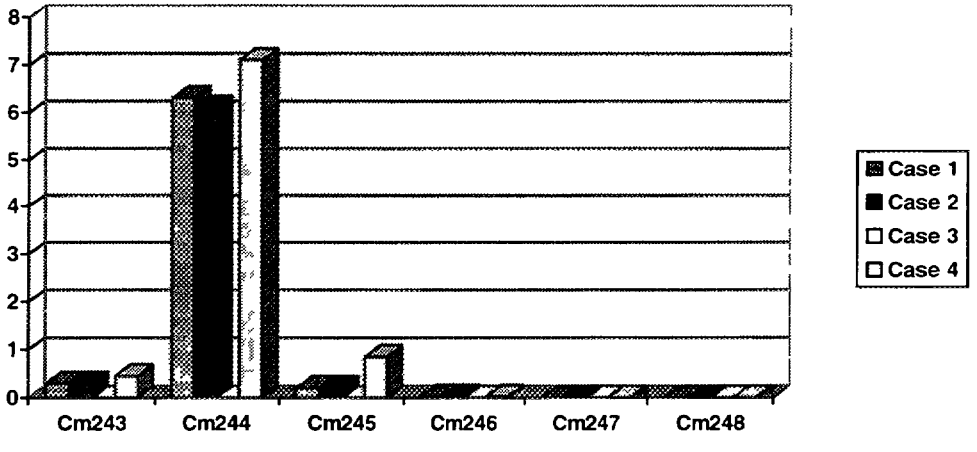

FIG 5 21 Accumulation of Cm isotopes for 4 cases

D.4.1.5.4 Physical Properties (Case 1).

D 4 1 5 4 1 Thermal Neutron Flux

Neutron flux Φ at the beginning of cycle is estimated as

$$\Phi \approx 0.5 * 10^{13} \text{ 1/cm}^2 \text{ sec}$$

By the end of fuel cycle (~ 6 years) fissile material mass decreases so that:

$$\Phi \approx 1.6 * 10^{13} \text{ 1/cm}^2 \text{ sec}$$

D.4.1.5.4.2. Capture and Decay of Pa233

Neutron capture by intermediate element Pa233 in the breeding process (conversion of Th232 into U233) results in a loss of neutron in the competition between neutron capture and radioactive decay and is proportional to neutron flux that brings about the loss of reactivity and consequently a decrease of breeding ratio. The loss of reactivity is estimated by the value:

$$dK/K \text{ (Pa233)} = - 0.13\%$$

After shut-down the of ABC F-T system the decay of Pa233 results in an increase of U233 concentration and consequently in reactivity increase. This effect was estimated for the end of fuel cycle:

$$dK/K(Pa233 \rightarrow U233) = + 0.45 \% \ (K=0.99 \rightarrow K=0.9945)$$

This low value may be explained by low neutron flux in T-blanket (In E-A system [1] a similar effect is estimated to be about 2%). It should be noted that multiplication factor K defined as the ratio :

[number of secondary neutrons emitted in fission] / [number of secondary neutrons emitted in fission + number of neutrons produced by external source]

for subcritical system is different from eigen-value K_e (that determines the properties of the system with external sources switched off). The corresponding values were:

K_e=0.9710 (instead of K=0.99); K_e=(Pa233→U233) =0.9777

As a matter of fact internal properties of the system and consequently safety conditions are governed by K_e that is less than K. In this sense the system remains in a deeper sub-critical state even after decay of Pa233.

D.4.1.5.4.3. Doppler reactivity effect.

Doppler reactivity effect was estimated by calculation of T-blanket cell for two different fuel temperatures - 800 K and 900 K. The difference in reactivity per 1 °C - Doppler reactivity effect is equal: dK/dT = -7.8 E-6 1/ °

D.4.1.5.4.4. Liquid Pb-Bi Void Reactivity Effect

Of much importance is the negativity of Pb-Bi void effect. Calculations with Pb-Bi density decreased twice led to the result:

$$dK/K_{void} = - 0.01\% / 1\% \text{ of void}$$

Loss of a half of Pb-Bi liquid (substitution for a void) leads to the loss of reactivity 0.5%.

D.4.1.5.4.5. Moderator Density (with Tc99 Dissolved) Reactivity Effects

The decrease of moderator density results in a reactivity effect that depends on the concentration of Tc99 dissolved in heavy water. As was estimated reactivity effect is negative or zero for weight concentration of Tc99 about 10 g/l. If this limit is exceeded the other ways of reactivity compensation should be applied : burn-able poisons - Gd for short period processes; Am241 (thermal capture cross-section 600 b, resonance integral 1500 b) and Am243 - for long periods; control rods; continual reloading at full or decreased level of power (like in CANDU reactors).

D.4.1.5.4.6. The Property of One-Directional Neutron Coupling

This property may be defined as having two features: 1) weak influence of multiplication capabilities in T-blanket on the number of secondary neutrons born in fission in F-blanket, 2)weak influence of physical properties changes in T-blanket on the reactivity of total system.

Calculations led to the following results:

$$1) \quad [\, d(nF)/\, nF)]_{F\text{-blanket}} \;/\; [\, d(nF)/\, nF)]_{T\text{-blanket}} = 0.005$$

$$2) \quad dK/dConc(Pu239) = 0.033\% \,/\, 1\%.$$

For a system without one-directional coupling (fission material removed from F-blanket and the same level of sub-criticality reached by an increase of initial Pu239 concentration ~1.5 times), the 2nd value occurred to be an order higher : 0.33%/ 1%. This means that total system may be operated at the level of sub-criticality with K=0.99 and have the same safety conditions as a system without this property with much deeper sub-criticality (K around 0.9-0.95) and consequently the system proposed here needs much lower (5-10 times) proton current of accelerator beam.

D.4.1.6. MONITORING AND CONTROLLING OF ADS INSTALLATION

In order to provide optimal and safe routine operation of the electro-nuclear installation, it is necessary to conserve all elements of traditional systems of controlling and protection of critical installation and to add to them some necessary specific elements to create by this a quite new system for monitoring and controlling the electro-nuclear installation.

The functions of quick response (with response time ~ 1 ms) will be implemented by a subsystem of interruption of the beam in the very beginning of the accelerator (after injector or/and the very first accelerating sections). This will allow to stop the beam of accelerator with practically any given rate of reliability.

The blanket must be equipped with well developed structures of operating heads of controlling and monitoring in order to provide:

- reliable shut-down of the blanket for periods of reloading or long stops;

-possibilities to flatten specific power production through the whole volume of the blanket to maintain satisfactory economical parameters of the installation.

Presence of a traditional subsystem of controlling and monitoring in the total system will allow to reach critical state of the installation (for specific experiments) and to rise significantly reliability of assessment of the level of subcriticality of the blanket.

But traditional system should be complemented with channels of continuous reactivity control. This system is based on analysis of back edge of a neutron pulse resulting due to time pause arising due to separation of H^- and H^+ beams as each type of accelerated beam irradiates its own blanket.

If this reactivity parameter falls out of the limits of a certain interval, the control system should correct the level of reactivity or to stop the whole NP installation by operating drives of the control system and by switching off the charged particles beam.

To guarantee the possibility to control power variations of the installation and to find out the reasons of these variations a special system capable to measure charged particle beam directly falling on the target is quite necessary.

D.4.1.7. FUEL CYCLE

The fuel cycle incorporates the operations of fresh oxide fuel manufacture for "fast" and "thermal" blanket zones, irradiation of finished fuels, cooling prior to reprocessing, chemical reprocessing of spent fuel and refabrication to produce a fresh fuel charge from fissionable materials recovered upon reprocessing with minor actinides (MA) included.

The fuel cycle does not directly involve operations of separation of short-lived transmutation products and conditioning of products of this type to chemical forms suited for the disposal, however, these operations are indispensable for the ecologically safe closure of the fuel cycle.

Fundamentally specific feature of the fuel cycle under discussion is the availability of two fissionable actinides (Pu-Th) in the primary charge and three ones (Pu-Th-U) in the spent fuel; Pu, Th and U being macrocomponents of the composition.

To-day there are no commercial or semi-commercial processes of both fabrication of Pu-Th oxide fuel and regeneration of Pu-Th-U compositions that are formed under irradiation. However, some fragments of such processes have been mastered adequately to form the process flow outline for the needed fuel cycle.

These main fragments cover:

- reprocessing U-Pu (discharged) fuel (Purex process and its versions);

- manufacture of mixed U-Pu oxide fuel (MOX);

- reprocessing Th-U (discharged) fuel (Thorex process, interim and their versions).

The above mentioned technological processes are basic ones in considering the fuel cycle route.

Fabrication of fuel. The fuel fabrication may be based on two main technologies, namely, dry blending of oxides and chemical coprecipitation of fuel components followed by processing the precipitate to prepare mixed oxide.

Dry blending of oxides. The process involves operations of blending Pu and Th oxides, briquetting, primary sintering, comminution with a binder (zink stearate), granulation, pellet pressing and sintering. The sintered pellets are checked for their geometric sizes, density, chemical composition and structure. Then, the operations of certifying pellet columns, fuel rod stacking, welding and tightness check-up are carried out.

The basic technology is the process used to fabricate U-Pu fuel for the complex "300" at the PU "Mayak".

The dry route can be considered to realizable for the primary charge of both "fast" and "thermal" blanket zones as well as for the refabrication of the thermal blanket charge. Problematic is the application of the dry route to the refabricated charge of "the fast" blanket that is to incorporate highly toxic oxides of Np, Am, Cm and long-lived fission products (e.g., Tc). The main obstacle is the available dust forming operations and problems relevant to the staff protection and gas clean-up.

Chemical coprecipitation of elements. Mostly mastered are carbonate and ammonia processes developed for the MOX fuel fabrication. For the fuel cycle under consideration the ammonia process is preferable. Ammonium hydroxide is a more universal precipitant and can be used for fabrication of both the primary charge of "fast" and "thermal" blanket zones and the refabricated charges containing oxides of MA and fission products.

Initial solution contains nitrates of Pu and Th in the specified ratio (the primary charge) and additionally nitrates of MA (the refabricated charge). Pu is stabilized in the tetravalent state. Metal hydroxides are precipitated with ammonia hydroxide in presence of surface-active substances as shape formers. The precipitate that is adequately flocculated granules is readily separable from a mother solution. After washing and drying the precipitate is calcined in an inert environment to form a homogenized oxide mixture. Pellet pressing and subsequent operations are the same as are used for the dry route of fuel fabrication. Incorporation of long-lived fission products into a fuel composition requires the process to be additionally mastered (e.g., Tc-99 may be also incorporated into the composition as TcO_2, however, the stage remains to be determined at which Tc can be added, Tc (IV) stabilization, precipitated and blended).

The basic technology is the "Granat" process also developed for the MOX fuel production at the complex "300", PU "Mayak".

Fuel irradiation. On one hand, duration of irradiation is governed by nuclear transmutation and, on the other, by life-time of oxide fuel rods. Real time of a fuel rod staying in "fast" and "thermal" blanket zones is 6 to 8 years.

Interim storage of fuel. The time of the interim storage of fuel prior to reprocessing is summed up of the time of the at-reactor storage (immediately after the discharge) and the time of holding in a cooling pond at a reprocessing facility. Storage condition differs in intensity of heat removal. If the spent fuel is not to be shipped transmutation reactor and reprocessing facility are sited at the same utility. A single special schedule of interim storage is feasible. The total time of interim storage must not be less than 3 years.

Spent fuel reprocessing. The process flow outline for spent fuel reprocessing integrates the most rational elements of known extraction routs (Purex, Impurex, Thorex), involving also additional operations such as evaporation and crystallization.

Since in both "fast" and "thermal" blanket zones new fuel - U-233 is generated and burnt, despite different rations of the main components (Th, Pu and U) in the spent fuel of the "fast" and "thermal" blanket zones it is advisable to co-reprocess it.

After removal of structural components of a fuel assembly and mechanical chopping fuel rods the fuel is dissolved in nitric acid under the conditions close to those used for the dissolution of power reactor fuel rods. Adjustments are possible as small additive of fluorine ion to dissolving solution to accelerate dissolution of thorium oxide. Then the solution is isolated from cladding elements and goes for filtration and acidity adjustment for extraction reprocessing. Fuel rod cladding components are washed and transferred to a special tank and their subsequent handling may be different (disposal, decontamination etc.).

While dissolving non-dissolvable residue may be available; it mainly consists of intermetallic phases of Rh, Pd, Ru, Tc and Mo. Handling of undissolvable residue is a special operation of deep dissolution and storage.

The solution as conditioned to extraction reprocessing goes to the first extraction cycle the objective of which is to extract and purify Th, Pu and U from fission products. Separation of Pu from Th and U and preparation of the cycle products, namely, Pu and Th-U streams. An extractant is a standard solution of TBP (30% vol.) in a hydrocarbon dilutant; the apparatuses are commercially operated equipment of any type (mixer-settlers, centrifugal extractors, counter-current columns). The operations of the cycle are co-extraction of U, Pu and Th, washing of an extract to remove fission fragments, reductive stripping of Pu and removal of Pu from the cycle, co-stripping of Th and U regeneration of an extractant. As a reductant it is advisable to use no-salt forming reagents on the basis of hydrazine or U (IV) derivatives from the U regenerate.

Pu extracted from the head end cycle is sent to the refinement cycle. The refinement cycle structure is not discussed since similar operations are well known and are a constituent port of commercial facilities for power reactor spent fuel reprocessing. From the refinement cycle Pu as a Pu nitrate solution purified is directed to the operations of refabrication of a fuel charge for the "fast" blanket.

The Th-U co-product is evaporated at the evaporation ration of 8-12 and cooled for hydrated thorium nitrate to be crystallized. If it is necessary thorium nitrate is subjected to recrystallization, washing and sent to the operations of the fuel charge refabrication for both "fast" and "thermal" blankets.

The mother solution from thorium nitrate crystallization containing U and Th (with U-Th increased proportionally to the evaporation ratio) is adjusted in terms of the HNO_3 content and reprocessed in the U-Th cycle with relatively low efficiency. The extractant of the cycle is similar to that of the head end cycle. The cycle operates under supercritical conditions with a partial discard of Th to the cycle raffinate since the objective of the cycle is to produce pure U product. The washing solutions of the cycle also containing thorium join the raffinate and the joint flow is transferred for reprocessing in the head (Th-Pu-U) end cycle. The purified U product of the cycle is used as a "plutonium substituting" fuel in the thermal blanket or is reprocessed to oxide (by the known processes and is stock-piled).

Thus, the products of chemical reprocessing spent fuel of "fast" and "thermal" blanket zones are purified nitrated of Pu, Th and U that are suited for refabrication into fuel.

Unburnt MA and fission products go to the high activity raffinate of the head end cycle. The raffinate is evaporated to recover nitric acid that is recycled.

The presented basic process flow outline does not involve operations of partitioning high-activity waste of the cycle and isolating the MA fraction to be incorporated into the fuel composition of a "fast" blanket zone. This operation is to be carried out jointly both for the major source of MA, namely, high-activity waste of power reactor spent fuel reprocessing and the waste of transmutation reactor fuel reprocessing. The products of this co-reprocessing are a MA stream arriving at the refabrication of "fast" blanket zone fuel and a stream of short- and medium-lived nuclides purified from long-lived nuclides; they are sent for the preparation of immobilizable forms (glass, mineral-like materials etc.) to be disposed of.

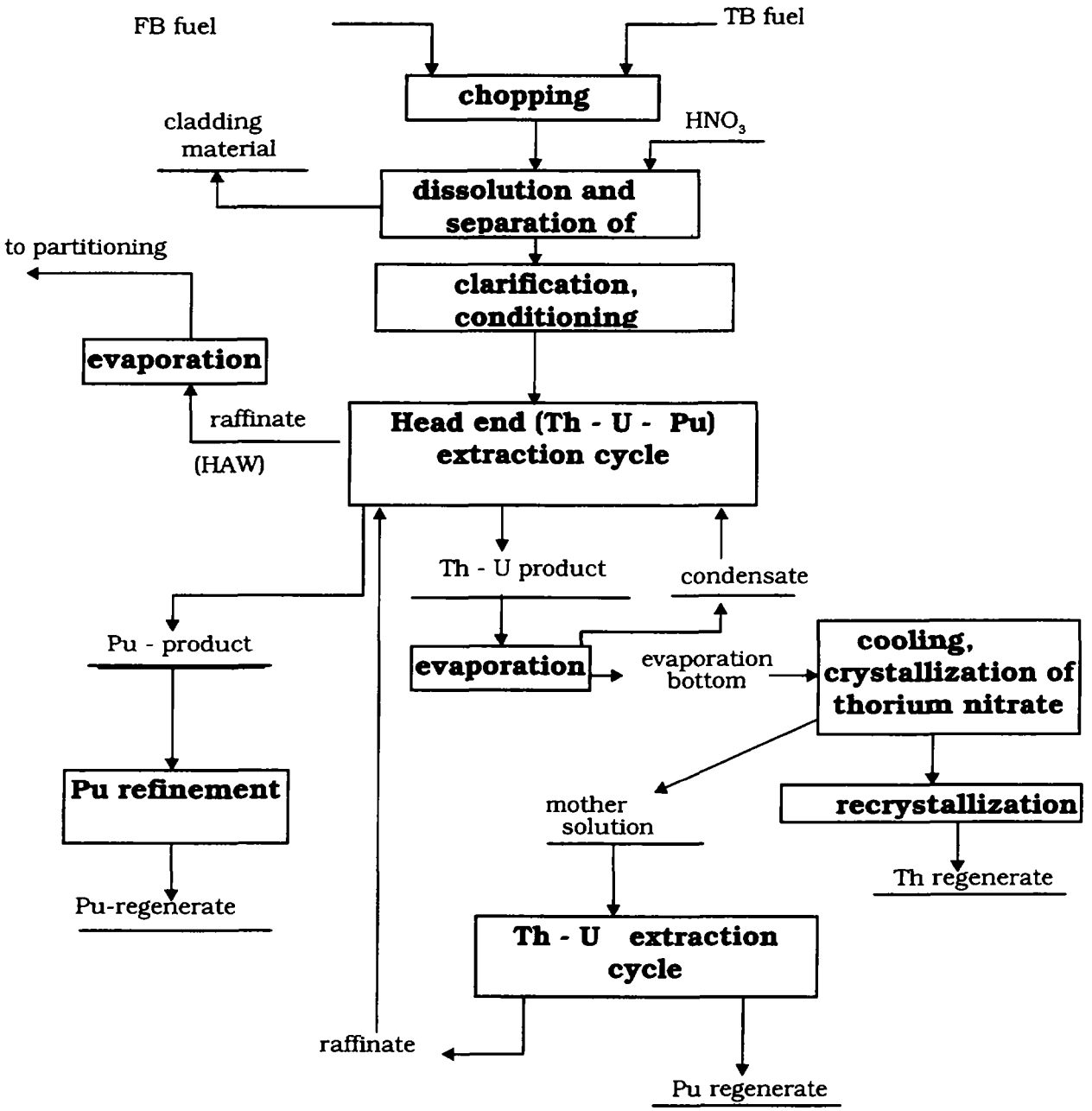

FIG. 7.1 Basic process flow outline of "fast" and "thermal" blanket spent fuel reprocessing.

D.4.1.8. WATER-CHEMICAL REGIME OF HEAVY-WATER BLANKET ZONE

The main parameters of the blanket of ADS are presented in Tables XVIII and XIX.

D.4.1.8.1. Water-chemical conditions of heavy-water loops

Water-chemical conditions are composited on basis of quality standards for heavy water medium, worked for all exploitation conditions (start of operation, stationary and transition states). Correctionless, near neutral water-chemical conditions are adopted in coolant and moderator loops. Quality standards are presented in Table XVIII.

In order to check characteristics of water medium it is necessary to find out: concentration of deuterium dissolved in water, radioactivity of water, stipulated by tritium and concentration of deuterium and oxygen in gaseous volumes of technological and auxiliary equipment.

D.4.1.8.2. Providing of settled water-chemical conditions

The rate of bypass flow (part of water loop, directed to purification) is usually measured by rate of entrance component in the water; in our situation – by product of corrosion in count on iron [38].

Rate of bypass flow ("blow off") for above mentioned loops is calculated from the equation [39]:

$$W = q_i / C_\varepsilon * \eta \qquad (8.1)$$

W – bypass flow, $t*h^{-1}$;

q_i – rate of i - component entrance in water medium, $q*h^{-1}$;

C_ε – standardized concentration of i - component, $q*m^{-3}$;

η – efficiency of water purification plant; this coefficient may be in range 0.6÷0.8 for iron corrosion products (oxides).

Corrosion rate of stainless steel under routine conditions in the loops according to [40,41]:

$1*10^{-4}$ – for coolant loop; $0.2*10^{-4}$ – for moderator loop.

Share of stainless steel corrosion products released in water in insoluble form (crud) at these conditions usually is accepted equal 0.2.

Then for coolant: $q_{Fe}^{C} = 0.006q \times h^{-1}; W^{C} = 1.7m^{3}h^{-1}$

for moderator: $q_{Fe}^{m} = 0.014\ q*h^{-1}$; $W^{m} = 0.4\ m^{3}*h^{-1}$

Summary value of bypass flow will be equal $2.1 m^3*h^{-1}$ or 3% of the volume of water loops, that is considered technically and economically reasonable in practice of nuclear power plant operation. Bypass flow enters on special water purification plant, where after preliminary degassing it is passed through ion exchange columns.

D.4.1.8.3. Evaluation of deuterium stationary concentration in heavy water loops

Basic factors, that define absolute stationary values of radiolysis of molecular products, including deuterium, are specific dose rate of radiation and standard values of water quality. Maximum values of deuterium stationary concentration that may be reached in modern powerful nuclear plants with specific power up to several $MW*dm^{-3}$ of core, can't exceed $5*10^{-4}$ $mol*dm^{-3}$ [42]. Power density in coolant (in water volume of core) and moderator of ENP is, accordingly: 130 $kW*dm^{-3}$ and 3.5 $kW*dm^{-3}$.

Stationary equilibrium concentration of deuterium in heavy water loops of coolant and moderator may be calculated, in particular, by dependence [42]:

$$[D_2]_{st} = [D_2]_{st}^{max} * \sqrt{N_{sp}} / \sqrt{N_{sp}^{max}} \qquad (8.2)$$

$[D_2]_{st}^{max}$ –stationary concentration of deuterium at power density in the water 10^3kW*dm^{-3} ,mol*dm^{-3};

N_{sp} – specific power in considered water system, kW*dm^{-3};

N_{sp}^{max} – specific power in high loaded water system, 10^3 kW*dm^{-3}.

for coolant $[D^2]_{st}^{c} = 1.8*10^{-4}$mol*dm^{-3} = 4 ml s.t.p./ dm^3

for moderator $[D^2]_{st}^{m} = 3.5*10^{-5}$ mol*dm^{-3} = 0.6 ml s.t.p./dm^3

Reliability of these results is confirmed by criterion evaluation. Received values of stationary, equilibrium concentration for deuterium in stationary conditions of coolant and moderator loops are presented in Table XIX

Deuterium in heavy water media of coolant and moderator must be in solved state and volume liberation of gases is impossible.

D.4.1.8.4. System for removing and catalytic recombination of radiolytic gas mixtures

Gas liberation (in particular liberation of deuterium) may take place from bypass flow of ADS heavy water medium. Rate of deuterium liberation from bypass flow in gas loop is calculated from values of bypass flows and stationary, equilibrium concentrations of dissolved gases in each loop. It is preferably to use helium as bearer gas in gas loop (cavity) of ADS, because this gas have high permissible limit of explosive concentration and small volume for dilution of radiolytic gas.

Productivity of radiolytic gases "blow off" system is calculated on the base of adopted standards on content of deuterium or explosive mixture and on the rate of entrance of these gases in gas volume (cavity) by following dependence:

$$Q = 10^2 * q_{D_2} * K / [D_2]_N \qquad (8.3)$$

Q – productivity of "blow off" system, m^3*h^{-1};

q_{D_2} – rate of deuterium liberation from liquid phase, m^3*h^{-1};

$[D_2]_N$ – standardized limit of deuterium concentration in gas cavity, % mol;

K – coefficient of multiplicity (K=2 or 3).

As above mentioned, flow rate of water on "blow off" from coolant loop is 1.7 m^3*h^{-1}, from moderator loop – 0.4 m^3*h^{-1}, concentration of deuterium in water of these loops is found at a level 4 ml s.t.p./dm^3 and 0.6 ml s.t.p./dm^3, accordingly. It follows from these data that flow rate of deuterium from "blow off" water in helium cavity is 6.8 dm^3*h^{-1} for coolant loop and 0.24 dm^3*h^{-1} for moderator loop.

Local productivity of "blow off" is calculated from equation (8.3) and adopting value of multiplicity coefficient equal 3 and standard on content of deuterium in helium loop (cavity) ≤ 5.5 % vol. is 0.4 m^{3}h^{-1}. Taking into account necessity of "blow off" deuterium from gas volume of auxiliary equipment and from technology volumes, given productivity must be increased by one order and will be 4 m^3*h^{-1} in first approximation.

D.4.1.8.5. Detritization and deprotonization of ADS heavy water medium

Radioactivity of water caused by tritium in heavy water is related with value of mean neutron flux. Thus, at flux 10^{14} n*cm^{-2}*c^{-1}, radioactivity of tritium rises by $2.146*10^{11}$ Bk*dm^{-3} per a year. Equilibrium concentration of tritium will be reached in 20 years of plant operation and will be equal

58 $Ci*dm^{-3}$. Supporting of tritium concentration in heavy water at level 1.0 $Ci*dm^{-3}$ for reactors is considered as technically sufficient.

In this connection plant for detritization and deprotonization must be provided in the technological scheme. Isotopic concentration of heavy water in coolant and moderator loops must be supported of level not less than 99,5 % mol. D_2O and concentration of tritium (DTO) at the level $3.7*10^{10}$ $Bk*dm^{-3}$ by means of continuous purification of heavy water from accumulative admixtures (HDO and DTO) should be provided.

TABLE XVIII. TECHNICAL REGUIREMENTS TO QUALITY OF HEAVY WATER COOLANT AND MODERATOR

Index of heave water quality	Unit of measuring	Normal value	
		First filling and make-up water	Loop water
Specific conductivity	$Sm*m^{-1}$	$\leq 2*10^{-4}$	$\leq 4*10^{-4}$
Value of pD	unit pD	5.5÷6.5	5.0÷7.0
Chlorides concentration	$mg*dm^{-3}$	$\leq 5*10^{-2}$	$\leq 5*10^{-2}$
Concentration of corrosion product (account on iron)	$mg*dm^{-3}$	$\leq 5*10^{-2}$	$\leq 5*10^{-2}$
Isotopic concentration of D in water	% mol	≥ 99.75	≥ 99.0

TABLE XIX. STATIONARY CONCENTRATION OF DEUTERIUM IN LOOPS OF COOLANT AND MODERATOR

Heave water loop	Equilibrium, stationary concentration of deuterium in loop water, dm^3 s.t.p./dm^3	Limit of deuterium solubility at exploitation parameters, dm^3 s.t.p./dm^3
coolant	$4*10^{-3}$	6.0
moderator	$6*10^{-4}$	$2*10^{-2}$

D.4.1.9. ELECTRO-NUCLEAR NEUTRON GENERATOR - PROTOTYPE OF ADS INSTALLATION

Electro-nuclear neutron generator planned to be constructed uses the ITEP decommissioned reactor HWR for housing of subcritical blanket with fast and thermal (heavy water) neutron multiplication zones (Fig.9.1).

Be-target irradiated by proton is from ISTRA-36 linear accelerator is the source of fast neutron.

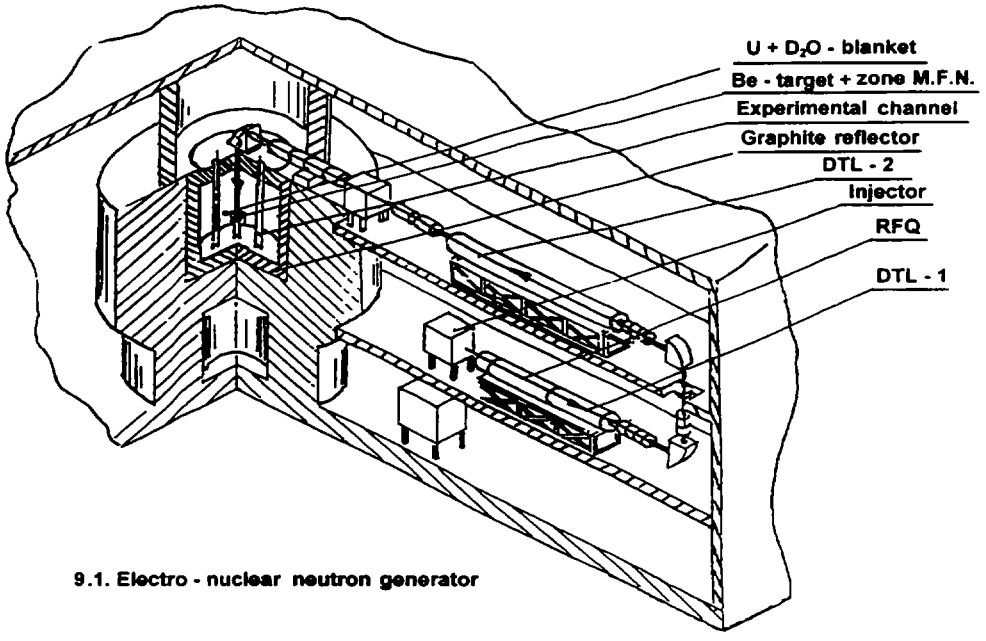

FIG. 9.1 Electro-nuclear neutron generator

Electro-nuclear neutron generator main parameters:

- Accelerator proton energy	36 MeV
- Proton pulse time	150 mks
- Proton pulse current	150 mÀ
- Mean proton current	0,5 mÀ
- Proton pulse frequency	25 Hz
- Target fast neutrons intensity	$1.5\ 10^{14}$ n/s
- K_{ef} start-up blanket	0.95
- Start-up blanket power	25 kW
- Reflector thermal neutron flux	$1.5\ 10^{12}$ n/sm^{2}s
- Start-up blanket load ^{235}U (90%)	2 kg

The purpose of the facility:

- application as a full scale physical model of ADS installation blanket;
- investigation of Th-heavy water cells;
- check and improvement of the control and protection system ADS installation;
- fundamental research (actinide constants for fast neutron parameters of proton interaction with target and accelerator materials).

D.4.1.10. ZERO POWER HEAVY WATER REACTOR MAKET AT ITEP

Zero power reactor MAKET is designed for precision experiments with full-scale lattice models of fast and heavy-water thermal blankets of ADS installations.

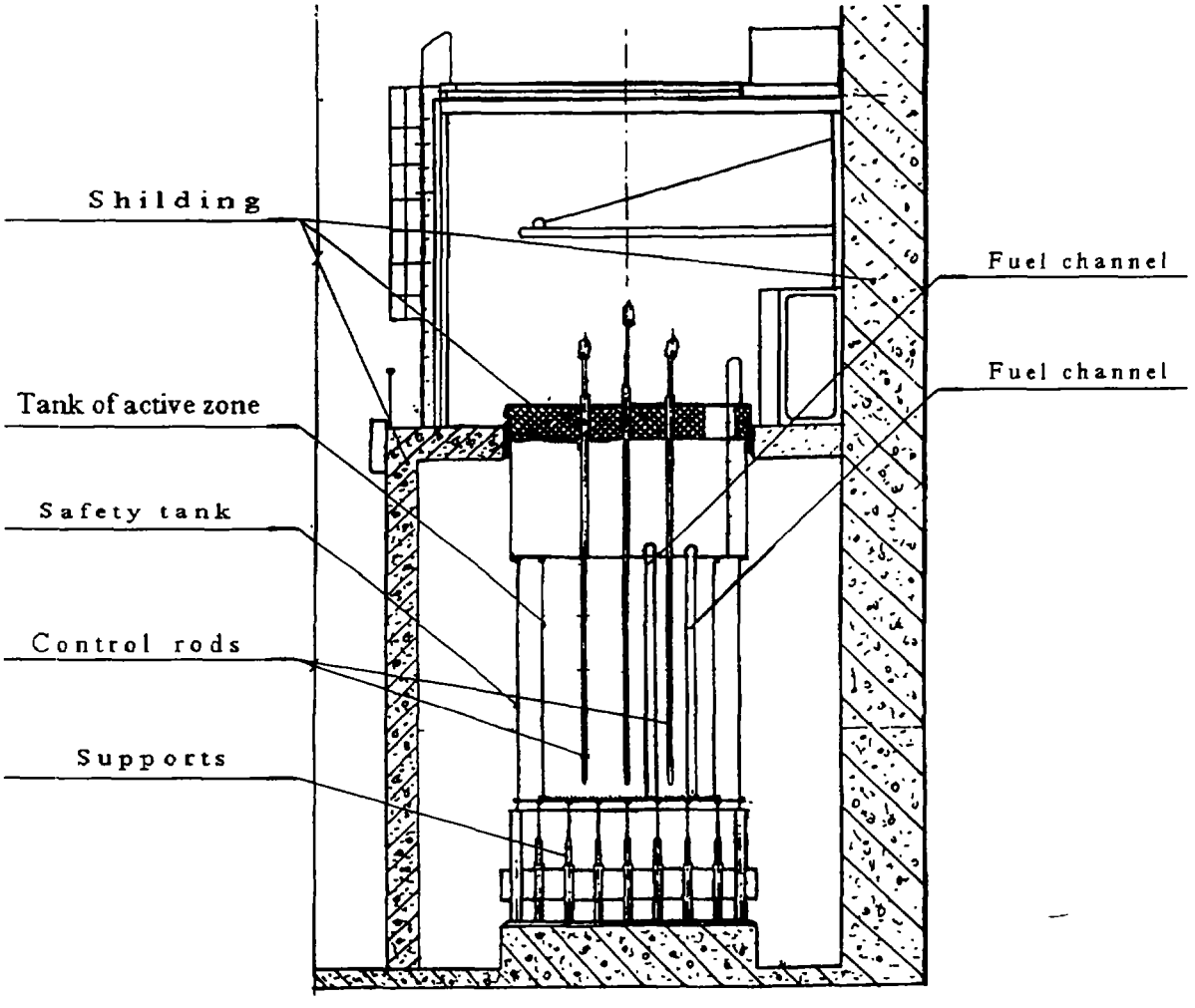

FIG.10.1. Zero power heavy water reactor MAKET.

Reactor main parameters:

- facility's maximum power	-	1 kWt
- core diameter / height	-	3,4 m/ 3,5m
- maximum volume of heavy water in the core	-	19 t
- number of power and reactivity control channels	-	7
- CPS rods number	-	7
- number of channels for control and limitation of the heavy water level in the core	-	4

- measurement accuracy of the heavy water absolute level in the core	-	1,5 mm
- measurement accuracy of the relative variations in heavy water level in the core	-	0,5 mm

D.4.1.11. ECONOMICAL ESTIMATIONS.

D.4.1.11.1. Expenditures for superconducting linear accelerator

Capital investments and expenditures for routine operation of superconducting 1 GeV, 10 mA 30 mA proton accelerator were defined on the costs of similar parameters devices of constructed accelerators, in particular of the linear accelerator of meson factory of INI of RAS and of the superconducting accelerator CEBAF. Full expenditures for accelerator with current 10 mA will be 150 million dollars. Their components are presented in the table:

Equipment	Expenditures (millions dollars)
Superconducting resonators with cryostats	60
HF channels with automatics systems	20
Automated control/parameters measurement systems	5
Standard equipment	40
Cost of construction	25

Expenditures for the accelerator with current 30 mA will be 185 million dollars. This rise is mainly caused by necessary increase of HF power. Annual expenditures for routine operation of the accelerator itself are estimated as 6 million dollars including 2 million dollars for salary.

Judging on experience of operation of linear accelerators life-time of the proposed accelerator is defined to be equal 30 years.

After decommissioning the accelerator and its main devices may be used for construction of other physical installations. The accelerator will be radioactive and ecologically "clean", without radioactive wastes. Costs necessary for decommissioning in this case will not be higher than 35 million dollars.

As to technical feasibility of the project it is possible to say that techniques of fabrication of the main devices of the accelerator is well experienced in the world though quite similar accelerators were not yet constructed. The accelerator of INI of RAS (protons energy is 600 MeV, average current - 1 mA) developed by MRTI of RAS jointly with invited institutions and superconducting electron accelerator CEBAF may be looked as prototypes. Time necessary for realization of the project is estimated as 7 - 10 years. If to invite to development and construction of the accelerator some of foreign laboratories and firms then this time may be decreased to 5 - 6 years.

At the stage of designing the cost of which is estimated as 40 million dollars and necessary time - 4 years, construction of three experimental installations is supposed: RFQ accelerator with a cryostat and a proton injector, cryomodules of the first and the main parts of the superconducting accelerator with HF and automation systems. Design solutions and the main procedures will be developed at these stands. Expenditures for creation of these stands will not be higher 10 million dollars; expenditures necessary for routine operation will be approximately 0.5 million dollars per a year.

Development and creation of equipment and of technologies of the accelerator will provide further progress in the area of HF superconductivity, powerful HF systems of continuous way of operation, effective systems of cryogenics under temperatures 2K. Significant numbers of specialists

in accelerators techniques and in adjacent specialities will obtain working places in the works on this project.

So full expenditures for the whole life of the accelerator will be

185 + 40 + 10 + 35 + 180 + 2 = 452 million dollars.

D.4.1.11.2. Expenditures for target-blanket part and the installation

A fast neutron reactor of BN-800 type and a heavy water gas-cooled reactor of TR-1000 type may be chosen as prototypes as real technical and economical foundations exist for them. In this case capital investments for creation of the installation (without accelerator) will be 1.5 billion dollars. Annual routine operation expenditures will be 160 million dollars. Cost of the project is 150 million dollars.

Costs for construction of a prototype of electro-nuclear generator of neutrons is 5 million dollars, expenditures for routine operation - 1 million dollars per a year. Costs for decommissioning of the power installation (by estimation of specialists of industrial association MAYAK) is 500 million dollars.

So for the whole life time of the installation (without accelerator) 1500 + 150 + 4800 + 500 + 5 + 30 = 6985 million dollars will be spent.

D.4.1.11.3. Expenditures for the whole installation

Total expenditures for the whole installation may be estimated by the sum 6985 + 452 = 7437 million dollars.

Relatively small expenditures for superconducting accelerator make full price of the electro-nuclear installation of such type quite comparable with the price of traditional NPS. All elaborated for NPS economical approaches and estimations may be fully applied to electro-nuclear systems with a superconducting accelerator.

Under power production of electric power 10 billion kW h all earlier presented expenditures will be recouped during the first years of operation of the installation as sale price of electric power in Russia is very high (6 cents per a kW h for February 1, 1996).

In accordance with the project of the reactor TR-1000 and estimations of MRTI on linear accelerator, total number of personnel necessary for routine operation of the Electro-Nuclear Power Installation, administration, technical and additional service will be approximately 2100 specialists.

All above presented estimations should be obligatory corrected by detailed technical and economical foundations but, nevertheless, accuracy of the presented estimations is comparable with estimations of the prices of traditional nuclear power installations at similar stages of development.

D.4.1.12. EFFECT ON ECOLOGY

The absence of appreciable losses of a beam of proton in a accelerator makes it relatively radioactive-safe in a operating time and in the process of removing it from operation.

Biological shielding of operating accelerator can be realized with the use of checked on Y-10 (ITEP) and Y-70 (IPHE) technical decisions in such a manner that outside a sanitarian zone characteristic radiation will not be above a background.

Fumes-off noble gases out of blanket will not be as much as indicated in [43]. Specific for heavy water system fumes-off tritium can be evaluated by a value not exceeding 1600 Ci per year in view of

measures on clearing heavy water of tritium, with maintenance of tritium concentration at a level not exceeding 1 Ci/l D_2O.

D.4.1.14. CONCLUSION

Presented data on superconducting linear accelerator show that such linear accelerator will possess unique characteristics:

- It will be capable to accelerate currents of protons and negative hydrogen ions up to 30 mA under losses not higher than 10^{-5}. Total efficiency on utilization of applied electric power will be approximately 60 %.

- The accelerator will be radioactive "clean" installation which will not require utilization of remote controlled techniques.

- Life time of the accelerator will be more than 30 years. After decommissioning there will not be necessity to bury separate elements and they may be used for other purposes.

ADS installation has Pb-Bi target and partitioned fast-thermal subcritical blanket. Total installation power is 2300 MWt. The coolant of fast blanket zone is Pb-Bi. The coolant and moderator of thermal zone is heavy water.

Analysis of accumulation of activity in Pb and Pb-Bi targets irradiated by protons has shown activity Po-210 to be not determining factor. It will allow to choose Pb-Bi (melting point 125°C) as a target and a heating agent in fast zone instead of Pb having relatively high-level melting point 327°C that essentially facilitates and makes cheaper operation of such system.

A general concept of ABC installation with an estimation of its main physical properties was presented above.

Fast spectrum blanket presents a source multiplying region that with a combination with thermal spectrum blanket and some elements of system composition (downward section of Pb-Bi coolant, steel walls of F- and T-blanket vessels and inner heavy water reflector) provides a property of one-directional coupling leading to a sufficient decrease of accelerator proton beam current (with (1-K) ~ 0.01) at safety conditions corresponding to much higher level of sub-criticality ((1- K) around 0.05-0.10) . On the other hand this section - F-blanket core - may be used for deeper incineration of actinides accumulated in both cores.

Deep burn-up values - about 70 GW-day/t in F-blanket and 35 GW-day/t in T-blanket - correspond to ~ 6 years of operation at full power without re-loading. About 90% of initial Pu239 in T-blanket is converted to fission fragments or higher isotopes during 6 years fuel cycle. The discharge of spent fuel (except fission fragments) - Pu and higher actinides - can be re-injected into F-blanket for further incineration .

During 30 years period of operation at full power about 25 of WG Pu is destroyed - converted in into Pu of different composition , other heavy nuclides and fission fragments, about 10 tons of Th are involved into fuel cycle with 6 t of U233 accumulated and 4 t spent in the installation for power production. A sufficient amount of Tc99 (dissolved in the moderator) or Am may be transmuted if they are used as a reactivity control materials in T-blanket.

Liquid Pb-Bi void reactivity effect is negative, reactivity effect of Pa233 decay (into U233) is small.

U233 accumulated in the system may be used in Th-U233 fuel cycle with conversion breeding ratio close to 1.

The system may effectively be used for destruction of WG Pu with power production and accumulation of U233 as a new fissile material that at the next stage can be used in a closed Th-U233 fuel cycle with breeding ratio close to 1.

It is shown that all stages of fuel cycle may be practically realized on the basis of technologies experienced in Minatom' plants in Russia.

Chemical technology defines reliability, technical safety and economy of electronuclear plant (ADS) in many respects. Significance of chemical technology is conditioned by using of heavy water, that is tied, besides problems of water preparation, special water purifying and degassing.

For successful realization of the project it is necessary to create a series of stands in substantiation of accelerator systems , to create stands for study of thermohydraulic parameters of Pb-Bi targets as well as parameters of fast zone cooled by Pb-Bi and at last to create accelerator driven generator of neutrons - a full scale model of power installation..

Significant part of technical solutions on accelerator, blanket, systems for monitoring and controlling may be checked and tested at the Electro-Nuclear Neutron Generator which is now under construction in ITEP. This Generator is based on the existing proton accelerator ISTRA-36 and the ITEP shut-down heavy water reactor HWR.

Neutron-physical blanket parameters of the electro-nuclear systems and physical foundations of the method of controlling reactivity by analysing the rear edge of a neutron pulse will be investigated at the experimental heavy-water reactor of zero power MAKET ITEP.

The problems of ecology and physical protection for offered ADS installation are traditional and do not differ from appropriate problems for critical NP installations in action and under design. The specific problem, connected with fume-off tritium formed in heavy water can be resolved with the help of installation on separating of hydrogen isotopes developed in ITEP, enabling to support tritium contents in heavy water at a level not exceeding 1 Ci/ l. In this case total annual tritium fume-off does not exceed 1600 Ci (experience of CANDU reactors).

Preliminary economic evaluations have shown that relatively small contribution of accelerator cost to total installation one permits to apply to ADS installation of such type all economic approaches and criteria, characteristic for traditional PN installations and makes the cost and recuperation of ADS installation comparable with appropriate NP installation.

Cooperation with Foreign Centers and Companies

1. Neutron physical properties of sub-critical systems with external sources (theoretical methods and computer codes, benchmark calculations, nuclear data, investigation of neutron physical properties of AD systems for current design) - collaboration **ITEP-LANL**

2. Design development and manufacturing of next subject:

- Superconducting cavities (with drift tubes and Cornell-type) - **Grumman (USA), CERN, KEK (Japan), CEBAF (USA), INFN (Legnaro, Italy).**

- Cryostat, cryogenic-system	-	**Grumman, USA, CERN**
- RFQ-accelerator	-	**Grumman, USA, LANL, USA, ANL, USA.**
- Permanent magnet quadruple lenses	-	**Grumman, USA, LANL, USA, JAERI, Japan.**
- High- intensity ion sources	-	**LANL, USA RAL - Rutherford Lab.**

- Beam loses, halo, emittance increase (research and suppression) - **LANL, USA,**

Maryland University,

GSI, Germany.

3. ITEP Neutron Generator Prototype of fuel-scale electro-nuclear plant (Linac+Target+HWR). Present - readiness is ~50%. Purchasing of modulators, finishing of construction and then participation in experiments on NG Complex

- Grumman, USA,

LANL, USA,

JAERI, Japan.

4. Calculation and analysis of target characteristics (isotope concentration long-lived activity etc) for Pb and Pb-Bi (and other alternative materials if necessary) targets irradiated by high energy proton beams using various computer codes;

- Testing of available input data (cross sections for spallation reactions and fission decay properties etc.) necessary for calculations, development of nuclear data base;

- Comparison between cat calculation results using various codes for standard spectra standard thermonuclear reactor spectrum here many results are available;

-Work out the recommendations for various hybrid systems - **LANL, USA,**

JAERI, Japan,

PSI, Switzerland.

REFERENCES

[1] C.Rubbia et al. Conceptual Design of a Fast Neutron Operated High Power Energy Amplifier. CERN/AT/95-44 (ET).

[2] Fitier N., Mandrillon P. A three-Stage Cyclotron for Driving Energy Amplifier, CERN/AT 95 03 (ET), Geneva, 1995

[3] Murin B.P., Fedotov A.P. Towards a Radiation - Free Linacs of Meson or Neutron Generator Type. Proc. of the 1976 Proton Linear Accelerator Conf. (Canada) - Chalk-River Nuclear Laboratories, 1976, p. 377 - 380.

[4] B.P.Murin et al. The New Concept in Designing of the CW High-Current Linacs. Internat. Conf on High-Energy Accelerators, Dallas, Texas, May 1 - 5, 1995.

[5] Cost Optimisation Studies of High Power Accelerators. R.Mc. Adams et al. in "AIP Conf. Proc 346, Las-Vegas, NV 1994.

[6] Proposals on linear accelerators of protons of continuous way of opera-tion to energy 1 GeV and currents 250/ 10 mA with utilisation of superconducting technics. Cipher of the theme "Kovyl", Resulting report of MRTI No 39-KL-95, 1995.

[7] Murin B.P., Fedotov A.P. Direction of development of powerful proton linear accelerators of continuous way of operation for nuclear-power goals. MRTI report, No 39-10-95, 1995.

[8] Weingarten W., Superconducting Cavities, CERN SL/94-15 (RF), 1994,

[9] Shepard K.W. at el. Construction of a superconducting RFQ structure. Proc. of the 1993 Particle Accel. Conf, USA, v.2, pp. 1042 - 1044.

[10] Wangler T.P. et al. Superconducting RFQ Development at Los-Alamos. 1992 Linear Accel. Conf. Proc. Canada, v. 2, pp. 627 - 629.

[11] Silaev S. Isoparametric Finite Element Analysis of Time-Harmonic Electromagnetic Field in Three Dimensions. Nuclear Instruments and Methods in Physics Research, A328, (1993), pp. 535 - 541.

[12] Proc. of the 4-th Workshop on RF Superconductivity, v.1, v.2, 1989, KEK, Tsukuba, Japan.

[13] Efremov V.M. et al. Improved Method for Electrochemical Polishing of Nb Superconducting Cavities. Proc. of the 5-th Workshop on RF Superconductivity, DESY, Hamburg, Germany, 1991, v.1, pp. 433 - 456.

[14] Korotkov A.M. at el. Special system of axial magnetron spraying of SC covers to operating surface of accelerating SHF structures of complex shape. Proc. of the Conf. "Vacuum science and techniques" Gurzuf, oct, 1994.

[15] Grigoriev A.D., Silaev S.A. Calculation of electromagnetic field of azymuthally-uniform modes of axially symmetrical resonators with arbitrary shape of the forming line. Serie Electronics of SHF, 1981, iss. 2, pp. 62 - 65.

[16] Kogen-Dalin V.V., Komarov E.V. Calculation and test of systems with permanent magnets. Moscow, Energy, 1977.

[17] B.P.Murin. Powerful sources of high frequency feeding for accelerators of charged particles. Preprint of MRTI ,No. 833, Moscow 1983.

[18] B.P.Murin. Stabilization and controlling of high frequency fields in linear accelerators of ions. Atomizdat, Moscow, 1971.

[19] Linear accelerators of ions. Under direction of B.P. Murin. V2, Atomizdat, Moscow, 1978.

[20] The LEP-II RF Power Generation System. H. Frischolz, CERN, Proc. of the 1983 Particle Accel. Conf. v. 2, p. 1247.

[21] Proposals on proton linear accelerators of continuous way of operation for energy 1 GeV and currents 250 and 10 mA with utilization of superconducting technics. Cipher of the theme - "Kovyl". Final report of MRTI No. 39-10-95, 1995.

[22] Kozodaev À.Ì., Lazarev N.V., Raskopin À.Ì. Pulsing mode of operations of linac-driver: advantages and peculiarities. The report on Third working meeting under Project No. 17. St.-Petersburg, on February 5-8, 1996.

[23] Lazarev N.V., Andreev V.A., Balabin A.I. et al. THIS YEAR. Technical lity of the radiation-safe linear accelerator at increase of a beam particles losses norm. The report on Third working meeting ISTC under Project No. 17. St.-Petersburg, on February 5-8, 1996.

[24] Lawrence G.P. Los Alamos High-Power Proton Linac Designs, Proc. of the Int. Conf. On Accelerator-Driven Transmutation Technologies and Applications, Las Vegas, NV, July 1994, p.177.

[25] Cost J.P., Brown P.D. et al. Radiating effects in REC-permanent magnets. Los Alamos, 1987, LA-UR-1455.

[26] Kozodaev À.Ì., Plotnikov V.K., Raskopin À.Ì. Reliability of RF systems of linacs. The report on Third working meeting ISTC under Project No. 17. St.-Petersburg, on February 5-8, 1996.

[27] Shvedov O.V., Vasilev V.V. et al.. Subcritical neutron generator of ITEP, conrolled by the accelerator of charged particles. Proc. of the Int. Conf. on Accelerator-Driven Transmutation Technologies and Applications, Las Vegas, NV, July 1994, p.425.

[28] Janni J.F. Proton Range-Energy Tables, 1 keV-10 GeV. Atomic Data and Nuclear Data,1982, v.27, p.417.

[29] Konobeev-A.Yu et.al. Helium production cross section in structural materials irradiated by protons and neutrons at energies up to 800 MeV. J.Nucl.Maters., 1992, v.195, p.286.

[30] Ireland J.R. ATW Aqueous Base Case Target/Blanket System Design. The Los Alamos Accelerator Transmutation of Nuclear Waste (ATW) Concept, Los Alamos, April 15-16, 1992.

[31] Takizuka T. et al. Conceptual Design of Transmutation Plant.Workshop on Nuclear Transmutation,July 1-5,1991,Obninsk.

[32] Harada H. et al. Transmutation of Fission Products, PSI-Procceed. of Specialist Meeting 92-02,ISSN 1019-6447,p.383.

[33] Takashita H.et al. Transmut. of Long-Lived Radioactive Nuclides. Global-93,Sept.12-17,1993,Seattle-Washingt.Proceedens,p.797.

[34] Konobeev-A.Yu., Korovin Yu.A. BISERM library for radiation damage analysis of the structural material, irradiated by 800 MeV nucleons At. Energy, 1992, v.72, ¹.2, p.190.

[35] Dementyev A.V et.al. SHIELD-Monte Carlo Hadron Transport Code. Proceedings of Specialist Meeting Intermediate Energy Nuclear Data: Models and Codes, Paris, France, 1994, p.237.

[36] Artisyuk V.V., et.al. Long-lived radionuclide formation in Lead and Lead-Bismuth targets irradiated by high energy protons. Izvestiya Vuzov, Yadernaya Energetica, 1994, v.1, p.41.

[37] Kochurov B.P., Kwaratzheli A.Yu., " Method of Calculation of Space-Time Processes in Subcritical Systems with External Source in 1D Cylindrical Geometry", Preprint ITEP 28-95, Moscow, 1995.

[38] Kulsky L.A. at. el. Technology of water purification on NP. Kiev, Sci. Thought, 1986.

[39] Honsharuk V.V. at el. Water-chemical technology of and ecology. Ref, Kiev, Sci.Th., 1993.

[40] Dowson Y.K. Sowden R.G. Chemical aspects of nuclear reactors, Vol.2, London, 1963.

[41] Gerasimov V.V. Corrosion of reactor materials. M.: AP, 1988.

[42] Trenin V.D. Research of water radiolysis in VVR-M reactor. Dissertation. LINP, L., 1975.

[43] Ermakov N.I., Murogov V.M. Role of fast reactors in the future of power engineering, the fuel supply and the environment. Reports on US /Russian Experts Meeting of long-time disposition of Plutonium. Los-Alamos, January 23, 1995.

D.4.2. ITEP CONCEPT OF THE USE OF ELECTRO-NUCLEAR FACILITIES IN THE ATOMIC POWER INDUSTRY

I. Chuvillo and Genadji Kiselev

Institute for Theoretical and Experimental Physics, 117259 Moscow, Russian Federation

D.4.2.1. INTRODUCTION.

In the last few years specialists from Russian and foreign research centers have been conducting conceptual investigations into the use of electro-nuclear facilities (ENFs) or Accelerator Driven Systems (ADS) in the atomic power industry. The ADS consists of a subcritical core (blanket), a neutron producing target and a charged particle accelerator.

The main goals of the ADSs are:

- To minimize the problems with radioactive waste that exist in the atomic industry and atomic power industry.
- Improvement of the environment.
- Provision of the conditions necessary for public acceptance of atomic power.

There are two important problems in the modern atomic power industry: the safety of NPP's and the large amount of high level radioactive waste (HLW). The safety problem of existing nuclear power plants (NPPs) is being solved through evolutionary improvement of control and protection systems (CPS). An increase in safety is effected by using the inherent features of self-protection, passive safety systems, "in-depth protection" principles, etc.

In most countries, including Russia, the main strategy of HLW management is surface burial in solidified form with further geological disposal.

In accordance with the "Concept of development of the atomic power industry in the Russian Federation" [1] a transfer to the closed nuclear fuel cycle (NFC) is being planned (at the present time a partially closed nuclear fuel cycle is implemented in Russia). In this case technically justified solutions for safe management of long-lived radioactive waste (LLRW) are required. Furthermore, other problems of equal importance in the atomic power industry should be kept in mind:

1) Storage of large amounts of spent nuclear fuel (SNF) from NPPs.
2) Storage of large amounts of depleted Uranium which has no application at the present time.
3) The large amount of highly enriched Uranium being released as a result of nuclear disarmament.
4) Large amounts of the weapon-grade and power (commercial) Plutonium.
5) The need to extend the fuel basis of the atomic power industry after 2010 in the case of further development.
6) Reduction in environmental effects.
7) Non proliferation problems associated with processing of weapons-grade Plutonium, its storage and the possibility of its use as nuclear fuel.
8) Economics.

As will be discussed later, ADSs could provide solutions to all the problems listed above in an integrated way whereas advanced power reactors could only partially solve the problems indicated.

The complexity of the solutions to the above problems requires the combination of the efforts of specialists from Russian institutes and foreign centers.

The following Russian institutes participate in the work dealing with the use of ADSs:

- State Scientific Center (SSC) Institute of Theoretical and Experimental Physics (ITEP), Moscow
- SSC Institute of Experimental Physics, Arzamas-16
- SSC Institute of Technical Physics, Chelyabinsk-70
- Russian Research Institute for Inorganic Materials (RRIIM) named after A.A. Bochvar, Moscow
- Scientific Production Association Radium Institute (SPA RI) named after V.G. Khlopin, S. Petersburg
- SSC Physics and Power Institute (SSC PPI), Obninsk
- Special Design Bureau for Machine Building (SDBMB), N.Novgorod
- Research and Design Institute for Power Technology (RDIPT), S. Petersburg
- Moscow Radiotechnical Institute, Moscow
- Design Bureau Hydropress (Podolsk, Moscow Region)
- Moscow Engineering Physics Institute (MEPI), Moscow
- Joint Institute for Nuclear Research (JINR), Dubna.

D.4.2.2. POSSIBLE SCHEMES FOR FUTURE DEVELOPMENT OF THE ATOMIC POWER INDUSTRY

The need to solve the problems indicated in the Introduction is determined by the prospects for development of the atomic power industry both worldwide and in Russia. Possible scenarios for the future development of the atomic power industry in Russia are:

1. The number of NPPs and their total electric power is kept constant over a long period of time.
2. The scale of NPP use will be increased compared to the existing level beginning at some point in time, e.g. following an increase in industrial production.
3. The atomic power industry for certain objective and subjective reasons, will cease to exist after a period of time.

It is quite obvious that the need for ADS development should be determined by the prospects for development of the atomic power industry in Russia. It is difficult to predict right now which direction will be chosen by the Russian atomic power industry for its further development. To answer the questions about the need to develop ADS as an alternative to power reactors and the existing technologies of LLRW management let us consider two mutually exclusive possibilities for the Russian atomic power industry (the second and third possibilities mentioned above):

1. The Russian atomic power industry will begin to develop progressively with a certain rate of commissioning of new capacities.

   In accordance with the "Concept" the period from the year 2000 to 2010 should be marked by an increase of capacity based on the new generation NPPs. Further development of full scale atomic power after 2010 is anticipated. It is noted in the "Concept" that the main designs of the third generation NPPs are improved NPPs with WWER-type reactors with a capacity of 1000 MW_e and about 630 MW_e. Construction of 3 BN-800 fast reactors at the South Urals NPP is expected to be completed.

   In the case of further development of the atomic power industry the amount of LLRW will grow progressively as NPPs are operated, as is shown in Fig. 1 curve 2 [2]. At the same time the adoption of ADSs in the atomic power industry will permit reduction of the amount of LLRW by several orders of magnitude compared with thermal (PWR) and fast (LMFBR) reactors. The NFCs for

fissile and fertile materials and LLRW are possible as a development of the atomic power industry for the period after 2010 as proposed by the present Concept.

2. The Russian atomic power industry ceases to exist at a certain time in the 21st century.

   In the case of cessation of the atomic power industry it is essential to have the technology for safe LLRW management including that associated with LLRW transmutation. Based on calculations performed in ITEP would be sufficient for the atomic power industry to have no more than a few (maybe one) ADS with optimum parameters for the purpose of transmutation of HLW generated during operation of the military nuclear industry and the atomic power industry.

D.4.2.3. ITEP APPROACHES TO ADS DEVELOPMENT

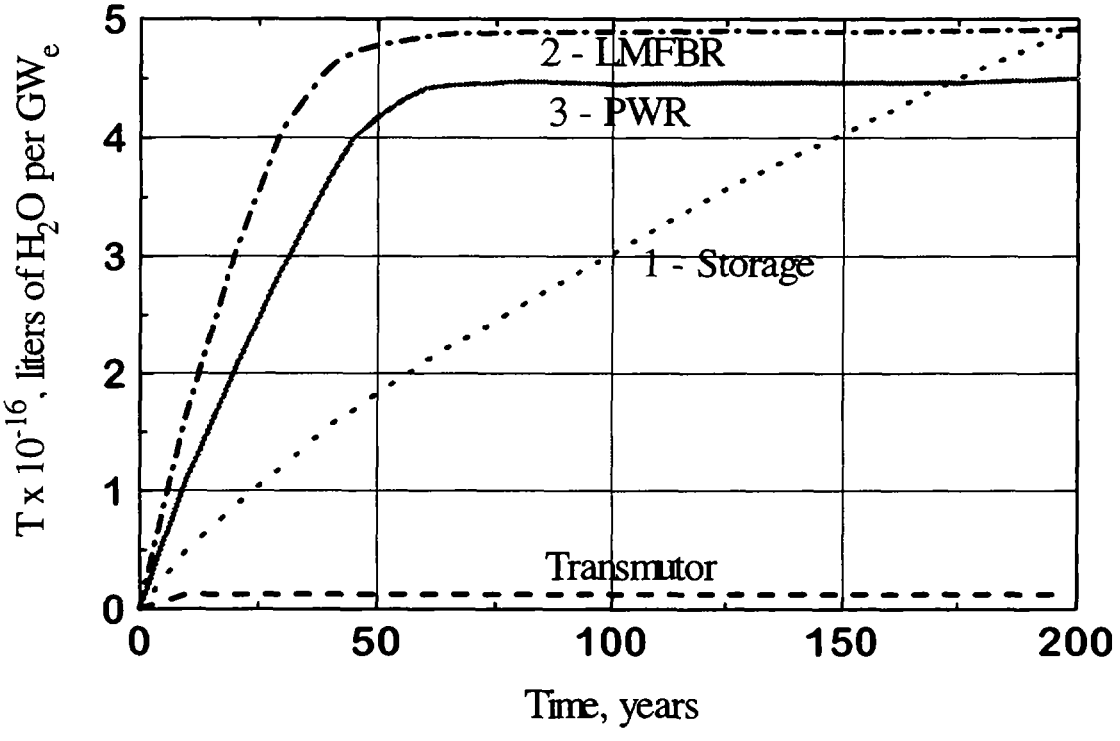

FIG. 1 The growth of the radioactivity for the long-lived wastes (LLRW) for the different nuclear power systems (in liters of water required for waste dilution in order to reach the regulatory limits).

ADSs represent a new type of nuclear power facility which in the opinion of ITEP, should be introduced into the atomic power industry in the 21st century. While conducting conceptual investigations and developments of ADS the ITEP experts are guided by the following criteria:

1. It is expedient to use the positive experience available and the technical approaches verified in the atomic power industry - the properties of inherent self-protection in particular, passive safety systems, "in-depth protection" principles, etc. The main criterion in this case is the increase in ADS nuclear and technical safety compared to NPP.

2 Experimental investigations should be conducted to substantiate the new technical approaches proposed; first of all the ADS blanket is the most complex and important component for the purpose of safety.

3. Experimental work should be done on the nuclear data base primarily for the radionuclides to be transmuted.
4. At the stage of conceptual investigations it is expedient to study various types of targets and blankets with estimates of their possible implementation, determination of technical and economical characteristics and then choose one version for further development.
5. The ADS operation should be performed with a positive power balance and decrease in radiotoxicity compared with the initial level.
6. The possibilities of ADS operation in combination with other improved power reactors, including fast reactors, should be investigated at the stage of conceptual studies.
7. Studies on the place of ADS in the future of the atomic power industry should be conducted with an estimation of the radiation load on operating staff and population

   (this has not been done because of the lack of financing).
8. The technical requirements and ADS criteria should be formulated as the result of conceptual investigations including:
   - Minimization of the amount of LLRW in the various technological processing stages of the future NFC.
   - The possibility of useful application of some transuranic elements from the LLRW list.
   - Power efficiency, i.e. the ratio of the useful power to consumed power.
   - Environmental efficiency, i.e. the reduction in LLRW radiotoxicity under irradiation in the ADS per unit of time.

D.4.2.4. PRINCIPLE POSSIBILITIES OF ADS

We shall indicate in the present section only the principle features of ADSs and the possibilities which should be justified as the result of conceptual studies. These possibilities are presented on Fig. 2, page 328.

D.4.2.4.1. Safety

The available operating experience of the atomic power industry allows us to specify three kinds of safety for nuclear facilities: nuclear, technical and radiation. Nuclear safety means the absence of conditions for self-sustaining chain fission reactions (SCFR), with an effective multiplication coefficient above unity, to develop.

Technical safety means the absence of conditions for core meltdown in non-stationary and emergency modes, in the event of vessel damage, damage to pipelines or other equipment failures which could Lead to dangerous consequences.

Radiation safety means the absence of conditions for increased radiation effects on operating staff or the population during normal operation or in the event of an accident.

At the present level of knowledge the ADS permits:

- exclusion of the class of accidents associated with a change in reactivity (reactivity margin); first of all, a power excursion of instantaneous neutrons in relation to the ADS blanket operation in subcritical mode with a sufficient margin for the value of the effective multiplication ratio with consideration for the feedback;
- to exclude in principle absorber rods in the emergency protection system as a possible cause of potential accidents;

- to use a new type of ADS passive emergency protection, without moving working heads at accelerator de-energization, which makes it possible to increase the speed of response several orders of magnitude compared to existing at the present time.

D.4.2.4.2. The use of NPP spent nuclear fuel as ADS fuel

ADS can use NPP spent nuclear fuel (SNF) as material for power generation, after its unloading from the power reactor and without radiochemical reprocessing. Estimations performed in ITEP suggest that in an ADS heavy-water blanket loaded with SNF from VVER-type reactors the specific power generation could be increased approximately a factor of two compared with the level of burnup achieved at the present time [3]. To implement this mode it is necessary to perform an analytical study of a particular blanket design scheme with consideration of material problems.

D.4.2.4.3. The use of depleted Uranium in ADS

A large amount of Uranium with a ^{235}U content of 0.25% or less is held in the stores of the Ministry of Russian Federation on Atomic Energy. The depleted Uranium is a potential source of power because of its transformation into Plutonium. The ADS could use the depleted Uranium as fertile material to produce Plutonium fuel and power at the same time (7-10% of ^{238}U is fissioned in a fast neutron spectrum) without any limitations on content of the ^{238}U. After the exhaustion of cheap natural Uranium resources in the future depleted Uranium will probably a valuable fuel.

D.4.2.4.4. The use of highly enriched Uranium

As the result of nuclear disarmament a possibility emerges of using highly enriched (90%) Uranium in the atomic power industry. It could be used either in the form of 90% Uranium dioxide or in the form of isotopic diluted dioxide, e.g. with 4.4% enrichment for VVER-type reactors. 90% Uranium, without its isotopic dilution, could be safely used in the ADS blanket for power generation and production of excess neutrons. In doing so the load of 90% Uranium dioxide into the blanket could, in principle, be less than the critical mass value. The excess neutrons are consumed for LLRW transmutation and production of new fissile materials.

D.4.2.4.5. The use of weapons-grade and power Plutonium

The ADS can use weapons-grade and power Plutonium as a nuclear fuel for power generation and production of excess neutrons which can be used for LLRW transmutation and production of new fissionable materials. The involvement of Plutonium in the NFC will make it possible to expand significantly the fuel basis of the atomic power industry.

D.4.2.4.6. The necessity to expand the fuel basis of the atomic power industry

One of the possibilities for expanding the fuel basis of the atomic power industry is the closure of the nuclear fuel cycle. In doing so a set of problems emerge which have a pronounced effect on the NPP nuclear fuel cycle and solutions are called for.

These are the following problems:

- ^{236}U buildup in the SNF as multiple irradiation of regenerated Uranium takes place that will require an increase in fuel enrichment,
- generation and continued increase in the amount of ^{232}U in the SNF as multiple irradiation of the regenerated Uranium takes place, that requires remote technology for fuel element manufacture starting from a certain cycle;
- extraction of the reactor-grade Plutonium from the NPP SNF and the need to use it as a fuel, with attendant problems (the need for remote technology for fuel element manufacture, nonproliferation, etc.),
- generation of a large amount of LLRW containing fission products and transuranium elements, especially with aqueous methods of SNF reprocessing,
- an increase in the amount of depleted Uranium with a low content of ^{235}U (0.1-0.2%).

Another way of extending of fuel basis of atomic power industry is to involve Thorium in the NFC for the purpose of generating new nuclear fuel, namely ^{233}U.

The problems indicated above could effectively be solved with the help of ADS, using previously elaborated approaches and techniques proved in NPP operation.

A formulation of the future problem of the atomic power industry in supplying itself with fuel is advisable. This could be solved not only through the use of fast reactors with breeding, but also by utilization of ADSs for breeding purposes. One possible conceptual solution is the utilization of a two-module ADS (a module consists of a target and a blanket) [4]. Depleted Uranium is loaded into the blanket of one module to produce Plutonium. Plutonium and actinides produced in that module are extracted from irradiated ^{238}U and directed into the power blanket to generate power and produce excess neutrons which could be used for LLRW transmutation or production of the new nuclear fuel. Such a two-module ADS will in principle permit implementation of ADS fuel self-supply.

D.4.2.4.7. Safe HLW management and environmental effects

The ADS can incinerate the main fission products except, for ^{90}Sr, ^{93}Zr, ^{151}Sm and transuranium elements, by a process of transmutation. This is characterized by the following parameters:

1. necessary neutron flux;
2. neutron consumption per one incinerated nucleus;
3. secondary radioactivity;
4. radiotoxicity.

As the result of the transmutation process the amount of HLW and the period required for storage is reduced as well as environmental effects.

D.4.2.4.8. Safeguards of fissionable materials and the problem of non-proliferation

The ADS makes new approaches available for preservation and non-proliferation of fissionable materials, most importantly weapon-grade Plutonium in connection with possibilities for its denaturation. The first technical possibility is irradiation of the mixture of Plutonium and fission products, e.g. Sr or Cs, to complicate their theft during storage, with subsequent irradiation of this mixture in the ADS blanket. It has been demonstrated that in this case no significant change in the ADS blanket reactivity takes place [5]. The second technical possibility is dilution of ^{239}Pu with ^{238}Pu either by addition of ^{238}Pu or by irradiation of the ^{237}Np and ^{239}Pu mixture. At specific ^{238}Pu content the mixture of ^{238}Pu + ^{239}Pu is unsuitable for

nuclear weapon manufacture. This possibility could be effectively implemented both in power reactors and in ADSs.

D.4.2.4.9. Economics

The ADS is at first glance a more expensive facility than a power reactor. The capital investment in ADS will be higher in connection with the accelerator and the target. The qualitative considerations, however, demonstrate the high profitability and economic efficiency of the ADS in a systematic approach rather than in comparison of individual facilities.

If we assume that a fast reactor of BN-800 type could transmute the minor actinides (MA) from 3 loads of VVER-1000 reactors and its own, 7 BN-800 reactors with total power of 3.6 GW_e are necessary to destroy MA from the existing Russian NPPs [6]. According to our estimation the cost of one reactor is nowadays appr. 2×10^9 US$ i.e. appr. 14×10^9 US$ are required for commissioning 7 BN-800 reactors.

One optimized ADS could in the limiting case transmute all the actinides from all NPPs existing in Russia. If we assume that capital investment in an ADS is twice as large as that for a BN-800 reactor owing to the accelerator and target, the amount is 4×10^9 US$. Moreover, it is necessary to commission 5 VVER-1000 reactors with a total capacity of 5 GW(e), and investment of appr. 5×10^9 US$, to compensate for the power generation by the BN-800 reactors. In this case the expense for LLRW transmutation with the use of BN-800 reactor is 1.5-2.0 times higher than for ADS. For a final conclusion on the economic efficiency of ADS, however, systematic investigations are necessary and these have not been yet performed.

The study of the possibilities for ADSs mentioned in the present section, and the place of ADSs in the future plans of the nuclear power industry, are the main purposes of this conceptual study.

D.4.2.5. POSSIBLE OPERATION MODES AND FUEL CYCLES

The following ADS operation modes could be considered:

1. A transmutation mode without power utilization.
2. A transmutation mode with concurrent power generation and utilization.
3. A mode with power generation and utilization as well as production of new fissionable materials and LLRW transmutation.
4. An after-burn mode for power generation with use of NPP spent fuel assemblies as nuclear fuel.

The ADS can also serve as a high intensity neutron source for producing radionuclides with high specific activity.

The ADS can have various fuel cycles depending upon the mode of operation. The following materials could be used as fuel materials for transmutation modes: enriched Uranium, power and weapon-grade Plutonium, actinides (in a mixture with Plutonium and without it), and ^{233}U. Depleted Uranium and Thorium could be used as fertile materials for the production of new fuel.

The possibility of implementing the following fuel cycles (FCs) in the ADS could be indicated:

1. The Uranium FC. In this version of the FC various Uranium fuels could be used in the blanket: 90% enriched Uranium released as the result of nuclear disarmament; regenerated Uranium produced after multiple irradiation and reprocessing cycles of the SNF with a high content of actinides and fission products (FPs) could be loaded into the blanket in various combinations and proportions for transmutation purposes. Depleted Uranium without any restriction in content should be loaded into the blanket in Plutonium production mode. ^{238}U could also be used as a nuclear fuel in the ADS blanket.

2. The Plutonium FC. Plutonium fuel with different isotopic compositions: weapon-grade Plutonium only, or power Plutonium only, or their mixture could be loaded into the blanket in this version. Actinides and FPs could be loaded into the ADS blanket for transmutation purposes. Depleted Uranium could be used for the purpose of nuclear fuel production in the ADS blanket. Neptunium or Plutonium fuel could be used for the special purpose of weapon-grade Plutonium denaturization.
3. The Uranium-Thorium and Plutonium-Thorium FCs. Enriched Uranium or Plutonium is used as a nuclear fuel in these FC versions (Thorium is used as fertile material for n purposes).
4. The actinide FC. In this version alternative actinides in various combinations with FPs are used as a nuclear fuel in the ADS blanket for transmutation purposes.

The form of the fuel, fertile, and target materials has been a matter of interest. Two main alternatives are possible for the application of fissionable fuel materials: a solid and a liquid form. Each alternative has its own advantages and disadvantages. If the available experience in production of the nuclear fuel for NPPs is kept in mind, it is advisable to chose dioxide fuel in Zirconium cladding. It will be a MOX-fuel in the case of power or weapon-grade Plutonium. In recent years Russian experts have conducted investigations on cermet and nitride fuels with increased burnup levels. In relation to the problem of non proliferation, Plutonium fuel in an inert matrix may be of interest. However, in the case of 3-5% actinide addition to the MOX-fuel, its radiation resistance should be experimentally verified; this requires substantial expense and is time consuming.

Some research groups in LANL, JAERI and ITEP are conducting investigations on liquid fuel based on fluoride molten salts of the type Li-BeF_2-ThF_4-PuF_4 .

The advantages of liquid fuel are the absence of radiation damage problems, the possibility of breaking away from metallurgical production of fuel assemblies, a reduction in amount of FPs and fissionable materials in the core, etc. The main objection in Russia against liquid fuel lies in the absence of a technological basis for its implementation in the atomic power industry, rather complex technical problems emerging in the reactor facility, etc. It could be argued that the problems of liquid fuel application are somewhat in advance of needs of the atomic power industry at the present time. However, R&D should be conducted on the prospects and possibilities for liquid fuel applications in ADSs in order to have a basis for decision making.

The variety of operation modes and fuel cycles in ADSs mentioned above requires certain priorities to be set in order to concentrate the small resources available into one or two R&D lines. For this purpose, systematic investigations have to be pursued which have not been performed yet because of lack of funding. However priorities in the fuel cycle development could be determined even now. The highest priority is the ADS Plutonium cycle, where Plutonium is used as nuclear fuel, to generate power and excess neutrons which in turn are directed toward transmutation of actinides and FPs. This could help solve the problems of nuclear weapons non-proliferation and the production of new fissionable fuel.

This is explained by the availability of large stocks of power and weapon-grade Plutonium with a high power potential and the need to prepare a technological basis for its safe use as a nuclear fuel in a future atomic power industry. Hence the transmutation mode with power generation and the use of the weapon-grade and power Plutonium, wherein a Plutonium FC with actinides and FPs is used as a target material has priority in R&D.

The second priority is a Plutonium FC wherein the ADS operates in the mode of power generation and Plutonium production from depleted Uranium. The priority of this mode and FC is explained by the availability of large amounts of depleted Uranium in storage in the nuclear nations, including Russia. The involvement of depleted Uranium makes it possible to increase nuclear fuel resources substantially as resources of cheap natural Uranium become exhausted. All necessary technologies are available for this version and have been verified on an industrial scale.

The third priority is a Plutonium FC wherein the ADS operates in the mode of power generation and ^{233}U production from Thorium. However, the involvement of FC implies that the development of new technologies will be necessary after all resources of natural Uranium have been exhausted.

In accordance with the decision of the Scientific and Technical Council of the Russian Ministry for Atomic Power, fast reactors are considered to be the main nuclear and power facilities for utilization of Russian weapon-grade Plutonium. At the same time the RF Ministry of the Atomic Power Industry supports the ADS development as an alternative line, keeping in mind the possibility of operating the ADS blanket in a subcritical mode which increases the nuclear safety level in the event of its loading with weapon-grade Plutonium.

D.4.2.6. PECULIARITIES OF THE TRANSMUTATION PROCESSES

The process of transmutation of FPs and actinides transmutation in neutron fluxes must has its own peculiarities which must be taken into account in the development of ADS. The transformation of FPs is performed mainly by (n,γ)-reactions through sequential capture of neutrons being transmuted by a nuclide and formed by intermediate nuclides. The destruction of actinides occurs mainly through fission reactions. Despite this difference the following LLRW transmutation processes are characterized by the following parameters:

1. A_i, the actinide destruction rate which is determined by the neutron flux density Φ and σ_i, the effective microscopic interaction cross-section.
2. The process power efficiency which is determined by the value of the power spent for the destruction of one nucleus of the nuclide being transmuted or by the number of neutrons spent for the destruction of one nucleus.
3. The secondary radioactivity which is formed as a result of the transmutation of LLRW.
4. The value of the radiotoxicity of nuclides before and after the transmutation.

Investigation of the mentioned above features allows us to determine the list of nuclides which are suitable for transmutation.

A short analysis of the features mentioned above is given below.

D.4.2.6.1 A_i destruction rate of the nuclide being transmuted

Since the value of A_i is proportional to $\phi\sigma_i$ for FPs it will be higher for the higher ϕ and σ_i values. The upper limit of ϕ which can be reached with present-day knowledge and experience is probably in the range of $7.\times10^{15}$ - $5.\times10^{16}$ n $cm^{-2}s^{-1}$. The value of σ_i depends on the neutron spectrum. It is advisable to use a thermal neutron spectrum for FP transmutation through (n,γ) reactions where interaction cross-section values are rather high. Actinide transmutation is possible both in thermal and fast neutron spectra. A comparison has been performed of neutron cross-sections for actinides at comparable neutron fluxes in a thermal blanket (10^{14} $cm^{-2}\cdot s^{-1}$) and in a fast reactor ($1.2\times10^{16}cm^{-2}\cdot s^{-1}$). As can be seen from the results given in Tables I and II, the effective cross-section of actinides in a thermal spectrum is in most cases much higher than for a fast reactor [7].

Specialists from ITEP and other institutes have estimated the value of the neutron flux density

TABLE I. EFFECTIVE CROSS-SECTIONS AND THE NUMBER OF NEUTRONS PER FISSION FOR THE FAST REACTOR.

(σ_c - cross section for capture, σ_f - Cross section for fission, σ_a - cross section for absorption, ν - number of neutrons per fission.)

Nuclide, I	σ_c (barn)	σ_f (barn)	σ_a (barn)	ν (n /fis.)
^{237}Np	1.4	0.3	1.7	2.9
^{238}Pu	0.5	1.1	1.6	3.0
^{239}Pu	0.5	1.8	2.3	2.9
^{240}Pu	0.5	0.4	0.9	3.1
^{241}Pu	0.4	2.4	2.8	3.0
^{242}Pu	0.4	0.3	0.7	3.0
^{241}Am	1.7	0.3	2	3.4
^{242m}Am	0.4	3.2	3.6	3.2
^{243}Am	1.0	0.2	1.2	3.6
^{242}Cm	0.288	0.185	0.473	3.5
^{243}Cm	0.3	2.6	2.9	3.8
^{244}Cm	0.6	.4	1	3.5
^{245}Cm	0.4	2.8	3.2	3.8
^{246}Cm	0.77	0.47	1.24	3.5

necessary for ^{90}Sr and ^{137}Cs [8] incineration. For ^{90}Sr separation the capture cross-section value is for σ= 0.014 [9] or 0.0097 [10] barn according to the latest data. According to older data it was believed that σ=0.8 ± 0.5 [11]. If we are adhere to contemporary data and believe that σ=0.01, then a neutron flux of 7.6×10^{16} $cm^{-2}\cdot s^{-1}$ is required for the ^{90}Sr transmutation rate to be equal to its radioactive decay rate ($T_{½}$=28.8 years). In this case the "half-destruction period" will be half of the half life, i.e. 15 years. Higher flux densities (more than 10^{17} $cm^{-2}\cdot s^{-1}$) would be required for more rapid destruction. Even though such flux densities could be achieved in the ADS, it is unlikely that this will be economically justified.

For ^{137}Cs σ=0.11 barn [12] or 0.25 barn [13]. For the transmutation rate to be equal to the radioactive decay rate ($T_{½}$=30 years) a flux density of 6.7×10^{15} or 2.9×10^{15} $cm^{-2}\cdot s^{-1}$ is accordingly necessary which is achievable in modern reactors. In this case the "half-destruction period" will be 15 years. Flux densities higher than 10^{16} n $cm^{-2}s^{-1}$ are required for more rapid destruction of ^{137}Cs. It should be kept in mind that the radiotoxicity of ^{90}Sr is significantly (37 times) higher than that of ^{137}Cs (the maximum permissible concentration of ^{90}Sr in water is 4.0×10^{-10} Ci/l, and that of ^{137}Cs is $^{1.5}\times10^{-8}$ Ci/*l*).

D.4.2.6.2. Transmutation process efficiency

It is quite obvious that the power consumption required for HLW destruction should be substantially less than the amount of power generated by NPPs. According to investigations carried out by specialists from the Moscow Engineering Physics Institute the FP transmutation process is effective if the power consumed for transmutation is appr. 30% of that generated in the NPP [14]. It is obvious that the power balance in actinide incineration is positive. The power consumption for HLW transmutation could only be determined after development of a particular ADS design. Therefore such a characteristic as R_i, the consumption of neutrons necessary to incinerate one FP nucleus, could be used to estimate the power consumption. The calculation results for R_i are tabulated in Table III [15]. It is evident from Table III that a considerable number of neutrons is required for transmutation of ^{93}Zr and ^{151}Sm. This demonstrates that their incineration in a neutron flux is ineffective from the power viewpoint. At the same time it is advisable to state the problem of their recycling in the NFC, for example ^{151}Sm is an absorbing material in the CPS rods. The transmutation of the other radionuclides listed in Table IV is energetically advisable.

D.4.2.6.3. Secondary radioactivity under transmutation

The process of neutron generation for transmutation is accompanied by electric power consumption from an external source for the accelerator supply. If we believe that this electric power is generated in the

TABLE II. EFFECTIVE CROSS-SECTIONS AND THE NUMBER OF NEUTRONS PER FISSION FOR THERMAL REACTORS.

($T_{1/2}$ - half-life, σ_c - cross section for capture, σ_f - cross section for fission, σ_a - cross section for absorption, ν - number of neutrons per fission.)

Nuclide, I	$T_{1/2}$ (years)	σ_c (barn)	σ_f (barn)	σ_a (barn)	ν (n/fis.)
^{237}Np	2.14×10^{6}	203.4	0.706	204.11	2.25
^{238}Np	2.12 days	62.	1773.	1835	2.8
^{239}Np	2.36 days	67.5	-	67.5	-
^{238}Pu	87.71	433.	17.1	450.1	2.9
^{239}Pu	2.41×10^{4}	268.	666.	934	2.877
^{240}Pu	6569	1050.	0.93	1050.9	-
^{241}Pu	14.35	316.	910.	1226	2.937
^{242}Pu	3.76×10^{5}	126.	0.7	126.7	-
^{243}Pu	4.96 hrs	97.	213.	310	-
^{241}Am	432.6	540.	4.01	544.01	3.21
^{242g}Am	16.1 hrs	-	1725.	1725.	3.26
^{242m}Am	141	1637.	6372.	8009	3.26
^{243}Am	7348.	243.	1.16	244.16	-
^{244}Am	10.1 hrs	-	1856.	1856.	-
^{244m}Am	26. min	-	1291	1291	-
^{242}Cm	161. days	23.	<4.	27	-
^{243}Cm	28.5	657.	127.	784	3.43
^{244}Cm	18.1	77.2	2.63	79.83	-
^{245}Cm	8500.	292.	1735.	2027	3.717
^{246}Cm	4700.	13.1	1.13	14.23	-
^{247}Cm	1560.	99.	142.	241	-
^{248}Cm	3.4×10^{5}	29.1	1.8	31.	-
^{249}Cm	64.15 min	1.3	-	1.3	-
^{249}Bk	329 days	995	-	995	-

NPP, then neutrons are produced as the result of fission reactions of the nuclear fuel in the reactor of the NPP which energizes the accelerator. Moreover, nuclear reactions generating neutrons also occur in the blanket of the ADS itself. Hence the transmutation process, i.e. the process of destruction one radioactivity unit is accompanied by generation of FPs, that is secondary radioactivity. Because in the first 100 years after unloading of the NPP's spent nuclear fuel (SNF) its activity will be determined to appr. 90% by activity of ^{90}Sr and ^{137}Cs, the secondary activity is mainly the activity of the medium-lived nuclides - ^{90}Sr and ^{137}Cs. The calculations of the secondary activity performed by ITEP specialists show that, with the elimination of all primary activity of the FPs (except for ^{90}Sr and ^{137}Cs), secondary radioactivity is generated which accounts for 10-12% of the radioactivity (see Table IV) [15]. In the event of elimination of 100% of the primary activity, including ^{90}Sr and ^{137}Cs, the secondary activity generated is equal to 40% of the ^{90}Sr and ^{137}Cs primary activity. This result can be interpreted in the following way. First, the long-lived activity is transformed to medium-lived with the help of an ADS. Second, we have to pay for this with the generation of an additional 10-12% of secondary activity of the medium-lived ^{90}Sr and ^{137}Cs radionuclides ($T_{½}$ up to 30 years). This is a very important result. It follows that with the use of an ADS all long-lived FPs (except ^{90}Sr) could be destroyed.

D.4.2.6.4. Radiotoxicity

The main radiobiological hazard is actinides with long half lives.

Taking into consideration the high radiation hazard of actinides a comparison of the radiotoxicity has been performed for fuel loads of the ADS thermal and fast blankets [7]. For the comparison to be representative a stationary operation mode has been chosen with continuous nuclear fuel replenishment such that the change in concentration of nuclides in the next cycle is the same as for the previous one. The

effective neutron flux density for the fast reactor was assumed to be equal to 1.2×10^{16} $cm^{-2}\cdot s^{-1}$; the effective cross-sections are listed in Table I. In Table II the cross-sections are listed for a thermal blanket and the effective neutron flux density averaged over a Maxwellian neutron spectrum was assumed to be equal to $5.\times10^{15}$ $cm^{-2}\cdot s^{-1}$. The results of the calculations are tabulated in Tables V, VI and VII. The following conclusions could be reached:

1. The equilibrium mass of all actinides in the fast reactor stationary mode is 40 times higher than in the thermal blanket.
2. The main contributions to the actinides mass are made by: ^{237}Np (18%), ^{238}Pu (26%), ^{241}Am (15%), ^{242}Cm (4%) and ^{243}Cm (9%) in the fast reactor and

   ^{237}Np (15%), ^{239}Pu (2.9%), ^{241}Am (4.9%), ^{242}Cm (37%), ^{244}Cm (16%) and ^{246}Cm (13%) in the thermal blanket.

TABLE III. NEUTRON CONSUMPTION FOR FP's TRANSMUTATION

Nuclide, I	$T_{1/2}$ (years)	σ_c	R_i
^{90}Sr	28.8	5.94×10^{-2}	2
^{137}Cs	30.17	6.23×10^{-2}	3
^{151}Sm	93	4.16×10^{-3}	30-250
^{99}Tc	2.14×10^{5}	6.15×10^{-2}	1.15-1.5
^{93}Zr	1.5×10^{6}	6.35×10^{-2}	150
^{126}Sn	1.0×10^{5}	5.72×10^{-4}	-
^{79}Se	6.5×10^{4}	4.49×10^{-4}	1.5
^{135}Cs	3.3×10^{6}	6.55×10^{-2}	-
^{107}Pd	6.5×10^{6}	1.42×10^{-3}	-
^{129}I	1.6×10^{7}	7.68×10^{-3}	2

TABLE IV. SECONDARY RADIOACTIVITY IN INCINERATION OF NUCLIDES CONTAINED IN 1 TONNE OF THE VVER-1000 SPENT NUCLEAR FUEL

Nuclide I	m_i, g/t	$m_iQ_i^{(0)}$, Ci/t	$m_iQ_i^{(2)}$, Ci/t	$m_iQ_i^{(2)}$, Ci/t
^{90}Sr	678	9.4×10^{4}	2.2×10^{4}	4.3×10^{4}
^{137}Cs	1460	1.3×10^{5}	4.8×10^{4}	9.1×10^{4}
^{151}Sm	14.9	405	4.5×10^{3} - 2.2×10^{4}	$(0.7 - .75)\times10^{4}$
^{99}Mo	950	16-2	2.0×10^{6}	4.0×10^{6}
^{93}Zr	907	2.3		
^{126}Sn	22.4	0.64		
^{79}Se	5.9	0.41	165	320
^{135}Cs	422	0.486		
^{107}Pd	254	0.13		
^{129}I	220	0.039	$5.\times10^{3}$	9.7×10^{3}
Total without Zr, Sm		2.4×10^{5}	9.2×10^{4}	1.7×10^{5}
Total without Zr, Sm, Cs, Sr			$(2.1-2.7)\times10^{4}$	$(4.1-5.1)\times10^{4}$

Note: The secondary radioactivity $m_iQ_i^{(2)}$ is caused basically by ^{90}Sr and ^{137}Sr

3. The long-lived activity of actinides in the fast reactor is 40 times higher than in the thermal blanket. The long-lived activity in the fast reactor is 34% due to ^{238}Pu and 54% to ^{244}Cm and is 90% due to ^{244}Cm in the thermal blanket.
4. T_l, the value of the radiotoxicity for long-lived actinides in the fast reactor is 100 times higher

than in the ADS thermal blanket. The value TI_{Ac} corresponding to a stationary amount of long-lived actinides in the fast reactor is 33 times higher than the TI_{Ac} for its own annual replenishment. For the thermal blanket the TI_{Ac} is 3 times less than TI_{Ac} for the annual replenishment. These results demonstrate the ecological hazard of actinide transmutation in fast reactors and the advantages of the ADS thermal blanket.

(Note: the above results have been obtained without considering the change in radiotoxicity of actinides during SNF radiochemical processing because of irreversible losses).

The analytical mentioned studies made it possible to chose FPs and actinides for transmutation. With consideration of the above mentioned characteristics, and taking into account conclusions made in the work performed by RRDIPT and the Radium Institute [16], it is advisable to transmute the following FPs and transuranium elements: ^{14}C, ^{79}Se, ^{99}Tc, ^{107}Pd, ^{126}Sn, ^{129}I, ^{135}Cs and ^{137}Cs (possibly during their isotopic separation) and Np, Am and Cm using Plutonium for the generation of excess neutrons.

D.4.2.7. THE USE OF THE WEAPON- AND REACTOR-GRADE PLUTONIUM IN ADS.

The investigations carried out by ITEP and other institutions demonstrate that existing power reactors and reactors under development are, despite the technical measures taken, are not guaranteed free from accidents such as those dealing with reactivity (accidents with a change in the core reactivity). The probability of an accident associated with reactivity increases when Plutonium fuel is used in thermal reactors because a decline in the safety parameters occurs. According to calculations performed by specialists from the Physical Power Institute RSC (Obninsk) for example the temperature and power coefficients of reactivity are increased in the VVER-500 reactor when MOX-fuel is used (4.8% and 2.7% instead of 3.6% and 2.1% respectively),the k_{eff} value is decreased (from 6.0×10^{-3} to 4.4×10^{-3}) with a condition that the efficiency of the operating groups of the CPS rods is decreased by a factor of 1.3 [17].

The addition of actinides to Plutonium fuel results in a degradation of the safety features of fast breeders. These features of Plutonium, especially of weapons-grade, require special approach for using Plutonium as a nuclear fuel for the atomic power industry. In the ITEP specialists opinion an ADS operation with a subcritical blanket permits us to exclude accidents associated with reactivity, firstly accidents such as reactor runaway on prompt neutrons. The ADS safety level could therefore be in principle substantially higher than that of power reactors with a critical core. This fundamental advantage gives grounds for using weapon-grade and power Plutonium as nuclear fuel for power generation and excess neutrons production in an ADS.

D.4.3. PHYSICAL FEATURES AND PERFORMANCE ACCELERATOR DRIVEN SYSTEMS (ADSs)

D.4.3.1. PHYSICAL FEATURES

D.4.3.1.1. Target

The ADS target principally transforms the energy of charged particles taken from an accelerator into the energy of neutrons produced by reaction with the target nuclei. The following factors have a significant effect on the efficiency of this transformation process:

1. The type, energy and intensity of the charged particle flux.
2. The possibility of developing a charged particle accelerator with specified parameters and minimum possible losses of charged particles in the acceleration process.
3. The target material.
4. The possibility to remove the heat generated in the target as a result of charged particle interaction with target nuclei.
5. Economic characteristics.

At the same time there is a simple criterion which can be used in considering items 1 and 2, that is n/p, the number of neutrons generated per proton interacting with the target nuclei.

The general requirement on ADS power efficiency has also been taken into consideration in the analysis of these factors. This requirement is related to the fact that ADS power consumption, especially in the HLW transmutation regime, should not exceed 30% of the power generated in a NPP as was demonstrated in studies conducted by specialists from the Moscow Physical Engineering Institute.

The following types of charged particles have been considered in ITEP during the conceptual study as possible for use in ADS: protons, deuterons, and α particles. Analysis of the available data on the neutron yield in spallation reactions of these particles at the same energy and with the same target material shows that the value of n/p is 10-15% higher for deuterons than for protons and α particles. It should be emphasized, however, that protons are preferable from the point of view of ensuring the required low level of particle losses in the acceleration process. It should be noted that such particle losses will determine the level of induced activity of accelerator structures and, consequently, the possibility of accelerator maintenance without use of remote technology and devices.

The available experimental data testify that the proton energy range of 1.0-1.5 GeV is preferable from the point of view of increasing the neutron yield in spallation reactions. A proton energy equal to 800 MeV has been chosen for an ADS demonstration facility bearing in mind the experience with development and operation of linear accelerators in LANL (USA) and the Institute of Nuclear Physics (Troitsk, Russia).

To increase the neutron yield, i.e. the value of n/p, it is necessary to use materials with a large mass number, for example, Plutonium, neptunium, Uranium, Thorium, Tungsten, Lead, and Bismuth, as target materials. A significant (up to 50%) absorption of neutrons generated in spallation reactions is observed in multiplication-type targets (made of such materials as Uranium, Thorium, neptunium, Plutonium) according to calculations performed in various Russian research institutes. Therefore, it is inadvisable to use targets made of fissile materials for ADS with target and blanket placed separately and designed for purposes of HLW transmutation. Lead and Lead-bismuth eutectic have the lowest absorption of neutrons generated in the target through spallation reactions.

The yield of neutrons per proton, or n/p, is 35 at a proton energy of 1000 MeV for Lead [21]. Comparison of Lead and Lead-bismuth eutectic demonstrates that they could be used as target materials. Lead, however, has some disadvantages: high melting temperature (327.44 °C), high coefficient of temperature expansion (28.5×10^{-6} K^{-1}). Pb-Bi eutectic (56.5% Pb, 43.5%) have the following features: melting temperature - 125 °C, a density of appr. 9.83 kg/m^3, a low thermal expansion coefficient [22]. The disadvantage of this eutectic is the production of ^{210}Po in a neutron flux. Taking into consideration the existing experience with application of Lead-bismuth eutectic in transport reactors it is advisable to accept it as the target material in ADS because of the existing advantages of this coolant (low melting temperature, high yield of neutrons per proton, mastered technology).

D.4.3.1.2. Types of fuel and associated fuel cycle technologies

Among fuel materials the oxides of Uranium, Plutonium, and their mixtures should first be noted. This is because all actinides are alike in their chemical properties and oxide fuel materials are the most advantageous for the production of fuel element cores with doping of minor actinides (MA) and fission products (FPs). If MA could reside in solid solutions with the oxides of the fuel elements, then some fragmented elements could form precipitates of excess oxide phases in the fuel matrix, or phases of more complex composition, and some elements (elements of the platinum group, alkaline elements) could form metallic precipitates. This, however, has little effect on the radiation resistance of the core. Oxides of Uranium and Plutonium, even with a doping of several percent of americium, have demonstrated good radiation resistance during their burnup at a level above 10% of the heavy atoms with fairly good economic feasibility for production. A sufficient data base of operational data has been accumulated on dioxides of Uranium, Plutonium, and their mixtures.

Fuel materials where the fissile component is distributed in an inert oxide matrix should also be designated as oxide fuel materials. Such compositions were considered for the first time during an assessment of the possibility of designing fast reactors with a core containing only Plutonium oxide and with breeding occurring only in the reflector which surrounds the core. A range of materials could be viewed as inert oxide diluents, including BeO, MgO, Al_2O_3, ZrO_2, CaO, La_2O_3, Nb_2O_5, SiO_2, SrO, TiO, V_2O_5, etc. The above mentioned set consists of rather high-melting and resistant oxides which have low parasitic capture of neutrons. Compact pellets for clads could be manufactured from a powder made of these materials mixed with an oxide powder of MA. Tentatively, the thermophysical features of the most preferred oxides are given in Table IV.

TABLE IV. THERMOPHYSICAL FEATURES OF INERT MATRIX OXIDES

Material	Melting temperature, °C	Thermal conductivity, W/mole °C (1000°C)	Heat capacity, kcal/mole °C
MgO^x	2825	7.5	12.31
ZrO_2	2700	1.65	18.72
Al_2O_3	2050	-	30.79
SrO^x	2650	-	13.38
CaO^x	2600	≈ 3.0	13.38

[x] Material interacts with water

The selection of materials, the design and technology of fuel element manufacturing should be looked at first of all from the viewpoint of economic feasibility of the whole closed fuel cycle. Reliability should not be provided at any cost. One of the main requirements is for ease of radiochemical reprocessing. This involves both cost assessments and environmental assessments. For example, the application of the fuel composition in the form of nuclear fuel dispersions in a neutral aluminum matrix has a clear disadvantage. Dissolution of the matrix material is necessary, and in spite of the low parasitic capture cross-section of neutrons in aluminum this produces a great amount of liquid radioactive waste which must be concentrated

and rendered harmless.

MA which are produced as matrix solid solutions with high thermodynamic characteristics are easily introduced into mononitride fuel. Besides, the recovery of the mononitride fuel (or carbide) could be performed using the technology of oxide fuel recovery (the PUREX-process) with the same equipment. In doing so the process of nitride fuel dilution in nitric acid proceeds quiescently with great completeness and a high rate. The above types of fuel allow rather economic manufacture of fuel elements and radiochemical reprocessing without clad dissolution. With a guaranteed provision that the temperature on the interface of the metallic fuel core, with metallic cladding of the fuel element, does not exceed 450-500°C in any of the possible modes of ADS operation, it is quite possible to use metallic fuel.

At the present time hydrometallurgical methods for radiochemical reprocessing of spent fuel elements are being industrially developed. They are based on the dissolution of SNF in nitric acid, with subsequent extraction of the fissile component and waste reprocessing. It has been demonstrated that completion of the radiochemical reprocessing of fuel elements by fractionation of radionuclides according to half lives and radiotoxicity is economically and environmentally advisable, as well as from the viewpoint of utilization of radioisotopes. In this case the possibility of keeping MA and long-lived FPs not subject to disposal for further transmutation can also be considered.

Although extraction technologies for actinide concentration permit a drastic reduction in the amount of liquid radioactive waste, the problem of its further concentration, thickening, solidification, and water purification exists. All these processes are power-intensive.

The possibilities for drastic reduction in the amount of water used are in the application of high-temperature methods of spent fuel element reprocessing. In the case of the use of power or weapon-grade Plutonium as a material for production of fuel without oxygen (mononitride, monocarbide) it is advisable to use an electrochemical process for the recovery of irradiated fuel in melts.

Also of some interest are technological processes for crystallization of MA dioxides of mixed composition from molten salts. Along this pathway the number of technological procedures in the cycle of spent fuel element reprocessing could be significantly reduced.

D.4.3.2. PERFORMANCE OF THE ADS SYSTEMS

D.4.3.2.1. ADS schematic diagram

There are two alternative designs of the ADS: one with a horizontal (version A) and the other with a vertical (version B) placement of the target and blanket (Fig.2). In accordance with an investigation conducted by specialists from the Special Design Bureau of Machine Building (SDBMB) in Nizhny Novgorod the vertical arrangement of target and blanket is preferable [18]. The use of one, two or more ADS modules operating from one accelerator is possible. The number of modules is determined by a number of factors, the first being the end use of the ADS.

The choice of a vertical arrangement predetermines the need to turn the beam 90° which requires the installation of a magnetic system. In the case when two or more modules are used it is necessary to divide the proton beam from the accelerator into two or more beams. In this event it is necessary to provide for the development and installation of the relevant device. Because a large amount of power is generated in the target and blanket, systems for heat removal and power utilization should be provided in ADS.

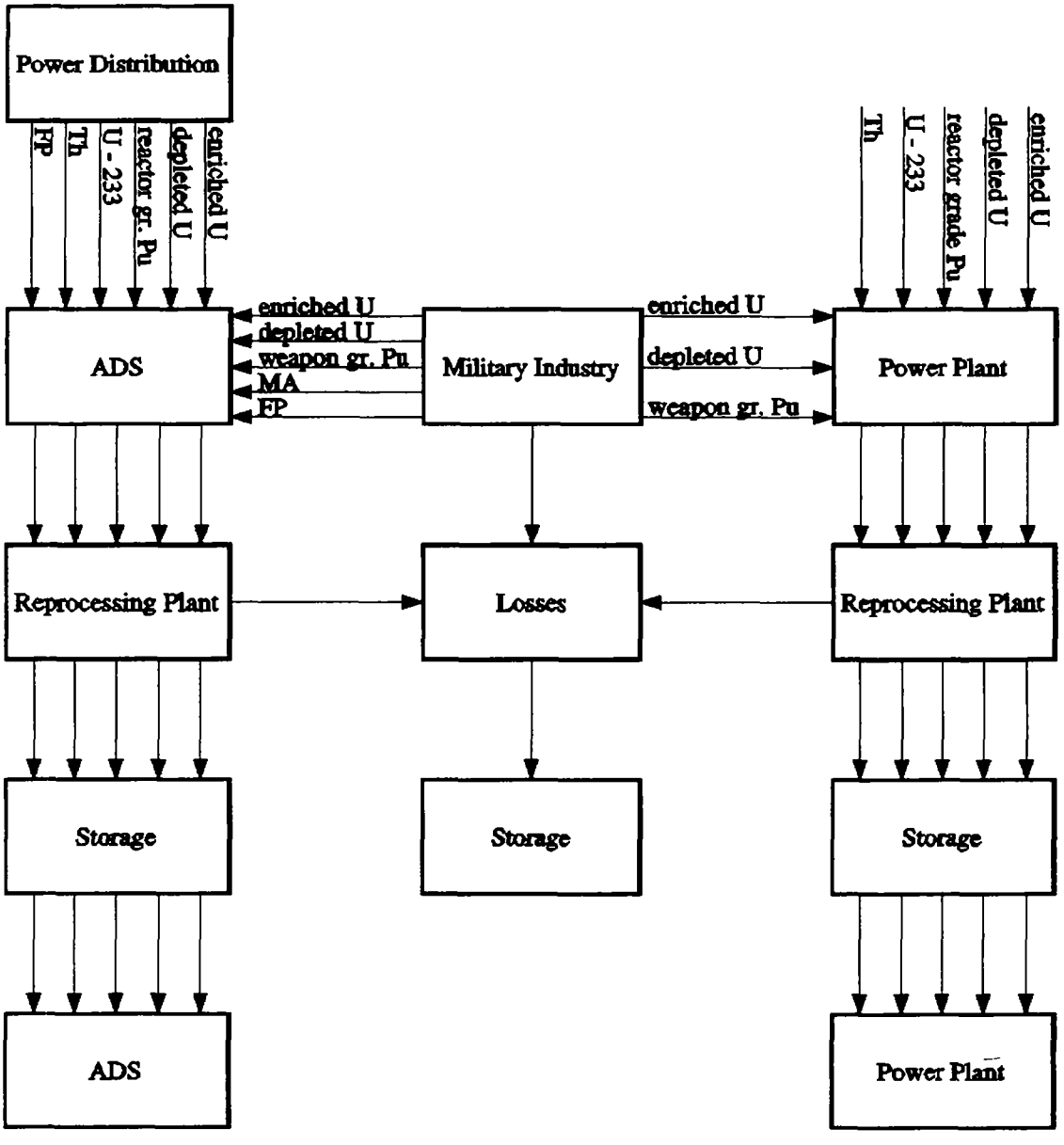

FIG.2 Closed fuel cycle at the nuclear power facility

D.4.3.2.2. The conceptual design of the blanket

In the present concept the development of the blanket design has been performed along several lines on the basis that heavy-water is used as coolant and moderator. The choice of heavy water is explained by the possibility of having significant irradiated space for placement of the target and fertile materials. Below a description is given of alternative conceptual blanket designs proposed by ITEP:

1. A blanket design with solid fuel.
2. A blanket design with liquid fuel and a modular (channel) blanket.
3. A design with liquid fuel and a homogeneous blanket.

In the solid fuel alternative a MOX-fuel or a Plutonium fuel without natural or depleted Uranium in

an inert matrix is considered. In this version targets and fertile materials could be used in a solid and liquid state located either in technological channels or in special loops. It should be emphasized that the solid fuel version is based on verified technical approaches which increase the possibility of its implementation. At the same time repeat radiochemical reprocessing of the SNF is necessary because of restrictions on the value of fuel burnup, which increases irretrievable losses during reprocessing.

In the second version the main units of the modular ADS are liquid fuel assemblies placed in the form of a channel array in the heavy-water moderator of the ADS proposed by ITEP specialists V.D. Kazaritsky, B.P. Kochurov and V.R. Mladov [19]. The design of the liquid-fuel heat generating assembly is shown in Fig.3 . As can be seen from Fig. 3 there are two circuits inside a channel: the fuel circuit (the solution or suspension of Plutonium dioxide in heavy water) and a circuit of heavy-water coolant under pressure. The coolant is circulated in the channel and leaves the blanket for chemical reprocessing only. Part of the fuel is continuously directed to reprocessing, is fractionated and actinides are returned into the fuel circuit; the remainder is subject to further reprocessing, fractionation, storage, transmutation and disposal.

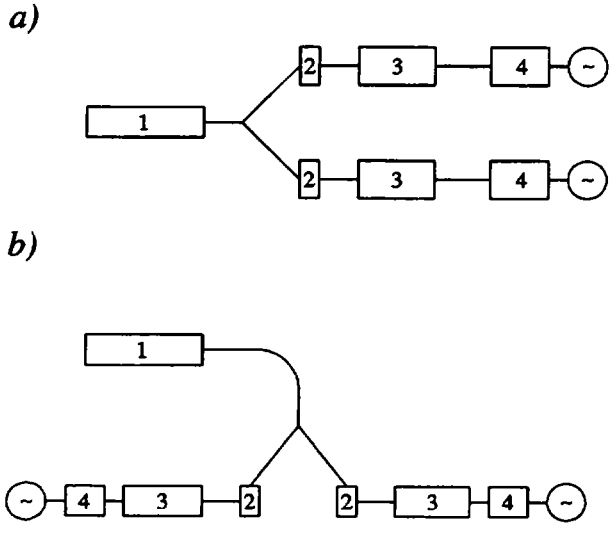

FIG. 3 A conceptual scheme of the accelerator-driven system. a) horizontal target system; b) vertical target system. 1 - linac, 2 - target, 3 - blanket, 4 - energy transformation system.

In the third version the blanket is a cylinder with a liquid metal target placed on the blanket axis and filled with liquid fuel in the form of a solution or suspension of MA in heavy water. A heat exchanger for heat removal is placed directly above the blanket so that the time that liquid fuel stays outside the irradiation zone is minimized. Maintaining the concentration of actinides at a level of appr. 10 g/l, the lack of constructional materials in the blanket and continuous purification from FPs makes it possible to provide a thermal neutron flux, averaged over the blanket, exceeding 10^{15} neutron/cm^2 s and to operate without nuclear fuel replenishment (or with small additions of Plutonium). One such facility proposed by B.R. Bergelson and S.A. Balyuk permits the destruction of actinide radioactivity generated by several tens of VVER-1000 power reactors.

Some performance data for these versions of blanket operation are given in Tables V, VI, VII.

D.4.3.3.3 The conceptual target design

ITEP specialists, together with specialists from the Physics Power Institute (Obninsk, Russia) and the Special Design Bureau for Machine Building (Nizhny Novgorod, Russia) are now studying two types of targets:

- a solid target made of tungsten and other materials for low values of the proton current (up to 30 mA);
- a solid target made of tungsten and other materials for low values of the proton current (up to 30 mA);
- a liquid target made of Lead or Lead-bismuth eutectic for high values of the proton current.

TABLE V. ADS BLANKET PERFORMANCE DATA FOR WEAPON-GRADE Pu.

ENR thermal power	2200 MW
ENR electrical power	680 MW
Linac electrical power	100 MW
Coolant pressure	10 MPa
Coolant temperature:	
input	226°C
output	310°C
Number of linacs	1
Number of target and blanket modules	2
Proton beam power	30-60 MW
Proton energy	800 MeV
Proton current	28 mA
Target:	
material (solid target)	Cu or W
cylinder size	3000×6000 mm^2
Neutron source intensity	3×10^{18} n/s
Power density in target	30 MW
Multiplication factor, k	0.97
Blanket power	1100 MW
Mode of the fuel replenishment	continuous
Number of channels in blanket	380
Lattice pitch	280 mm
Weapon-grade Plutonium consumption	850 kg/a

TABLE VI. ADS MAIN PERFORMANCE DATA FOR ^{237}Np TRANSMUTATION

ACCELERATOR	
proton energy	1.6 GeV
proton current	0.3 A
TARGET	
inner diameter	0.38 m
material	Pb
proton to neutron conversion ratio	50 n/proton
neutron source intensity	9.36×10^{19} n/s
BLANKET	
thermal power	1.8 GW
core height	2.5 m
diameter of the core with Np	2.12 m
multiplication factor, k	0.572-0.598
thermal neutron flux	3×10^{15} n/cm^2·s
Np incineration rate	484.6 kg/a

There are two important problems related to normal operation of the target:

- the permissible target power with consideration for the need to divide and expand the proton beam;
- the possibility to operate without a separating membrane ("window") so as to exclude losses of protons and the need for removal of the membrane in the process of ADS operation.

D.4.3.3. LINAC [23]

The proton linear accelerator has been selected on the basis of a set of considerations. Among these are:

- the high level of scientific and technical R & D based on new methods of charged particle acceleration (RFQ - radio frequency quadrupole) which have been developed and verified at ITEP and have been

TABLE VII. PERFORMANCE OF THE ADS MODULES

TARGET	
material	Pb
BLANKET	
height	2.5 m
diameter (with reflector)	5 m
type of assemblies	CANDU with pressure tubes
number of assemblies	250
pressure tube size:	
Inner tube radius	5.42/5.0 cm
outer tube radius	6.23/5.81 cm
pitch (hexagonal lattice)	23.8 cm
tube material	Zr-Nb
moderator	D_2O with dissolved nitrite salts, Tc, Th
Module thermal power	1800 MW
Module electric power	600 MW
ADS life cycle	30 years
Pu initial load in each module	305 kg
Subcriticality level	0.97-0.98
Pu consumption in 30 years	100 tonnes
^{233}U production in 30 years	78 tonnes
Transmutation of ^{99}Tc, ^{129}I, and partially Sm from ADS	

widely used in modern accelerators in various countries worldwide;

spallation reactions in the target;

- the possibility to achieve a low value of proton losses at a high beam density.

- the high efficiency of medium energy protons (1000 - 1500 MeV) for neutron generation because of The linear accelerator consists of 3 parts: initial, intermediate, and final (see Fig. 3). The initial part is an electrostatic generator with a voltage level less than 100 kV and an accelerator with a RFQ and a proton energy equal to 3 - 5 MeV. The intermediate part is an Alvarez accelerator (a Drift Tube Linac, DTL) to accelerate protons from the initial energy up to 100 - 150 MeV. The final part provides acceleration of protons to an energy of 1.5 GeV using disk and washer or DAW-structures.

The selection of operational frequencies for RFQ, DTL, and DAW should provide a margin for channel throughput necessary from considerations of radiation safety. An optimum relation should be found, however, since the rise in throughput, which requires a decrease in operational frequencies is accompanied by a sharp increase in geometric size and the weight of resonators, the area of the working surfaces and losses of RF power in the copper, i.e. a sharp rise in the cost of construction and operation. The selection of the transition energy from one structure to another should also be optimized.

The Moscow Radio Technics Institute has also proposed another design for the initial part of the accelerator with focusing which uses a superconducting solenoid. This is supposedly possible, although practical implementation will require the solution of a variety of complex technical problems (thermal isolation of the external superconducting solenoid and thermal resonator, marginal effects, etc.).

The following part of the DTL is an Alvarez accelerator with drift tubes as studied comprehensively on pulse accelerators. We must note that positioning of the focusing lenses in the narrow space of the drift tubes seems to be a problem which is difficult to solve. Quadrupole lenses with rare-earth magnets (REMs) provide the necessary focusing, have small overall dimensions, high operational frequency, and reduce the RF power consumed. The radiation resistance of REM materials is insufficient compared to electromagnetic lenses with mineral isolation of the windings, however, which could make one abandon REM lenses, although this will increase the overall lens dimensions and the power consumed noticeably.

As regards the final part of the accelerator, there are at least 3-4 types of resonators with the necessary parameters. The first is the disk and washer (DAW) type proposed and developed by V.G. Andreev at MRTI. The peculiarity of the structure proposed by V.G. Andreev is its lower sensitivity to drift in geometric size (for example, under temperature deformation) and it is preferable in our opinion.

One of the possible circuits for a high current (up to 300 mA) linac is a design with one acceleration channel proposed by ITEP. Detailed calculations confirm the possibility of constructing such a linac. A characteristic feature of the proposed design is the reduction in the bunch phase extension at the transition from one structure to another. The existing abrupt change (from 150 to 900 MHz, i.e. an increase by a factor of 6) in the operational frequencies of the DTL and DAW sections gives rise to certain concerns. At the present time other alternatives in the selection of operational frequencies are being considered at ITEP, especially as we have already accumulated practical experience in operating 300 MHZ resonators.

The operation of the multiresonator linac can not be ensured without systems which maintain the design parameters of the accelerating RF field within specified tolerances. Among such systems are:

- the field amplitude automatic control (AAC);
- the phase automatic control (PAC) between resonators;
- the master oscillators with quartz crystals;
- the multifunctional timer in the form of a specialized computer connected to simpler computers which control processes in each technological system.

The great power of the accelerated beam and the hazard of radiation contamination of the linac equipment determine the importance of developing a rigid hierarchy of command algorithms in all interrelated automatic control systems which manipulate the operation mode of the machine.

The most complex part, from a technological point of view, is the RF power supply system, namely its reliability and efficiency. The industrial facility should operate 75% of the total service time, that is 6,570 hrs per year with a reliability of no less than 85%, the reliability of the RF system in this case should not be worse than 90%. In the 25% of the time planned for stops, all scheduled and unscheduled preventive maintenance, as well as machine adjustment and tuning with and without beam should be carried out. These requirements are very stringent, and to meet them new generating devices should be developed which are optimized for the parameters specified by the design of the facility.

D.4.3.4. RESEARCH AND DEVELOPMENT

D.4.3.4.1. Technical problems of ADS development. New technologies

The blanket is the most complex unit in ADS. It is complex because it is desirable to provide a high value of the thermal neutron flux exceeding $5x10^{15}$neutron/cm^2 s. Therefore it is necessary, firstly, to find a possibility of increasing the density of power generation in comparison with the value achieved in existing power reactors, without a decrease in safety level. Secondly, it is essential to experimentally substantiate the possibility of using a sectioned blanket [20] with a neutron valve without a decrease in safety level. Thirdly, in the case of fuel and target in liquid form it is necessary to develop a technology for removing undesirable impurities from the irradiated materials. It is also essential to substantiate the radiation resistance of Plutonium fuel with the addition of minor actinides if such a version is to be accepted. It is necessary to check the possibility of implementing ADS protection from a sudden loss of the electric power supply or a break in the rods of the accident protection system.

In the case of a liquid target a problem emerges of developing the membrane ("window") which divides the space used by the target and accelerator, it should have a minimum absorption of neutrons, should be manufactured of heat-conducting material (or have cooling) and should be remotely replaceable when a specified neutron fluence has been achieved. It is also advisable to investigate the possibility of

using a separating membrane. It is a difficult problem. A technology for purification of the target material should be developed. To provide an acceptable value of power generation in the target from interaction with a proton beam, two complex technical problems should be solved:

1. Separation of the proton beam into several beams with lower intensity;
2. Expansion of the proton beam to the size needed.

Rather complex technical problems face the proton accelerator designers. One of these problems is related to the development of a reliable RF-power supply for the accelerator. Existing 1 MW klystron generators with an efficiency of 60-70% have a short service life and poor reliability. The second problem is to guarantee the required level of proton losses at various stages of acceleration. In accordance with calculations performed at ITEP by Prof. Kapchinsky the beam losses should be appr. 10^{-6} of the rated value. Specialists at ITEP and other institutes dealing with these problems reason that existing technical problems in ADS development could be solved, provided that the necessary finance and specialist effort will be concentrated on them.

D.4.3.4.2. Need for ADS R&D

To justify the feasibility of ADS a set of experimental studies should be carried out to verify parameters obtained analytically, as well as safety and reliability levels. The main design solutions should be verified for the following systems and technologies:

- blanket;
- target;
- accelerator;
- control and protection system (CPS);
- technology of the rapid purification of fuel and target materials in a liquid state.

A large amount of work should be done to compile the necessary nuclear data bases. In accordance with the decision of the Scientific and Technical Council of the Ministry of Atomic Power of the Russian Federation a program of R&D has been set out for 1995-2000 which provides for R&D on both ADS and fast reactors for incineration of actinides.

With regard to ADS the following experimental studies are included in this program:

1. Modeling of various alternative designs of the blanket with a subcritical assembly driven by a 36 MeV proton accelerator. For this purpose the program provides for the construction of an experimental facility called the "Transmutation Neutron Source" (TNS) using the building and biological shielding of the heavy-water research reactor (HWR) existing at ITEP. Beryllium will probably be used as the target material. The "Istra-36" experimental proton accelerator already exists at ITEP and when tested at a pulse current of 200 mA, will also be used.

The main goals of the experimental facility are [24]:

- its application as a full-scale physical model of the blanket for a power transmutation facility;
- development and verification of the ADS control and protection system;
- fundamental investigations (values of constants for actinides and FPs from interaction of protons with matter, production and use of ultracold neutrons, etc.).

The Transmutation Neutron Source will have the following parameters:

- proton energy, E_p = 36 MeV;
- proton pulse duration, T_p = 150 μs;
- proton pulse current, I_p = 150 mA;

- average proton current $I_p = 0.5\ \mu A$;
- proton pulse energy, $W_p = 5.4$ MW;
- intensity of the target fast neutron flux $1.5 \times 10^4\ s^{-1}$;
- k_{eff} of the starting blanket 0.95
- starting blanket power 25 kW;
- thermal neutron flux $1.5.10^{12}$ neutron/cm^2 s;
- blanket load with ^{235}U (90%) 2 kg.

The commissioning of this facility will be determined by the level of funding, which is insufficient at present.

2. The study of heat deposition in various targets as the result of interaction with protons, investigations of the yield of neutrons and gamma-quanta in spallation reactions and rates of reactions.

3. Investigation of the interaction cross-sections of protons and neutrons with FPs and actinides.

4. Analysis of the hydrodynamics of the liquid target models.

5. Experimental verification of certain accelerator units.

6. Analytical studies of the radiation load on population and operating staff during ADS service.

This work will permit the start of ADS design development not earlier than 1998. At the same time an analysis of ADS feasibility and a site selection for construction of a demonstration facility will be performed.

D.4.3.4.3. Engineering problems of materials

The selection of structural materials depends on the accepted design and the end use of the ADS. Information is given below about possible technical approaches to the selection of structural materials for various designs of the target and blanket.

1. Target materials

It was pointed out above that tungsten, Lead or Lead-bismuth eutectic could act as possible target materials. The selection of the target material will be performed at the stage of conceptual studies. At the present moment it is possible only to note the fact that experimental data on the radiation and thermal behaviour of these materials under the prolonged effect of proton and neutron fluxes are unavailable although they are rated in the radiation resistant class. Their behaviour should therefore be studied during operation of the demonstration ADS.

The technology of Lead-bismuth eutectic has been mastered fairly well in relation to its use as a coolant in the nuclear reactors of Russian submarines. As far as Lead is concerned as a target material, the technology for its use has not been mastered.

Besides target material selection, the selection of construction materials for the target/blanket vessel and the "separating" window between target space and accelerator should also be made in the period of conceptual studies. At this stage austenitic stainless steels are targeted for use, characterized by a maximum fluence of damaging neutrons of appr. $2\text{-}3 \times 10^{23}$ neutron/cm^2. Preliminary data are available on the possibility to increase this value. This means that a possibility for vessel and "window" replacement should be provided in the ADS design.

2. Blanket materials

The selection of structural materials for the blanket is determined by the requirement to ensure high radiation, thermal and corrosion resistance during operation. In the case of the solid-fuel design the selection is facilitated by the fact that positive experience is available from the application of construction

materials in nuclear power reactors of various types. Zirconium alloys and stainless steels are used in reactors using water and liquid metals as coolants, and austinite and special steels are used for reactor vessels. The only point which is unclear is the selection of the material for technological channels in the case when liquid-phase target materials are used. For the design with liquid fuel in the form of Plutonium or actinide salts dissolved in heavy water the selection will be performed at the stage of conceptual studies. At the same time there are grounds for optimism on this point in relation to the experience available in operation of equipment in radiochemical plants.

3. Problems associated with radiolysis

The problem of radiolitic generation of hydrogen is of fundamental importance for heavy-water designs with a high neutron flux density. In this respect the problems of safety provision are also of great importance.

Radiolysis of the coolant in pressurized water reactors is determined first of all by the specific character of the reactor design, mode of operation, and water-chemical conditions in the first circuit: high temperature (up to 600°K) means a considerable (up to 0.05 dm^3kg^{-1}) hydrogen concentration in the first circuit water. The total decomposition reaction could be presented as

$$2H_2O = 2H_2 + O_2$$

In this case the reaction is strongly displaced to the left even at hydrogen concentrations higher than $2x10^{-4}$ mole kg.

For water homogeneous reactors the problem of radiolysis is the most serious. In these reactors all fission energy is essentially released in water, with the major part in the form of kinetic energy of highly ionizing fission fragments. The results of this are high yields of molecular products, radiolysis and insignificant yields of radicals.

Heavy-water nuclear reactors, pool-type research reactors, and power reactors supplied with a de-aerator can be fitted into the group of reactors with a renewed atmosphere. In some of these reactors the water surface is continuously blown by an inert gas.

In the of nuclear power facilities with VVER-type reactors the hydrogen concentration, from $1.3x10^{-3}$ to $2.8x10^{-3}$ mole/dm^3, is kept in stationary conditions in the circuit water. This guarantees virtually complete suppression of radiolysis. Ammonia is used for maintaining such concentrations of hydrogen. In this case its content in solution is kept in the range of $1.76x10^{-3}$ to $3.5x10^{-3}$ mole/dm^3 respectively. About one quarter of the ammonia is subjected to radiolytic decomposition; the yield of the ammonia decomposition is proportional to the ratio of ammonia to hydrogen in the coolant. The effect of a high concentration of hydrogen on this ratio depends on the competition between hydrogen and ammonia when reaction with OH radical is in progress. The stationary ammonia concentration, once established, is maintained through the use in the water purification system of a cationic exchanger in ammonia or ammonia-potassium form which has superior buffer effect.

All kinds of conceptual approaches to the development of ADS and transmutation facilities wherein the application of heavy-water media is anticipated are repeatedly hindered by the need to solve of the radiolytic gas emission problems, which actually seen to be tractable on the basis of the results of targeted investigations and reactor tests. It has been determined, in particular, that some materials dissolved in heavy water containing, for example, ions of Copper, Nickel, Cobalt, Lead, etc. are capable of acting as homogeneous catalysts for thermal combination of Deuterium and Oxygen. The effect of salts containing bivalent Copper has been studied in most completely. The creation of a certain concentration of bivalent copper in the heavy-water medium (solution of the fissionable radionuclide salt or suppression based on fissionable radionuclides) at certain temperatures and pressure is capable of reducing radiolytic gas emission practically to zero. In doing so, the concentration of Copper ions remains at the initial level because there are no conditions for Copper restoration in the operational volume. This does not lead to a

need for additional introduction of a Copper containing compound in the circuit and, which is more important, does not establish conditions for metallic Copper deposition on the metalwork.

Corresponding analytical and pilot data demonstrate that the value of bivalent Copper concentration necessary to suppress radiolytic gas emission depends, for a specific facility, upon the optimum combination of the specific power density and temperature of the Deuterium partial pressure, via a system whereby the concentration of the bivalent Copper and Deuterium dissolved in the aqueous medium would be kept at a technically acceptable level.

With a concentration limit for bivalent Copper of ≤ 0.1 mole/dm^3 corresponding to the macroscopic cross-section of 2.2×10^{-4} cm^{-1} and a technically acceptable concentration of Deuterium dissolved in the heavy-water medium corresponding to a partial pressure of 1.0 MPa, the permissible specific power density should not exceed a value of 20 kW/dm^3 (at 523°K) or 130 kW/dm^3 (at 573 K) in the event of the application of heavy-water salt solutions, and 100 kW/dm^3 (at 523°K) or 260 kW/dm^3 (at 573°K) in the event of the application of heavy-water suspensions.

Taking into consideration the importance of the problem of radiolysis, as well as tritium build up in heavy-water systems a R&D program is being developed to investigate this problem under real reactors conditions.

ACKNOWLEDGEMENTS

Author would like to acknowledge an invaluable assistance of the experts from SSC RF ITEP: Drs B.Bergelson, A.Gerasimov, B.Kochurov, V.Lazarev and O.Shvedov and of MEPI prof.A.Shmelyov who examined this review.

REFERENCES

[1] N.N. Egorov. Organization of the Nuclear Wastes Management in Russia. Information Bulletin, No. 5, 1993, pp. 22-27.

[2] B.R. Bergelson, S.A. Balyuk. Parameters of a facility for minor actinides transmutation without use of nuclear fuel and with small additions of Plutonium. ITEP preprint No. 10-94, 1994.

[3] T.S. Zaritskaya, G.V. Kiselev, A.K. Kruglov, A.P. Rudik. Physics of light-water reactor spent nuclear fuel burnuot in heavy-water reactors. VANT, Physics of nuclear reactors series, 1991, issue 6.

[4] B.R. Bergelson, S.A. Balyuk. The Concept of the Double Purpose Electro-Nuclear Facility. Report for International Conference on Accelerator-Driven Transmutation Technologies and Application, July 25-29, 1994, Las Vegas, USA.

[5] A.S. Gerasimov, T.S. Zaritskaya, G.V. Kiselev. Possibilities to lower requirements for Plutonium purification as nuclear fuel. ITEP report No. 889, 1994.

[6] A.N. Shmelyov, G.G. Kulikov, V.A. Apse. Physical aspects of the weapon-grade Plutonium conversion in fast reactors. Izvestiya Vuzov, Ser. Yadernaya energetika, No. 1, 1993, pp. 59-64.

[7] A.S. Gerasimov, T.S. Zaritskaya, G.V. Kiselev, A.P. Rudik. Comparison of the radiological hazard of fast neutron reactors and electro-nuclear reactors under LLRW and Plutonium transmutation. ITEP preprint No. 14-94, 1994.

[8] G.V. Kiselev, I.V. Chuvilo, O.V. Shvedov, A.S. Gerasimov, E.V. Kulikov. The application of electro-nuclear facilities in perspective nuclear power industry. Atomic power, 1994, v. 77, No 3, pp. 167-174.

[9] L. A. McVey, R.L. Brodzinski, T.M. Tammer. J.Radioanal. Chem.76(1983),131.

[10] M.A. Lone, W.J. Edwards, R. Collins. Cross section of the $^{90}Sr(n, \gamma)^{91}Sr$ for a D_2O moderated Reactor Fuel. Proceedings of International Conference Future Nuclear Systems: Emerging Fuel Cycle&Waste Disposal Options, September 12-17,1993, Seattle, Washington.

[11] G. Zeisel. Acta Phys.Austr.,23(1966),223.

[12] Stupegia, J.JNE,12,16(1960).

[13] H.Harada, W.Watanabe, T. Sekine at. al. J. Nucl. Sci. Tech. 27, 577 (1990).

[14] N.G. Basov, N.I. Belousov, et. al. Requirements for power and nuclear physical parameters of the nuclear power systems with a transmuter. MPEI preprint No. 011-92, 1992.

[15] A.S. Gerasimov, T.S. Zaritskaya, A.P. Rudik, I.V. Chuvilo. Stationary Transmutation of the Long-lived Fission Products in Nuclear Power Engineering and Secondary Radioactivity Produced in Transmutation of Long-lived Fission Products. Global-93 Proceedings, v. 1, p. 301.

[16] Physical, radiochemical and ecological fundamentals of the nuclear transmutation of fission products and nuclear fuel cycle actinides. ARDIPT and RI report, No. 6014, 1990.

[17] V.M. Murogov, V.I. Subbotin, M.F. Troyanov et. al. The Use of Weapon-Grade Plutonium in Atomic Power Industry (A Concept of U-Pu Fuel Cycle Implementation). Information Bulletin, No. 11, 1993, p. 22.

[18] The solid target - a heavy-water blanket system for electronuclear facility. Explanatory note to SDBMB design investigation, 1994.

[19] V.D. Kazaritsky, N.N. Blagovolin, V.R. Mladov. An Approach to an Accelerator-Driven Thermal Reactor and Requirements in Nuclear Data Improvement. ITEP preprint No. 32-94, 1994.

[20] The nuclear power facility. Vasiliev A.A, Grebyonkin K.F., Danilov M.M. et. al. Russian patent No. 93025526/21 of 27.04.1993.

[21] Vasillkov R.G., Barashenko V.S. et. al. Nuclear-physical aspects of the electronuclear method. OYa IP patent R2-11071,1977, Atomic Energy, 1970, v. 29, p. 151.

[22] Physical data. A handbook. Editor I.S. Grigorieva, E.Z. Meilikhova. Moscow, Energoatomizdat, 1991.

[23] I.M. Kapchinskiy, I.V. Chuvilo, A.A. Kolomiets at al. Linear Accelerator for Plutonium Conversion and Transmutation of NNP Waste. Proceedings of International Conference on Particle accelerator, May 17-20, 1993, Washington, USA.

[24] O.V. Shvedov, I.V. Chuvilo, E.V. Kulikov, V.V. Vasiliev, M.M. Igumnov, A.M. Kozodaev, E.B. Volkov, A.V. Lopatkin. ITEP subcritical neutron generator driven by charged particle accelerator. Report for International Conference on Accelerator-Driven Transmutation Technologies and Application, July 25-29, 1994, Las Vegas, USA.

D.5. BROOKHAVEN NATIONAL LABORATORY ADS CONCEPTS (USA)

Hiroshi Takahashi
Brookhaven National Laboratory
Upton, New York, 11973.

Presently three types of accelerator driven system have been studied at BNL. The first is the accelerator driven energy producer (ADEP) which is intended for energy production, incineration of minor actinides (MA) and long-lived fission products (LLFP) using a small power accelerator like a segmented cyclotron [1]. The second is the Phoenix concept [2] aimed at transmuting large amounts of MA and LLFP using a high current linear accelerator. The third is the accelerator driven particle fuel transmutor (ADPF) [3] which also transmutes the MA and LLFP at high rate by using a high neutron flux.

D.5.1. ACCELERATOR DRIVEN ENERGY PRODUCER (ADEP)

The ADEP concept is very close to the conventional Pu-fueled fast reactor which has been developed by heavy investment over the last few decades. In contrast to the fast reactor, which is run in critical conditions, ADEP runs in slightly subcritical conditions of k_{eff}=0.98-0.99 [4] by providing the small spallation source created by the segmented cyclotron with a few mA current and 3 GeV energy protons.

The Pu-fueled fast reactor has a superior neutron economy compared to a thermal reactor; the η value of Pu increases as the neutron spectrum becomes harder. However this results in a positive Na coolant void coefficient, smaller Doppler coefficient, smaller delayed neutron fraction and short neutron life time. Thus the operation of the reactor in critical condition requires very careful control [5].

By running this fast reactor even in a slightly subcritical condition these safety problems related to the criticality, especially a sudden increase of the reactivity, become greatly alleviated. The flattening of core geometry which is adopted in the fast reactor [6] for reducing the positive Na void coefficient is not necessary and the solid core with D/H can be close to 1 so that the neutron economy is improved. Thus the inventory of fissile material can be reduced, and the internal conversion from fissile or from MA material to fissile material can be increased. This will lengthen the period for which the fuel can be burnt without reprocessing, provided that the fuel can withstand radiation damage, or that the accumulation of fission products does not affect the fuel's metallurgic properties. Consequently the superior neutron economy in the subcritical reactor can be improved for transmuting LLFPs.

This reactor has Thorium oxide instead of Uranium oxide in the blanket region [7] and ^{233}U produced will be supplied to a light water reactor as fuel in place of ^{235}U. This reduces the production of MA, and due to the larger η value of ^{233}U than ^{235}U the inventory of fissile material required to start this fuel cycle can be reduced by about 70% compared the ^{235}U-fuel cycle.

The geometry of the ADEP is cylindrical as shown in Fig. 1. The proton beam is injected from the top directly into the central target through a window.

The fuel composition in the ADEP core region is ^{239}Pu + ^{238}U, and MA in the form of metal and oxide. The composition of MA is the same as that coming out of the LWR reactor (see Tables I-VI). For transmuting the LLFP such as ^{99}Tc and ^{129}I, the moderator region is installed between the outer core and the blanket region; these LLFP are transmuted by neutron capture. This installation of a moderator region makes the positive Na void coefficient lower and a smaller core makes it negative. Since it also provides a large Doppler coefficient and longer neutrons life-time, the safety of the reactor can be improved.

To increase the production of ^{233}U, this moderator region can be filled with Thorium oxide.This makes the Na void coefficient less positive without sacrificing the production of ^{233}U. The production rate of fissile

material and the transmutation rate of LLFP are shown together with the initial multiplication factor in Table I.

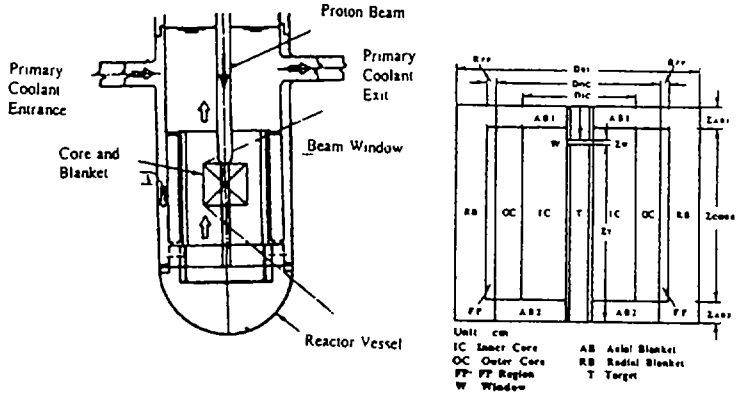

Fig. 1 The geometry of ADEP system.

TABLE I. MULTIPLICATION FACTOR, NEUTRON LIFE-TIME, PRODUCTION OF ^{239}Pu & ^{233}U. TRANSMUTATION OF MA AND LLFP, AND INITIAL BREEDING RATIO OF VARIOUS CONFIGURATIONS OF THE REACTOR

	Multiplication Factor Neutron life-time (10^{-8} s)	Production of ^{239}Pu & ^{233}U MA or LLFP Transmutation (kg)	Initial Breeding Ratio
Uranium Blanket [a]	1.0343 ± .0043 129.4	^{239}Pu 243.8	0.96026
Thorium Blanket [b]	1.025431 ± .0011 134.56 1.02423 ± .0011 1.02060 ± .0011	^{239}Pu 126.3 ^{233}U 137.9 Sum 264.2	0.98544
Thorium Blanket with 30% Th 70% YH1 in moderator region [d]	1.00154 ± .0012 0.99649 ± .0012	^{239}Pu	1.00723
Thorium Blanket Core [c]	0.9503 ± .0042 123.94	^{233}U 265.5	1.0528
Thorium Blanket 5 w% MA in core [d]	0.9808 ± .0042 123.49	^{239}Pu 122.2 ^{233}U 106.2 MA (cap.) 41. MA (fiss.) 10.9	1.02716
Thorium Blanket ^{99}Tc [e]	.9920 ± .0012 353.77	^{239}Pu 112.7 ^{233}U 60.1 ^{99}Tc 34.7	0.698
Thorium Blanket ^{129}I (30%)	1.002 ± .006 462.18	^{239}Pu 173.6 ^{129}I 34.4	0.7014

[a] Uranium-oxide (UO_2) in core and blanket (BL), [b] Thorium-oxide (ThO_2) in BL, [c] ThO_2 in core and BL, [d] ThO_2 in BL & 5 w% MA in core, [e] ThO_2 in BL & ^{99}Tc with YH1.7, [f] UO_2 in BL & ^{129}I (30%) with YH1.7.

TABLE II. SUBCRITICAL CORE COMPOSITION AND DIMENSION

Subcritical core type	ADEP (A)	ADEP (B)	ADEP (C)	ADEP (D)	ADEP (E) Blanket
Material composition Fuel/Clad+struct./ Coolant	Pu+^{238}U+MA	Pu+^{238}U+MA	Pu+^{238}U+MA	Nitrate Coated $^{232}ThO_2$ Particle Fuel	
Chemical form of fuel	Solid oxide fuel	Metal	Solid	Solid	Solid Oxide blanket
Coolant	Na	Na	Pb	He	Na
Averaged fresh fuel composition U/Pu/MA/LLFP(%)	PuO_2+UO_2+MA 72/16/10/0	Pu+U+MA+Zr 67/21/12/0	PuO_2+UO_2+MA 72/16/10/0	0/34/66/0	
Averaged composition of LLFP	93% ^{99}Tc/ 7%^{129}I	93% ^{99}Tc/ 7%^{129}I	93% ^{99}Tc/ 7%^{129}I	93% ^{99}Tc/ 7%^{129}I	93%^{99}Tc/ 7%^{129}I
Core diameter (cm)	150.	130.	150.	130.	25. Thickness
Core height (cm)	150.	130.	150.	150.	150.

TABLE III. SPECIFICATION OF FUEL AND BLANKET ELEMENTS (ADEP,ADPF)

	Pu-oxide Na coolant (A)	Pu-metallic Na coolant (B)	Pu-oxide Pb coolant (C)	Th-oxide blanket Na coolant (D)
Fuel pin diameter (mm)	7.44	5.22	9.6	9.6
Clad thickness (mm)	0.425	0.3	0.525	0.525
Fuel pellet diameter (mm)	6.43	4.4	8.6	8.6
Wire spacer diameter (mm)	1.43	1.22	2.0	2.0
Fuel smearing density (%TD)	87.6	90.	87.6	87.6

TABLE IVa. Pu ISOTOPIC RATIO

Pu	238	239	240	241	242
Oxide+Metallic	0	58	24	14	4
Particle Fuel	15.8	49.6	35.7	8.4	4.6

TABLE IVb. MA FRACTIONAL WEIGHT (%) SPECIFICATION

MA Nuclide	^{237}Np	^{241}Am	^{242}Am	^{243}Am	^{243}Cm	^{244}Cm
Oxide+Metallic	53.6	23.1	0	17.4	0	5.9
Particle Fuel	56.7	26.2	0	11.8	0.3	5.0

TABLE V. TARGET COMPOSITION AND DIMENSION

Target	A	B*	C	D
Diameter (cm)	10.	10.	10.	7.
Height (cm)	100.	100.	100.	60.
Target material	Solid Pb	Liquid Pb	Molten Salt of 60%NaCl 40%$MACl_3$	W
Coolant	Pb or Na**	Pb	Molten Salt	He

* Take out a few central fuel assemblies and use as the Pb coolant as the target

** The cooling material for a liquid target depend on the cooling material chosen for the core cooling

TABLE VI. REACTOR SPECIFICATION OF ADEP AND ADPF

Fuel Type	Pu and ^{238}U oxide fuel Na coolant (A)	Pu and ^{238}U metallic fuel Na coolant (B)	Pu oxide Pb coolant (C)	Particle fuel (D)
Actinide inventory (kg)	3000	2500	2700	2000
k_{eff}	0.98-0.99	0.98-0.99	0.98-0.99	0.98-0.99
Mean neutron energy (keV)	720	800	760	740
Neutron flux ($n\ cm^{-2}\cdot s^{-1}$)	4×10^{14}	4.5×10^{15}	4.5×10^{15}	8.4×10^{15}
Thermal and electric power (MW)	850 323	850 325	850 340	1000 370
Power density (MW/m^3)	700	850	700	3400
Linear power density (kW/m)	51	53	53	77

D.5.2. PHOENIX CONCEPT [2]

The idea of a large-scale accelerator incinerator was studied by enlarging the early Euratom-BNL-CERN concept using state-of-the-art technology [1]. The Phoenix concept consists of modules of accelerator-driven subcritical lattices containing minor actinide fuel (see Fig. 2). Classical fast-reactor technology is assumed, such as oxide fuel elements and sodium cooling. Each module resembles the core of the Fast Flux Test Facility (FFTF) with a $k_{eff} = 0.9$; however, from 1 to 8 target modules are aligned in front of a 104 mA beam of 1.6GeV protons. The entire bank of reactor modules serves as a target for a proton beam that is expanded before entering the core region. With these parameters, eight modules would generate 3600 MW_t. The target chamber as viewed from three perspective and fuel assembly lattice based on FFTF oxide fuel are shown in Figures 3 and 4.

The study showed that after 2 years of operation at 73% capacity, the fuel reaches an average burn-up of 8.6%, with an additional 12.7% converted to Plutonium. Using a 2-year cycle assures that most of the Plutonium (> 83%) is ^{238}Pu, which is valuable as a long-term remote source of power, and also reduces any concerns about degradation in the fuel or in the structural steels. During the 2-year reprocessing step, the Plutonium and fission products are replaced by new minor actinides from the LWRs. Plutonium that is not useful for isotopic applications could be blended with the highly fissile Plutonium from the LWR waste steam, so that the resulting mixture would contain enough ^{238}Pu and ^{236}Pu to make weapon production difficult.

Burn-up calculations were carried out for six two-year cycles; they reach equilibrium after two years, and produce little ^{239}Pu and only a modest amount of ^{242}Pu. The fraction of ^{238}Pu varies between 83% and 87% after each cycle. There is little variation of ^{237}Np, but a noticeable increase of ^{243}Am and ^{241}Am.

The combined neptunium and americium inventory decreases by about 2.6 Tones/a, with 1.33 tones/yr being converted to Plutonium. Thus, one incinerator unit would transmute the minor actinide wastes from about seventy three 1 GW_e LWRs.

In this concept, a number of modules are irradiated by one high-current proton beam; the beam must be spread significantly to reduce radiation damage and the steep power distribution. This necessitates a long

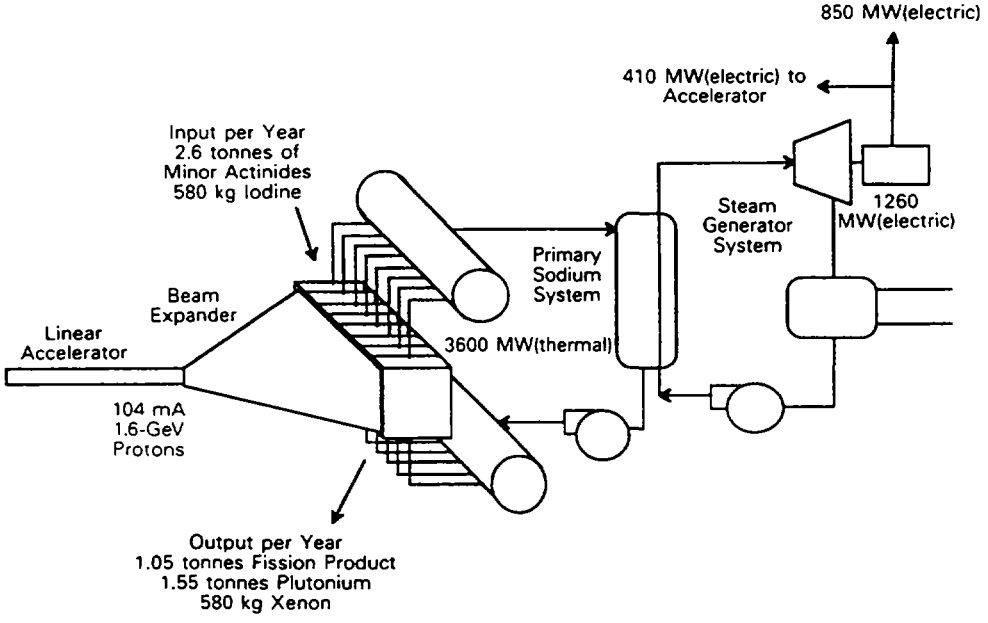

Fig. 2 The PHOENIX concept (intermediate sodium system not shown)

beam-spreading section and causes a large leakage of neutrons from the irradiated surface. To avoid this shortcoming, the high current beam should be split into a number of small beams, and injected into a number of small reactors so avoiding the inconvenience of a failure in the accelerator or in one module that would stop the whole system.

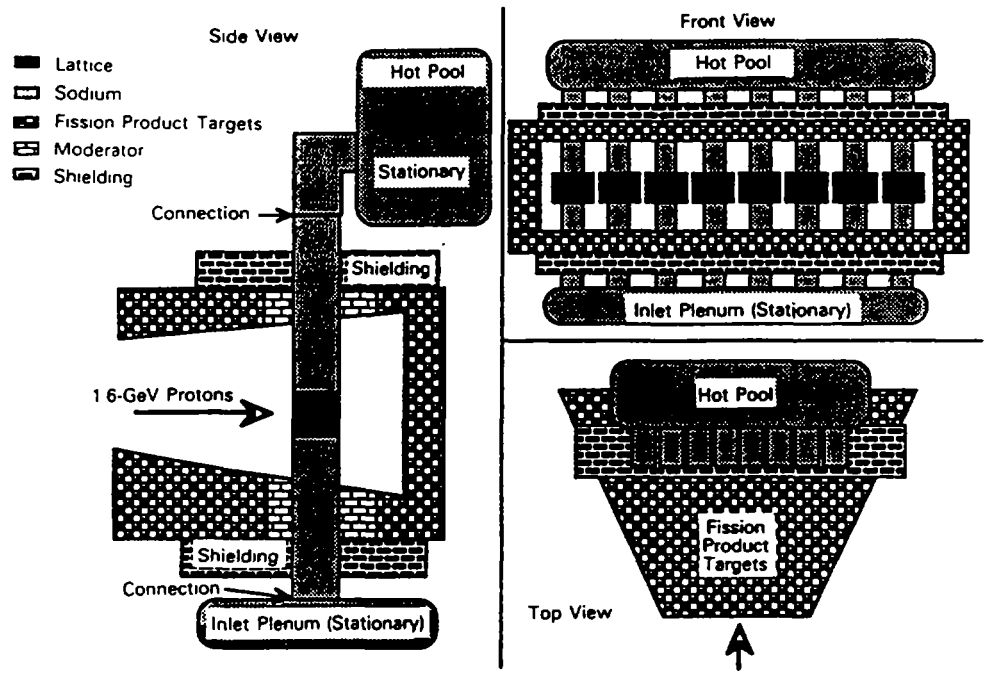

Fig. 3 PHOENIX target chamber from three perspectives

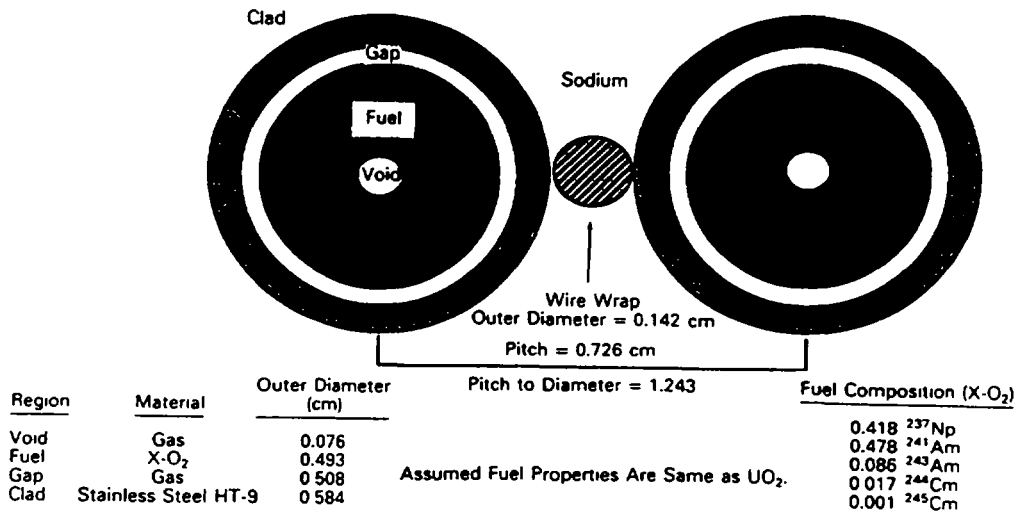

Fig. 4 PHOENIX lattice fuel pins based on FFTF oxide fuel.

D.5.3. ACCELERATOR DRIVEN PARTICLE FUEL TRANSMUTER

To increase transmutation efficiency of the MA or LLFP, a high neutron flux is required and it can be created by using a particle fuel [3]. Similar to liquid fuels, such as molten salt and slurry fuels, a particle fuel that is directly cooled has several advantages over a regular, solid fuel. Particle fuel has an extremely large heat-transfer area (of the order of 100 C m^2/cm^3), and the small size (less than 1 mm) of the particles confers three major benefits:

1) very high power densities,

2) a small temperature difference between the fuel and coolant,

3) minimum thermal stress and shock in the fuel.

Thermal power densities in the packed bed can be 10MW/l or more because of the large heat-transfer area. Due to this large power density, this fuel is suitable for transmuting LLFP or MA at a high rate.

Loading and unloading of the particle fuel can be performed with high-pressure coolants. In the case of an emergency, rapid unloading from the core can quickly lower the multiplication factor of the core assembly. Also, dumping the particle fuel into a large pit of liquid coolant removes the decay heat from the burned fuel, so that it can reduce the risk associated with the melt-down of solid fuel by decay heat. This problem of removing decay heat is more serious for regular rod-type solid fuel where decay heat is removed by natural circulation of coolant liquid through the solid fuel components.

In contrast to liquid fuel, for the purpose heat removal the particle fuel can remain in the core where it is irradiated by neutrons, so that the neutrons are effectively used for burning the fuel or transmuting the MA or LLFP.

For liquid fuel, unless a heat exchanger is included in the core region, the fuel is circulated outside the core and so the effective neutron flux for transmutation is reduced; also a larger inventory of fuel is needed.

To transmute the LLFP or MA quickly and more effectively, the transmuted products, which have a large neutron-capture cross-section, should be removed as soon as they are produced. Thus, the neutrons are not wasted as is the case when they remain in the reactor. If the cost of separating the transmuted FP from the particle fuel is not great, the particle fuel can be taken out of the reactor core frequently, and these products can be removed by chemical methods.

D.5.4. FUEL AND COOLANT MATERIALS AND TARGET

Use of metal fuel, for which technology has been developed at Argonne National Laboratory [6], has several advantage over oxide fuel.

Due to high heat conductivity an inherently safe operation can be achieved. Pyrometallurgical fuel processing will decrease the capital cost of the fuel processing plant.

This metal fuel has large a content of fissile material so the neutron spectrum can be hardened and transmutation of the MA can be increased. Although this hardening of the neutron spectrum increases the positive Na void coefficient, operation in subcritical conditions solves the safety problem. Another advantage of this metal-fuel reactor over the oxide-fuel reactor is that it has only a small swing in reactivity during fuel burn-up, so that very few control rods are required to control the excess reactivity; alternatively, the reactivity-worth of a single control rod can be much lower. Thus, the probability of having an accident after withdrawing a control rod can be reduced.

The coolant material of the ADEP and Phoenix reactor is Na; the option to use Pb is also reserved. Although high-temperature liquid Pb coolant is more corrosive than Na, it has many interesting features which improve the neutronic characteristics beneficial for transmuting MA. A harder neutron energy spectrum can be obtained, making this system resistant to recriticality in the case of a core-melt accident because the mass density of Pb is comparable to that of the fuel material. In the case of Na coolant, the

melted core is much heavier than the Na, so that the possibility that a melted core might sink to the bottom of the core vessel and bring the reactor into a critical condition is higher than in the case of Pb coolant. Furthermore, due to the high mass density of Pb, the volume ratio of coolant to fuel can be increased without lowering the neutron energy, and a large amount of Pb coolant can be used to remove heat from the core.

For the particle fueled reactor ADPF, He is chosen as the coolant because of a large data base of information has been accumulated from the high temperature reactor.

As the target material for ADEP and ADPF, liquid Lead has been adopted because of the lack of a radiation damage problem and the efficient heat removal capacity. When Pb is very corrosive, the following three types of target materials will be chosen; solid Lead, molten salt ^{237}Np, and solid tungsten. The composition of the molten salt MA target, including ^{237}Np, is $60NaCl\text{-}40MACl_3$, and due to the small fission cross section of the MA material for low energy neutrons, the amount of heat generated is not as great as in a target composed of fissile material.

The size of the double-shelled target is determined from the heat generated and from the heat-removal capacity of the coolant, as shown in Table V.

When Pb is chosen as the coolant, the target need not be contained in a double-shelled wall. By taking out the some of the fuel assemblies from the center section, the liquid coolant material irradiated by high energy protons, can be used as target.

In the Phoenix concept, the proton beam is expanded by a magnetic field to reduce the beam density which is injected directly into the core assembly, and to flatten the power density.

D.5.5. SUBCRITICALITY AND SAFETY ISSUE

The degree of subcriticality adopted for an accelerator-driven system is very important for many aspects of safety and economy. Although some proposals have suggested having large subcriticality to avoid recriticality conditions occurring in the melt-down accident, a large subcriticality creates other kinds of safety problems, such as a high power-peaking factor when the accelerated proton beam is injected locally. Furthermore, larger power of a proton beam accelerator requires a more stringent design of the beam window, and radiation damage to the target material and its surrounding area is much more serious. In addition to this problem of radiation damage, a high current beam has to be controlled very strictly to avoid instability, such as breakup and beam spilling which makes any hands-on maintenance of the accelerator difficult and very expensive. These problems become a considerable burden in the running of a large current accelerator in addition to the economical problems of the high initial cost.

To decrease the difficulties associated with a high powered accelerator, our ADEP and ADPF is operated with a slightly subcriticality such as k=0.98-0.99. Although a small number of control rods will then be needed to adjust the reactivity change due to burn up of the fuel, the reactor safety problem associated with critical operation can be substantially reduced. This small subcriticality is enough to avoid a sudden change of the power of the reactor due to a small change of reactivity [8].

Due to this advantage, the amounts of minor actinides that are mixed into to the Pu fueled reactor can be increased and hence, the transmutation rate of MA also increases.

The Phoenix concept which use a high current proton beam power, has a rather large subcriticality of k=0.9.

D.5.6. USE OF THORIUM, CROSS PROGENY FUEL CYCLE (^{233}U PRODUCTION AND TRANSMUTATION OF MINOR ACTINIDES) AND NEUTRON ECONOMY

At the last international fuel-cycle evaluation (INFCE), several options for producing ^{233}U were proposed; however, this study was carried out before the end of the cold war, and so the use of Pu was not considered. The United States has accumulated a great deal of military Pu from the last 40 years of Cold War era, and also large quantities of Pu from operating LWRs. To incinerate military Pu completely it was suggested that an accelerator could be used, as well as a LWR. However Pu is a very valuable fuel for future generations and we should consider using this surplus Pu to start up a ^{233}U and Thorium fuel cycle in addition to a Pu-fuel cycle.

Instead of producing ^{233}U fuel in a thermal reactor as discussed in the Thorium cycle, in our concept, ^{233}U fuel is produced in the blanket region of the Pu fueled fast reactor. Due to the larger η-value of ^{233}U compared to ^{233}U for thermal neutrons, the inventory of the fissile material for a LWR can be reduced to about 70% of ^{235}U fuel. The production of MA from ^{233}U is extremely small and reduces the burden of transmutation or disposal of MA.

^{233}U is produced with ^{232}U, whose descendant nucleus ^{208}Tl emits high-energy γ-radiation so that it is a more theft-resistant fissile material. Until a few years ago, using the Thorium and ^{233}U fuel-cycle system was opposed because of this high-energy γ-radiation generated by ^{208}Tl. Now, with the general endorsement for mixing minor actinides into the fuel cycle, the prospects for using it are far better.

To prevent the removal of pure ^{233}U, ^{232}Th should be mixed with a small amount of ^{238}U.

From the point of view of neutron economy, transmutation of MAs is much simpler than that of LLFPs, because neutrons are produced by fission processes in the MA transmutation process; LLFP transmutation requires neutron capture. A LWR reactor produces substantial quantities of long-lived radioactive ^{93}Zr from the neutron capture process of Zr fuel-cladding material, as shown in Table VII. Thus, transmutation of these long-lived radioactive isotopes requires a transmutor which has a higher neutron economy, like a Pu-fueled fast reactor, than the thermal reactor, because it has high η value for high-energy neutrons and small parasitic neutron capture by structural and fission products in a thermal reactor. Subcritical operation of a fast reactor provides a higher neutron economy suitable for transmuting LLFP. To incinerate LLFP and ^{93}Zr isotopes efficiently, the spallation neutrons should be multiplied by coupling this neutron source to a Pu-fueled subcritical reactor with a hard spectrum. As shown in Table VII, the reduction of the k_{eff} value by neutron capture is large, so it is not an easy task to get a long burn-up time. As an alternative way of solving the transmutation of LLFP such as ^{99}Tc and ^{129}I we are studying the disposal of these isotopes into outer space a the small accelerator instead of the rocket proposed by NASA [9].

D.5.7. ISSUE OF NON-PROLIFERATION (SEPARATION OF POWER PRODUCTION AND FUEL PROCESSING)

From the point of view of non-proliferation, it is desirable to separate power production and fuel-processing facilities; a small number of fuel processing facilities, which are internationally controlled, is particularly beneficial for purposes of inspection.

In contrast to fuel production by a breeder reactor, fuel production by an accelerator does not require any fissile material, only electricity and fertile material. If and when the world needs a large amount of fissile material within a short period due to a rapid growth in energy demand, then a high-power proton accelerator can produce fissile material from fertile material and electricity only, without needing any fissile material. Although the cost of producing fissile material in this way is higher than it is with a breeder reactor, this high cost can be reduced somewhat by using a subcritical assembly.

Since a breeder reactor can only produce the fissile fuel by producing energy, it should be located near an area where this energy will be consumed. An accelerator fuel producer does not necessarily produce

TABLE VII. LLFPs FISSION YIELD, HALF-LIFE TIMES, THERMAL AND FAST (N,Γ) CROSS SECTION, TRANSMUTATION FLUXES

	^{90}Sr	^{137}Cs	^{99}Tc	^{129}I	^{85}Kr	^{93}Zr	^{135}Cs
Fission yield (%)	5.91	6.15	6.12	3.56	1.33	5.45	
sub sum		12.06				16.46	
total sum						28.52	
Half-life (years)	29.	30.2	2.1×10^{5}	1.6×10^{7}	10.73	1.5×10^{6}	$3.\times10^{6}$
σ_{th}(b)	0.01	0.25	20	31	1.7	1.	8.7
σ_{fast}(b)	0.4	0.4	0.2	0.2	2.0 (R.I.)	15. (R.I.)	62. (R.I.)
ϕ_{th} (n $cm^{-2}\cdot s^{-1}$) ~3 y HL_{eff}*	7.7×10^{17}	$3.\times10^{16}$	4.0×10^{14}	2.5×10^{14}	4.5×10^{15}	7.7×10^{16}	8.9×10^{15}
ϕ_{fast} (n $cm^{-2}\cdot s^{-1}$) ~10y HL_{eff}	$2.\times10^{16}$	$2.\times10^{16}$	$4.\times10^{16}$	$4.\times10^{16}$	$4.\times10^{16}$	5.1×10^{14}	1.2×10^{14}

*- HL_{eff} - effective half-life, R.I. - resonance integral

more energy than is required to run it, so that fuel production facilities can be located in a remote area, as can the facilities for processing the fuel and transmuting high-level waste. A remote location where there is a fossil-fueled bunning power plant or a hydraulic power generator is an ideal place for an accelerator producer, and if asubcritical reactor is used, the electric energy required for operating the accelerator can easily be obtained.

By locating such facilities in this way, the risk of proliferation of fissile material can be reduced, although transportion of the fuel elements and spent fuel must be protected.

A subcritical reactor gives a flexible choice between fuel production and power production. When there is plenty of electricity in the remote area, the accelerator can operate with a fission-suppressed reactor with a small k_{eff}; fission is suppressed, so that the accelerator's power can be increased to get a higher rate of fuel production without jeopardizing safety with an overpowered condition.

Fuel production and power production can be adjusted by the subcriticality. Thus, there are many options and much flexibility which cannot be obtained in a reactor system operated in the critical condition. In operating a subcritical target, k_{eff} can be less than one, and the neutrons which are needed to maintain the critical condition can be diverted into producing fuel. Hence, the rate of fuel production can be increased by running the operation at a low k_{eff} value. The initial requirement for fissile material will depend on the reactivity; this can be adjusted by the initial inventory of the fuel.

D.5.8. ACCELERATOR

For accelerator fuel production, we have promoted the high power linear accelerator of about 300-450 MW. In this scheme, we assumed that the target is a fission-suppressed core with large subcriticality. With a higher beam current of more than 100 mA, the linear accelerator has higher efficiency than the cyclotron, which is efficient at less than 10 mA. ADEP and ADPF can be operated by a small size segmented cyclotron of the order of a few MW. This circular machine does not require a long beam transport building and proton energy can be increased without jeopardizing the economy of the accelerator; we envisage using a high energy of 3 GeV instead of the 0.8-1.0 GeV energy customarily used for our previous conceptual design study and for the linear accelerator. This use of high energy protons can reduce the beam current to produce the same number of spallation neutrons, the current required is almost inversely proportional to proton energy. Furthermore, the use of high energy protons can reduce the radiation damage in the material of the beam's window section and the surrounding sections of the target region because of the

smaller proton beam current. The range of high energy protons is longer than that of low energy ones; thus, the axial distribution of the spallation neutron source is flattened and this is beneficial for heat removal from the core.

For the Phoenix concept which requires a large proton current accelerator, a linac of 100 MW beam power has been considered. For high the powered accelerator, the superconductor linac (SC-linac) has been studied. The SC-linac has a higher efficiency and a higher accelerating electric field with a larger iris aperture than a conventional linac so that the linac can be shortened. The linac can also accommodate a wide range of β by the supply RF to each cavity without reducing the accelerator efficiency compared to the regular conductor linac, although the radiation heating and damage in the superconductor requires further study, and the practicality of SC-linac is being investigated [10].

The splitting of the high current beam and its injection into many reactors is desirable to reduce the inventory cost per beam power. A negatively charged H^- beam or $H122^-$ molecular beam accelerated by a linac can be slit with a gas jet, using laser irradiation, or by ionizing the beam and extracting it with magnetic field. When the beam is slit time-wise, we must take into account the thermal shock generated in the target by injecting pulsed beams. To avoid thermal shock, the proton beam should be slit in such a way that the interval between pulses is smaller than the thermal relaxation time of the target assembly.

Although one large accelerator can run several reactor targets with higher efficiency than can a cyclotron, a failure of the large accelerator would result in the shutting down of all reactors; therefore, it might be practical to use numbers of small cyclotrons. Cost might be increased by independently operating several small reactors, but it would alleviate several difficulties, such as splitting and controlling the high current beam.

Besides the transmutation of MA and LLFP, other projects concerning accelerator tritium production and spallation neutron sources have been going on. The concept of ATP was developed in1980, just after studying the accelerator breeder, and collaborative work continued with Los Alamos National Laboratory and Hanford Westinghouse Laboratory untill 1987. After temporary closure the project started again 1992 in collaboration with Los Alamos National Laboratory (LANL) and Lawrence Livermore National Laboratory(LLNL).

D.5.8.1 Cyclotron for proton accelerator

As mentioned before it might be practical to use numbers of small cyclotrons instead of a linac. At present a cyclotron of 1.1 MW beam power has been developed at PSI for a 600 MeV proton accelerator [11].

As discussed earlier, to incinerate the minor actinides produced from 10 units of LWR, it is sufficient to use medium-energy proton with a 15-30 MW current. Because of the nearly linear energy-dependence on number, if the spallation neutrons have energies ranging from 1-3 GeV then beam intensity and beam energy are exchangeable. These factor may favor the use of "multistage-parallel" cyclotrons over the linear accelerator.

While the price is almost proportional to the energy requirement for the latter system, doubling or tripling the energy of a cyclotron is much less costly. On the other hand, the maximum achievable beam current of a cyclotron is rather limited, especially at low energies.

These conditions lead to the concept of the so-called "multistage-parallel" cyclotron arrangement, consisting of several low-energy, low-current cyclotrons feeding into one high energy cyclotron.

For example, (as shown in Fig. 5) a multistage cyclotron arrangement providing 15 mA at an energy of at least 2 GeV would require the following assembly:

- Three sources of 60-70 keV ions,
- a low-energy 2 Mev, 5 mA injector stage, consisting of three radio-frequency quadrupole linacs (37 MHz), developed by Müller from Darmstadt (Split Coaxial Resonator)
- an intermediate stage, made of the same number of four-sector cyclotrons with a phase width of 36 and frequency of 36 MHz accelerating the 5 mA proton current to the upper limit around 200 MeV.

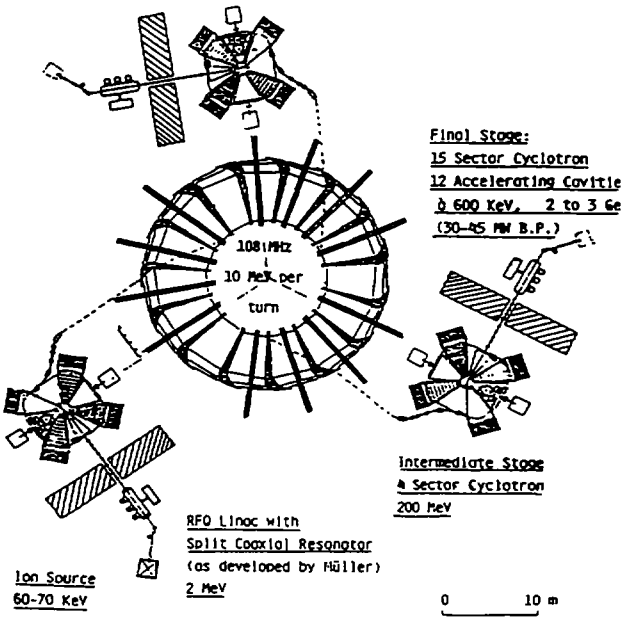

Fig. 5. Multistage cyclotron arrangement

- a final-stage 15-sector cyclotron, fed by the three intermediate stages (3x5 mA at 200 MeV).

This cyclotron works at 3x36=108 MHz, using 12 accelerating cavities of 600 keV. The final stage can reach a proton energy of 2 to 3 GeV at a beam power of 30-45 MW.

As the next generation of neutron sources a spallation neutron source using 3 GeV protons from synchrotron has been studied. In addition, intermediate energy proton and neutron cross-section data, which is required to evaluate ADS has also been obtained.

REFERENCES

[1-1] P. Bonnaue, H. Rief, P. Mandrillon, and H. Takahashi: "Actinide Transmutation by Spallation in the Light of Recent Cyclotron Development"; NEACRP-A-910, Session B.1.2 (1987). (European American) Reactor Physics Committee Report. and ICENES 86, Madrid, July 1986.

[1-2] H.Takahashi'" Actinide Transmutation by the Spallation Process," presented at Workshop Feasibility of Resarch Program in Actinide Transmutaiion by Spallation Process, Ispra, Varese, Italy, June 18- 21, 1985.

[2] G.Van Tuyle, M.Todoso, M.Geiger, A.Aronson and H.Takahashi, "Accelerator-Driven Subcritical Target Concept for transmutation of Nuclear Wastes, Nucl. Tech. p.1, Vol. 101, 1993

[3] H. Takahashi, The Role of Accelerator in the Nuclear Fuel Cycle, Proc. of 2nd Internat. Symp. on Advanced Nucl. Energy Research, p.77, Mito, JAERI, Jan. 24-26 (1990).

[4-1] H. Takahashi, A Fast Breeder and Incinerator Assisted by a Proton Accelerator, Fusion

Technology, 20 (1991) 657.

[4-2] H. Takahashi."Safe Economical Operation of Subcritical Fast Reactor and Transmutor with a Small Proton Accelerator" Proc. Int. Conf. on Reactor Physics and Reactor Computations, P.79, edited By Y. Ronen and E.Elias, Tel-Aviv, Jan 23-26,1994.Ben-Gurion Unv. of the Negev Press (1994).The 8th Juness SATURNE Accelerator Applied to the Nuclear waste Problem held at Saclay on May 5-6, 1994.

[5-1] X. Elie and J. M. Chanmont, Operation Experience with the Phenix Prototype Fast Reactor, Internat. Conf. on Fast Reactor and Related Fuel Cycles (ICFRRFC) 5.1-1, (1991)

[5-2] J. Mchaumont, D. Goux and L. Matin, Some Safety Related Characteristics of Phenix, a 250 MWe Fast Reactor 1989 and 1990 Negative Reactivity Trip Investigations, Internat. Conf. on Design and Safety of Advanced Nuclear Power Plants (ICDSANPP) Oct. 25-29, 1992, Tokyo Japan.

[6] C. L. Cockey and M. L. Thompson, ALMR Potential for Actinide Consumption, Internat. Conf. on Fast Reactor and Related Fuel Cycles (ICFRRFC), P3.4-1, (1991).

[7] H. Takahashi, and X.Chen " Accelerator Driven Cross-Progeny Nuclear Fuel Cycle" International Conference on Evaluation of Emerging Nuclear Fuel Cycle Systems. Global,1995, P.1436, Sept.11-14,1995 Palais des Congres, Versailles, France.

[8] H. Rief and H.Takahashi, Safety and Control of accelerator-driven Subcritical System. International Conference on Accelerator-driven Transmutation technologies and Applications.p.159, Las Vegas, NV 1994 AIP Conf. Proc. 346.

[9-1] Takahashi, H. and Chen, X. (1995) "Alternative Way to Dispose of High-Level Waste in Outer Space," Twelfth Symposium on Space Nuclear Power and Propulsion, AIP Conference, Proc. 324:347-354." Disposal of Type II Fission Products into Outer Space" Thirteenth Symposiumon Space Nuclear Power and Propulsion, AIP Conference, Proc. 361:967-973.

[9-2] Takahashi, H. and Chen, X. (1996) "Disposal of type -II long-lived fission products into outer space" Thirteenth Symposium on Space Nuclear Power and Propulsion, AIP Conference, Proc. 361: 967-973.

[10] A. Ruggiero, Personal Communication (1995)

[11-1] T. Stammbach "Experience with the High Current Operation of the PSI Cyclotron Facility, Proc. of the 13-th Internat. Conf., Vancouver, 1992, p.28-36, ed. G. Dutto and M. K. Craddick, World Scientific New Jersey.

[11-2] S. A. Martin, E. Zaplatin, P. F. Meads, Jr., Wuestefeld and K.Ziegler, Study of an FFAG Synchrocyclotron for a Pulsed Neutron Source, Proc. of the 13-th Internat. Conf., P. 701-704, Vancouver, 1992, ed. G. Dutto and M. K. Craddick, World Scientific New Jersey.

D.6. THE EUROPEAN COMMUNITY PROJECTS

D.6.1. IMPACT OF ACCELERATOR BASED TECHNOLOGIES ON NUCLEAR FISSION SAFETY - SHARE COST PROJECT OF THE EUROPEAN COMMUNITY

D.6.1.1. INTRODUCTION

Over the last few years the interest in ADS has grown in many European countries. As a result of this some European institutes have decided to establish a shared cost project in the framework of the European Community. The overall objective of this project is to make a European assessment of the possibilities of accelerator-driven hybrid reactor systems from the point of view of safe energy production, minimum waste production and transmutation capabilities. In particular:

a) **to perform system studies on accelerator driven hybrid systems**

b) **to assess the accelerator technology**

c) **to study the radiotoxicity of the fuel cycle for ADS and its nonproliferation aspects**

d) **to provide basic nuclear and material data for ADS by means of evaluation and experiments**

The final objective is to concentrate and coordinate different efforts from member states to create a European scientific and technological basis for further projects aimed at developing environmentally friendly, more publicly acceptable and safer nuclear fission energy sources. The final results will be models, tools, validated routines and some new experimental data for future experimental activity on a larger scale.

D.6.1.2. WORK CONTENTS

This project is divided into 4 tasks presented in Fig. 1:

1. system studies on the accelerator driven hybrid
2. assessment of the accelerator technology
3. basic nuclear and material data
4. studies of the fuel cycle for ADS

Task 1: System studies of an accelerator driven hybrid

System studies will be focused on the following systems :

a) Energy production using the Thorium fuel cycle

b) Energy production using LWR spent fuel and burning of TransUranium elements

c) Dedicated Plutonium burning with energy production

d) Transmutation of fission products combined with burning of TransUranium elements

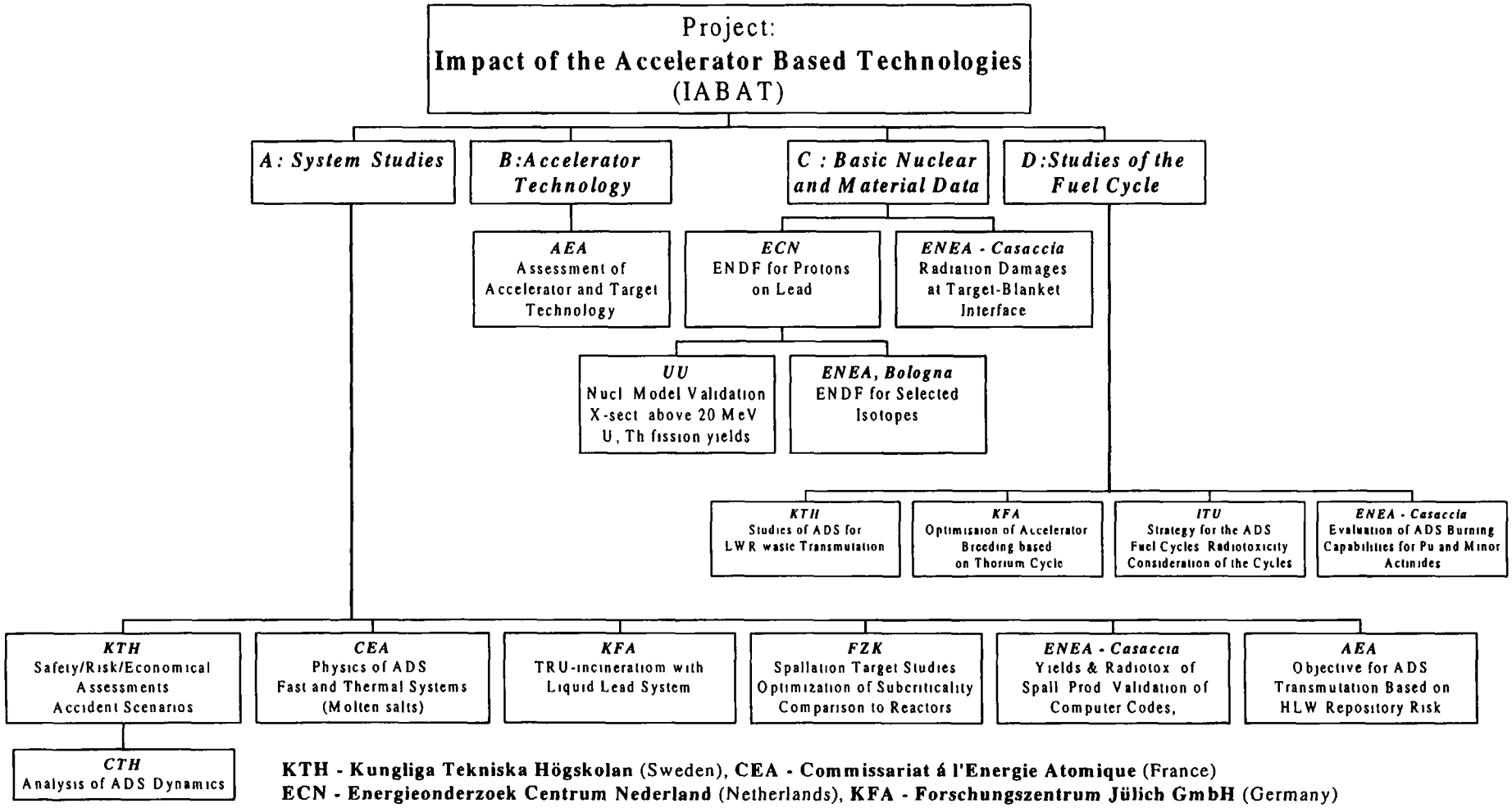

FIG. 1 Task structure of the European project: Impact of the Accelerator Based Technologies on Nuclear Fission Safety

These studies will be performed for thermal, fast and intermediate neutron energies to optimize the performance of the system. The neutron energy range strongly determines the choice of the materials used for the coolant and reflectors/moderators and requires multidimensional optimization which has to be performed in respect of material compatibility, engineering aspects, corrosion, safety, economy and other factors.

In Europe large quantities of Pu from reprocessed spent LWR fuel are available. These can be recycled to some extent in existing LWRs using the MOX option, or by using fast reactors. However, multiple recycling of MOX in thermal reactors is not very efficient in LWRs. The possibilities of using recycled Pu in hybrid systems will be investigated.

It is also very important for Europe to monitor and, if required, to help to destroy excess Russian weapons Plutonium. Therefore the potential of **ADS** to efficiently burn weapon Plutonium with a simultaneous energy production has to be investigated.

The spallation target will be chosen and optimized with respect to proton energy, neutron production, thermodynamics and radiotoxicity of spallation products.

The safety/risk assessment of the different ADS will be performed and reference scenarios for severe accidents will be worked out for these different systems. Optimization of the subcriticality level with respect to safety and efficiency will be investigated. Transient behaviours of the ADS will be investigated.

The environmental and economical impact of the ADS on the geological repository of HLW will be estimated.

A preliminary economic assessment, based on the results of studies in this project, will be made in order to estimate the feasibility of these ideas as well as to validate the results.

Task 2: Assessment of the accelerator technology

Accelerator technology will be assessed with respect to: construction (cyclotron vs linac), proton current and energy levels. These results will strongly influence the economical aspects of the system studies.

Task 3: Basic nuclear and material data

A relatively high yield of neutrons up to several hundreds of MeV is produced by the proton interactions in the thick, heavy element ADS target. Nuclear reaction calculations will be performed and experimental data will be collected in order to create an evaluated data file.

Nuclear model codes will be validated for basic nuclear reaction cross section data of importance for ADS neutronic calculations. The validation is based on a number of protons and neutrons induced cross section measurements performed at the The Svedberg Laboratory, Uppsala in the energy range 50 to 200 MeV. Measurements will also be made of the thermal fission yield for ^{233}U and the fast fission yield for ^{232}Th.

Task 4: Studies of the fuel cycle for ADS

The use of the Thorium cycle for energy production seems to be extremely attractive due to the breeding potential generated by the excess neutrons in the system. Apart from operating in a self-sufficient mode supplying large amounts of energy, there is simultaneous production of fissile material and negligible production of TRU-elements.

A combined Th and LWR-spent fuel cycle is another attractive option opening new possibilities for synergetic coexistence of conventional nuclear reactors and ADS. Generic aspects of the Th-cycle will be studied in the framework of another project entitled "Thorium cycles, a nuclear waste management option",

coordinated by W.M.P. Franken, ECN. In our project we shall only concentrate on specific aspects of the hybrid systems and the studies will be coordinated with ECN.

The following fuel options will be investigated:

- inert matrix using liquid Lead as a carrier/cooling material
- inert matrix using molten salt (fluoride, chloride) as a carrier/cooling material
- aqueous systems with heavy water
- oxide fuels
- metallic fuel

The proliferation and radiotoxicity characteristics of the different fuel cycles and fuel options will be investigated. The efficiency and costs of fission products transmutation will also be assessed.

D.6.1.2. EXPECTED BENEFITS

The strategic aim of the project is to **broaden the nuclear power option** and to make it **more attractive and acceptable to the general public, for the benefit of present and future generations**. By addressing some of the most important problems of nuclear power, namely improving safety and reducing the burden of the waste radiotoxicity, we may significantly contribute to the permanent solution of the world long term energy supply. The strategic studies planned in this project will result in the comparison of different options in the form of the cost/benefit impact of accelerator based transmutation on different strategies such as: direct geological disposal of irradiated fuel, with or without reprocessing and Pu recycling in reactors etc. Up to now, individual studies have been very difficult to compare due to the significant differences in hypothesis, method and data. This difficulty has been compounded when comparisons have been attempted on the use of different fuel cycles and/or different neutron spectra for transmutation. This project will prepare the platform for future analysis of diverse nuclear power systems.

In the frame of this project, the problems of **weighting the long-term low-level risks versus short-term higher-level risks will be addressed for comparison of geological repositories with the transmutation option**.

Many questions have also been raised concerning the economic costs of introducing accelerators into nuclear power. Even at this very early stage it is necessary to make a **preliminary economic assessment to prepare the ground for future decisions concerning the eventual construction of such systems**. This project addresses these issues.

In conclusion, the project will result in the following benefits:

1. preparation of the platform for future analysis of diverse nuclear power systems
2. grounds for weighting the long-term low-level risks versus short-term higher-level risks for comparison of geological repositories with the transmutation option
3. preliminary economic assessment to prepare the ground for future decisions concerning the eventual construction of accelerator driven systems
4. a framework for future international collaboration aimed at performing an ADS integral experiment will be prepared.

D.6.2. SWEDISH PERSPECTIVE ON THE ACCELERATOR DRIVEN NUCLEAR SYSTEM

Waclaw Gudowski and Henri Condé
Sweden

D.6.2.1. INTRODUCTION

The nuclear power programme in Sweden consists of 12 nuclear reactors located at four different sites and with a combined capacity of 10 000 MW net electric power. The nuclear power plants generated about 42% of the total Swedish electric power produced in 1993.

These nuclear power plants are owned by four companies which have formed the Swedish Nuclear Fuel and Waste Management Company, SKB (SKB - Svensk Kärnbränslehantering AB). SKB's duties are to develop, plan, construct and operate facilities and systems for the management and disposal of spent nuclear fuel and radioactive wastes from the Swedish nuclear power plants. On behalf of its owners SKB is responsible for all handling, transport and storage of nuclear waste outside of the nuclear power production facilities [1]. SKB is also in charge of a comprehensive research programme in the radwaste field.

A complete system has been planned for the management of all radioactive residues from the 12 nuclear reactors and from the research facilities. The system is based on the projected generation of waste up to the year 2010. A central interim storage facility, CLAB, was put into operation in July 1985 for the storage of spent fuel. This facility has a current capacity of 5 000 tonnes of spent fuel. The spent fuel will be stored in CLAB for about 40 years. It will then be encapsulated in corrosion-resistant canisters and deposited at depth in the Swedish bedrock. The construction of the deep repository will be made in stages. The first stage of the repository, for 5 - 10% of the fuel, is planned to be put into operation in 2008. The next stage for the full repository will only be built after thorough evaluation of the experience of the first stage and renewed licensing. The site for the deep repository has not yet been chosen.

The estimated costs for the Swedish deep rock repository amounts to about 40 billion SEK. One attractive option to reduce these costs would be to transmute the most cumbersome components of the spent fuel using accelerator-driven transmutation technology.

D.6.2.2. ACCELERATORS ENTER THE NUCLEAR ENERGY FIELD

As described in this Status report, new concepts for treating spent fuel from fission reactors have been developed in recent years. This has initiated rapidly growing international research activities in which a number of Swedish, mostly university-linked, groups participate. It is believed that Accelerator-Driven Systems can effectively convert the long-lived radioactivity in the burned nuclear fuel, to short-lived and by so reduce the need for geological repositories. ADS offers in the long-term a possibility to produce cleaner fission energy over an indefinite period, a concept which would fit Swedish needs and technological skill. However, due to environmental requirements the Swedish parliament decided that the two dominating energy sources - nuclear power and fossil fuels - will be either shut down (nuclear power) or its use will be limited (fossil fuels), so in the long run the Swedish energy supply is a problem area. The parliamentary decisions are based on the perceived risks which in the first case are linked to a possible release of radioactivity from a large reactor accident and/or the handling of the highly radioactive spent fuel and also to proliferation concerns. In the second case the decisions are linked to the risk of a global environmental catastrophe through the "green house effect". Although research on alternative renewable energy sources has been in progress, no large scale solutions which can meet the future energy demands have been found so far. At the same time the research problems connected with the utilization of fusion

energy are still numerous. Today it is difficult to predict when the basic problems in this field will be solved. Finally, the import of energy negatively effects the balance of trade and makes Sweden dependent upon the political and economic decisions of foreign countries.

With the threefold aim (1) to find *methods for treating the high level nuclear wastes* which could be more easily accepted by the public than a direct geological deposition, (2) to design *a nuclear power system which would be more acceptable to the public (safer performance and reduced waste streams)* and at the same time (3) *to recruit students to the nuclear energy field*, a national collaboration has been initiated in the research of accelerator driven systems. The ambition to start research in this field was positively influenced by the Specialists' Meeting on "Accelerator-Driven Transmutation Technology for Radwaste and other Applications" which was held at Saltsjöbaden, Sweden on 24-28 June 1991.

The "Group for Spallator Research" conducts - so far - concerted research at Chalmers University of Technology (CTH), the Royal Institute of Technology (KTH), the Manne Siegbahn Laboratory-Stockholm University and Uppsala University.

The main task of this Group is to stimulate and to coordinate research and development projects in the accelerator driven transmutation technologies. These projects - as shown on Fig. 1 - aim to :

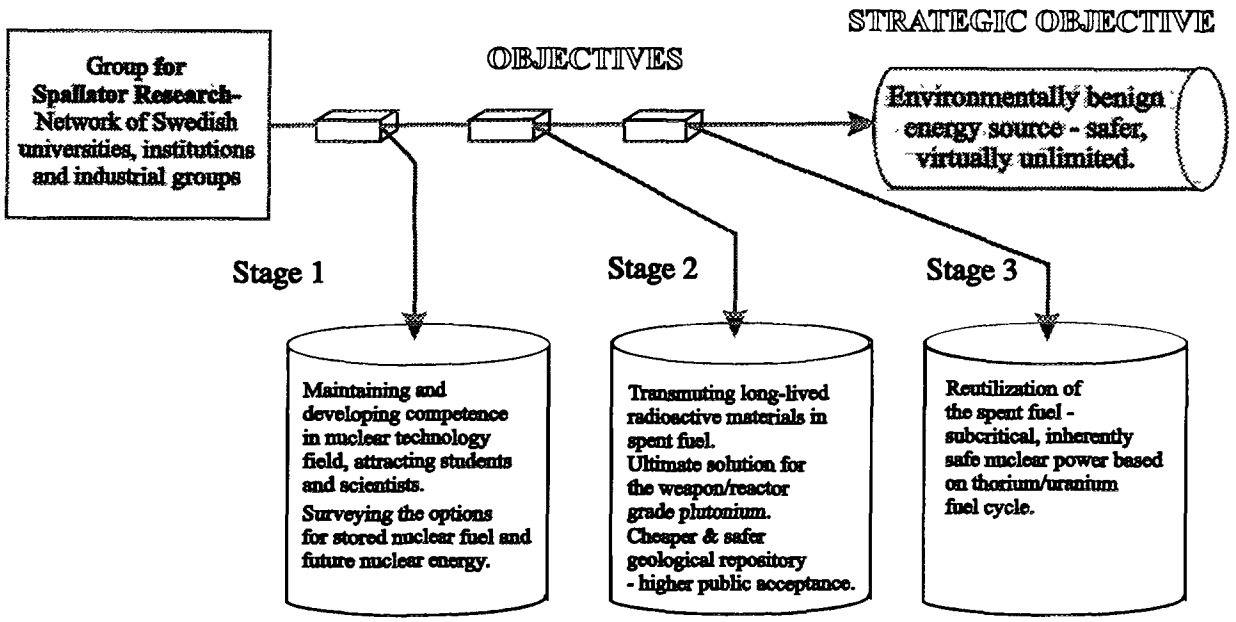

FIG. 1. Objectives of the Swedish cooperation in accelerator-driven nuclear systems

1) Find practical solutions for accelerator driven transmutation of longlived radioactive material (e.g. Plutonium, minor actinides, fission products) into shortlife or stable elements. This may result in cheaper and safer storage in geological repository;

2) Investigate of new options for nuclear energy production with inherently safe systems, either with Uranium or Thorium fuel and with reduced longlived radioactive waste production. If successful, this will result in a new, environmentally friendly, safe, cheap and virtually unlimited source of energy. The proposed systems for transmutation of spent fuel and production of energy are subcritical and inherently safe.

3) Open new, exciting research and occupation possibilities for students and young specialists, which will ensure the proper level of competence needed for our nuclear power utilities, governmental agencies etc. The existing nuclear power facilities will need qualified personnel for at least two generations, even in the case of a shut-down of all the Swedish nuclear power plants by the year 2010.

The Group is now in the process of establishing long term financing for this national collaboration.

D.6.2.3. RESEARCH WITHIN THE SPALLATOR GROUP

The research projects are so far driven by the scientific interests of particular groups:

Department of Nuclear Chemistry Chalmers University of Technology (CTH) is studying separation processes proposed for use in connection with nuclear transmutation. The project, conducted in cooperation with research groups in the US, Japan and the EC contains both experimental investigations as well as modeling of different separation systems. The project is mostly directed towards fundamental research and aims to help judge whether different proposed separation and transmutation processes are realistic.

Department of Neutron and Reactor Physics and Centre for Safety Research, the Royal Institute of Technology is conducting a research program focused on conceptual studies based on computer simulations of ADS, safety and system assessments.

Department of Neutron Research and Department of Radiation Science, Uppsala University (UU) has for many years been carrying out research on basic nuclear data such as cross sections for neutron and proton induced reactions, fission yields, half-life of short lived fission products, delayed neutron yields etc.

Manne Siegbahn Laboratory (MSL) - Stockholm University has a long tradition in accelerator design and operation and conducts studies of space-charge current-limitation in the low energy part of the accelerator and a minimization of the particle losses due to residual gas collisions in the vacuum system.

An industrially oriented group of reactor physicists, formerly at ABB Atom, and neutron physicists from Uppsala University and KTH is also taking part in this collaboration and have investigated the technical and economical possibilities of implementing an inherently safe reactor concept for an accelerator driven system.

D.6.2.4. INTERNATIONAL PERSPECTIVE

The research activities of the Group for Spallator Research have been primarily devoted to system and feasibility studies together with participation in a number of international efforts mainly in the US (Los Alamos), Russia (ITEP-Moscow, IPPE-Obninsk), France (Saturne) and in the future possibly in Japan (PNC-JAERI), CERN and Switzerland (PSI).

Collaborative projects on ADS research are already in progress with leading international laboratories as described above. In particular, a project aimed at the construction and testing of a 1 MW liquid lead-bismuth spallation target has been started as a collaboration between the U.S.A., Russia, France and Sweden. It is anticipated that the Swedish groups (coordinated and financed through the Centre for Spallator Research) will prepare some part of the experimental equipment and take responsibility for its installation and performance.

The Group for Spallator Research is also going to work actively to create an international organisation or centre for advancement of ADTT.

D.6.2.5. FINAL REMARKS

Accelerator-driven nuclear systems can become an important complement for nuclear reactors opening new options for the nuclear fuel cycle and furthermore, in countries like Sweden, where of conventional

nuclear power has no future prospects, these systems can make nuclear energy an attractive source of environmentally friendly energy again. Also the idea of burning weapon grade Plutonium in accelerator driven systems has a lot of advantages and should be thoroughly exploited. The best way to achieve these goals is through intensive international cooperation and common efforts to build the first demonstration facility.

REFERENCE

[1] SKB Annual Report 1993, Stockholm May 1994

D.6.3. ADS PROGRAMS IN FRANCE

D.6.3.1 FRENCH PROGRAMS FOR ADVANCED WASTE MANAGEMENT OPTIONS

M. Salvatores *, J.P. Schapira**, H. Mouney***

* CEA-DRN, ** CNRS-IN2P3, *** EDF-DE

Several organisms (CEA, CNRS, EdF, etc) are cooperating in France on Accelerator-Driven Systems. The major motivation is the investigation of innovative options for the radioactive waste management. The paper describes the ongoing activities and future directions of the cooperative efforts.

D.6.3.1.1 INTRODUCTION

The management of long-lived radioactive wastes, has been the subject in France of a Parliament law (December 1991), which requires that R and D work should be performed, in particular by research organism , on : partitioning/transmutation (P/T); underground laboratories for deep storage assessment; intermediate storage technology, in order to provide the scientific elements to evaluate advantages/disadvantages of the different options to be submitted to the Government for a decision in 2006. As far as transmutation, most work has been done up to now on the potential of standard (or advanced) fission reactors. However, the national body Commission Nationale d´ Evaluation (CNE) in charge of evaluating step by step the R and D work performed, has recently recommended to explore also more advanced solutions for waste management and in particular for transmutations. Accelerator-Driven System fall clearly in this category.

D.6.3.1.2 THE ISAAC PROGRAM AT CEA

D.6.3.1.2.1 Background

As mentioned above, most work on transmutation is focused on the potential of fission reactors (thermal or fats). The CEA is conducting a research program [1] in the frame of the wider SPIN program (which includes actinide chemistry) in partnership with EdF, FRAMATOM and COGEMA.

From a strictly point of view, "transmutation" is a matter of neutron availability [2], and standard fission reactors can provide them : a PWR with increased fuel enrichment or a Fast Neutron Reactor used in the "burner" mode [3] . Accelerator-Driven System can provide extra neutrons [2] and can play a role in a long term P/T strategy, or, in general, they can play a role in the assessment of different long term options for the back-end of the fuel cycle.

D.6.3.1.2.2 The Fields of Activity of the ISAAC Program

At CEA, different laboratories have been working in recent years on several aspects of the technology and of the physics of Accelerator-Driven Systems (high intensity accelerator technology, physics of source-driven multiplying systems, spallation physics). It has been decided in 1995 to launch a program, devoted to the experimental validation of the major items related to a generic accelerator-driven system (namely, accelerator technology, target physics and multiplying sub-critical system physics). The program of research concerns the physics of multiplying subcritical systems, in the feasibility of high intensity accelerators, the physics and the experimental validation of spallation phenomena modelisation and system studies, devoted both to minor actinide transmutation potential and to feasibility/safety studies.

D.6.3.1.2.3 The Physics of Multiplying subcritical Systems

It is recognized that, whatever the application, the multiplying subcritical core will play a central role. The physics of such systems (I. e. source-driven subcritical systems) is known in principle. However, no specific experimental program has been performed, in particular for near-critical subcritical systems. Methods and data needed are fairly sophisticated, in terms of geometrical configurations, neutrons modes superposition, spatial flux distribution, etc, and in a specific experimental program is needed to gain confidence in the assessment of the performances of hybrid systems.

An experimental program has been launched at the MASURCA facility in CADARACHE. A first experiment (MUSE) has been performed in December 1995 and it will be reported in a companion paper at this conference [4]. These experiments can help to understand the role of the neutron importance of the source and the impact of the source spectrum and environment , at different levels of subcriticality. The "homogenisation" of the results will be indicated at this conference. The first MUSE-1 experiment did allow to confirm that the high accuracy measurements can be performed to evaluate the system subcriticality $\Delta\rho$ (to less than 3%), the reaction rate spatial distributions (to $\pm$ 1%), and the neutron source effectiveness φ^* [4].

The next phase, MUSE-2, will be devoted to the study of the influence of neutron diffusing medium around the source (see Figs 1 and 2) . This program has been performed in late summer 1996.

A MUSE-3 experiment, to be performed in early 1997 is under study , possibility using a lead buffer around the source and attempting delayed neutron effective fraction measurement in the subcritical medium.

In the frame of these studies , actinide and fission product neutron cross-sections have been or will also be measured at the Geel LINAC (in particular ^{237}Np, ^{99}Tc). Moreover, a large scale experiment is underway at SUPERPHENIX (the SUPERPROFIL experiment), in which a large number of pure, separated isotope samples are irradiated in two standard fuel pins in a clean environment inside the core. In particular samples of ^{237}Np ,^{239}Pu, ^{241}Am, ^{243}Am, ^{244}Cm will be analyzed after irradiation and transmutation rates will be determined with high accuracy.

D.6.3.1.2.4 Feasibility of High Intensity Accelerators

Studies are underway on accelerator structures with coupling cells, on halo phenomena and the dynamics of the beam and on radiofrequency chains. Theoretical studies are completed by an experiment on the beam dynamic (FODO experiment) and by the design of a proton source of 100 mA at SATURNE. Of course, this activity has wider scope than hybrid system applications. At present, no unique specifications for a high intensity accelerator have been given, since the role and applications of hybrid systems are still to be fully defined (see section D.6.3.2.6).

D.6.3.1.2.5 Physics and Modelisation of Spallation

The experimental programs at SATURNE will be detailed in other companion papers at this conference (thin and thick targets, spallation residual nuclei measurements, double differential cross-sections measurements, neutron production etc) [6].

New code systems are developed and validated on these experiments. In particular, a project for a new code system, dedicated to the physics of spallation, has been launched at CEA (1996-1998). This code system (called "SPARTE") will handle intranuclear cascades (with improved models) , high energy particle transport, neutron transport below a threshold energy E_t (initially E_t=20 MeV, later E_t=150 MeV) with

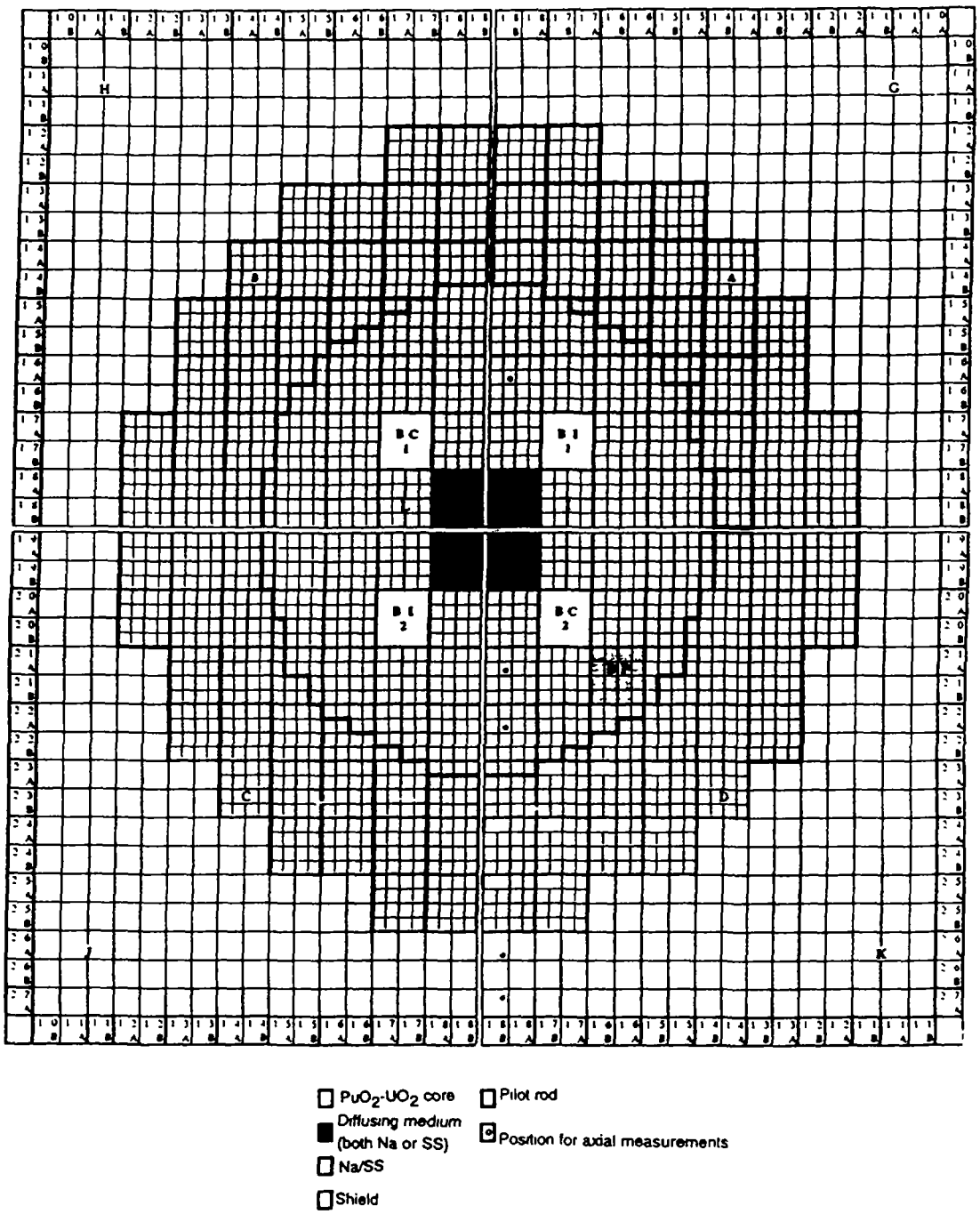

FIG. 1. Proposed configuration for the MUSE-2 experiment

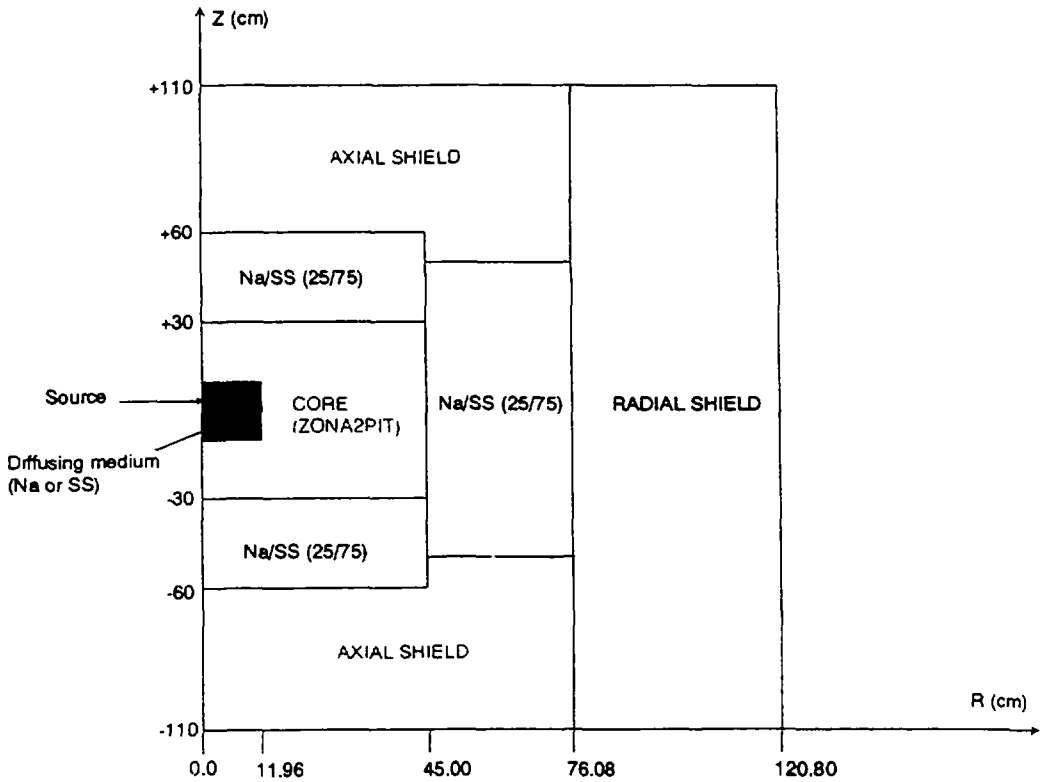

FIG. 2. RZ model for the proposed configuration of the MUSE-2 experiment

the continuous Monte Carlo code TRIPOLI, and full nuclide time evolution description (activity, decay heat, toxicity) by the code DAEWIN (developed for standard applications).

Nuclear data bases will be enlarged, as far as possible in the frame of international collaborations (like Working Party on Evaluation Collaboration of the OECD-NEA). The coupling with the standard neutronics code systems (e. g. ERANOS [7]) will be realized. A principle scheme of SPARTE is given in Fig.3 .

D.6.3.1.2.6 System Studies

The physics of the accelerator driven system has been the object of studies and the main conclusions and present views have be presented in a paper by M. Salvatores and I. Slessarev [8]. The main potential role for accelerator driven systems can be found in cases where the external neutron supply can help to shape a radioactivity clean nuclear power (RCNP), i. e. concentrate radioactive wastes (e. g. Am and Cm) in a very limited number of installations inside a standard nuclear power park of reactors, also dedicated if possible to eliminate long-lived fission products.

This approach is close to the "double strata" concept proposed by JAERI [9].

Two more fields of application of hybrid systems seem to be promising:

-Optimized use of the Uranium cycle in a large subcritical fast reactors, with long burn-up and low reactivity loss per cycle.

-Enhanced and adaptable neutron source, for driving small power systems with high subcriticality for innovative irradiation studies and fundamental physics studies. This last type of system could be eventually used as pilot experiment for hybrid system feasibility demonstration.

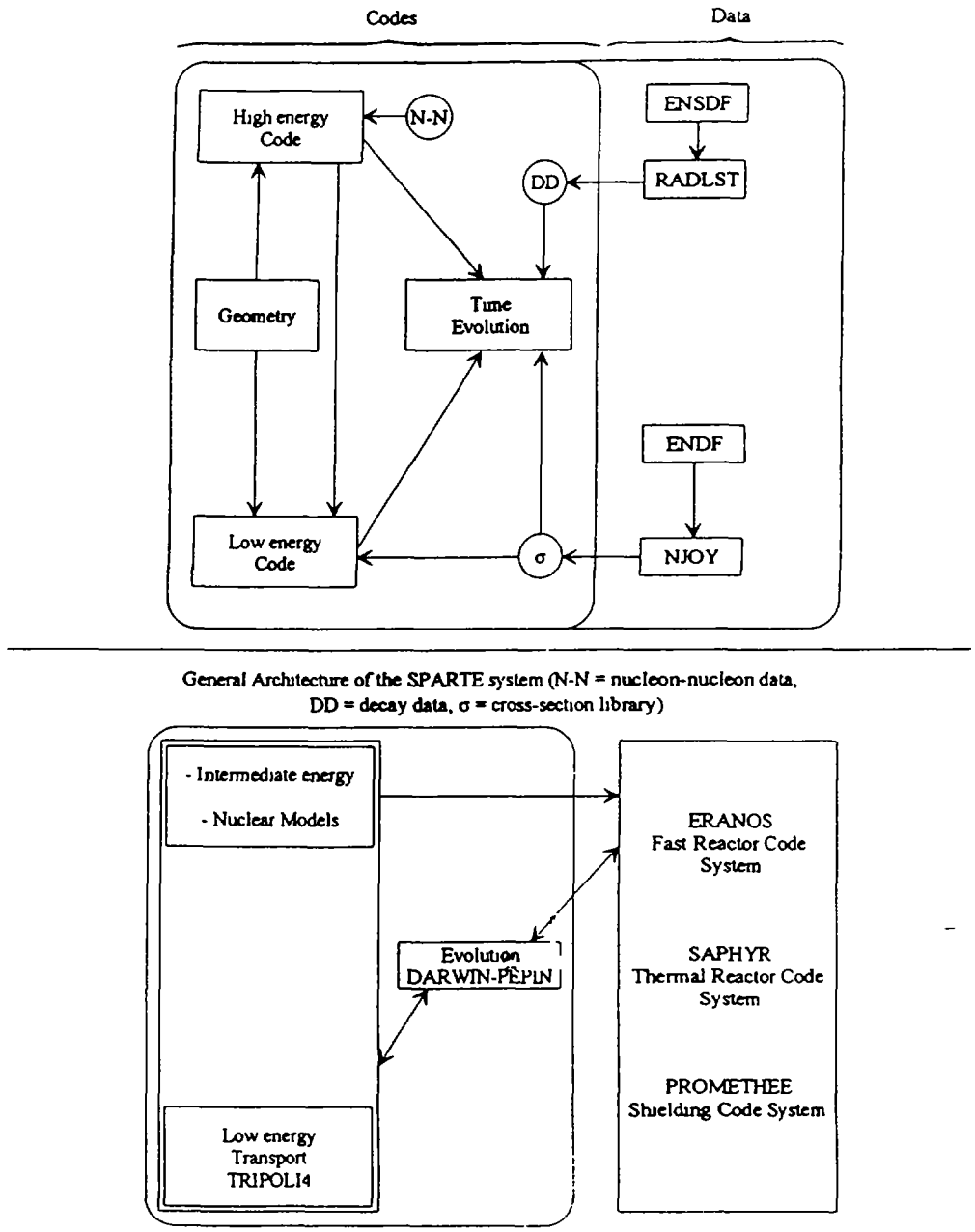

FIG. 3 The SPARTE computer code system

D.6.3.1.3 THE PRACEN RESEARCH PROGRAM AT IN2P3

In France, basic research in nuclear and particle physics are carried out by IN2P3 (Institute National de Physique Nucleaire et de Physique des Particles), which is a part of CNRS (Centre National de la Recgercge Scientifique), as well as by a part of CEA (Direction Des Sciences de la Materie). The activity of IN2P3, related to nuclear waste management was restricted to a radiochemistry and nuclear chemistry studies, at least until 1993 when it was decided to make larger contribution on certain aspects of the back end of the fuel cycle for which basic research could be needed.

In June 1993 , a coordinated research program, called PRACEN (Programme de Recherche sur l' Aval du Cycle ElectroNucleaire) was officially set up on two subjects, in accordance with the above mentioned 1991 law (article 4) and with the competencies identified among the radiochemists and physicists of IN2P3:

-Radiochemical studies related to the physico-chemical conditions of deep geological storage as well as to the chemical separation of certain long-lived radioelements.

-Nuclear storage properties and accelerator studies in relation with accelerator driven systems.

The first theme is up to now the most active, and it is carried out, since 1995, in the frame of a national program called PRACTIS (Physicochimie des Actinides at Autres Radioelements en Solutions et aux Interfaces), with part of CEA (Direction du Cycle du Combustible) and the department of Chemical Sciences of CNRS. On the other hand, IN2P3 is partner to an EC program on "Thorium Cycles as Nuclear waste Management Option" and is specifically in charge of the mining aspects and of the residual risks in deep geological storage.

The main activity on the second theme is carried out in the frame of collaboration with the Rubbia's group ET at CERN. Physicists from various IN2P3 laboratories (Grenoble, Bordeaux and Orsay) have taken a very active part in the first experimental study carried out in 1994 at CERN to establish the Energy Amplifier concept [10]. In relation with the new C. Rubbia's proposal of subcritical fast reactor, driven by a cyclotron , and cooled by lead, IN2P3 has recently designed a lead structure to be used near the Grenoble cyclotron, which produces a pulsed neutron beam. Such a device is designed for neutron transport studies in lead and for some transmutation rates measurement at various neutron energy, the lead being used as a slowing down spectrometer [11]. It is also part of the project TARC (Transmutation by Adiabatic Resonance Crossing) developed at the ET group of CERN, which should be applied to the transmutation of some long-lived fission products (such as ^{99}Tc).

D.6.3.1.4 THE "GEDEON" COLLABORATIVE PROGRAM

At the national level, a joint research program has been recently established among CNRS, EDF, and CEA. The program covers the common areas of interest of the ISAAC and PRACEN programs. The objective is to explore innovative options in common for radioactive waste management. The Hybrid Systems potential evaluation is at the core of the GEDEON program, but the potential of alternative fuel cycles (e. g. Thorium) is also explored . Starting in 1996 , efforts are put in common to run the previously mentioned experiments (e.g. the MUSE and the Grenoble lead experiments), and to plan future experiments and activities. Moreover, the international collaboration (underway with PSI-Switzerland, CERN, ENEA-Italy, FZK-Germany, GSI-Germany, RIT-Sweden, ECN-Netherlands, Politecnico di Torino etc), should strongly expand in the near future.

REFERENCES

[1] Viala, M. Salvatores, M. "An overview of the SPIN Programme". Proc. 3rd Int. Information Exchange Meeting on Partioning an Transmutation, Cadarache, Dec. 1994 (OECD-NEA/PT Report n. 13).

[2] Salvatores, M. et al., Nucl. Sci. Eng. 116, 1 (1994).

[3] Languille , A. et al. "CAPRA core studies", Proc GLOBAL' 95 Int. Conference, Versailles, Sept. 1995.

[4] Salvatores, M. et al. "MUSE-1 : A first experiment of MASURCA to validate the physics of sub-critical multiplying systems relevant to ADS", this conference.

[5] D' Angelo, A. et al. Nucl. Sci. Eng. 105, 244 (1990).

[6] Leray, S. "Spallation Neutron Studies at SATURNE", this conference.

[7] J. Y. Doriath, J. M. Ruggieri, G. Buzzi , J. M. Rieunier, P. Smith, P. Fougeras, A. Maghnouj, "Reactor Analysis Using a Variational Nodal Method Implemented in the ERANOS System", ANS Topical Meeting, Knoxville, TN, USA, vol. II, p. 20 (April 1994).

[8] Salvatores, M. , Slessarev, I. "Nuclear Power Development and hybrid system role", 2nd International Conference on Accelerator Driven Transmutation Technologies and Applications, 3 - 7 June 1996, Kalmar, Sweden.

[9] Mukaiyama, T. "Importance of the Double Strata Fuel Cycle for Minor Actinide Transmutation".. Proc. III Int. Information Exchange Meeting on Partitioning and Transmutation, Cadarache, Dec 1994 (OECD-NEA/PT Report n. 13).

[10] Andriamonie, S. et al., "Physics letters" B348 (1995) 697-709.

[11] Asghar, M. et al., "Lead slowing-down time spectrometer at SARA", ISN Report 96-42, Grenoble (1996).

D.6.3.2. MUSE-1 : A FIRST EXPERIMENT AT MASURCA TO VALIDATE THE PHYSICS OF SUB-CRITICAL MULTIPLYING SYSTEMS RELEVANT TO ADS

M. Salvatores, M. Martini, I. Slessarev, R. Soule, J. C. Cabrillat, J. P. Chauvin, Ph. Finck, R. Jacqmin, A. Tchistiaakov

CEA - Nuclear Reactor Directorate - Cadarache

ABSTRACT

In the framework of CEA programme ISAAC, devoted to Accelerator-Driven Systems, several experiments activities have been launched. A significant experimental programme is underway in MASURCA experimental reactor in Cadarache to validate the physics of subcritical multiplying media. The first experiment MUSE-1 performed in December 1995 is described in the present paper, and a first analysis of the result obtained is geven.

D.6.3.2.1 INTRODUCTION

External source-driven subcritical systems (here called "hybrid systems) have been widely discussed in recent years.. The behavior of the subcritical reactor is mostly determined by the inherent neutronics characteristics related to the Boltzmann operator of that system. A flexible installation like the MASURCA experimental facility in Cadarache can be used to investigate experimentally a large range of different configurations (geometry, composition etc) at different subcriticality levels (k_{eff} ~ 0.9 to 1). As far as analysis is concerned, one can decouple the study of the spallation neutron source and its validation from the study of the neutronic behavior of the subcritical system. In that case the subcritical system can be driven by a known (I. E. in space and energy spectrum) source.

D.6.3.2.2 THE PHYSICS OF SUBCRITICAL MULTIPLYING SYSTEMS

The simplest way to represent the steady state condition in a source-driven subcritical system (k_{eff}<1) is as follows:

$$S_{ext} + \bar{\nu} = \frac{\bar{\nu}}{k_{eff}} \tag{1}$$

where $\bar{\nu}$ is the average number of prompt neutrons per fission and S_{ext} is the external neutron source (expressed in neutrons/fission).

The neutron flux distribution ϕ inside the multiplying system is given by the solution of :

$$A\phi = M\phi + S \tag{2}$$

where A and M are, respectively the net neutron loss and fission production operators of the standard Boltzmann equation.

More explicitly :

$$A\phi = \chi(E)\int \nu\Sigma_f(E',r)\phi(E',r)dE' + S(E,r)\int\Sigma_f(\tag{3}$$

where the source can be represented as :

$$S(E,r) = \chi_s(E)P(r) \tag{4}$$

with the following normalization :

$$\int S(E,r)dEdr = \int P(r)dr = \Gamma \ (neutrons/fission) \tag{5}$$

where Γ is the total number of spallation neutrons which feed the subcritical system, if all the fission energy is transformed in proton current.

It is easy to verify that the true balance equation is :

$$\Gamma\varphi^* + \bar{\nu} = \frac{\bar{\nu}}{k_{eff}} \tag{1'}$$

where φ^* is the neutron source effectiveness, defined as the ratio of the importance of the source neutrons to the importance of the fission neutrons :

$$\varphi^* = \frac{S^*}{\chi^*} \tag{6}$$

where (using the notation $< > \equiv \int dE$) :

$$\left.\begin{aligned} S^* &= \int dr <\phi^*, S> \\ \chi^* &= \frac{\int dr <\phi^*, \chi> <\Sigma_f, \phi>}{\int dr <\Sigma_f, \phi>} \end{aligned}\right\} \tag{7}$$

and ϕ^* is solution of :

$$A^*\phi^* = \frac{\nu\Sigma_f(E)}{k_{eff}} \int \chi(E')\phi^*(E',r)dr \tag{8}$$

φ^* is in general $\neq 1$, and affects in a significant way the energy balance of the system. A $\varphi^*>1$ value is desirable, since in that way once can reduce, for example, the current needed to feed the system.

In case of a known source S (neutron/s), corresponding to W_0 fissions/s, one can measure $\varphi^*/\bar{\nu}$:

$$\varphi^*/\bar{\nu} = \left[W \times 3.1 \times 10^{10}(1 - k_{eff})/k_{eff}\right]/s$$

where W (in watts) is the power in the multiplying system, which can be measured, together with the subcriticality level $(1-k_{eff})/k_{eff}$.

Obviously , in a subcritical system, one can measure physical quantities, such as reaction rates, which are directly related to the neutron flux spatial distribution, with and without external source.

D.6.3.2.3 THE EXPERIMENTAL PROGRAM

The MASURCA zero-power critical facility in Cadarache allows to set up a wide range of critical configurations with fast neutron spectrum, using a variety of different fuels and simulated coolant materials (like Na), in different proportions. For the MUSE-1 experiment in December 1995, and in order to reduce the time needed to unload/load the core, an existing loaded core was used (fueled with UO_2-PuO_2 with a ratio of Pu/(Pu+U) approximately equal to 0.25 , and with simulated Na coolant). The core axial and radial dimensions were, respectively, h = 60 cm and r = 45 cm. In the central channel of the core it was possible to load a ^{252}Cf neutron source (s = 7.55×10^7 n/s), which was located successively at three axial position (in the midplane, at +15 cm and at +25 cm above the midplane). The geometrical arrangement of the experiment is shown in Fig. 1. The core composition is given in Table I.

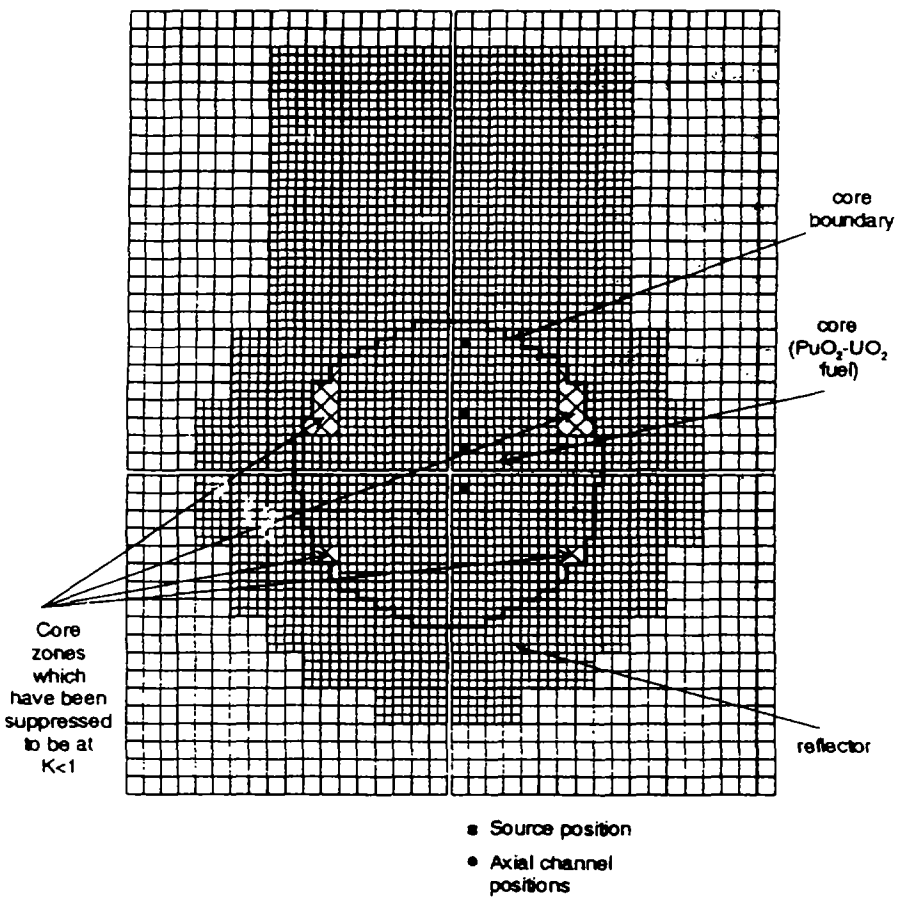

FIG. 1. MUSE-1 configuration - XY section at midplane

TABLE I. MUSE-1 CORE COMPOSITION

	Volume Fraction
Fuel: UO_2-PuO_2 Pu/(Pu+U) = 0.25	34%
Simulated coolant : Na	43%
Structural material : SS	12%
Void	11

Starting from a critical configuration without external source), the core was made subcritical , by unloading some peripheral fuel elements.

The following measurements have been performed :

-sub-criticality level,

- ^{235}U fission rate radial and axial distributions,

- φ^* measurement.

D.6.3.2.3 EXPERIMENTAL RESULTS AND ANALYSIS

The reactivity of the subcritical configuration has been measured by modified source multiplication method (MSM) .

The analysis has been performed with the latest version of ERANOS code system [1], used for the neutronic analysis of fast reactors. In particular fixed-source 3-dimensional transport methods have been used, since diffusion theory is not adequate for this type of configurations. A comparison of calculation and experiment of reactivity is given in Table II.

TABLE II. CALCULATION/EXPERIMENT COMPARISON FOR REACTIVITY

	Experiment	Calculation		
		3D(XYZ) Diffusion Finite Differences	3D(XYZ) Diffusion Nodal	3D(XYZ) Transport Nodal
k_{eff}	0.98345±0.00250	0.96729	0.96821	0.98111
E-C		0.01515	0.01524	0.00234
$\Delta\rho$	-0.01572±.00060	-	-	-0.01560
E-C		-	-	0.00012±.00060

The agreement is very satisfactory. The relative distributions of ^{235}U fission rates were measured using fission chambers both in a radial channel at core mid-plane and in three axial channels located at three radial positions (see Fig. 1).

The relative precision of the measurement was high enough (±1%), to make it possible to detect the perturbations caused by the presence of the Californium source. Some typical results are shown in Figs 2 and 3. Figure 2 shows a radial profile of the ^{235}U fission rate measured both with and without the external source.

Figure 3 shows the three axial distributions of the ^{235}U fission rate, relative to the cases when the external source, which becomes less pronounced when the fission rate is measured in an axial channel far from the center.Calculations have been performed using the same calculation scheme as indicated previously. Excellent C/E agreement was found as illustrated in Figs 4 and 5. Most C/E values are inside the experimental error bars (±1 ÷ 2%).

Finally Table III compares the measured and calculated $\varphi^*/\bar{\nu}$ values relative to the external source: good agreement is observed, often within experimental uncertainties.

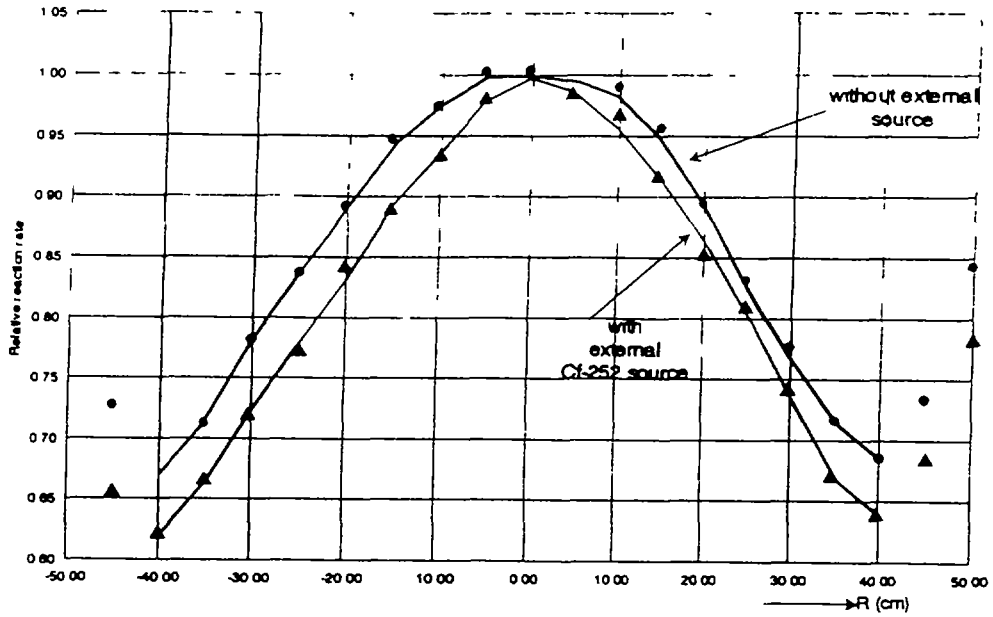

FIG. 2 Radial ^{235}U fission rate in MUSE-1.

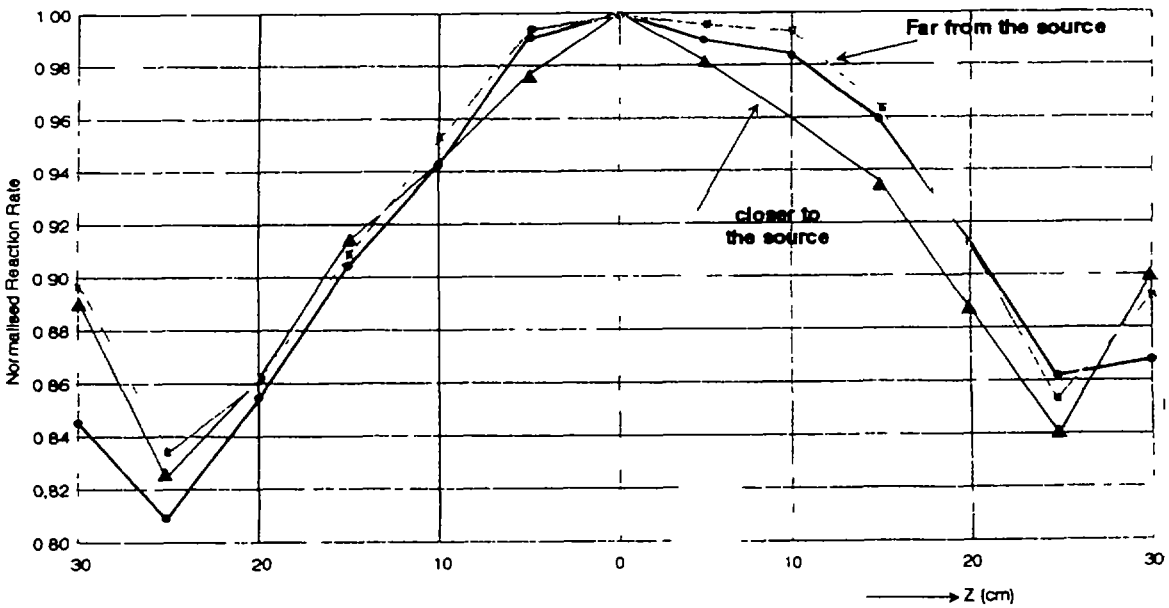

FIG 3. Axial ^{235}U fission rate in MUSE-1.

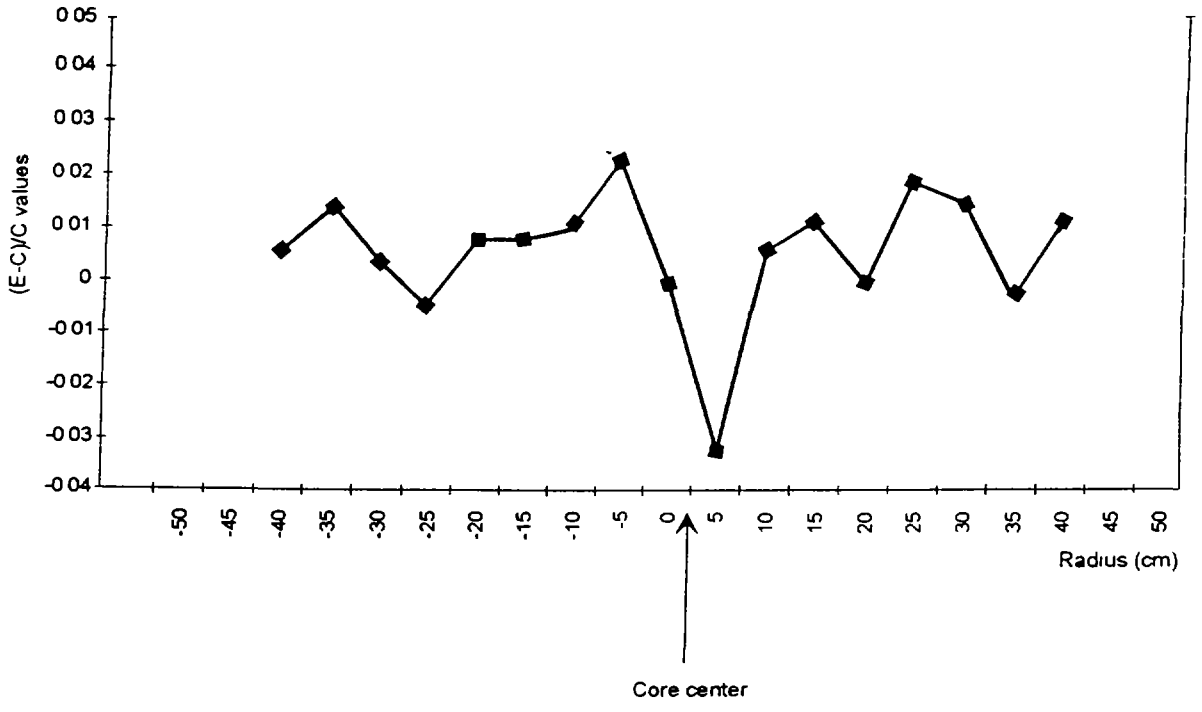

FIG. 4. C/E values for the radial ^{235}U fission rate at midplane (^{252}Cf source at midplane)

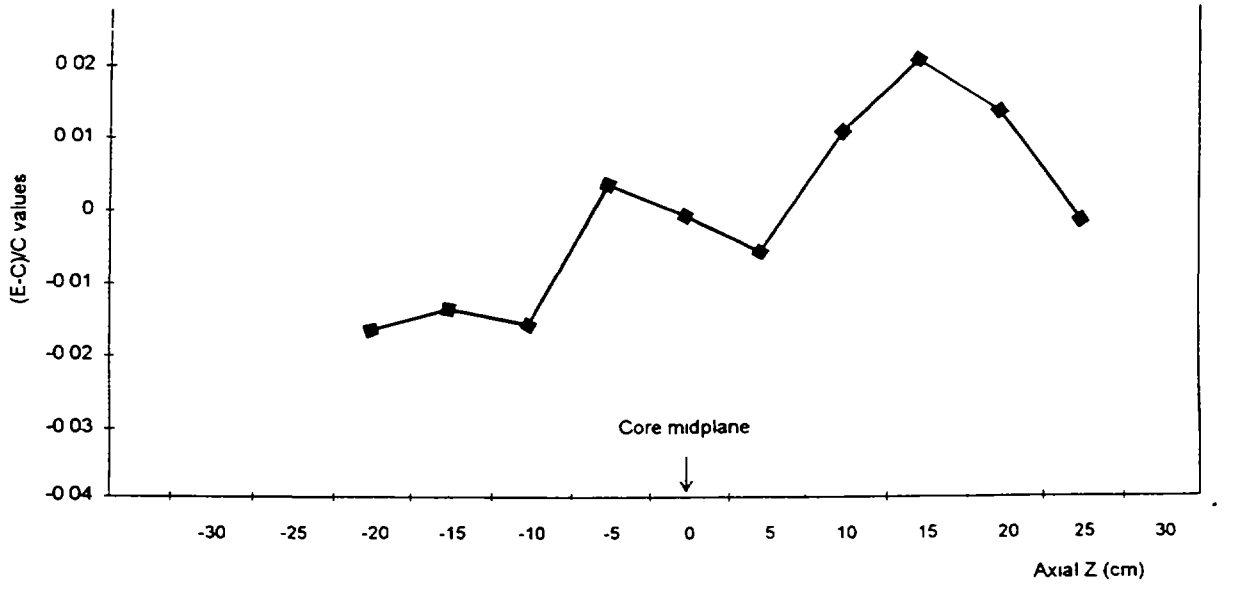

FIG. 5. C/E values for the axial ^{235}U fission rate at midplane (^{252}Cf source at +25 cm with respect to midplane)

TABLE III. CALCULATION/EXPERIMENT COMPARISON FOR $\varphi^*/\bar{\nu}$

^{252}Cf Source Position:	At core center	+15 cm [a]	+25 cm[b]
	E=0.495±4%	0.460±4%	0.380±4%
	C=0.534	0.468	0361
	(E-C)/C=-7.1±4%	-1.7±4%	+5.3±4%

(A) : Z with respect to midplane

D.6.3.2.4 CONCLUSIONS AND FUTURE PLANS

The MUSE-1 experiment performed on the MASURCA assembly in Cadarache has shown the potential of that facility to investigate the physics of subcritical multiplying systems in the presence of an external source. The accuracy of the measurements is very high, and known experimental techniques, used in standard experiments to validate the physics of fast neutron cores, can be applied with confidence.

The short, exploratory MUSE-1 programme has provided some insight into the physical behavior of the neutron population in the subcritical system.

Moreover, a relevant integral parameter , I. e. the external neutron source effectiveness φ^*, was defined and measured with high accuracy. This point is very relevant, since φ^* can be a key parameter in the optimization of a hybrid system, to improve the energy balance and to provide an optimized neutron importance distribution.

Future experiments will focus on the study of neutron diffusing media placed around the source, with different positions of the source and at different levels of subcriticality.

Kinetics parameters (like β_{eff}) will be measured, to gain insight in the time dependent behavior of a subcritical system.

REFERENCE

[1] J. Y. Doriath, J. M. Rggieri, G. Buzzi , J. M. Rieunier, P. Smith, P. Fougeras, A. Maghnouj, "Reactor Analysis Using a Variational Nodal Method Implemented in the ERANOS System", ANS Topical Meeting, Knoxville, TN, USA, vol. II, p. 20 (April 1994).

D.6.4. ADS PROGRAM IN THE CZECH REPUBLIC

D.6.4.1 APPROACHES TO A NATIONAL ADS PROGRAM IN THE CZECH REPUBLIC

František Janouch
The Royal Institute of Technology, Stockholm, Sweden and
The Institute of Nuclear Physics, Czech Academy od Sciences, Řež,
Miloslav Hron
Nuclear Research Institute, Řež, Czech Republic
Rostislav Mach
The Institute of Nuclear Physics, Řež, Czech republic
V. Valenta
Škoda, Nuclear Machinery, Ltd., Czech Republic

D.6.4.1.1. NUCLEAR ENERGY IN THE CZECH REPUBLIC

The Czech Republic is a highly developed industrial country with a dense population.The country is very poor in conventional energy resources: hydroenergy - fully exploited - provides less than 3% of the total electricity production; fossil reserves are reduced to coal only, most of it being low quality and sulphur rich brown coal and lignites. Its use for electricity production caused, and still causes, heavy environmental damage especially in the northern part of the Czech republic which is internationally declared to be an ecological disaster region. The atmospheric pollution caused by coal power stations is causing grave concerns even in the neighboring countries. At the end of the eighties, Czechoslovakia, having a population of about 0.3% of the total world population, was burning app.10% of the total world production of lignites. At the beginning of the nineties, about 90% of Czechoslovakia's oil and natural gas were imported from the former USSR i.e. from abroad, making the country's economics very vulnerable and dependent.

The Czech republic had considerable reserves of Uranium ores. Although a large part of it was exploited between 1945 and the seventies, a reasonable amount of Uranium ore is still available.

These are the main reasons why the Czech Republic decided to build several nuclear power stations. Four of them, Russian designed VVER-440 (V-213) reactors have been in operation at Dukovany since the middle of eighties. Two additional reactors, VVER-1000, are near to completion in Temelín, South Bohemia.

The completion of the Temelín nuclear power plant initiated hectic discussions both at the national and international levels. Although the VVER-1000 is the most modern russian designed NPP, provided with a very solid containment, additional significant steps were undertaken to increase its safety standards. The American company Westinghouse is in charge of further modernization the NPP, providing modern instrumentation and control system and newly designed fuel elements.

D.6.4.1.2. SPENT FUEL MANAGEMENT

Until 1986 the spent fuel did not present any problems since the country manufacturing the fuel - i.e. the USSR - had a contract obligation to take care of it. Since the end of 1991a Russian Federation law prohibits the acceptance of spent fuel from abroad, so the Soviet/Russian option for handling of the spent fuel has been out of the question.

This is why the Czech Republic since 1992 has had to reconsider the whole problem of the spent fuel waste. The Czech energy board tried unsuccessfully to negotiate the storage of spent fuel abroad in Germany, Italy, Finland, Belgium and Sweden - i.e. in countries with spare storage capacity. After rejecting

the reprocessing option, the only remaining solution was to build both an interim and a final repository in the Czech republic. Due to considerable public opposition, spent fuel management has become a serious political problem in the Czech republic during the last couple of years. According to present political plans, the final underground repository should not be opened before 2050-2070; therefore enough time exists for a thorough investigation of alternative solutions.

D.6.4.1.3. THE 1994 AND 1995 LIBLICE SYMPOSIUM

The above are, in brief the reasons why the new ideas presented on the Los Alamos ATW project and by the Rubbia energy amplifier project met a positive response not only in political quarters but also in the nuclear power industry and utilities. Even the mass-media reacted positively and published several reports about the Los Alamos project.

In 1994 the Ministry of Industry and Commerce asked a group of Czech scientists to prepare a preliminary study on projects dealing with accelerator driven nuclear reactors and nuclear waste transmutation. The study has been completed in the spring of 1994 and published in Czech [1].

The Initiative Group for the accelerator driven transmutation of waste was set up in September 1993. Its activities were financially supported by the Czech Energy Board (ČEZ), Czech Ministry of Industry and Commerce and the ŠKoda industrial group.

This financial support has allowed small symposiums to be convened on June 27-29, 1994 and then on September 1995 at the Liblice castle near Prague on accelerator driven reactors and nuclear waste management projects in the Czech Republic [2].

The symposiums met with a considerable interest from Czech scientists and nuclear engineers. Over 40 people, including several scientists from Sweden, the U.S., Slovakia and Russia, took part in its work and around 20 papers, covering different aspects of this problem and reporting related activities in the Czech republic were presented. The participation of a group of engineers from ŠKODA NM Ltd who presented several papers was encouriging, showing that these new ideas are seriously discussed and studied in the industry.

The Liblice symposiums reviewed the competencies of Czech scientists and engineers in the field of accelerator driven reactor and transmuters. Many interesting proposals and topics were presented at the symposium [3].

In the spring of 1995, the Iniative Group presented another more detailed and complex study to the Czech Ministry of Industry and Commerce under the title "Possibilities of incineration of spent fuel and radioactive wastes by new methods" [4].

The nuclear program was initiated in the former Czechoslovakia in the late fifties. Since then Czech and Slovak scientists and engineers and the nuclear industry gained considerable experience in nuclear science and technology:

(1) several accelerators, research and experimental reactors were successfully operated for several decades;

(2) considerable experience was also gained in the field of hot chemistry - separation, partitioning and solidification;

(3) jointly with Russian specialists, a new type of nuclear power reactor was designed, constructed and operated between 1972-1977. The nuclear power station, called A1, had a graphite moderated gas-cooled (CO_2) reactor using natural Uranium with a designed net electrical output of 150 MW_e;

(4) the Škoda nuclear engineering factory produced 14 NPP, twelve of them with VVER 440 power reactor units with modernized design and two with VVER-1000 reactors.

The Liblice symposiums allowed assessment of both the interest and the competences available in the Czech republic for the transmutation projects. The main centers in the Czech Republic which possess

know-how and competence for the future accelerator driven systems and transmutation studies are described here:

Nuclear Research Institute, Řež [1]:

Two research reactors (LVR-15 for material testing and LR-0 developed for testing cores of the VVER reactors)

Research reactor department.

Division of reactor physics.

Division of radiation chemistry (hot cells).,

Division of fuel cycle.

Division of metallurgy of Uranium and of reactor materials, .

Institute of Nuclear Physics, Řež near Prague:

Cyclotron (U120M, energy for protons 36 MeV, alpha-particles 40 MeV)

Van de Graaf (protons 2-5 MeV).

Accelerator department.

Department of Nuclear reactions.

Department of Nuclear spectroscopy.

Collaboration with the Joint Institute for Nuclear studies in Dubna, Russia and access to its facilities.

Institute of Special Inorganic Chemistry, Řež

Partition, extraction, solidification etc.

Institute of Physics, Czech Academy of Sciences, Prague

High Energy physics, detectors.

Collaboration with CERN.

Faculty of Mathematics and Physics and Faculty of Nuclear Physics and Engineering, Prague

Experimental reactor VR-1

Nuclear Physics

High Energy Physics

Dosimetry

Nuclear Chemistry

Neutron Physics,

Reactor Engineering.

Reactor Safety.

---

[1] Nuclear Research Institute originally belonged to the Czechoslovak Academy of Sciences, and later to the Czechoslovak Atomic Energy Commission. It was privatized in 1993.

Škoda Nuclear Machinery Co, Plzeň.

This company has built 14 reactors (12 VVER 440, 2 VVER 1000), many testing loops, transport and storage casks for spent fuel and performed reactor safety studies.

Institute of Thermomechanics, Czech Academy of Sciences, Prague:

Fluid dynamics

Thermodynamics

Dynamic fracture and impact problems

Vibrations

Institute of Nuclear Fuel, Zbraslav

Encapsulation of nuclear fuel

The Liblice symposiums and numerous discussions after it concluded that the Czech ADS program will deal with the following topics:

- Review of the present knowledge on feasibility of transmutation of actinides and fission products
- Investigation of nuclear processes in a spallation target hit by a high energy particle beam. Determination of optimal target-projectile combination(s).
- Specific problems of transmutation of long-living nuclides and neutron economics. Photonuclear reactions.
- Studies of subcritical systems, their geometry and their static and dynamic behaviour. Control of such systems.
- Trends in development of separation techniques. Dicarbollides Extraction and Sorption. Assessment of approaches developed in other countries.
- Studies on technical and economical efficiency of subcritical systems.
- Studies of thermodynamical processes in subcritical systems.
- Studies of suitable materials for the most exposed parts of subcritical systems.
- Feasibility studies of the application of an ADS in the framework of the national nuclear power program conditions and Škoda's own nuclear power technology manufacturing tradition.

The 1994 and 1995 Liblice symposiums concluded that the Czech Republic has significant theoretical, experimental and engineering potential and know-how in several fields important for the rapid development at accelerator driven systems.

Reflecting the strong interest of Czech scientists and engineers and the favorable attitude of Czech industry and Czech policy makers it was decided to establish an information and coordination center, based at the Institute of Nuclear Physics in Prague. The main task of this Center will be the formulation and coordination of national policy in this field. The center will also collect information about the development of transmutation technologies and assist in establishing contacts and collaboration with similar centres abroad.

The interest and financial support for this initiative group both from the Czech Energy Board and Škoda company and the interest shown to these programs by the Ministry of Industry and Commerce is noted as positive and promising.

6.3.1.4. INDUSTRIAL PARTNERSHIP

Being one of the first European industrial companies traditionally involved in nuclear power technology manufacturing, Škoda Nuclear Machinery (NM), Ltd. started the first feasibility studies of the application of an ADS in the framework of the national nuclear power program conditions and its own nuclear power technology manufacturing tradition [3,5-8].

Škoda NM decided to concentrate on the LANL liquid fuel (molten salt) concept of the blanket with an accelerator concept adjusted to the applicability of the redundance principle (modular system). For example: Several accelerators of lower power could be employed. The use of their integrated proton beams to bombard the lead target will not only raise the strength of the neutron source but will play one of the most significant roles of the above mentioned modular systems:

One of the accelerators can be used as a spare in case of e.g. malfunction of one of the other machines, periodic maintenance and inspection, etc. A concept that assumes accelerated proton beams bombarding several different targets in various reactor/blanket units also seems to be feasible for the Škoda NM designers.

The first results of the study mention a series of engineering problems in the area of materials and their degradation in the fields of intensive high energy particles, both charged and neutrons. The problem of the window and its life time, the problem of the target and others are proposed to be solved by the already mentioned modular system principle. The proton channel section, including the window, will be designed as remotely replaceable, by a vacuum preservation at an optimal level and by a proton channel contamination prevention. A replaceable window design solution has been proposed as well with the design of a proton channel closing valve and a quick-operating valve for a window break emergency event.

The obviously high level of complexity, and thus also the price, of such systems produces a need to accelerate the procedure to reduce the number of options and to go rather into more detailed system design and engineering in order to reach a realistic technological and economical image of the concept and project itself.

D.6.4.1.5. CONCLUSIONS

Czech scientists and engineers are fully aware of the fact that the accelerator driven transmutation and reactors are projects which are too large to be handled individually by small European nations. Scientists and engineers from the Czech republic consider therefore that a large scale international collaboration is an essential condition for further progress in this important and promising project and would welcome a creation of an international coordination body as the first step. In a more - but not too - distant perspective also the creation of an international institute, laboratory or center specializing in accelerator driven transmutation and energy production is desirable and will be supported by Czech specialists.

REFERENCES

[1] Jech Č., Niederle J., Pospíšil S.: New possibilities of obtaining nuclear energy from radioactive wastes by means of accelerators. Study report for the Ministry of industry and Commerce (In Czech), Prague 1994.

[2] Accelerator driven reactors and nuclear waste management. Abstract from the Liblice symposium, June 27-29, 1994.

[3] Janouch F., Mach R., Accelerator driven reactors and nuclear waste management projects in the Czech republic. International conference on Accelerator-Driven Transmutation Technologies and applications. Las Vegas, July 25-29, 1994.

[4] Z. Dlouhý, M. Hron, F. Janouch, L. Kuča, A. Kugler, M. Kuzmiak, M. Kyrš, V. Lelek, R. Mach, L. Nachmilner, M. Šumbera, M. Vognar, A. Vokál. Possibilities of liquidation of burnt nuclear fuel and radioactive wastes by new methods (In Czech). Report for the Ministry of Industry and Commerce of the Czech Republic, released in Prague, March 1995.

[5] Some comments by Škoda, Nuclear Machinery, Ltd., Plzen, to Accelerator Driven Reactor (ADR) problems, personal communication, 1995

[6] Valenta V., Hep J., : Safety Aspect of Reactors Controlled by Accelerator for Transuranides Burn-up Symposium on Accelerator Driven Reactors and Nuclear Waste Management, Liblice, Czech Republic, June 20-29, 1994

[7] Jílek M., Valenta V., Lelek V. : Temporary Storaging of Burned Fuel from Nuclear Power Stations in the Light of New Technologies, Symposium on Accelerator Driven Reactors and Nuclear Waste Management, Liblice, Czech Republic, June 20-29, 1994

[8] Jílek M., Hep J., Hosnedl P., Hejplík K., Pedal L., Valenta V. : Nuclear Waste Management Projects with Regard to ADR in Škoda Nuclear Machinery, Plzen, Co. Ltd., Internal Report Škoda,1995

D.6.4.2. ACHIEVEMENT OF ACCELERATOR PARAMETERS NEEDED FOR ENERGY PRODUCING AND WASTE TRANSMUTING ADS

Miloslav Hron[†] and Mikulas Kuzmiak[‡],

[†]Nuclear Research Institute Rez, plc, CZ-250 68 Rez

[‡]The Institute of Nuclear Physics of the Academy of Sciences of the Czech Republic, CZ-250 68 Rez

D.6.4.2.1. INTRODUCTION

The accelerators needed for ADS, especially for the systems producing energy and burning waste, have to satisfy some minimum technological requirements. This is not a principal problem as for reaching the necessary level of beam energy. High energy accelerators are quite common in the field of fundamental particle physics. The accelerator needed for power production, at an energy of 800 MeV, is in the mid-range of energies for such devices, much higher than those used for cancer therapies in hospitals (tens of MeV) but much lower than those used for fundamental physics research at the biggest world centers (thousands of MeV and beyond). This energy is sufficiently high that a single proton colliding with several nuclei as it moves through the heavy metal target releases about 20 to 30 neutrons which are then multiplied in number in the surrounding blanket as reported by the scientists of LANL, USA [1].

There are two types of accelerators that could drive the system at approximately 1 GeV and average currents in the range of 10 to 100 mA. The first option is to use a linear accelerator that would be an advanced, high intensity version of, e.g. the Los Alamos Meson Physics Facility (LAMPF) 800 MeV accelerator. The second is to use a circular accelerator, e.g. the 500 MeV ring cyclotron operating at the Paul Scherer Institute in Switzerland or a series of others of that or similar type. Both of the options can achieve energy required without difficulty but both require technology development to achieve the necessary beam intensities. The cyclotron machines, in particular, are limited to currents of 10 to 15 mA due to the difficulty in adequately confining the beam.

Linear accelerators are foreseen to be able to deliver perhaps 100 to 300 mA of beam current. They already produce such current in pulsed mode but the technology will have to be extended to provide the near-continuous operation which would be needed for the highest currents. Although the beam physics for a continuous operation is a modest extrapolation of that for pulsed operation, significant engineering development is still needed. A system delivering 15 mA of protons and 800 MeV (12.5 MW of beam power) can drive a blanket assembly to produce 200 MW of electrical power and so a circular accelerator is an attractive option at this power level.

To achieve the usual level of approximately 1,000 MW_e it possible to apply the LAMPF-like linear accelerator with much higher current capability, which would allow a single accelerator to drive either a large transmutor or a small cluster of separate blanket assemblies with a total system power of 1.200 MW_e. In either case only about 15% of the electrical power would be used to drive the accelerator. However, the exclusive use of only one accelerator unit would represent a weak point of such a systems operational reliability. On the other hand, the employment of more than one accelerator of such a class would be an extremely costly approach.

An attractive approach to the achievement of the accelerator parameters needed to employ circular machines that beside others have an advantage of being more compact systems, has recently been proposed by Czech scientists [2]. A brief description of their idea is introduced in the following paragraph.

The proposal is based upon an octupole magnet. A transversal cross-section of such an octupole magnet is schematically outlined in Figure1.

This octupol magnet has two focusing planes (Θ =0 and Θ=π/2) and two defocusing planes (Θ = π/4 and Θ=3π/4). Taking the octupol magnet symmetry into account and maintaining the terms up to the fifth order in the expansion we may obtain the magnetic field components from the general expressions for the magnetic field expansion:

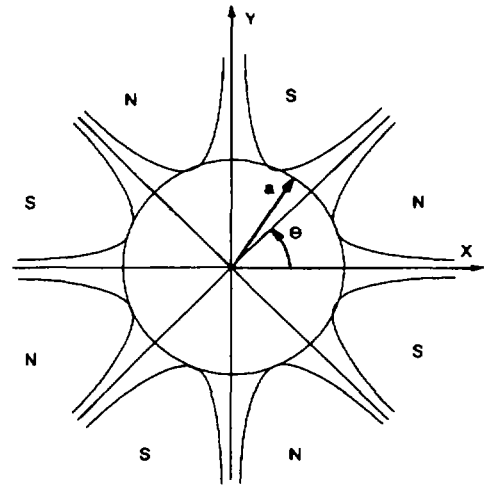

FIG. 1. Cross section of an octupole magnet

$$B_x = \frac{B_0}{a^3}\left[f(z)y(3x^2-y^2) + f''(z)\frac{y}{20}(y^4-5x^4)\right]$$
$$B_y = \frac{B_0}{a^3}\left[f(z)x(x^2-3y^2) + f''(z)\frac{x}{20}(5y^4-x^4)\right] \quad (1)$$
$$B_z = \frac{B_0}{a^3}\left[f'(z)xy(x^2-y^2)\right]$$

with B_0 the field on the pole, a the aperture radius of the octupole magnet, f(z) the function describing the field distribution along the z axis; the prime denotes a derivative with respect to the z variable.

The joining of two beams into one beam is schematically outlined in Figure 2.

Let us note that this scheme can be applied to both twins of the focusing and defocusing planes of the octupole magnet as mentioned above, so that totally 4 individual beams being generated by 4 individual accelerators can be joined to one beam with an integrated intensity through the following process:

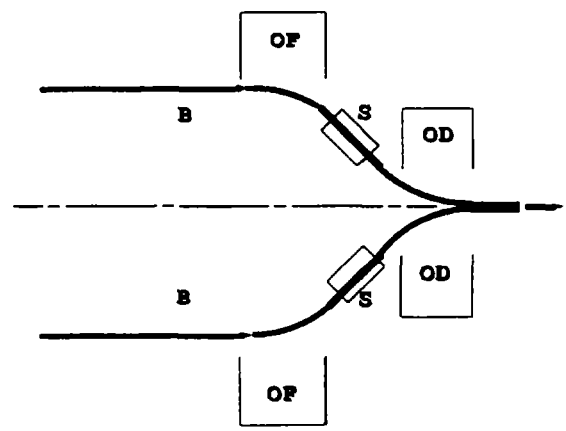

FIG. 2. Funnel of beams

The charged particle beams (B) enter an octupole focusing magnet (OF) which deflects them towards the longitudinal axis z. Behind this octupole focusing magnet, the beams transit through solenoids (S). These solenoids focus the beams in a transverse direction. There is an octupol a defocusing magnet (OD) behind the solenoids. It deflects the beams towards the longitudinal axis z. The proximity to the longitudinal axis can be expressed either by the transverse coordinate of the central trajectory of the beam or by the angle between the central trajectory and the longitudinal axis. If these two values are in the range of the

emittances of the entering beams, then the joining is complete.

The general trajectory equations of a particle with charge e and momentum p in the magnetic field of the octupole magnet take the following form:

$$x'' = \frac{B_0}{B\rho a^3}\left\{ f\left[x(3y^2-x^2)\left(1+\frac{3x'^2+y'^2}{2}\right) + x'y'y(y^2-3x\right.\right.$$
$$\left.\left. + f'xyy'(y^2-x^2) + \frac{1}{20}f''x(5y^4-x^4)\right\}\right.$$
$$y'' = \frac{B_0}{B\rho a^3}\left\{ f\left[y(3x^2-y^2)\left(1+\frac{3y'^2+x'^2}{2}\right) + + x'y'x(3y^2-x\right.\right. \quad (2)$$
$$\left.\left. + f'xyx'(y^2-x^2) + \frac{1}{20}f''y(y^4-5x^4)\right\}\right.$$

where B =pc/e is the magnetic rigidity. By approximating the field distribution in the octupole magnet along the axis by a rectangular model (f(z)=1 within the octupole magnet and f(z)=0 outside the octupole magnet) and by confining to the third order terms only, the trajectory equation in an octupole magnet takes the following simple form:

$$x'' = \frac{B_0}{B\rho a^3}x(3y^2 + x^2)$$
$$y'' = \frac{B_0}{B\rho a^3}y(3x^2 + y^2) \quad (3)$$

which can easily be applied for checking of the sufficient proximity of the central trajectory to the longitudinal axis as mentioned above. By varying B_0 and a the prescribed precision can be easily reached.

D.6.4.2.3. CONCLUSION

The issue of the achievement of the accelerator parameters needed for energy producing and waste transmuting ADS plays an important role in the strategy of a convenient technology choice and an overall optimization of the system. Therefore, the problem was briefly discussed and the current status of accelerator technology available or that expected in the near future has been outlined. There exists a series of specific approaches to the achievement of the accelerated charged particle beam intensity. However, one which was proposed recently [2] seems to be very efficient and in spite of the fact that it is still currently being analyzed and developed to a practical application in ADS technology it has been introduced here. It is likely, that such an approach would allow employment, in ADS of broadly applied circular accelerators, with a lower level of beam intensity, in a similar manner and with comparable efficiency to the high beam current producing LINACs. Moreover, the principal features of the complex employment of several units which can adjust their output parameters in a certain interval will very likely allow to leave at least one unit to be left out of operation for repair or exchange while the whole ADS remain in full power operation.

REFERENCES

[1] VENNERI, F., HEIGHWAY, E. and BOWMAN, C., Accelerators Add a New Option to our Energy Future , Los Alamos National Laboratory, Los Alamos, personal communication, 1995

[2] HRON, M., KUZMIAK, M.: The proposal of a funnel for joining more beams into one, The Institute of Nuclear Physics, Rez (in preparation).

E. SAFETY ASPECTS

H.U. Wider, JRC Ispra, EC, Italy

E.1. BASIC SAFETY FEATURES OF ADS

E.1.1. ACCIDENT TYPES

In this overview it is assumed that in an accelerator-driven system (ADS) the same type of accidents can be envisaged as in critical reactors. The ADSs proposed in this State-of-the-Art report include fast systems with solid fuel and Lead or *sodium* cooling *(also gas cooling was discussed at one time)*, fast systems with circulating molten salt/minor actinides, thermal systems with circulating molten salt/minor actinide/Pu and graphite moderation and thermal systems in which the latter mixture or a water/oxide slurry is circulated in pipes and heavy water is used as moderator.

The generic accidents that can occur in low pressure fast or thermal systems are cooling-failure accidents, either due to a rapid primary flow decay caused by loss of power to the pumps (Loss-of-Flow: LOF) or due to the loss of the heat sink (LOHS) due to loss of power to the pumps in the heat removal loops or to the feedwater pumps. For a gas-cooled fast reactor the loss of coolant accident (LOCA) is a possibility if a sudden depressurization occurs due to a leak. For the low pressure systems the loss of coolant accident is of low probability and a guard vessel should assure that the coolant cannot escape completely. Decay heat removal problems can also lead to accidents, e.g. if the diesels driving the blowers for the forced convection cooling in a gas-cooled system fail to start.

The ADS systems mentioned in the Studies of Accidents in Reactors (SOAR) are also susceptible to reactivity accidents which are called Reactivity Induced Accidents (RIAs) for thermal reactors and Transient Overpower (TOP) accidents for fast reactors. All types of ADSs that have some control rods could experience an inadvertent withdrawal of the latter. In pressurised systems the blow-out of one control rod cluster is considered to be a possibility. Since ADSs will probably use fewer control rods than a critical reactor this will reduce the potential for reactivity accidents. Different types of reactivity insertions can also be postulated due to the inadvertent insertion of moderator material in a fast system, accumulations of fissile material in a system with circulating salt/fuel or earthquakes causing core distortions. The proposed sodium-cooled fast ADS will probably have a positive void coefficient which could lead to a reactivity excursion if the sodium overheats and boils. If the core of a fast ADS melted down there would be the potential for the core to slump down and form a molten pool in which molten fuel sloshing can occur. These fuel motions can also cause reactivity ramps.

Whether an ADS-specific accident due to a sudden and significant increase of the accelerator power above its nominal value is possible, is not clear at this time but it should be investigated whether such increases are possible.

E.1.2. PREVENTION OF ACCIDENTS IN ADSs

As for critical reactors a high quality of the safety grade components, their inspectability and an in-service inspection programme during the whole reactor life are necessary. Components which should be particularly reliable are the accelerator shut-off system and the decay heat removal systems. The design of the ADS should ideally be such that it cannot lead to a severe accident or that accidents develop slowly enough so that there is time for a corrective response. Because the shut-off of the neutron source is of major importance for cooling-failure accidents it is discussed below and compared with shutdown systems in critical reactors.

E.1.3. SWITCHING OFF THE ADS NEUTRON SOURCE IN CASE OF AN ACCIDENT

The reactor part of an ADS is a subcritical neutron-multiplying medium with a more or less powerful

neutron source. If one switches the external (spallation) neutron source off, the power will decrease to decay power levels. This will occur at a faster rate for larger neutron sources and their corresponding initial subcriticalies.

As will be discussed in the later sections on major cooling-failure accidents without beam shut-off, the rapid turning off of the neutron source is central for avoiding a core melt at least in fast systems with solid fuel. This is because the neutron source prevents a rapid power decrease even if some negative feedbacks come in [1] - see also the later discussion of cooling failure accidents in ADSs without beam shut-off.

For reactivity accidents in ADSs - even rather strong ones - the switch-off of the source may only be necessary after some time in order to prevent a limited core damage. The reasons for this will also be discussed in the later sections on reactivity accidents in which the source is left on.

E.1.3.1 Scramming a Regular Critical Reactor in Case of an Accident

To switch off the neutron source in an ADS is similar to the scramming of a critical reactor by rapidly inserting control rods. In reactor types in which a loss of coolant doesn't lead to a strong negative reactivity (i.e. gas cooled thermal reactors or thermal CANDU and sodium cooled fast reactors which even lead to positive void reactivities) a scram is an essential safety requirement in a major cooling failure accident at full power. PWRs or BWRs shut down by themselves in LOCA or station blackout accidents but it will be impossible to establish proper decay heat cooling if the scram is not actuated. The only type of reactor that could have survived a major cooling disturbance (LOF, LOHS) without scram would have been the now abandoned US Integral Fast Reactor (IFR) with metal fuel [1]. Even the Swedish PIUS concept uses a scram by adding large amounts of borated water into the core region in case of a cooling failure accident [2].

Reactivity insertions in LWRs or fast reactors at full power due to the inadvertent withdrawal of control rods, the ejection of a control rod cluster in a PWR or the dropping of such a cluster in a BWR require a fast scram in order to avoid core damage. The introduction of cold and unborated emergency cooling water into an LWR can also introduce an RIA which has to be terminated by a scram. All reactors have a certain potential for reactivity accidents and the main line of defence against them is the scram. The fact that an ADS can overcome sizeable reactivity insertions without a fast scram (see E.1.5.1 and E.1.5.2) is a unique property of this system.

E.1.3.2 Comparison of a Reactor Scram and Switching-off an Accelerator Beam

The delay time from the trip signal to a control rod release is about 0.5s for an LWR [3] and this delay will be similar for activating the beam shut-off system of an ADS. However, turning off the current to an accelerator should be considerably faster than the mechanical insertion of control rods which takes about 1.5 - 3s in an LWR [3] and should be less for fast reactors cores which are smaller.

Comparing the redundancy and diversity of a shutdown system with that of the beam shut-off system, the latter has a disadvantage because it is only one beam that can be shut off whereas many - even different - control rods can be inserted and e.g. in an LWR and an alternate shutdown mode is possible through the insertion of borated water. However, many diverse trip signals can feed into the beam shut-off.

Because the beam shut-off is mainly important for cooling failure accidents, the current to the accelerator should be coupled to the electrical current driving the primary pumps, the pumps for the secondary and - if existing - tertiary loops and also to the feedwater pumps. A different and fully passive system to shut the neutron source off, could involve the dropping of the spallation target by using a support made of a low melting point metal which would heat up and melt in a cooling failure or slow reactivity accident. The target could also be magnetically supported and if the magnets reached the Curie temperature, the target would drop. Another shut-off system could consist of deflecting the proton beam by demagnetising a magnetic lens through the cutting off of its current by bi-metallic devices located at the core outlet. In the ADS design by Rubbia, which is described earlier in this report, a passive beam interrupt devise is based on the rising Lead coolant level due to a cooling failure and leads to the overflow of the Lead into a container which is in the path of the proton beam. This appears to be a reliable and clearly transparent passive beam

shut-off system.

E.1.4. COOLING-FAILURE ACCIDENTS IN ADSS WITH THE SPALLATION SOURCE STILL ON

E.1.4.1 Loss-of-Flow Accident in a Sodium-cooled Fast ADS

In chapter E.1.7 calculations of LOF accidents in a large fast ADS (800MWe) are discussed and compared with those of a corresponding critical reactor. The main results are that fast sodium-cooled ADSs with their source still on Lead to much lower and wider power peaks than in the critical reactor. These power increases are caused by the positive sodium void reactivity. The power in the ADS also rises somewhat earlier because the negative feedbacks due to Doppler, axial expansion and structure feedbacks do not decrease the power as much as in a critical system (see also [1]). The sodium voiding phase is considerably longer lasting but pin failures still occur earlier in an ADS. Once strong negative feedbacks come in due to dispersive fuel motion, the power decreases much less than in a critical system. This is due to the neutron source which makes the ADS less sensitive to feedbacks (positive and negative ones). This "inertia" of the ADS to feedbacks has been recognised earlier [4].

The more subcritical an ADS, the more the above statements hold, i.e. the initial power peak becomes even lower, but after a strong negative feedback comes in, the power doesn't decrease much. The latter will lead to a complete core meltdown unless the spallation source is switched off. Two calculations with a simulated beam switch-off show that the ADS can be safely brought to decay power levels if the turning off is done before much sodium voiding has occurred. The later the switch-off takes place, the more core damage is likely. If the switch-off is too late, the meltdown will proceed by fuel slumping down leading to a molten fuel pool. Fuel sloshing around can lead to recriticalities and a power excursion [5]. A basic reason for this possibility is that a fast system is not in its most critical configuration initially.

On balance a sodium-cooled ADS would have advantages over a critical fast reactor with regard to LOF and probably LOHS accidents in which no beam switch-off or reactor scram is considered. This is mainly because no rapid power excursions are possible at least when the ADS is in its initial configuration. A smaller but still important point is that the phenomena such as sodium boiling and pin failures in different parts of the core are stretched out in time and therefore easier to detect. That a beam switch-off is necessary for an ADS during a LOF accident is similar to the necessity for a scram in a regular fast reactor. Both systems have the potential for recriticalities if the beam isn't shut off or a scram is not activated. With regard to regular decay heat removal, both systems can rely on passive natural convection cooling with the liquid sodium. With regard to post-accident heat removal both systems have equal uncertainties whether an in-vessel coolability is possible or not. Also both systems have the potential for sodium fires and sodium/water interactions.

E.1.4.2 Cooling Failure Accidents in Gas-Cooled Fast ADSs

Relative to sodium-cooled fast ADS, a gas cooled variant has the advantage that there is no chemically reactive coolant and that there will be no positive reactivity effect due to a decrease in the coolant density. Moreover, it may be possible to use water cooling in a post-accident heat removal situation if a properly designed in-vessel or ex-vessel core catcher could be designed that avoids recriticalities.

On the other hand there is the possibility of a LOCA accident if a leak occurred in the pressurised primary system. LOF and LOHS accidents are also possible. In all these cooling failure type accidents the timely switch-off of the accelerator beam is also crucial for avoiding a core melt. If a core melt occurred it could lead to recriticalities as in the sodium-cooled ADS. A significant disadvantage is that the regular decay heat removal can not be done in a passive natural circulation mode (or at least not for larger systems). In a shutdown condition with no electricity available, the forced convection cooling has to rely on diesel generators.

E.1.4.3 Cooling Failure Accidents in Lead Cooled Fast ADSs

Lead cooling has many safety advantages relative to sodium cooling. Hot Lead does not react chemically with air or water. Equally or more important is that it is a very weak moderator that will not lead to a significant spectrum change or positive reactivity effect when the coolant should experience a decrease in density due to heating of the coolant or due to boiling and voiding. In comparison to a gas coolant, Lead would be at much lower pressure and would not be susceptible to a Loss-of-Coolant Accident (LOCA). A leak of the primary vessel would only lead to the flowing of the low pressure coolant into the surrounding guard vessel.

A disadvantage of a Lead coolant is its high melting point of 327°C which probably requires electrical heaters during reactor start-up and possibly also at very low decay power levels. The failure of such electrical heaters could lead to some Lead freezing and blockage formation which could impede the coolant flow in the core. However, it should be investigated whether conduction cooling would not be sufficient for very low power conditions.

In the conceptual design of C. Rubbia (see chapter D.3), presented earlier in this SOAR, Loss-of-Flow (LOF) accidents due to pump failures cannot occur because the Rubbia design is based on natural convection cooling. However, a Loss-of-Heat Sink (LOHS) accident is still conceivable if e.g. the steam generators dried out due to a loss of feedwater. For the LOHS accident or for slow but long lasting reactivity insertions (see chapter E.1.7) these could lead to a partial or full meltdown of an ADS if the proton beam was not interrupted or the accelerator switched off. The Rubbia design includes a passive shutdown device based on the rise of the coolant level caused by the heating up of the Lead coolant. As explained earlier this will lead to the overflow of the Lead into a container that is in the path of the proton beam which will thus become a new target on top of the reactor. This would rapidly decrease the reactor power, and thus, the coolant temperature.

However, the decay heat would slowly increase the coolant temperature again. In the Rubbia design, the renewed and further level swell will lead to an overflow of the Lead into the relatively small gap between the main and the guard vessel and will largely increase the heat transfer between the two vessels. this will start a natural air convection cooling of the guard vessel. This type of decay heat removal, which was earlier proposed by the US ALMR programme, has the disadvantage that the containment has to have openings (which could possibly be closed in an emergency). An alternate way for the decay heat removal could be in-vessel Lead-air heat exchangers.

E.1.4.4 Coolant Failure Accidents in Thermal ADS with a Circulating Salt/Fuel Mixture.

An important advantage of thermal systems is that they have a lower power density than fast systems (for the same power, their cores are therefore much larger than those of fast ADSs). This makes the heating up of a core slower in a LOF or LOHS accident and allows more time for the detection of off-normal conditions. Moreover, the thermal expansion and the potential boiling of the salt/fuel mixture will reduce its density and will decrease the full power to a certain degree. However, this would lead soon (possibly within minutes) to extensive boiling and pressure generation if the accelerator wasn't switched off. If the switch-off wouldn't take place, the spallation source might melt, disintegrate and lead to neutronic shutdown before the primary system would be challenged.

A positive safety feature of this system is also that a problem with the decay heat removal does not lead to a rapid heating up of the primary system but allows tens of hours to re-establish the regular decay heat removal (Bell, 94). This is due to the fact that about 2/3 of the fuel is not in the core but in a natural circulation mode in the primary system which therefore gets heated up in its entirety. A smaller fluid fueled ADS ($< 800\ MW_t$) will probably loose all the decay heat to the surrounding. For a larger ADS of this type, the salt/fuel mixture will eventually have to be drained into a cooled reservoir. (In contrast a fast ADS with liquid coolant could have relatively small coolant/air heat exchangers which can passively remove all the decay heat from the primary system).

Another advantage relative to ADS systems with solid fuel is the on-line removal of short - lived fission products which will considerably reduce the fission product inventory.

Certain problems with the salt/fuel ADS could be due to the precipitation of the heavy fuel or minor

actinides which might lead to a temporary increase in density of the latter in the core. As will be discussed under reactivity accidents, this would lead only to a limited increase in power. However, one could also imagine that such a precipitation could lead to an accumulation somewhere in the primary system away from the graphite moderator and lead to a fast criticality. However, such an accumulation may blow apart without doing damage to the strong primary system.

An interesting problem for fluid fuel/molten salt systems may be a strongly positive temperature coefficient for a pure salt / Pu / minor actinide mixture because no ^{238}U or ^{232}Th, with their absorption resonances, is present [6]. If this were true, a LOF or LOHS would lead to some power increase rather than decrease during the heating up of the salt/fuel mixture if the beam was not switched off.

A potential problem is also the explosive interaction between molten salt and water [7] which could occur in the Russian design in which molten salt / fuel is pumped through pipes which are surrounded by heavy water. In such a system a leak could lead to a molten salt / water explosion which could destroy other pipes and lead to a propagating explosion. In the LASL design there could also be a potential problem if water was used in the secondary loop .

A general weakness of a molten salt / fuel design is that it is a relatively "dirty" system in which radioactive material gets into the pumps and heat exchangers and makes the inspection of these important components difficult. A related problem is that the vessel is the first safety boundary and if a leak occurred, the whole containment would be radioactive.

E.1.5. REACTIVITY ACCIDENTS WITH THE ACCELERATOR BEAM STILL ON

E.1.5.1 TOP Accident in a sodium cooled fast ADS

In chapter E.3. calculations of reactivity accidents in the same sodium-cooled ADSas used for the case described in E.2. are discussed and compared with reactivity accidents in an equivalent critical fast reactor. The results are rather clear. The sodium cooled ADS has no significant problems to cope with very fast and medium ramp rates (170 \$/s for a total insertion of up to 2.65 \$ and 6 \$/s for a total insertion of up to 3\$) - the subcriticality of the ADS was -3\$ in the first case and -5\$ in the second. The corresponding runs for the critical system gave power peaks of around 2000 times nominal and led to complete core destructions.

For a rather slow ramp of 10 c/s inserted for 30 s to give a total insertion of 3\$, the critical reactor will lead to pin failures in 1 out of 10 calculational channels. The negative feedback from the fuel dispersal makes the net reactivity low enough to prevent further failures. In the corresponding ADS case with a - 3\$ subcriticality, a failure of one channel occurred also - but later, for a -5\$ subcriticality it occurred even later, and for a subcriticality of -10\$ not at all.

For fast ramp rates, which could not be counteracted in a timely manner by a scram in a regular reactor, the ADS behaves benignly. For slow ramp rate accidents the ADS may lead to late failures and limited core damage if the beam is not shut off and the subcriticality is not large enough. However, since a beam shut-off system has to be in place for cooling - failure accidents, there is probably no need to go to low subcriticalities to avoid late pin failures. The unscrammed regular reactor will definitely experience some limited core damage for slow ramps which will probably not spread to the rest of the core.

E.1.5.2 TOP and RIA Accidents in other ADSs

The gas cooled fast ADS should behave similarly benignly when subjected to fast transients. For slow ramp rates and late pin failures, the fuel dispersal may be more limited in a gas cooled system and give less of a negative feedback which could lead to further pin failures.

A thermal ADS with a molten salt/fuel mixture will also react benignly to fast ramp rate insertion [Bell, 94]. For slow reactivity insertions, the advantage is certainly that no pins can fail in the fluid-fueled system and that it can probably survive an enhanced power situation without problems.

E.1.6 CONCLUSIONS

The ADS has a clear advantage for coping with fast ramp rate accidents which would occur too rapidly for scram systems in regular reactors. This ability to overcome fast reactivity insertions is important to avoid Chernobyl type power excursions.

In cooling-failure accidents without beam shut-off, rapid power excursions are not possible - even for positive void worth cores. However, the power of an ADS cannot be decreased very much due to negative feedbacks. The only way to decrease the power to decay heat levels is the switching off of the accelerator beam - otherwise a core melt will occur in a cooling failure accident (which would eventually happen in LWRs too if no scram were activated). Therefore emphasis will have to be put on a highly reliable beam shut-off system in an ADS. If the ADS had a low pressure cooling system and a guard vessel there could be no problems with Loss-off-Coolant Accidents (LOCA). Of general importance for safety in any reactor type as well as for ADSs is a reliable emergency decay heat removal system which should preferably be a passive system.

Comparing fast ADS with solid fuel and thermal ADS with a circulating salt/fuel mixture a few points are important. The thermal systems have a slower response time in accident situations which makes the detection of the off-normal conditions easier. In severe accident situations without beam switch-off, the salt/fuel will expand and boil and could lead to leakages whereas the fast system could melt down and possibly lead to a recriticality which could cause a power excursion. In the salt/fuel system pumps and primary heat exchangers are all radioactive and therefore difficult to inspect. Moreover, there are uncertainties about the precipitation and accumulation of fuel and minor actinides leading to mild excursions and there is also an uncertainty about the temperature coefficient of reactivity.

E.2. FIRST INVESTIGATIONS OF THE BEHAVIOUR OF AN ACCELERATOR DRIVEN FAST OXIDE REACTOR DURING AN UNPROTECTED LOSS-OF-FLOW ACCIDENT

E.2.1 INTRODUCTION

A new concept for an Energy Amplifier (EA) has been proposed by C. Rubbia [8]. It consists of a subcritical fast system that is driven by the proton beam of a compact cyclotron which hits a target in the reactor and generates about 50 fast neutrons per proton through a spallation process. The proposed F-EA is cooled by Lead and uses $^{233}U/^{232}Th$ fuel.

Safety considerations of such new approaches and in particular the investigation of severe accident conditions are important. An investigation of a severe reactivity accident was earlier undertaken [9]. Although the reactivity ramp used was rather steep and it started from initial reactor conditions this study showed that accelerator driven fast systems are rather insensitive to fast reactivity insertions.

The present study deals with a Loss-of-Flow accident in which the primary pumps are assumed to coast down (e.g. due to a station blackout) and which can lead to a major coolability problem for a fast reactor if no scram occurs. Different from the study above in which only the point kinetics and the Doppler feedback were considered, this study used the EAC2 code [10,11] which calculates coolant heating up and voiding, fuel pin heating up and axial expansion, pin ruptures and subsequent molten fuel motion inside the pins and in the coolant channels. The reactivity feedbacks due to axial pin expansion, sodium voiding, fuel motion as well as the Doppler feedback are considered. So far only sodium cooling has been considered. The subcriticality is simulated by a programmed negative reactivity. To simulate the spallation neutrons coming from the target a source was introduced into the point kinetics module. This represents a source that is uniformly distributed in the reactor which is only a simple approximation for the real case of a central neutron source. The reactor under consideration is a 800 MWe reactor design used in the European WAC benchmark calculations [12]. The pump coastdown times and a negative ramp of -2 cent/s, which roughly simulates a structural expansion feedback, were taken from the WACLOF benchmark. The core set-up with half of the fuel near fresh and the remainder with a burnup of 275 days and the dividing of the core into 10 representative calculational "channels" were also taken from the WACLOF benchmark. Since this benchmark dealt with a sodium coolant, the comparison calculations were also made for sodium cooling. The investigation of the accident behaviour with Lead cooling may be a further step.

E.2.2. CALCULATIONAL RESULTS

Figs 1 and 1a show the EAC-2 results for the standard WACLOF case. The important reactivity effects all occur within one second. Sodium voiding gets the total reactivity to prompt critical despite negative Doppler and axial pin expansion reactivities. Subsequently the fuel pins fail near the midplane and some in-pin fuel motion towards the failure location leads to positive reactivity effects (see the small positive peak of the total reactivity) and this leads to superprompt critical conditions and a power peak of 1800 times nominal. Once the fuel moves in the coolant channels away from the midplane, the fuel motion reactivity becomes strongly negative and shuts the reactor down. However more than 85 % is of the fuel is now molten. The integrated power measured from the first pin failure is 4.5 full power seconds

Fig.2 and 2a show a modified WACLOF case for which stress failure criteria were used for failing the pins. These mechanistic criteria lead to earlier pin failures than the melt fraction criteria in the original case. This leads to a more limited in-pin fuel motion to the pin rupture site, and thus, only to a power peak of 265 times nominal and only 1.8 full power seconds integrated power after the first pin failure .

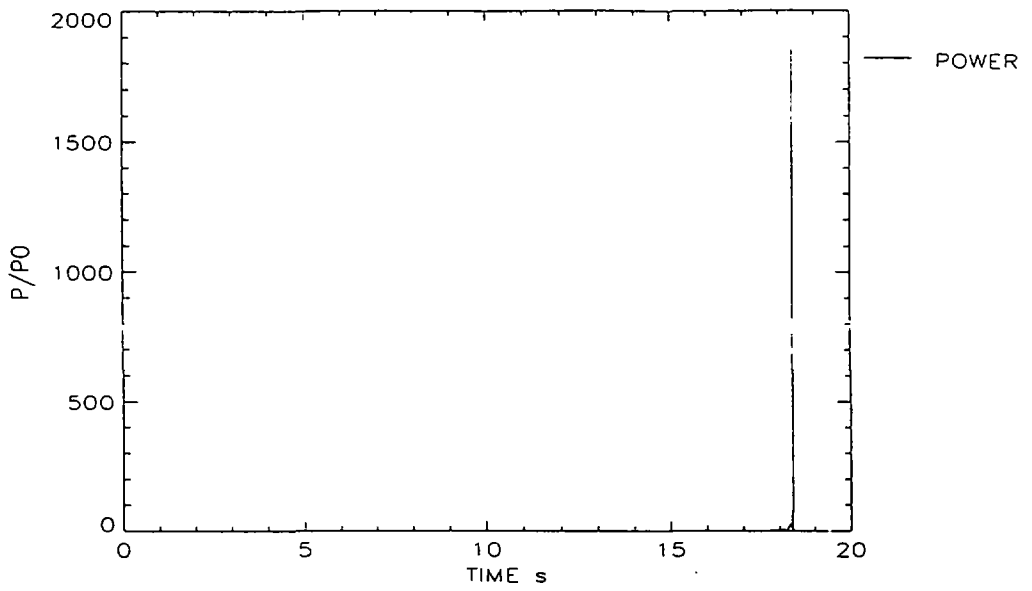

FIG. 1. Power history in the original WACLOF case (pin failures based on melt fraction criterion).

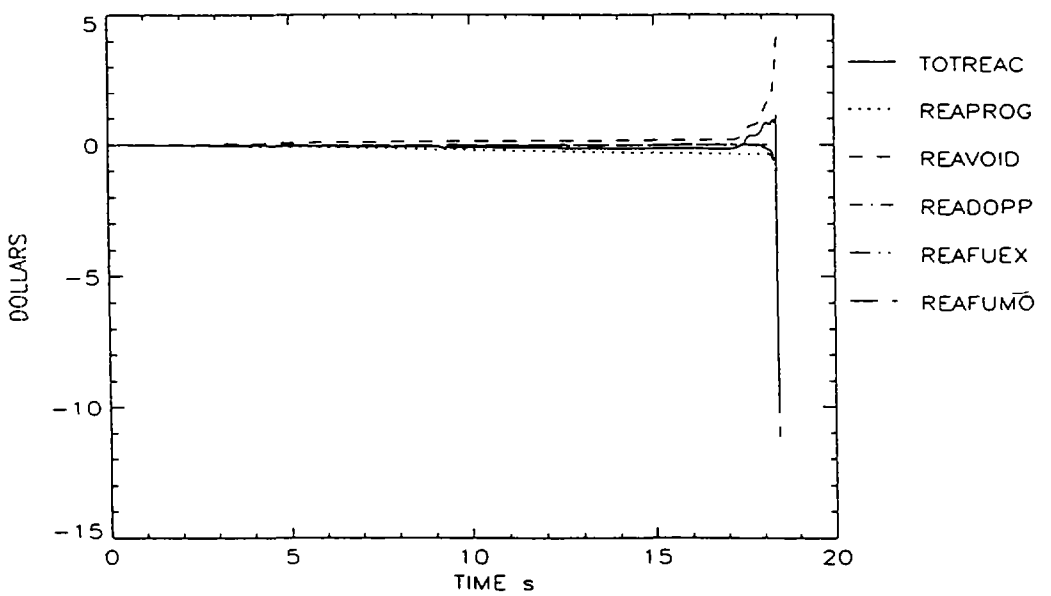

FIG. 1a. Reactivities causing the power history in Fig.1.

Fig.3 and 3a show the results of a run in which the WAC reactor was initially subcritical by -3$ and an accelerator driven neutron source was active and provided the neutrons necessary to maintain nominal power. The negative ramp of -2 cents/s was maintained in order to compare with the WACLOF case. For the pin failure criteria the melt fraction criteria from the WACLOF benchmark were also kept (70% maximum areal melt fraction for irradiated pins and 90% for fresh pins). The main difference in this

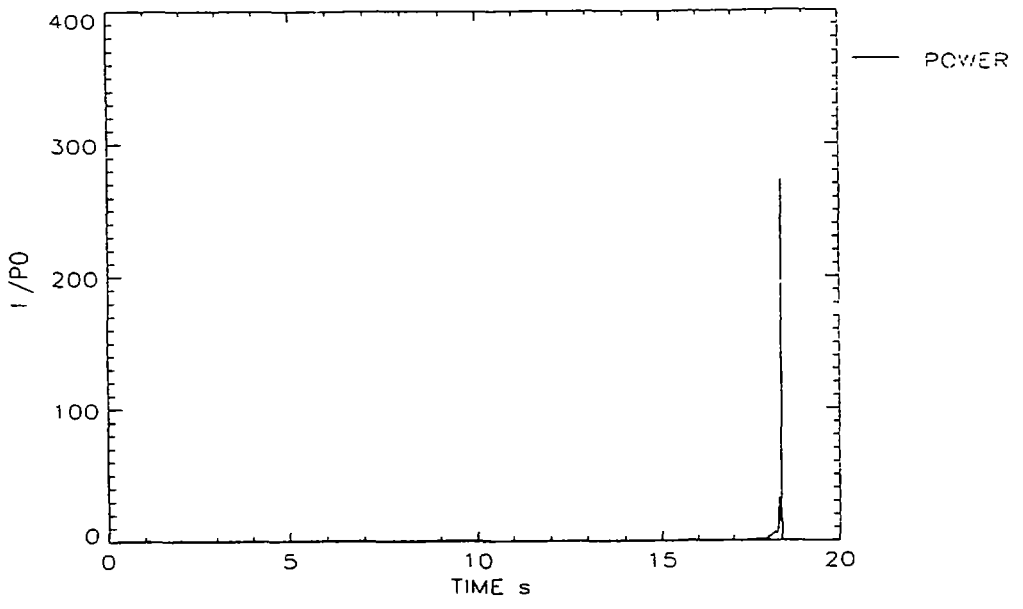

FIG. 2. Power of WACLOF case with more realistic pin failure criteria.

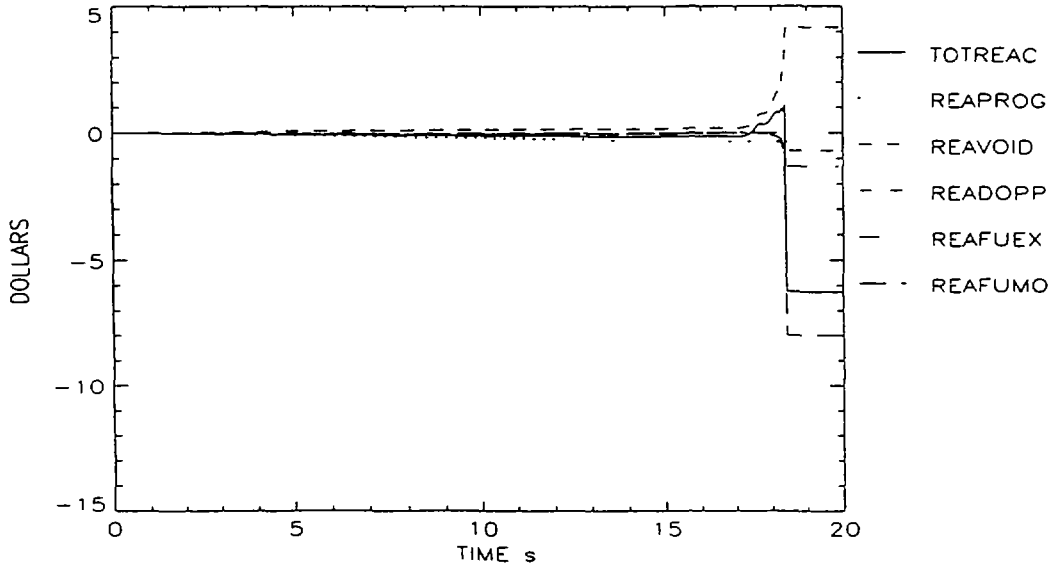

FIG. 2a. Reactivities causing the power history in Fig. 2.

calculation is that the power rises to only 5 times nominal and that the total reactivity gets only slightly above delayed critical. It can also be seen that the time from the onset of sodium voiding to the onset of fuel motion (i.e. pin failures) is about 3s, and thus, about 3 times longer than in Fig.1. However, fuel melting also occurs and leads to the failure of 3 of the 10 calculational channels. The subsequent fuel dispersal reduces the total reactivity to -10$, but the power reduces only to 0.3 times nominal because the neutron source is still on. This is further addressed in the discussion of Fig.5 below The integrated power

from the first pin failure to reaching 0.3 times power is 1.5 full power seconds.

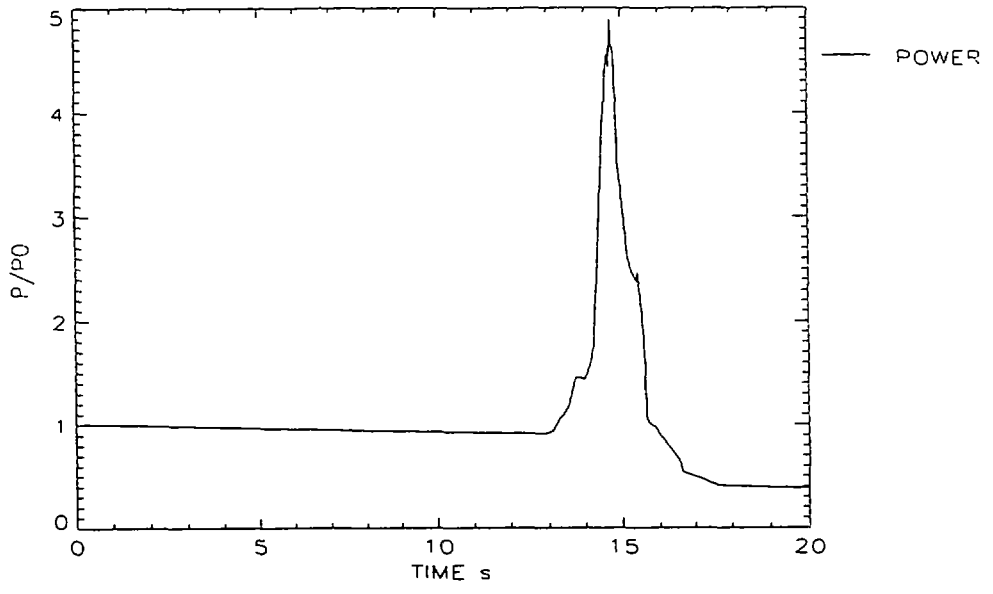

FIG. 3. Power history of WACLOF case with -3$ and neutron source

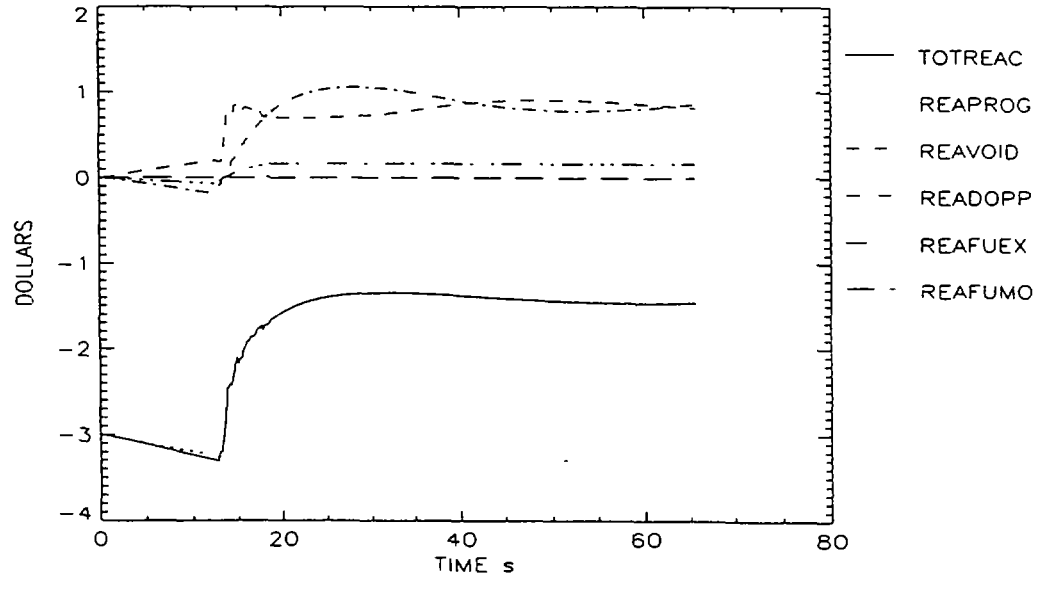

FIG. 3a. Reactivities causing the power history in Fig. 3.

In Figs. 4 and 4a the WAC reactor was initially at -10$ and the neutron source active and providing more neutrons than in the previous case. The power rises to only 1.4 times nominal and the time between voiding onset and pin failures is extended to 6s. The pins fail in 3 calculational channels and lead to molten fuel dispersal which causes a decrease in the total reactivity to -15$. However, the power only decreases

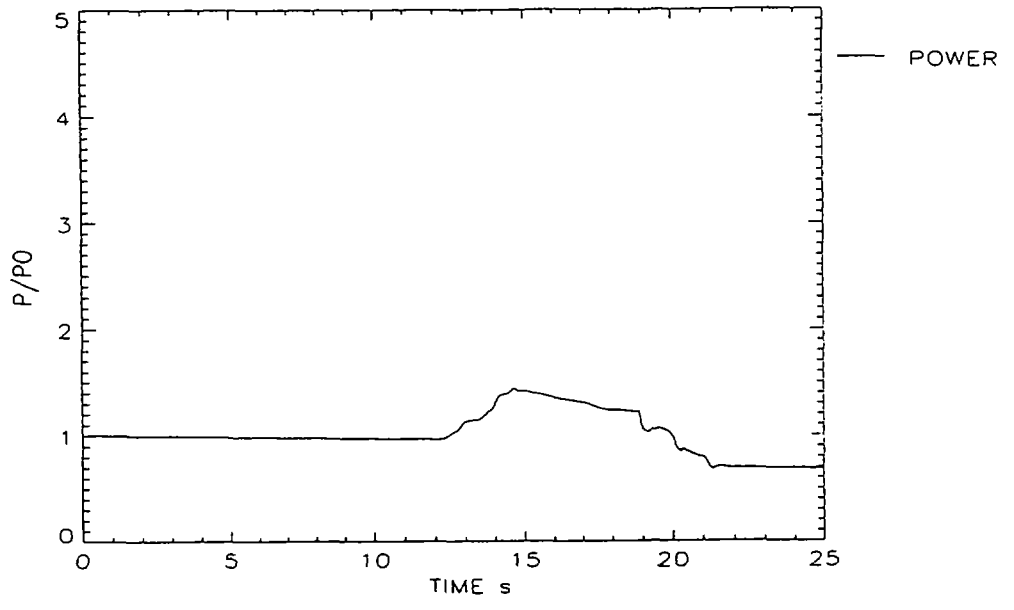

FIG. 4. Power history of WACLOF case - 10$ and neutron source

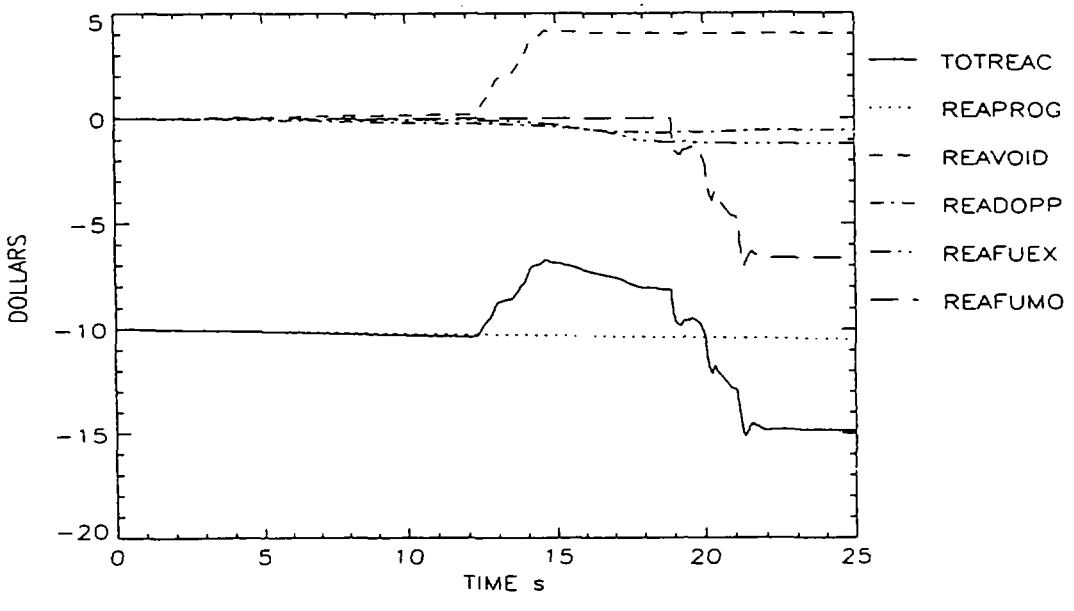

FIG. 4a. Reactivities causing the power history in Fig. 4.

to about 0.7 times nominal because of the relatively strong neutron source which is assumed to be still active. This rather high longer-term power level will lead to more core melting (see discussion of Fig.5). The integrated power from the first pin failure to reaching 0.7 times nominal power is 2.8 full power seconds. However, with the power remaining at 0.7 the integrated power would continue to increase with each additional second by 0.7 full power seconds . The EAC2 results presented in Figs. 4 and 4a cannot be considered very reliable because the cladding melted in this case before the fuel and EAC2 does not model molten cladding motion. The latter would have introduced additional positive reactivity and reduced

the fuel dispersal.

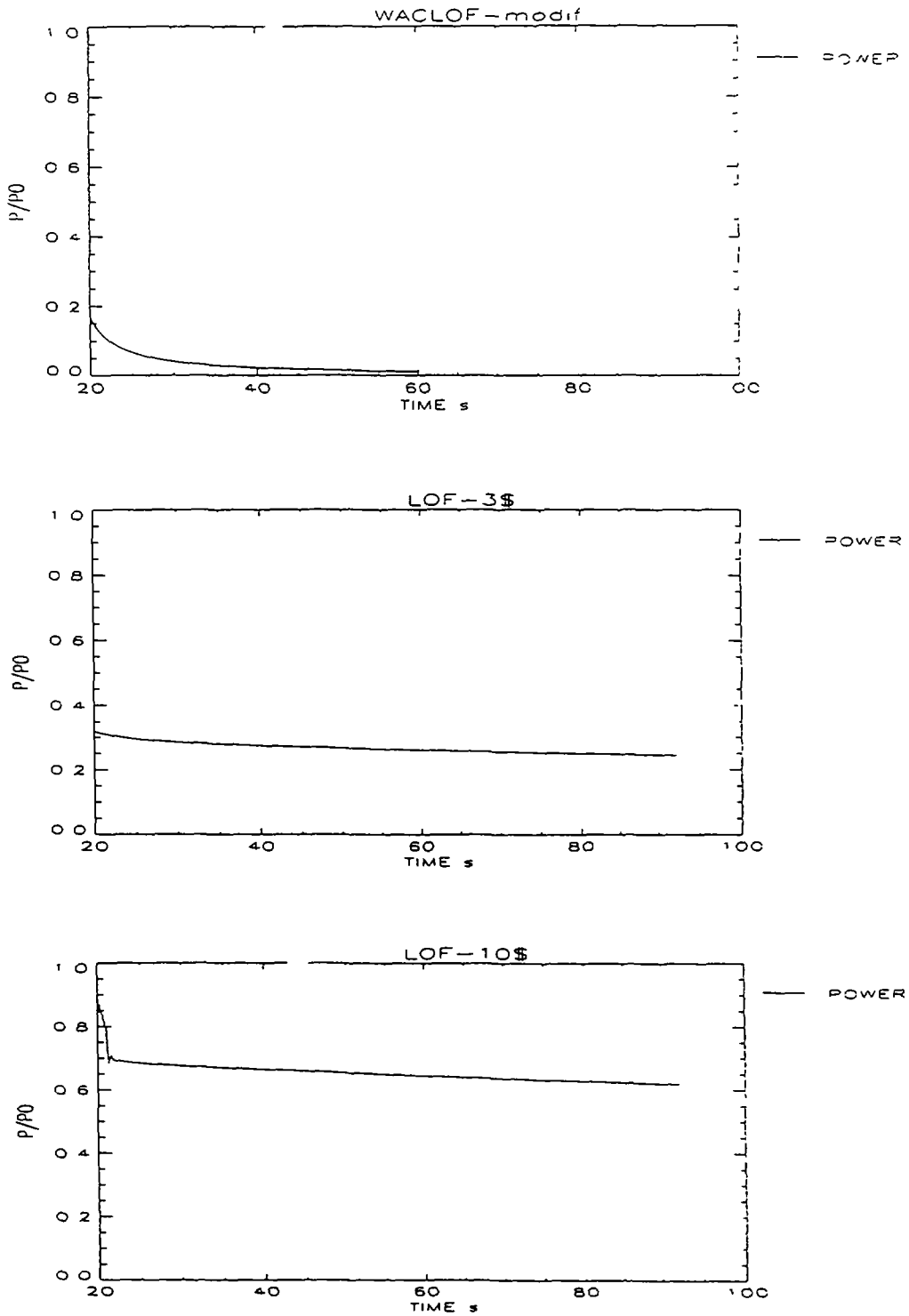

FIG. 5. Comparison of later power histories with core configuration fixed.

Fig 5 shows the later power histories in three cases no initial subcriticality, -3$, and -10$ initial subcriticality These power traces are based on the final configurations calculated by the thermo-hydraulic models (near the ends of Figs 2, 3, and 4) and a continuation of the calculation solely with the point kinetics model It can be seen that the power in the subcritical cases decreases only rather slowly (and the decrease is even partially due to the negative ramp of -2 cents/s which is still introduced) The maintaining of a relatively high power level due to the still active neutron source will cause the reactor core to melt down further unless the neutron source is switched off

Figs 6 and 6a shows the power history and the reactivity histories for the -10$ case including a switch-off of the accelerator beam starting at 12 3 s and decreasing with

$$e^{-t/\tau}$$

where was chosen to be 0 1 s The switching off of the source reduces the power level drastically The effect of the switching-off of the source is similar to the introduction of many control rods in a critical fast reactor When the source was switched off the core was already hot enough to cause sodium boiling However, the latter removed enough heat from the core so that the liquid sodium could re-enter and the

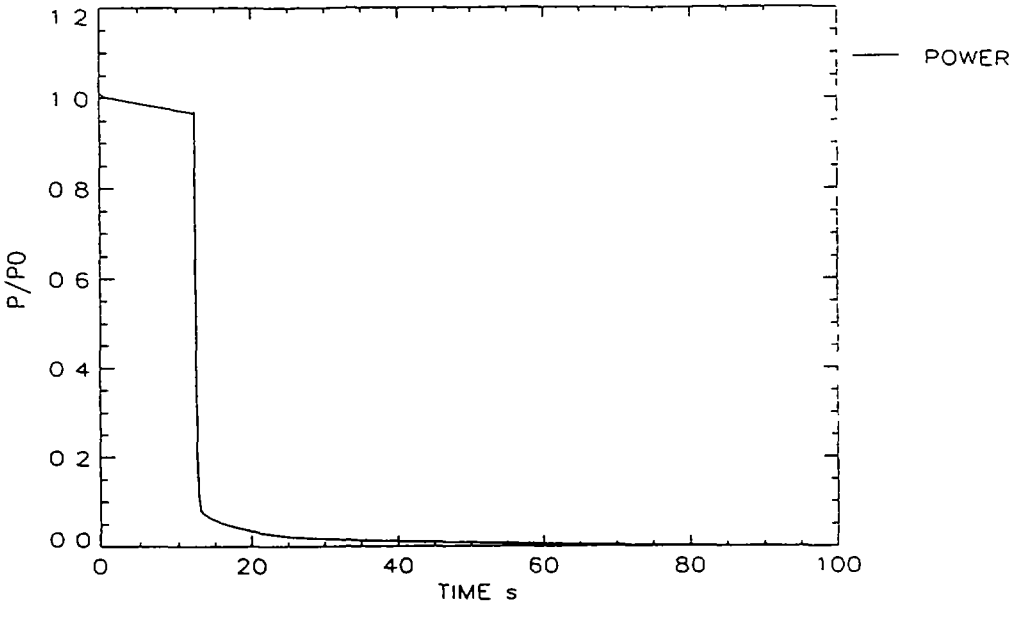

FIG 6 Power for case - 10$ but neutron source switched off at 12 3s

remaining small flowrate suffices to cool the core at the low power

Fig 7 and 7a show the power and reactivity histories for the -3$ case with the same switch-off of the beam as in Fig 6 However, due to the smaller subcriticality, the power doesn't drop as fast as in the case with the 10$ subriticality and the lead channel becomes vapour bound i e the liquid Na cannot penetrate anymore Whether the cladding in this channel will start melting or whether the liquid sodium can eventually get back into the channel depends on a more detailed calculation At any rate, it would have been better to shut the beam off earlier

E.2.2.1 Means of shutting off the beam

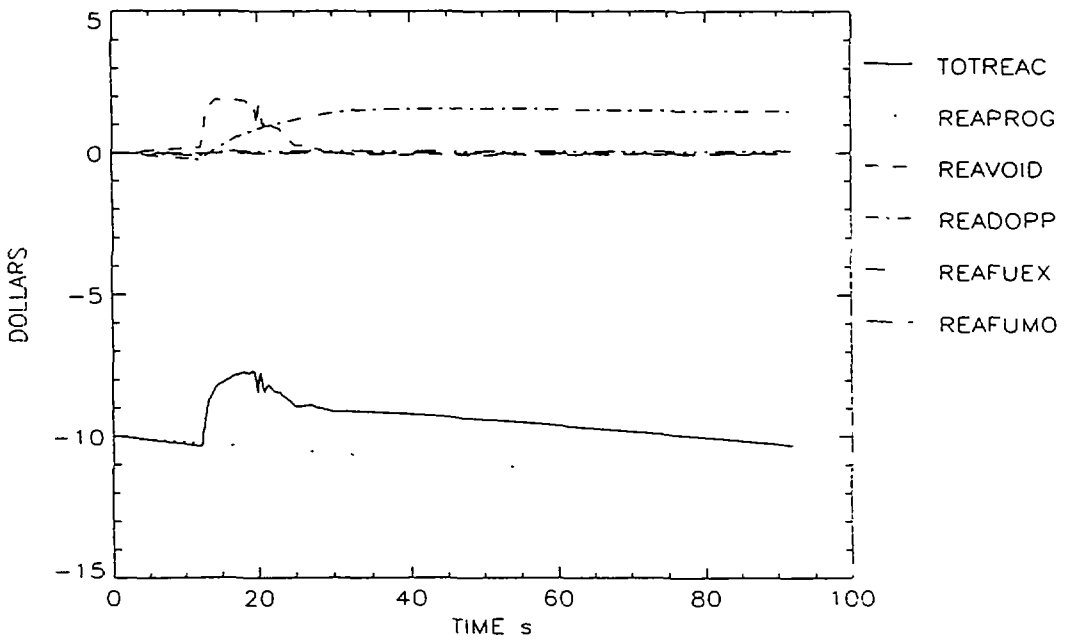

FIG. 6a. Reactivity changes responsible for power history in Fig. 6.

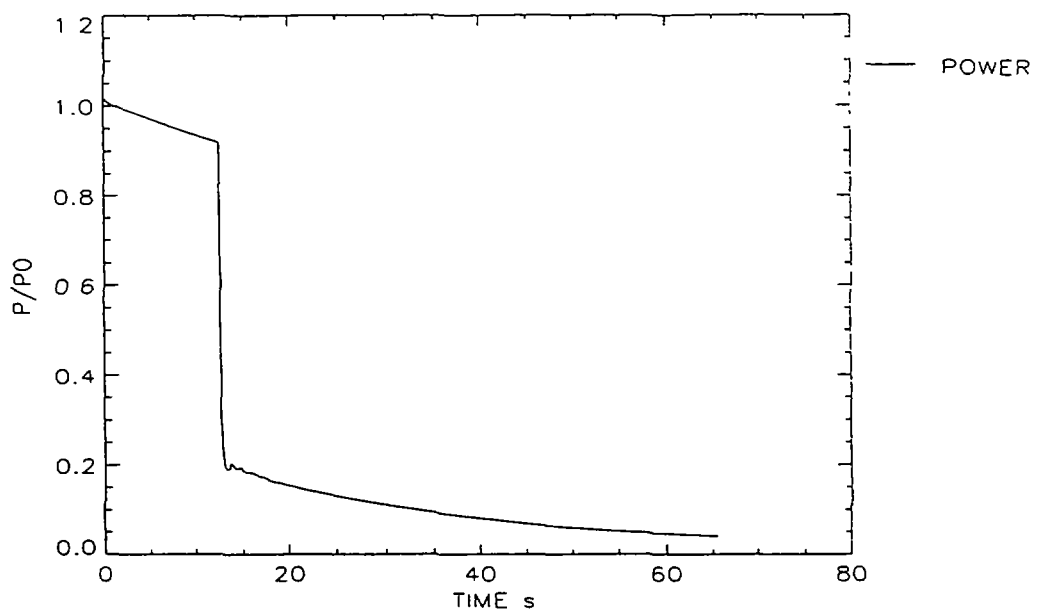

FIG. 7 Power of -3$ case with source switched off a little too late.

One can think of passive means to switch off the effect of a spallation source in case of an accident in which the coolant heats up. For a liquid lead target that is located in the middle of the core and hit by a

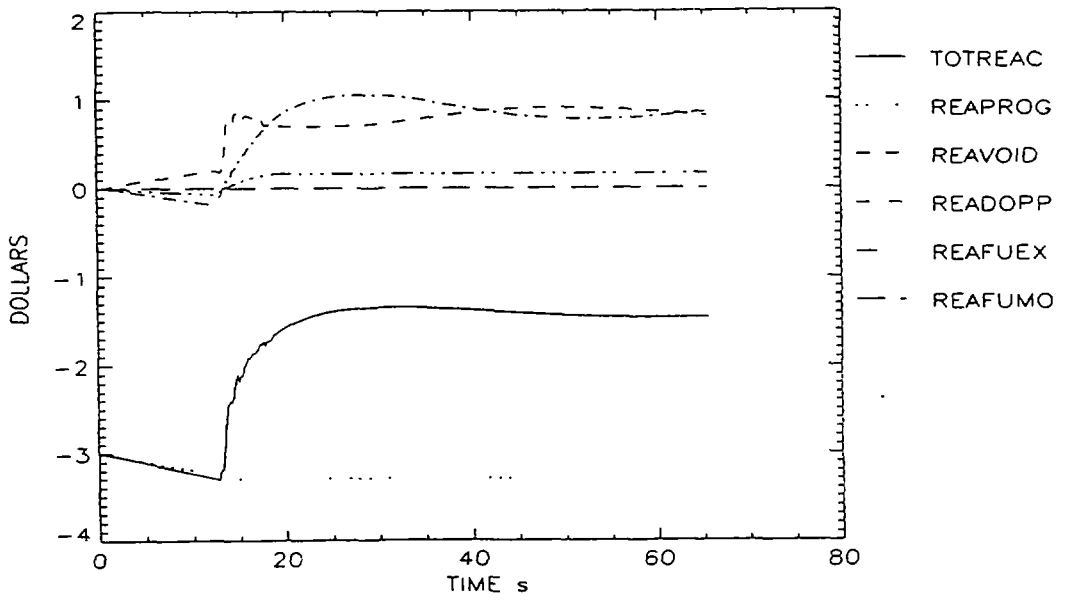

FIG 7a. Reactivity changes responsible for power history in Fig. 7

proton beam from above, one could use a metal plate with a low melting point as the bottom of a container for the target. If the cooling of the core and the target decreased, this bottom plate would melt and the liquid target would run down. The proton beam would then hit the target below the core where the neutron multiplication is low. - Off course all means for detecting coolant overheating (many different thermocouple indications, the de-magnetising of magnets) which are used in present LMFBRs for activating control rod insertion could also be used to switch off the cyclotron. Moreover there could be a connection between the electric current to the coolant pumps and the cyclotron which would cut the current to the latter off when the current to the primary or secondary pumps decreased.

E.2.3. CONCLUSIONS

The main safety advantage of a subcritical fast system driven by a spallation source is that no power excursions leading to high power levels are possible for positive reactivity additions which are of the order of the subcriticality. The possibility of power excursions during the initiation phase in present Fast Reactors is a disadvantage with regard to safety (recriticalities in the subsequent transition phase, post-accident coolability problems and sodium fires are the other ones)

An important remaining problem for subcritical fast systems undergoing a Loss-of-Flow or Loss-of-Heat-Sink accident is that a core melt-down cannot be prevented unless the spallation source is switched off (in present fast reactors the control rods have to be inserted to prevent a core melt down - it could be argued that the activation and the insertion of control rods is more complex than switching off an accelerator beam). If the spallation source is not switched off in any accident at full power, the latter will not decrease strongly even if a considerable negative reactivity has been introduced (e.g. negative Doppler feedback, ..)

As a general tendency it was confirmed that accelerator driven systems react benignly to the introduction of rather strong positive reactivities. On the other hand, massive cooling disturbances lead to core melting at low power if the accelerator beam is not switched off. Therefore investigations into passive means for shutting off the proton beam are of importance.

E.3. INVESTIGATION OF REACTIVITY ACCIDENTS IN A LARGE SODIUM-COOLED ADS

In this study the same 800 MWe fast reactor design is used as in the study of LOF accidents in chapter E.2. However, in this investigation all 10 channels which represent the core were irradiated for 275 days. Different reactivity ramp rates of 170$/s, 6$/s and 10 cents/s were investigated and the total reactivity insertions were limited to $2.65 and $3. The source strengths and the corresponding subcriticalities were also varied in some cases (between -3$ and -20$).

E.3.1. 170 $/S TOP CASES WITHOUT AND WITH SPALLATION SOURCE

The first case considers no external source and an insertion of up to 2.65 $. It is based on an old FZK benchmark case for space-time kinetics [13]. It should be mentioned that this ramp rate starting from steady state is probably unrealistic but it's slope is similar to the calculated voiding ramp rate shown in Fig. 10a. This benchmark case was earlier investigated by [9] with a point kinetics model and a point model for a reactor taking into account only the Doppler reactivity feedback. By recalculating this case with the EAC-2 code [10] important additional feedbacks due to axial fuel expansion, sodium voiding and fuel motion are also being considered. The results for the regular reactor case are shown in Fig.1. The first two power peaks are due to the driving ramp and the counteracting Doppler and axial expansion feedbacks. The second peak is lower because of the axial expansion feedback which gets more negative due to fuel melting and

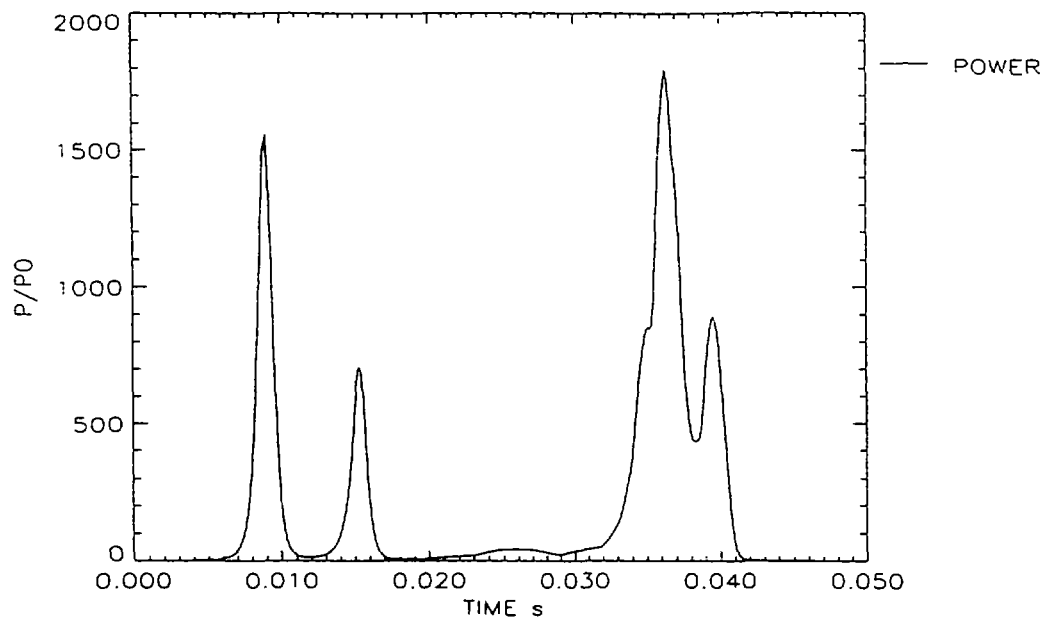

FIG. 1. Power history for 170 $/s TOP case without the neutron source.

expansion. The first pin failures due to cladding strain occur soon afterwards and lead to some voiding and fuel dispersal. At some time the voiding reactivity is not compensated anymore by the negative fuel reactivity and goes above prompt critical. The rapid power rise leads to stress failures which cause more voiding and the large power peak. However, eventually the fuel dispersal dominates and terminates this power excursion. At the end the entire core is molten and about 18 full power seconds of energy went into this power pulse.

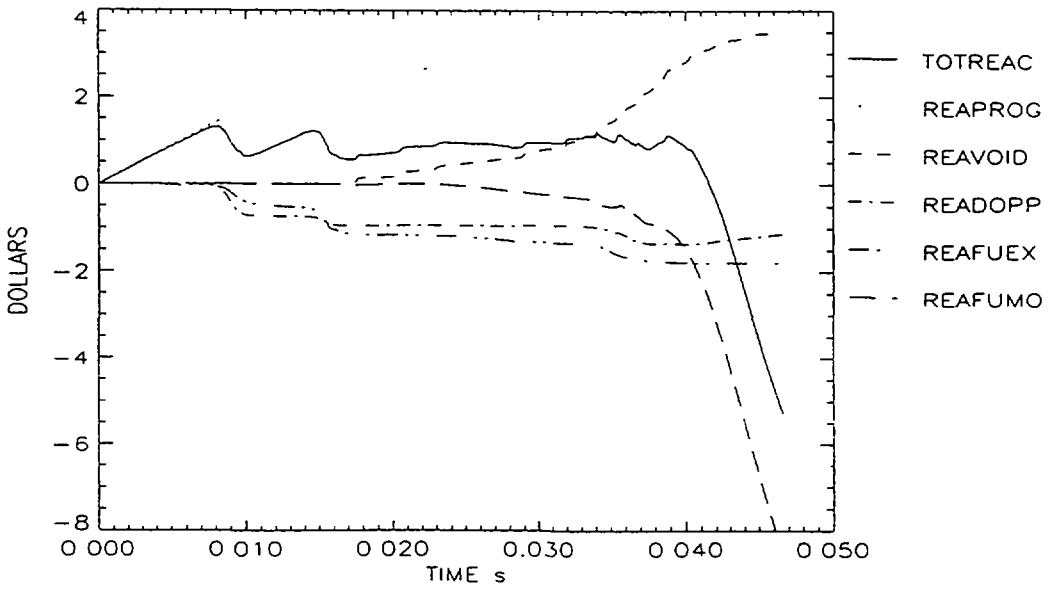

FIG. 1a. Reactivities causing the power history in Fig. 1.

The corresponding case with an external neutron source and a -3 $ subcricticality behaves benignly as can be seen in Fig. 2. The case was actually run up to 92 seconds when the power was 1.27 times nominal. After 60 s a few pin meshes indicated strain failures. But no fuel ejection was predicted because EAC-2 starts fuel ejection only when 25% areal melt fraction is reached and this did not happen. Most likely fission

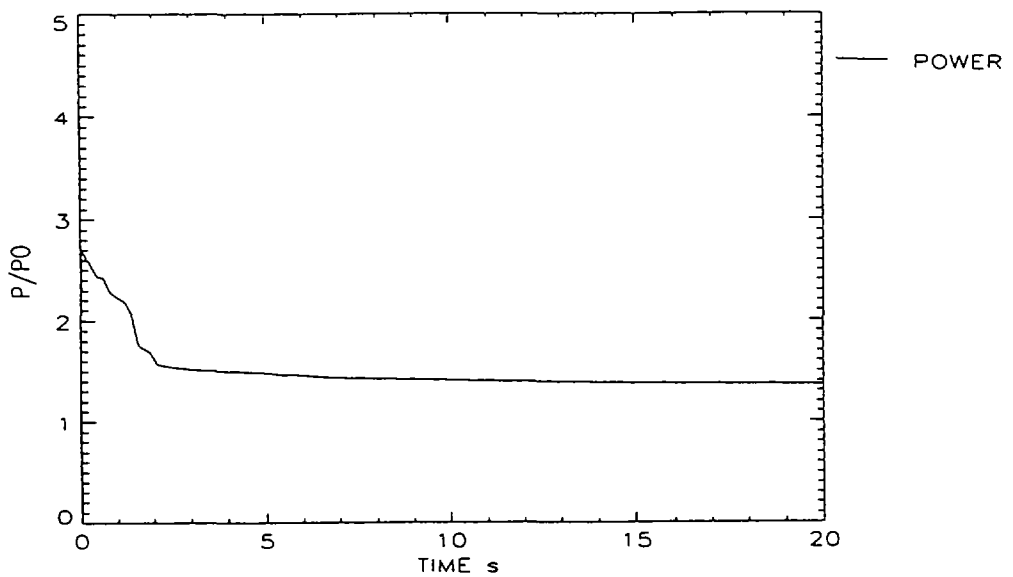

FIG. 2. Power history for 170 $/s case with the spallation source and -3 $ subcriticality.

gases will get released under these conditions. On the one hand there is some time to switch off the spallation source and on the other hand one could make the subcriticality larger.

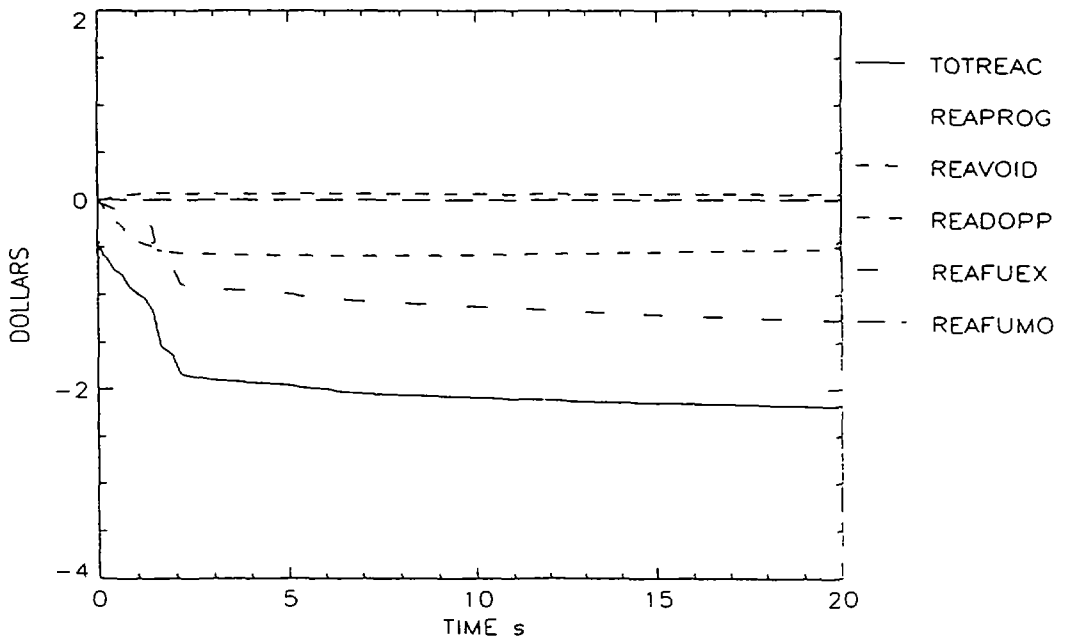

FIG 2a. Reactivity changes responsible for power history in Fig 2.

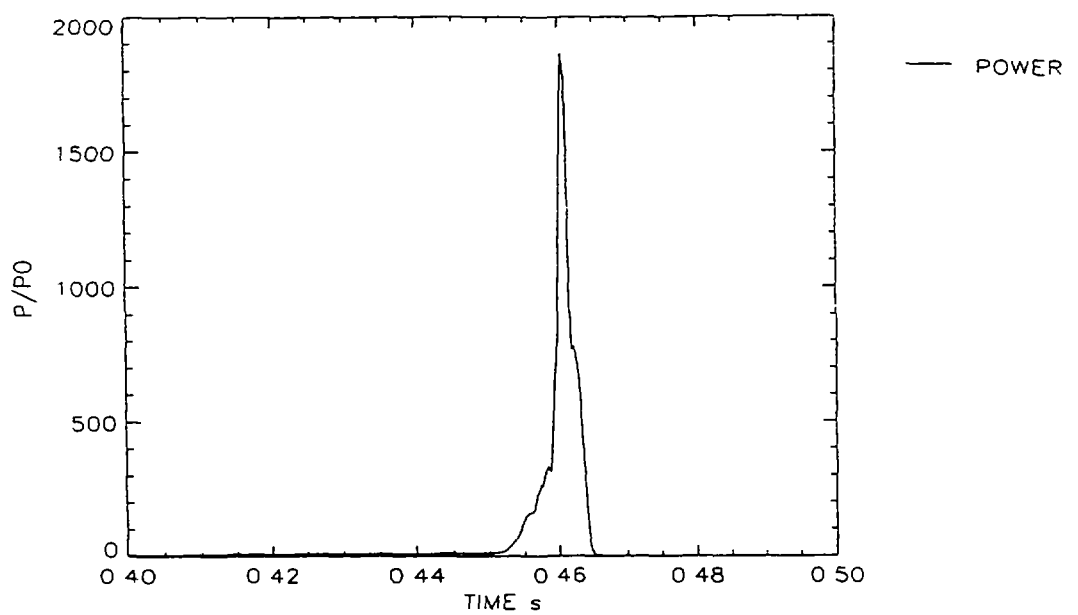

FIG. 3 Power history for 6 $/s TOP case without the spallation source.

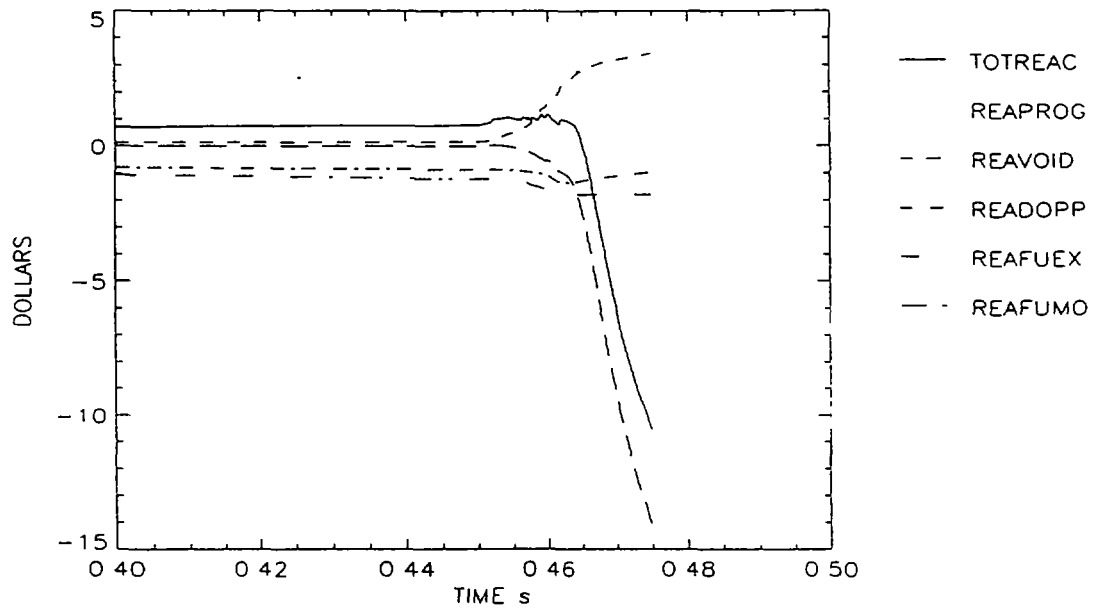

FIG. 3a Reactivities causing the power history in Fig. 3.

E.3 2. 6 $/S TOP CASES WITHOUT AND WITH SPALLATION SOURCE

The first case is without external source and the ramp is introduced up to 3 $. It should also be mentioned here that this is a very unlikely ramp rate Figs 3 and 3a show only the time interval from 0.4 to 0.5 s because nothing special happens before When the pins start failing and ejecting fuel, a rapid sodium voiding starts. The energy produced is about 9 full power seconds and the core is about 90%

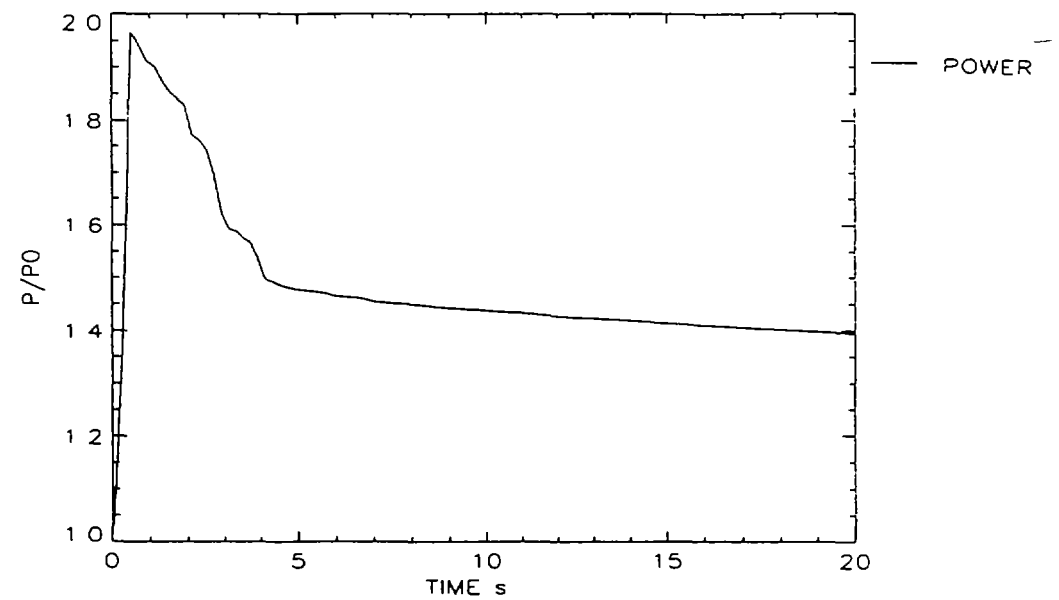

FIG. 4. Power history in 6 $/s TOP case with source and -5$ subcriticality

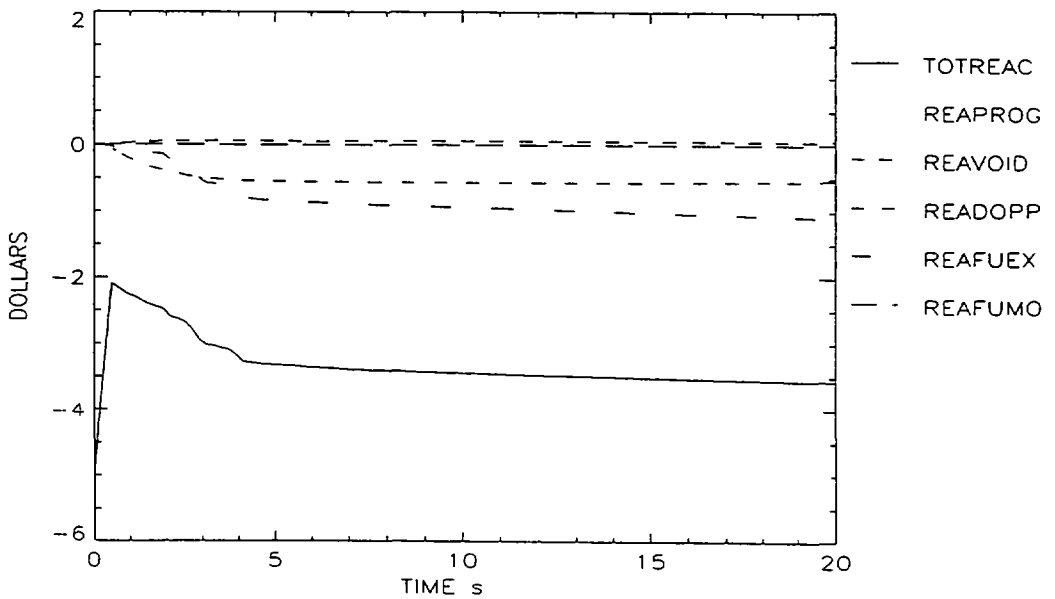

FIG 4a Reactivities causing the power history in Fig 4

molten This large peak is still less powerful than the one shown in Fig 1a This is due to an earlier rapid fuel dispersal in this case and in turn due to initial failure locations that are higher up

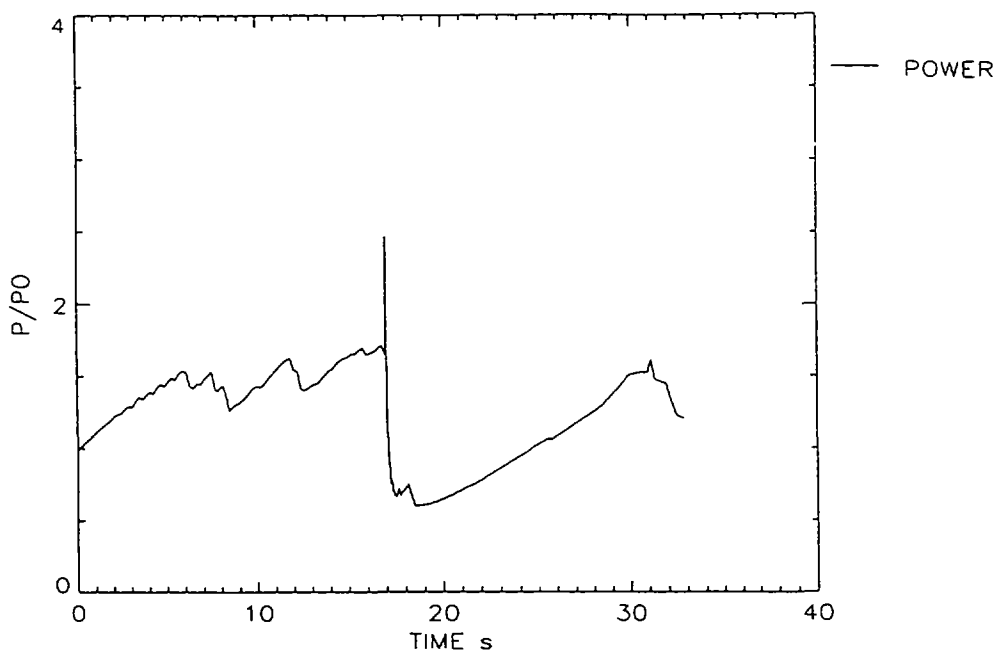

FIG 5 Power history for 10 cents/s TOP without the spallation source

The case with external source and a -5$ subcriticality is shown in Figs 4 and 4a The case was run out to 92 s and did not show any failure although the power at 92 s was 1 37 times nominal With a

subcriticality of only -3$ a strain failure led to fuel ejection in one channel. This caused enough of a negative reactivity to prevent failures in the other channels.

E.3.3. 10CENT/S TOP CASE WITHOUT AND WITH EXTERNAL SOURCE

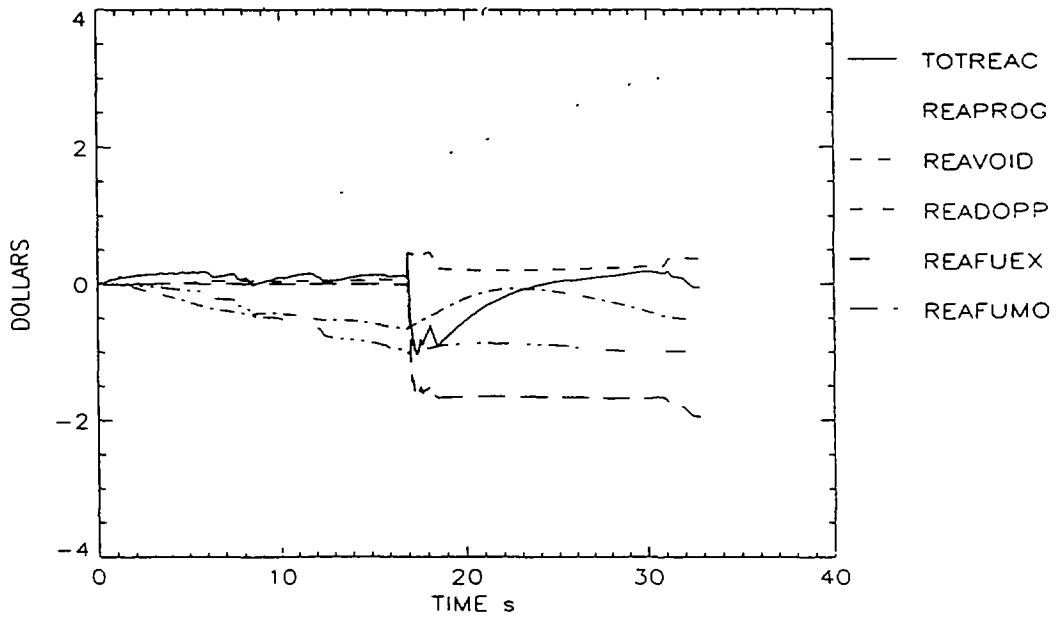

FIG. 5a. Reactivities causing the power history in Fig. 5.

The first calculation is for a regular fast reactor and the ramp inserts up to 3$. These slower ramp rates are considered more realistic but still of low probability. The power and reactivity histories are shown in Fig. 5 and 5a. The power rise is rather uneven and this is due to the axial fuel expansion reactivity which reflects the loss of fuel/clad contact in different channels which is modelled in the TRANSURANUS pin behaviour code [4] which is part of EAC2. This case leads inevitably to the failure of one calculational channel. The negative reactivity from the fuel dispersal just prevents another failure.

The alternate case with source uses a -10 $ subriticality to avoid any failure - Figs 6 and 6a. At 92 s the power level is about 1.3 times nominal. In another case a -$20 subcriticality was tried. This led to a power level of 1.15 times nominal at 92 s. With a -3$ subcriticality a strain failure occurred at 30 s at a power level of 1.65 times nominal power. With a -5$ subcriticality a strain failure occurred at 60s at 1.4 times nominal power. This means that one still gets the failures leading later than for a critical reactor and if one wants to avoid these failures one has to go to a larger subcriticality.

E.3.4. CONCLUSIONS

For fast or medium fast reactivity ramps the ADS has a major advantage in coping with such serious reactivity accidents. For slower ramps there is still somewhat of an advantage because pin failures will occur later or one can avoid them with a larger subcriticality. Moreover, they can be avoided with larger subcriticalities

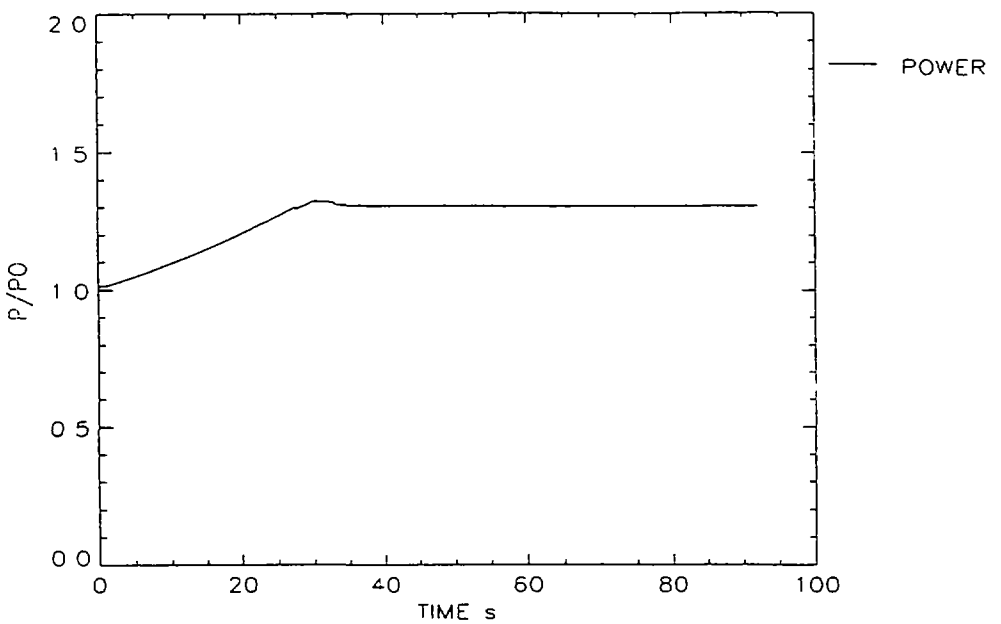

FIG 6 Power history in 10 cents/s TOP case with the spallation source and -10$subcriticality

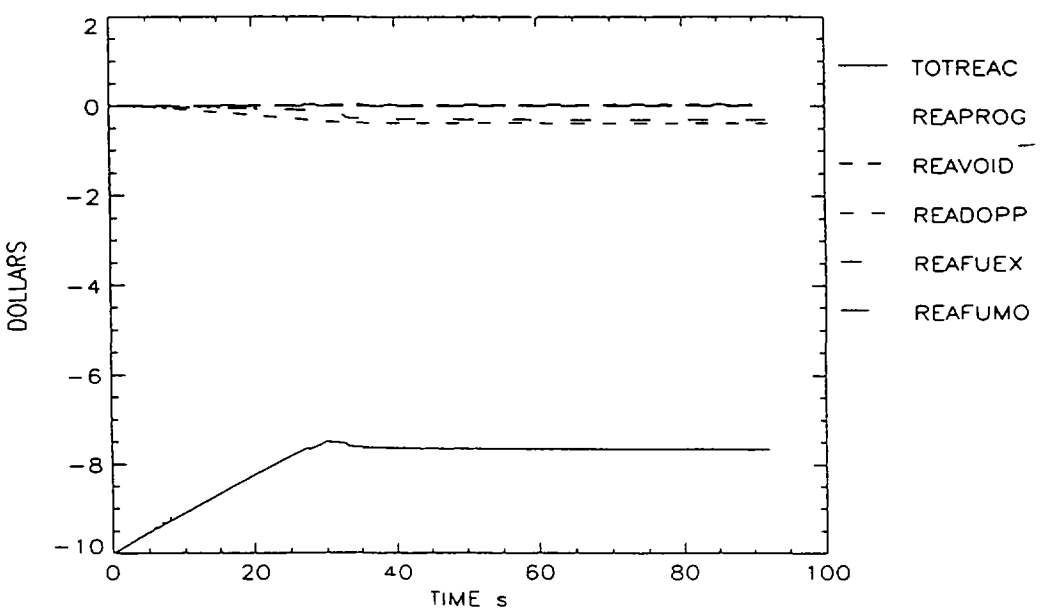

FIG 6a Reactivities causing the power history in Fig 6

REFERENCES

[1] F. Lypsch, and R. N. Hill, "Development and Analysis of a Metal-fueled Accelerator-Driven Burner", Int. Conference on Accelerator-Driven Transmutation Technologies ans Applications, Las Vegas, USA, 1994.

[2] B. Pershagen, "Light Water Reactor Safety", Pergamon Press

[3] D.J. Diamond, "The Control Rod Ejection Accident", Proc. of the First Technical Committee Meeting on Reactivity Transient Accidents, IAEA, Vienna, 1987

[4] C.R. Bell, "Safety Features of Subcritical Fluid Fueled Systems", International Conference on Accelerator-Driven Transmutation Technologies ans Applications, Las Vegas, USA, 1994.

[5] T.G. Theofanous, C.R. Bell, "An Assessment of CRBR Core Disruptive Accident Energetics", Proc. of the Int. Topical Meeting on Fast Reactor Safety, Vol. 1, Knoxville, USA, 1985

[6] Landeyro, ENEA, Rome, private communication

[7] H. Hohmann, H. Kottowski, H. Schins and R.E. Henry, "Experimental Investigations of Spontaneous and Triggered Vapour Explosions in the Molten Salt/Water System", Int. Meeting on Thermal Nuclear Safety, Chicago, USA, 1982

[8] C. Rubbia, "A High Gain Energy Amplifier Operated with Fast Neutrons", Int. Conf. on Accelerator-Driven Transmutation Technologies and Applications, Las Vegas, USA, July 1994

[9] H. Rief and H. Takahashi, "Safety and Control of Accelerator-Driven Subcritical Systems", Int. Conf. on Accelerator-Driven Transmutation Technologies and Applications, Las Vegas, USA, July 1994

[10] H. Wider et al., "The European Accident Code-2: Overview and Status", Proceedings of the 1990 International Fast Reactor Safety Meeting, Snowbird, Utah, USA, Aug. 1990

[11] Lassmann K. et. al., "Analysis of CABRI Experiments Using the TRANSURANUS Code and the Coupled Codes TRANSURANUS-CAMDYN", Technical Note K 0292158, CEC Institute for Transuranium Elements, Karlsruhe, 1992

[12] H. Wider et al. , "Comparative Analysis of a Hypothetical Loss-off-Flow Accident in an Irradiated LMFBR Core Using Different Computer Models for a Common Benchmark Problem", Nuclear Science and Technology, EUR 11925 EN, 1989

[13] L. Väth et al. "Survey of the Results of a Two-Dimensional Kinetic Benchmark Problem Typical for a Fast Reactor", Proc. Joint NEACRP/CSNI Specialist Mtg. on New Developments in the Three Dimensional Neutron Kinetics Benchmark Calculations, Garching, FRG, 1975

F. CONCLUSIONS AND RECOMMENDATIONS

ADS have the attractive potential to broaden and revitalize nuclear power. ADS address the main concerns and worries of the public regarding nuclear energy. There are still many questions which have to be answered before the engineering design of ADS can become a reality but already today the following points can be made:

(1) ADS offer a subcritical mode of operation for nuclear power systems, and make them flexible from the operational point of view.

(2) ADS reduce the long-lived waste burden and offer the way to transmute existing nuclear reactor waste.

(3) A well designed ADS can ensure a proliferation-resistant fuel cycle and fuel treatment.

(4) ADS open a promising way to utilize Thorium resources for energy production.

(5) ADS offer an alternative way to utilize the existing excess of weapons-grade Plutonium for energy production.

Economic and technical developments throughout the world should not be achieved at the expense of the environment. In this context ADS is an attractive option which research institutes and industry should develop and offer to the international community.

The international cooperation under the auspices of international organizations could be focused on:

1. Encouraging and stimulating ADS research in the different countries, particularly in the fields of:
   - a) Assessment of accelerators as drivers for nuclear subcritical systems
   - b) Transmution of nuclear wastes from commercial nuclear power plants, with special attention to reactor grade Plutonium stocked in the wastes
   - c) Utilization of the excess of weapons-grade Plutonium for power production
   - d) Introduction of the Thorium nuclear fuel cycle
   - e) Non-proliferation / aspects of the ADS-fuel cycle
   - f) Safety assessment of ADS
   - g) Impact of ADS on the radiotoxicity of the fuel cycle
3. Preparing the evaluation of possible synergetic nuclear energy systems based on different scenarios e.g. LWR - FBR - ADS, LWR - ADS etc.
4. Supporting international efforts to organize demonstration experiments on ADS
5. Extending the nuclear data research into the reactions and energy regions of interest for ADS
6. Organizing meetings for information exchange and for coordination of further international efforts.

LIST OF CONTRIBUTERS TO DRAFTING AND REVIEW

Czech Republic	Miloslav Hron The Institute of Nuclear Physics Czech Academy of Sciences, Rez
	František Janouch The Institute of Nuclear Physics Czech Academy of Sciences, Rez
	Mikulas Kuzmiak The Institute of Nuclear Physics of the Academy of Sciences of the Czech Republic
	Rostislav Mach The Institute of Nuclear Physics Czech Academy of Sciences, Rez
	V. Valenta Skoda, Nuclear Machinery, Ltd. Czech Republic
France	J.C. Cabrillat CEA - Nuclear Reactor Directorate Cadarache
	J.P. Chauvin CEA - Nuclear Reactor Directorate Cadarache
	Ph. Finck CEA - Nuclear Reactor Directorate Cadarache
	R. Jacqmin CEA - Nuclear Reactor Directorate Cadarache
	M. Martini CEA - Nuclear Reactor Directorate Cadarache
	H. Mouney EDF-DE
	M. Salvatores CEA-DRN
	J.P. Schapira CNRS-IN2P3

	I. Slessarev CEA, Cadarache
	R. Soule CEA - Nuclear Reactor Directorate Cadarache
	A. Tchistiaakov CEA - Nuclear Reactor Directorate Cadarache
Italy	S. Buono Sincrotrone Trieste Trieste
	N. Fiétier Laboratoire du Cyclotron Nice
	P. Mandrillon Laboratoire du Cyclotron Nice
	H.U. Wider EC JRC Ispra
Japan	K. Hasegawa Japan Atomic Energy Research Institute Tokai-mura, Naka-gun, Ibaraki-ken 319-11 Japan
	Kenji Ishibashi Kyushu University Hakozaki Higashi-ku, Fukuoka-shi Fukuoka-ken 812
	N. Ito Japan Atomic Energy Research Institute Tokai-mura, Naka-gun, Ibaraki-ken 319-11 Japan
	Hiroji Katsuta Japan Atomic Energy Research Institute Tokai-mura, Naka-gun, Ibaraki-ken 319-11 Japan
	Masumitsu Kubota Japan Atomic Energy Research Institute Tokai-mura, Naka-gun, Ibaraki-ken 319-11 Japan

Mr. J. Kusano
Japan Atomic Energy Research Institute
Tokai-mura, Naka-gun, Ibaraki-ken
319-11 Japan

Shin-ichirou Meigo
Japan Atomic Energy Research Institute
Tokai-mura, Naka-gun, Ibaraki-ken
319-11 Japan

M. Mizumoto
Japan Atomic Energy Research Institute
Tokai-mura, Naka-gun, Ibaraki-ken
319-11 Japan

H. Murata
Japan Atomic Energy Research Institute
Tokai-mura, Naka-gun, Ibaraki-ken
319-11 Japan

Tatsushi Nakamoto
Kyushu University
Hakozaki
Higashi-ku, Fukuoka-shi
Fukuoka-ken 812

N. Nakamura
Power Reactor and Nuclear Fuel Development Corporation

Takahiko Nishida
Japan Atomic Energy Research Institute
Tokai-mura, Naka-gun, Ibaraki-ken
319-11 Japan

Toru Ogawa
Japan Atomic Energy Research Institute
Tokai-mura, Naka-gun, Ibaraki-ken
319-11 Japan

H. Oguri
Japan Atomic Energy Research Institute
Tokai-mura, Naka-gun, Ibaraki-ken
319-11 Japan

Y. Okumura
Japan Atomic Energy Research Institute
Tokai-mura, Naka-gun, Ibaraki-ken
319-11 Japan

K. Sakogawa
Japan Atomic Energy Research Institute
Tokai-mura, Naka-gun, Ibaraki-ken
319-11 Japan

Toshinobu Sasa
Japan Atomic Energy Research Institute
Tokai-mura, Naka-gun, Ibaraki-ken
319-11 Japan

Yasufumi Suzuki
Japan Atomic Energy Research Institute
Tokai-mura, Naka-gun, Ibaraki-ken
319-11 Japan

Hiroshi Takada
Japan Atomic Energy Research Institute
Tokai-mura, Naka-gun, Ibaraki-ken
319-11 Japan

Takakazu Takizuka
Japan Atomic Energy Research Institute
Tokai-mura, Naka-gun, Ibaraki-ken
319-11 Japan

S. Tani
Power Reactor and Nuclear Fuel Development Corporation

Russian Federation

V.F. Batyaev
Institute for Theoretical and Experimental Physics
Moscow

P.P. Blagovolin
Institute for Theoretical and Experimental Physics
Moscow

P.V. Bogdanov
MNP

I. Chuvillo
IPPE
117259, Moscow

E.I. Efimov
EDO "Hydropress"
Podolsk, Moscow

V.P. Eismont
V.G. Khlopin Radium Institute
St-Petersburg

Yu.T. Gorschkov
EDO "Hydropress"
Podolsk, Moscow

V.D. Kazaritsky
Institute for Theoretical and Experimental Physics
Moscow

Genadji Kiselev
IPPE
117259, Moscow

B.P. Kochurov
ITEP
Moscow

V.R. Mladov
Institute for Theoretical and Experimental Physics
Moscow

B.P. Murin
MRTI
Moscow

M.L. Okhlopkov
Institute for Theoretical and Experimental Physics
Moscow

Yu. I. Orlov
Institute of Physics and Power Engineering
Obninsk, Kaluga Region

V.A. Shulyndin
EDO "Hydropress"
Podolsk, Moscow

S.G. Yavshits
V.G. Khlopin Radium Institute
St-Petersburg

V.V. Seliverstov
Institute for Theoretical and Experimental Physics
Moscow

Yu.N. Shubin
IPPE
Obninsk, Kaluga Region

O.V. Shvedov
ITEP
Moscow

N.V. Stepanov
Institute for Theoretical and Experimental Physics
Moscow

V.I. Volk
Institute of Inorganic Materials
Moscow

Sweden

H. Condé
Uppsala University
Uppsala

W. Gudowski
Royal Institute of Technology
Stockholm

Switzerland

C. Rubbia
European Organization for Nuclear Research
CERN
Geneva

J.A. Rubio
European Organization for Nuclear Research
CERN
Geneva

F. Carminati
European Organization for Nuclear Research
CERN
Geneva

J. Galvez
European Organization for Nuclear Research
CERN
Geneva

C. Gelès
European Organization for Nuclear Research
CERN
Geneva

Y. Kadi
European Organization for Nuclear Research
CERN
Geneva

R. Klapisch
European Organization for Nuclear Research
Cern
Geneva

J.P. Revol
European Organization for Nuclear Research
CERN
Geneva

Ch. Roche
European Organization for Nuclear Research
CERN
Geneva

USA

E.D. Arthur
Los Alamos National Laboratory
Los Alamos, NM 87545

C.A. Beard
Los Alamos National Laboratory
Los Alamos, NM 87545

Charles D. Bowman
LER-ADTT
Los Alamos National Laboratory
Los Alamos, NM 87545

R.R. Bracht
Los Alamos National Laboratory
Los Alamos, NM 87545

J.J. Buksa
Los Alamos National Laboratory
Los Alamos, NM 87545

W. Chavez
Los Alamos National Laboratory
Los Alamos, NM 87545

B.G. DeVolder
Los Alamos National Laboratory
Los Alamos, NM 87545

E. Heighway
Los Alamos National Laboratory
Los Alamos, NM 87545

L. Ning
LER-ADTT Project Office
Los Alamos National Laboratory
Los Alamos, NM 87545

J.J. Park
Los Alamos National Laboratory
Los Alamos, NM 87545

R.B. Parker
Los Alamos National Laboratory
Los Alamos, NM 87545

C. Pillai
Los Alamos National Laboratory
Los Alamos, NM 87545

E. Pitcher
Los Alamos National Laboratory
Los Alamos, NM 87545

R.C. Potter
Los Alamos National Laboratory
Los Alamos, NM 87545

R.S. Reid
Los Alamos National Laboratory
Los Alamos, NM 87545

G.J. Russell
Los Alamos National Laboratory
Los Alamos, NM 87545

H. Takahashi
Brookhaven National Laboratory
Upton, New York 11973

D.A. Trujillo
Los Alamos National Laboratory
Los Alamos, NM 87545

F. Venneri
Los Alamos National Laboratory
Los Alamos, NM 87545

M.A. Williamson
LER-ADTT Project Office
Los Alamos National Laboratory
Los Alamos, NM 87545

S.A. Wender
Los Alamos National Laboratory
Los Alamos, NM 87545

D.J. Weinacht
Los Alamos National Laboratory
Los Alamos, NM 87545

W.B. Wilson
Los Alamos National Laboratory
Los Alamos, NM 87545

K.A. Woloshun
Los Alamos National Laboratory
Los Alamos, NM 87545

IAEA

V. Arkhipov
(Scientific Secretary)
International Atomic Energy Agency
Wagramerstrasse 5, A-1400, Vienna.